ISSN (Print): 2734-259X | ISSN (electronic): 2734-2603

# NIGERIAN JOURNAL OF ENVIRONMENTAL SCIENCES AND TECHNOLOGY (NIJEST)

In Affiliation with The Nigerian Environmental Society (NES)

https://www.nijest.com Volume 5 | Number 1 | March 2021

# NIGERIAN JOURNAL OF ENVIRONMENTAL SCIENCES AND TECHNOLOGY (NIJEST)

https://nijest.com

Volume 5 | Number 1 | March 2021

A

PUBLICATION OF

FACULTY OF ENVIRONMENTAL SCIENCES

UNIVERSITY OF BENIN

IN

AFFILIATION WITH

THE NIGERIAN ENVIRONMENTAL SOCIETY

Published by:
The Faculty of Environmental Sciences
University of Benin
P.M.B 1154, Benin City, Edo State, Nigeria
E: editor-in-chief@nijest.com

In Partnership with
Mindex Publishing Co. Ltd.
22, Benin Technical College Road,
Ugbowo, P. O. Box 5089, Benin City, Nigeria
Tel: +234802 345 3848, 803 740 4398, 805 475 5695
Email: info@mindexpublishing.com, mindexpublishing@gmail.com
website: www.mindexpublishing.com

*Benin *Lagos *Abuja *Aba



**Services**

For advertisements (online or in print copy of NIJEST), journal reprints and general enquiries please contact the secretariat or email the Editor – editor-in-chief@nijest.com

**Address for Correspondence**

The Nigerian Journal of Environmental Sciences and Technology (NIJEST) is Managed by:

The Faculty of Environmental Sciences,
University of Benin
PMB 1154, Benin City, Edo State, Nigeria
E: editor-in-chief@nijest.com

NIGERIAN JOURNAL OF ENVIRONMENTAL SCIENCES AND TECHNOLOGY (NIJEST)
https://www.nijest.com

# EDITORIAL BOARD

ISSN (Print): 2734-259X | ISSN (electronic): 2734-2603

**Purpose**

The Nigerian Journal of Environmental Science and Technology (NIJEST) is dedicated to promoting high standards and excellence in the generation and dissemination of scientific research findings, reviews and case studies to both the academic communities and industries locally, nationally and globally. It focuses on publishing original and high quality articles covering a wide range of topics in Environmental Sciences and Technology.

**Scope**

The areas of focus include but not limited to the following:

Environmental Sciences; Applied Earth Sciences; Built Environment; Civil Engineering; Climate, Energy and Environment; Water Resources and Environmental Engineering and Computer and Information Science and Technology.

Papers in other related areas not listed above can be considered for publication, provided they meet the journal's requirements.

**Manuscript Submission**

Details on how to submit your article for publication in the Nigerian Journal of Environmental Sciences and Technology and the format to follow are provided at the end of this publication or can be accessed online at http://www.nijest.com.

**Nigerian Journal of Environmental of Environmental Sciences and Technology (NIJEST)**
Journal available online at http://www.nijest.com **Vol 5 No. 1 March 2021**

ISSN (Print): 2734-259X | ISSN (electronic): 2734-2603

# Contents

Nigerian Journal of Environmental Sciences and Technology (NIJEST)

www.nijest.com

ISSN (Print): 2734-259X | ISSN (electronic): 2734-2603

Vol 5, No. 1 March 2021, pp 1 - 12

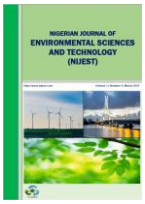

# Multilinear Regression Model to Estimate Mud Weight

Oloro J. O.[1,]* and Akhihiero T. E.[2]

[1]Department of Chemical and Petroleum Engineering, Faculty of Engineering, Delta State University, Delta State, Nigeria

[2,3]Department of Chemical Engineering, Faculty of Engineering, University of Benin, Benin City, Edo State, Nigeria

Corresponding Author: *olorojo@delsu.edu.ng

https://doi.org/10.36263/nijest.2021.01.0229

## ABSTRACT

*Estimation of mud weight poses a serious challenge to mud industries. In this study, a model was developed to tackle the problem of estimation of mud weight using multilinear regression techniques. The model was developed using data obtained from production records. The data include mud weight, water and other chemicals (materials) for nine different samples. The data were analysed to establish linearity and the data was substituted into the multiple regression to form a matrix with nine unknown regression parameters which was substituted into the regression equation to form the model. T-test and F –test was used to validate the model. Results from the test suggest that the developed model was reliable. The model was used to estimate mud weight for four samples and the results are reliable. The effect of each variable was also considered and results also show that each of the variables affects the mud weight.*

**Keywords:** Regression, Fluid, Mud weight, Caustic soda, Barite

## 1.0. Introduction

Mud is usually prepared to meet certain properties which enable it to perform the basic intended functions. Mud is an element that characterized the quality of the drilling. The researches and survey conducted; there are likelihoods of having environmentally friendly mud. The operators of gas and oil industries are faced with the challenge of getting a solution to this problem by formulating high-quality mud and also negative environmental conventional diesel oil base mud effects. The more environmentally welcoming acceptable alternative to oil-base mud (OBM) found is water base mud (Sir Dele and Joseph, 2014).

Drilling mud varies in degrees of toxicity. It is very costly and tedious to dispose of it in an environmentally friendly way. Protection of the environment from pollutants is important in every drilling operation. Mud Companies have restrictions placed on some materials they use and the methods of their disposal. At the beginning of the 1990s, the restrictions are becoming more stringent and restraints are becoming worldwide issues (Enamul *et al*., 2016).

Regular interval testing of mud properties will help Mud Engineers to determine the proper functioning of mud (Fadairo *et al*., 2012). Mud is classified into:

1. Pneumatic fluids: Pneumatic fluids are used for drilling low fluid zones or an area where unusual little formation pressures may be experienced. Pneumatic fluids are better than other liquid mud systems since it increases penetration rates. Air/gas mud fluids are not effective in an area where large volumes of formation fluids are experienced. Hence, the chances of losing circulation or damaging a productive zone are greatly increased. One other factor when considering the selection of pneumatic fluids is the well depth. They are not approved for wells below 10,000 ft since the volume of air essential to lift cuttings from the bottom of the hole can become larger than the surface apparatus can deliver.

2. Oil-based mud: The main use of oil-based fluids is to drill difficult shale. They are also used in the drilling of exceedingly deviated holes because of their high performance of its lubricity and tendency to stop hydration of clays. They may also be chosen for distinct applications such as high pressure /high-temperature wells, lessening formation damage, and native-state coring. Another reason for selecting oil-based fluids is that they are resilient to contaminants such as anhydrite, salt, and $CO_2$ and $H_2S$ acid gases.
3. Water-based mud; Water-based fluids are the most widely used drilling fluids. They are normally easy to build, inexpensive to maintain, and can be prepared to overcome most drilling problems.

Testing of mud is not limited to the kind of drilling mud for each hole interval but also to properties of such mud; density, rheology (flow properties), filtration and solid content and also chemical properties. Mud properties are field controlled and properly maintained at their preselected values; to avoid drilling problems. But this work is restricted to mud weight (density). Mud density is the weight per unit volume. The unit is given as pounds per gallon (lb/gal). Mud weight is a significant parameter which is controlled during a drilling operation. To avoid formation fluids to flow into the wellbore and to seal the wellbore with a low permeability filter cake, the weight of the mud must be greater than the pore pressure of the formation. However, the mud weight column should not be high enough to cause formation fracture. The weighting agents used in mud building are barite, hematite, galena, calcium carbonate. Statistically, barite is the most wildly used weighing agent. All materials present in mud contribute to its weight (Sharif *et al*., 2017). The resulting mud mixture from all the additives and water is assumed to be ideal. Hence, the total volume is the addition of the component volumes and the total weight (density) is equal to the sum of the component weight add depending on the function (Øyvind, 2017).

Mud weight is employed to subsurface pressure and stabilizes the wellbore; mud weight is commonly measured with a mud balance capable of +0.1lb/gal accuracy. A mud balance calibrated with the freshwater of 70o ± 5o should give a reading of 8.3lb/gal. Mud weight is usually reported in g/ml or lb/gal, lb/cuft, or psi/100ft of depth.

Mud balance is an instrument used in the laboratory to calculate mud weight. This instrument was manufactured by Fann. The name of the mud balance is Model 140. It has a range of 7 to 24 lb/gal. The measurement taken was reported to the nearest 0.1 lb/gal.

Estimation of mud weight poses is a serious challenge in the mud industry. Therefore in this study, a model was developed to tackle the problem of estimation of mud weight using multilinear regression techniques. The model was developed using data obtained from the production record. The data include the quantity of mud produced and mud utilize for nine different samples (Sample 1 – Sample 9). The data was analysed to establish linearity and the data was substituted into the multiple regression to form a matrix with nine unknown regression parameters which was substituted into the regression equation to form the model.

## 2.0. Methodology

### *2.1. Materials*

Materials and method investigation involved a series of laboratory works which was initiated with the preparation of water base mud as the continuous phase system. The mud sample is prepared as per field formulations, which comprised of freshwater, potassium chloride, caustic soda, soda ash, PAC R, PAC L, XCD. The weighting materials were then added into the mud separately to form the required mud weight, ranging from 9ppg to 14ppg. Different ppg was gotten as a result of using different quantities of materials (chemicals). Multiple regression was developed using the least square method. The different mud weights gotten are plotted against each material (chemical) to determine the linearity of the regression (Burgoyne *et al*., 1986; John *et al*., 2018; Bill and Nicole, 2018). The regression parameters obtained using excel program were plugged into the regression model to obtain the required equation. Thereafter the model was tested for validity using t-test and F-test (Andy, 2000) The materials and equipment used for work are summarized in Table 1. The mud weight of the mud samples was determined by using the conventional mud balance, whilst the retort apparatus was used

to find the solid content of the mud sample. All the laboratory works were conducted according to the API standard procedures (API, 2003; Paulauskiene, 2017).

**Table 1:** Equipment and materials (chemical)

| Materials | Equipment |
|---|---|
| Water | Mud balance |
| Barite | Retort kit |
| Carboxymethyl cellulose (CMC) | Halminton Beach Mixer |
| Potassium chloride (KCl) | Electrical weighing balance |
| Polyanionic Cellulose (Pac-R) | Round bottom flask |
| Caustic Soda | Rotary viscometer |
| Soda Ash | API filter press |
| XCD Kelzan | pH meter |
| Calcium Carbonate | |

*2.2. Relationship between variables*

Often in practice, a relationship is found to exist between two or more variables. For example; weights of mud depend on calcium carbonate; soda ash; Potassium chloride (KCl); polyanionic cellulose (Pac-R); barite; carboxymethyl cellulose (CMC) and caustic Soda. Figure 1 to Figure 9 is plotted to determine the mathematical relationship between mud weight and other variables.

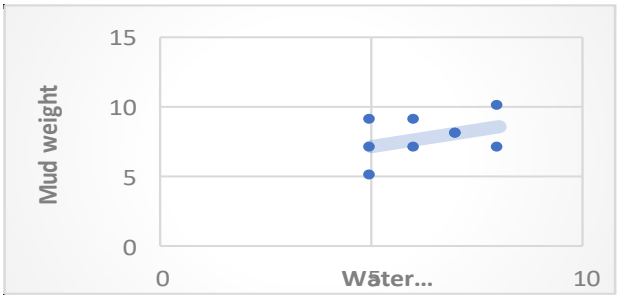


**Figure 1:** Quantity of water ($X_1$) used to produce total mud weight

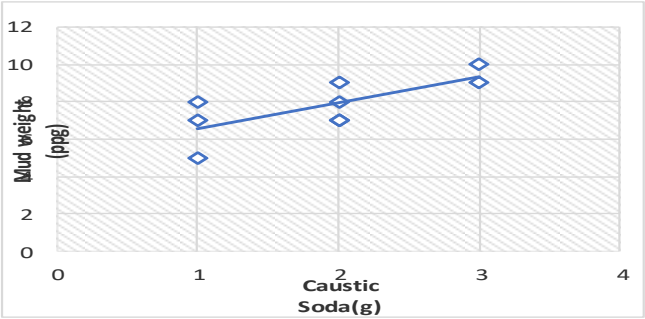


**Figure 2:** Quantity of caustic soda ($X_2$) used to produce total mud weight

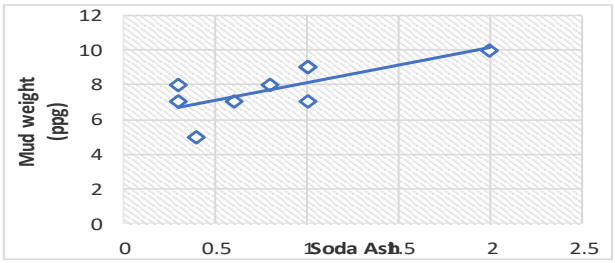


**Figure 3:** Quantity of soda ash ($X_3$) used to produce total mud weight

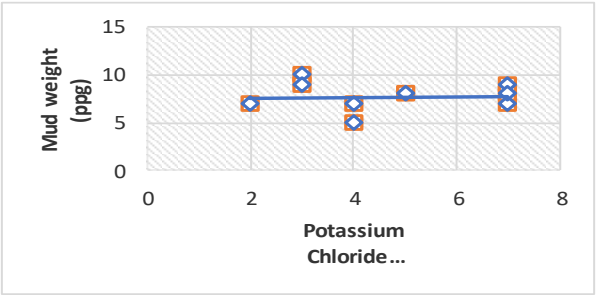


**Figure 4:** Quantity of potassium chloride ($X_4$) used to produce total mud weight

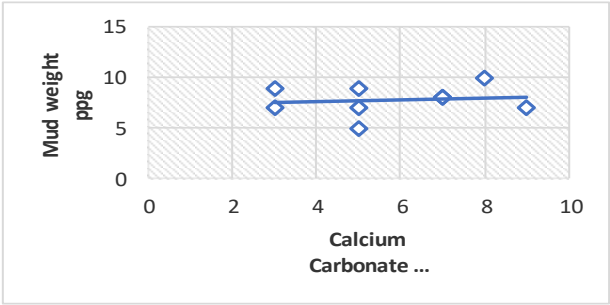


**Figure 5:** Quantity of calcium carbonate, $CaCO_3$ ($X_5$) used to produce total mud weight

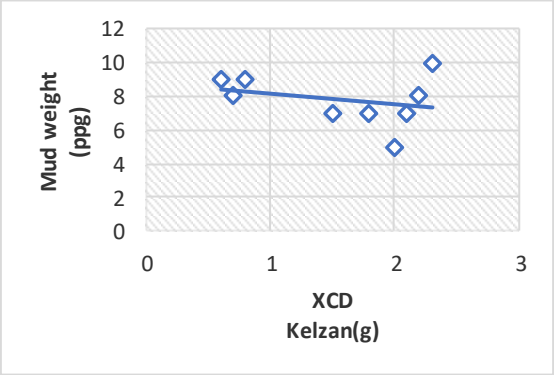


**Figure 6:** Quantity of XCD Kelzan ($X_6$) used to produce total mud weight

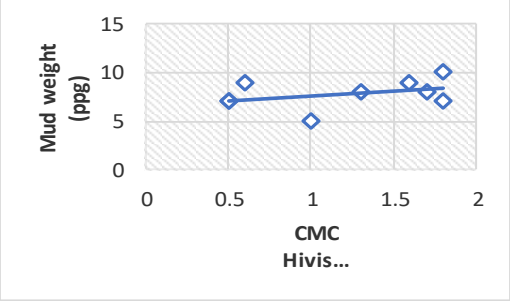


**Figure 7:** Quantity of PAC-R ($X_7$) used to produce total mud weight

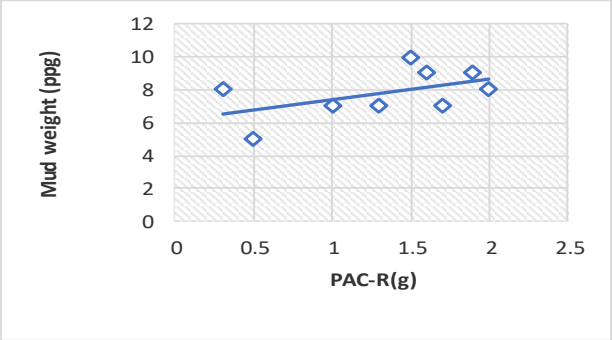


**Figure 8:** Quantity of PAC-R ($X_8$) used to produce total mud weight

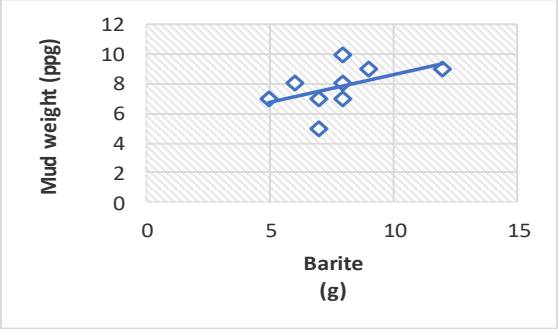


**Figure 9:** Quantity of barite ($X_9$) used to produce total mud weight

**Table 2:** Data to prepare mud weight

| S/N | Mud weight (ppg) | Water $X_1$(litre) | Caustic soda(g) $X_2$ | Soda ash $X_3$ | Potassium chloride (KCl)(g) $X_4$ | Calcium carbonate ($CaCO_3$) $X_5$(g) | XCD Kelzan(g) $X_6$ | CMC Hivis (g) $X_7$ | PAC-R(g) $X_8$ | Barite (g) $X_9$ |
|---|---|---|---|---|---|---|---|---|---|---|
| 1 | 10 | 8 | 3 | 2 | 3 | 8 | 2.3 | 1.8 | 1.5 | 8 |
| 2 | 7 | 5 | 2 | 1 | 2 | 9 | 1.8 | 1.8 | 1.3 | 8 |
| 3 | 5 | 5 | 1 | 0.4 | 4 | 5 | 2 | 1 | 0.5 | 7 |
| 4 | 7 | 6 | 2 | 0.3 | 7 | 3 | 1.5 | 0.5 | 1 | 7 |
| 5 | 8 | 7 | 1 | 0.3 | 5 | 7 | 2.2 | 1.7 | 2 | 8 |
| 6 | 9 | 6 | 3 | 1 | 3 | 5 | 0.6 | 0.6 | 1.6 | 9 |
| 7 | 9 | 5 | 2 | 1 | 7 | 3 | 0.8 | 1.6 | 1.9 | 12 |
| 8 | 7 | 8 | 1 | 0.6 | 4 | 5 | 2.1 | 0.5 | 1.7 | 5 |
| 9 | 8 | 7 | 2 | 0.8 | 7 | 7 | 0.7 | 1.3 | 0.3 | 6 |

*2.3. Methods*

In this paper, $Y$ is the dependent variable, while the independent variables are $X_1$, $X_2$ ……., $X_9$ (Andy, 2000) The regression equation was formed using the parameters in Table 2 as given in Equation 1 below:

The normal equations to Equation (1) are Equation (2) through to Equation (10).

$$Y = nb_0 + b_1X_1 + b_2X_2 + b_3X_3 + b_4X_4 + b_5X_5 + b_6X_6 + b_7X_7 + b_8X_8 + b_9X_9 \quad (1)$$

where:

$Y$ mud weight
$X_1$ volume of water
$X_2$ caustic soda
$X_3$ soda ash
$X_4$ potassium chloride (KCl)

$X_5$ calcium carbonate ($CaCO_3$)
$X_6$ XCD Kelzan
$X_7$ CMC Hivis
$X_8$ PAC-R
$X_9$ Barite

$$\sum YX_1 = b_0\sum X_1 + b_1\sum {X_1}^2 + b_2\sum X_1X_2 + b_3\sum X_1X_3 + b_4\sum X_1X_4 + b_5\sum X_1X_5 + b_6\sum X_1X_6 + b_7\sum X_1X_7 + b_8\sum X_1X_8 + b_9\sum X_1X_9 \quad (2)$$

$$\sum YX_2 = b_0\sum X_2 + b_1\sum X_1X_2 + b_2\sum {X_2}^2 + b_3\sum X_2X_3 + b_4\sum X_2X_4 + b_5\sum X_2X_5 + b_6\sum X_2X_6 + b_7\sum X_2X_7 + b_8\sum X_2X_8 + b_9\sum X_2X_9 \quad (3)$$

$$\sum YX_3 = b_0\sum X_3 + b_1\sum X_1X_3 + b_2\sum X_2X_3 + b_3\sum {X_3}^2 + b_4\sum X_3X_4 + b_5\sum X_3X_5 + b_6\sum X_3X_6 + b_7\sum X_3X_7 + b_8\sum X_3X_8 + b_9\sum X_3X_9 \quad (4)$$

$$\sum YX_4 = b_0\sum X_4 + b_1\sum X_1X_4 + b_2\sum X_2X_4 + b_3\sum X_3X_4 + b_4\sum {X_4}^2 + b_5\sum X_4X_5 + b_6\sum X_4X_6 + b_7\sum X_4X_7 + b_8\sum X_4X_8 + b_9\sum X_4X_9 \quad (5)$$

$$\sum YX_5 = b_0\sum X_5 + b_1\sum X_1X_5 + b_2\sum X_2X_5 + b_3\sum X_3X_5 + b_4\sum X_4X_5 + b_5\sum {X_5}^2 + b_6\sum X_5X_6 + b_7\sum X_5X_7 + b_8\sum X_5X_8 + b_9\sum X_5X_9 \quad (6)$$

$$\sum YX_6 = b_0\sum X_6 + b_1\sum X_1X_6 + b_2\sum X_2X_6 + b_3\sum X_3X_6 + b_4\sum X_4X_6 + b_5\sum X_5X_6 + b_6\sum {X_6}^2 + b_7\sum X_6X_7 + b_8\sum X_6X_8 + b_9\sum X_6X_9 \quad (7)$$

$$\sum YX_7 = b_0\sum X_7 + b_1\sum X_1X_7 + b_2\sum X_2X_7 + b_3\sum X_3X_7 + b_4\sum X_4X_7 + b_5\sum X_5X_7 + b_6\sum X_6X_7 + b_7\sum {X_7}^2 + b_8\sum X_7X_8 + b_9\sum X_7X_9 \quad (8)$$

$$\sum YX_8 = b_0\sum X_8 + b_1\sum X_1X_8 + b_2\sum X_2X_8 + b_3\sum X_3X_8 + b_4\sum X_4X_8 + b_5\sum X_5X_8 + b_6\sum X_6X_8 + b_7\sum X_7X_8 + b_8\sum {X_8}^2 + b_9\sum X_8X_9 \quad (9)$$

$$\sum YX_9 = b_0\sum X_9 + b_1\sum X_1X_9 + b_2\sum X_2X_9 + b_3\sum X_3X_9 + b_4\sum X_4X_9 + b_5\sum X_5X_9 + b_6\sum X_6X_9 + b_7\sum X_7X_9 + b_8\sum X_8X_9 + b_9\sum {X_9}^2 \quad (10)$$

*. 2.3. Creation of matrix*

In creating a matrix, the values of each material in Table 2 were substituted into Equations 2 to 10 to form the matrix notation. This can be written as *A* x *R* = *C*. These unknown parameters *R* (i.e. $b_o$, $b_1$, $b_2$, $b_3$, $b_4$, $b_5$, $b_6$, $b_7$, $b_8$, $b_9$) was determined using an Excel program. The results are shown below.

$$\begin{bmatrix} 9 & 57 & 17 & 7.4 & 42 & 52 & 14 & 10.8 & 11.53 & 70 \\ 57 & 373 & 108 & 48.3 & 265 & 335 & 91.1 & 68 & 75.8 & 433 \\ 17 & 108 & 37 & 16.5 & 77 & 100 & 24.6 & 20.8 & 22.5 & 137 \\ 7.4 & 48.3 & 16.5 & 8.34 & 77 & 46.6 & 11.53 & 10 & 10.16 & 60.1 \\ 42 & 265 & 77 & 31.3 & 226 & 223 & 60.7 & 49.1 & 53.1 & 330 \\ 52 & 335 & 91.1 & 100 & 46.6 & 223 & 336 & 85.3 & 65.4 & 67.5 \\ 14 & 91.1 & 24.6 & 11.53 & 60.7 & 85.3 & 25.52 & 17.47 & 18.95 & 104.6 \\ 10.8 & 68 & 20.8 & 10 & 49.1 & 65.4 & 17.47 & 15.48 & 14.68 & 87.8 \\ 11.8 & 75.8 & 22.5 & 10.16 & 53.1 & 67.5 & 18.95 & 14.68 & 18.34 & 96.4 \\ 70 & 433 & 137 & 60.1 & 330 & 396 & 104.6 & 87.8 & 96.4 & 576 \end{bmatrix} \begin{Bmatrix} b_0 \\ b_1 \\ b_2 \\ b_3 \\ b_4 \\ b_5 \\ b_6 \\ b_7 \\ b_8 \\ b_9 \end{Bmatrix} = \begin{Bmatrix} 70 \\ 449 \\ 139 \\ 62.1 \\ 327 \\ 408 \\ 107 \\ 86.4 \\ 95.4 \\ 556 \end{Bmatrix} \quad (11)$$

## 3.0. Results and Discussion

The matrix shown above was solved by using excel program to determine regression parameters. The parameters are as follow:
$b_o$ = 5.445, $b_1$ = 0.4148, $b_2$ = 0.1571, $b_3$ = 2.0377, $b_4$ = -0.0117, $b_5$ = -0.3814, $b_6$ = -0.7673, $b_7$ = 0.7188, $b_8$ = 0.8722, $b_9$ = 88.41448

Substituting these parameters into Equation 1 above gives:

$$Y = 5.445 + 0.4148x_1 + 0.1571x_2 + 2.0377x_3 - 0.0117x_4 - 0.3814x_5 - 0.7673x_6 + 0.7188x_7 + 0.8722x_8 + 88.4144x_9 - 0.186828 \quad (12)$$

Equation 12 is the model to determine mud weight. The model is used to estimate the mud weight as shown in Table 3.

**Table 3:** Estimated mud weight actual quantity of materials

| Samples | Actual mud weight $X_1$(ppg) | Estimated mud weight $X_2$(ppg) |
|---|---|---|
| 1 | 10 | 10.03032 |
| 2 | 7 | 6.43063 |
| 3 | 5 | 5.232352 |
| 4 | 7 | 6.788532 |
| 5 | 8 | 6.636182 |
| 6 | 9 | 8.730792 |
| 7 | 9 | 9.385392 |
| 8 | 7 | 7.705802 |
| 9 | 8 | 7.380422 |

*3.1. Testing the validity of the model*

$H_0$; $b_0 = b_1 = b_2 = b_k = 0$
$H_1$; At least one $b_i$ is not equal to zero (Bill and Nicole, 2012)
If at least one $b_i$ is not equation to zero, the model is valid.

$$\bar{\sigma}_{Y_1-Y_2} = \sqrt{\left(\frac{Y_1 + Y_2}{N_1 + N_2}\right)\left(\frac{N_1 + N_2}{N_1 \times N_2}\right)} \quad (13)$$

where:
$Y_1$ Sum of squares for actual mud weight
$Y_2$ Sum of squares for estimated mud weight
$N_1$ Sample size for actual mud weight
$N_2$ Sample size for estimated mud weight
$\bar{\sigma}_{Y_1-Y_2}$ for the data is

$$\sqrt{\left(\frac{70 + 68.380422}{9 + 9 - 2}\right)\left(\frac{9 + 9}{9 * 9}\right)} = 1.306774$$

$$\overline{X}_1 = 7.777$$

$$\overline{X}_2 = 7.5911$$

$$t = \frac{\overline{X}_1 - \overline{X}_2}{\bar{\sigma}_{Y_1-Y_2}} = 0.1428$$

The degree of freedom is $N_1 + N_2 - 2 = 16$

The obtained *t*-ratio was compared with the table t-ratio for degree of freedom using a two-tailed test ($H_O$ is being tested).

The obtained *t*- *t*-ratio is 0.0004472 and tabled *t*-ratio (α = 0'.05) for 16 degree of freedom is 1.746. Since obtained *t*-ratio is less than that of the tabled value, $H_O$ is rejected.
The conclusion drawn the *t*-test carried out, therefore, is that there is no significant difference between actual mud weight and the estimated one.

To know whether this assumption is met, the unbiased sample variance of actual mud weight and estimated mud weight subjected to an *F*-test.

The *F*-test is given as (Andy 2000):

$$F = \frac{S_1^2}{S_2^2} \tag{14}$$

where:
$S_1^2$ the greater variance of the two samples
$S_2^2$ the lesser variance of the two samples

The standard deviations for actual mud weight and estimated mud weight are given as Equation 15 and 16 respectively.

$$S_1 = \sqrt{\frac{\sum(X_1 - \bar{X}_1)^2}{N_1}} \tag{15}$$

$$S_2 = \sqrt{\frac{\sum(X_2 - \bar{X}_2)^2}{N_2}} \tag{16}$$

where:
$X_1$ actual mud weight
$X_2$ estimated mud weight
$\bar{X}_1$ mean of actual mud weight
$\bar{X}_2$ estimated mud weight

From Table 3,
$\bar{X}_1 = 7.777$
$\bar{X}_2 = 7.5911$

From Equation 15 and 16,
$S_1^2 = 2.110232$
$S_2^2 = 1.950618$

Therefore, from Equation 14,
$F = \frac{2.110232}{1.950618} = 1.081827$

Degree of freedom for greater variance of the mud weight = 9 – 1 = 8
Degree of freedom for lesser variance of the mud weight = 9 – 1 = 8

Checking the significance of the obtained *F*-ratio of 1.081827 with the critical *F*-ratios in the *F*-table, we find that the obtained *F*-ratio is less than the critical *F*- ratios at both $\alpha$ = 0.05 (F = 3.44) and $\alpha$ = 0.01 (F = 6.03). The homogeneity of both variances is thus confirmed.

Figure 2 through to Figure 9 it has been shown linearity of the model, it shows that the model is reliable. And control of the production of mud weight is now very easy. If the different quantity of materials is used, the estimated mud weights are shown in Table 4.

**Table 4:** Estimation of mud weight using different of materials (chemicals)

| Samples | Water (litre) $X_1$ | Caustic soda (g)($X_2$) | Soda ash (g) $X_3$ | Potassium chloride (KCl) (g) ($X_4$) | Calcium carbonate ($CaCO_3$) (g) $X_5$ | XCD Kelzan (g) $X_6$ | CMC Hivis $X_7$ | PAC-R (g) $X_8$ | Barite (g) $X_9$ | Estimated mud weight (ppg) Y |
|---|---|---|---|---|---|---|---|---|---|---|
| 1 | 4 | 2 | 2.5 | 4 | 10 | 3 | 5 | 10 | 8 | 17.635 |
| 2 | 0.01 | 0.01 | 0.02 | 10 | 15 | 3 | 4 | 10 | 6 | 8.1289 |
| 3 | 1 | 0.11 | 0.4 | 6 | 10 | 5 | 4 | 7 | 20 | 5.6552 |
| 4 | 0.004 | 2 | 0.6 | 6 | 0.6 | 3 | 2 | 5 | 26 | 7.2513 |

Water is the most significant material involved in drilling fluid technology. It is usually readily available at relatively low cost. Among the unusual properties of water in contrast with other liquids are the highest surface tension, dielectric constant, heat of fusion, the heat of vaporization, and the superior ability of water to dissolve different substances. As the quantity of water is increased, the mud weight increases (Brini *et al*., 2017). The effect of water is in Figure 10.

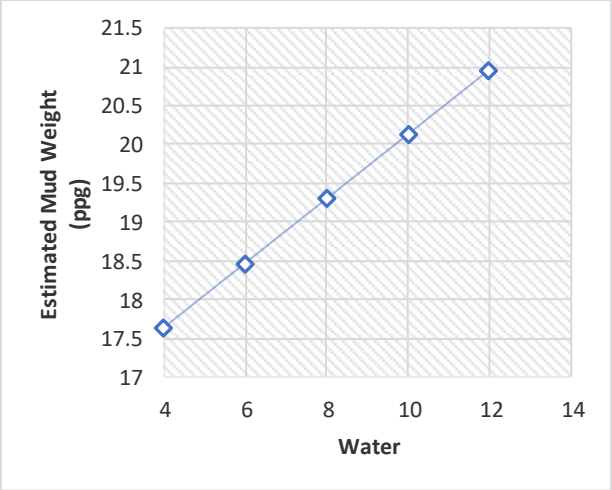


**Figure 10:** Effect of water used on mud weight

The most important part of these samples is the concentration of $CaCO_3$ as a weighting agent. It is used to increase the densities of samples from 9.0 to 11 pounds per gallon (ppg). The density of mud is the main parameter to consider during the study as it directly affects the formation of a filter cake. The most common additive to increase the mud weight in production (Raheem *et al*., 2019) as shown in Figure 11.

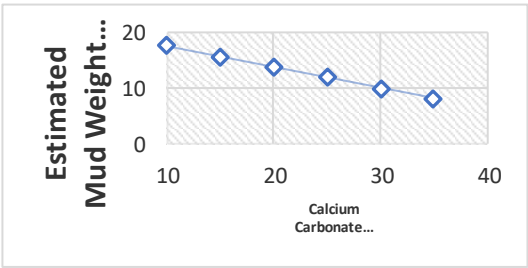


**Figure 11:** Effect of calcium carbonate ($CaCO_3$)(g) used on mud weight

Barite one of the vital roles of drilling mud is the control of formation fluid pressure to avoid blowouts. The density of the mud must be elevated at times to stabilize fragile formations (Ibrahim and Sami, 2017). The effect of Barite is illustrated in Figure 12.

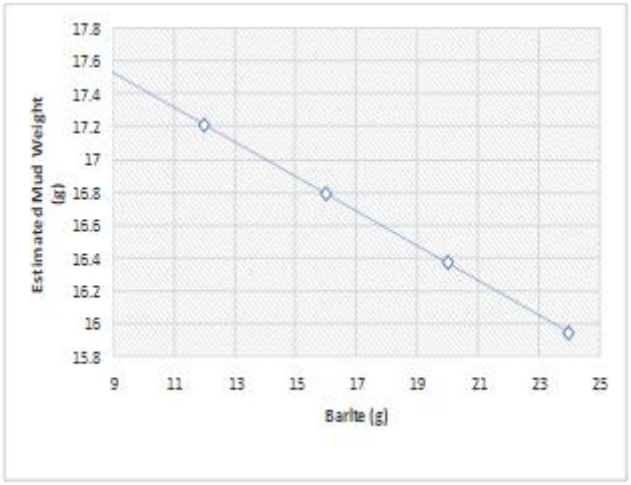


**Figure 12:** Effect of Barite used on mud weight

Caustic soda is used in water-based mud to increase its pH, to offset corrosion and to counteract hydrogen sulphide. Also, some achievement can be attained by addition of caustic soda to the freshwater sideways with the bentonite to perform as a dispersing agent. Soda ash the principal use of soda ash or sodium carbonate ($Na_2CO_3$) is for the exclusion of soluble salts from the makeup of waters and muds and to recover the yield of clay (Annis and Smith, 2012) as shown in Figure 13.

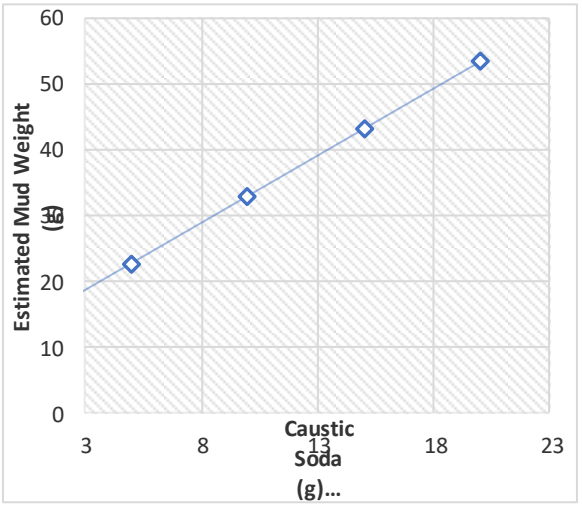


**Figure 13:** Effect of caustic soda used on mud weight

The experimental data show that rheological properties of a water base mud (plastic viscosity and yield point) are altered when shale formation is encountered when KCl is use as shown in Figure 14.

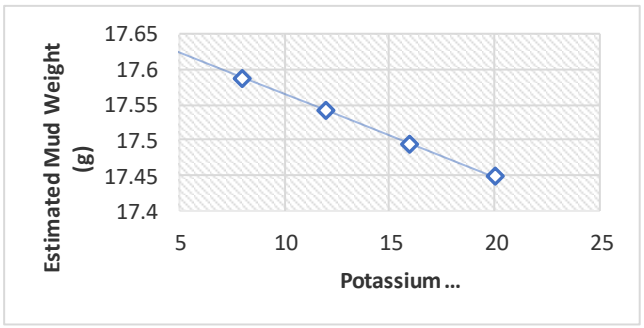


**Figure 14:** Effect of potassium chloride (KCl)(g) used on mud weight

The principal use of soda ash or sodium carbonate ($Na_2CO_3$) is for the removal of soluble salts from the makeup of waters and muds and to enhance the yield of clay. The effect of Soda ash is shown in Figure 15.

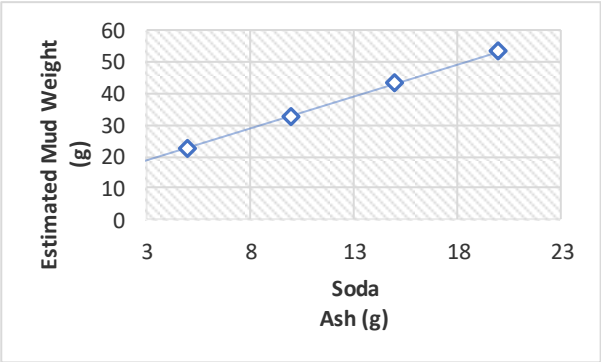


**Figure 15:** Effect of soda ash (g)used on mud weight

## 4.0. Conclusion

In this study, a model was developed using data obtained from production records. The data include mud weight, water and other Chemicals (Materials) for nine different samples. The data were analysed to establish linearity and the data was substituted into the multiple regression to form a matrix with nine unknown regression parameters which was substituted into the regression equation to form the model. T-test and F –test was used to validate the model. Results from the test suggest that the developed model was reliable. The model was used to estimate mud weight for four samples and the results are reliable. The effect of each variable was also considered and results also show that each of the variables affects the mud weight.

## References

Andy, I. J. (2000). Fundamental for Education and the Behavioral Science's, pp.183-187.

Annis, M. R. and Smith. Drilling Fluids Technology, Published on Sep 10, (2012) 3.1

API Recommended Practice 13B-1, I. 1.-1 Recommended Practice for Field Testing water-based Drilling Fluids. American Petroleum Institute, (2003).

Bill and Nicole. Multiple Regression, burkewiz@stanford.edu,(2012).

Brini, E., Christopher, I., Fennell, M., Fernandez-Serra, B., Hribar-Lee, M., Luksic and A. D. Ken, (2017). How Water's Properties Are Encoded in Its Molecular Structure and Energies, Chem. Rev. 117(19), pp. 12385–12414. https://doi.org/10.1021/acs.chemrev.7b00259

Burgoyne, A. T., Chenevert, M. E., Mulheim, K. K. and Young, F. S. (1986) Applied Drilling Engineering's Textbook Series, 2(53), pp. 76-77

Enamul, M., Hossain and Mohammed Wajheeuddin, (2016). The use of grass as an environmentally friendly additive in water-based drilling fluids. *Petroleum Science*, 13, pp. 292–303.

Fadairo, A., Ameloko, A., Adeyemi,G., Ogidigbo, E. and Airend, O. (2012). Environmental Impact Evaluation of a Safe Drilling Mud. SPE, (2012)

Ibrahim, D. S. and Sami, N. A. (2017). Balasubramanian. Effect of barite and gas oil drilling fluid additives on the reservoir rock characteristics. *Journal of Petroleum Exploration and Production Technology*, 7(1), pp. 281-292. DOI: 10.1007/s13202-016- 0258-2

John, I. L and Ogbonna, J. (2018) Effect of Weighing Agent on Rheological Properties of Drilling Fluid. *IJERT*, 7(4), IJERTV7IS040322

Multiple Regression, https://www.utdallas.edu/~scniu/OPRE- 6301/documents/Chapter-18. (2019).16.,24.

Øyvind, B. (2017) Drilling fluid properties and design Posted 12.01.

Paulauskiene, T. (2017). Petroleum Extraction Engineering, Intech Open, 2017.DOI: 10.5772/intechopen.70360.

Raheem, I., Zubair, M., Pirzada, F. Abro, A. Muhammad, V. Avinashi (2019). An Experimental Study on the Performance of Calcium Carbonate Extracted from Eggshells as Weighting Agent in Drilling Fluid. *Engineering, Technology and Applied Science Research*, 9(1), pp. 3859

Sharif, M. D. A., Nagalakshmi, N. V. R. S., Srigowri, R., Vasanth, R. G. and Uma Sankar, K. (2017) Drilling Waste Management and Control the Effects. *J Adv Chem Eng*, 7(1), DOI: 10.4172/2090- 4568.1000166.

Sir Dele, O. and Joseph, O. (2014). Building Pad Mud (Arkleen Oil and Gas Manual).

.

**Cite this article as:**
Oloro J. O. and Akhihiero T. E., 2021. Multilinear Regression Model to Estimate Mud Weight. *Nigerian Journal of Environmental Sciences and Technology*, 5(1), pp. 1-12. https://doi.org/10.36263/nijest.2021.01.0229

Nigerian Journal of Environmental Sciences and Technology (NIJEST)

www.nijest.com

ISSN (Print): 2734-259X | ISSN (electronic): 2734-2603

Vol 5, No. 1 March 2021, pp 13 - 18

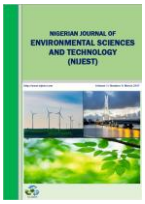

# Assessment of Uncharred Palm Kernel Shell as a Filter Medium in Low Rate Filtration

Jeje J. O.[1,*] and Oladepo K. T.[1]

[1]Department of Civil Engineering, Obafemi Awolowo University, Ile Ife, Nigeria

Corresponding Author: *jemails2000@yahoo.co.uk

https://doi.org/10.36263/nijest.2021.01.0246

## ABSTRACT

*This study examined the use of uncharred palm kernel shells as a filter medium in low rate filtration as a water treatment alternative. The filter column was made of 150 mm diameter PVC pipe about 1.8 m high. The filter medium (uncharred palm kernel shells) with size range 0.15 – 0.60 mm overlying two layers of graded gravels. The raw water passed through the filter medium and the effluent collected in a metal tank. The effluent was evaluated by monitoring the flow rate, turbidity, filtration rate, bacteriological quality and headloss across the filter bed for a daily six hour run for 14 days. The filter bed was cleaned using the throwing-over method after the filtration rate became appreciably very low at 1.20 l/min-m$^2$. It was found from the results obtained that uncharred palm kernel shells could serve as an effective filter for low rate filtration relative to sand. An average hydraulic loading and filtration rate of 120.35 l/min-m$^2$ and 5.5 l/min-m$^2$ were achieved respectively. The turbidity of the filtered water reduced below 5.5 NTU after the eleventh day and the bacteriological treatment level though excessively high at 65 coliform/100 ml showed reducing tendencies (120/100 ml to 65/100 ml).*

**Keywords:** Filtration, Uncharred palm kernel shells, Headloss, Low rate filtration, Potable water

## 1.0. Introduction

The primary aim of the World Health Organization (WHO, 2006) guidelines for drinking water quality is the protection of public health. These guidelines emphasize microbiological safety which is due to the fact that more than half the world's population is still exposed to waters that are not free from pathogenic organisms.

A typical water treatment plant consists of aeration, coagulation and flocculation, sedimentation, filtration, disinfection and distribution units. The treatment is necessitated by the possible presence of some impurities such as dissolved gases, dust, minerals, organic matters, microorganisms and other pollutants (Hammer, 1977).

The slow sand filter was studied in this project and it precludes any chemical pre-treatment as against the rapid sand filter which is mostly used in most treatment plants because of its ability to remove about 99.9% of the bacteria present if it is not overloaded (Alam *et al*., 2007). This filtration technique employs the use of the filter medium, uncharred palm kernel shells in this case, as a mechanical and microbiological purifier of water. The mechanical purification is due to the straining effect of the filter medium and the microbiological removal due to the action of a biological layer called the schmutzdecke, which develops on the bed's surface (Rust and McArthur, 1991).

The Schmutzdecke is the layer that provides the effective purification of potable water treatment. It is a gelatinous layer or biofilm called the hypogeal layer or schmutzdecke. This sticky film, which is reddish brown in colour, consists of decomposing organic matter, iron, manganese and silica and therefore acts as a fine filter media that contributes to the removal of turbid particles in the raw water (Buzunis, 1995). It also doubles up as an initial zone of biological activity and providing some degradation of soluble organics in the raw water, which is useful for reducing tastes, odours and colour. It is formed in the first few weeks of operation and consists of organic matter including

bacteria, fungi, protozoa, rotifer and various aquatic insect larvae. It consists of alluvial mud, organic matter, bacteria, diatoms, zooplankton, thread-like algae formed by the excretion of microorganisms. It is the layer of aquatic life that is responsible for purifying the water (Ranjan and Prem, 2018). As water passes through this biological layer, foreign particles are trapped and essentially eaten by bacteria forms on this layer. As the water slowly passes down through the layers of sand, impurities are left behind, leaving the water between 90% and 99% free from bacteria (Elliott *et al*., 2008; Lee *et al*., 2014)

Generally, filters operate by the water passing through the sand from top to bottom. Larger suspended particles are left behind in the top layers of sand and the smaller particles of organic sediment left in the sand filter are eaten by microscopic organisms including bacteria and protozoans which stick in the layers of slime that form around the sand particles and the clean water which passes through the filter is safe to drink (Babayemi and Onukwuli, 2016; Uzun *et al*., 2010). Provided that the grain size is around 0.1 mm in diameter, a sand filter can remove all faecal coliforms and virtually all viruses (Uzun *et al*., 2010). Submission of a paper to NIJEST implies that the corresponding author has obtained the permission of all authors, and that all authors have read the paper and guarantee that the paper is an original research work, that the data used in carrying the research will be provided to NIJEST Editors if requested, and that the paper has not been previously published and is not currently under review for publication by another journal.

## 2.0. Methodology

### *2.1. Materials*

The filter medium used for the project was uncharred palm kernel shells. The material was sieved though sieves 0.15 – 0.60 mm. It was bought and milled to the required size ranges using a Hammer mill and pulveriser. The milled and sieved portion was thoroughly washed and rinsed until the water became clear. The materials were then sun-dried, sieved and stored in polythene bags for use. Two layers of gravel, obtained at Opa dam waterworks, were also used for the study.

### *2.2. Experimental equipment*

A circular cross sectional filter made of PVC sewer pipe was used. The filter diameter was 150 mm with a depth of 1800 mm. the surface area was 0.0177 $m^2$. The bottom was sealed with a concrete base and a hole was placed centrally just above the base to collect the effluent from the filter. Headloss and overflow outlets were also made along the sides of the tube; this was to maintain a constant head during filtration. The headloss and sampling ports were made up of 1/8 inches brass pipes with fine mesh wire gauge to prevent the media from blocking the ports.
A manometer and HACH 21004 turbidimeter were also used. The raw water sample was taken from the Opa dam waterworks and the treated water from the dam was used as a control. 19 mm pipes, gate valves, elbow joints and back nuts were also used.

### *2.3. Methods*

The effective sizes (D10) of the uncharred palm kernel shells were determined along with its uniformity coefficients (Gonzalo *et al*., 2012).

The filter column was placed in the proper position and an inlet pipe, about 5 cm in size, was placed near the bottom of the pilot column to collect the effluent. The two layers of graded gravel was placed at the bottom and a plug-hole was placed at the bottom. A 750 mm layer of the prepared uncharred palm kernel shells was placed on top of the plate. The schmutzdecke was developed at the surface of this medium and a flat stone was placed on top to prevent disturbance of the schmutzdecke layer. The outlet and overflow pipes were then inserted (Figure 1). Before the first use, the filter was filled with a solution of 100 mg/l chlorine, left for 12 hours and emptied through the plug-holes. Clean water was also introduced into the filter from the bottom; this was to remove air bubbles from the medium.

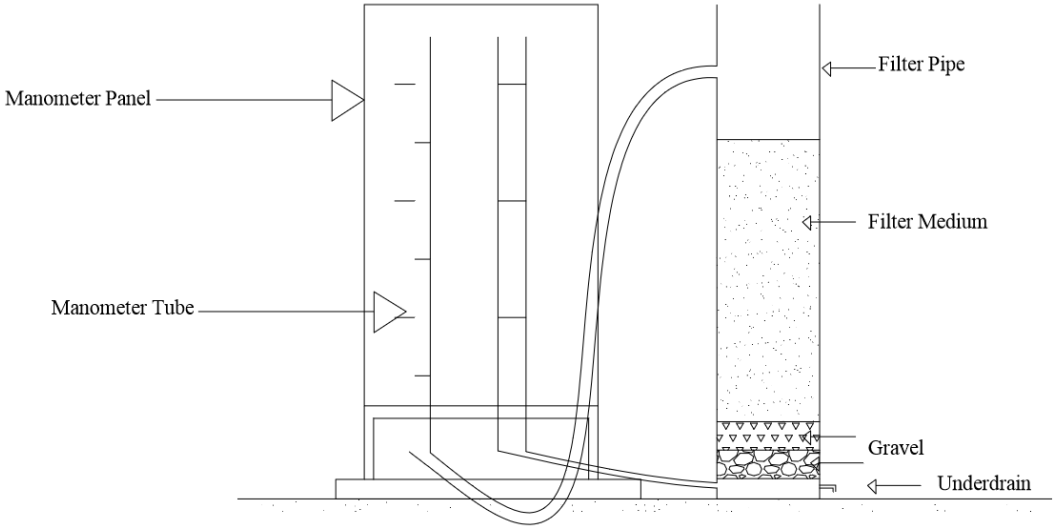


**Figure 1:** Schematic diagram of filter setup (Babayemi and Onukwuli, 2016)

*2.4. Experimental procedure*

After charging the filter, the influent water was allowed into the filter while a constant head was maintained above the filter head during filtration. The filtration process was started once the tap was closed. The headloss and flow rate was then measured simultaneously. The headloss and flow rate were measured at every two hours interval until the experimental run was terminated. An experimental run terminates when the rate of headloss build up, i.e. pressure drop across the filter, over time reaches an unacceptably high (terminal) headloss and thus the filter bed needs to be cleaned. The filter bed was due for cleaning when the setup reached a flow rate of 1.20 l/min-m2 and the headloss was high. The filter medium was cleaned by reducing the water in the system to about 100 mm below the top of the filter medium. The top 20 mm was then scraped off and washed in a flowing steram of water. The entire schmutzdecke layer was not scraped off in order to reduce the ripening period of the new schmutzdecke layer that would be formed. The filter medium and support gravels required additional washing in order to remove dirt particles and to meet the desired cleanliness of less than 0.1% passing the number 200 screen.

## 3.0. Results and Discussion

*3.1. Headloss and filtration rate*

The filtration rate was set to 6.5 l/min-m2 at the start of the operation and it was observed to decrease with the filtration run time until it became relatively low at 1.2 l/min-m2 (Figure 2). The headloss was measured on a daily basis at two hours interval. Figure 3 shows the average daily headloss across the filter medium. It was observed that as the headloss was increasing with time, the filtration rate was also declining with time. The relative headloss standard when treated water was passed into the system was 43 cm as compared to the net terminal headloss of 117 cm; this shows that the performance of the system had considerably reduced.

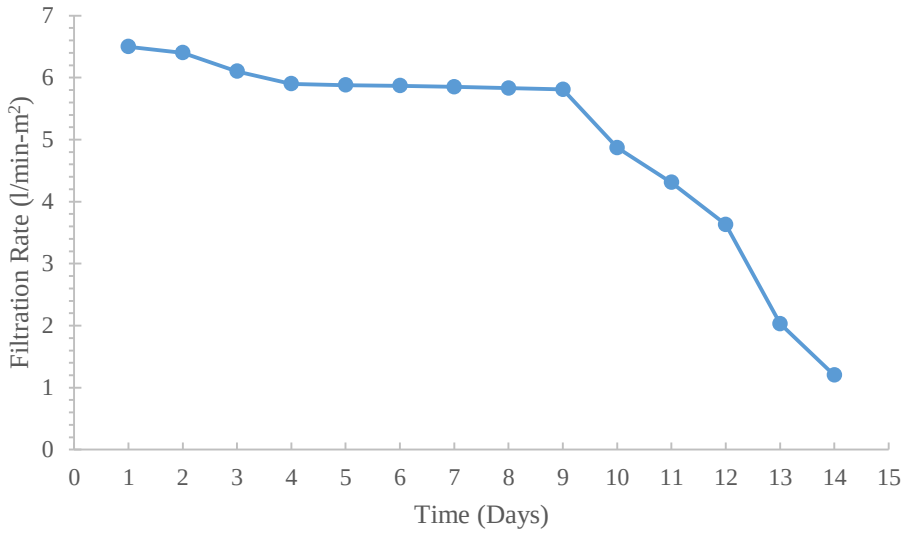


**Figure 2:** Filtration rate with time

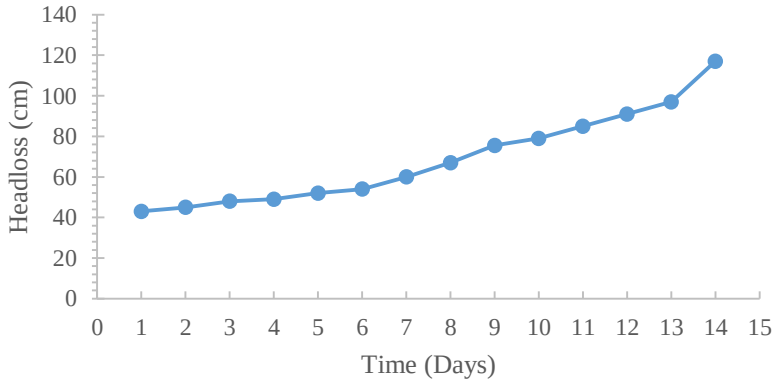


**Figure 3:** Headloss development with time

*3.2. Turbidity removal and bacteriological analysis*

Figure 4 shows the average daily turbidity removal. It shows the turbidity of the water before filtration and after filtration. It was observed that the rate of turbidity removal with time increased tremendously around the twelfth and fourteenth day.

The schmutzdecke, which is responsible for the bacteriological treatment of the raw water gradually built up as the raw water entered the system. This layer is believed to be responsible for the reduction of coliform count on the thirteenth day (Babayemi and Onukwuli, 2016); the coliform count for raw water was 120/100 ml which reduced to 65/100 ml after filtration.

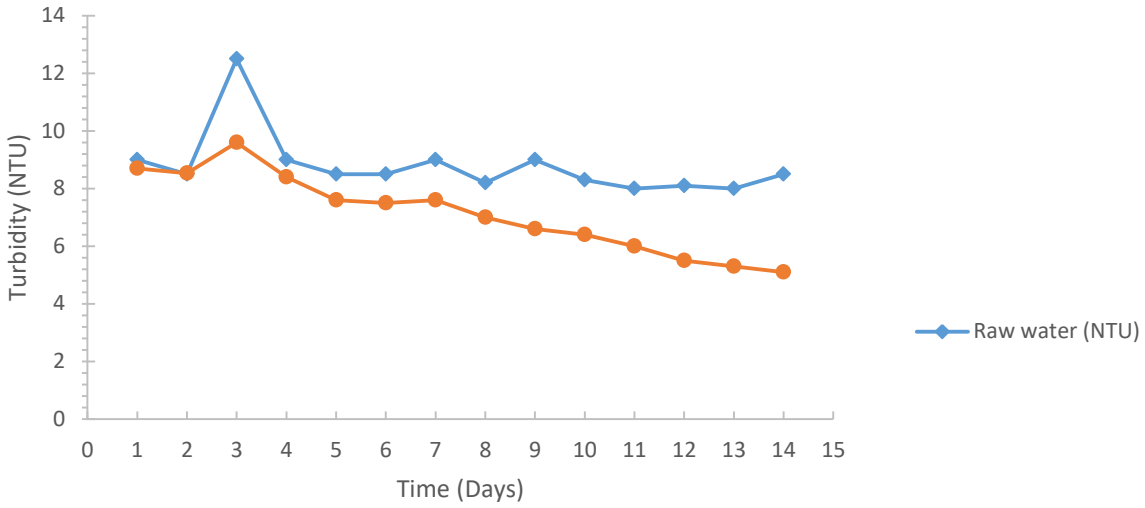


**Figure 4:** Turbidity removal with time

## 4.0. Conclusion

Based on the singular run carried out, the filtered water maximum turbidity at the time the filter skin is functional was 5.5 NTU, at an average filtration rate of 5.5 l/min-$m^2$. The volume of filtered water at a bed surface area of 0.0017 $m^2$ and length of run of 14 days is reasonable. The average operational flow rate for this system is 120.50 l/min-$m^2$ which produced a filtration rate of 5.5 l/min-$m^2$ at a head of 650 mm. The microbial count is 65/100 ml.

## References

Alam, M. Z., Muyibi, S. A., Mansor, M. F. and Wahid, R. (2007) Activated carbons derived from oil palm empty-fruit bunches: Application to environmental problems. *J. Environ. Sci.* 19, pp. 103–108.

Babayemi, A. K. and Onukwuli, O. D. (2016) Adsorption Isotherms, Thermodynamics and Statistical Modeling of Phosphate Removal from Aqueous Solution by Locally prepared Bio-Sorbent. IOSR *Journal of Applied Chemistry*, 9, pp. 46-50.

Buzunis, B. J. (1995). Intermittently operated slow sand filtration: a new water treatment process. Civil Engineering, University of Calgary

Elliott, M. A., Stauber, C. E., Koksal, F., DiGiano, F. A. and Sobsey, M. D. (2008). Reductions of E. coli, echovirus type 12 and bacteriophages in an intermittently operated household-scale slow sand filter. *Water Research*, 42(10), pp. 2662-2670.

Gonzalo, V., Olga, M., Sonia, F., Gervasio, A. and Julia, G. A. (2012). Alkaline Pre-treatment of waste chesnut shell from a food industry to enhance cadmium, copper, lead and zinc ions removal. *Chemical Engineering Journal*, 184, pp. 147-155.

Hammer, M. J. (1977). Water and Wastewater Technology. John Wiley and Sons Inc., New York.

Lee, T., Zubir, Z. A., Jamil, F. M., Matsumoto, A. and Yeoh, F. Y. (2014). Combustion and pyrolysis of activated carbon fibre from oil palm empty fruit bunch fibre assisted through chemical activation with acid treatment. *J. Anal. Appl. Pyrolysis.* 110, pp. 408–418.

Ranjan, P. and Prem, M. (2018). Schmutzdecke- A Filtration Layer of Slow Sand Filter. *International Journal of Current Microbiology and Applied Sciences*, 7, pp. 637-645.

Rust, M. and McArthur, K. (1991). Slow sand filtration. Civil Engineering Department, Virginia Tech.

Uzun, B. B., Apaydin-Varol, E., Ates, F., Ozbay, N. and Putun, A. E. (2010). Synthetic fuel production from tea waste: Characterization of bio-oil and bio-char. *Fuel*, 89, pp. 176-184.

World Health Organization (2006). Guidelines for drinking-water quality [electronic resource], Incorporating First Addendum. Vol. 1, Recommendations. 3rd ed.

**Cite this article as:**
Jeje, J. O. and Oladepo, K. T. 2021. Assessment of Uncharred Palm Kernel Shell as a Filter Medium in Low Rate Filtration. *Nigerian Journal of Environmental Sciences and Technology*, 5(1), pp. 13-18. https://doi.org/10.36263/nijest.2021.01.0246

Nigerian Journal of Environmental Sciences and Technology (NIJEST)

www.nijest.com

ISSN (Print): 2734-259X | ISSN (electronic): 2734-2603

Vol 5, No. 1 March 2021, pp 19 - 31

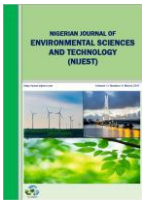

# Electrical Conductivity of PA6/Graphite and Graphite Nanoplatelets Composites using Two Processing Streams

Umar M.[1,*], Ofem M. I.[2], Anwar A. S.[1] and Usman M. M.[3]

[1]Department of Chemical Engineering, Kaduna Polytechnic, Kaduna, Nigeria

[2]Department of Mechanical Engineering, Cross Rivers University of Technology, Calabar, Nigeria

[3]Department of Chemical Engineering, Federal Polytechnic, Nasarawa, Nigeria

Corresponding Author: *michaeliofem@crutech.edu.ng

https://doi.org/10.36263/nijest.2021.01.0251

## ABSTRACT

*The percolation threshold (PT) of any polymer/particulate carbon composite depends on the processing, the dispersed state of the filler, the matrix used and the morphology attained. Sonication technique was used to make PA6/G and PA6/GNP composites employing in situ polymerisation, after which their electrical conductivity behaviours were investigated. While overhead stirring and horn sonication were used to distribute and disperse the carbon fillers, the composites were made in 2 streams 40/10 and 20/20. The 40/10 stream implies that while dispersing the carbon fillers in PA6 monomer, 40% amplitude of sonication was applied for 10 minutes whereas the 20/20 stream implies 20% amplitude of sonication for 20 minutes. In both streams, the dispersing strain imparted on the monomer/carbon mixture was 400 in magnitude. Purely ohmic electrical conductivity behaviour was attained at 9.75 G wt. % for IG 40/10 system. For composites in the IG 20/20 system, same was attained at 10.00 G wt. %. Electrical conductivity sufficient for electrostatic discharge applications was achieved above 15 G wt. % in the IG 40/10 system. Using the power law percolation theory, percolation threshold was attained at 9.7 G wt. % loading in IG 40/10 system, while same was attained at 7.6 G wt. % loading in IG 20/20 system. For the GNP based systems, percolation threshold occurred at 5.2 GNP wt. % in the INP 40/10 system whereas same occurred at 7.4 GNP wt. % in the IG 20/20 system.*

**Keywords:** Electrical-conductivity, Graphite, Percolation-threshold, Amplitude, Sonication

## 1.0. Introduction

Polymers are essentially insulators except for the natural double conjugates. To introduce electrical conductivity to polymers, conductive constituents such as metals and carbon are used as fillers. Fillers are carefully selected and added in quantity that will not compromise other important physical properties of the matrix. Without much loss to other significant matrix properties, threshold quantities just above which an electrically percolated conductive state is attained is needed. At higher loading above the threshold amount, the risk of the composite becoming too brittle and loss of ability to perform other functions is expected. For the conductive regimes, usefulness is found when the electrical conductivity attained can sufficiently prevent lightning strikes, shield electromagnetic effects, provide anti-statics to components and in applications related to strain sensors (Marsden *et al*. 2018).

Polymer/micro-particulate composites, such as polymer/G composites, are usually made using high weight percentages of the fillers, sometimes, up to 40 wt. % (Clingerman *et al*., 2002). This is mainly done to attain significant property improvements such as converting a composite from an electrical insulator to a conductor (Clingerman *et al*., 2002). This transition takes effect at the percolation threshold (PT) which corresponds to that conductive filler loading level just above which, composites transform from being an electrical insulator to electrical conductor. The transition is usually marked by a sharp rise in electrical conductivity due to the formation of an electrically-conductive network by the filler. A plot of conductivity against filler loading takes the characteristic S-shape which represents the insulating, percolating and conductive regimes (Marsden *et al*., 2018).

For each filler/matrix combination, the PT depends on the blending method used, the type, shape, size and orientation of the filler in the polymer composite and the filler-matrix interaction or, how considerable the matrix wets the filler (Clingerman, 2001). Many properties including electrical conductivity of composites may follow the power law percolation theory. When written for electrical conductivity; the critical filler loading at percolation, $p_c$, and the power constant, *t*, can be determined from Equation 1 (Marsden *et al*., 2018);

$$\sigma(p) = \sigma_c(p - p_c)^t \text{ for } p > p_c \quad (1)$$

Where $\sigma$, is the specific composite conductivity; $\sigma_c$, the conductivity at the filler loading above which the composites conductivity raises in an order of magnitude and, $p$ is the filler loading in wt. %. The power constant, *t*, indicates the dimensionality of the filler network. Its typical value may range between 1.3-2.0 for systems in which the filler network dimension (D) lays between 2D and 3D (Sandler *et al*., 2003). As a class of polymer/carbon particulate composites, electrically conductive polymer composites find application in electromagnetic shielding, antistatic protection, batteries (Zheng *et al*., 2002), in aerospace and sports goods (Krupa and Chodak, 2001).

The use of graphite nanoplatelets (GN) is not often common due to the need of high weight percentage. The GN density of 2.26 g/cm$^3$ (Sengupta *et al*., 2011) tends to increase the density of the final products. In addition, the accompanying rise in melt viscosity makes processing more difficult and energy consuming (She *et al*., 2007). Notwithstanding, using a solution blending process with poly (methyl methacrylate) (PMMA), an electrical conductivity percolation threshold is reported at 3.61 G wt. % (Moniruzzaman and Winey, 2006). Again, using G, the critical exponent of *t* (in Equation 1) is approximately 1.8 as reported by Zheng *et al*. (2002). This suggests that a 3 dimensional conductive filler network was formed. The authors ascribed the low electrical conductivity PT to a '*tunnelling*' phenomenon between adjacent conductive clusters. In a comparative study involving G and expanded graphite (EG) using polystyrene (PS) matrix, PT was attained at 6 G wt.% (Chen *et al*., 2003b). In a similar investigation for PMMA/G composites, a PT of 3.19 vol.% was achieved using *in situ* polymerisation (Chen *et al*., 2003a). Both *in situ* polymerisation and solution blending usually result in lower PT values compared to melt blending (Sengupta *et al*., 2011). Clingerman (2001) used an additive equation to describe, among other properties, the electrical percolation behaviour of synthetic graphite (SG) here referred to as G in PA6, 6 and polycarbonate (PC) matrices. The PA6, 6/G composite was estimated to have a PT of about 11 vol. %. Significant electrical conductivity of 2 x 10$^{-3}$S/cm was only attained at a much higher loading of 25 vol. %. Other studies (She *et al*., 2007; Lu *et al*., 2005) of G and EG with polyethylene showed that only at significantly large amounts (22.2 and 18 vol. % for G and EG, respectively) did composites became electrically conductive.

It is also common for G composites to show sluggish percolation behaviour. In such instances, the change from insulator to a conductor is not sharp, and the electrical conductivity at PT obtained will not be high enough for many practical applications. For instance, Zheng *et al*. (2004) melt compounded high density polyethylene, (HDPE) with G; the first steep rise in conductivity occurred at 5G wt. % but the conductivity achieved was only 1 x 10$^{-11}$ S/cm. However a steeper rise followed at about 8G wt. % to give conductivity of about 1x10$^{-6}$ S/cm sufficient for electrostatic discharge applications (Moniruzzaman and Winey, 2006).

The high volume fractions of micron-scale fillers such as G required improving the properties leads to high viscosities during processing. To prevent forming highly dense product, co-blending two or more polymers with the filler helps. The concept being to make the filler preferentially dispersed in one phase while the volume of the other phase becomes effectively excluded (Thongruang *et al*., 2002). Alternatively, increasing the degree of crystallinity (Gubbel *et al*., 1995) of composites when a semi-crystalline matrix is used can also be used as a strategy. During crystal growth, fillers are pushed aside into the amorphous phase. Mixtures of micron-scale carbon fillers (Clingerman *et al*., 2002; Elwell *et al*., 2004) can also be used to attain early electrical conductivity PT.

Adding nano-sized particulate carbon fillers such as GNP can also be made to attain property gains such as electrical conductivity. This could be attained at loading levels where processing the composite is not severely altered compared to the unfilled matrix (Kalaitzidou *et al*., 2007a). A low

PT of 0.75 vol. % was attained using *in situ* polymerisation of EC to produce PA6/GNP composites (Weng *et al*., 2004). The highest electrical conductivity attained was $10^{-3}$ S/cm. The synthesis was assisted by sonication which continued until the system's viscosity increased. The attainment of low PT was ascribed to good dispersion, the structure and aspect ratio of the GNP. It is observed that washing the product by boiling for one hour will improve conductivity by the elimination of diluents while sonication during synthesis may shorten polymerised chains, reduce molecular weight and increase the levels of water soluble oligomers.

Percolation behaviour of conductive fillers can also be investigated for already conductive conjugated polymers such as Polyaniline (PANI). The electrical conductivity and percolation behaviour of PANI was determined using *in situ* polymerisation of aniline with GNP where at 0.32 GNP vol. %, conductivity of 420 S/cm was obtained as against 5 S/cm for unfilled PANI. The nanocomposites' conductivity increased gradually to 522 S/cm at 4.5 vol. % which doubled the former in order of magnitude. Applying percolation theory, a critical exponent of $t = 0.85$ was obtained which is lower than the universal value (1.3-2). In this wet process, the impressive result was assigned to the high aspect ratio of GNP which led to the formation of an effective conductive network.

Another wet process, (solution blending) was employed by Vadukumpully *et al*. (2011) in an effort to determine the PT in poly (vinyl chloride)/GNP nanocomposites. Relative to the unfilled PVC for composites with GNP loading level less than 0.1 vol. %, no electrical conductivity was attained. However, some electrical conductivity was attained from 0.1-0.6 GNP vol. % which was not even sufficient to attain the basic practical applications such as preventing the accumulation antistatic charges. Useful electrical conductivity was attained from 1.3 GNP vol. %. The authors reported that the rapid rise in electrical conductivity around 6 GNP vol. % was assumed to correspond with the PT. Nonetheless, wet processing does not always guarantee low PT for polymer/GNP composites although it is always likely to be lower relative to melt processing. In a comparative study, high PT values were obtained at 12 and 15 wt. % for solution blending and counter-rotating twin-screw extrusion respectively using low linear density polyethylene (LLDPE)/GNP nanocomposites. The GNP loading levels were up to 20 wt. % (Kim *et al*., 2009). Here, the solution process was employed alongside a series of twin-screw extrusion melt compounding processes. Overall, solution mixing gave the best dispersion. Among the melt compounded composites; the counter-rotating screw arrangement gave the highest PT. Reasons for the high PT values were not given, however, the GNP aspect ratio of 1500 suggests that it was GNP-15 which has a moderate surface area of 100 $m^2/g$ (Kalaitzidou *et al*., 2007c). DSC results showed decreased crystallinity relative to unfilled LLDPE on both the solution blending and melt compounding. This decrease does not favour the lowering of PT (Zang *et al*., 2007).

Kalaizidou *et al*. (2007c) made a series of investigations on the properties PP/GNP nanocomposites. The objective is to study the effect on the electrical conductivity of three mixing methods namely; melt compounding, solvent processing and polymer coating/melt compounding. The processes are followed by compression or injection moulding. Two GNP fillers, GNP-1 and GNP-15 with the same surface area of about 100 $m^2/g$ were used with the latter having higher aspect ratio. Polymer coating followed by melt compounding was found to be as efficient as solvent processing. SEM micrographs indicated uniform dispersion of the GNP particles in the polymer coated/melt compounded nanocomposites. The authors observed that at the same volume fraction, GNP-1 had about 200 x more particles than GNP-15. This increased the ability of GNP-1 to efficiently coat PP there by inducing electrical conductivity at lower loadings. With regard to the GNP-coated melt compounded nanocomposites (the best among the melt processed systems), followed with compression moulding gave better properties than injection moulding. The complex 3D particle orienting effects found in the fountain-flow in injection moulding as against the 2D planar orientation generated during compression moulding may have contributed to this (Kim and Mascoko, 2009). For the coated melt compounded/injection moulded nanocomposites of GNP-15, PT was attained at 5 vol. %. When uncoated melt extrudates with injection moulded, PT was attained at approximately 7 vol. %.

In a related investigation by Kalaizidou *et al*. (2007b), an SEM micrograph showed that due to the higher surface area of GNP-15 (implying more flexibility) it may fold and roll up. Therefore, it suffices to say that the PT of any polymer/particulate carbon composite depends on the processing, the dispersed state of the filler, the matrix used and the morphology attained. Fukushima and Drzal

(2006) conducted a research to identify the PT of PA6, 6/carbon nanocomposites using co-rotating twin screw extrusion, the carbon fillers used were GNP-1 and GNP-15. PA6, 6/GNP-15 had a lower PT of 6 vol. % compared to the PT of PA6, 6/GNP-1 at 10-12 vol. %. The variation could be attributed to the processing which allowed the retention of the natural morphology of GNP-15 leading to early formation of an electrically-conductive percolated network. Just as high aspect ratio is expected to decrease thermal contact resistance (Kalaitzidou *et al*., 2007c) so it is expected to facilitate smooth flow of electric charges.

In the light of the above in this research, a micro-composite PA6/graphite (G) and a nanocomposite, PA6/graphite nanoplatelets (GNP) are synthesized *in situ* employing a novel approach. Overhead stirring and horn sonication will be used to distribute and disperse the carbon fillers, using two streams 40/10 and 20/20. The 40/10 stream implies that while dispersing the carbon fillers in PA6 monomer, 40% amplitude of sonication will be applied for 10 minutes while the 20/20 stream implies that 20% amplitude of sonication was applied for 20 minutes. The electrical conductivity for the two streams at different filler loading will be investigated. At what filler loading will *'purely ohmic behaviour'* of composite be achieved? The percolation threshold (PT) for the two streams will be examined for the *in situ* for graphite (IG) and *in situ* polymerised for nanoplatelets (INP).

## 2.0. Methodology

### *2.1. Materials*

Pristine commercial grade PA6 was donated by Akulun Germany. The monomer Epsilon Caprolactam (C6H11NO, coded as EC) was purchased from Sigma-Aldrich, with purity level of 99 % and a molecular weight of 113.16. The pristine PA6 and the EC were vacuum dried overnight at 50º C before usage which adequately removed moisture. Methyl Magnesium Bromide (coded as MMB, molecular weight 119.26,) is a Grignard catalyst precursor which forms the catalyst, (Caprolactam Magnesium Bromide (CMB)) *in-situ,* was purchased Fisher Scientific as a 100 ml bottle containing a 3.0 M solution of MMB in diethyl ether. *Activator*: or co-catalyst, is a monofunctional Nacetylcaprolactam ($C_8\ H_{13}NO_2$), coded as NAC), supplied by Sigma-Aldrich with purity; 99 % and molecular weight of 155.19. Graphite Filler: Synthetic graphite, (coded as G) is ≤ 2 μm in particle size was supplied by Sigma-Aldrich. *Graphite Nano-Platelets:* GNP-15, (coded as GNP) with surface area 107±7 $m^2$/g, diameter of 15 μm, aspect ratio of 1500 and density of 2 g/cm3 was bought from XG-Sciences, UK. Prior to use G and GNP are kept overnight in an oven at 160 °C.

### *2.2. Methods*

Details of production of composite can be found elsewhere (Umar *et al*. 2020). Briefly, graphite (G) and graphite nanoplatelets **(**GNP**)** were cumulatively added to the molten monomer EC and dispersed by simultaneous sonication and mechanical stirring. This was followed by the addition of the catalysing species at the designated temperatures. The reaction took place *in situ* in a 100ml beaker which served as the reaction vessel. Catalyst precursor and a co-catalyst were employed to ensure that the reaction to form the composites occurred. For the PA6/G composites, G loading ranged between 5-25G wt. % loading while for the GNP, the loading was between 0.5-2.5 GNP wt. %. Two similar sonication processing streams with magnitudes theoretically similar in processing streams were used. In one, the amplitude of sonication was kept at 40% and sonication was conducted for 10mins. In the other, sonication was conducted for double the time, 20mins but half the sonication amplitude, 20%. The first was designated as the IG 40/10 and IGNP 40/10 streams while the others are the IG20/20 and IGNP 20/20 streams. After the synthesis solid products were withdrawn from the reaction vessel and crushed without washing while, dog bone specimens were prepared on a Haake Mini-Lab injection moulding machine. To prepare the specimens for electrical conductivity the straight and central portions of the dog-bones were used for all the carbon loadings and for unfilled PA6.

### *2.3. Characterization for electrical conductivity*

The electrical conductivity of pure PA6, G- and GNP-based composites were investigated using an impedance spectrometer; a numeric Q phase sensitive multi-meter (PSM 1735). The meter is a 2 channelled, 4 wire kind which was operated in the inductance, current and resistance or LCR mode. The resistance displayed by test specimen as the frequency of the applied voltage varied from 1-$10^6$ Hz indicates the electrical conductivity of the measured test specimen.

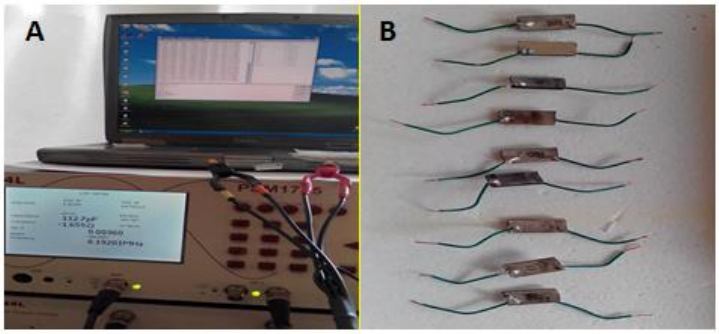


**Figure 1:** (a) Numeric Q phase sensitive multi-meter (PSM 1735) used to measure electrical conductivity, (b) specimens prepared for testing

A specimen's electrical conductivity was measured across its thickness and perpendicular to the direction of any filler alignment imposed by injection moulding. Silver paint was applied on both faces and specimens were then allowed to dry. Using a silver-epoxy conductive paste, copper wires were alternately attached on opposite faces. Figure 1a and 1b shows the test set up and ready-to-test specimens. Each specimen test was repeated 3 times. For all the carbon loadings at least 5 separate specimens were tested. The resistance recorded was converted to electrical conductivity in S/m using the dimensions of the samples according to Equation 2.

$$\sigma(\mathrm{S/m}) = \frac{1}{\mathrm{R}} \mathrm{X} \frac{\text{Specimen thickness}}{\text{specimens}' \text{cross sectional area}} \tag{2}$$

where $\sigma$ is the electrical conductivity; $R$ is the resistance of the materials.

## 3.0. Results and Discussion

### *3.1. Electrical conductivity behaviour for in situ polymerised PA6/G composites (IG 40/10 and the IG 20/20 Systems)*

Figures 2a and 2b depicts frequency dependence conductive behaviour of 2 *in situ* polymerised PA6/GNP composites systems, IG 20/20 and IG 40/10. In both, the conductivity patterns remain somewhat similar even as the frequency of the current increases at higher carbon loadings. The frequency dependence of electrical conductivity for both systems show a *'purely ohmic behaviour'* (Sandlera *et al*., 1999) as can be seen in the figures. This was achieved at 9.75 G wt. % loading in IG 40/10 system and above 10 G wt. % loading in IG 20/20 system. The relatively early lower frequency independent electrical conductivity in IG 40/10 system may be related to the higher tendency of its broken G particles agglomerate to form a conductive path. The sonication amplitude of 40% breaks more particles reducing their aspect ratios. The smaller the particles are, the more their tendency to attract each other and agglomerate. Agglomeration supports the formation of an electrically conductive network (Alig *et al*., 2008). In some cases, lower aspect ratio particles cause the formation of an electrically conductive path at lower carbon content. This is due to higher number of particles at equivalent weight fractions in comparison to higher aspect ratio particles (Kalaitzidou *et al*., 2007a). Such promotes the formation of a conductive path via agglomeration. On the one hand, with the smaller sized particle, surface tension increases in polymers (Supova *et al*., 2011) while particle/particle attraction increases making it easier formation of agglomeration-based conductive path. Again, the tendency for particles to agglomerate increases with decreasing particle size (Keledi *et al*., 2012) though with smaller sized particles, transport resistances also increases at particle/particle junctions.

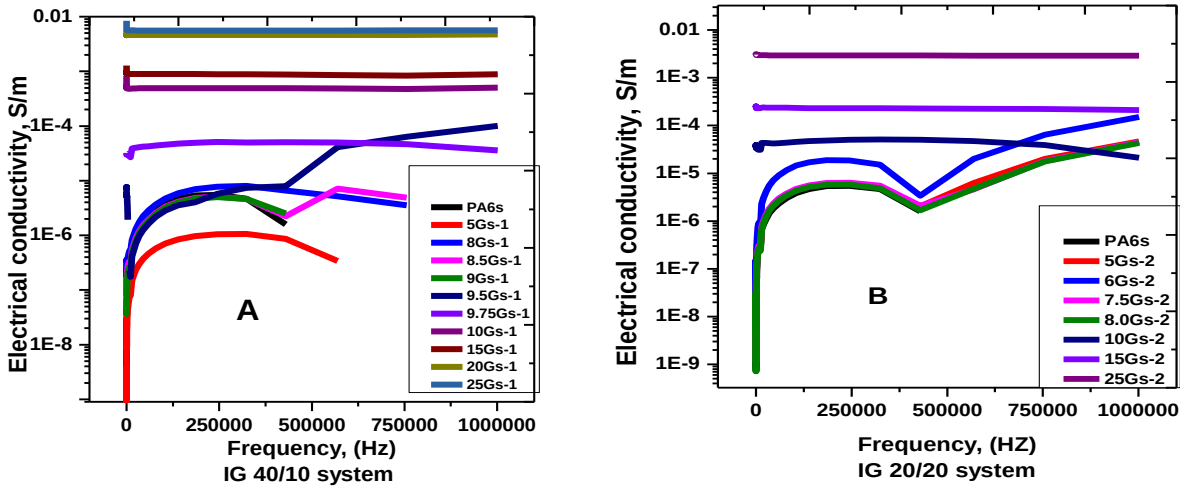


**Figure 2:** Frequency dependence of electrical conductivity in-(a) IG 40/10 system (sonication amplitude of 40% applied for 10 minutes) (b) IG 20/20 system (20% amplitude applied for 20 min)

Figure 3 depicts the percolation behaviour of the IG 40/10 system by fitting it to the power law equation. It seemed not to correspond well with the commonly reported sigmoidal curve trends. A similar behaviour with carbon loading, the electrical conductivity continues to grow defying the sigmoidal curve pattern was previously reported (Chandrasekaran *et al*., 2013). Such trends may suggest that there is a significant growth in the volume of the conductive path formed above critical carbon loading. In the IG 40/10 system, electrical conductivity sufficient for electrostatic discharge applications ($10^{-5}$-$10^{-4}$ S/m (Moniruzzaman and Winey, 2006)) is achieved above 15 G wt %. Kang and Chung (2003) attained this by incorporating 8 wt. % G and 4 wt. % oil in a PA6 hydrolytic based *in situ* polymerisation process. Most likely, oil had excluded a significant volume of the composite thereby reducing the volume required to form a conductive path.

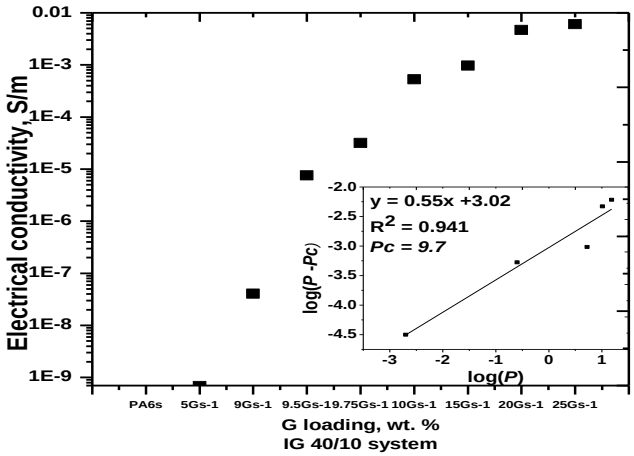


**Figure 3:** Electrical conductivity percolation curve for the G 40/10 system (40% sonication applied for 10 min). Inset is the corresponding power law fit

The inset in Figure 3 is the power law fitting of the percolation curve. The estimated percolation threshold (PT) loading is about 9.7 G wt. % which is significantly lower than some reported values in studies containing polymer/G composites (Kang and Chung, 2003; Chen *et al*., 2003b; Chen *et al*., 2001). This observed disparity may have to do with the variation in the matrix type, the effect arising from same and the inclusion of oil. Crystal formation in semi-crystalline polymers like PA6 also enhances electrical conductivity. As crystals are formed they push away filler particles thereby narrowing the total volume required to form a conductive path (Krupa and Chodák, 2001). When a very low PT loading of close to 6 G wt. % was reported with a HDPE matrix (Zheng *et al*., 2004), the success was associated with filler shape, the mixing viscosity and the effect of the actual blending process (Cheng *et al*., 2010). Additionally all polymers differ in their intrinsic dielectric properties. Although *in situ* polymerisation (as applied here ) has the advantage of providing good wetting of carbon fillers (Chen *et al*., 2003a), it also limits direct conduction of electric current since the carbon particles become coated (Weng *et al*., 2005). A similar effect also occurs when the filler is

encapsulated, for instance when master-batch processing precedes melt extrusion. In such cases, electron flow switches from a contact-based mechanism into an electron tunnelling type (Li and Chen, 2007).

In percolation data fittings, the critical constant, *t*, describes the shape of the fillers as it relates to the dimensionality of the conductive path attained (Weng *et al*., 2005; Yamamuro *et al*., 1999). In the G 40/10 system, a critical constant of 0.55 is obtained with the regression coefficient above 0.9 which justifies the value. Conventionally, *t* values close to 2 implies that the electrical conductive network is 3 dimensional (Schmidt *et al*., 2007). Deviations to higher values are considered to be a manifestation of a non-universal phenomenon (Foulger, 1999b; Chen *et al*., 2003a; Foulger, 1999a). Chen *et al*. (2003a) suggests *t* values between 1.65 to 2.0 to correspond to a 3 dimensional filler connectivity network while, extreme filler geometry causes deviations to higher values. This results in other forms of conductive mechanism, for instance tunnelling (Foulger, 1999B) to occur in parallel with the contact type. Filler connectivity can also be such that a two dimensional network forms. Values around 1.1 (Yamamuro *et al*., 1999) , those within the range of 1.2-1.30 (Schmidt *et al*., 2007) and even up to 1.33 (Bauhofer and Kovacs, 2009) have all been considered to describe an electrically conductive path with a dimensionality of 2. Values of *t* far away from the range typically associated with both the two and three dimensional connectivity are sometimes observed especially when, sonication is used in dispersing the fillers (Bauhofer and Kovacs, 2009). For instance, a *t* value of 7.6 (Ha *et al*., 2007) was obtained as well as a *t* value of less than 1 (Wang and Dang, 2005), both in processes involving carbon dispersion by sonication. Therefore, the *t* value of ≈ 0.6 obtained in the G 40/10 system is not an isolated finding. It appears that the harsh sonication conditions applied in 40/10 created small particles of diverging geometries as evident in Figure 4 below. The red arrow points at somewhat distorted cone among other intricate shapes. Such mixed geometries are anisotropic thus, lacking any definable central or rotational symmetry to fit proper aspect ratio description (Supova *et al*., 2011) .

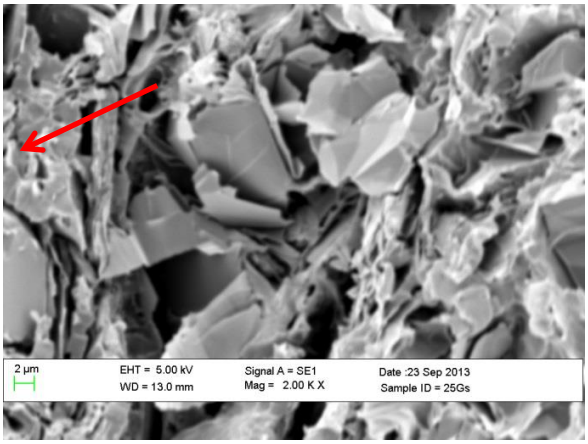


**Figure 4:** SEM photo for tensile fractured PA6/G of the IG 40/10 system (40% sonication applied for 10 min)

Figure 5 shows the PT fitting for IG 20/20 system where the PT forms at a lower loading of 7.6 G wt. % with a regression coefficient, R = 0.994. The PT value compares favourably with that achieved in G 40/10 system at 9.7 G wt. % with R = 0.941. This is an indication of a better retention of the aspect ratio in G 20/20 system despite a higher value of the sonication. The *t* value of 2.26 obtained here is an approximate to a 3 dimensional connectivity network as reported in literature (Bryning *et al*., 2005; Yuen *et al*., 2007; Yoshino *et al*., 1999; Mierczynska *et al*., 2007). It also shows that formation of an electrically conductive network occurred preferentially with a well dispersed G compared to that based on agglomerated conductive path.

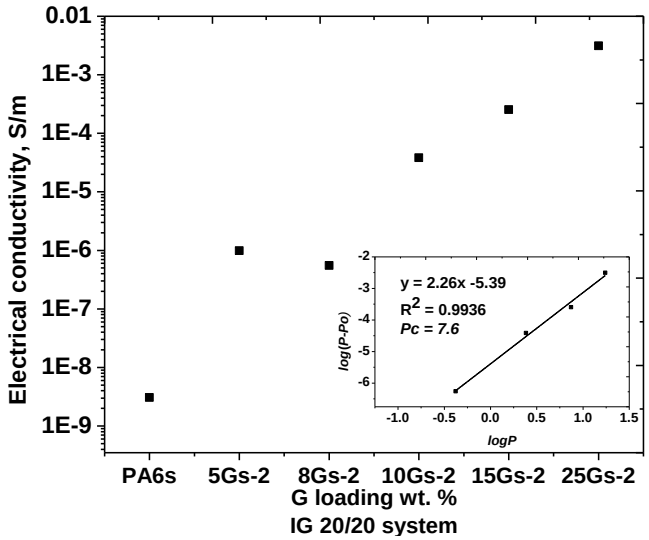


**Figure 5:** Electrical conductivity percolation curve for IG 20/20 system where 20% amplitude of sonication was applied for 20 min. Inset is the corresponding power law fit

*3.2. Electrical conductivity behaviour for in situ polymerised PA6/G composites (INP 40/10 and the INP 20/20 systems)*

A significant deviation of *t* values found in literature occurs in the INP 40/10 system as represented in Figure 6. The deviation is believed to be strongly associated with the nano filler size and shape of the GNP due to 40/10 harsh sonication conditions. Formation of large quantity of relatively small particles of different shapes is linked to sonication conditions. There seems to be no studies with which to compare these results, i.e. where GNP is incorporated *in situ* during synthesis of PA6 using fast anionic polymerisation which follows concurrent direct horn sonication and mechanical stirring. The two dimensional lateral structure of GNP combined with harsh sonication conditions can alter the GNP geometry and as such, the measured *t* value of 22.7 may not be unusual since a value close to 8 was reported when one dimensional CNT was dispersed by sonication (Ha *et al*., 2007). Ideally, *t* values describe both the geometry and dimensionality of connectivity networks (Foulger, 1999A; Foulger, 1999B). The percolation theory may have limitations when it comes to carbon particles as reported by Gojny *et al*. (2006) where higher PT values are predicted. The higher PT for INP 40/10 system is also likely associated to filler agglomeration on the nano-scale. This can negate the formation of a sufficiently large conductive path all across the specimen. The degree of crystallisation (DoC) reported in Marsden *et al*. (2018) did not vary significantly, relatively higher DoC did occur for INP 40/10 system. The lowest and highest values are 33.9±0.9 and 37.8±1.0 GNP wt. % respectively. This compares to 26.0±0.9 and 35.7±1.7 GNP wt. % in the INP 20/20 system. Hence INP 40/10 which has a higher DoC is more likely to have a higher volume excluded. This will surely aid formation of a lower PT in INP 40/10 system.

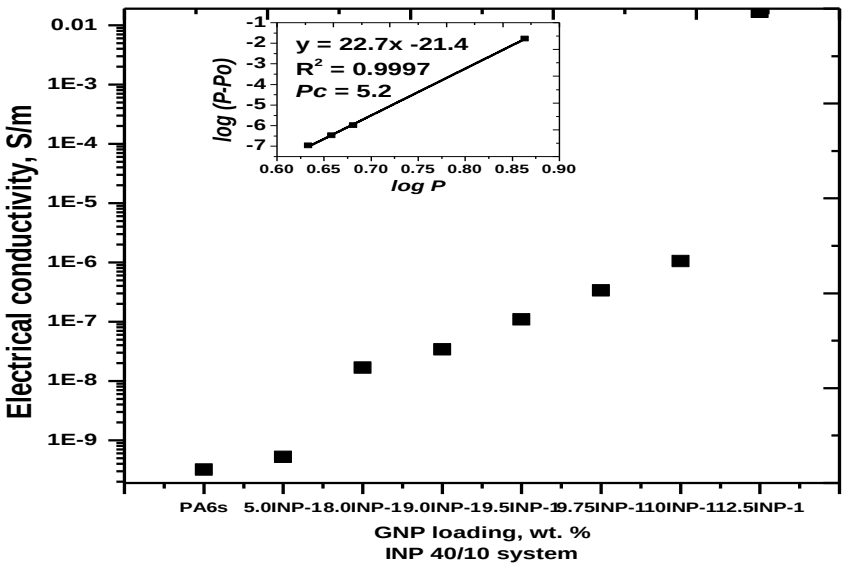


**Figure 6:** Electrical conductivity percolation curve for the INP 40/10 system where 40% sonication amplitude applied for 10 min. Inset is the corresponding power law fit

In the INP 20/20 system, electrical conductivity improvement seems quiet gradual as depicted in Figure 7. The effect of a milder sonication manifests with *t* value of 7.4 which remains within reported range where sonication is applied (Ha *et al*., 2007). It also agrees with the micrographs shown in Figure 8 where, better maintenance of the lateral structure of the GNP occurs in A for the INP 20/20 with a milder sonication condition. Under the 40/10 sonication condition, the GNP has a more fragmented structure. The higher PT value of 7.4 in the INP 20/20 system relative to 5.2 in the INP 40/10 system gives a difference of 2.2 GNP wt. % and most likely corresponds to their percolation behaviours.

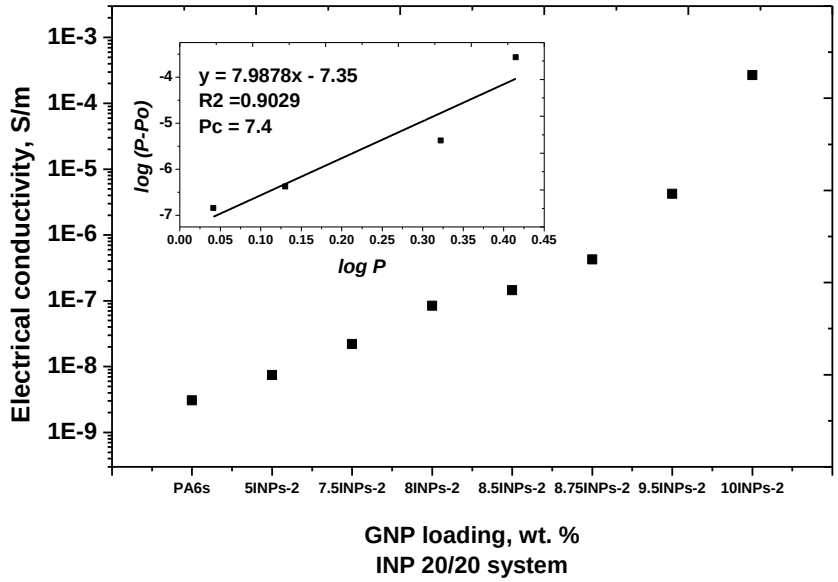


**Figure 7:** Percolation curve for the INP 20/20 system where 20% sonication amplitude was applied for 20 min. Inset is the corresponding power law fitting

(a) (b)

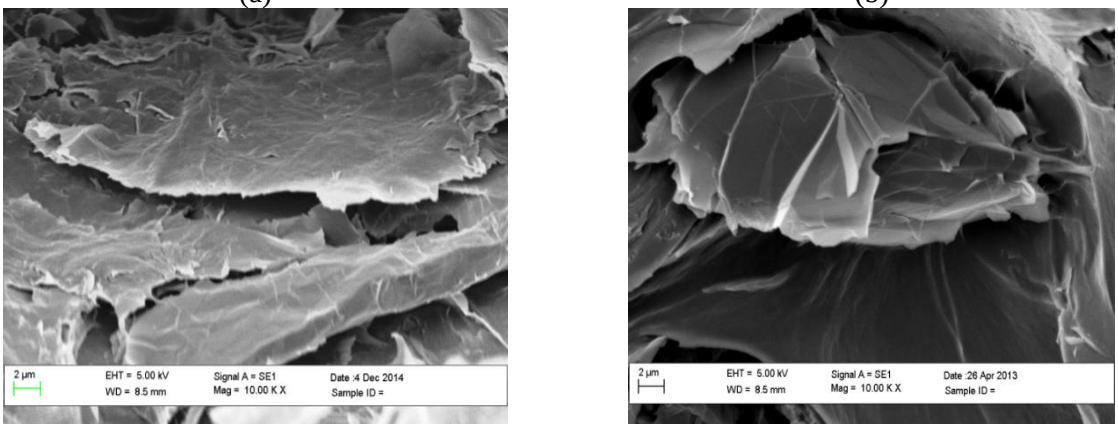


**Figure 8:** Morphologies of the GNP in (a) the INP 20/20 system (sonication amplitude of 20% for 20 min), and (b) the INP 40/10 system (40% amplitude for 10 min)

## 4.0. Conclusion

Using *in situ* polymerisation and two processing streams of theoretically equivalent carbon filler dispersion strain rates, micron and nano sized carbon composites of PA6 were made and their electrical conductivities and percolation thresholds were investigated. The two dispersion processing streams used were the 40 % amplitude for 10 min (40/10) and the sonication amplitude of 20% for 20 min (20/20). Each G and GNP composites were made at five cumulative filler loading levels. A purely ohmic electrical conductivity behaviour was attained at 9.75 G wt. % for the G composites in IG 40/10 system. For composites in the IG 20/20 system, ohmic electrical conductivity was attained at 10.00 G wt. %. Percolation threshold was attained at 9.7 G wt. % loading in IG 40/10 system while, same was attained at 7.6 G wt. % loading in IG 20/20 system. For the GNP based systems, percolation threshold occurred at 5.2 GNP wt. % in the INP 40/10 system whereas same occurred at 7.4 GNP wt.% in the IG 20/20 system.

## References

Alig, I., Skipa, T., Lellinger, D. and Pötschke, P. (2008). Destruction and formation of a carbon nanotube network in polymer melts: rheology and conductivity spectroscopy. *Polymer*, 49(16), pp. 3524-3532.

Bauhofer, W. and Kovacs, J. Z. (2009). A review and analysis of electrical percolation in carbon nanotube polymer composites. *Composites Science and Technology*, 69(10), pp. 1486-1498.

Bryning, M. B., Islam, M. F., Kikkawa, J. M. and Yodh, A. G. (2005). Very Low Conductivity Threshold in Bulk Isotropic Single-Walled Carbon Nanotube–Epoxy Composites. *Advanced Materials*, 17(9), pp. 1186-1191.

Chandrasekaran, S., Seidel, C. and Schulte, K. (2013). Preparation and characterization of graphite nano-platelet (GNP)/epoxy nano-composite: Mechanical, electrical and thermal properties. *European polymer journal*, 49(12), pp. 3878-3888.

Chen, G., Weng, W., Wu, D. and Wu, C. (2003A). PMMA/graphite nanosheets composite and its conducting properties. *European Polymer Journal*, 39(12), pp. 2329-2335.

Chen, G., Wu, C., Weng, W., Wu, D. and Yan, W. (2003B). Preparation of polystyrene/graphite nanosheet composite. *Polymer*, 44(6), pp. 1781-1784.

Chen, G. H., Wu, D. J., Weng, W. G., He, B. and Yan, W. (2001). Preparation of polystyrene–graphite conducting nanocomposites via intercalation polymerization. *Polymer international*, 2001. 50(9), pp. 980-985.

Cheng, H. K. F., Sahoo, N. G., Pan, Y., Li, L., Chan, S. H., Zhao, J. and Che, G. (2010). Complementary effects of multiwalled carbon nanotubes and conductive carbon black on polyamide 6. *Journal of Polymer Science Part B: Polymer Physics,* 48(11), pp. 1203-1212.

Clingerman, M. L. (2001). Development and modelling of electrically conductive composite materials, PhD Thesis Michigan Technological University England.

Clingerman, M. L., Weber, E. H., King, J. A. and Schulz, K. H. (2002). Synergistic effect of carbon fillers in electrically conductive nylon 6, 6 and polycarbonate based resins. *Polymer Composites,* 23(5), pp. 911-924.

Elwell, J. King, J., Konell, J. and Sutter, L., (2004). Shielding effectiveness of carbon-filled nylon 6,6. *Polymer Composites,* 25, pp. 407- 416.

Foulger, S. H. (1999A). Reduced percolation thresholds of immiscible conductive blends. *Journal of Polymer Science Part B Polymer Physics,* 37(15), pp.1899-1910.

Foulger, S. H. (1999B). Electrical properties of composites in the vicinity of the percolation threshold. *Journal of Applied Polymer Science,* 72(12), pp.1573-1582.

Fukushima, H. and Drzal. L. T., (2006). Nylon-exfoliated graphite nanoplatelet (xGnP) nanocomposites with enhanced mechanical, electrical and thermal properties. *Technical Proceedings of the 2006 NSTI Nanotechnology Conference and Trade Show, (NSTI-Nanotech 2006),* 1, pp. 282-285.

Gojny, F. H., Wichmann, M. H. G., Fiedler, B., Kinloch, I., Bauhofer, W., Windle, A. and Karl, S. (2006). Evaluation and identification of electrical and thermal conduction mechanisms in carbon nanotube/epoxy composites. *Polymer,* 47(6), pp. 2036-2045.

Gubbels, F., Blacher, S., Vanlathem, E., Jerome, R., Deltour, R., Brouers, F. and Teyssie, Ph (1995). Design of electrical composites: determining the role of the morphology on the electrical properties of carbon black filled polymer blends. *Macromolecules,* 28(5), pp. 1559-1566.

Ha, M., Grady, B., Lolli, G., Resasco, D. and Ford, W. (2007). Composites of Single-Walled Carbon Nanotubes and Styrene-Isoprene Copolymer Latices. *Macromolecular chemistry and physics,* 208(5), pp. 446-456.

Keledi, G., Hári, J. and Pukánszky, B. (2012). Polymer nanocomposites: structure, interaction, and functionality. *Nanoscale,* 4(6), pp. 1919-1938.

Kalaitzidou, K., Fukushima, H. and Drzal, L. T. (2007A). A new compounding method for exfoliated graphite–polypropylene nanocomposites with enhanced flexural properties and lower percolation threshold. *Composites Science and Technology,* 67(10), pp. 2045-2051.

Kalaitzidou, K., Fukushima, H. and Drzal, L. T. (2007B). Mechanical properties and morphological characterization of exfoliated graphite–polypropylene nanocomposites. *Composites Part A: Applied Science and Manufacturing,* 38(7), pp. 1675-1682.

Kalaitzidou, K., Fukushima, H. and Drzal, L.T. (2007C). Multifunctional polypropylene composites produced by incorporation of exfoliated graphite nanoplatelets. *Carbon,* 45(7), pp. 1446-1452.

Kang, S.-c. and Chung, D.-w. (2003). Improvement of frictional properties and abrasive wear resistance of nylon/graphite composite by oil impregnation. *Wear,* 254(1), pp.103-110.

Kim, H. and Macosko, C. W. (2009). Processing-property relationships of polycarbonate/graphene composites. *Polymer,* 50(15), pp. 3797-3809.

Krupa, I. and Chodák, I. (2011). Physical properties of thermoplastic/graphite composites. *European Polymer Journal*, 37(11), pp. 2159-2168.

Li, J., Sham, M. L., Kim, J. and Marom, G. (2007). Morphology and properties of UV/ozone treated graphite nanoplatelet/epoxy nanocomposites. *Composites Science and Technology*, 67(2), pp. 296-305.

Lu, J. R., Weng, W. G., Chen, X. F., Wu, D. J., Wu, C. L. and Chen, G. H. (2005). Piezoresistive Materials from Directed Shear-Induced Assembly of Graphite Nanosheets in Polyethylene. *Advanced functional materials*, 15(8), pp. 1358-1363.

Marsden, A. J., Papageorgiou, D. G., Vallés, C., Liscio, A. Palermo, V., Bissett, M. A., Young, R. J. and Kinloch, I. A. (2018). Electrical percolation in graphene–polymer composites. *2D Materials* 5(3), pp. 2003-2021.

Moniruzzaman, M. and Winey, K. I. (2006). Polymer Nanocomposites Containing Carbon Nanotubes. *Macromolecules,* 39(16), pp. 5194-5205.

Mierczynska-Vasilev, A., Mayne-L'Hermite, M., Boiteux, G., Jeszka, J. (2007). Electrical and mechanical properties of carbon nanotube/ultrahigh-molecular-weight polyethylene composites prepared by a filler prelocalization method. *Journal of Applied Polymer Science*, 105(1), pp. 158-168.

Sandler, J., Kirk, J. E., Kinloch, I., Shaffer, M. S. P. and Windle, A. (2003). Ultra-low Electrical Percolation Threshold in Carbon–Nanotube–Epoxy Composites. *Polymer*, 44(19), pp. 5893-5899.

Sandlera, J., Shaffera, M. S. P., Prasseb, T., Bauhoferb, W., Schultea, K. and Windle, A. H. (1999). Development of a dispersion process for carbon nanotubes in an epoxy matrix and the resulting electrical properties. *Polymer*, 40(21), pp. 5967-5971.

Schmidt, R., Kinloch, I., Burgess, A. and Windle, A. (2007). The Effect of Aggregation on the Electrical Conductivity of Spin-Coated Polymer/Carbon Nanotube Composite Films. *Langmuir: the ACS journal of surfaces and colloids.* 23(10), pp. 5707-5712.

Sengupta, R., Bhattacharya, M., Bandyopadhyay, S. and Bhowmick, A. K. (2011). A review on the mechanical and electrical properties of graphite and modified graphite reinforced polymer composites. *Progress in Polymer Science*, 36(5), pp. 638-670.

She, Y., Chen, G. and Wu, D. (2007). Fabrication of polyethylene/graphite nanocomposite from modified expanded graphite. *Polymer International*, 56(5), pp. 679-685.

Supova, M., Martynkova, G. S. and Barabaszova, K. (2011). Effect of nanofillers dispersion in polymer matrices: a review. *Science of Advanced Materials*, 3(1), pp. 1-25.

Thongruang, W., Balik, C. M., and Spontak, R. J. (2002). Volume-exclusion effects in polyethylene blends filled with carbon black, graphite, or carbon fiber. *Journal of Polymer Science Part B: Polymer Physics*, 40(10), pp. 1013-1025.

Umar, M., Ofem, M. I. Anwar, A. S. and Salisu, A. G. (2020). Thermo gravimetric analysis (TGA) of PA6/G and PA6/GNP composites using two processing streams. Journal of King Saud University - Engineering Sciences (in the press) doi.org/10.1016/j.jksues.2020.09.003

Vadukumpully, S., Paul, J., Mahanta, N. and Valiyaveettil, S. (2011). Flexible conductive graphene/poly (vinyl chloride) composite thin films with high mechanical strength and thermal stability. *Carbon*, 49(1), pp. 198-205.

Wang, L. and Dang, Z.-M. (2005). Carbon nanotube composites with high dielectric constant at low percolation threshold. *Applied Physics Letters*, 87(4), pp. 042903-042905.

Weng, W., Chen, G., Wu, D., Chen, X., Lu, J. and Wang, P. (2004). Fabrication and characterization of nylon 6/foliated graphite electrically conducting nanocomposite. *Journal of Polymer Science Part B: Polymer Physics,* 42(15), pp. 2844-2856.

Weng, W., Chen, G. and Wu, D. (2005). Transport properties of electrically conducting nylon 6/foliated graphite nanocomposites. *Polymer,* 46(16), pp. 6250-6257.

Yamamuro, S., Sumiyama, K., Hihara, T. and Suzuki, K. (1999). Geometrical and electrical percolation in nanometre-sized Co-cluster assemblies. Journal of Physics: *Condensed Matter*, 11(16), pp. 3247

Yoshino, K., Kajii, H., Araki, H., Sonoda, V., Take, H. and Lee, S. (1999). Electrical and optical properties of conducting polymer-fullerene and conducting polymer-carbon nanotube composites. *Fullerene science and technology,* 7(4), pp. 695-711.

Yuen, S., Ma, C., Wu, H., Kuan, H., Chen, W., Liao, S., Hsu, C. and Wu, H. (2007). Preparation and thermal, electrical, and morphological properties of multiwalled carbon nanotube and epoxy composites. *Journal of Applied Polymer Science,* 103(2), pp. 1272-1278.

Zhang, W., Dehghani-Sanij, A. A. and Blackburn, R. S. (2007). Carbon based conductive polymer composites. *Journal of materials science,* 42(10), pp. 3408-3418.

Zheng, W., Wong, S.-C. and Sue, H. J. (2002). Transport behavior of PMMA/expanded graphite nanocomposites. *Polymer,* 43(25), pp. 6767-6773.

Zheng, W., Lu, X. and Wong, S. C. (2004). Electrical and mechanical properties of expanded graphite-reinforced high-density polyethylene. *Journal of Applied Polymer Science,* 91(5), pp. 2781-2788.

**Cite this article as:**
Umar M., Ofem M. I., Anwar A. S. and Usman M. U., 2021. Electrical Conductivity of PA6/Graphite and Graphite Nanoplatelets Composites using Two Processing Streams. *Nigerian Journal of Environmental Sciences and Technology*, 5(1), pp. 19-31. https://doi.org/10.36263/nijest.2021.01.0251

Nigerian Journal of Environmental Sciences and Technology (NIJEST)

www.nijest.com

ISSN (Print): 2734-259X | ISSN (electronic): 2734-2603

Vol 5, No. 1 March 2021, pp 32 - 46

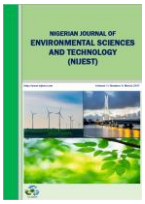

# Vulnerability Assessment of Components in a Typical Rural Nigerian Power Distribution System

Omoroghomwan A. E.[1,*], Igbinovia S. O.[2] and Odiase F. O.[3]

[1,2,3]Department of Electrical Engineering, Faculty of Engineering, University of Benin, Benin City, Nigeria

Corresponding Author: *efosaarnoldomoroghomwan@gmail.com

https://doi.org/10.36263/nijest.2021.01.0237

## ABSTRACT

*The major aim of any power system is the continuous provision of safe, quality and reliable electric power to the customers. One of the greatest challenges to meeting up with this goal is the failure of components in the system. In this article, the frequency of outages caused by failure of different components in the distribution system was investigated to ascertain the ones that are more susceptible to failure by comparing their proportions in the entire failure events. The outage data obtained from Irrua Transmission Station comprising Ehor, Ubiaja and Uzebba 33kV feeders were analyzed using Microsoft Excel while the hazard rates were measured using the failure rate index. Findings revealed that 93.77% of all the forced outages in the distribution subsystem in the power sector are caused by the high exposure rate of the bare aluminum conductors used in the construction of the various overhead feeders. Subsequently, the yearly failure rates of aluminum conductors, cross arms, relay, insulators, fuses, electric poles, breakers, transformers, isolators, cables lightning surge arresters were found to be 836.0, 17.5, 17.0, 10.3, 4.3, 2.0, 1.5, 1.3, 1.0, 0.5 and 0.3 respectively in the studied network. A comparison between this study and a related work showed that the rural feeders are more prone to faults as compared to the ones in the urban areas. It was therefore recommended that regular tree trimming along the network corridor should be done. Proper conductor size should be used in every subsequent construction and every segment with undersized conductor should be replaced with the appropriate size. This study will help the power system engineers in the design, construction, maintenance and operation of the distribution power system for optimum and improved system performance.*

**Keywords:** Vulnerability assessment, Power system components, Nigeria power sector, NEMSA, Bathtub curve, Failure rate, NERC

## 1.0. Introduction

Components are those hardware necessary to effect the proper functioning and operation of a process. While vulnerability in this context is a measure of weakness as a result of wear, tears, production lapses etc. of any component which can lead to its failure. A system is a common entity which comprises many components to carry out specific objective. The major objective of a power distribution system is the supply of safe and quality power to the customers (Brown, 2009). However, the level of the success of this objective is subject to the health and capacity of the installed components in the system. Hence, the arrangement and sizing of components in a power system has become a major aspect in system planning and design because the configuration, architecture and capacity can influence the component failure rate, cost and operational flexibility (Brown, 2009).

In an electrical system, all the components are connected together either in parallel, series, meshed or a combination of these. Therefore, the performance of a power system is a function of the performance state of these constituent components. According to IEEE, the definition of reliability of a system or components is simply their ability to perform the intended functions under stated conditions for a specified period of time. Hence the major point of interest in distribution system reliability assessment is the rate of component failure, repair rates and the general interruptions suffered by the customers (Akintola and Awosope, 2017). This is because the flow of power requires that all the components should be healthy and energized (except standby) before electricity can get to customers.

The adequacy of any power system is defined by the capacity of the installed component. System adequacy has become a major subject in the field of electric power system studies due to the impact on the performance of the power system (Eminoglu and Uyan, 2016). This is a situation whereby there are enough facilities to cater for the generation, transmission and distribution needs of all the served customers. This implies that the point of interest as far as system adequacy is concerned are the network structural architecture and the capacity of the installed components (Billinton and Allan, 1996; Wang, 2012).

Some of the components in the power system include conductors, electric poles, switch gears, lightning arresters, isolators, fuses, transformers and insulator (Gupta, 2005; Brown, 2009; Eke, 2003). Studies have shown that these items are susceptible to failure thereby causing interruption of power supply to the customers. Sometimes, the failure of a component can cause cascaded failure in the power system as a result of the interconnection relationship that exists between the various components.

Power outages are unpalatable events for power users whether they were scheduled or abrupt. The unscheduled events are mainly due to failure of network components. Hence, component failure is the major technical cause of power outages (Akinloye *et al*., 2016). The effect of the outages caused by both line faults and components failures on the power system can last for long period if not quickly resolved. Some line faults could be transient and could be resolved within few seconds by operation of well-planned network switches. However, the failure of network equipment such as transformers, breakers, poles etc can take time to either replace or repair leading to long power outage duration. These system disturbances as a result of faults and failures are the major causes of outages in advanced countries like the United States and the United Kingdom where there are no issue of system inadequacy unlike in Nigeria and Ghana (Godfrey *et al*., 2006). The side effects of such outages are enormous and far worse when compared to scheduled outages because of the customers' unpreparedness for seamless transfer of their load to back-up sources to ensure continuation of operations. The scheduled events are usually as a result of the need to carry out maintenance operations on the equipment, construction and on consumer requests. Most often, customers are pre-informed of such outages in advance so they could make alternative arrangements for any critical activity that may require quality electric power.

One of the major menaces of faults on the distribution networks is the negative impact on the system reliability while also increasing the operational and maintenance costs (Gana *et al*., 2017). To this end, the utility companies have devised different means to contain the excesses of faults on the network reliability by adopting enhanced preventive maintenance policies and deployment of standard protection mechanisms in their systems.

One of the cost-effective methods to improve reliability is by attending to the identified network component that can improve power availability at minimum cost (Canazise *et al*., 2010). Hence in many reliability assessments, the focus of system level of stability are on the failure related characteristics of the components without necessarily considering the number of customers affected by the breakdown. The attention on component failure is even more crucial in series connected power system because according to Canizes *et al*. (2017), the failure of any of the major line components in such a network will result to an outage in the entire circuit due to lack of redundancy in the network. This can influence choice of equipment vendor(s)/manufacturer(s) to rely on for supply of components based on established reliability of products of different brands over time. This is sequel to the fact that the Utility Industry is expected to ensure that operation and maintenance funds are spent wisely to meet customer expectations (Layton, 2004).

The impact of the failures of these component and the consequences on the reliability of the entire power system are usually measured using their failure/hazard rates and repair times. Some of the parameters used in such assessment include permanent short circuit failure rate ($\lambda_P$), temporary short circuit failure rate ($\lambda_T$), open circuit failure rate ($\lambda_{OC}$), mean time to repair (MTTR) and probability of operational failure (POF). Others are scheduled maintenance frequency ($\lambda_M$) and mean time to maintain (MTTM) (Brown, 2009).

The study about the failure of components in the power system has become a very interesting area amongst scholars (Sambo *et al*., 2010; Brown, 2009; Xie *et al*., 2004; Min *et al*., 2009; Musa *et al*., 2015; Wang and Wu, 2011; Akintola and Awosope, 2017; Adegboyega and Dawal, 2012; Etu *et al*., 2015; Okoronkwo and Nwagu, 2006; Adoghe *et al*., 2013). This high popularity enjoyed by this field of study is not unconnected with the vital role played by these components in the distribution of electricity to customers. These studies have helped in highlighting the behavior, characteristics, importance and performance of these components in the power system. However, there is still dearth in the study of the proportion of breakdown suffered by each component in the power system. The analysis of causes of power outages presented by Brown (2009) lumped the proportion of the entire component breakdown together against other factors. The components considered by Adoghe *et al*. (2013) in their study were very few. Though, Akintola and Awosope (2017) analyzed more components and presented their proportion of failures in the studied network nevertheless, the scarcity of studies which focus on comparison of component susceptibility levels in the power system warrant more researches. Hence, in this article, the failure of components in a typical rural distribution system in Nigeria will be analyzed to ascertain the proportions of vulnerability of each component to failure. This has become very necessary in order to improve understanding on vital issue bothering on the efficient management of the power distribution industry such as 'what proportion of the forced outages is caused by the failure of a certain or any component in the system?' Hence, such knowledge will help to identify the major items responsible for forced outages thereby assisting the utility providers to plan for effective and efficient maintenance methods. Also, such information can assist in the modification of future network designs to mitigate such failures. The rest of this work will be structured as follows: The materials and method used will be presented in Section 2. The finding will be discussed in Section 3 while the conclusion and suggestion will be done in Section 4.

### *1.1 The power system*

Typical power system consists of different components which are necessary for the generation, transmission, and distribution of electricity to the different load points as shown in Figure 1. In order to successfully achieve this, step-up transformers are used to step up the output voltage of the generators (G) for efficient transmission of the produced power. One of the advantages of transmitting electricity at high voltage is the reduction of line losses as the energy travel through long distances from point of generation to point of utilization. The high transmission line voltage requires stepping down for the purpose of distribution (Prakash *et al*., 2016). The final voltage step down is usually achieved by the distribution transformers which are fed through the primary distribution feeders. Depending on the congestion of any place and policy, the distribution conductors could be placed overhead or underground with it inherent advantages.

The efficiency and reliability of the power system largely depends on the robustness of the implemented design architecture which could be radial, ring or mesh. Mesh is the most reliable and also most complicated to operate followed by ring and then radial (Prakash *et al*., 2016). The system performance can also be affected by natural disaster, such as earthquake and cyclone. Given the fact that every power network was designed under natural disaster rated units, the damages sustained under fault conditions can affect the Mean Time To Restore/Repair (MTTR) depending on the design, control and management of that particular system (Siemens, 2008; Mariam *et al*., 2013). Though the power system comprises generation, transmission and distribution, however findings showed that 80% of all the faults in the system occur at the distribution level (Filomena *et al*., 2011).

The major role of the power distribution system is the stepping down of the transmission voltage to an appropriate level that can be safely utilized by the different customers as presented in Figure 2 (Electrical4u, 2018), and it is radial in our study such that any feeder interruption will affect the customers downstream with failure model presented in Figure 3. Thus, all the components must be in good working condition before power can be delivered to the end users due to lack of redundancy in such systems (Anthony, 2014).

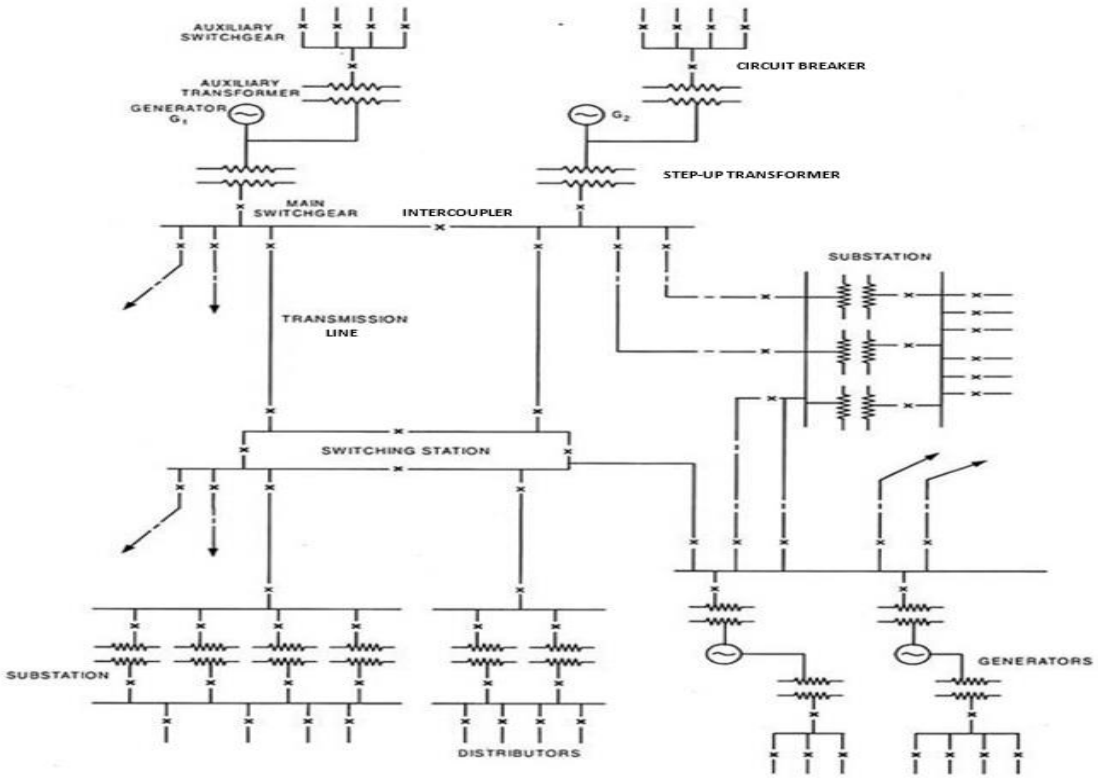


**Figure 1:** Simplified single line diagram of a typical power system (Anshika, 2017)

*1.2. Faults in distribution systems*

Faults are unhealthy system or network events. According to Meier (2006), fault is an accidental electrical connection of any live component and another conductive body at a different voltage level which results to short circuit. Research has shown that the causes of fault in the power system include vegetation and animals contact with the live lines, human errors, adverse weather conditions, damaged transformer windings, failed lightning arresters, shattered insulators etc. (Min *et al*., 2009; Airoboman *et al*., 2017; Hines *et al*., 2009; Akinloye *et al*., 2016).

The pattern of events and the phases in the life-time of components with respect to failure rates is defined by a bathtub shape to includes early infant mortality failure resulting from factory errors, wrong handling and poor workmanship, constant/random failures dependent on component functions and exposure rate to hazardous environment, and wear-out failures that are age dependent (Zhang, 2007; Neubeck, 2004; Lienig and Bruemmer, 2017; Dhillon, 2002; Brown, 2009; Xie *et al*., 2004; Akintola, 2017). Every fault results to power failure or outage in the power system. Hence there is no hardline drawn between the usage of these terms (i.e. faults and failures) in this study. For the purpose of operation, faults are broadly categorized to either line or equipment faults.

Power distribution lines are susceptible to faults of varying types and magnitudes, classified as either single phase to ground, double phase to ground, phase to phase, three phases to ground or three-phase faults (Ewesor, 2003). In analyzing these faults, we have balanced (symmetrical) three-phase faults (i.e. short circuit/shunt fault), unbalanced (unsymmetrical) faults, one line/series faults and simultaneous faults. The associated fault level can be classified as low impedance and high impedance faults, distinguished by the fault current values which resulted from the arching between the phase to the surface of contact. Unlike low impedance, high impedance faults are difficult to be detected (Wester, 1998). It requires customized approaches that can extract information of these high impedance faults from the available data occurrence (Gana *et al*., 2017). The shunt faults have been researched to be more severe than the series faults.

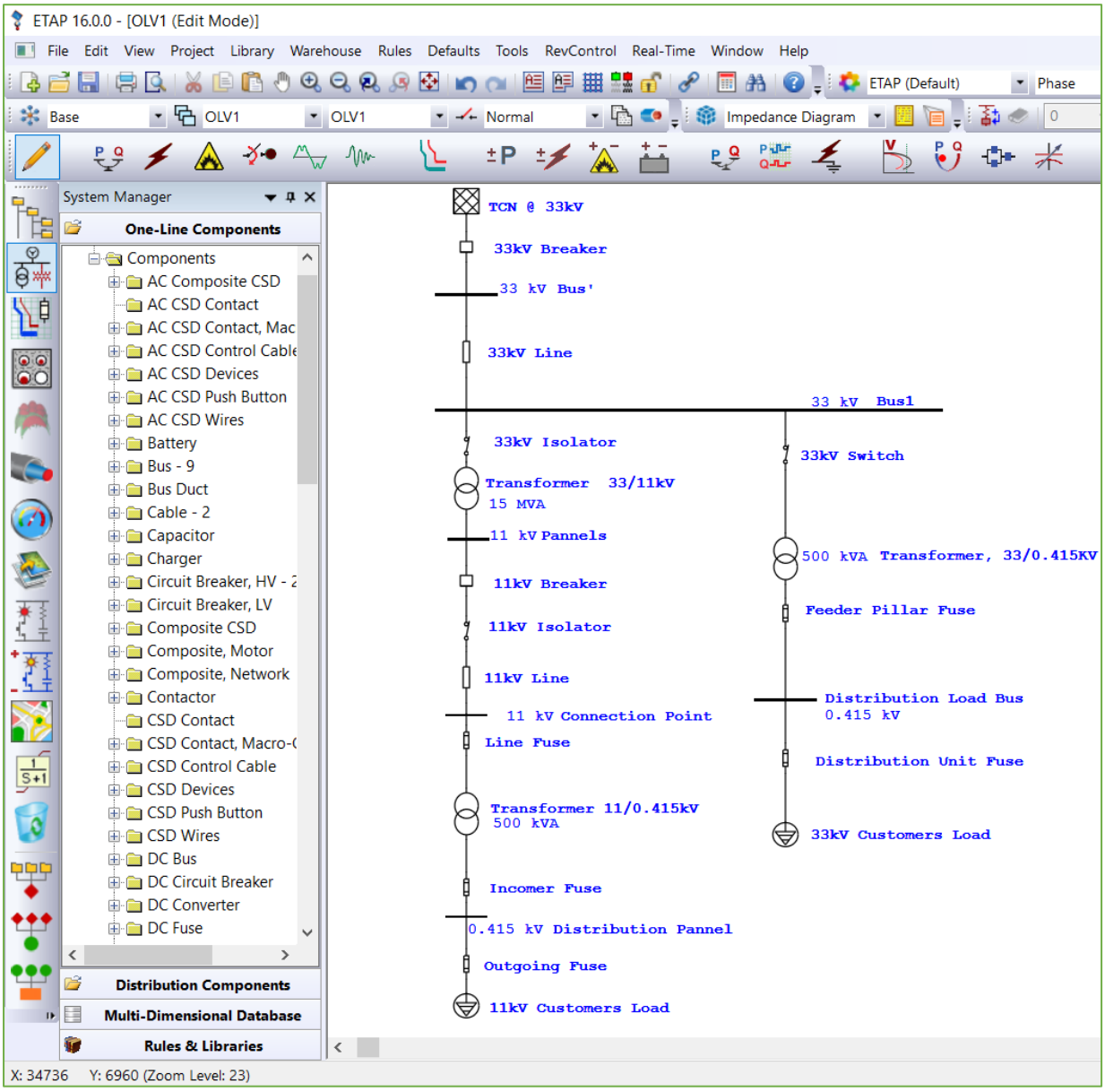


**Figure 2:** An ETAP software presentation of a typical Single-End Radial Network Configuration


**Figure 3:** Series network structure (Dorji, 2009).

Where $\lambda_p$, = Failure rate
r = Component repair time

Apart from line faults presented, there are also instances of fault conditions on the power system because of breakdown of equipment and these affect the system reliability. Some of the equipment that are susceptible to breakdown include transformers arising from insulation failure of windings, shattered bushings and oil leakage. These can result to rise in winding and oil temperature, oil shortage, fire outbreak and total failure of the transformer (Gupta, 2005; Dhakal, 2000). Another component that can break down are breakers, which have to do with their arc quenching medium and operations mechanism failures (Gupta, 2005). Other vulnerable components include line isolators, electric poles, lightning arresters and insulators (Anshika, 2017).

The findings from the study carried out in the US as presented in Figure 4 showed that the outages in the power system were as a result of trees, lightning, animals, overload, traffic accidents and dig ins (excavation activities), and the highest cause of outages are equipment failures (Brown, 2009). Figure 5 is a graphical representation of the failure rates of the different components in the distribution substation. The chart shows that fuses, line conductors and switchgear are the susceptible components in a power system with very high failure rates. However, it should be noted that faults such as failed joints/terminations are not specific to a particular equipment due to the fact that there are vibration in some equipment as current flows through them and lead to increase in resistance at such points, which can lead to high wastage of energy and fire outbreak if not properly maintained (Gupta, 2005).

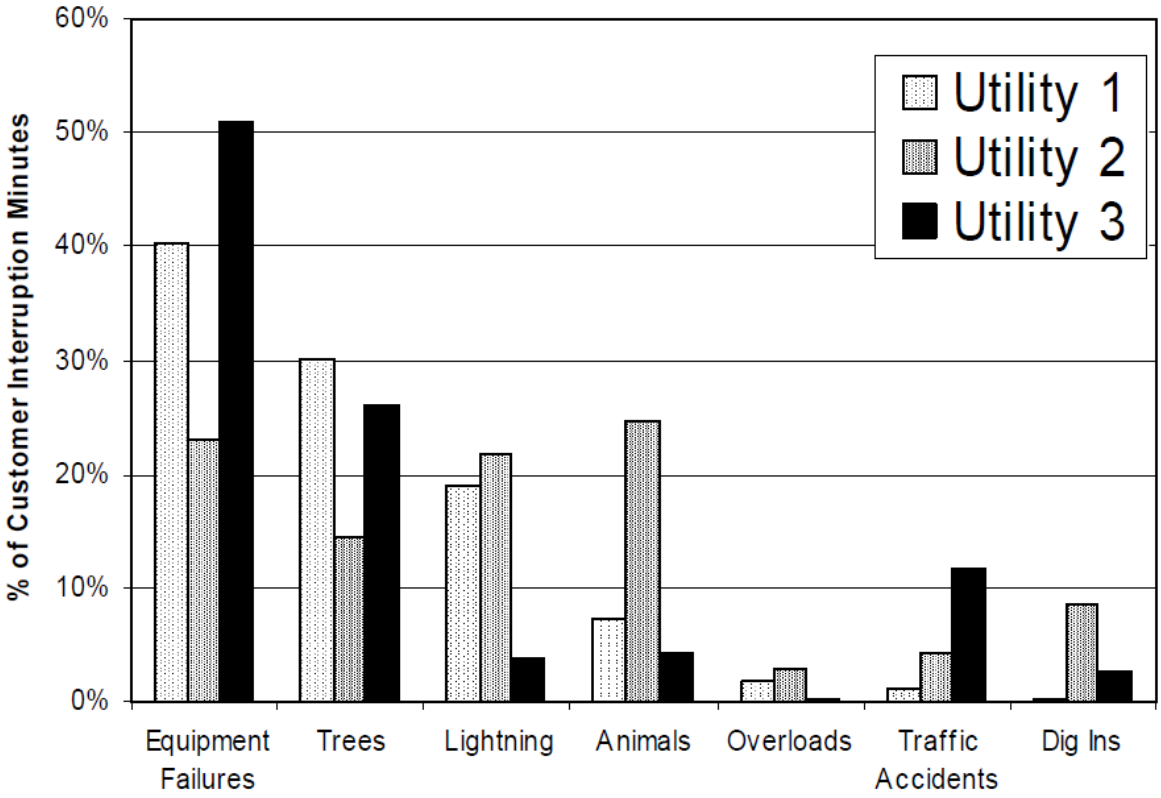


**Figure 4:** Major causes of power outages for three US utilities (Brown, 2009)

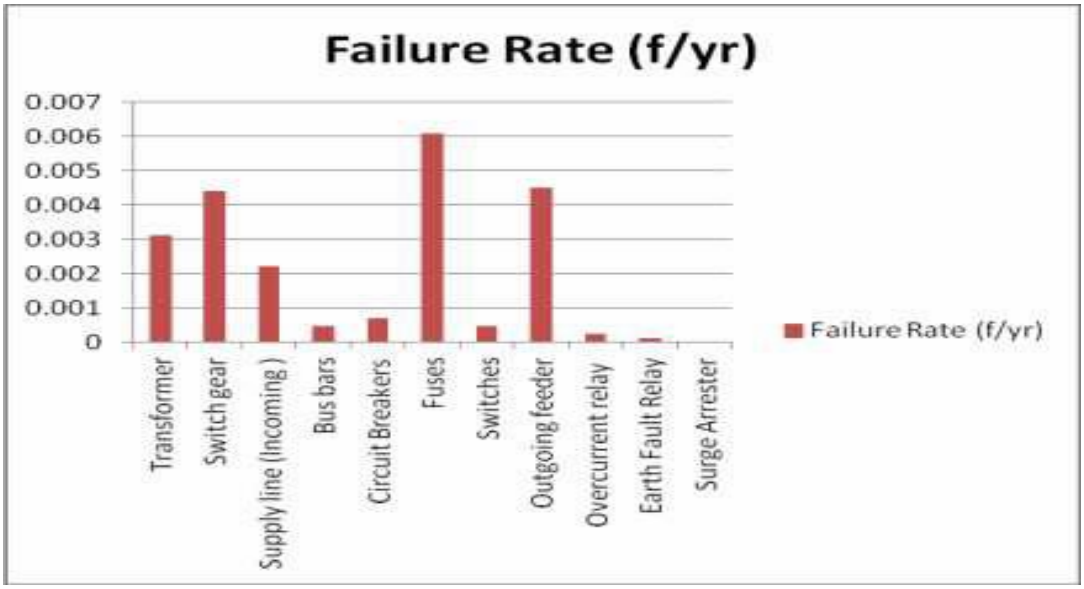


**Figure 5:** Bar chart showing the failure rate of each component (Akintola and Awosope, 2017)

## 2.0. Methodology

The data for this study were obtained from the outage records of some 33kV feeders in Irrua Transmission Station, Transmission Company of Nigeria (TCN). This comprises Ehor, Ubiaja and Uzebba feeders and the event duration was from 2015 to 2018. Special focus was placed on those forced outages which are caused by component failures hence outages caused by load management and maintenance purposes where not considered The components investigated includes Aluminum conductors, cross arms, relays, insulators, fuses, poles, breakers, transformers, isolators, cables and lightning arresters.

The raw data as presented in Table 1 was processed using Microsoft Excel application to obtain and present the counts of events in tabular form. Summarized annual outage events as a result of failure of components in the network are presented in Table 2.

**Table 1:** Sample of the interruption data of Ehor, Ubiaja and Uzebba 33kV Feeders.

| FEEDER | DAY OUT | TIME OUT | REASONS |
|---|---|---|---|
| UZEBBA 33KV FDR | 20-12-15 | 19:40 | Wire Snap |
| UZEBBA 33KV FDR | 22-12-15 | 11:32 | Wire Snap |
| UBIAJA 33KV FDR | 23-12-15 | 11:47 | Fallen tree/Vegetation Interference |
| UZEBBA 33KV FDR | 24-12-15 | 6:37 | Wire Snap |
| EHOR 33KV FDR | 25-12-15 | 10:40 | Fallen tree/Vegetation Interference |
| UBIAJA 33KV FDR | 25-12-15 | 10:48 | Fallen tree/Vegetation Interference |
| UZEBBA 33KV FDR | 28-12-15 | 18:56 | Fallen tree/Vegetation Interference |
| UZEBBA 33KV FDR | 31-12-15 | 6:00 | Phase Imbalance |
| UBIAJA 33KV FDR | 02-01-16 | 10:50 | Fallen tree/Vegetation Interference |
| EHOR 33KV FDR | 03-01-16 | 10:52 | Fallen tree/Vegetation Interference |
| EHOR 33KV FDR | 11-01-16 | 12:40 | Wire Snap |
| UZEBBA 33KV FDR | 12-01-16 | 11:00 | Insulator Failure |
| EHOR 33KV FDR | 13-01-16 | 12:33 | Twisted Conductors |
| UBIAJA 33KV FDR | 14-01-16 | 9:48 | Wire Snap |
| UBIAJA 33KV FDR | 14-01-16 | 14:00 | Broken X arm |
| EHOR 33KV FDR | 15-01-16 | 6:54 | Fallen tree/Vegetation Interference |
| UZEBBA 33KV FDR | 15-01-16 | 22:44 | Phase Imbalance |
| UBIAJA 33KV FDR | 17-01-16 | 13:40 | Jumper/Upriser cut |
| UBIAJA 33KV FDR | 17-01-16 | 18:24 | Fallen tree/Vegetation Interference |
| UZEBBA 33KV FDR | 24-01-16 | 7:40 | Pulled out conductor from pin insulator |
| UZEBBA 33KV FDR | 26-01-16 | 10:40 | Insulator Failure |
| UZEBBA 33KV FDR | 30-01-16 | 20:42 | Wire Snap |
| UZEBBA 33KV FDR | 07-02-16 | 8:39 | Uncordinated tripping |
| UZEBBA 33KV FDR | 07-02-16 | 14:48 | Wire Snap |
| UBIAJA 33KV FDR | 11-02-16 | 11:25 | Broken X arm |
| UBIAJA 33KV FDR | 11-02-16 | 18:24 | Broken X arm |
| EHOR 33KV FDR | 02-03-16 | 13:09 | Uncordinated tripping |
| UBIAJA 33KV FDR | 03-03-16 | 10:30 | Fallen tree/Vegetation Interference |
| UBIAJA 33KV FDR | 03-03-16 | 20:57 | Fallen tree/Vegetation Interference |
| UBIAJA 33KV FDR | 05-03-16 | 3:23 | Fallen tree/Vegetation Interference |
| EHOR 33KV FDR | 05-03-16 | 10:55 | Jumper/Upriser cut |
| EHOR 33KV FDR | 05-03-16 | 15:02 | Twisted Conductors |
| EHOR 33KV FDR | 05-03-16 | 19:23 | Jumper/Upriser cut |
| UBIAJA 33KV FDR | 06-03-16 | 7:14 | Fallen tree/Vegetation Interference |
| UBIAJA 33KV FDR | 08-03-16 | 2:50 | Broken X arm |
| EHOR 33KV FDR | 08-03-16 | 13:31 | Fallen tree/Vegetation Interference |
| EHOR 33KV FDR | 10-03-16 | 20:30 | Animal bridges |
| UZEBBA 33KV FDR | 12-03-16 | 9:32 | Broken X arm |
| UZEBBA 33KV FDR | 18-03-16 | 3:41 | Fallen tree/Vegetation Interference |
| UZEBBA 33KV FDR | 20-03-16 | 23:50 | Broken X arm |
| UBIAJA 33KV FDR | 24-03-16 | 9:35 | Jumper/Upriser cut |
| EHOR 33KV FDR | 26-03-16 | 19:45 | Fallen tree/Vegetation Interference |
| UZEBBA 33KV FDR | 07-04-16 | 6:20 | Breaker Failure |
| UBIAJA 33KV FDR | 10-04-16 | 19:27 | Pulled out conductor from pin insulator |

**Table 2:** Summary of component failure incidences

| Feeders | 2015 | 2016 | 2017 | 2018 |
|---|---|---|---|---|
| Ehor | 289 | 348 | 361 | 482 |
| Ubiaja | 259 | 307 | 293 | 336 |
| Uzebba | 131 | 250 | 242 | 268 |

Table 3 represents the distribution system components and the identified causes of their failures/breakdowns.

**Table 3:** Components and their major causes of failure in the system (Source: TCN)

| Serial Number | Components | Causes of failure |
|---|---|---|
| 1 | Bare Aluminum Conductor | Overgrown vegetation, Jumper/Upriser cut, detached conductor from support, wire snap, animal activities, twisted conductors. |
| 2 | Cross Arms | Broken cross arms. |
| 3 | Relays | Poor calibration, poor selectivity, poor sensitivity. |
| 4 | Insulators | Insulation failure |
| 5 | Fuses | Ruptured fuses |
| 6 | Poles | Broken poles and vehicular collision. |
| 7 | Breakers | Breaker failure |
| 8 | Transformers | Transformer faults |
| 9 | Isolators | Faulty isolators |
| 10 | Cables | Punctured cables |
| 11 | Lightning Arresters | Arrester failure |

Based on detailed analysis of the raw data, Table 4 shows the major components and equipment used in the power systems for the distribution of electric power and their level of susceptibility to failures. The grand total is the summation of total failure counts of each contributory cause of interruption to the equipment failures. For instance, according to Table 3, electric poles are susceptible to fault conditions such as broken pole and vehicular collision hence the grand total of outages comprises the count of failures from both scenarios.

**Table 4:** The frequencies, proportions and causes of components' failure induced outages

| | Bare Aluminum Conductor | | | | | | | | Cross Arms | Relays | Insulators | Fuses | Poles | | Breakers | Transformers | Isolatotrs | Cables | Lightning Arresters | Grand Total |
|---|---|---|---|---|---|---|---|---|---|---|---|---|---|---|---|---|---|---|---|---|
| FEEDERS & PROPORTION OF INTERRUPTION | Intermittent Outages | Fallen tree/Vegetation Interference | Jumper/Upriser cut | Pulled out conductor from insulator | Wire Snap | Animal bridges | Twisted Conductors | Phase Imbalance | Broken Cross Arm | Uncoordinated Tripping | Insulator Failure | Ruptured fuse | Broken pole | Vehicular Collision | Breaker Failure | Transformer fault | Isolator Fault | Punctured Cable | Lightning Arrester Failure | |
| **EHOR (41.50%)** | | | | | | | | | | | | | | | | | | | | |
| 2015 | 207 | 35 | 12 | 5 | | 4 | 6 | | 6 | 4 | 8 | 1 | | | | | | | 1 | 289 |
| 2016 | 292 | 23 | 5 | 1 | 2 | 4 | 2 | | 6 | 3 | 3 | 1 | | | 1 | 2 | 2 | 1 | | 348 |
| 2017 | 298 | 16 | 6 | 8 | 2 | 3 | | | 8 | 12 | 5 | | 2 | | | | 1 | | | 361 |
| 2018 | 367 | 42 | 3 | 16 | 1 | 2 | 1 | | 7 | 29 | 8 | 3 | | 1 | 2 | | | | | 482 |
| **SUBTOTAL** | **1164** | **116** | **26** | **30** | **5** | **13** | **9** | | **27** | **48** | **24** | **5** | **2** | **1** | **3** | **2** | **3** | **1** | **1** | **1480** |
| **UBIAJA (33.51%)** | | | | | | | | | | | | | | | | | | | | |
| 2015 | 204 | 32 | 4 | 2 | | | 1 | | 3 | 5 | 3 | 4 | 1 | | | | | | | 259 |
| 2016 | 230 | 50 | 5 | 5 | 2 | 2 | | | 9 | | 1 | 1 | | 1 | 1 | | | | | 307 |
| 2017 | 232 | 43 | 3 | | 1 | 3 | | 1 | 4 | 3 | 2 | 1 | | | | | | | | 293 |
| 2018 | 273 | 39 | 1 | 3 | 1 | | | | 8 | 5 | 1 | 2 | 2 | | 1 | | | | | 336 |
| **SUBTOTAL** | **939** | **164** | **13** | **10** | **4** | **5** | **1** | **1** | **24** | **13** | **7** | **8** | **3** | **1** | **2** | | | | | **1195** |
| **UZEBBA (24.99%)** | | | | | | | | | | | | | | | | | | | | |
| 2015 | 93 | 15 | 4 | | 12 | | | 4 | | | 2 | | | 1 | | | | | | 131 |
| 2016 | 190 | 32 | 3 | 2 | 9 | | | 1 | 6 | 1 | 3 | 1 | | | 1 | 1 | | | | 250 |
| 2017 | 191 | 29 | 2 | | 6 | | | | 8 | 1 | 2 | 1 | | | | | 1 | 1 | | 242 |
| 2018 | 215 | 27 | 2 | 1 | 5 | 1 | | | 5 | 5 | 3 | 2 | | | | 2 | | | | 268 |
| **SUBTOTAL** | **689** | **103** | **11** | **3** | **32** | **1** | | **5** | **19** | **7** | **10** | **4** | | **1** | **1** | **3** | **1** | **1** | | **891** |
| **Total** | **2792** | **383** | **50** | **43** | **41** | **19** | **10** | **6** | **70** | **68** | **41** | **17** | **5** | **3** | **6** | **5** | **4** | **2** | **1** | **3566** |
| **Proportion (%)** | **78.30** | **10.74** | **1.40** | **1.21** | **1.15** | **0.53** | **0.28** | **0.17** | **1.96** | **1.91** | **1.15** | **0.48** | 0.14 | 0.08 | **0.17** | **0.14** | **0.11** | **0.06** | **0.03** | |
| **Grand Total** | | | | **3344** | | | | | **70** | **68** | **41** | **17** | 8 | | **6** | **5** | **4** | **2** | **1** | |
| **Proportion (%)** | | | | **93.77** | | | | | **1.96** | **1.91** | **1.15** | **0.48** | 0.22 | | **0.17** | **0.14** | **0.11** | **0.06** | **0.03** | |

The proportion (%) of the grand total of the identified causes to the entire failure events (which is a measure of their level of relative susceptibility) is also presented. These proportions were determined using Equation 1 (Peter *et al*., 2011).

$$C_P = \frac{\sum C_O}{\sum O} x100 \quad (1)$$

$C_p$ Percentage proportion of each component contribution to total outages (Vulnerability)
$\sum C_o$ Sum of outages cause as a result of failure of each component
$\sum O$ Sum of all outages caused by failure of components (3566)

The failure rates (λ) of each of the components were determined using Equation 2.

$$\boldsymbol{\lambda} = \frac{\sum F}{\sum D} \quad (2)$$

$\lambda$ Failure Rate
$\sum F$ Sum of failure of each component
$\sum D$ Total duration of study

In order to obtain the proportion (%) of the failures recorded in the system as a result of the any component like aluminum conductor, the following steps were taken;

i. The total counts of failure events that have anything to do with aluminum conductors were identified. These information which can be found in Table 4 include;
    a. Intermittent outages (2792 cases)
    b. Fallen trees/vegetational encroachment (383 cases)
    c. Jumper/upriser cut (50 cases)
    d. Pulled out conductors from insulators (43 cases)
    e. Wire snap (41 cases)
    f. Animal bridges (19 cases)
    g. Twisted conductors (10 cases)
    h. Phase imbalance (6 cases)
ii. These numbers of cases were then substituted into equation 1 as follows:

$$C_p = \left(\frac{2792 + 383 + 50 + 43 + 41 + 19 + 10 + 6}{3566}\right) * 100$$
$$= \frac{3344}{3566} * 100$$
$$= 93.77$$

These steps were replicated for the other component and the results are presented in Table 5.

## 3.0. Results and Discussion

Table 5 shows that there were 3566 outages as a result of equipment and components failures, the failure distribution are: the bare aluminum conductors accounted for 93.77% of the failures, cross arms (1.96%) as a result of manufacture defects or old age, relays (1.91%) due to improper relay coordination of the 11kV protection zones which do result to trippings of the 33kV protection schemes by faults that occurred on the 11kV networks, insulators (1.15%) due to manufacture defects or old age, fuses (0.48%) in response to a fault condition or overloading condition in the system, poles (0.22%) due to old age or accidental vehicular collision. Also, outages could occur due to faults on the breakers (0.17%), transformers (0.14%), isolators (0.11%), cables (0.06%) and lightning arresters (0.03%). Figure 6 gives a graphical depiction of these realities.

**Table 5:** Vulnerability report of component in the distribution power system

| Components | Total Failures | Proportion of contribution to total forced outages in the system (%) |
|---|---|---|
| Bare Aluminum Conductor | 3344 | 93.77 |
| Cross Arms | 70 | 1.96 |
| Relays | 68 | 1.91 |
| Insulators | 41 | 1.15 |
| Fuses | 17 | 0.48 |
| Pole | 8 | 0.22 |
| Breakers | 6 | 0.17 |
| Transformers | 5 | 0.14 |
| Isolators | 4 | 0.11 |
| Cables | 2 | 0.06 |
| Lightning Surge Arresters | 1 | 0.03 |
| Total | 3566 | 100 |

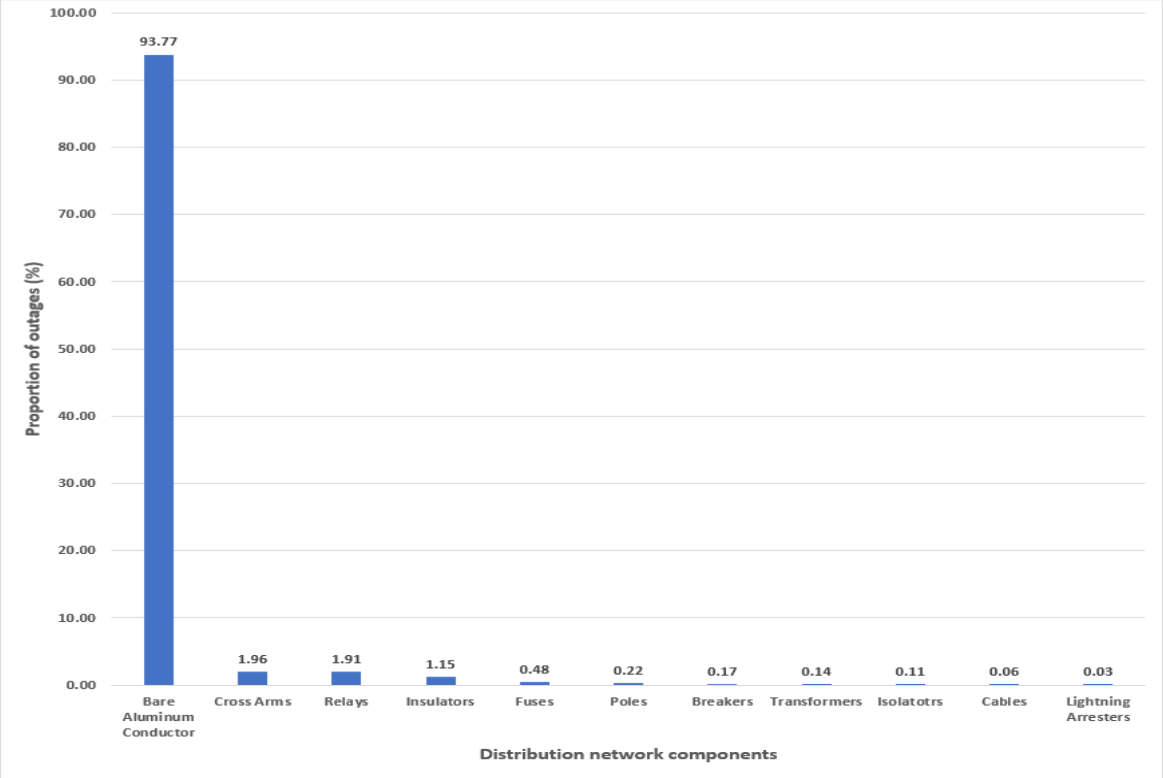


**Figure 6:** Contribution of major components to the forced outage incidences

The most visible reason for line fault is fallen trees that rest on the network and this account for 10.74% of all the faults as presented in Table 4. This result agrees with the earlier findings of Short (2004) and Okorie and Abdul (2015) which stated that vegetation issues are the major causes of faults on the distribution network resulting in overcurrent earth fault.

Components like insulators, cross arms and poles are very important supports for the conductors have been found to be prone to failures at varying degrees resulting to power outages to the customers. This agrees with the findings of Adegboye and Dawal (2012). Sometimes, weak and obsolete cross arms can also cause power outages when they break and make the live conductors to be earthed.

Considering the grand total of 3,344 outage events connected to aluminum conductor out of 3,566 events in Table 5, it is evident that 93.77% of the faults in the power sector in Nigeria are connected to the susceptible nature of the aluminum conductors that are used for the distribution of power to the various load points. This high level of bare aluminum related faults is due to many factors such as the high vegetation density of the environments where these feeders transverse.
Overloading increases the thermal characteristics of the conductors which leads to snapping of the lines (including jumpers and uprisers), while other incidents that affect the bare aluminum conductors include detachment from supports, animals bridging the lines (Brown, 2009), phase imbalance due to disconnected phase and twisted conductors' issues.

From Table 5, transformer failure is very minimal in the network (about 0.14%). This is due to the high level of protection given to it by the fuses, relays, breakers and lightning arresters in the design stage. However, it is found to fail more than the circuit breakers.

Equation 2 was used to determine the failure rate of each of the component on hourly, daily, monthly and yearly basis as presented in Table 6. The table shows that the aluminum conductors had issues 3,344 times during the period of study (2015 - 2018) within the studied distribution system. Consequently, this resulted to a failure rate of 0.09537 per hour, 2.2888 per day, 69.667 per month and 836 per year for the component.

**Table 6:** Failure rate of each component

| Components | Total Failures | Failure Rate | | | |
|---|---|---|---|---|---|
| | | Hourly | Daily | Monthly | Yearly |
| Bare Aluminum Conductor | 3344 | 0.09537 | 2.2888 | 69.667 | 836.0 |
| Cross Arms | 70 | 0.00200 | 0.0479 | 1.458 | 17.5 |
| Relays | 68 | 0.00194 | 0.0465 | 1.417 | 17.0 |
| Insulators | 41 | 0.00117 | 0.0281 | 0.854 | 10.3 |
| Fuses | 17 | 0.00048 | 0.0116 | 0.354 | 4.3 |
| Pole | 8 | 0.00023 | 0.0055 | 0.167 | 2.0 |
| Breakers | 6 | 0.00017 | 0.0041 | 0.125 | 1.5 |
| Transformers | 5 | 0.00014 | 0.0034 | 0.104 | 1.3 |
| Isolators | 4 | 0.00011 | 0.0027 | 0.083 | 1.0 |
| Cables | 2 | 0.00006 | 0.0014 | 0.042 | 0.5 |
| Lightning Surge Arresters | 1 | 0.00003 | 0.0007 | 0.021 | 0.3 |

Furthermore, the yearly failure rate of cross arms, relay, insulators, fuses, electric poles, breakers, transformers, isolators, cables lightning surge arresters are 17.5, 17.0, 10.3, 4.3, 2.0, 1.5, 1.3, 1.0, 0.5 and 0.3 respectively. These values are other ways of conveying the information on Table 5 and Figure 6 with regards to the measurement of each component hazard/failure/susceptibility rates relatively to one another with regards to proportion, causes and effects which have been discussed.

Table 7 represents a comparison of findings from this study and a similar one conducted by Akintola and Awosope (2017). To make up for the observed nomenclature variances amongst the network components in the two studies, some of the names were reconciled as follows: switches were taken as isolator, overcurrent and earth relays were presented as relays, incoming and outgoing feeders were named as aluminum conductors. Both studies showed that the line conductors are responsible for most of the forced outages. Also, both studies showed that the least failure prone component in the distribution system is the lightning arresters. The proportion of feeder conductor was 30.12% in Akintola and Awosope (2017) as against 93.77% found in this study. It was observed that the proportions (%) of failures reported in both studies (This Work : Akintola and Awosope, 2017) for relays (1.91 : 1.56), fuses (0.48 : 27.41), circuit breakers (0.17 : 3.07), transformers (0.14 : 13.93) and isolators (0.11 : 2.06) varied. This is likely due to the fact that both studies were conducted in different power systems, environments, duration and time. The difference in urbanization level in both studied areas is another key factor in the observed disparity in the obtained results. The network used in this study are mainly in rural location with a lot of vegetation on its corridor as against the other study which was done in Ayetoro I Substation located in the heart of Lagos state. It is therefore established from this study that networks in the rural areas are more susceptible to forced outages than those in the urban areas. Some of the components were not studied in each work hence no values were found for them and these are presented as NA (Not Available).

**Table 7:** Comparison between the findings from related work and this study

| S/N | Components | Percentage relative failure proportion (%) | |
|---|---|---|---|
| | | This work | Akintola and Awosope (2017) |
| 1 | Bare Aluminum Conductor | 93.77 | 30.12 |
| 2 | Cross Arms | 1.96 | NA |
| 3 | Relays | 1.91 | 1.56 |
| 4 | Insulators | 1.15 | NA |
| 5 | Fuses | 0.48 | 27.41 |
| 6 | Poles | 0.22 | NA |
| 7 | Circuit Breakers | 0.17 | 3.07 |
| 8 | Transformers | 0.14 | 13.93 |
| 9 | Isolators | 0.11 | 2.06 |
| 10 | Cables | 0.06 | NA |
| 11 | Lightning Surge Arresters | 0.03 | 0.00 |
| 12 | Switch gear | NA | 19.77 |
| 13 | Bus bars | NA | 2.08 |

## 4.0. Conclusion

In this article, the failure of components in a typical distribution system in Nigeria was analyzed to measure the proportions of vulnerability of each component to failure. Such information is useful in identifying the key components responsible for forced outages thereby assisting the utility providers to apply the appropriate maintenance methods.

The results showed that almost all the forced outages (93.7%) in the distribution network occur as a result of temporary and permanent current leakage to earth from the aluminum conductors (feeders). The rest proportion of outages are as a result of the failure of other components such as cross arms (1.96%), relays (1.91%), insulators (1.15%), fuses (0.48%), poles (0.22%), breakers (0.17%), transformers (0.14%), isolators (0.11%), cables (0.06%) and lightning arresters (0.03%). The failure rate of each of these components was also determined on hourly, daily, monthly and yearly basis to give insight to their hazard rates. Based on the findings, it is therefore recommended that proper trace clearing should be regularly carried out on the distribution networks to avoid the intermittent tripping of the lines. There should be legislation for the enactment of laws prohibiting the use of wooden cross arms and wooden poles in future power network construction in Nigeria. This will help to reduce failures of these components to the barest minimum in the network. The use of protective equipment should be sustained and improved upon to eliminate the failure of vital and expensive network component such as transformers. The appropriate wire gauge should be selected for the conductor sizes used for network construction to avoid wire snap due to overloading of conductors. Proper component inventory should be kept so as to help identify the obsolete component to effect replacement before they finally fail. Any policy or technique (such as condition monitoring (CM), predictive and reliability centered maintenance (RCM) techniques) that could reduce component failures in the network will go a long way to enhance the reliability, cut maintenance cost and reduce probable hazards in the system.

## References

Adegboye, B. A. and Dawal, E. (2012). Outage analysis and system integrity of an 11kV distribution system. *Advanced Material Research*, 367, pp. 151 – 158.

Adoghe, U. A., Awosope, C. O. and Ekeh, J. C. (2013). Asset maintenance planning in electric power distribution network. *Elsevier Journal of Electrical Power and Energy Systems,* 47, pp. 424 – 435.

Airoboman, A., Ogujor, E. and Okakwu, I. (2017). "Reliability analysis of power system network: a case study of transmission company of Nigeria, Benin City." *IEEE PES-IAS Power Africa Conference. June 27-30. The Gimpa, Accra, Ghana,* pp. 99-104. DOI: 10.1109/PowerAfrica.2017.7991206.

Akinloye, B., Oshevire, P. and Epemu, A. (2016). Evaluation of system collapse incidences on the Nigeria power system. *Journal of Multidisciplinary Engineering Science and Technology (JMEST)*, 3(1), pp. 3707 – 3711.

Akintola, A. A. (2017). Reliability evaluation of secondary distribution system in nigeria: a case study of Ayetoro 1 substation, Aguda, Lagos State. Master of Science Thesis, Department of Electrical and Information Engineering, Faculty of Engineering, Covenant University, Ota, Ogun State, Nigeria, pp. 1-78.

Akintola, A. A. and Awosope, C. O. A. (2017). Reliability Analysis of Secondary Distribution System in Nigeria: A Case Study of Ayetoro 1 Substation, Lagos State. *The International Journal of Engineering and Science (IJES)*, 6(7), pp. 2319 – 1805.

Anshika, R. (2017). Components of a power system (with diagram). *Electrical Engineering*. Retrieved from: www.engineeringenotes.com:http://www. engineeringenotes.com/ electrical-engineering/power-system/components-of-a-power-system-with-diagram-electrical-engineering/28186.

Anthony, R. (2014). Reliability analysis of distribution network. Master of Science Thesis, Faculty of Electrical and Electronic Engineering, Universiti Tun Hussein Onn, Malaysia, pp. 1- 38.

Billinton, R. and Allan, R. N. (1996). *Reliability evaluation of power systems*. 2nd ed. New York and London: Plenum Press, pp. 1 – 13.

Brown, R. E. (2009). Electric Power Distribution Reliability. Boca Raton, Florida: CRC Press, pp. 1-462.

Canizes, B. Soares J., Hugo, M. and Costa-Lobo M.C. (2017) Optimal Approach for Reliability Assessment in Radial Distribution Networks. *IEEE Systems Journal*, 1(3), pp. 1-11.

Canizes, B., Soares., Vale Z. and Lobo C. (2010) "Increase of the Delivered Power Probability in Distribution Networks using Pareto DC Programming. IEEE Power and Energy Society General Meeting, Vancouver, pp. 1-5.

Dhakal, P. (2000). Computer aided design of substation switching schemes. Ph.D Thesis, University of Saskatchewan, Canada. Retrieved from www.collectionscanada.gc: https://www.collectionscanada.gc.ca/obj/s4/f2/dsk1/tape4/PQDD_0033/NQ63860.pdf.

Dhillon, B.S. (2002). "Engineering Maintenance A Modern Approach" *CRC Press, Boca Raton New York London Washington DC*, pp. 1-222.

Dorji, T. (2009). Reliability assessment of distribution systems. M.Eng. Thesis, Norwegian University of Science and Technology, Bhutan, Norway, pp. 9 – 20.

Ekeh, J.C. (2003). "Electric Power Principles" 1st Edition, Amflitop Publishing. ISBN 978-2983-41-1, pp.1-427.

Electrical4u (2018). Electrical power distribution system, radial and ring main. Retrieved from electrical4u.com: https://www.electrical4u.com/electrical-power-distribution-system-radial-ring-main-electrical-power-distribution-system.

Eminoglu, U. and Uyan, R. (2016). Reliability Analyses of Electrical Distribution System: A Case Study. *International Refereed Journal of Engineering and Science (IRJES)*, 5(12), pp. 94 – 102.

Etu, I. A., Ahmed, E. A. and Jack, K. E. (2015). Assessment of Nigeria's power situation and the way forward. *International Journal of Latest Research in Engineering and Technology (IJLRET)*, 1(4), pp. 23 – 31.

Ewesor, P. O. (2003). *Practical electrical systems installation*. Sam Adex. Nigeria. pp. 1 - 170.

Filomena, A. D., Resener, M. and Salim, R. H. (2011). Distribution systems fault analysis considering fault resistance estimation. *Int J Electr Power Energy Syst*, 33, pp. 1326 – 1335.

Gana, N., Aziz, N. A., Ali, Z., Hashim, H. and Bahisham, Y. (2017). A comprehensive review of fault location methods for distribution power system. *Indonesian Journal of Electrical Engineering and Computer Science,* 6(1), pp. 185 – 192.

Godfrey, M., Quarshie, E., & Robiou, M. P. (1996). *Suppressed demand-causes, measurement and cures.* Paper presented at the Proceedings of IEEE. AFRICON'96, pp. 962-967.

Gupta, J.B. (2005). "A Course in Electrical Power". Dariaganj Dehli: S.K. Katarina and Sons, 1-583.
Lakervi, E. and Holmes E. J. (1995). Electricity distribution network design, *IEEE Power Engineering Series 21*.

Layton, L. (2004). Electric System Reliability indices. *Retrieved May, 22, 2018* from https://www.researchgate.net/file.PostFileLoader.html?id=57e7af1396b7e4d28151fe14&assetKey=AS%3A410161068953600%401474801427090

Mariam, L., Basu, M. and Michael, F. (2013). A review of existing distributed network. *Architectures Journal of Engineering*. pp. 1 – 8.

Meier, A. V. (2006). *Electric power system*. John Wiley and Sons, Hoboken, New Jersey, USA., pp. 1-309.

Min, G., Pahwa, A. and Das, S. (2009). Analysis of animal-related outages in overhead distribution systems with wavelet decomposition and immune systems-based neural networks. *IEEE Transactions on Power Systems*, 24(4), pp. 1765 – 1771.

Musa B. Ngaja T. Kali B., and Tijani B. (2015). Outage Analysis on Distribution Feeder in North East Nigeria. *Journal of Multidisciplinary Engineering Science and Technology (JMEST)*, 2(1), pp. 149-152

Neubeck K. (2004). Practical Reliability Analysis, Pearson Prentice Hall, New Jersey, USA.

Okorie P. U. and Abdul A. I. (2015). Reliability Evaluation of Power Distribution Network System in Kano Metropolis of Nigeria. *International Journal of Electrical and Electronic Science.* 2(1), pp. 1 – 5.

Okoronkwo, C. and Nwangwu, E. O. (2006). Distribution System Reliability Assessment of Enugu District of Power Holding Company of Nigeria (PHCN) for Three Years. *Journal of Science and Engineering Development*, 1(1), pp. 27 – 38.

Peter, B., Michael, E., David, H., Janine, M., Bill, P., et al. (2011). Percentages. [online] Numbers and Algebra. Available at: http://amsi.org.au/teacher_modules/pdfs/Percentages.pdf [Accessed 24 Mar. 2021].

Popoola, J. J., Akinlolu A. P. and Ale T. O. (2011). Reliability Worth Assessment of Electric Power Utility in Nigeria: Residential Customer Survey Results. *Assumption University Journal, Thailand.* 14(3), pp. 217-224.

Prakash, K., Lallu, A., Islam, F. R. and Mamun, K. A. (2016). Review of power system distribution network architecture distribution power system network designs. *IEEE*, pp. 124 – 130.

Sambo, A. S., Garba, B., Zarma, I. H. and Gaji, M. M. (2010). Electricity Generation and the Present Challenges in the Nigerian Power Sector. Energy Commission of Nigeria, Abuja-Nigeria. pp. 1-17.

Short, T. A. (2004). *Electric power distribution handbook*. CRC Press LLC Boca Raton, Florida, USA.

Siemens Power Distribution and Control, Technical (2007-2008). Types of power distribution systems, *ED-1*, 18, pp. 3 – 5.

Wang, F. (2012). Reliability evaluation of substations subject to protection failures. Master of Science Thesis, Department of Electrical Engineering, Mathematics and Computer Science, Division of Electrical Power System, Delft University of Technology, Delft, the Netherlands.

Wang, T. and Wu, Y. (2011). The reliability evaluating method considering component aging for distribution network. *International Conference on Future Energy, Environment, and Materials*, 16, pp. 1613–1618. doi:10.1016/j.egypro.

Wester, C. G. (1998). High impedance fault detection on distribution systems. *Rural Electric Power Conference*, 5, pp. 1 – 5.

Xie, M., Goh, T. N and Tang, Y. (2004). On changing points of mean residual life and failure rate function for some generalized Weibull distributions. *Reliability Engineering and System Safety*, 84, pp. 293 – 299.

Zhang, X., Gockenbach, E., Wasserberg, V. and Borsi, H. (2007). Estimation of the lifetime of the electrical components in distribution networks. *IEEE Transactions on Power Delivery*, 22(1), pp. 515 – 522.

**Cite this article as:**
Omoroghomwan A. E., Igbinovia S. O. and Odiase F. O., 2021. Vulnerability Assessment of Components in a Typical Rural Nigerian Power Distribution System. *Nigerian Journal of Environmental Sciences and Technology*, 5(1), pp. 32-46. https://doi.org/10.36263/nijest.2021.01.0237

Nigerian Journal of Environmental Sciences and Technology (NIJEST)

www.nijest.com

ISSN (Print): 2734-259X | ISSN (electronic): 2734-2603

Vol 5, No. 1 March 2021, pp 47 - 56

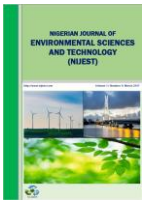

# Physicochemical Characteristics of Selected Sachet and Bottled Water in Abraka, Delta State

Otobrise C.[1,*], Azuh T. C.[2], Mmakwe E. I.[3], Ogbakpa E.[4] and Tolorun C. O.[5]

[1,2,3,4,5]Department of Chemistry, Faculty of Science, Delta State University, Abraka, Delta State, Nigeria

Corresponding Author: *otobrisec@delsu.edu.ng

https://doi.org/10.36263/nijest.2021.01.0248

## ABSTRACT

*Some physicochemical properties of five brands of sachet and five brands of bottled water sold/produced in Abraka; Ethiope East Local Government Area of Delta State was investigated. Amounts of heavy in the water samples were also determined. The results were compared with World Health Organization (WHO) standards and Nigerian Standard for Drinking Water Quality (NSDWQ) respectively. Seventy percent of the samples had pH levels below the minimum level of 6.50 recommended by WHO and NSDWQ, suggesting that the water samples are acidic. The slight acidity of the water samples may not be unconnected to impurities from poor treatment techniques. Results for other physicochemical parameters: EC (78.60 ± 34.06 µs/cm), TDS (42.80 ± 18.46mg/l), Temperature (30.02 ± 0.46 $^{O}$C), $Cl^-$ (16.88 ± 7.01mg/l), $NO_3^-$ (0.12 ± 0.05mg/l), $NO_2^-$ (<0.001mg/l), TH(10.60 ± 7.09mg/l), Cu(0.05 ± 0.00mg/l), Fe(0.34 ± 0.19mg/l), Zn(0.11 ± 0.02mg/l) and Mn (0.03 ± 0.00mg/l) for sachet water samples; EC (99.60 ± 76.18 µs/cm), TDS (54.20 ± 41.84mg/l), Temperature (29.96 ± 0.21 $^{O}$C), $Cl^-$ (20.85 ± 17.44mg/l), $NO_3^-$ (0.12 ± 0.03mg/l), $NO_2^-$ (0.01 ± 0.01mg/l), TH(15.00 ± 16.36mg/l), Cu(0.04 ± 0.01mg/l), Fe(0.20 ± 0.15mg/l), Zn(0.11 ± 0.03mg/l) and Mn (0.09 ± 0.01mg/l) for bottled water samples; were within permissible limits, indicating that the water samples are good enough for human consumption.*

**Keywords:** Sachet water, Bottled water, Physicochemical characteristics, Potable, Abraka

## 1.0. Introduction

Water is very crucial for the sustenance of lives (Gangil *et al.*, 2013; Thliza *et al.*, 2015). Virtually all processes of life in the atmosphere, lithosphere or hydrosphere require water (Aroh *et al.*, 2013). Water is an essential part of human diet and is required for maintaining personal hygiene, for drinking, domestic, industrial and agricultural uses (Isikwue and Chikezie, 2014; Thliza *et al.*, 2015). In many developing countries, availability of potable water is a perennial challenge and has become a matter of concern to families and communities (Maduka *et al.*, 2014). Studies have shown a gross inadequacy of access to potable water amongst the world's population (Akinde *et al.*, 2011; Oyelude and Ahenkorah, 2011).

In Nigeria, the situation is worrisome. Several studies have corroborated the inadequacy of the country's potable water supply (Gbadegesin and Olorunfemi, 2007; Aderibigbe *et al.*, 2008; Maconachie, 2008; Adamu, 2009; Omalu *et al.*, 2011).This has occasioned an increase in water related illnesses that has continued to be one of the foremost health burdens worldwide (Onifade and Ilori, 2008; Omalu *et al*., 2011). According to Akunyili (2003), the Government's persistent inability to provide the required quality and quantity of water for the growing population contributed in no small measure to the proliferation of the so-called 'pure water' companies in Nigeria. The proliferation of sachet and bottled drinking water products brings to fore the argument as to whether they are hygienically produced, especially when the poor sanitary conditions in most urban and rural areas of Nigeria coupled with irregular and insufficient monitoring of sachet and bottled water producers by regulating agencies is taken into cognizance (Adekunle *et al*., 2004).

Akpoborie and Ehwarimo (2012) analyzed a variety of common packaged water products in Warri. The potability of the water samples was determined by investigating coliform count, selected physical

and chemical properties as well as presence of heavy metals like cadmium, chromium and lead. Sachet and bottled water samples were procured from street vendors, wholesale shops and production plants. The results showed that pH ranged from 7.1 to 8.2; Total dissolved solids (TDS) was between 2.26 to 89.6mg/l; Turbidity: 0.45 to 2.55 NTU; Calcium: 0.11 to 1.21mg/l; Magnesium: 0.03 to 0.31mg/l; Sulphate: 0 to 1.21mg/l; chloride: 0.5 to 3.1mg/l; nitrate: 0.2 to 0.25mg/l. The cadmium level in three brands of the water samples ranged from 0.001 to 0.002mg/l. Lead concentrations ranged from 0.001 to 0.003mg/l and chromium levels ranged from 0.001 to 0.002mg/l. The parameters analysed were well below regulatory guidelines. However, the authors observed a significantly small amount of TDS in the water samples.

An investigation into the potability of sachet water available to residents of Kano metropolitan area was carried out by Ezeugwunne *et al.* (2009). The concentrations of metals (Zn, Pb, Fe, and Cu), conductivity, dissolved solids and hardness were within the World Health Organization's (WHO) permissible limits. However, some of the pH values were above the WHO permissible limits. Adekunle *et al.* (2004) assessed the socio-economic and health implications sachet water in Ibadan Nigeria. The authors reported that the physical parameters were within the WHO limits for drinking water quality, except for pH. Some chemical properties studied were also within the WHO limits. However, aluminum, fluoride and cyanide concentrations in the water samples were not within the WHO limits.

Sachet and bottled water are regulated as food products in Nigeria by the National Agency for Food and Drug Administration and Control (NAFDAC). The agency relies on WHO and NSDWQ standards for the product regulation, registration and certification. Packaged water is relatively affordable and convenient to carry and has increasingly become popular. However, many local manufacturers of sachet and bottled water do not adhere strictly to NAFDAC guidelines. This undermines the safety of such water for human consumption. The need to investigate the quality of packaged water therefore becomes imperative. The objective of this study is to investigate the quality of packaged water produced or sold in Abraka town.

## 2.0. Methodology

### *2.1. Description of study area*

Abraka is a sprawling University town situated between latitude 5°45'and 5°50' N and longitude 6° and 6°15'E. It is unevenly lowland with a gradient that slopes gently towards the River Ethiope. It is a collection of a number of linear communities in Ethiope East Local Government Area of Delta State, Nigeria. It is majorly populated by students, civil servants, farmers and small scale business owners, because it hosts the three sites of the Abraka campus of the Delta State University and a large market respectively.

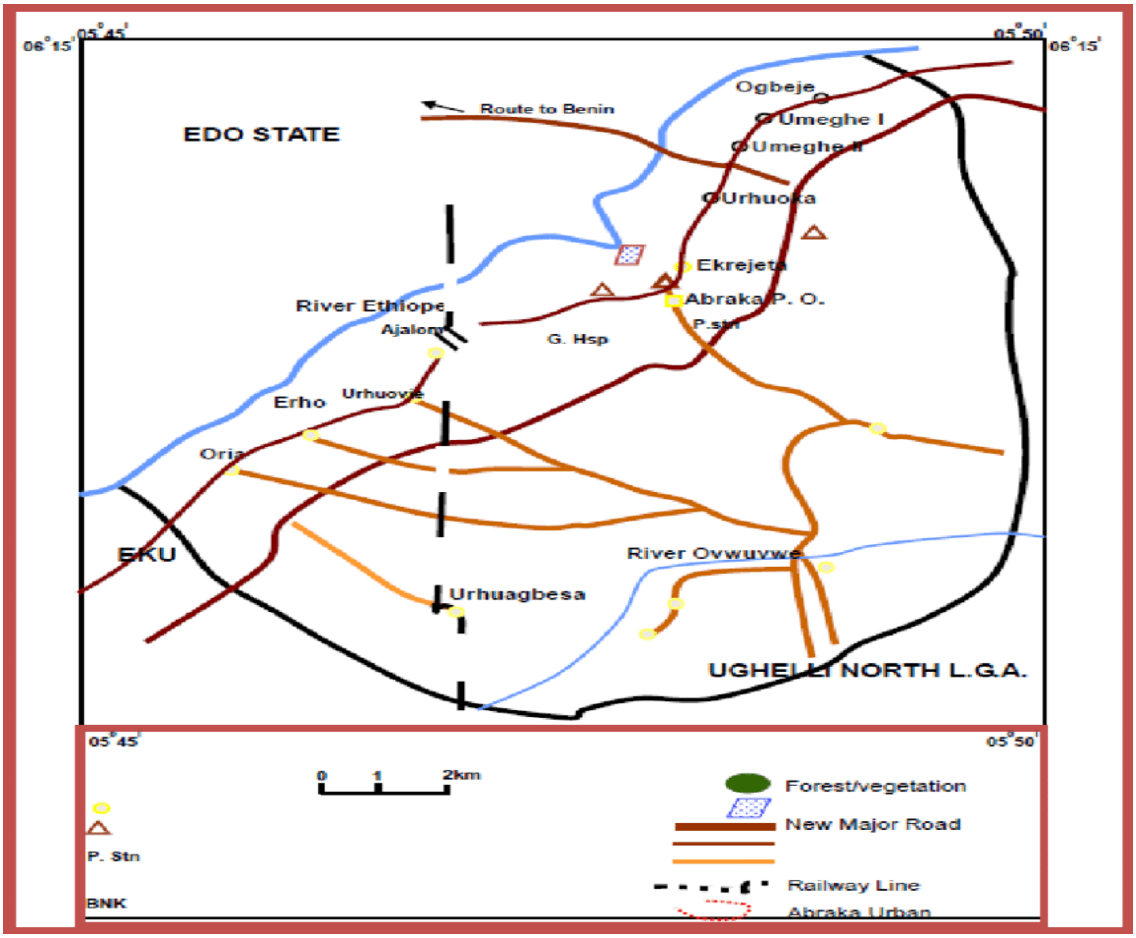


**Figure 1:** Map of Abraka showing its several linear settlements
*Source:https://www.researchgate.net/figure/Map-of-Abraka-Ethiope-East-LGA-Delta-State-Nigeria*

### *2.2. Collection/preservation of samples*

Ten (10) different bottled and sachet water brands were procured at random on the 12th of March, 2020 from the different communities that constitute Abraka town. Particular attention was on popular brand names commonly consumed in Abraka. Five (5) samples of each brand were purchased to obtain a composite sample of each sachet and bottled water brand. To protect the identity of each brand, they were labelled sample A to J. Samples A to E are sachet water, while F to J are bottled water samples. The samples were stored in the refrigerator at 4°C prior analyses.

### *2.3. Methods*

#### 2.3.1. pH and Temperature

The pH of each water sample was determined with a pH meter as described in standard methods (APHA 4500-$H^+$ Electrometric, 2017). The temperature of each water sample was measured with a digital thermometer (APHA 2550B Electrometric, 2017). About 200ml of water sample was measured into a conical flask. The thermometer was lowered into the sample until the mercury bulb was sufficiently covered by the sample and the temperature was read and recorded.

#### 2.3.2. Conductivity and turbidity

The conductivity of each sample was determined using digital conductivity meter (APHA 2510B Electrometric, 2017). The turbidity was determined by the nephelometric method with the aid of a laboratory nephelometer (APHA 2130B Nephelometric, 2017).

#### 2.3.3. Total Dissolved Solids

Total Dissolved Solids (TDS) was determined with TDS meter. The electrode was rinsed with deionised water followed by the water sample. The rinsed electrode was allowed to stabilize in the

sample for 1 minute after which the TDS value was read directly inmg/l (APHA 2540C Gravimetric, 2017).

2.3.4. Colour

Colour was determined by the method reported in the work of Dinrifo *et al.* (2010). A Lovibond visual colour comparator (APHA 2120B Visual) was used. Ten tubes of Lovibond visual colour comparator were filled with each water sample and the eleventh tube was filled with distilled water as standard control. The tubes were placed in the comparator and aligned by rotating the disc until a nearest colour match was observed. Total Hardness (TH) was determined by the EDTA titrimetric method using Eriochrome black T as indicator. The titration was done at pH = 10 (APHA 2340C Titrimetric, 2017).

2.3.5. Chloride, nitrate and nitrite concentrations

Chloride content was determined by Argentometric/Titrimetric method (APHA 4500-Cl-B Titrimetric, 2017). Nitrate ($NO_3^-$) and nitrite ($NO_2^-$) contents were determined by colorimetric method using a potable UV-visible spectrophotometer (Searchtech Instrument, 752N model, India) (APHA 4500E Colorimetric, 2017) and (APHA 4500-$NO_2$ Colorimetric, 2017) respectively.

2.3.6. Heavy metals

Heavy metals such as copper (Cu), lead (Pb), iron (Fe), zinc (Zn), manganese (Mn) were determined by Flame Atomic Absorption Spectrophotometry (FAAS) using acetylene/air with Atomic Absorption Spectrophotometer, Varian Spetra AA 600 model (USA) (APHA 3111B FAAS, 2017). Arsenic (As) was determined using AAS-Hydride method (APHA 3111B AAS-Hydride, 2017).

2.3.7. Statistical analysis

Data analysis was done by independent samples t-test using Statistical Package for Social Sciences (SPSS) version 20 Software. At a significant level ($p$ – value) of 0.05; differences between the means of the two sets of data for each parameter were considered not significant at $p > 0.05$.

## 3.0. Results and Discussion

Tables 1 and 2 show the physical and chemical properties of the sachet and bottled water samples determined in this study. A comparison of the average values of physicochemical parameters and heavy metals concentration of the water samples with international and national guidelines for drinking water is presented on Table 3. Samples A to E are sachet water samples while samples F to J are bottled water samples.

The pH values of the sachet water samples ranged from 4.11 – 6.65, while that of the bottled water ranged from 5.17 – 7.77. There is a significant deviation in the pH values of most of the water samples from acceptable standards as can be observed in Figure 1. Only samples E, F and I had values within the acceptable limit. The pH values of the other water samples were below acceptable limits. This is similar to the observations of Oyelude and Ahenkorah (2012). At a degree of freedom (df) equal to 8 and a p-value of 0.116, there was no significant difference between the pH values obtained for the sachet and bottled water samples. The pH of water affects transformation processes of the various forms of nutrients and metals. Extreme pH values poses health risks to humans.

**Table1:** Physicochemical properties of the sachet water samples

| Parameter | Sachet water samples | | | | |
|---|---|---|---|---|---|
| | A | B | C | D | E |
| pH @ 25 (°C) | 6.40 | 4.57 | 4.50 | 4.11 | 6.65 |
| EC (µs/cm) | 20 | 88 | 91 | 109 | 85 |
| TDS (mg/l) | 11 | 48 | 50 | 59 | 46 |
| Turbidity (NTU) | <0.1 | <0.1 | <0.1 | <0.1 | <0.1 |
| Temp. (°C) | 30.10 | 30.20 | 29.80 | 29.90 | 30.10 |
| Colour (Pt-Co) | <1 | <1 | <1 | <1 | <1 |
| $Cl^-$ (mg/l) | 6.00 | 17.90 | 20.24 | 24.85 | 15.39 |
| $NO_3^-$ (mg/l) | 0.10 | 0.09 | 0.07 | 0.21 | 0.12 |
| $NO_2^-$ (mg/l) | <0.001 | <0.001 | <0.001 | <0.001 | 0.080 |
| TH(mg/l) | 6.00 | 7.00 | 10.00 | 7.00 | 23.00 |
| Cu(mg/l) | 0.05 | ND | ND | ND | ND |
| Pb(mg/l) | ND | ND | ND | ND | ND |
| Fe(mg/l) | 0.20 | ND | ND | ND | 0.47 |
| Zn(mg/l) | 0.09 | 0.12 | 0.14 | 0.11 | 0.09 |
| Mn (mg/l) | ND | ND | ND | ND | 0.03 |
| As (mg/l) | ND | ND | ND | ND | ND |

*ND = Not Detected*

**Table2:** Physicochemical properties of the bottled water samples

| Parameter | Bottled water samples | | | | |
|---|---|---|---|---|---|
| | F | G | H | I | J |
| pH @ 25 (°C) | 7.21 | 5.17 | 5.93 | 7.77 | 6.33 |
| EC (µs/cm) | 142 | 36 | 83 | 209 | 28 |
| TDS (mg/l) | 78 | 19 | 45 | 114 | 15 |
| Turbidity (NTU) | <0.1 | <0.1 | <0.1 | <0.1 | <0.1 |
| Temp. (°C) | 30.10 | 29.70 | 29.80 | 30.20 | 30.00 |
| Colour (Pt-Co) | <1 | <1 | <1 | <1 | <1 |
| $Cl^-$ (mg/l) | 28.04 | 8.10 | 14.12 | 47.99 | 6.00 |
| $NO_3^-$ (mg/l) | 0.14 | 0.15 | 0.09 | 0.15 | 0.08 |
| $NO_2^-$ (mg/l) | <0.001 | <0.001 | 0.009 | 0.018 | <0.001 |
| TH(mg/l) | 44.00 | 5.00 | 8.00 | 11.0 | 7.0 |
| Cu(mg/l) | 0.05 | ND | 0.03 | ND | ND |
| Pb(mg/l) | ND | ND | ND | ND | ND |
| Fe(mg/l) | 0.01 | ND | 0.24 | 0.37 | 0.18 |
| Zn(mg/l) | 0.09 | 0.11 | 0.15 | 0.06 | 0.13 |
| Mn (mg/l) | ND | ND | 0.10 | 0.08 | ND |
| As (mg/l) | ND | ND | ND | ND | ND |

*ND = Not Detected*

**Table3:** Comparison of physicochemical properties of the water samples with National and International Guidelines

| Parameter | Sachet Water Mean ± SD | Bottled Water Mean ± SD | WHO | NSDWQ |
|---|---|---|---|---|
| pH @ 25 (°C) | 5.25 ± 1.18 | 6.48 ± 1.03 | 6.50-8.50 | 6.50-8.50 |
| EC (µs/cm) | 78.60 ± 34.06 | 99.60 ± 76.18 | NG | 1000.00 |
| TDS (mg/l) | 42.80 ± 18.46 | 54.20 ± 41.84 | 1000.00 | 500.00 |
| Turbidity (NTU) | <0.1 | <0.1 | 0.2 | 5 |
| Temp. (°C) | 30.02 ± 0.46 | 29.96 ± 0.21 | Ambient | Ambient |
| Colour (Pt-Co) | <1 | <1 | 15 | 15 |
| $Cl^-$ (mg/l) | 16.88 ± 7.01 | 20.85 ± 17.44 | 250.00 | 250.00 |
| $NO_3^-$ (mg/l) | 0.12 ± 0.05 | 0.12 ± 0.03 | 50.00 | 50.00 |
| $NO_2^-$ (mg/l) | <0.001 | 0.01 ± 0.01 | 3.00 | 0.20 |
| TH(mg/l) | 10.60 ± 7.09 | 15.00 ± 16.36 | 500.00 | 150.00 |
| Cu(mg/l) | 0.05 ± 0.00 | 0.04 ± 0.01 | 2.00 | 1.00 |
| Pb(mg/l) | ND | ND | 0.01 | 0.01 |
| Fe(mg/l) | 0.34 ± 0.19 | 0.20 ± 0.15 | 1.00 | 0.30 |
| Zn(mg/l) | 0.11 ± 0.02 | 0.11 ± 0.03 | 5.00 | 3.00 |
| Mn (mg/l) | 0.03 ± 0.00 | 0.09 ± 0.01 | 0.40 | 0.20 |
| As (mg/l) | ND | ND | 0.01 | 0.01 |

*WHO = World Health Organization (2017), Guideline for drinking water quality, 4th edition*
*NSDWQ = Nigerian Standard for Drinking Water Quality*
*NG = No Guideline*
*ND = Not Detected*

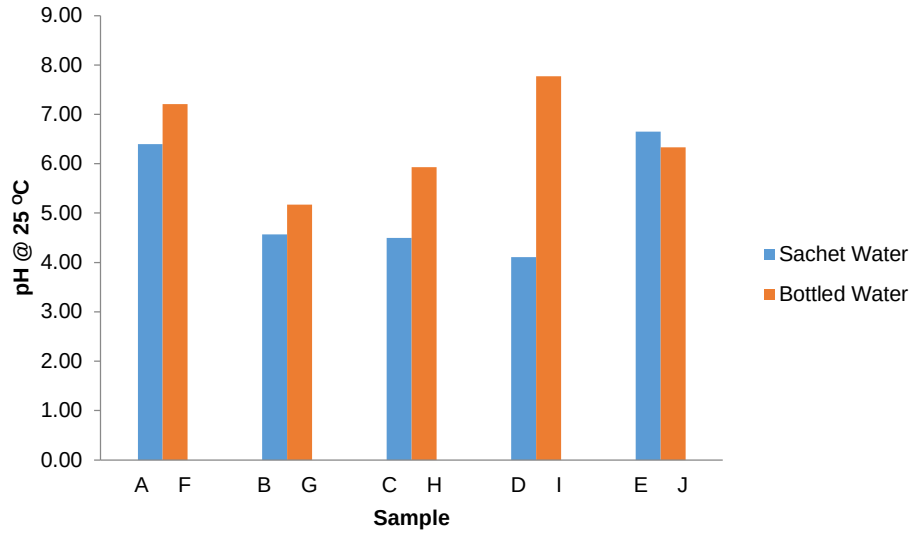


**Figure 1:** pH of Water Samples

Electrical conductivity (EC) of the sachet water samples ranged from 20.00 to 109.00µscm$^{-1}$; while that of bottled water samples ranged from 28.00 to 209.00µscm$^{-1}$. At a df of 8 and a p-value of 0.589, there was no significant difference between the EC values obtained for the sachet and bottled water samples. The EC values were far below the maximum of 1000µscm$^{-1}$ recommended for drinking water by NSDWQ. According to Nwidu *et al*. (2008) low EC values indicate the presence of minimal amount of dissolved salts (mineral elements such as calcium, magnesium and fluoride) in water. The long term drinking of packaged water with EC value that is lower than 40µscm$^{-1}$ constitute a number of health risks such as higher probability of fracture in children, pregnancy disorder (preeclampsia), diuresis, premature or low baby weight at birth and increased tooth decay (Guler and Alpalsan, 2009).

TDS of the bottled water samples ranged from 15.0 – 114.0mg/l; that of the sachet water samples was 11.0 – 59.0mg/l. At a df of 8 and a p-value of 0.592, there was no significant difference between the TDS values obtained for the sachet and bottled water samples. However, TDS of all the water samples was observed to be within the WHO and NSDWQ standards of 1000mg/l and 500mg/l respectively. TDS above the WHO upper limit of 1000mg/l affect the taste of drinking water negatively, making it unacceptable for drinking purpose. In the same vein, a very low level of TDS gives water a flat taste, this for many people is undesirable.

The salinity of the water samples was within the limit recommended for potable water. The Turbidity of drinking water is purely dependent on presence of particulate matter. Turbidity has effects on taste, odour and colour of water (Ndinwa *et al.,* 2012). The turbidity of all the sachet and bottled water samples was less than 0.1 NTU. This is within the 0.2 NTU recommended standard of WHO.

The temperature of sachet water samples ranged from 29.80 - 30.20°C; the bottled water samples had a temperature range of 29.80 - 30.20°C. At a df of 8 and a p-value of 0.626, there was no significant difference between the temperature values obtained for the sachet and bottled water samples. Variation in temperature for packaged potable water is probably due to increased hours of exposure to sunlight during the day and improper storage of water. High temperature reduces the amount of dissolved oxygen in water, (Sawyer *et al.,* 2000). The temperatures of the water samples were within the standard guidelines for drinking water.

Chloride ions concentration in the water samples varied from 6.00 – 47.99mg/l for bottled water, with sample I having the highest concentration, while the range for sachet water was 6.00 – 24.85mg/l as shown in Figure 2. At a df of 8 and a p-value of 0.649, there was no significant difference between the Chloride ion concentrations obtained for the sachet and bottled water samples. The values were however, within the WHO maximum permissible concentration of 250mg/l desirable for drinking water. This limit is primarily based on taste considerations. However, intake of water containing higher concentrations of chloride, have not been widely reported to have adverse health effect on humans (Ndinwa *et al.,* 2012). Higher levels of chloride ions in drinking water can become very

evident in the taste of water. The values observed in this study were higher than 0.31- 3.03mg/l reported for sachet water analysis in Warri and Abraka, Nigeria (Ndinwa *et al.*, 2012).

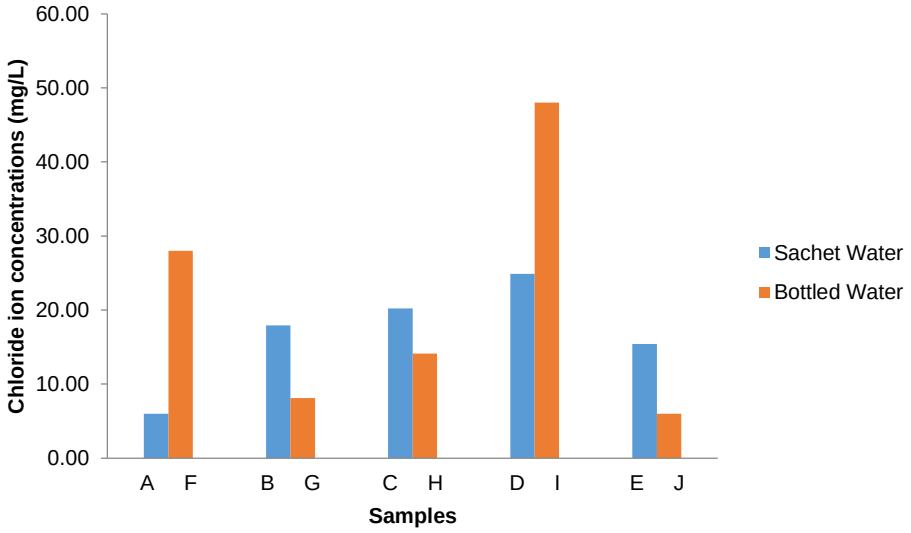


**Figure 2:** Chloride ion concentrations in the water samples

The range of nitrate ion levels in the water samples was 0.07 - 0.21mg/l for sachet water and 0.08 - 0.15mg/l for bottled water. At a df of 8 and a p-value of 0.893, there was no significant difference between the nitrate ion levels obtained for the sachet and bottled water samples. The results showed nitrate content to be relatively lower than the WHO and NSDWQ permissible limit of 50mg/l. Excessive amounts of nitrate ions can cause water quality problems, as well as contribute to the illness known as methemoglobinemia in infants (Zhang, 2007).

The concentration of nitrite ions in sachet water ranged from less than 0.001 to 0.08mg/l. The concentration is in compliance with the 3.0mg/l maximum standard (WHO, 2017). The bottled water samples had a nitrite concentration range of less than 0.001 to 0.02mg/l. There was no significant difference in the nitrite ion levels for sachet and bottled water.

The distribution pattern of heavy metals concentrations in the study as observed on Table 3 is: Fe > Zn > Mn > Cu > Pb> Ar for sachet water and Fe > Zn > Cu > Mn > Pb > Ar for bottled water respectively. Copper occur naturally in water in only minute quantity (few micrograms per litre) in drinking water (Saleh *et al.*, 2001). In all the water samples investigated, only three sample A (sachet water) with samples F and H (bottled water) contained this trace element at concentrations 0.05, 0.05 and 0.03mg/l respectively. Copper was not detected in 70% of the samples. They were all within the 2.0mg/l standard for drinking water (WHO, 2017). Higher level of copper is not desirable in drinking water as it could causes gastrointestinal disorder (SON, 2007).

Lead and Arsenic were not detected in all the samples. Iron as a trace element was not detected in about 40% of the water samples. Iron concentrations of 0.20 and 0.47mg/l were observed in sachet water samples A and E. In four brands of bottled water samples (G, H, I and J) iron levels ranged from 0.01 – 0.37mg/l. These observed values fall within the limit of 1.0mg/l stipulated by World Health Organization (WHO, 2017) for drinking water. However, the levels of iron in samples F and J were slightly above the guideline set by NSDWQ.

Manganese concentration of 0.03mg/l was detected in one sachet water sample, while concentrations of 0.10 and 0.08mg/l respectively were observed in two bottled water samples (H and I). These values are within the baseline values of 0.40 and 0.20mg/l respectively set by WHO and NSDWQ respectively. Large quantities of manganese have an effect on water taste and enhance the growth of bacteria. Large doses of manganese have also been reported to cause lethargy, irritability, headache, sleeplessness, and leg weakness, which might induce psychological symptoms like violent behavior, inexplicable laughter, impulsive acts and absent-mindedness (Saleh *et al.*, 2001).

Zinc was detected in all the water samples. Its concentration ranged from 0.09 – 0.14mg/l and 0.06 – 0.15mg/l for sachet and bottled water respectively as shown on Figure 3. At a df of 8 and a p-value of 0.916, there was no significant difference between the zinc concentration values obtained for the sachet and bottled water samples. The values obtained were within the permissible level of 5.0mg/l and 3.0mg/l recommended by WHO and NSDWQ respectively.

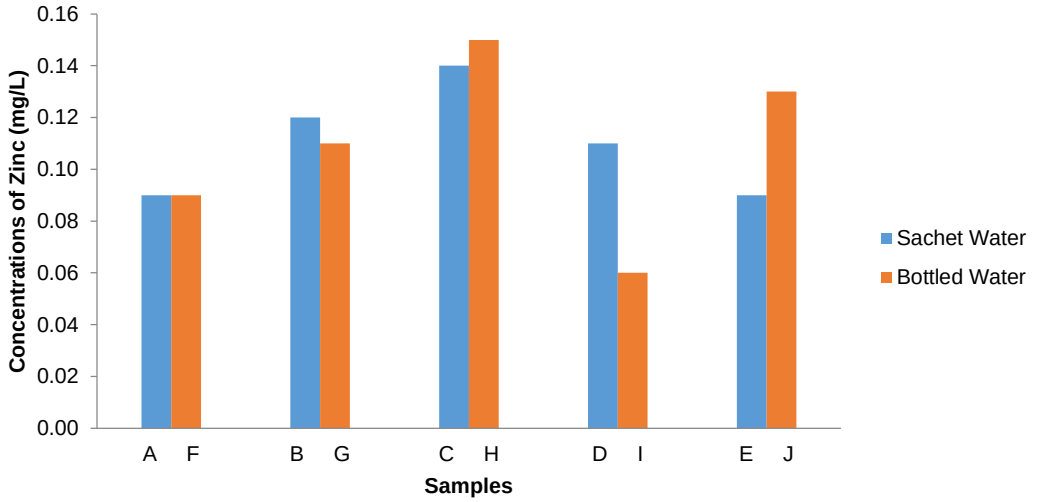


**Figure 3:** Zinc ion concentrations in the water samples

## 4.0. Conclusion

Sachet and bottled water play important roles in providing readily accessible water to the general populace; however, the quality of such water must be of paramount interest to all: producers, consumers and regulatory authorities alike. Samples of sachet and bottled water were collected from various retail outlets in Abraka and subjected to different analytical procedures to determine values of a range of physicochemical properties. The findings of this study revealed that the pH of 70% of the sachet and bottled water samples investigated was below permissible limits. The values of other parameters in the study such as: turbidity, colour, temperature, total dissolved solids, total hardness, electrical conductivity, chloride ion, nitrate ion, nitrite ion, and heavy metals such as copper, iron, zinc, and manganese were within the national and international guidelines. On the average, the sachet and bottled water samples were of good quality.

## References

Adamu, S. (2009). Tackling Water Shortage in Kaduna. *The Herald, Daily*, Jan. 2, 2009, P. 5.

Adekunle, L. V., Sridhar, M. K. C., Ajayi, A. A., Oluwade, P. A. and Olawuyi, J. F. (2004). An Assessment of The Health and Social Economic Implications of Sachet Water in Ibadan Nigeria: A Public Health Challenge. *African Journal of Biomedical Research* 7, pp. 5-8.

Aderibigbe, S. A., Awoyemi, A. O. and Osagbemi, G. K. (2008). Availability, Adequacy and Quality of Water Supply in Ilorin Metropolis, Nigeria. *European Journal of Scientific Research*, 23(4), pp. 528-536.

Akinde, S. B., Nwachukwu, M. I. and Ogamba, A. S. (2011). Storage effects on the quality of sachet water produced within Port Harcourt metropolis, Nigeria. *Journal of Biological Sciences* 4, pp. 157-164.

Akpoborie, I. A. and Ehwarimo, A. (2012). Quality of packaged drinking water produced in Warri Metropolis and potential implications for public health. *Journal of Environmental Chemistry and Ecotoxicology*, 4(11), pp.195-202.

Akunyili, D. N. (2003). The Role of Pure Water and Bottled Water Manufacturers in Nigeria. *Paper presented at the 29th Water, Engineering and Development Centre International Conference*, in Abuja, Nigeria.

APHA, (2017). American Public Health Association, American Water works Association, Water Environment Federation, Standard Methods for the Examination of Water and Wastewater" 23rd Edition., Washington, DC.

Aroh, K. N., Eze, E., Ukaji, D., Wachuku, C., Gobo, A. E., Abbe, S. D., *et al*. (2013). Health and environmental components of sachet water consumption and trade in Aba and Port Harcourt, Nigeria. *Journal of Chemical Engineering and Materials Science*, 4(2), pp. 13-22.

Dinrifo, R. R., Babatunde, S. O. E., Bankole, Y. O. and Demu, Q. A. (2010). Physico-Chemical Properties of Rain Water Collected from Some Industrial Areas of Lagos State Nigeria. *European Journal of Scientific Research*, 41(3), pp. 383-390.

Ezeugwunne, I. P., Agbakoba, N. R., Nnamah, N. K. and Anahalu, I. C. (2009). The prevalence of bacteria in packaged sachets water sold in Nnewi, South East, Nigeria. *World Journal of Dairy & Food Sciences*, 4(1), pp.19-21.

Gangil, R., Tripathi, R., Patyal, A. and Dutta, P. (2013) Bacteriological Evaluation of Packaged Bottled Water sold at Jaipur city and its Public Health Significance. Vet World 6(1), pp. 27-30. doi:10.5455/vetworld.2013.27-30.

Gbadegesin, N. and Olorunfemi, F. (2007). Assessment of Rural Water Supply Management in Selected Rural Areas of Oyo State. *ATPS Working Paper*, Series No. 49.

Guler, C. and Alpalsan, M. (2009). Mineral content of 70 bottled water brands sold on the Turkish market: Assessment of their compliance with current regulations, *Journal of Food Composition and Analysis*, 22, pp. 728–737

Isikwue, M. O. and Chikezie, A. (2014). Quality assessment of various sachet water brands marketed in Bauchi metropolis of Nigeria. *International Journal of Advances in Engineering and Technology*, 6, pp. 2489-2495.

Maconachie, R. (2008). Surface Water Quality and Periurban Food Production in Kano, Nigeria. *Urban Agriculture Magazine*, No. 20

Maduka, H. C. C., Chukwu, N. C., Ugwu, C. E., Dike, C. C., Okpogba, A. N., Ogueche, P. N., *et al*. (2014). Assessment of commercial bottled table and sachet water commonly consumed in Federal University of Technology, Owerri (FUTO), Imo State, Nigeria using Microbiological indices. *Journal of Dental and Medical Sciences*, 13, pp. 86-89.

Ndinwa, C. C. G., Chukumah, O. C., Edafe, E. A., Obarakpor, K. I., Morka, W. and Osubor-Ndinwa, P. N. (2012).Physiochemical and Bacteriological Characteristics of Bottled and Sachet Water in Warri and Abraka, Southern Nigeria. *Journal of Environmental Management and Safety*, 3(2), pp. 145–160.

Nwidu, L. L., Oveh, B., Okoriye, T. and Vaikosen, N. A. (2008). Assessment of the water quality and prevalence of water borne diseases in Amassoma, Niger Delta, Nigeria. *African Journal of Biotechnology*, 7(17), pp. 2993-2997.

Omalu, I. C. J., Eze, G. C., Olayemi, I. K., Gbesi, S., Adeniran, L. A., Ayanwale, A.V., Mohammed, A. Z. and Chukwuemeka, V. (2011). Contamination of sachet water in Nigeria: Assessment and health impact. *Online Journal of Health Allied Sciences*, 9(4), p15.

Onifade, A. K. and Ilori, R. M. (2008). Microbiological analysis of sachet water vended in Ondo State, Nigeria. *Environmental Research Journal*, 2(3), pp. 107-110.

Oyelude, E. O. and Ahenkorah, S. (2012). Quality of Sachet Water and Bottled Water in Bolgatanga Municipality of Ghana. *Research Journal of Applied Sciences, Engineering and Technology,* 4(9), pp. 1094-1098.

Saleh, M. A., Ewane, E., Jones, J. and Wilson, B. L. (2001). Chemical Evaluation of Commercial Bottled Drinking Water from Egypt. *Journal of Food Composition and Analysis,* 14(2), pp. 127-152.

Standards Organization of Nigeria SON (2007) Nigerian Standard for Drinking Water Quality. Abuja, Nigeria: *SON Publishing Company*, pp.15-33.

Thliza, L. A., Khan, A. U., Dangora, D. B. and Yahaya, A. (2015). Study of some bacterial load of some brands of sachet water sold in Ahmadu Bello University (Main Campus), Zaria, Nigeria. *International Journal Current Science,* 14, pp. 91–97.

Wetzel, R. G. (2001). Limnology; lake and River Ecosystem 3rd ed. Academic Press New York 1006 pp.

World Health Organisation WHO (2017), Guideline for Drinking Water Quality, 4th Edition. World Health Organisation, Geneva, Switzerland.

Zhang, J. (2007). Increasing Antarctic Sea Ice under Warming Atmospheric and Oceanic Conditions. *Journal of Climate*, 20, pp. 2515-2529.

**Cite this article as:**
Otobrise C., Azuh T. C., Mmakwe E. I., Ogbakpa E. and Tolorun C. O., 2021. Physicochemical Characteristics of Selected Sachet and Bottled Water in Abraka, Delta State. *Nigerian Journal of Environmental Sciences and Technology,* 5(1), pp. 47-56. https://doi.org/10.36263/nijest.2021.01.0248

Nigerian Journal of Environmental Sciences and Technology (NIJEST)

www.nijest.com

ISSN (Print): 2734-259X | ISSN (electronic): 2734-2603

Vol 5, No. 1 March 2021, pp 57 - 66

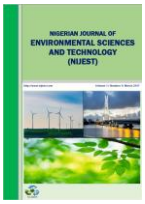

# Design Mix Formulation and Optimization of Metakaolin Based Alkali Activated Geopolymer Concrete with the Taguchi Method

Okovido J. O.[1] and Yahya I. A.[2]

[1]Department of Civil/Structural Engineering, Faculty of Engineering, University of Benin, Benin City, Nigeria

[2]Department of Civil Engineering, School of Engineering and Engineering Technology, Moddibo Adama University of Technology, Yola, Adamawa State, Nigeria

Corresponding Author: [2]ismakola2012@gmail.com

https://doi.org/10.36263/nijest.2021.01.0249

## ABSTRACT

*Concrete mix formulation is the science of deciding relative proportions of ingredients of concrete, to achieve desired properties in the most economical way. Formulation of concrete mix requires adequate knowledge of the properties of its constituents. Aluminosilicate materials have recently found applications in construction industry due to their unique and flexible properties. The metakaolin used for this study was the locally sourced kaolin calcined at $750^0C$. The alkali activating reagents include a fixed concentration of sodium silicate solution and sodium hydroxide solutions of three different concentrations. Strength development of metakaolin – based geopolymer concrete is quite different from that of ordinary Portland cement concrete due to differences in their constituents, hence, the need for special formulation, most especially when high strength is required. Taguchi method was adopted in this study to formulate mix proportion for high compressive strength of geopolymer concrete at ambient curing condition. Four parameters were selected that are more likely to influence the compressive strength of metakaolin – based geopolymer concrete, these include aggregate content, alkali – binder ratio, alkali reagent ratio and alkali reagent concentration. The effect of these parameters on the density, workability and compressive strength at 3, 7 and 28 days are determined. The result showed that an optimum mix obtained from a formulation formula ($2.75SiO_2$ * $Al_2O_3$ * $0.55Na_2O$ * $6.8H_2O$) produced a compressive strength of 62MPa at 28 days of open air curing. It was revealed that the molar concentration of the alkali reagent (sodium hydroxide) should be kept within 10M range for an open air curing, the alkali reagents to binder ratio should be kept at 0.7 or less with no addition of water to achieve reasonable workability. Also, it has been observed that the bulk density of metakaolin – based geopolymer concrete that yielded substantial strength fall within 2250kg/$m^3$ and 2350 kg/$m^3$.*

**Keywords:** Aluminosilicate Material, Geopolymer Concrete, Taguchi Method, Mix Formulation, Mix Optimization

## 1.0. Introduction

Concrete is a global construction material that has impacted the environment more than any other construction material, because it can be produced under a plethora of innovative technology, material and conditions. According to Ikponmwosa *et al.* (2014), the fact that concrete allows innovations and creativity in its production, either by altering its composition during mix designs, or by the addition of chemical admixtures or mineral additives etc., has led to the development of many types of concrete with different properties and for different applications. One of such type of concrete is metakaolin – based alkali – activated geopolymer concrete, a construction material that is yet to be developed in Nigeria despite the abundance deposit of kaolin in the country.

Geopolymers are solid materials that can be synthesised by the reaction of an aluminosilicate powder with an alkaline solution (Pouhet, 2016). Theoretically, any material containing aluminium and silicon can be a solid source of aluminosilicate for geopolymerization (Ahmed Al - Dujaili *et al.*, 2020). However, past studies have shown that the most often used materials are blast furnace slags, fly ash

and calcined clay. The most common clay is the kaolin which upon thermal activation within temperature range of 650°C to 800°C becomes metakaolin (Pera, 2001). Metakaolin – based geopolymer is said to be purer and can be readily characterised hence, they are referred to as model – system without the complexities associated with other aluminosilicate source such as fly ash (Shihab *et al.*, 2018).

The activating reagent is an aqueous form of alkaline compound. The common used compounds are hydroxides ($Na^+$ and $K^+$), silicates ($Na^+$ and $K^+$) and silica gel (Ahmed Al - Dujaili *et al.*, 2020). The silicate solution increases the $SiO_2$ content in the mix while the hydroxide solution increases the level of alkalinity of the mix. The origin of the element composing the geopolymer mixture is as shown in Figure 1. The reaction mechanism of geopolymer is a chemical process that involves the transformation of vitreous structures into a stable and compact composite. This chemical process only takes place in alkaline environment which help to dissolve the silica and alumina in the solid material.

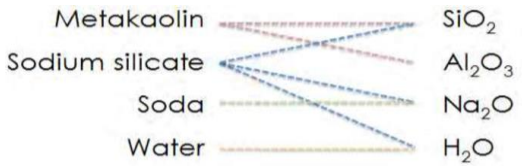


**Figure 1:** Origin of the element composing the geopolymer (Pouhet, 2016)

The properties of geopolymer depend on crystallographic and microstructural features of the alkali – activated product which are directly affected by the mix formulation of the individual element that composed the geopolymer. Mix formulation of metakaolin – based alkali – activated geopolymer concrete is predicated upon four compounds (i.e. $SiO_2$, $Al_2O_3$, $Na_2O$ and $H_2O$). The metakaolin powder provides silica and aluminium with a fixed $SiO_2/Al_2O_3$ ratio. The sodium silicate solution contributes silica, sodium and water in fixed proportions. The sodium hydroxide in different molar concentration allows for $Na_2O$ and $H_2O$ to vary in each mix formulation.

The composition ranges of alkaline/binder, $SiO_2/Al_2O_3$, $Na_2O/Al_2O_3$, $H_2O/Na_2O$ ratios of the component materials can be used to formulate the right mix for alkaline – activated products. These composition ranges are determined by such parameters as aggregate content, alkali reagent ratio, alkali/binder ratio and alkali concentration. However, the measure of successes or failures of every mix formulation can be based on the compressive strength properties of the geopolymer products (Hardjito *et al.*, 2004; Fernandez – Jimenez *et al.*, 2006; Shindunata *et al.*, 2006).

Studying the effects of these parameters on the strength properties of geopolymer concrete by the full factorial design tends to be too cumbersome to yield efficient results. To overcome this problem, suitable methods of design of experiment, such as Taguchi method was used to ascertain the effect of four parameters on the compressive strength property of metakaolin – based geopolymer concrete. Taguchi and Konishi (1987) developed Taguchi method as a statistical method for conducting minimal number of experiment with potential of giving full information of all factors that determine the performance properties of the product. Taguchi method is a design of experiment (DOE) approach which seek to develop products and processes that are robust to environmental factors and other sources of variation (Montgomery, 2013). Taguchi method helps reduce time and cost on testing all possible combinations by using one factor at a time to fulfil Full Factorial Experiment (FFE) (Olivia, 2011).

Taguchi optimization method has been used by researchers in different areas such as the optimization of blended cements (Wu and Naik, 2003), the optimization of mineral admixture and assessment of mix proportion for self – compacting concrete (Ozbay *et al.*, 2009), and recently for the optimization of the properties of metakaolin based geopolymer pastes (Ahmed Al - Dujaili *et al.*, 2020), and to determine the proportion of materials with optimal replacement of cement for optimum compressive strength properties of mortar (De Side *et al.*, 2020). However, at present there is no study in relation to the use of Taguchi method to establish a mix formulation for high strength metakaolin – based geopolymer concrete. This study therefore aims to determine the right mix formulation for metakaolin – based geopolymer concrete with high compressive strength as a prerequisite for further investigation into other important properties of geopolymer concrete.

## 2.0. Methodology

### *2.1. Metakaolin*

It was decided that the materials for this study must be locally sourced. Ten bags of powder kaolin were supplied by local supplier from Ikpeshi in Edo State. The raw kaolin was pinkish white in colour. The calcination process of the kaolin took place in the Structural laboratory at University of Benin, with a portable electric furnace presented in Figure 2. The calcination process involved filling of a metal container with kaolin and placed in the furnace where it is heated up to 750°C over a period of 4 hrs. Then the hot material is left in the oven to cool till the next day.

The raw kaolin has a dull pinkish colour and the metakaolin turned out to be smooth pinkish white colour after calcination. A sample of the metakaolin was taken for analysis of its oxide composition by x – ray fluorescence (XRF) analysis and the result is as presented in Table 1.

**Figure 2:** Calcination process of kaolin

**Table 1:** Chemical composition of metakaolin

| Comp. (%) | $SiO_2$ | $Al_2O_3$ | $Fe_2O_3$ | CaO | MgO | $Na_2O$ | $K_2O$ | $P_2O_5$ | $TiO_2$ | LOI |
|---|---|---|---|---|---|---|---|---|---|---|
| MK (%) | 49.10 | 37.93 | 0.38 | 0.34 | 0.11 | 0.28 | 1.32 | 0.12 | 1.14 | 1.03 |

### *2.2. Alkaline solution*

The alkaline activators are the sodium silicate solution and sodium hydroxide solution at specific molarity.

The NaOH flake of 99% purity grade was obtained from a local supplier at Onitsha market. Sodium hydroxide solutions were prepared in three molar concentrations (10M, 12M and 15M). For a typical 15M concentration, 600g of sodium hydroxide flakes was dissolved in 1 litre of distilled water to make a 15M solution. The preparation of sodium hydroxide solution took place 24hours before use, to ensure that the generated heat during preparation was completely dissipated.

The sodium silicate solution used has a modulus silicate (Ms) of 2.0 and was obtained from a local supplier with chemical characteristics as presented in Table 2.

**Table 2:** Chemical characteristics of sodium silicate

| Prop. | $SiO_2$ (%) | $Na_2O$ (%) | $SiO_2/Na_2O$ | $H_2O$ (%) | pH | Density ($g/cm^3$) |
|---|---|---|---|---|---|---|
| Value | 29.4 | 14.7 | 2.0 | 55.9 | 12.6 | 1.35 |

### *2.3. Aggregates*

Coarse aggregates for this study were crushed granite obtained from local supplier. The particle sizes that passed through 10mm sieve were used for this study. The fine aggregates used were the natural sand obtained from local supplier and the maximum nominal size of 1.18mm was used throughout the project. The aggregates were treated with little amount of water a day before mixing to ensure that they are dust – free and to achieve saturated surface dry condition.

### *2.4. Water*

Deionize/distilled water was used during the course of this study so as to ensure minimal chloride ions content so as to reduce chloride – induced corrosion. Water was used for preparation of sodium hydroxide solution, since the sodium silicate was obtained in liquid form. No addition of water in the mix for geopolymer concrete, except the water in the activating solutions, because of the open air curing method adopted in this study.

### *2.5. Mix formulation by Taguchi method*

The four parameters with direct effects on the compressive strength of geopolymer concrete are selected as presented in table 3. The aggregate content in percentage of the total mass of concrete is considered most critical factor (Factor A), the alkali activator – binder ratio (factor B), then sodium silicate – sodium hydroxide ratio (factor C) and finally sodium hydroxide molarity (factor D). Each of these factors is considered under three trial levels to ascertain their influence on the strength development of metakaolin – based geopolymer concrete.

**Table 3:** Parameters and level of trials

| Parameter | Factors/Levels | 1 | 2 | 3 |
|---|---|---|---|---|
| Aggregate Percent | A | 60 | 65 | 70 |
| A/B ratio | B | 0.70 | 0.75 | 0.80 |
| SS/SH ratio | C | 1.5 | 2.0 | 2.5 |
| SH Molarity | D | 10M | 12M | 15M |

The parameters were distributed using Taguchi's orthogonal array method for ($3^4$) mix trials to produce nine trial mixes as shown in Table 4. The orthogonal array distribution produced the mix proportion presented in Table 5.

**Table 4:** Taguchi's orthogonal arrays method of distribution of factors and levels

| Factor/Mix trial | T1 | T2 | T3 | T4 | T5 | T6 | T7 | T8 | T9 |
|---|---|---|---|---|---|---|---|---|---|
| A | 1 | 1 | 1 | 2 | 2 | 2 | 3 | 3 | 3 |
| B | 1 | 2 | 3 | 1 | 2 | 3 | 1 | 2 | 3 |
| C | 1 | 2 | 3 | 2 | 3 | 1 | 3 | 1 | 2 |
| D | 1 | 2 | 3 | 3 | 1 | 2 | 2 | 3 | 1 |

**Table 5:** Summary of mix formulation for metakaolin–based geopolymer concrete

| ($kg/m^3$) | T1 | T2 | T3 | T4 | T5 | T6 | T7 | T8 | T9 |
|---|---|---|---|---|---|---|---|---|---|
| MK750 | 565 | 549 | 533 | 494 | 480 | 467 | 424 | 411 | 400 |
| Fine Agg. | 720 | 720 | 720 | 780 | 780 | 780 | 840 | 840 | 840 |
| Coarse Agg. | 720 | 720 | 720 | 780 | 780 | 780 | 840 | 840 | 840 |
| SS sol. | 237 | 274 | 305 | 231 | 257 | 224 | 211 | 185 | 213 |
| SH Sol. | 158 | 137 | 122 | 115 | 103 | 149 | 85 | 124 | 107 |
| A/B | 0.70 | 0.75 | 0.80 | 0.70 | 0.75 | 0.80 | 0.70 | 0.75 | 0.80 |
| SH Mol. | 10M | 12M | 15M | 15M | 10M | 12M | 12M | 15M | 10M |
| SS/SH | 1.5 | 2.0 | 2.5 | 2.0 | 2.5 | 1.5 | 2.5 | 1.5 | 2.0 |
| Agg. (%) | 60 | 60 | 60 | 65 | 65 | 65 | 70 | 70 | 70 |
| MK (%) | 23.5 | 23 | 22 | 21 | 20 | 19.5 | 18 | 13 | 13 |
| Alk. (%) | 16.5 | 17 | 18 | 14 | 15 | 15.5 | 12 | 13 | 13 |
| $SiO_2/Na_2O$ | 5.00 | 4.74 | 4.42 | 4.98 | 5.18 | 4.24 | 5.21 | 4.42 | 4.76 |
| $SiO_2/Al_2O_3$ | 2.75 | 2.86 | 2.95 | 2.81 | 2.90 | 2.83 | 2.85 | 2.79 | 2.90 |
| $Na_2O/Al_2O_3$ | 0.55 | 0.60 | 0.67 | 0.57 | 0.56 | 0.67 | 0.55 | 0.63 | 0.61 |
| $H_2O/Na_2O$ | 12.30 | 11.54 | 10.81 | 11.20 | 12.42 | 11.37 | 11.66 | 10.97 | 12.40 |

### *2.6. Concrete casting and curing*

The metakaolin – based geopolymer concrete specimens were prepared by mixing a measured dry aggregate with a measured metakaolin powder before the addition of alkaline solutions, which are separately prepared. The combined materials were thoroughly mixed until homogenous mixture was obtained. The fresh mixture was placed in slump cone for workability determination according to EN206 – 1. Low slump class S2 was observed in the concrete having 70% by mass of aggregate, despite the increase in alkaline/binder ratio from 0.7 to 0.8. Moderate slump class S3 was observed in the concrete having 65% by mass of aggregates. The 60% by mass of aggregates, showed a collapsed slump class S4 – S5.

After the slump determination, the fresh concrete was re - mixed and placed in 100 x 100 x 100 mould and compacted on vibratory table. The moulds were initially coated with releasing agent to prevent sticking to the mould. The specimens in the mould were covered with thick polythene sheet for the next 24 hours before they were demoulded and kept in open air for continuous curing until test days.

### *2.7. Control specimen preparation*

The use of Portland cement concrete in this study was to serve as control specimen for the purpose of comparative analysis. Its mix design did not serve as a control mix for metakaolin – based geopolymer concrete because their mix procedure differs. OPC concrete mix design was done for three different aggregates content in comparison with geopolymer concrete of the same aggregate content. Table 6 shows the summary of mix proportioning for OPC concrete for three aggregate contents, which are represented as control trial (CT01, CT02 and CT03). The OPC concrete specimens were prepared following the same procedure as geopolymer with the use of water instead as the main activating agent and as curing medium after demoulding.

**Table 6:** Mix proportioning for Portland cement concrete

| Mix No | Concrete Mix (kg/m$^3$) | | | | | | |
|---|---|---|---|---|---|---|---|
| | Cement | F.A | C.A | Add. $H_2O$ | Agg. (%) | w/c ratio | Slump (mm) |
| CT01 | 662 | 720 | 720 | 298 | 60 | 0.45 | 75 |
| CT02 | 579 | 780 | 780 | 261 | 65 | 0.45 | 60 |
| CT03 | 497 | 840 | 840 | 223 | 70 | 0.45 | 50 |

## 3.0. Results and Discussion

### *3.1. XRF analysis of metakaolin sample*

The result of the plot of the x–ray fluorescence analysis of the metakaolin for this study is as presented in Figure 3. It is clearly seen that the major oxide constituent of the metakaolin are the silicon oxide and aluminium oxide both of which constitute 87% of the total chemical oxide of the sample. In view of the large percentage of $SiO_2$ and $Al_2O_3$ in the metakaolin, most of the characteristics of the metakaolin as binder in geopolymer concrete are traceable to the interaction between these two major chemical oxides, and in essence they both determine the possible mix formulation for desired strength properties of metakaolin – based geopolymer concrete.

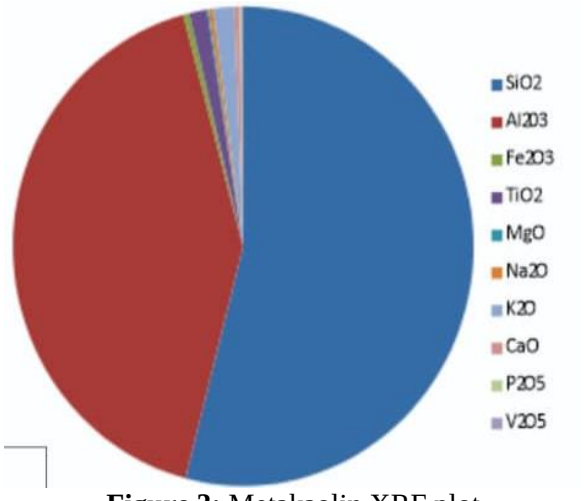


**Figure 3:** Metakaolin XRF plot

### *3.2. Bulk density and workability of geopolymer concrete*

The workability of the geopolymer concrete as measured by slump value and the density of hardened concrete at three different test days are as presented in Table 7. It could be observed that the bulk density is influenced by the aggregate content in the geopolymer mix. The mix with 70% aggregate content has the highest range of bulk density, while there is insignificant difference in the mix with 65% and 60% aggregate content. This could be due to adequate amount of activated metakaolin in the mix for aggregate content of 65% and 60%. The slump value obtained in this study can only be attributable to the alkali content since there is no additional water except the amount in the alkali

solution. The slump value indicates the impact of the sodium silicate/sodium hydroxide ratio as the mix with the highest amount of sodium hydroxide of lowest concentration produced the highest slump value, and also exhibited the same property as the self – compacting concrete. This could be due to low viscosity of sodium hydroxide solution as compared with sodium silicate solution.

**Table 7:** Bulk density and slump value for metakaolin–based geopolymer concrete

| Mix | T1 | T2 | T3 | T4 | T5 | T6 | T7 | T8 | T9 |
|---|---|---|---|---|---|---|---|---|---|
| 3 day density ($kg/m^3$) | 2335 | 2400 | 2390 | 2250 | 2280 | 2300 | 2450 | 2465 | 2400 |
| 7 day density ($kg/m^3$) | 2330 | 2350 | 2350 | 2250 | 2270 | 2285 | 2450 | 2430 | 2390 |
| 28 day density ($kg/m^3$) | 2300 | 2395 | 2330 | 2200 | 2265 | 2285 | 2435 | 2470 | 2420 |
| Slump (mm) | 205 | 195 | 190 | 155 | 150 | 135 | 75 | 75 | 60 |

*3.3. Compressive strength of geopolymer concrete*

Compressive strength was used in the evaluation of mixes using the Taguchi method. As shown in Table 8, the compressive strength results of metakaolin – based geopolymer concrete was obtained as the average of three samples for each test. It was observed that the strength varies significantly between 1 and 7 days, due to rapid geopolymerization process, and there was insignificant change in strength between the 7 and 28 days of open air curing. The highest strength was recorded for trial mix T1 at 28 days with 62MPa. The mix T1 contained the lowest $SiO_2/Al_2O_3$ ratio and the highest metakaolin content in comparison with other mixes, hence the mix was favored by the low SS/SH ratio and SH molarity to keep the additional $SiO_2$ from sodium silicate in check. In order to achieve the mix formulation for optimum strength it is required to control the $SiO_2/Al_2O_3$ ratio using the activating solution, since the $SiO_2/Al_2O_3$ of the metakaolin is already fixed. Also, it can be observed that mixes with 10M concentration of sodium hydroxide performed better in comparison with higher molarity. It can then be argued that the metakaolin used for this study requires low molar concentration of sodium hydroxide for activation, and this may be traced to its high $Al_2O_3$ content.

**Table 8:** Compressive strength of geopolymer and Portland cement concrete

| Comp. Str. (MPa) | T1 | T2 | T3 | T4 | T5 | T6 | T7 | T8 | T9 |
|---|---|---|---|---|---|---|---|---|---|
| 3 day | 48 | 21 | 29 | 35 | 33 | 36 | 38 | 33 | 29 |
| 7 day | 60 | 30 | 40 | 39 | 36 | 40 | 39 | 34 | 30 |
| 28 day | 62 | 31 | 42 | 41 | 40 | 40 | 39 | 34 | 30 |

The mechanical strength of geopolymer concrete is completely governed by the binding strength of alkali – activated metakaolin in the mix. The essence of seeking optimum mix proportioning is to ensure right amount of metakaolin for a given amount of aggregate and the sufficient amount of alkali – activator required for complete activation of the metakaolin for efficient binding property. In hundred percent metakaolin – based alkali – activated concrete, there is no strength to be gained where metakaolin serves as the mineral filler, due to insufficient amount of activator or as a result of excessive amount of metakaolin in the mix. The mix formulation equation 1 produced the maximum strength value and it is typical of metakaolin – based geopolymer concrete for ambient curing condition. The amount of water (both in the activating reagent and added water) required for desired workability may be varied depending on the type of curing and the nature of exposure condition.

$$2.75SiO_2 * Al_2O_3 * 0.55Na_2O * 6.8H_2O \quad (1)$$

From the mix design, the only water content in the mix is that with which the alkaline reagents were prepared, hence, with correct molarity of sodium hydroxide and adequate concentration of sodium silicate, no extra water is required to achieve significant strength of metakaolin – based geopolymer concrete. Excess amount of water in the mix, beyond the need of the alkaline activators would only fill and displace the void meant for activated paste for optimum binding effect on the aggregate, leading to weak concrete product.

The compressive strength results for OPC concrete are as presented in Table 9 for 7, 14 and 28 days of water curing.

**Table 9:** Compressive strength of Portland cement concrete

| Mix No | Compressive Strength (MPa) | | |
|---|---|---|---|
| | 7 day | 14 day | 28 day |
| CT01 | 38 | 45 | 49 |
| CT02 | 37 | 44 | 47 |
| CT03 | 32 | 38 | 42 |

3.3.1. Compressive strength analysis by Taguchi method

In Taguchi method, Signal/Noise ratio analysis are carried out in order to study the response of experiment that combine repetitions and the effect of trial levels in one data point. Using the Signal/Noise ratio analysis in this study, a response index was established in the experiment. The average contribution of each level of a factor to the final strength was calculated by adding the strength of mixtures corresponding to each level and dividing the sum by the number of repetition for the level and the results are as shown in table 10 – 12. The plots of compressive strength response index against the selected factors for the mix formulation are presented in Figure 4 – 6.

Table 10 shows the results of Taguchi analysis for the 3 – day compressive strength of metakaolin – based geopolymer concrete. The ranking of the result indicates that the most influential factors on the compressive strength is the alkali/binder (A/B) ratio. It shows that the selected factors keep their order of importance from A/B ratio to SH molarity with the exception of aggregate content which indicate the least effect. Figure 4 shows the plot of the major effect for the compressive strength during 3 – day of geopolymer concrete. The plot shows that the larger the signal – to – noise the better for each of the compressive strength results. It also indicates that factor B, C and D tend to pick up positive momentum at level three while factor A shows a downturn which could be interpreted as a negative effect on the compressive strength development of geopolymer concrete.

Table 11 shows the results of 7-day compressive strength analyzed by Taguchi method for geopolymer concrete and the corresponding plot of the major effects is as presented in Figure 5. It can be seen that the alkali/binder (A/B) ratio has the major effect while the least impact on the 7 – day compressive strength of geopolymer concrete was recorded for molarity of sodium hydroxide as initially proposed. This indicates that the activated metakaolin is still binding on the aggregates in the mix as the concrete ages. The plot in Figure 5 shows clearly that the negative impact associated with increasing aggregate content persist at 7-day maturity of geopolymer concrete.

Table 12 presents the results for 28–day compressive strength as analyzed by Taguchi method. It could be seen that the same pattern of strength development as 7–day compression strength is maintained at 28 days. It shows that the alkali/binder (A/B) ratio remained the most affecting factor in the compressive strength of geopolymer concrete at 28 days. The corresponding plot of the major effects of the selected factors is presented in Figure 6. It could be seen from Figure 6 that the downward trend associated with increasing aggregate content in the mix persist at 28–day. The highest A/B ratio (0.8) yielded lowest 28–day strength, despite the fact that it gave highest 7 - day strength. This may be due to excess of alkali in the concrete matrix after active geopolymerization period, which cause weakness in the interface of aggregates. In general, it can be seen that the middle level for each of the selected factors except the aggregate content has the lowest impact on compressive strength as the geopolymer concrete ages.

**Table 10:** Response value for 3–day compressive strength of geopolymer concrete

| Level/Factors | A | B | C | D |
|---|---|---|---|---|
| 1 | 32.7 | 40.3 | 39.0 | 36.7 |
| 2 | 34.7 | 29.0 | 28.3 | 31.7 |
| 3 | 33.3 | 31.3 | 33.3 | 32.3 |
| S. Deviation | 0.84 | 4.88 | 4.37 | 2.20 |
| Rank | 4 | 1 | 2 | 3 |

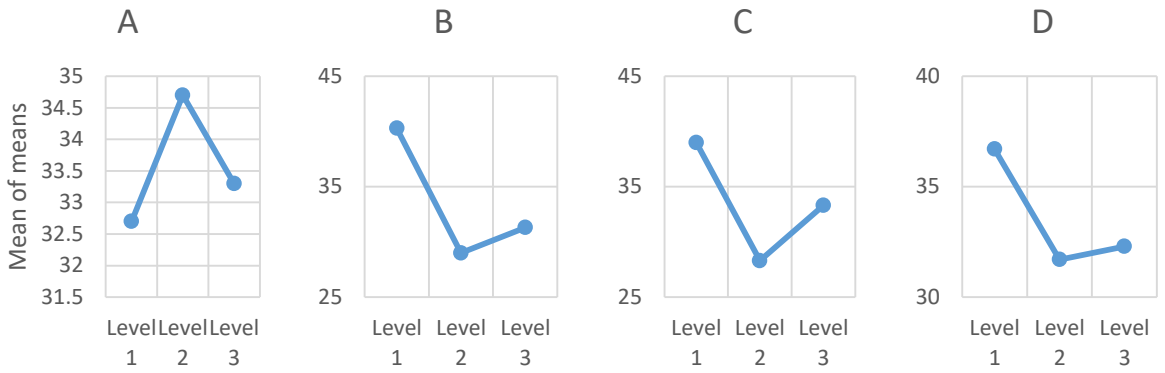


**Figure 4:** Major effect for the 3 – day compressive strength of geopolymer concrete

**Table 11:** Response value by Taguchi method for 7 – day compressive strength

| Level/Factors | A | B | C | D |
|---|---|---|---|---|
| 1 | 43.3 | 46.0 | 44.7 | 42.0 |
| 2 | 38.3 | 33.3 | 33.0 | 36.3 |
| 3 | 34.3 | 36.7 | 38.3 | 37.7 |
| S. Deviation | 3.68 | 5.37 | 4.78 | 2.43 |
| Rank | 3 | 1 | 2 | 4 |

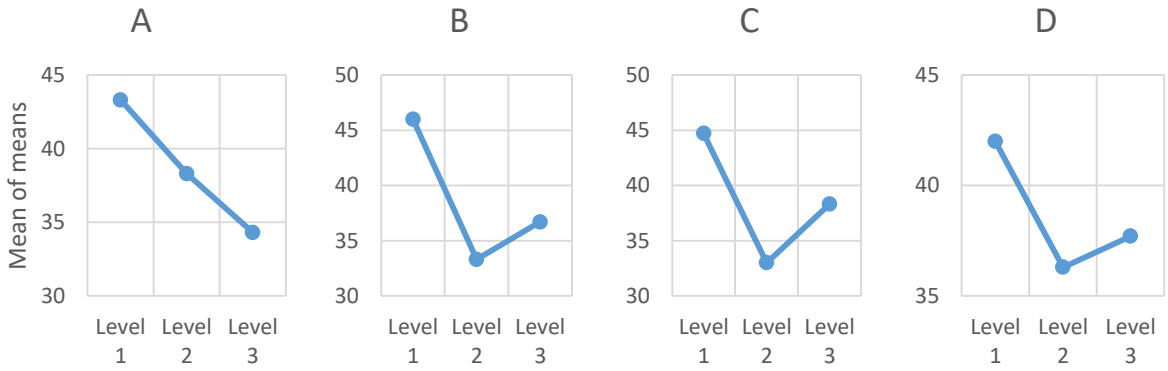


**Figure 5:** Major effect for the 7 – day compressive strength of geopolymer concrete

**Table 12:** Response value by Taguchi method for 28 – day compressive strength

| Level/Factors | A | B | C | D |
|---|---|---|---|---|
| 1 | 45.0 | 47.3 | 45.3 | 44.0 |
| 2 | 40.3 | 35.0 | 34.0 | 36.7 |
| 3 | 34.3 | 37.3 | 40.3 | 39.0 |
| S. Deviation | 4.38 | 5.34 | 4.62 | 3.05 |
| Rank | 3 | 1 | 2 | 4 |

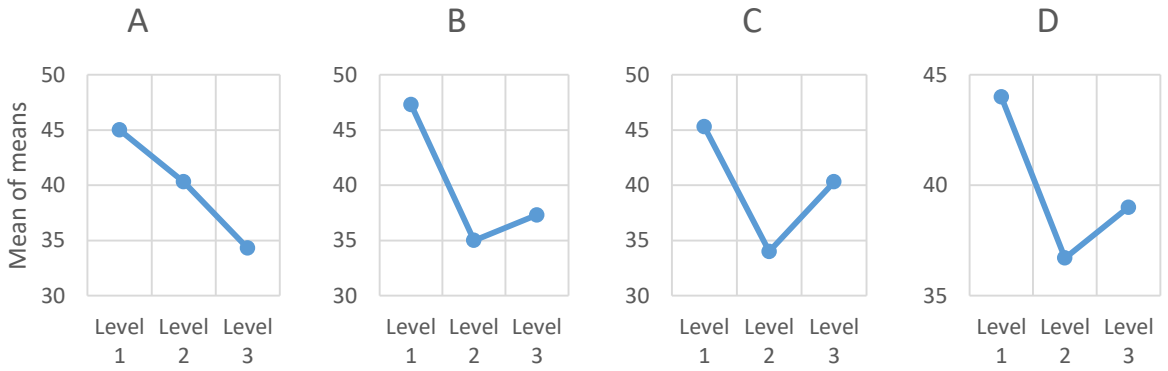


**Figure 6:** Major effect for the 28 – day compressive strength of geopolymer concrete

*3.4. Comparative analysis of geopolymer concrete and Portland cement concrete*

The comparative analysis of the 7 and 28 - day's compressive strength pattern of geopolymer and Portland cement concrete is as presented in Figure 7.

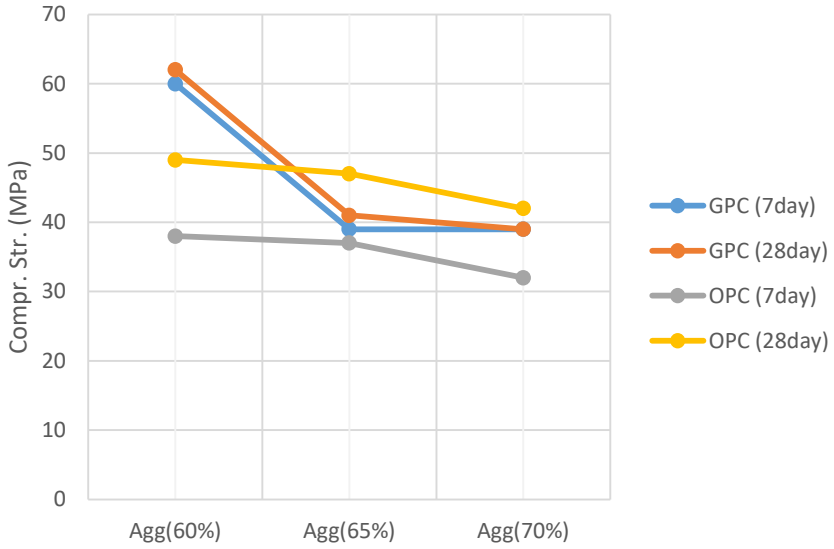


**Figure 7:** Compressive strength comparison between metakaolin – based geopolymer concrete and Portland cement concrete

From Figure 7 it is clear that the aggregate content in concrete has significant effects on strength development of both concretes however, these effects are quite different in terms of strength development for both type of concrete. While the 7 – day and 28 – day strength of geopolymer concrete are very close and concave in shape as a result of connecting the three aggregate contents, that of Portland cement concrete is wider and convex in shape. This is a pointer to the fact that these two concrete cannot be treated the same and the difference cannot be traced to difference in aggregate content but rather to other factors like the chemistry and difference in chemical composition between the two materials.

## 4.0. Conclusion

In this study, nine mixes based on Taguchi Orthogonal array was used to reduce the number of trial mixes required to achieve a high strength geopolymer concrete under open air curing condition, considering various mix parameters ranging from aggregate content, alkali – binder ratio, sodium silicate – sodium hydroxide ratio and sodium hydroxide molarity. An optimum mix with formulation formula of $2.75SiO_2$ * $Al_2O_3$ * $0.55Na_2O$ * $6.8H_2O$ was obtained for metakaolin – based geopolymer concrete mix for open air curing. With the compressive strength results obtained and the insights into the effects of the selected mix parameters on the compressive strength of geopolymer concrete as a result of the analysis by Taguchi method, this method was found suitable for optimization of metakaolin – based geopolymer concrete mixtures.

## References

Ahmed Al – dujaili, M. A., Disher Al – hydary, I. A. and Zayer Hassan, Z. (2020). Optimizing the properties of metakaolin – based (Na, K) – geopolymer using Taguchi design method. *International Journal of Engineering*, 33(4), pp. 631 – 638.

De Side, G. N., Kencanawati, N. N. and Hariyadi (2020). An application of Taguchi experiment design methods on optimization of mortar mixture composition with silica fume as a partial substitution for cement. *IOP Conference Series: Earth and Environmental Science*, 413(1), pp. 012012.

Fernandez-Jimenez, A., Palomo, A. and Lopez-Hombrados, C. (2006) Engineering properties of alkali-activated fly ash concrete. *ACI Materials Journal*, 103(2), pp. 106-112.

Hardjito, D., Wallah, S. E., Sumajouw, D. M. J. and Rangan, B. V. (2004). On the development of fly ash based geopolymer concrete. *ACI Materials Journal*, 101(6), pp. 467-472.

Ikponmwosa, E., Falade F. and Fapohunda C. (2014). A review and investigation of some properties of foamed aerated concrete. *Nigeria Journal of Technology (NIJOTECH)*, 33(1), pp. 1 – 9.

Montgomery, D. C. (2013). Design and analysis of experiments, John Wiley & Sons, Inc.

Olivia, M. (2011). Durability related properties of low calcium fly ash based geopolymer concrete. *Department of Civil Engineering, Curtin University of Technology*. PhD Thesis

Ozbay, E., Oztas, A., Baykasoglu, A. and Ozbebek, H. (2009) Investigating mix proportions of high strength self - compacting concrete by using Taguchi method. *Construction and Building Materials*, 23(2), pp. 694-702.

Pera, J. (2001). Metakaolin and calcined clays, *Cement Concrete Composition*, 23

Pouhet, R. (2016). Formulation and durability of metakaolin – based geopolymers. *Civil Engineering Universite paul Sabastier* – Toulouse III, NNT:2015TOU30085

Shihab, A. M., Abbas, J. M. and Ibrahim, A. M. (2018). Effects of temperature in different initial duration time for soft clay stabilized by fly ash based geopolymer. *Civil Engineering Journal*, 4(9), pp. 2082 – 2096.

Shindunata, van Deventer J. S. J., Lukey, G. C. and Xu, H. (2006) Effect of curing temperature and silicate concentration on fly ash based geopolymerization. *Industrial & Engineering Chemistry Research*, 45(10), pp. 3559-3568.

Taguchi, G. and Konishi, S. (1987). Taguchi methods, orthogonal arrays and linear graphs, tools for quality American Supplier Institute. *American Supplier Institute*, pp. 8-35.

Wu, Z. and Naik, T. R. (2003). Chemically activated blended cements. *ACI Materials Journal*, 100(5), pp. 434-440.

**Cite this article as:**
Okovido J. O. and Yahya I. A. 2021. Design Mix Formulation and Optimization of Metakaolin Based Alkali Activated Geopolymer Concrete with the Taguchi Method. *Nigerian Journal of Environmental Sciences and Technology*, 5(1), pp. 57-66. https://doi.org/10.36263/nijest.2021.01.0249

Nigerian Journal of Environmental Sciences and Technology (NIJEST)

www.nijest.com

ISSN (Print): 2734-259X | ISSN (electronic): 2734-2603

Vol 5, No. 1 March 2021, pp 67 - 75

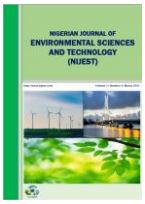

# Protection of Ecosystem and Preservation of Biodiversity: The Geospatial Technology Approach

Ogunlade S. O.

Department of Surveying and Geoinformatics, Federal University of Technology, Akure, Nigeria

Corresponding Author: soogunlade@futa.edu.ng

https://doi.org/10.36263/nijest.2021.01.0253

## ABSTRACT

*The protection of ecosystem and preservation of biodiversity through the approach of geospatial technology was the aim of this research. The channel was monitoring the spatial transformation of the Federal University of Technology, Akure, Nigeria between year 2002 and year 2018 using Satellite Remote Sensing and Geographical Information System techniques. Landsat 7 Enhanced Thematic Mapper (ETM) plus of year 2002, Landsat 8 Operational Land Imager (OLI) and Thermal Infrared Sensor (TIRS) of year 2014 and year 2018 all of 32m resolution were the satellite images obtained for the study. These images were processed with supervised maximum likelihood classification algorithm using ArcGIS 10.3 software. To validate the classification and ensure high accuracy, an accuracy assessment was performed using training samples from 60 points on each of the satellite imagery on a reference image from google earth combined with ground data collected on actual visitation to the study area to verify the true land-cover type existing on the site. The resultant images deemed fit for analyses were classified into built-up, thick vegetation, light vegetation and bare land, land cover classes. Microsoft Excel spreadsheet was used to perform land cover area calculations through which the land cover dynamics and the spatial expansion were identified. The result showed built-up (13.58%, 14.59%, 20.75%); thick vegetation (33.78%, 26.26%, 12.18%); Light vegetation (24.57%, 32.29%, 30.51%); Bare land (28.08%, 26.26%, 36.56%) for the three years respectively. A special focus was put on the general depletion of the (thick and light) vegetation of which trees are a major actor. This depletion was adduced to the positive transformation of other land cover classes through the underlining landuse. The study concluded that alteration, depletion and consequent disappearance of trees in the green ecosystem is a threat to environment's sustainability and the protection of ecosystem and preservation of biodiversity. The study recommended the research as a tool to controlling the removal of trees and thick forest, growing more trees and plants among other factors to protect ecosystem and preserve biodiversity.*

**Keywords:** Ecosystem, Geospatial Technology, Land cover, Land use, Satellite Images

## 1.0. Introduction

Jamie (2019), United Nations (2020) Szaro *et al*. (1998) affirmed the protection of the ecosystem and preservation of biodiversity as inevitable in the sustainability of the ever dynamic environment, and as an all-important concern of the global sustainable development agenda, thus requiring the attention of the research world. The duos are two inseparable twin-concern of the United Nation (UN) in the quest to transform the world by the year 2030 and beyond. According to Caballero (2016), the global Sustainable Development Goals (SDGs) or "2030 Agenda" (2015-2030) is a clarion call to all developing and developed countries to partner globally to achieve sustainable developments by the year 2030. The quest began as millennium development goals (MDGs) in 2000 and supposed to attain full achievement by 2015 (United Nations, 2015) but got further extended as sustainable development goals (SDGs) to year 2030 (Caballero, 2016). In the environmental management part of these global goals; sustainable landscape development constitutes an important transition pathway to the SDGs (United Nations, 2017). Embedded in the sustainable landscape development are the inevitable protection of the ecosystem and the preservation of biodiversity (United Nations, 2020). Ogunlade (2018b; 2020a) attested that in the transition to and actualization of sustainable development goals the

geospatial environment remains a major player. The environment is ever dynamic and the monitoring of the dynamics remains a crucial pathway in the transition (Ogunlade, 2018a). Spatial dynamics according to Ogunlade (2019), Igbokwe *et al.* (2016) is an important factor in the sustainability of of the environment. The indicator of the dynamics of the environment is the land use land cover change (Lackey, 1998). Hence, through the measurement of the LULC transformation, spatial expansion are monitored thus the ecosystem and biodiversity are well managed. In the ecosystem, there is a communal systemic interaction between living organisms (plants and animals) and their environment non-living components. The interactions are mainly on the terrestrial or aquatic platforms. The terrestrial interaction can be in the form of green (forest, grassland), tundra, and desert ecosystems; while the aquatic platform is either in form of fresh water or marine ecosystems. Management of the ecosystem is a salient in getting the best of the natural resources. Ecosystem resilience and sustainability, and its constant evaluation are inevitable in its protection and in the preservation of biodiversity (Meffe *et al.*, 2013; Szaro *et al.*, 1998; United Nations, 2020). The role and supremacy of geospatial technology in measuring and monitoring the earth surface have become so germane in the modern days primarily due to advent of computers, advancement in technology through availability of sophisticated digital instrument and highly researched and innovated methodologies (Ogunlade, 2020b). In-depth multifaceted discovery, large volume of data acquisition and management, speedy multipurpose transformation of data, diversified high level applications are some of the benefits of the involvement of geospatial technology in the management of the environment and the ecosystem (Oyinloye *et al.*, 2018). Integration of Satellite Remote Sensing and GIS techniques has excelled in the recent times above conventional techniques for speed, coverage and unlimited reach Ogunlade (2018a, 2018b). Thus, this research premised on the rich profitability of geospatial technology to monitor and evaluate the protection of the green ecosystem and preservation of biodiversity from the view point of land use land cover dynamics of the study area.

## 2.0. Methodology

Satellite images of Ondo state (Landsat ETM+ 2002, Landsat OLI/TIRS 2014, and Landsat OLI/TIRS 2018) downloaded from U.S. Geological Survey.; the boundary map of the study area from Surveying Department Federal University of Technology Akure Nigeria; and coordinates of ground control points through dual frequency Global Navigation Satellite System (GNSS) survey from the study area, were the materials obtained for the research. The satellite imageries were all subjected to algorithms of geometric and radiometric correction in ArcGIS 10.3 software environment. The boundary map of the study area was in AUTOCAD format (.dwg file) and was converted to shape-file (.shp) in the ArcGIS 10.3 environment and used to clip out the study area from the satellite imagery. To enhance visualization of features in the imagery, creation of false colour composite images was performed using ArcGIS 10.3 (Figure 1) by the combination of Near Infrared (NIR), Red (R) and Green (G) bands of each imagery (Table 1).

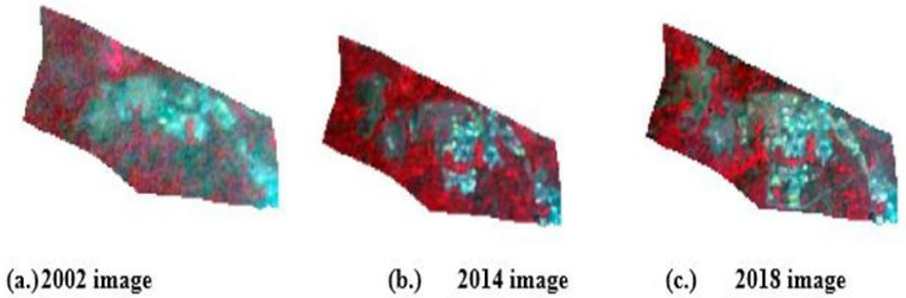


**Figure 1:** False colour composite for each year of study

**Table 1:** Landsat band combinations.

| Image | 2002 (Landsat 7 ETM+) | 2014 Landsat 8 (OLI/TIRS) | 2018 Landsat 8 (OLI/TIRS) |
|---|---|---|---|
| Spectral Band Combination | 4,3,2 | 5,4,3 | 5,4,3 |
| Spectral Band Names | NIR, Red, Green | NIR, Red, Green | NIR, Red, Green |

To further enhance visualization of features in the composite images, ESRI pan-sharpening method in ArcGIS 10.3 was performed on the composite images by fusing the higher-resolution panchromatic 8$^{th}$ band of each Landsat image with the low spatial resolution composite image.

The image classification was performed using supervised classification with maximum likelihood. The images were classified under the following four classes in Table 2.

**Table 2:** Showing the LULC classes and description

| LULC classes | Description |
|---|---|
| Built up Areas | Residential (staff quarters and student hostels), academic and administrative buildings, commercial centres, all other levels of housing |
| Thick vegetation | Heavy green areas, thick forest and trees. |
| Light vegetation | Grassland, horticultural gardens, farmlands, vegetated open spaces |
| Bare land | Sand plains, non-vegetated areas (pavements, rocks, roads, open spaces) |

To validate the classification and ensure high accuracy, an accuracy assessment was performed to compare the classified image to what actually obtained on the ground. Training samples from 60 points on the each of the satellite imagery were used on a reference image from Google earth combined with ground troth data collected on actual visitation to the study area to verify the true land-cover type existing on the site. The ground troth data was compared with the classified image and it was discovered to have relatively matched with what was obtainable on the image. The high number of training samples was chosen due to the fact that the areal extent being studied is small, hence the need for more training sample to ensure a high accuracy of classification. The size of the study area helped in actual visitation for on-the-site verification.

*2.1. Land cover/use Area Calculation*

After image classification, the area covered by each LULC class was calculated with Microsoft Excel spreadsheet using the formula:

$$A = \frac{C_t . C_s^2}{10000} \quad (1)$$

where:

$A$ Areal extent of each LULC class in Hectares

$C_t$ COUNT, the number of pixels in a LULC class. The COUNT value for each class was obtained from the attribute table of the classified map.

$C_S$ Cell size of the classified image for each year, which was 15m by 15m.

## 3.0. Results and Discussion

Four land cover classes were generated from the supervised image classification performed (Table 2). The areal extent for each land cover class in each year was calculated using Microsoft Excel spreadsheet and tabulated (Table 3). The corresponding landuse/landcover (LULC) maps were generated for the year 2002 (Figure 3), 2014 (Figure 4) and 2018 (Figure 5). The transformation that occurred within the LULC classes in the epochs of study was calculated (Table 4).

**Table 3:** Areal extent of LULC classes

| Year | 2002 | | 2014 | | 2018 | |
|---|---|---|---|---|---|---|
| LULC Type | Areal extent | | | | | |
| | (Ha) | (%) | (Ha) | (%) | (Ha) | (%) |
| Built Up | 78.48 | 13.58 | 84.33 | 14.59 | 119.90 | 20.75 |
| Bare Land | 162.25 | 28.08 | 151.76 | 26.26 | 211.25 | 36.56 |
| Thick Veg. | 195.19 | 33.78 | 155.21 | 26.86 | 70.40 | 12.18 |
| Light Veg | 141.98 | 24.57 | 186.59 | 32.29 | 170.33 | 30.51 |
| Total | 577.89 | 100.00 | 577.89 | 100 | 577.89 | 100 |

**Table 4:** LULC Transformations in two epochs

| Year | 2002 | | 2014 | | 2018 |
|---|---|---|---|---|---|
| LULC Type | Areal Extent | | | | |
| | (%) | Δ% | (%) | Δ% | (%) |
| Built Up | 13.58 | 1.01 | 14.59 | 6.16 | 20.75 |
| Bare Land | 28.08 | -1.82 | 26.26 | 10.3 | 36.56 |
| Thick Veg. | 33.78 | -6.92 | 26.86 | -14.68 | 12.18 |
| Light Veg | 24.57 | 7.72 | 32.29 | -1.78 | 30.51 |

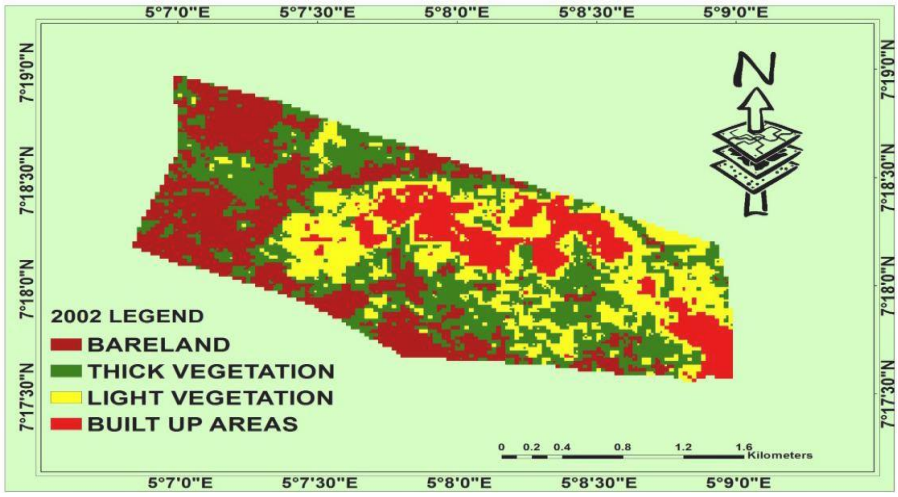


**Figure 3:** Land use/Land cover map of FUTA in 2002

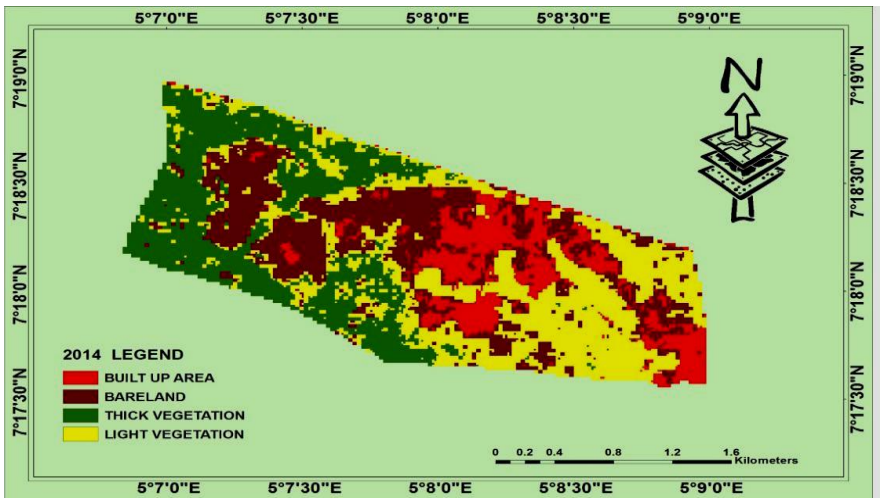


**Figure 4:** Land use/Land cover map of FUTA in 2014

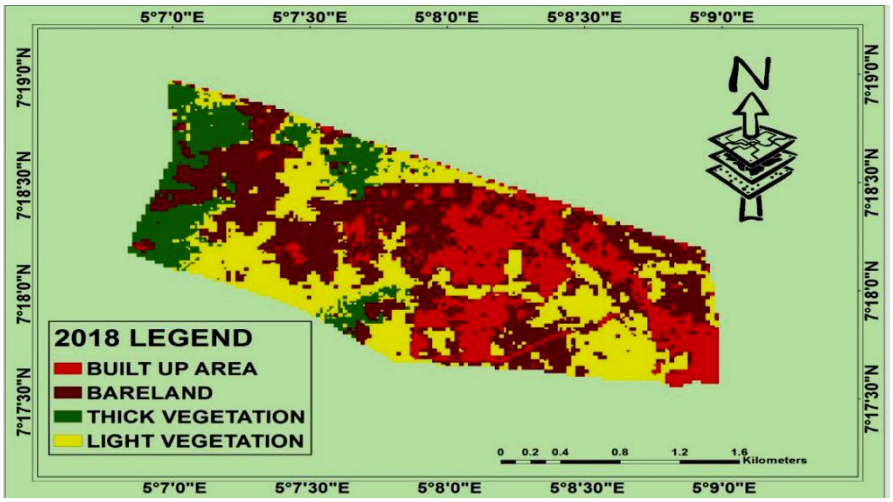


**Figure 5:** Land use/Land cover map of FUTA in 2018

The transformation in the land cover classes for the two epochs in Table 4 showed that Built-Up and Bare Land classes had an appreciable gain of 7.17% and 8.48% respectively. These are all at the expense of the thick forest with an overall loss of 21.8%. Light vegetation has commenced depletion by 1.78% in the second epoch. The overall perception is shown in Figure 6 and the transformation of individual land cover class is shown in Figure 7.

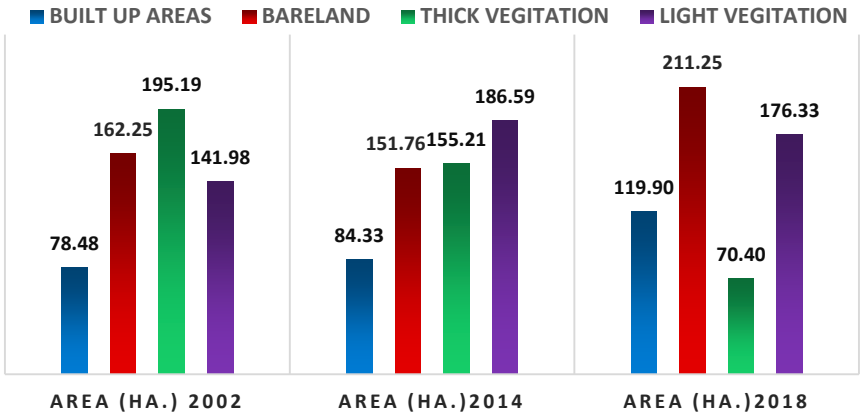


**Figure 6:** Overall view of the land cover transformation in the two epochs

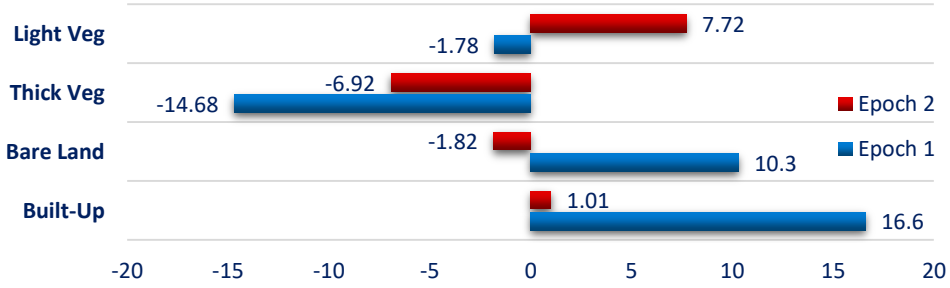


**Figure 7:** Individual land cover transformation

Observation in Figure 7 showed that the green ecosystem (vegetation land cover) is suffering the overall loss. There was a reduction of the light vegetation to -1.78 between 2014 and 2018, a space of four years. Worse still the thick vegetation depleted by a lump sum of 14.68% within a space of four years! All these are ripple effect of positive transformation of other land cover through the underlining landuse (Ogunlade 2018a). The ripple effect majorly affects the thick forest (trees) which are being lost at very alarming rate!

*3.1. Effect of vegetation (green ecosystem) loss on the Ecosystem and Biodiversity*

Szaro *et al.* (1998); Lackey (1998); Meffe *et al.* (2013) attested that humans are the life wire and the colour of the ecosystem. NC State University (2021), Precision Land Scape and Trees (2021), Keystone Ten Million Trees Partnership (2021) observed that plants are a carbon-sink in the ecosystem as they absorb carbon dioxide released by man and release oxygen that is highly needed for the survival of man. According to the findings of Treepeople (2020), UNFAO (2016) research has shown that a single tree can absorb up to 150kg (330lb) of $CO_2$ in a year. Thus plants reduce carbon emission. A deficiency in the plant-man carbon-sink flow amounts to danger for the man such as ill-health, social vices, and even death. Russell (2014), Christopher (2019), Precision Land Scape and Trees (2021) observed that man do experience more stress due to harsh weather as climate change are escalated by atmospheric pollutants.

Absence of green ecosystem makes stress to sky rocket. Christopher (2019) revealed that from research into magnetic resonance imaging (MRI) scan, cities and natural features receives different perception in our brains. He explained that while cities are found in the part of the brain responsible

for hostile environments, natural features are found in the part of the brain responsible for empathy and compassion. Thus, according to INSH (2018) the presence of the green ecosystem regulates the brain's hostile perception of the city's harsh environment in city inhabitants thereby cushioning the inevitable anxiety, depression and aggression in an already violent, de-stabilized world.

The loss of the green ecosystem will make the city environment louder. Szaro *et al.* (1998); Lackey (1998); Meffe *et al.* (2013) attested that trees are good absorber of sound waves. Thus trees and green vegetation thus protect the ecosystem by attenuating the noise resulting from traffic and construction (United Nations 2020).

Loss of the green ecosystem according to Treepeople (2020) and UNFAO (2016) exposes the whole ecosystem to direct sun's rays resulting to severe temperature change. Bau-Show and Yann-Jou (2010) and Extension (2019) revealed that the ecosystem can be cooled by trees by as much as 45°F. Temperature change is a major actor in the sustainability of the ecosystem.

Green ecosystem enhances the quality of fresh air (INSH 2018). Russell (2014); Christopher (2019); Precision Land Scape and Trees (2021) affirmed that trees supply oxygen which is major in the survival of not only man but many living organisms. Oregon Forest Research Institute (OFRI) (2020), Precision Land Scape and Trees (2021) and Russell (2014) observed that from research, a supply of oxygen from an acre of trees can sustain 18 people per day. Thus the quality of air drops where the green ecosystem is absent or depletes (INSH 2018, Extension 2019).

Loss of green ecosystem affects the terrain. According to John (2010); NC State University (2021) and Treepeople (2020), trees are natural water filters. Trees and grasses filter heavy down pour and prevent free flow of storm water thus preventing topography hazards like erosion, landslides and flooding. Voichita (2005) with Treepeople (2020) and UNFAO (2016) agreed that trees protect the soil by absorbing the water that can cause increased run off resulting in higher mud and sediments getting into our water reserves thus making water becoming unsafe for drinking and contaminated for growing foods

Olivia (2018) attested that green ecosystem brings a welcoming environment and that research has shown that there is more violence where there is less green economy. Recreation, relaxation and sports that take the mind from crime and many vices thrives more in green ecosystem like under trees, on green grassland etc. (INSH 2018). Thus, absence of green ecosystem is a breeding medium for crimes of all sorts (Olivia 2018).

Green ecosystem boosts commerce and productivity. Oregon Forest Research Institute (OFRI) (2020), Szaro *et al.* (1998). Russell (2014), Precision Land Scape and Trees (2021) attested that research has shown that trees grow sales and that for instance, on tree-lined streets consumers shop longer and pay 10% more for goods. Treepeople (2020) and UNFAO (2016) observed that people tend to be comfortable buying where there are trees, grassland than just open spaces. View of nature according to Christopher (2019) and INSH (2018) has been found to enhance health as workers who do not have a view of nature from their desks call in sick 23% more often.

## 4.0. Conclusion

Investigation of the depletion of the green ecosystem and its attendant consequences have been the platform upon which the possibility of the protection of the ecosystem and preservation of biodiversity was examined. The wellbeing of the ecosystem is a major factor in the achievement of the Sustainable Development Goals (SDGs), and the protection of the green ecosystem is vital to the survival of the rest ecosystem as it directly affect the man who is the main player in the survival. From the approach of geospatial technology adopted for the study, it was discovered that there was transformations in the land cover of the study area in the year 2002, 2014 and 2018 studied, and a corresponding glaring depletion of duo component the green ecosystem: the thick vegetation (33.78%, 26.26%, 12.18%) and Light vegetation (24.57%, 32.29%, 30.51%). The transformation in the land cover classes for the two epochs 2002-2014 and 2014-2018 were examined and showed an appreciable gain of 7.17% and 8.48% for Built-Up and Bare Land classes respectively at the expense of the thick vegetation (forest) with an overall loss of 21.8%. Light vegetation was observed to

commence depletion by 1.78% in the second epoch. These depletion bears generally on the green ecosystem, and the trees are the major actor in the transformation. The alteration and depletion of the green ecosystem and the consequent disappearance of trees is observed to pose very gruesome threat on living and life in general. The sustainability of the environment has become questionable and doubtful, thus endangering the protection of the ecosystem and preservation of the biodiversity. Unstable sustainability of the environment does not guarantee a protected ecosystem or a preserved biodiversity (UNFAO 2020).

Consequent upon the findings in this research and the corresponding grave consequences observed the study hereby recommend that the regulation and control of the removal of the green ecosystem (vegetation) around us should be taken with all seriousness so as to ensure a proper protection of the ecosystem and preservation of the biodiversity. The various consequence of the disappearance of trees should be avoided by the replacement of felled trees and strong afforestation. The ecosystem and biodiversity must be consciously protected and preserved. The soil and the terrain require great preservation from climatic conditions: direct heat from the sun, erosion, flooding and many natural and anthropogenic hazards of the environment. The negative consequences observed and envisaged must be avoided while the positive consequences should embraced at all governmental and most especially individual level. There is need for public education and awareness at all level on the protection of the ecosystem and the preservation of the biodiversity as a matter of urgency, spelling out in clear terms the implication and the benefits to mankind's survival.

**References**

Bau-Show, L. and Yann-Jou, L. (2010). Cooling Effect Of Shades Trees With Different Characteristics In a Subtropical Urban Park. *American society of horticultural science*, 45(1), pp. 83-86.

Caballero, P. (2016). A Short History of the SDGs . Available at: https://impakter.com/short-history-sdgs/ Accessed: 18th November 2017.

Christopher, B. (2019): Psychology Today-The Neuroscience of Empathy -Neuroscientists identify specific brain areas linked to compassion. Available at: https://www.psychologytoday.com/us/blog/the-athletes-way/201310/the-neuroscience-empathy Accessed: 9th February 2021.

Extension (2019).Trees For Energy Conservation. Available at: https://trees-energy-conservation.org/how-do-trees-cool-the-air/ How do trees cool the air?

Igbokwe, J. I., Ogunlade, S. O., Ejikeme, J. O. and Igbokwe, E. C. (2016). Mapping and Monitoring Deforestation in Ondo State Using Remote Sensing Techniques for Forest Resource Management. *Nigerian Journal of Surveying and Geoinformatics*, 5(1), pp. 108-117.

INSH (2018). What If Urban Forest Disappear? Backyard Media Inc. Toronto, Ontario M6R 3A9 Canada.

Jamie, O. (2019). What are the four ecosystem Types? Available at: Sciencing. http//:sciencing.com/four-ecosystem-types-8102476.hmtl

John, R. (2010).Trees play key role in purifying our water. AJC.com

Keystone Ten Million Trees Partneship (2021): For a Clean Pennsylvani- All about Trees.http://www.tenmilliontrees.org/trees/all about trees Retrieved 9 February 2021

Lackey, R. T. (1998). Seven pillars of ecosystem management. *Landscape and Urban Planning*, 40 (1–3), pp. 21–30. doi:10.1016/S0169-2046(97)00095-9.

Meffe, G., Nielsen, L., Knight, R. and Schenborn, D. eds. (2013). *Ecosystem Management: Adaptive, Community-Based Conservation*. Island Press. ISBN 978-1-55963-824-1.

NC State University (2021): Trees of strength-tree facts. Available at: https://projects.ncsu.edu/project/treesofstrength/treefact.htm. Retrieved 9 February 2021.

Ogunlade, S. O. (2018a). Mapping and Analysis of Spatiotemporal Landuse Dynamics of Akure and Environs, Ondo State Nigeria. [Unpublished Doctoral Desertation]. Nnamdi Azikiwe University, Awka-Nigeria.

Ogunlade, S. O. (2018b). Monitoring the spatial transformation of the Federal University of Technology, Akure between 2002 and 2018: 2nd World Environmental Conservation Conference (WECC)-Transition Pathways to SDGs: Integrated Landscape Approach, Economic Well Being and Inclusive Climate Resilience. 5th -8th June, 2019 FUTA

Ogunlade, S. O. (2019). Spatiotemporal Landuse Pattern Mapping For Sustainable Development Of Akure City. *Journal of Environmental Technology,* 1(1), pp. 21-28.

Ogunlade, S. O. (2020a). Decadal Analysis of Land Cover Trend of Federal University of Technology Akure, Ondo State, Nigeria Using Medium Resolution Multi-Temporal Satellite Images. *International Journal of Innovative Research & Development,* doi: 10.24940/ijird/2020/v9/i7/JUL20084.

Ogunlade, S. O. (2020b). Site Suitability Mapping For Fish Farming: a Geospatial Approach. 3rd World Environmental Conservation Conference (WECC)- 'Strategies for Improved Quality of Life: Inclusive, Innovative, Integrated and Multi-stakeholder's Participation' Wesley University Ondo, Ondo State, Nigeria. 6th July, 2020

Olivia, W. (2018). Reduce Crime And Violence With Trees In Your Neighbourhood. Winconsin DNR Forestry News., WI DNR Urban Forestry Coordinator, 414-750-8744, Olivia.Witthun@wisconsin.gov Online.

Oregon Forest Research Institute (OFRI) (2020) Sustainable forest management is key. www.oregonforests.org retrieved on January 25th 2020

Oyinloye, M. A., Owoeye, J. O. and Ogunlade, S. O. (2018). Impact of Water Hyacinth on Resident Living in Coastal Areas of Ondo State, Nigeria: A Focus on Ilaje Local Government Area. *International Journal of Environmental Monitoring and Protection.* 5(3), pp. 52-63.

Precision Land Scape and Trees (2021): 14 fun facts about trees. https://www.precisiontreemn.com/tips/14-fun-facts-about-trees.html Retrieved 9 February 2021

Russell, M. (2014). 21 reasons why forests are important. Mother Nature Network. www.mnn.com/earth-matters/wilderness-resources/blogs/21-reasons-why-forests- are-important

Szaro, R., Sexton, W. T. and Malone, C. R. (1998). The emergence of ecosystem management as a tool for meeting people's needs and sustaining ecosystems. *Landscape and Urban Planning,* 40(1–3), pp. 1 –7. doi:10.1016/s0169-2046(97)00093-5.

Treepeople (2020).Top 22 benefits of trees https://www.treepeople.org/tree-benefits

UNFAO (2016). Building greener cities: nine benefits of urban trees. www.fao.org

United Nations (2015a). Transforming our world: the 2030 Agenda for Sustainable Development. Sustainable Development Knowledge Platform. (https://sustainabledevelopment.un.org/post2015/transformingourworld)

United Nations (2015b). Sustainable Development Goals 2050. Forests of the future fundamental to achieving Sustainable Development Goals – UN agency. https://www.un.org/sustainabledevelopment/blog/tag/2050/

United Nations (2017). Development, World Commission on Environment and. Our Common Future, Chapter 2: Towards Sustainable Development - A/42/427 Annex, Chapter 2 - UN Documents: Gathering a body of global agreements. *www.un-documents.net*. Retrieved 17 November 2017.

United Nations (2020): Biodiversity and ecosystems https://sustainabledevelopment.un.org/topics/biodiversityandecosystems

Voichita, B. (2005).Urban Forest Acoustics. Pacs 43.28.Fp INRA, Centre de Recherches Forestières de Nancy UMR 1093 – Laboratoire d'Etudes et Recherches sure le Matériau Bois 54280 Champenoux. France.

**Cite this article as:**
Ogunlade S. O. 2021. Protection of Ecosystem and Preservation of Biodiversity: The Geospatial Technology Approach. *Nigerian Journal of Environmental Sciences and Technology*, 5(1), pp. 67-75. https://doi.org/10.36263/nijest.2021.01.0253

Nigerian Journal of Environmental Sciences and Technology (NIJEST)

www.nijest.com

ISSN (Print): 2734-259X | ISSN (electronic): 2734-2603

Vol 5, No. 1 March 2021, pp 76 - 90

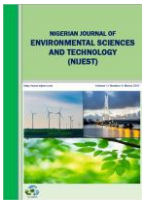

# Evaluating the Quality of Spatial Data for the Analysis of Climate Variability in the Coastal Region of Nigeria

Agbonaye A. I.[1,*] and Izinyon O. C.[2]

[1,2]Department of Civil Engineering, University of Benin, Benin City, Nigeria

Corresponding Author: *augustine.agbonaye@uniben.edu

https://doi.org/10.36263/nijest.2021.01.0236

## ABSTRACT

*The lack of truly reliable data for climate change analyses and prediction presents challenges in climate modeling. Needed data are required to be hydrologically/statistically reliable to be useful for hydrological, meteorological, climate change, and estimation studies. Thus, data quality and homogeneity screening are preliminary analyses. In this study, the homogeneity of the climatic data used for analyses of climate variability was conducted in the coastal region of Nigeria. Climatic Research Unit (CRU 0.5× 0.5) gridded monthly climatic data for sixty years (1956- 2016) for nine states of the coastal region of Nigeria obtained from internet sources were validated with the Nigerian Meteorological Agency (NiMet) data to assure adequacy for use. The data were tested for normality using the Shapiro-Wilk (S-W) test, D'Agostino-Pearson omnibus test, and skewness test. Four homogeneity test methods were applied to 257 locations in the nine states of the coastal region of Nigeria and they include Pettit's, Standard Normal Homogeneity Test (SNHT), Buishand's and Von Neumann Ratio (VNR) tests. The results of the validity analysis indicated that the CRU data are very reliable and thus justified their use for the further analysis carried out in the study. Also, the results obtained indicated that CRU climatic data series were normally distributed and parametric methods could be used in further analysis of the data. Rainfall data homogeneity was detected for Bayelsa, Delta, Edo, Lagos, Ogun, and Ondo states and inhomogeneity for Akwa Ibom, Cross Rivers, and Rivers States. Also, temperature data inhomogeneity was detected for all the states in the study area.*

**Keywords:** Climatic data, Normality, Homogeneity, Climate change, CRU

## 1.0. Introduction

Reliable and accurate estimates of climate are not only crucial for the study of climate variability but are also important for water resource management, agriculture, weather, climate, and hydrological forecasting (Sarojini *et al*., 2016). Unfortunately, there is the dearth of satisfactory climatic data in developing countries. The rain-gauge measurement is the traditional and oldest method for monitoring rainfall. However, because of the practical observational limitations, this measurement often suffers from numerous gaps in space and time, due to weather stations being limited in numbers and often unevenly distributed, resulting in missing data problem, a short period of observation, incomplete areal coverage, and deficiencies over most oceanic and sparsely populated areas (Kidd *et al*.,2017), thus making its use in climate change diagnostic studies less reliable in initial data processing and calibration problems of subjecting non-continuous rainfall and temperature data into the Water Balance and TREND software. This may arise as this software often recognizes only continuous data of long duration over fifty (50) years. Unfortunately, available data from NIMET either had missing data or are not up to 50 years in some locations. Often, this basic requirement for use is not met and the situation is compounded by sparse data coverage challenge in the region due to the few weather stations per state most of which are located in the airports. Studies have shown that a major constraint in climatic change research identified in the past is the lack of long-term climatic data on a temporal basis (Nnamchi *et al*., 2008). Mitchel and Jones (2005) recommended that a large proportion of such data needs can be met through providing a standard set of 'climate grids', in terms of monthly variations over a century-long time scale on a regular high-resolution (0.5°) latitude-longitude grid.

The extensive application of data the CRU TS datasets for studying climatic variability has been used by converting climatic datasets into formats that are more commonly used and therefore can be directly utilized in GIS. In long-term modeling of climatic variability, the application of the CRU dataset is well documented.

Data taken from the observation stations should be tested for reliability and homogeneity before their use in the research studies. Homogeneity testing is one of the most important analyses in climate-related studies as it underpins the reliability of any inferences (Yozgatligil and Yazici, 2015). The accuracy and reliability of the model result in the studies about climate change, classification, flood and drought modeling, water resources planning and modeling related to hydrology and meteorology vary according to the quality of the data used. Inhomogeneous observation records may occur in the stations making meteorological observations unreliable due to the method used, the conditions around the station and the reliability of the measurement tool, etc.

Homogeneous climate series may be defined as a series only influenced by the variations in climate. However, it is difficult to find reference stations with a high correlation and a homogeneous structure in wide regions. For this reason, the absolute method was used for the homogeneity test in our study owing to the high spatial variation of precipitation stations. The standard procedure is to apply four tests: the Pettit, Standard Normal Homogeneity (SNH), Buishand (BR), and Von Neumann (VNR) tests at a significance level of 0.05 (Agha *et al*., 2017). The temperature series were tested using the annual mean temperature while the Precipitation series were tested using the annual mean rainfall. The use of derived annual variables avoided autocorrelation problems with testing daily series.

There are some differences between SNHT, BRT, and Pettitt test. SNHT test is known to find change point towards the beginning and the end of the series, whereas BRT and Pettitt tests are sensitive to find the changes in the middle of a series (Martínez *et al*., 2009). These three tests are capable of detecting the year where a break occurs. Meanwhile, VNRT assumes the same null hypothesis as the previous three tests but for the alternate hypothesis, it assumes that the series is not randomly distributed. VNRT assesses the randomness of the series but does not give information about the year of the break. Homogeneity of consistency implies that all the collected hydrologic time series data belong to the same statistical population having a time-invariant mean. Therefore, the tests to check the homogeneity or consistency of the data series are based on evaluating the significance of changes in the mean value. To be accurate, the climate data used for long-term climate analyses, particularly climate change analyses, must be homogeneous. A homogeneous climate time series is defined as one where variations are caused only by variations in weather and climate. Unfortunately, most long-term climatological time series have been affected by several non-climatic factors that make these data unrepresentative of the actual climate variations occurring over time.

Climate data homogenization aims to adjust observations, if necessary so that the temporal variations in the adjusted data are caused only by climate processes.

## 2.0. Methodology

### *2.1. Description of study area*

The study area is the coastal region of Nigeria. The area is geographically located between latitude $4^oN - 8^oN$ and longitude $3^oE - 9^oE$. Figure 1 presents the map of Nigeria showing the coastal region station coordinates of representative cities in the coastal region of Nigeria and other states details are presented in Table 1. The Nigeria coastline which is about 853km long runs through nine states of Nigeria namely: Lagos, Ogun, Ondo, Edo, Delta, Bayelsa, Rivers, Akwa-Ibom and Cross River states, bordering the Atlantic Ocean. Nine stations, each from these states, were selected for representative coverage. Nigerian coastal zone experiences a tropical climate consisting of the rainy season (April to November) and dry season (December to March). High temperatures and humidity as well as marked wet and dry seasons characterize the Nigerian climate. The coastal areas have an annual rainfall ranging between 1, 500, and 4,000 mm. The coastline area is humid with a mean average temperature of $24 - 32^oC$ (Kuruk, 2004). The coastal area is low lying with heights of not more than 3.0m above sea level and is generally covered by freshwater swamp, mangrove swamp, lagoon marshes, tidal channels, beach ridges, and sand bars (Nwilo and Badejo, 2006).

The station coordinates of representative cities in the coastal region of Nigeria and the map of the area are presented in Table 1 and Figure 1 respectively.

**Table 1:** Station coordinates of representative cities in the coastal region of Nigeria and other states details

| S/N | Coastal state | Land Area ($km^2$) | Population density (Persons/$km^2$) | Selected city | Longitude | Latitude | Years of available MIMET data |
|---|---|---|---|---|---|---|---|
| 1 | Akwa-Ibom | 8,421 | 466 | Uyo | 7.53°E | 5.10°N | 60 |
| 2 | Bayelsa | 21,100 | 81 | Yenogoa | 6.26°E | 4.92°N | 60 |
| 3 | Cross Rivers | 23,074 | 125 | Calabar | 8.20°E | 4.57°N | 60 |
| 4 | Delta | 17,011 | 241 | Warri | 5.75°E | 5.5°N | 60 |
| 5 | Edo | 15,650 | 206 | Benin City | 5.31°E | 6.20°N | 60 |
| 6 | Lagos | 3577 (787 in water) | 2520 | Ikeja | 3.45°E | 6.2°N | 60 |
| 7 | Ogun | 16720 | 223 | Abeokuta | 3.35°E | 7.16°N | 60 |
| 8 | Ondo | 14769 | 233 | Akure | 5.5°E | 7.15°N | 60 |
| 9 | Rivers | 11,225 | 462 | Port Harcourt | 7.10°E | 4.4°N | 60 |

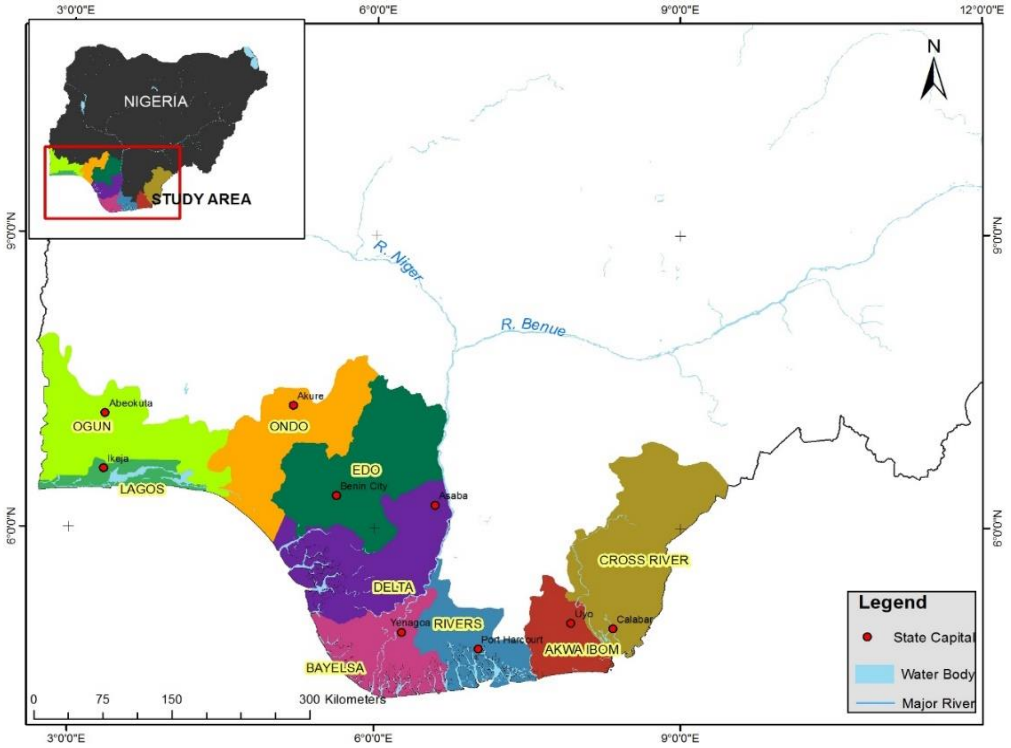


**Figure 1:** Map of Nigeria showing the coastal region
*[Source: Adapted from Office of the Survey General of the Federation (OSGOF)]*

*2.2. Data collection/validation*

Climatic data collected were mean monthly rainfall and temperature for a period of 60 years (1956-2017) for selected cities in the coastal region of Nigeria. Climate Research Unit (CRU 0.5× 0.5) gridded monthly climatic data for two climatic periods ((1956- 1986 and 1987-2016), obtained from the internet (http://badc.nerc.ac.uk), were sorted into annual rainfall series and validated with the Nigerian Meteorological Agency (NiMet) data obtained from Central Bank of Nigeria (CBN) website https://www.cbn.gov.ng/documents/Statbulletin.asp. The validation was carried out using the following goodness of fit statistics: Coefficient of Determination ($R^2$), Nash-Sutcliffe Efficiency (NSE) and Ratio of Standard Deviation of observations to Root Mean Squared (RSR). These data series from 257 locations in nine states of the region were tested for normality and homogeneity. The value of $R^2$ obtained is considered very good when its value is within the range of $0.75 < R^2 \leq 1$ (see Table 2). The lack of truly reliable data is a problem that complicates the analysis of climate trends, increasing the challenges of related relevant research, hence data validation was done.

**Table 2:** General validation rating used

| $R^2$ (adj $R,)^2$ | RSR (-) | K tau | Validation rating | MAPE (%) | Validation rating | Cp | Capability |
|---|---|---|---|---|---|---|---|
| $0.75 \leq R^2 \leq 1$ | $0 < RSR \leq 0.5$ | $0.75 < K \leq 1$ | Very Good | 0 < 10 | Highly accurate | 0 < 1 | Incapable |
| $0.65 \leq R^2 \leq 0.75$ | $0.5 < RSR \leq 0.6$ | $0.65 < K \leq 0.75$ | Good | 10-20 | Good | 1 < Cp < 3 | capable |
| $0.5 \leq R^2 \leq 0.65$ | $0.6 < RSR \leq 0.7$ | $0.5 < K \leq 0.65$ | Satisfactory | 20-50 | Reasonable | 3 < Cp | Very capable |
| $R^2 \leq 0.5$ | RSR > 0.7 | $K \leq 0.5$ | Unsatisfactory | > 50 | Inaccurate | | |

Note that adjusted-$R^2$ can have a negative value, unlike $R^2$, which is always between 0 and 1. We also mentioned that adjusted-$R^2$ is roughly equal to $R^2$. Adjusted R-squared more than 0.75 indicates a very good value for showing the accuracy. The interpretations of Kendall's tau and Spearman's rank correlation coefficient are very similar and thus invariably lead to the same inferences.

### *2.3. Preliminary data analysis*

#### 2.3.1. Descriptive statistics

The descriptive statistics of annual rainfall time series which includes; minimum, maximum, range, mean, standard deviation, variance, standard error of the mean, kurtosis, and skewness with their standard error's computations were implemented by using XLSTAT software. Basic equations for descriptive statistics are presented in Table 3.

**Table 3:** Equations for descriptive statistics

| Statistical text | Applicable formula | Remark |
|---|---|---|
| Mean | $\bar{R} = \frac{\sum(R)}{N}$ | It is obtained by adding together all the variates, $\sum(R)$ and dividing by the total number of variates, **N**. |
| Standard Deviation | $\sigma = \sqrt{\frac{\sum(R-\bar{R})^2}{N}}$ | It is the square root of the mean-squared deviation of individual observations from their mean Standard deviation. |
| Variance | $\sigma^2 = \frac{\sum(R-\bar{R})^2}{N}$ | |
| Coefficient of Variation | Coefficient of variation, $\mathbf{C_v} = \frac{6}{\bar{R}}$ | It is obtained by dividing the standard deviation of the data set by its mean. |
| Determination of coefficient of variation | $CV = \frac{SD\ x\ 100}{\bar{X}}$ | This is a measure of the variability of data |
| Skewness | $\alpha = \frac{1}{N} \sum(R - \bar{R})^3$ | Where R is a variate, $\bar{R}$ is the mean of the data set and N is the total number of variates. |
| Kurtosis | $K = n \frac{\sum_{i=1}^{n}(R_i-\bar{R})^4}{\left(\sum_{i=1}^{n}(R_i-\bar{R})^2\right)^2}$ | Kurtosis is the degree of peakedness of distribution, usually taken relative to a normal distribution. A distribution having a relatively high peak is called leptokurtic, while a curve that is flat-topped is called platykurtic. The normal distribution which is not very peaked or very flat-topped is called isocratic. |

#### 2.3.2. Simple *t*-test

This test is data-driven and provided a known change point. It was used to check the null hypothesis of whether equal means in two different periods are different (Mu *et al*., 2007). The simple *t*-test assumes that the data are normally distributed. The relationship is expressed as follows:

$$t = \frac{\left|\bar{x} - \bar{y}\right|}{S\sqrt{\frac{1}{n_1} + \frac{1}{n_2}}} \quad (1)$$

$$S = \sqrt{\frac{(n_1 - 1)s_1^2 + (n_2 - 1)s_2^2}{n - 2}} \quad (2)$$

where $\bar{x}$ and $\bar{y}$ in Equation 1 stand for the means of the observed and simulated data respectively, while $n_1$ and $n_2$ are the numbers of data in the observed and simulated respectively, and $S$ is the standard deviation of sample (of the entire $n_1$ and $n_2$ observations, $n = n_1 + n_2$). We considered the $t$

statistic test statistic and the degrees of freedom to determine the *p*-value. The *p*-value is the probability that a *t* statistic having *n* - *2* (22) degrees of freedom is very much greater than 1.725. Since this is a two-tailed test, "very much greater" means greater than 1.725 or less than -1.725.

2.3.3. Test of normality

Normality test, which was employed to determine whether the dataset could be described by a normal distribution, was carried out using Shapiro Wilk Test (SWT), D`Agostino-Pearson Test, and Skewness Test. This enabled data screening, outlier identification, description, assumption checking, and characterizing differences among sub-populations.

The basic test of a hypothesis that guides in deciding on normality is stated as follows:

Null hypothesis $H_0$: Data follow a normal distribution

Alternative hypothesis $H_1$: Data do not follow a normal distribution

**The Shapiro-Wilk**

This test is one of the most popular tests for normality assumption diagnostics which has good properties of power and is based on correlation within given observations and associated normal scores. The Shapiro-Wilk test statistics derived by Shapiro and Wilk (1965) is as shown below:

$$W = \frac{\left(\sum a_i y_{(i)}\right)^2}{\sum (y-\bar{y})^2} \tag{3}$$

where (i ) y is the $i^{th}$ order statistics and $I_a$ is the i-th expected value of normalized order statistics. For independently and identically distributed observations, the values of *I* can be obtained from the table presented by Shapiro and Wilk (1965) for sample sizes up to 50. W can be expressed as a square of the correlation coefficient between $I_a$ and *(i)y*. So *W* is the location and scale-invariant and is always less than or equal to 1. In the plot of *(i)y* against *I* an exact straight line would lead to *W* very close to 1. So if *W* is significantly less than 1, the hypothesis of normality will be rejected. Although the Shapiro-Wilk *W* test is very popular, it depends on the availability of values of $I_a$, and for large sample cases their computation may be much more complicated.

**D'Agostino-Pearson Omnibus Test**

An alternative test of the same nature for samples larger than 50 was designed by D'Agostino (1973).

To assess the symmetry or asymmetry generally, skewness is measured and to evaluate the shape of the distribution kurtosis is overlooked. D'Agostino-Pearson (1973) test standing based on skewness and kurtosis test and these are also assessing through moments. The equation is given as:

$$K^2 = Z^2\left(\sqrt{b_1}\right) + Z^2\left(b_2\right) \tag{4}$$

where $Z^2\left(\sqrt{b_1}\right)$ and $Z^2\left(b_2\right)$ are the normal approximation equivalent to $\sqrt{b_1}$ and $b_2$ are sample skewness and kurtosis respectively. This statistic follows a chi-squared distribution with two degrees of freedom if the population is from a normal distribution. A large value $K^2$ leads to the rejection of the normality assumption.

For the skewness test, the skewness coefficient of a time series *X(t)* is estimated as follows (Karamouz *et al*., 2003):

$$\hat{S} = \frac{\frac{1}{N}\sum_{i=1}^{N}\left(X_{(t)} - \overline{X}\right)^3}{\left[\frac{1}{N}\sum_{i=1}^{N}\left(X_{(t)} - \overline{X}\right)^2\right]^{\frac{3}{2}}} \tag{5}$$

where $N$ is the number of sample data and $X$ is the sample mean for time series $X(t)$. The skewness test is based on the fact that the skewness coefficient of a normal variable is zero. If the series is normally distributed, $\hat{S}$ is asymptotically normally distributed with the mean of zero, variance of 6/N, hence, (1−α) ×100% confidence limit on skewness is defined as,

$$S \in \left[ -Z_{\left(\frac{\alpha}{2}\right)}\sqrt{\frac{6}{N}},\ Z_{\left(\frac{\alpha}{2}\right)}\sqrt{\frac{6}{N}} \right] \tag{6}$$

where $Z_{(\alpha/2)}$ is the (1−α/2) quantile of the standard normal distribution. Therefore, if ˆS falls within the limits of Eq.6, the hypothesis of normality cannot be rejected. The test is found to be reasonably accurate for $N > 150$.

The Shapiro-Wilk (S-W) test, D'Agostino-Pearson omnibus test, and skewness values are also displayed as the output of descriptive statistic explained in the last section and the result is presented in Section 3.1.2.

*2.4. Data analysis*

2. 4.1. Test for homogeneity

Homogeneity tests help in assessing trend reliability and identifying suitable sub-periods for the analysis. Homogeneity test was carried out by use of Pettit's test, Standard Normal Homogeneity Test (SNHT), Buishand's test, Von Neumann Ratio which was implemented by the XLSTAT software.
The basis of these tests corresponds to the alternative hypothesis of a single shift. For all tests, p-values were being calculated using Monte Carlo resampling. Test of hypothesis would guide in taking a decision on from results of homogeneity on the tables. The hypothesis is stated as follows:

Null hypothesis: $H_0$: Data are Homogeneous
Alternative hypothesis: $H_a$ There is a date at which there is a change in the data

Test interpretation:
$H_0$: Data are homogeneous
*Ha*: There is a date at which there is a change in the data. The p-value shows that the null hypothesis is rejected; we can conclude that there is a shift between two parts of our time series. The associated pilot confirms this result. The SNHT test (Standard Normal Homogeneity Test) is usually applied to a series of ratios that compare the observations with an average. The ratios are then standardized. The null hypothesis are: $H_0$: The obtained ratios follow an N(0,1) distribution.

Since the *p*-value is very small, we reject the null hypothesis and thus conclude that there exists a shift in the time series. This result confirms the result of the first test. The Buishand's test can be used on variables following any type of distribution. It is based on the null hypothesis: $H_0$: The $T$ variables follow one or more distributions that have the same mean. Since the p-value is very small, this hypothesis is rejected and the alternative hypothesis will be: there exists a time t from which the variables change of mean. Finally, the von Neumann ratio is based on the sum of the square's differences between each pair of following time measures. The mean of this ratio is equal to 2 when the average of the time series is constant. The *p*-value is equal to 0.002, which leads us to reject the null hypothesis of homogeneity of the time series. This also confirms the preceding results. Von Neumann does not determine the time of change.

When $p$ is smaller than the specified significance level, e.g. 0.05, the null hypothesis is rejected. In other words, if a significant change point exists, and the time series was divided into two parts at the location of the change point. For all these four tests, if the test statistic exceeds the critical value at a certain confidence level, the null hypothesis will be rejected at that confidence level.

The statistical analyses of every climatic time series must always be carried out for studying important time series characters, i.e., normality, homogeneity, seasonality, presence of trends and changes, etc.

2.4.2. Pettit's test (Non-Parametric Rank Test)

This test developed by Pettitt is a nonparametric test, which is useful for evaluating the occurrence of abrupt changes in climatic records (Smadi and Zghoul, 2006). One of the reasons for using this test is that it is more sensitive to breaks in the middle of the time series (Wijngaard *et al*., 2003). Pettitt's test is a nonparametric test that requires no assumption about the distribution of data. Pettitt's test is an adaptation of the rank-based Mann-Whitney test that allows identifying the time at which the shift occurs. The statistic used for Pettitt's test is computed as follows: The null and alternative hypotheses in this test are the same as in the Buishand test, and this test is also more sensitive to the breaks in the middle of the series (Costa and Soares, 2009). The ranks $r_1...r_n$ of the $Y_1...Y_n$ is used to calculate the statistics.

$$X_k = 2\sum_{i=1}^{k} r_i - k(n+1) \qquad \text{k = 1,2,….,n} \tag{7}$$

If a break occurs in year *K*, then the statistic is maximal or minimal near the year $k = K$:

$$X_k = \max_{1\le k\le n} |X_k| \tag{8}$$

2.4.3. Standard Normal Homogeneity Test (SNHT)

SNHT is one of the most popular homogeneity tests in climate studies. The null and alternative hypotheses in this test are the same as in the Buishand test; however, unlike the Buishand test, SNHT is more sensitive to the breaks near the beginning and the end of the series (Costa and Soares, 2009). Alexandersson and Moberg (1997) proposed a statistic *T(k)* to compare the mean of the first *k* years of the record with that of the last $(n - k)$ years:

$$T(k) = kz_1^{-2} + (n-k)z_2^{-2} \qquad \text{k = 1,2,….,n} \tag{9}$$

$$\textit{Where, } \overline{z_1} = \frac{1}{n}\frac{\sum_{i=1}^{k}\left(Y_i - \overline{Y}\right)}{S} \textit{ and } \overline{z_2} = \frac{1}{n-k}\frac{\sum_{i=k+1}^{n}\left(Y_i - \overline{Y}\right)}{S} \textit{ and } S = \frac{1}{n}\sum_{i=1}^{k}\left(Y_i - \overline{Y}\right) \tag{10}$$

If a break is located at the year *K*, then *T(k)* reaches a maximum near the year $k = K$. The test statistic $T_0$ is defined as:

$$T_0 = \max_{1\le k\le n} T(k) \tag{11}$$

The null hypothesis is rejected if $T_0$ is above a certain level, which is dependent on the sample size.

2.4.4. Buishand's test (Parametric test)

This test is used to detect a change in the mean by studying the cumulative deviation from the mean. It bases on the adjusted partial sums or cumulative deviation from the mean. According to Al-Ghazali, and Alawadi (2014) the null hypothesis is that the data are homogenous and normally distributed and the alternative hypothesis is that there is a date at which a change in a mean occurs.

This test supposes that tested values are independent and identically normally distributed (null hypothesis). The alternative hypothesis assumes that the series has a jump-like shift (break). This test is more sensitive to breaks in the middle of the time series (Costa and Soares, 2009). The test statistics, which are the adjusted partial sums (Buishand, 1982), are defined as $S_0^* = 0$ and

$$S_k^* = \frac{n\sum_{i=1}^{k}\left(Y_i - \overline{Y}\right)}{\sum_{i=1}^{n}\left(Y_i - \overline{Y}\right)^2} \qquad \text{k = 1, 2, …. , n} \tag{12}$$

When series are homogeneous, the values of $S_k$* will fluctuate around zero because no systematic deviations of the Yi values concerning their mean will appear. Q-statistics: if a break is present in year *K*, then $S_k$* reaches a maximum (negative shift) or minimum (positive shift) near the year $k = K$.

$$Q = \max_{0 \le k \le n} S_k \tag{13}$$

R-statistics (Range Statistics) are,

$$R = \left( \max_{0 \le k \le n} S_k^* - - - \min_{0 \le k \le n} S_k^* \right) \tag{14}$$

Buishand (1982) gives critical values for *Q* and *R* for different data set lengths random values; the alternative hypothesis is that the values in the series are not randomly distributed.

2.4.5. Von Neumann Ratio Test (Non-Parametric Test)
Von Neumann proposed a nonparametric test where the statistic is defined as the ratio of the mean square successive (year-to-year) difference to the variance. The null hypothesis is that the data are independent, identically distributed random quantities and the alternative' is that the time series is not randomly distributed. Under the null hypothesis of a constant mean, the expected value of the test statistic is equal to two. The von Neumann ratio test is not location-specific, which means that it gives no information about the date of the break.

In this test, the null hypothesis is that the data are independent identically distributed. The von Neumann ratio N is defined as the ratio of the mean square successive (year to year) difference to the variance (von Neumann):

$$N = \frac{\sum_{i=1}^{n-1} \left( Y_i - Y_{i+1} \right)^2}{\sum_{i=1}^{n} \left( Y_i - \overline{Y} \right)^2} \tag{15}$$

Hereafter, for each of the test descriptions, $n$ is the data set length, $Y_i$ is the $i^{th}$ element of the data set, is the mean value of the data set. When the sample is homogeneous the expected value is $N = 2$. If the sample contains a break, then the value of $N$ tends to be lower than this expected value. If the sample has rapid variations in the mean, then values of $N$ may rise above two (Klein, 2007). This test gives no information about the location of the shift. Critical values for $N$ for different data set lengths.

XLSTAT statistical software used a hypothesis testing method to detect homogeneity of the rainfall data. This software was used to execute the homogeneity analysis. The results were categorized into three classes, which are useful, doubtful, and suspect according to the number of tests rejecting the null hypothesis. Based on an alpha value of 0.05 (95% significance level), for *p*-value bigger than alpha value, the series was considered to be homogeneous.

## 3.0. Results and Discussion

### *3.1. Test result for reliability of CRU data (preliminary data validation)*

The descriptive statistics of NiMeT and CRU mean annual rainfall and temperature are presented in Tables 4 and 5. Table 4 shows that the mean annual rainfall varies from 3074.098 mm in Bayelsa and 1263.575 mm in Lagos. The standard deviation varies from 96.9369mm to 160.7266mm while the skewness and Kurtosis vary from 0.06751 to - 0.01484 and -1.61271 to -0.57684 respectively. These values of skewness and Kurtosis are indicative that the rainfall series approximate to normal distribution.

**Table 4:** Descriptive statistics of NiMeT and CRU mean annual rainfall (1956- 1986 and 1987-2016)

| Climatic Station | Climatic Data | Mean mm | SD mm | Variance | Min Mm | Max mm | Range mm | Sum mm | Skewness | Kurtosis |
|---|---|---|---|---|---|---|---|---|---|---|
| Akwa | NIMET | 377.4364 | 235.4844 | 55452.89 | 35 | 800.125 | 765.125 | 4151.8 | 0.201617 | -0.78341 |
| Ibom | CRU | 236.5422 | 150.7492 | 22725.32 | 34.13 | 458.181 | 424.049 | 2838.5 | -0.01484 | -1.55418 |
| Bayelsa | NIMET | 237.1409 | 139.3913 | 19429.94 | 33.27 | 428.725 | 395.45 | 2608.55 | -0.2039 | -1.55741 |
| | CRU | 256.1748 | 160.7266 | 25833.04 | 45.39 | 464.289 | 418.903 | 3074.098 | 0.067378 | -1.51304 |
| Cross | NIMET | 257.3424 | 147.4242 | 21733.91 | 23 | 449.8 | 426.8 | 2830.767 | -0.3454 | -1.16572 |
| River | CRU | 230.2533 | 153.8214 | 23661.02 | 22.58 | 448.109 | 425.52 | 2763.039 | -0.0152 | -1.61271 |
| Delta | NIMET | 176.484 | 120.079 | 14418.97 | 4.1 | 377.63 | 373.53 | 1941.33 | -0.1477 | -0.8333 |
| | CRU | 206.0484 | 142.8669 | 20410.94 | 25.08 | 404.26 | 379.176 | 2472.581 | 0.037337 | -1.60228 |
| Edo | NIMET | 191.7341 | 128.3811 | 16481.72 | 0.55 | 413.375 | 412.825 | 2109.075 | -0.04404 | -0.74626 |
| | CRU | 170.348 | 117.3442 | 13769.66 | 16.55 | 335.84 | 319.286 | 2044.176 | -0.09218 | -1.60147 |
| Lagos | NIMET | 114.870 | 0.88266 | 5024.352 | 9.55 | 241.75 | 232.2 | 1263.575 | 0.443287 | -0.58833 |
| | CRU | 136.2877 | 99.56 | 9912.54 | 15.364 | 331.068 | 315.70 | 1635.453 | 0.504882 | -0.57684 |
| Ogun | NIMET | 114.7036 | 79.180 | 6269.618 | 2.86 | 209.74 | 206.88 | 12 | -0.32077 | -1.79549 |
| | CRU | 140.0217 | 96.9369 | 9396.777 | 13.88 | 280.636 | 266.76 | 1680.26 | 0.06751 | -1.53347 |
| Ondo | NIMET | 119.3667 | 67.100 | 4502.435 | 0 | 221.5 | 221.5 | 1313.03 | -0.50953 | -0.46507 |
| | CRU | 167.3427 | 116.23 | 13509.37 | 17.12 | 344.131 | 327.013 | 2008.1 | 0.055487 | -1.43844 |
| Rivers | NIMET | 215.2455 | 133.545 | 17834.28 | 20.35 | 344.1312 | 369.75 | 2367.7 | 0.039566 | -1.66506 |
| | CRU | 246.76 | 154.04 | 23729.21 | 44.17 | 456.724 | 412.55 | 2961.13 | 0.030139 | -1.58832 |

**Table 5:** Descriptive statistics of NiMeT and CTU mean annual temperature (1956- 1986 and 1987-2016)

| Climatic Station | Climatic Data | Mean mm | SD mm | Variance | Min Mm | Max mm | Range mm | Sum mm | Skewness | Kurtosis |
|---|---|---|---|---|---|---|---|---|---|---|
| Akwa | NIMET | 27.074 | 1.0575 | 1.118 | 25.775 | 28.891 | 3.116 | 297.8 | 0.482552 | -0.8468 |
| Ibom | CRU | 30.569 | 1.328 | 1.764 | 28.31 | 32.332 | 4.022 | 366.83 | -0.32776 | -1.00893 |
| Bayelsa | NIMET | 26.66 | 0.9298 | 0.864 | 25.4 | 28 | 2.6 | 293.3 | -0.03137 | -1.3631 |
| | CRU | 30.39 | 1.3242 | 1.7534 | 28.267 | 32.046 | 3.7786 | 364.717 | -0.43492 | -1.31231 |
| Cross | NIMET | 26.86 | 1.1483 | 1.3187 | 25.24 | 28.77 | 3.525 | 295.46 | 0.242124 | -0.92303 |
| River | CRU | 30.562 | 1.431 | 2.0476 | 28.064 | 32.490 | 4.43 | 366.74 | -0.33311 | -0.85852 |
| Delta | NIMET | 27.45 | 1.1794 | 1.391 | 25.687 | 29.025 | 3.338 | 301.98 | -0.2685 | -1.1837 |
| | CRU | 30.579 | 1.561 | 2.438 | 28.077 | 32.501 | 4.42 | 366.95 | -0.45921 | -1.31496 |
| Edo | NIMET | 27.27 | 1.4263 | 2.035 | 25.068 | 29.068 | 4 | 300.05 | -0.31898 | -1.39383 |
| | CRU | 30.447 | 1.838 | 3.378 | 27.507 | 32.729 | 5.22 | 365.366 | -0.40085 | -1.34195 |
| Lagos | NIMET | 26.96 | 1.1604 | -1.3419 | 25.2 | 28.6 | 3.4 | 296.6 | -0.11815 | -1.42984 |
| | CRU | 30.597 | 1.629 | 2.6558 | 28.046 | 32.490 | 4.44 | 367.162 | -0.43246 | -1.4675 |
| Ogun | NIMET | 27.08 | 1.336 | 1.786 | 25.1 | 29.1 | 4 | 297.9 | -0.02428 | -1.2389 |
| | CRU | 30.81 | 1.856 | 3.444 | 27.826 | 33.063 | 5.24 | 369.73 | -0.3822 | -1.444 |
| Ondo | NIMET | 25.38 | 1.415 | 2.003 | 23.2 | 27.2 | 4 | 279.2 | -0.26792 | -1.38252 |
| | CRU | 30.664 | 1.8259 | 3.3339 | 27.746 | 32.949 | 5.20 | 367.97 | -0.368 | -1.391 |
| Rivers | NIMET | 27.017 | 0.972976 | 0.947 | 25.76 | 28.508 | 2.75 | 297.187 | 0.2653 | -1.2259 |
| | CRU | 30.512 | 1.299 | 1.688 | 28.368 | 32.157 | 3.79 | 366.14 | -0.3456 | -1.1793 |

The descriptive statistics of mean annual temperature (1956-2016), in the coastal region of Nigeria are presented in Table 5. The table was obtained by use of XL Statistic software as explained in Section 3.3.1. The table shows that the mean annual temperature varies from 369.73°C in Ogun and 293.3°C in Bayelsa. The standard deviation varied from 1.856°C to 1.3242°C while the skewness and Kurtosis varied from -0.45921 to -0.32776 and -1.4675 to -0.85852 respectively. These values of skewness and Kurtosis are indicative that the rainfall series approximate to normal distribution.

### *3.2. Result for differences in mean annual rainfall during the two climatic periods (simple t-Test)*

The results of values obtained from the computer output are presented in Table 6. The table depicts the values of the means in the two climatic periods in the states for which the Student t-test was used to establish if there were differences between them. The Pearson correlation, the number of observations (*n*) the degree of freedom (df = n-1) are shown. The computed *t* statistics, as well as the *t* critical for one tail and two-tail test, are also presented.

The hypothesis is stated as follows:
The null hypothesis is that there is no statistical difference in mean seasonal rainfall distribution between the NIMET and CRU data**.** The alternate hypothesis is that there is a statistical difference in mean seasonal rainfall distribution between the NIMET and CRU data:

Null hypothesis $H_0$: $\mu_1 = \mu_2$
While the alternative hypothesis is $H_a$: $\mu_1 \neq \mu_2$ i.e. $\mu_1 > \mu_2$ or $\mu_1 < \mu_2$.

Hence, two-tail tests are used for the analysis. Based on the *t* statistic test statistic and the degrees of freedom, we determine the *P*-value. The *P*-value is the probability that a *t* statistic having 11 degrees of freedom is more extreme than 1.725. Since this is a two-tailed test, "more extreme" means greater than 1.725 or less than -1.725 i.e. $-1.725 < T_0 < 1.725$.

**Table 6:** Results of Simple t - test on comparison of NIMET and CRU data for rainfall

| Location | Simple t-test ($T_0$) Computed | Df (n-2) | Alpha | P-value (Two tail) | Decision |
|---|---|---|---|---|---|
| AKWA IBOM | 1.660 | 22 | 0.05 | 1.725 | Cannot Reject Ho |
| BAYELSA | 0.295 | 22 | 0.05 | 1.725 | Cannot Reject Ho |
| CROSS RIVER | 0.420 | 22 | 0.05 | 1.725 | Cannot Reject Ho |
| DELTA | 0.523 | 22 | 0.05 | 1.725 | Cannot Reject Ho |
| EDO | 0.406 | 22 | 0.05 | 1.725 | Cannot Reject Ho |
| LAGOS | 0.429 | 22 | 0.05 | 1.725 | Cannot Reject Ho |
| OGUN | 0.569 | 22 | 0.05 | 1.725 | Cannot Reject Ho |
| ONDO | 1.181 | 22 | 0.05 | 1.725 | Cannot Reject Ho |
| RIVERS | 0.511 | 22 | 0.05 | 1.725 | Cannot Reject Ho |

Hence, there is no significant statistical difference in mean of seasonal rainfall distribution between the NIMET and CRU data at a significance level of 0.05.

To determine the suitability/ adequacy of the CRU rainfall and temperature data for sixty-one years (1956-2017) for further analysis, the data were further subjected to validation with observed NIMET data covering the same period by comparison of their descriptive statistics using simple t test and the goodness of fit criterion such as Coefficient of Determination ($R^2$), adjusted-$R^2$, Mallows' Process Capability ($C_p$), Kendall Tau (K tau), Root Mean Squared (RSR) and Mean Absolute Percentage Error (MAPE). This is shown in Table 7 and 8 for rainfall and temperature respectively.

**Table 7:** Comparison between NIMET and CRU data for rainfall

| State | $R^2$ | Rating | Adj $R^2$ | Rating | K tau | Rating | RSR | Rating | MAPE | Rating | Cp | Rating |
|---|---|---|---|---|---|---|---|---|---|---|---|---|
| Akwa Ibom | 0.924 | V.good | 0.901 | V.good | 0.782 | V.good | 0.315 | V.good | 18.6 | Good | 2 | OK |
| Bayelsa | 0.931 | V.good | 0.907 | V.good | 0.782 | V.good | 0.302 | V.good | 19.2 | Good | 2.8 | OK |
| Cross River | 0.935 | V.good | 0.912 | V.good | 0.801 | V.good | 0.293 | V.good | 30.3 | R | 2 | OK |
| Delta | 0.865 | V.good | 0.83 | V.good | 0.818 | V.good | 0.41 | V.good | 66 | I | 2 | OK |
| Edo | 0.890 | V.good | 0.867 | V.good | 0.709 | V.good | 0.369 | V.good | 23.48 | R | 2 | OK |
| Lagos | 0.774 | V.good | 0.709 | V.good | 0.709 | V.good | 0.539 | Good | 44.79 | R | 2 | OK |
| Ogun | 0.888 | V.good | 0.850 | V.good | 0.745 | V.good | 0.381 | V.good | 50 | R | 2 | OK |
| Ondo | 0.882 | V.good | 0.869 | V.good | 0.782 | V.good | 0.362 | V.good | 15.37 | Good | 2 | OK |
| River | 0.927 | V.good | 0.903 | V.good | 0.818 | V.good | 0.312 | V.good | 18.17 | Good | 2 | OK |

R = Reasonable, I = Inaccurate, OK = capable or Reliable

**Table 8:** Comparison between NIMET and CRU data for temperature

| State | $R^2$ | Rating | Adj $R^2$ | Rating | K tau | Rating | RSR | Rating | MAPE | Rating | Cp | Rating |
|---|---|---|---|---|---|---|---|---|---|---|---|---|
| Akwa Ibom | 0.933 | V.good | 0.925 | V.good | 0.927 | V.good | 0.272 | V.good | 0.679 | H | 2 | OK |
| Bayelsa | 0.954 | V.good | 0.949 | V.good | 0.891 | V.good | 0.225 | V.good | 0.588 | H | 2 | OK |
| Cross River | 0.973 | V.good | 0.97 | V.good | 0.964 | V.good | 0.173 | V.good | 0.523 | H | 2 | OK |
| Delta | 0.949 | V.good | 0.94 | V.good | 0.891 | V.good | 0.227 | V.good | 0.659 | H | 2 | OK |
| Edo | 0.976 | V.good | 0.973 | V.good | 0.855 | V.good | 0.165 | V.good | 0.634 | H | 2 | OK |
| Lagos | 0.931 | V.good | 0.923 | V.good | 0.823 | V.good | 0.227 | V.good | 0.987 | H | 2 | OK |
| Ogun | 0.946 | V.good | 0.94 | V.good | 0.844 | V.good | 0.244 | V.good | 0.772 | H | 2 | OK |
| Ondo | 0.883- | V.good | 0.87 | V.good | 0.771 | V.good | 0.36 | V.good | 1.379 | H | 2 | OK |
| River | 0.905 | V.good | 0.922 | V.good | 0.855 | V.good | 0.278 | V.good | 0.623 | H | 2 | OK |

H = Highly Reliable, OK = capable or Reliable

Tables 7 and 8 shows the values of $R^2$ obtained from the comparison. They range from 0.935 (Cross River) to 0.774 (Lagos) for rainfall and from 0.976 (Edo) to 0.883 (Ondo) for temperature. Following Table 2, the performance rating of $R^2$ is very good as $0.75 < R^2 \leq 1$. With the minimum value of 0.77788 for both rainfall and temperature, the performance rating of $R^2$ in validating the CRU data is very good.

The results of this validity analysis indicate that the CRU data obtained is very reliable and thus justified their use for the further analysis carried out in the study.

RMSE close to zero and R-Square value approaching 1 is indicative of high accuracy between observed and predicted values. Based on a rule of thumb, it can be said that RMSE values between 0.2 and 0.5 show that the model can relatively predict the data accurately.

$C_{p,}$ processes capability sometimes referred to as *Mallows' $C_p$*, shows whether the distribution can potentially fit inside the specification. $C_p$ is an index used to assess the width of the process spread in comparison to the width of the specification. It is calculated by dividing the allowable spread by the actual spread. The allowable spread is the difference between the upper and lower specification limits. The actual spread is 6 times the estimated standard deviation.

$$C_p = (USL - LSL)/6\sigma \quad (16)$$

Where USL and LSL are upper and lower specification limits, σ estimated standard deviation.

*3.3. Normality tests*

Three common normality tests were carried out, namely the Shapiro Wilk Test (SWT), D`Agostino-Pearson Test, and Skewness Test. The results are presented in Tables 9 to 12. When the *p*-value is larger than the significance level, the decision is to fail to reject the null hypothesis because we do not have enough evidence to conclude that our data do not follow a normal distribution. The results indicate that the three normality tests were in agreement that rainfall series follow a normal distribution. Normal distribution assumption is very crucial for the reliability of results especially for parametric tests. The tables show values of test statistics, the *p*-values, and significant level alpha = 0.05. It also provided for confirmation of normality as it indicated YES. To determine whether the data do not follow a normal distribution, we compare the p-value to the significance level. Usually, a significance level (denoted as α or alpha) of 0.05 works well. A significance level of 0.05 indicates that the risk of concluding the data do not follow a normal distribution—when the data do follow a normal distribution—is 5%.

**Table 9:** Results of test for normality of spatial rainfall data (normality acceptable if -0.59 < s < 0.59)

| Location | SHAPIRO WILK TEST (SWT) | | | | D`AGOSTINO-PEARSON TEST | | | | SKEWNESS TEST | | |
|---|---|---|---|---|---|---|---|---|---|---|---|
| | W STAT | P value | Alpha | normal | DA STAT | P value | alpha | normal | S | alpha | |
| Akwa Ibom | 0.93868 | 0.50511 | 0.05 | YES | 02.0182 | 0.36455 | 0.05 | YES | -0.01484 | 0.05 | YES |
| Bayelsa | 0.91194 | 0.25706 | 0.05 | YES | 1.9496 | 0.3773 | 0.05 | YES | 0.067378 | 0.05 | YES |
| Cross River | 0.92222 | 0.33758 | 0.05 | YES | 2.438 | 0.2955 | 0.05 | YES | -0.0152 | 0.05 | YES |
| Delta | 0.92559 | 0.36799 | 0.05 | YES | 2.2248 | 0.3287 | 0.05 | YES | 0.037337 | 0.05 | YES |
| Edo | 0.92490 | 0.36169 | 0.05 | YES | 1.985 | 0.3706 | 0.05 | YES | -0.09218 | 0.05 | YES |
| Lagos | 0.96089 | 0.7828 | 0.05 | YES | 0.5076 | 0.7758 | 0.05 | YES | 0.504882 | 0.05 | yes |
| Ogun | 0.94230 | 0.54799 | 0.05 | YES | 1.9859 | 0.3704 | 0.05 | YES | 0.06751 | 0.05 | YES |
| Ondo | 0.94946 | 0.63700 | 0.05 | YES | 1.4617 | 0.4815 | 0.05 | YES | 0.055487 | 0.05 | YES |
| Rivers | 0,92684 | 0.37975 | 0.05 | YES | 2.2976 | 0.3170 | 0.05 | YES | 0.030139 | 0.05 | YES |

**Table 10:** Results of test for normality of spatial temperature data (normality acceptable if -0.59 < s< 0.59)

| Location | SHAPIRO WILK TEST (SWT) | | | | D`AGOSTINO-PEARSON TEST | | | | SKEWNESS TEST | | |
|---|---|---|---|---|---|---|---|---|---|---|---|
| | W STAT | P-value | Alpha (α) | Normal (p>α) | DA STAT | P value | alpha | Normal (p>α) | S | alpha | |
| Akwa Ibom | 0.94954 | 0.66381 | 0.05 | YES | 1.2855 | 0.5258 | 0.05 | YES | -0.32776 | 0.05 | YES |
| Bayelsa | 0.91966 | 0.3158 | 0.05 | YES | 2.5974 | 0.2729 | 0.05 | YES | -0.43492 | 0.05 | YES |
| Cross River | 0.95524 | 0.71132 | 0.05 | YES | 0.9932 | 0.6086 | 0.05 | YES | -0.33311 | 0.05 | YES |
| Delta | 0.9069 | 0.2242 | 0.05 | YES | 2.7698 | 0.2503 | 0.05 | YES | -0.45921 | 0.05 | YES |
| Edo | 0.9123 | 0.2594 | 0.05 | YES | 2.756 | 0.2520 | 0.05 | YES | -0.40085 | 0.05 | YES |
| Lagos | 0.9080 | 0.23108 | 0.05 | YES | 3.009 | 0.2221 | 0.05 | YES | -0.43246 | 0.05 | YES |
| Ogun | 0.9136 | 0.2689 | 0.05 | YES | 2.899 | 0.2346 | 0.05 | YES | -0.38228 | 0.05 | YES |
| Ondo | 0.9143 | 0.274 | 0.05 | YES | 2.864 | 0.2387 | 0.05 | YES | -0.36835 | 0.05 | YES |
| Rivers | 0.9593 | 0.7775 | 0.05 | YES | 1.094 | 0.5787 | 0.05 | YES | -0.34561 | 0.05 | YES |

The five tests scored $H_0$ for Edo, Lagos, Ogun, and Ondo state Rainfall data and $H_a$ for Cross Rivers and Rivers States rainfall data. Three tests scored $H_a$ and two tests scored $H_0$ for Akwa Ibom rainfall

data. The average score could be considered as $H_a$. Also, three tests scored $H_0$ and two tests scored $H_a$ for Bayelsa and Delta States rainfall data. The average score could be considered as $H_0$.

**Table 11a:** Summary of homogeneity test for rainfall data (Pettit's test and SNHT)

| State | PETTIT'S TEST | | | | SNHT | | | |
|---|---|---|---|---|---|---|---|---|
| | K-Value | Year | P-Value | T | To-Value | Year | P-Value | T |
| Akwa Ibom | 321 | 1971 | 0.17 | Ho | 9.894 | 1969 | 0.020 | Ha |
| Bayelsa | 243 | 1969 | 0.62 | Ho | 9.39 | 2011 | 0.032 | Ha |
| Cross River | 618 | 198 | 0.00 | Ha | 21.44 | 1984 | 0.000 | Ha |
| Delta | 258 | 1980 | 0.48 | Ho | 8.917 | 2012 | 0.038 | Ha |
| Edo | 149 | 2011 | 0.32 | Ho | 3.429 | 2011 | 0.618 | Ho |
| Lagos | 278 | 1970 | 0.36 | Ho | 7.883 | 1970 | 0.157 | Ho |
| Ogun | 192 | 1986 | 0.83 | Ho | 4.131 | 1970 | 0.414 | Ho |
| Ondo | 244 | 1986 | 0.54 | Ho | 3.033 | 1958 | 0.701 | Ho |
| Rivers | 466 | 1980 | 0.00 | Ha | 14.12 | 1969 | 0.002 | Ha |

**Table 11b:** Summary of homogeneity test for rainfall data (Bush and Von Neumann test)

| State | BUISHAND TEST | | | | VON NEUMANN | | | | | |
|---|---|---|---|---|---|---|---|---|---|---|
| | Q-Value | Year | P-Value | T | R-Value | P-Value | T | N | P-Value | T |
| Akwa Ibom | 10.303 | 1971 | 0.04 | Ha | 11.94 | 0.065 | Ho | 1.26 | 0.002 | Ha |
| Bayelsa | 6.616 | 2011 | 0.369 | Ho | 8.227 | 0.547 | Ho | 1.42 | | Ha |
| Cross River | 18.04 | 1984 | 0.000 | Ha | 18.043 | 0.000 | Ha | 0.000 | 0.00 | Ha |
| Delta | 7.669 | 1999 | 0.216 | Ho | 9.617 | 0.238 | Ho | 1.284 | 0.002 | Ha |
| Edo | 3.998 | 20.11 | 0.895 | Ho | 7.572 | 0.669 | Ho | 1.675 | 0.10 | Ho |
| Lagos | 9.276 | 1970 | 0.062 | Ho | 11.842 | 0.028 | Ha | 1.679 | 0.088 | Ho |
| Ogun | 6.715 | 1970 | 0.346 | Ho | 10.151 | 0.193 | Ho | 1.618 | 0.061 | Ho |
| Ondo | 5.835 | 1986 | 0.509 | Ho | 8.625 | 0.452 | Ho | 1.655 | 0.098 | Ho |
| Rivers | 13.33 | 1980 | 0.002 | Ha | 13.899 | 0.011 | Ha | 1.124 | 0.00 | Ha |

**Table 12a:** Summary of homogeneity test for temperature data

| Location | PETTIT'S TEST | | | SNHT | | |
|---|---|---|---|---|---|---|
| | K-Value | Year | Trend | To-Value | Year | Trend |
| Akwa Ibom | 652.00 | 1980 | Ha | 23.011 | 1980 | Ha |
| Bayelsa | 708.00 | 1980 | Ha | 27.490 | 1980 | Ha |
| Cross River | 648.00 | 1986 | Ha | 22.561 | 1980 | Ha |
| Delta | 718.00 | 1980 | Ha | 28.073 | 1980 | Ha |
| Edo | 708.00 | 1980 | Ha | 27.287 | 1980 | Ha |
| Lagos | 630.00 | 1980 | Ha | 20.504 | 1980 | Ha |
| Ogun | 642.00 | 1980 | Ha | 21.647 | 1980 | Ha |
| Ondo | 684.00 | 1980 | Ha | 24.723 | 1980 | Ha |
| Rivers | 688.00 | 1980 | Ha | 25.900 | 1980 | Ha |

**Table 12b:** Summary of homogeneity test for temperature data

| Location | BUISHAND TEST | | | VON NEUMANN | | | |
|---|---|---|---|---|---|---|---|
| | Q-Value | Year | Trend | R-Value | Trend | N | |
| Akwa Ibom | 18.357 | 1980 | Ha | 18.357 | Ha | 1.078 | Ha |
| Bayelsa | 20.064 | 1980 | Ha | 20.064 | Ha | 0.995 | Ha |
| Cross River | 18.177 | 1980 | Ha | 18.177 | Ha | 1.100 | Ha |
| Delta | 20.278 | 1980 | Ha | 20.276 | Ha | 0.992 | Ha |
| Edo | 19.990 | 1980 | Ha | 19.990 | Ha | 1.001 | Ha |
| Lagos | 17.328 | 1980 | Ha | 17.418 | Ha | 1.134 | Ha |
| Ogun | 17.805 | 1980 | Ha | 17.886 | Ha | 1.096 | Ha |
| Ondo | 19.027 | 1980 | Ha | 19.027 | Ha | 1.016 | Ha |
| Rivers | 19.475 | 1980 | Ha | 19.475 | Ha | 0.978 | Ha |

Test interpretations of rainfall data continued

| Case 1 | Case 2 |
|---|---|
| $H_0$: Data are Homogeneous<br>$H_a$: There is a date at which there is a change in the data. As the computed *p*-value is greater than the significance level alpha = 0.05, one cannot reject the null hypothesis $H_0$. We have to accept the null hypothesis that the data is homogeneous | $H_0$: Data are Homogeneous<br>$H_a$: There is a date at which there is a change in the data. As the computed *p*-value is lower than the significance level alpha = 0.05, one should reject the null hypothesis $H_0$, and accept the alternate hypothesis $H_a$ that the data is inhomogeneous |

3.3.1. Test interpretations of temperature data

The five tests scored $H_a$ for all the States in the study area for temperature data

$H_0$: Data are Homogeneous
$H_a$: There is a date at which there is a change in the data

As the computed *p*-value (<0.0001) is lower than the significance level alpha = 0.05, one should reject the null hypothesis $H_0$, and accept the alternate hypothesis $H_a$ that the data is not homogeneous.

CRU TS is not specifically homogeneous. Some National Meteorological Agencies (NMAs) homogenize their station observations, either before release or at a later stage (requiring a re-release). Therefore, many CRU TS observations have been homogenized (and also quality controlled) within each country. However, performing additional homogenization on the CRU TS databases would be complicated and not completely possible because of elements of the process, such as partly synthetic variables and the use of published climatology. The result obtained from homogeneity test is presented in Figures 2a to 2j and Table 13.

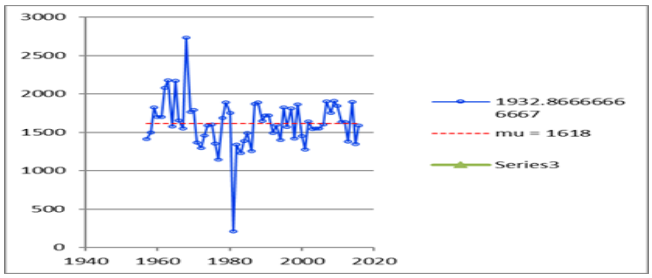


**Figure 2a:** Lagos State rainfall Petitt test

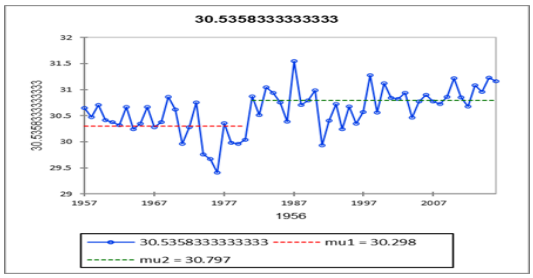


**Figure 2b:** Lagos State temperature Pettitt Test

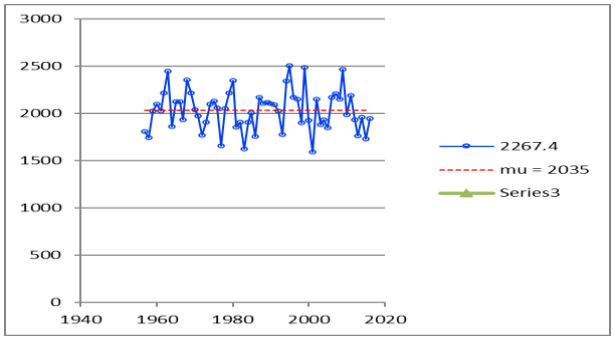


**Figure 2c:** Edo State rainfall Pettitt test

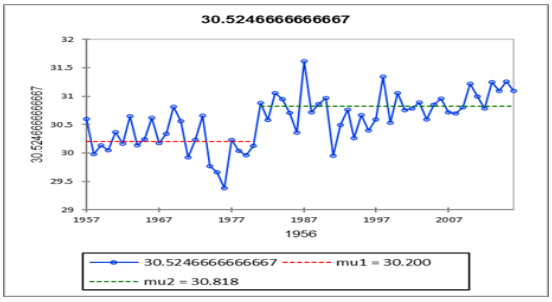


**Figure 2d:** Edo State temperature Pettitt test

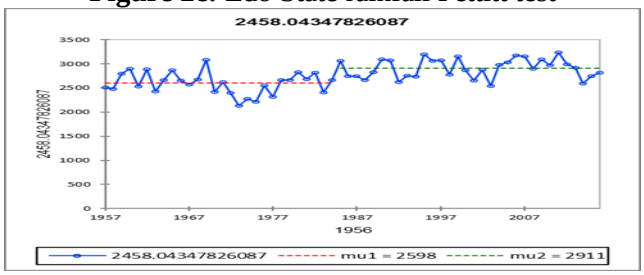


**Figure 2e:** Cross River State rainfall Petitt test

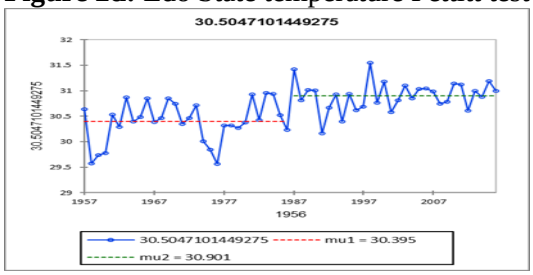


**Figure 2f:** Cross River State temperature Pettitt test

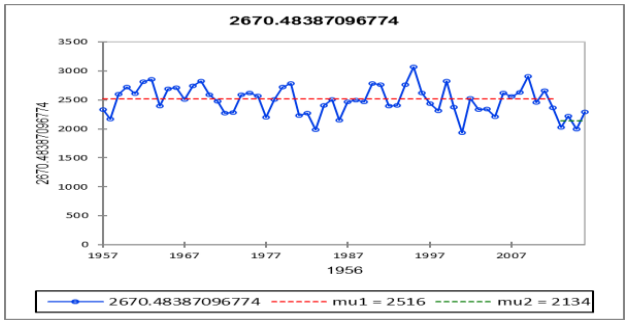


**Figure 2g:** Delta State rainfall SNHT test

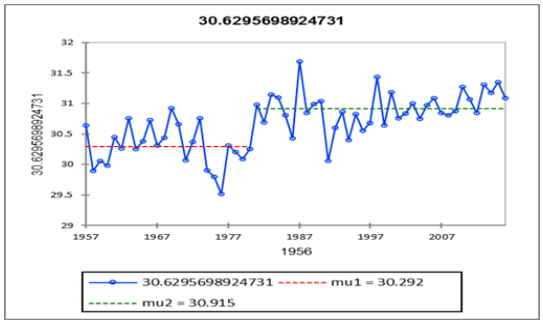


**Figure 2h:** Delta State temperature SNHT test

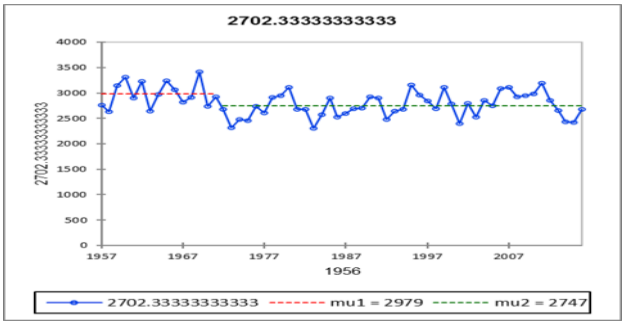


**Figure 2i:** Akwa Ibom State rainfall Buishand's test

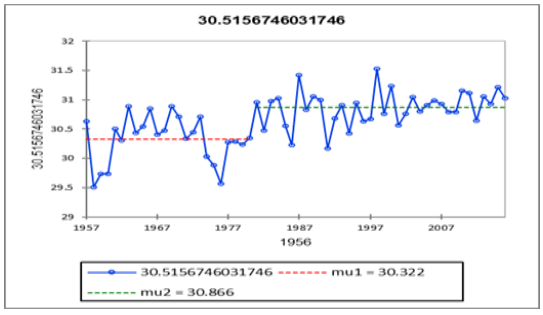


**Figure 2j:** Akwa Ibom State temperature Buishand's test

**Table 13:** Summary of abrupt change result obtained from homogeneity test (Figure 2a to 2j)

| State | Year of abrupt change for rainfall | Year of abrupt change for temperature |
|---|---|---|
| Akwa Ibom | 1971 | 1980 |
| Bayelsa | 2011 | 1980 |
| Cross River | 1984 | 1986 |
| Delta | 1980 | 1980 |
| Edo | 2011 | 1980 |
| Lagos | 1970 | 1980 |
| Ondo | 1970 | 1980 |
| Ogun | 1986 | 1980 |
| Rivers | 1980 | 1980 |

## 4.0. Conclusion

The five homogeneity tests conducted indicated that CRU rainfall data for Bayelsa, Delta Edo, Lagos, Ogun, and Ondo states are homogeneous those for Akwa Ibom, Cross Rivers, and Rivers States are inhomogeneous. Also, the five homogeneity tests conducted indicated that CRU temperature data for all the States in the study area are inhomogeneous.

National Meteorological Agencies (NMAs) homogenize their station observations, either before release or at a later stage (requiring a re-release). Therefore, many CRU TS observations have been homogenized (and also quality controlled) within each country. Hence, inhomogeneity observed may not be due to data quality but to climate variability and climate change. For temperature, the year of significant abrupt change was likely in 1980 where there were breakpoints. The study also indicated that 1980 was the driest year in Lagos state.

## References

Agha, O. M. A., Bağçacı, Ç. S. and Şarlak, N. (2017). Homogeneity analysis of precipitation series in North Iraq. *IOSR Journal of Applied Geology and Geophysics*, 5, pp. 57–63.

Alexandersson, H. and Moberg, A. (1997). Homogenization of Swedish Temperature Data Part I: Homogeneity Test for Linear Trends. *International Journal of Climatology*, 17, pp. 25–34.

Al-Ghazali, N. O. S. and Alawadi, D. A. H. (2014). Testing the Homogeneity Of Rainfall Records for Some Stations in Iraq. *International Journal of Civil Engineering and Technology (IJCIET)*, 5, pp. 76-87.

Buishand, T. A. (1982). Some Methods for Testing the Homogeneity of Rainfall Records. *Journal of Hydrology*, 58, pp. 11-27.

Costa, A. C. and Soares, A. (2009). Homogenization of climate data: review and new perspectives using geostatistics. *Math. Geosci.* 41, pp. 291–305.

D' Agostino, R. and Pearson, E. S. (1973). Test for departure from normality: Empirical results for the distributions of b2and -4131. *Biometrika*, 60, pp. 613-622.

Karamouz, M., Szidarovszky, F. and Zahraie, B. (2003). Water Resources Systems Analysis, Lewis Publishers, pp. 159-160.

Klein, T. A. M., Zwiers, F. W. and Zhang, X. (2009). Guidelines on Analysis Adaptation. Geneva: WMO.

Kidd, C., Becker, A., Huffman, G. J., Muller, C. L., Joe, P., Skofronick-Jackson, G. and Kirschbaum, D. B. (2017). So, how much of the Earth's surface is covered by rain gauges? *Bulletin of the American Meteorological Society*, 98, pp. 69–78.

Kuruk, P., (2004): Customary Water Laws and Practices: Nigeria. Available at: http://www.fao.org/legal/advserv/FAOIUCNcs/Nigeria.pdf

Ma, Z., Kang, S., Zhang, L., Tong, L. and Su, X. (2008). Analysis of impacts of climate variability and human activity on streamflow for a river basin in the arid region of northwest China. *Journal of Hydrology*, 352**,** 239-249.

Martínez, M. D., Serra, C., Burgueño, A. and Lana, X. (2009). Time Trends of Daily Maximum and Minimum Temperatures in Catalonia (Ne Spain) for the Period 1975–2004. *International Journal of Climatology*,30(2), pp. 267–290.

Mitchell, T. D. and Jones, P. D. (2005). An Improved Method of Constructing A Database Of Monthly Climate Observations And Associated High-Resolution Grids. *International Journal Of Climatology Int. J. Climatol.* 25, pp. 693–712.

Nnamchi, H. C., Anyadike, R. N. C. and Emeribe, C. N. (2008). Spatial patterns of the Twentieth Century mean seasonal precipitation over West Africa. *Nigeria Journal of Space Research*, 6, pp 89-101.

Nwilo, P. C. and Badejo, O. T. (2006). Impacts and Management of Oil Spill Pollution along with the Nigerian Coastal Areas. *Administering Marine Spaces: International Issues*, 119, pp. 1-15.

Sarojini, B. B., Stott, P. A. and Black, E. (2016). Detection and attribution of human influence on regional precipitation. *Nat. Clim. Change*, 6(7), pp. 669–675.

Shapiro, S. S. and Wilk, M. B. (1965). An analysis of variance test for normality (complete samples). *Biometrika*, 52, pp. 591–611.

Smadi, M. M. and Zghoul, A. (2006). A Sudden Change in Rainfall characteristics in Amman, Jordan during the Mid 1950s. *Am J Environ Sci* 2(3), pp. 84–91.

Wijngaard, J. B., Klein Tank, A. M. G. and Können, G. P. (2003). Homogeneity of 20th Century European Daily Temperature and Precipitation Series 23, pp. 679–692.

Yozgatligil, C., Purutcuoglu, V., Yazici, C. and Batmaz, I. ( 2015). The validity of homogeneity tests for meteorological time series data: a simulation study, In Proceedings of the 58th World Statistics Congress (ISI2011), Dublin, Ireland. . http://2011.isiproceedings.org/ papers/950636.pdf (accessed 27 March 2015).

**Cite this article as:**
Agbonaye A. I. and Izinyon O. C. 2021. Evaluating the Quality of Spatial Data for the Analysis of Climate Variability in the Coastal Region of Nigeria. *Nigerian Journal of Environmental Sciences and Technology*, 5(1), pp. 76-90. https://doi.org/10.36263/nijest.2021.01.0236

Nigerian Journal of Environmental Sciences and Technology (NIJEST)

www.nijest.com

ISSN (Print): 2734-259X | ISSN (electronic): 2734-2603

Vol 5, No. 1 March 2021, pp 91 - 101

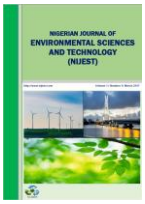

# Storage Moduli of *in situ* Polymerised and Melt Extruded PA6 Graphite (G) Composites

Umar M.[1], Ofem M. I.[2,]*, Anwar A. S.[1] and Usman M. M.[3]

[1]Department of Chemical Engineering, Kaduna Polytechnic, Kaduna State, Nigeria

[2]Department of Mechanical Engineering, Cross River University of Technology, Calabar, Nigeria

[3]Department of Chemical Engineering, Federal Polytechnic, Nasarawa, Nigeria

Corresponding Author: *michaeliofem@crutech.edu.ng

https://doi.org/10.36263/nijest.2021.01.0252

## ABSTRACT

*Four PA6/graphite (G) composites systems were made. Two in situ polymerisation equivalent in mixing strain and two melt extrusion of equivalent processing strain. The effective modulus of the carbons, room temperature storage modulus and storage modulus at 80 ºC were evaluated using Dynamic Mechanical and thermal Analysis (DMTA). Melt processing, was employed to make PA6/carbon composite systems over a range of loadings of Graphite (G) and Graphite Nano Platelets (GNP) fillers. Melt extrusion was carried out using 100/6 processing condition, which indicates an extrusion screw rotation frequency of 100 rpm applied for 6 minutes (min) and 200/3 processing conditions, of 200 rpm for 3 min. For in situ polymerised systems G and GNP dispersion was made using two similar conditions designated as 40/10 and 20/20. Here, 40/10 indicates that sonication amplitude of 40% was applied for 10 min, whereas in the 20/20 conditions, amplitude of 20% was applied for 20 min. For in situ Nano P INP 40/10 systems weak interaction between PA6 and GNP is indicated by the very low modulus enhancement above glass transition temperature ($T_g$). The modulus behaviour shows that the reinforcement provided by GNP is not significant relative to unfilled PA6, despite the low loading levels. A similar, but less pronounced, behaviour is observed for INP 20/20 system. Effective modulus for the in situ polymerised systems INP 40/10, was 4.8 GPa. Due to the low loading level of GNP used and the better reaction rates, an extrapolated modulus of 22.4 GPa is obtained in the INP 20/20 system. For G200/3 and G100/6 the trend of increasing modulus with GNP loading is not followed exactly. On all levels of loading, the relative modulus values of the INP 20/20 system are higher than those of the 40/10 system, a reflection of retention or improvement in the aspect ratio of the GNP due to less intensive sonication.*

**Keywords:** In situ-polymerisation, Melt-extrusion, Effective-modulus, Storage-modulus

## 1.0. Introduction

Carbon can be used in different forms. Carbon Fibres, micro-particulates and nano-particulates are the common forms of carbon. To improve existing properties of carbon or develop an entire new properties, different processing techniques; melt, solution or *in situ* polymerisation can be applied (Keledi *et al.,* 2012; Sengupta *et al.,* 2011; Supova *et al.,* 2011). The size-scale and structure of a particulate carbon are very important as these control the inherent properties. The dimensionality of the particulate carbon determines the structure in addition to whether it is pristine or modified. Different dimensional (1, 2 or 3) structures of Particulate carbon fillers create room for wide range of alternatives for making carbon composites. Particulate carbons thus, provide a variety of carbon fillers suitable for polymer composites and whose basic building block is the graphene sheet.

The selection of an appropriate processing technique to make particulate carbon composites using well dispersed or percolated carbon filler will lead to desired properties. Properties such as light, weight and toughness may be maintained in addition to the good mechanical and electrical conductivity. The processing techniques determines the state of the filler in the composite following compounding; including dispersion - how well the filler is reduced down to its primary particles and

distribution - the distance between neighbouring filler particles within the composite and how well the positions of the particles are randomised. Poor compounding frequently lead to agglomeration of filler displaying lower aspect ratio and surface area to volume ratio.

Graphite (G), whether synthetic or natural, is mostly polycrystalline or granular. Due to anisotropy (Howe, 1952) properties graphite exhibits metallic and non-metallic properties concurrently (Wissler, 2006). Howe (1952) described G as highly polycrystalline and anisotropic due to the difference between covalently bonded in-plane carbon networks and out-of-plane weak van der Waals forces (Sengupta *et al.,* 2011*).* This makes it possible for small molecules to intercalate into the G galleries (Celzard *et al*., 2005) and also results in G being non-conductive out-of-plane since the layers in the stack are held only by weak van der Waals forces (Howe, 1952). The in-plane properties of G makes it stronger than diamond (Sengupta *et al*., 2011), semi-conductive, as well as thermally and electrically conductive.

This is why G is used for making polymer composites that are electrically (Clingerman 2001; Clingerman *et al*., 2002) and thermally (Weber *et al*., 2003; Miller *et al*., 2006) conductive. In contrast, the weak attraction out-of-plane has produced wide application for G as a solid lubricant. Therefore, polymer/G composites are specifically used in abrasion related applications regarding wear (Kang *et al*., 2003), tribology (Horský *et al*., 2001) and in evaluating performance of nanosized particulate carbons in polymer composites where G mainly serves as a control (Ramanathan *et al*., 2007; Debelak and Lafd, 2007). Despite the low cost of G, its limited use in advanced polymer composites perhaps has to do with its high density, 2.26g/cm$^3$ (Sengupta *et al*., 2011) and very low aspect ratio (1.68-1.7) (Heiser *et al*., 2004) which may necessitate the use of higher loadings.

In the graphene family, graphite nano platelets (GNP) is widely employed because of its 2D structure, reasonably high aspect ratio (about 1500 (Kalaitzidou *et al*., 2007; Fukushima *et al*., 2006), high surface area (theoretically between 2630-2965m$^2$/g (Viculis *et al*., 2005) and chain segment constraining ability. Due to this, GNP have the potential to improve or induce multiple functions in polymers, such as a combination of improved barrier, mechanical, thermal and electrical functions, whilst at the same time retaining light weight and transparency (Li *et al*., 2011). However, the transfer of these properties to the matrix depends strongly on dispersion level, interaction and maintaining the size and shape of the GNP after processing (Sadasivuni *et al*., 2014). It is also possible to improve the aspect ratio of GNP by further exfoliation using techniques such as intercalation followed by polymerisation, oxidation, heat treatments and sonication. This will make GNP production cost effective compared to other nanocarbon fillers (Li *et al*., 2011).

Two graphitic platelet-structured carbon fillers were used in this research, graphite (G) an example of micro-scale filler, and graphite nanoplatelets, (GNP) comparative nano-scale filler. The size scale of the fillers is considered in fixing the level of loading with that of the GNP-based nanocomposites being an order of magnitude lower than that of the G-based microcomposites. This is considered to be a better basis for comparison against the traditional (Ramanathan *et al*., 2007) same-weight comparison. The same weight comparison disregards the scale of interaction occurring in these diverse systems due to the significant disparity in surface area and aspect ratio between the two fillers. The disparity has significant implications for polymer/filler interactions and the property changes expected relative to the unfilled polymer matrix. The class of polymer matrix available to be selected from include the thermosets, elastomers or thermoplastics (amorphous or semi-crystalline) but this study is concerned with polyamide-6 (PA6)/particulate carbon composites. The semi-crystalline nature of PA6 and its strong intermolecular hydrogen bonding confers on it properties which suits applications such fibre, film and injection mouldings for engineering applications. In addition, its formation via ring-opening polymerisation provides the opportunity for processes such as casting, reaction injection moulding and vacuum-infusion of continuous fibre composites (all of which provide opportunity to construct complex shapes directly) (Van-Rijswijk *et al*., 2006).

Melt processing, which still maintains a lead in the commercial production of polymeric composites (Hussain *et al*., 2006), was employed using a twin-screw extruder, TSE, (Thermo-Haake Minilab) to make PA6/carbon composite systems over a range of loadings. Melt extrusion was carried out using 100/6 processing condition, which indicates an extrusion screw rotation frequency of 100 rpm applied for 6 minutes (min) and 200/3 processing conditions, of 200 rpm for 3 min. For *in situ* polymerised

systems G and GNP dispersion was made using two similar conditions designated as 40/10 and 20/20. Here, 40/10 indicates that sonication amplitude of 40% was applied for 10 min, whereas in the 20/20 conditions, amplitude of 20% was applied for 20 min. Comparing the acquired properties between melt extruded and *in situ* polymerised polymer/filler composites is not new (Tung *et al*., 2005), but here the comparisons are more extensive.

## 2.0. Methodology

### *2.1. Materials*

Pristine commercial grade PA6 was donated by Akulun Germany. The monomer Epsilon Caprolactam ($C_6H_{11}NO$, coded as EC) was purchased from Sigma-Aldrich, with purity level of 99% and a molecular weight of 113.16. Pristine PA6 and EC were vacuum dried overnight at 50°C before usage which adequately removed moisture. Methyl Magnesium Bromide (coded as MMB, molecular weight 119.26,) is a Grignard catalyst precursor which forms the catalyst, (Caprolactam Magnesium Bromide (CMB)) *in situ*, was purchased Fisher Scientific as a 100ml bottle containing a 3.0M solution of MMB in diethyl ether. Activator or co-catalyst, is a mono-functional Nacetylcaprolactam ($C_8H_{13}NO_2$, coded as NAC), supplied by Sigma-Aldrich with purity of 99% and molecular weight of 155.19. Graphite Filler: Synthetic graphite, (coded as G) is $\leq 2\mu m$ in particle size was supplied by Sigma-Aldrich. Graphite Nano-Platelets: GNP-15, (coded as GNP) with surface area $107\pm7 m^2/g$, diameter of 15µm, aspect ratio of 1500 and density of $2g/cm^3$ was bought from XG-Sciences, UK. Prior to use G and GNP were kept overnight in an oven at 160°C.

### *2.2. Method*

Details of experimental procedure for making the composites can be found elsewhere (Umar *et al*., 2020). Since storage modulus is obtained using Dynamic Mechanical and thermal Analysis (DMTA). DMTA is used to investigate the viscoelastic behaviour of polymers and composites by subjecting the test specimens to a dynamic sinusoidal stress or strain within a temperature range, a time frame or a frequency range. Melt processing, was employed to make PA6/carbon composite systems over a range of loadings of G and GNP fillers. Melt extrusion was carried out using 100/6 processing condition, which indicates an extrusion screw rotation frequency of 100 rpm applied for 6 minutes (min) and 200/3 processing conditions, of 200 rpm for 3 min. For *in situ* polymerised systems G and GNP dispersion was made using two similar conditions designated as 40/10 and 20/20. Here, 40/10 indicates that sonication amplitude of 40% was applied for 10 min, whereas in the 20/20 conditions, amplitude of 20% was applied for 20 min. A TA Instruments Q800 dynamic mechanical analyser was used to determine the thermo-mechanical responses. Specimens (approximately 5.00 x 1.55 x 17.50mm) were cut from within the gauge length of injection moulded dog-bones made using Haake Minilab injection moulding machine. At least 3 specimens were tested for each material. The specimens were tested using single cantilever mode and applying a Poisson's ratio of 0.35 for PA6 and its composites. The tests were carried out using a temperature ramp/frequency sweep in multi-frequency- strain operation mode, at a strain rate of 0.2%, and a temperature ramp of 3° C/min within the region of 0-200°C. Five carbon loadings were made at equivalent incremental steps. For the micro composites, a G loading of 5-25 Wt.% was used and for GNP composites, 0.5-2.5 Wt.% were used.

## 3.0. Results and Discussion

### *3.1. Storage modulus of the INP 40/10 and INP 20/20 systems*

Weak interaction between PA6 and GNP is indicated by the very low modulus enhancement above $T_g$ as can be seen in Figure 1a and 1b and from Table 1 (modulus at 80°C). Although it is understood that the matrix-filler interaction is weak this may be compensated to some extent by the large surface area available with GNP-15 (Keledi *et al*., 2012), the wetting EC provides on GNP and any intercalation of EC between the carbon sheets (as established for EG (Pan *et al*., 2000). However, the modulus behaviour in Figure 1a shows that the reinforcement provided by GNP is not significant relative to unfilled PA6, although the loading levels are low. A similar, but less pronounced, behaviour is shown in Figure 1b.

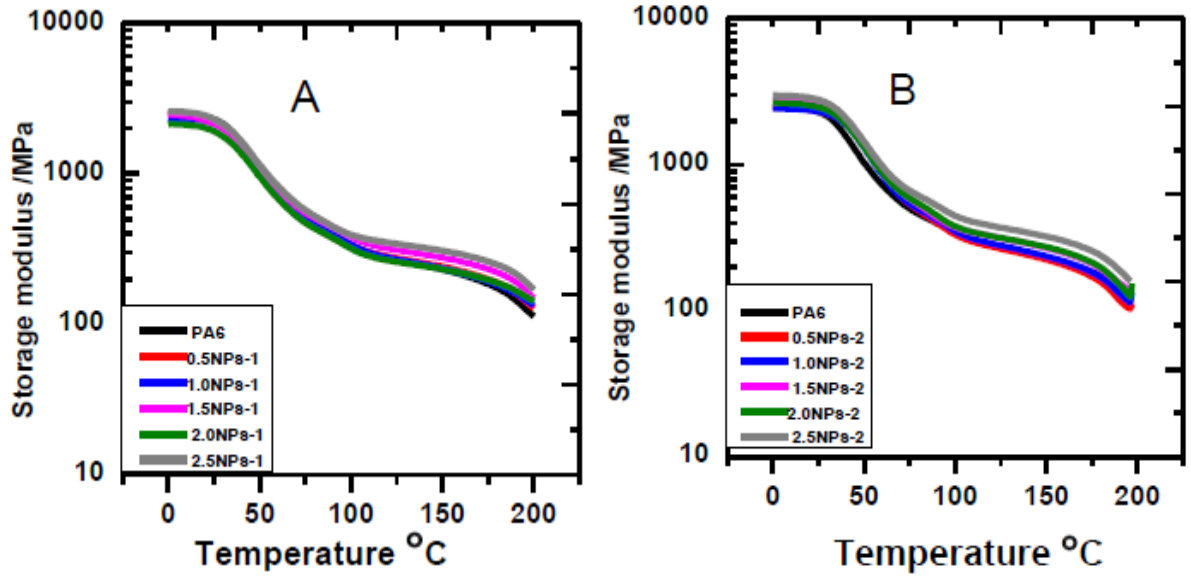


**Figure 1:** Storage modulus (E') versus temperature data for (a) INP 40/10 system where 40% indicates amplitude of sonication for 10 min and (b) for INP 20/20 system where 20% indicates the amplitude of sonication for 20 min. (INPs 40/10 (labelled-1) and INPs 20/20 (labelled-2) systems)

From Table 1, there appears to be slightly higher storage modulus reinforcement with the INP 20/20 system, probably due to better retention of the aspect ratio of the GNP. Attaining only low levels of modulus reinforcement with GNP loading has occurred with other systems, using epoxy and HDPE matrices (Pan *et al*., 2000; King *et al*., 2013) with the loading level used exceeding that of the present study. The fluctuation in E25 is attributed to effect of the diluents left after polymerisation especially in INP 40/10 system. This leads to a very poor effective modulus of GNP in INP 40/10 system of 4.8GPa after excluding the lowest modulus data of 1.9GPa corresponding to 2.0 GNP wt. % loading. However, due to the low loading level of GNP used in the present work and the better reaction rates in the INP 20/20 system, an extrapolated modulus of 22.4GPa is obtained. This value is higher by an order of magnitude relative to the 7.5GPa and 8.8GPa estimated for the IG 40/10 and IG 20/20 systems, respectively. The highest filler effective modulus for GNP occurs with the 20/20 processing regime. This may still reflect the influence of the aspect ratio of the smaller GNP particles since mild sonication with 20% amplitude for 20 min. may fragment the GNP particles such that its high aspect ratio is maintained. Direct horn sonication (Penu *et al*., 2010) (as used in present work) for only 10s was reported as sufficient to disperse CNT in molten EC and lowering in the rate of reaction was dependent both on exposure time and sonication amplitude. Some studies (Kalaitzidou *et al*., 2007; Fukushima *et al*., 2006) ascribe better mechanical property enhancement to smaller GNP fillers. However, in these synthesis systems, maintaining higher aspect ratio is expected to be a plus for mechanical property gains; whereas extrusion may cause folding, buckling and rolling of GNP-15 while GNP-5 maintains its lateral structure. Although higher aspect ratio is meant to be an advantage in terms of reinforcement, GNP-15 has been shown to be more flexible and easier to fold (Vadukumpully *et al*., 2011) which leads to loss of the original aspect ratio, shape and probably dimensionality. This event is more likely to occur in melt mixing processing. Extending similar extrapolation to the work by Ramanathan *et al*. (2007) on PMMA/GNP, where high modulus enhancements were obtained alongside increased Tg, the effective modulus of GNP is 42.9GPa almost double what obtains here, (22.4GPa). The work of Vadukumpully *et al*. (2011) gave effective modulus of GNP of 65.8GPa which almost triples the best obtained in the present study in the INP 20/20 system. Notwithstanding, these results shows that the potential for impressive modulus improvements of PA6/GNP nanocomposites can be improved by tackling issues of dispersion, uncontrolled fragmentation (in the case of *in situ* polymerisation) and balancing up with optimised amounts of catalysing species to maintain high monomer conversion. Besides in the mentioned studies (Ramanathan *et al*., 2007; Vadukumpully *et al*., 2011) solution blending which ensures better retention of filler morphology was used. Additionally, Vadukumpully *et al*. (2011) modified the particle/polymer interaction to an organic/organic type which informs the greater interaction observed.

**Table 1:** DMTA data for composites in the INP 40/10 (labelled-1) and INP 20/20 (labelled-2) systems

| GNP *in situ* polymerised | E' at 25° C MPa | E' at 80°C MPa | $T_g$ °C (DMTA) |
|---|---|---|---|
| PA6s | 2224±179 | 440±39 | 49.3±1.5 |
| 0.5NPs-1 | 2355±393 | 446±16 | 50.0±0.9 |
| 1.0NPs-1 | 2160±47 | 465±29 | 52.8±1.6 |
| 1.5NPs-1 | 2354±194 | 538±35 | 53.8±1.3 |
| 2.0NPs-1 | 1917±248 | 434±63 | 51.3±2.3 |
| 2.5NPs-1 | 2305±18 | 543±17 | 51.8±1.6 |
| 0.5NPs-2 | 2348±185 | 499±46 | 60.2±0.3 |
| 1.0NPs-2 | 2311±148 | 495±51 | 58.2±0.8 |
| 1.5 NPs-2 | 2598±113 | 543±36 | 54.3±0.2 |
| 2.0NPs-2 | 2497±157 | 550±36 | 56.5±1.8 |
| 2.5NPs-2 | 2784±54 | 613±10 | 52.8±1.3 |

*3.2. Storage modulus of the NP 200/3 and NP100/6 systems*

Modulus versus temperature data for the GNP based melt processed system is shown in Figure 2a and 2b while the derived data are presented in Table 2. Compared to the synthesized systems (Section 3.1), it can be seen that the trend of increasing modulus with GNP loading is not followed exactly though there is some resemblance. The major difference between the two systems is the grouping of $T_g$ in A and its broad division into two groups in B, which was discussed previously in Section 3.1.

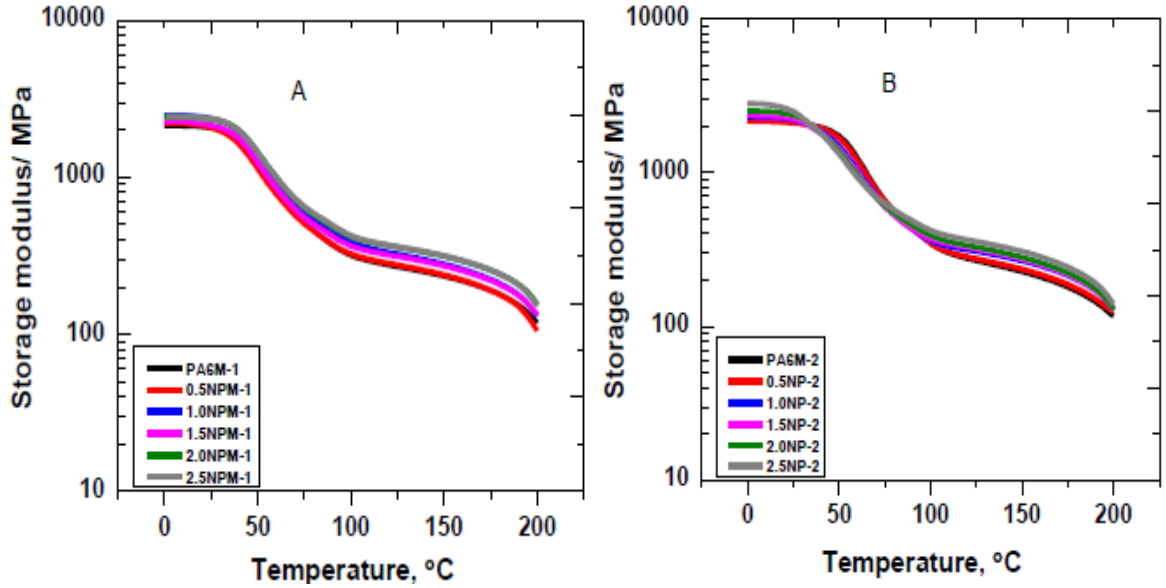


**Figure 2:** Storage modulus (E') versus temperature data for (a) NP 200/3 (screw speed of 200 rpm for 3 min) and (b) NP 100/6 (screw speed of 100 rpm for 6 min) systems. (NPM 200/3 (labelled-1) and NPM 100/6 (labelled-2) systems)

**Table 2:** DMTA derived data for composites in NP 200/3 (labelled 1) and NP100/6 (labelled 2) systems

| GNP melt extruded nanocomposites | E' at 25 ° C MPa | E' at 80° C | $T_g$° C (DMTA) |
|---|---|---|---|
| PA6M-1 | 2066±50 | 461±39 | 58.2±4.2 |
| 0.5NPM-1 | 2069±78 | 454±26 | 54.7±0.3 |
| 1.0NPM-1 | 2371±223 | 539±42 | 54.2±0.3 |
| 1.5NPM-1 | 2154±10 | 502±36 | 55.7±0.0 |
| 2.0NPM-1 | 2338±120 | 579±29 | 56.5±0.9 |
| 2.5NPM-1 | 2357±141 | 591±24 | 56.3±0.6 |
| PA6M-2 | 2124±126 | 562±21 | 67.7±0.6 |
| 0.5NPM-2 | 2104±121 | 558±30 | 66.7±0.6 |
| 1.0NPM-2 | 2207±83 | 531±74 | 65.0±1.7 |
| 1.5NPM-2 | 2240±54 | 527±10 | 64.7±0.6 |
| 2.0NPM-2 | 2357±40 | 533±9 | 63.0±1.0 |
| 2.5NPM-2 | 2500±151 | 572±17 | 60.8±0.8 |

*3.3. Room temperature storage moduli (E25) of the INP 40/10 and INP 20/20 systems*

The INP 40/10 system shows no significant changes in E25 for the nanocomposites relative to unfilled PA6 as shown in Figure 3a. However, it is observed, that 1.5NP-1 nanocomposite has the highest $T_g$ and E25, which relate to their higher reaction rate that raises the number of reaction activation sites (Van-Rijswijk *et al*., 2006) and eventually leads to increased crystallinity and modulus. E25 drops at 2.0 NP wt. % loading and rises again at 2.5GNP wt. % loading in both the INP 40/10 and INP 20/20 systems. This reflects the dynamics of mixing (stirring and dispersion by sonication) imparted on the GNP particles as its loading level increases in molten EC. The efficiency of dispersion by sonication is not independent of loading (Hielscher, 2005) and the extent of particle deagglomeration, dispersion and fragmentation attained depends on the mixing dynamics. Therefore, the mechanical properties of nanocomposites reflect the dispersed state and the interfacial contact (Gao *et al*., 2006) with the polymer. In addition, processing using *in situ* polymerisation without washing to remove remnants of catalysing species or unconverted EC means that plasticization cannot be entirely ruled out.

The INP 20/20 system shows higher E25 values relative to the INP 40/10 system due to better wetting of GNP by EC and retention of the GNP aspect ratio. When composites of parallel loading are compared (Table 1), a semblance of a pattern is seen with nanocomposites in the INP 40/10 system reflecting the stepping-up of the mole % of catalysing species, thus preventing the fall in rate of reaction. It is possible to improve the physical properties of PA6 by changing the catalysing specie concentrations (Tüzün, 2008). However, the effective modulus of GNP filler in INP 20/20 system estimate as 22.4GPa and that of INP 40/10 system being only 4.8GPa probably indicates poor GNP morphology and aspect ratio of the GNP (due to the sonication condition applied). The effective GNP modulus value of 22.4GPa for INP 20/20 is in the same order of magnitude with that of GO (32GPa) and GNP (42GPa) measured in the tensile mode (Dikin *et al*., 2007) However, the effective modulus of GNP in INP 20/20 system is much lower than the theoretical value of 1TPa reported for pristine graphene (Geim and Novoselov, 2007). The value is, notwithstanding, higher than the values estimated for G in all the G based systems.

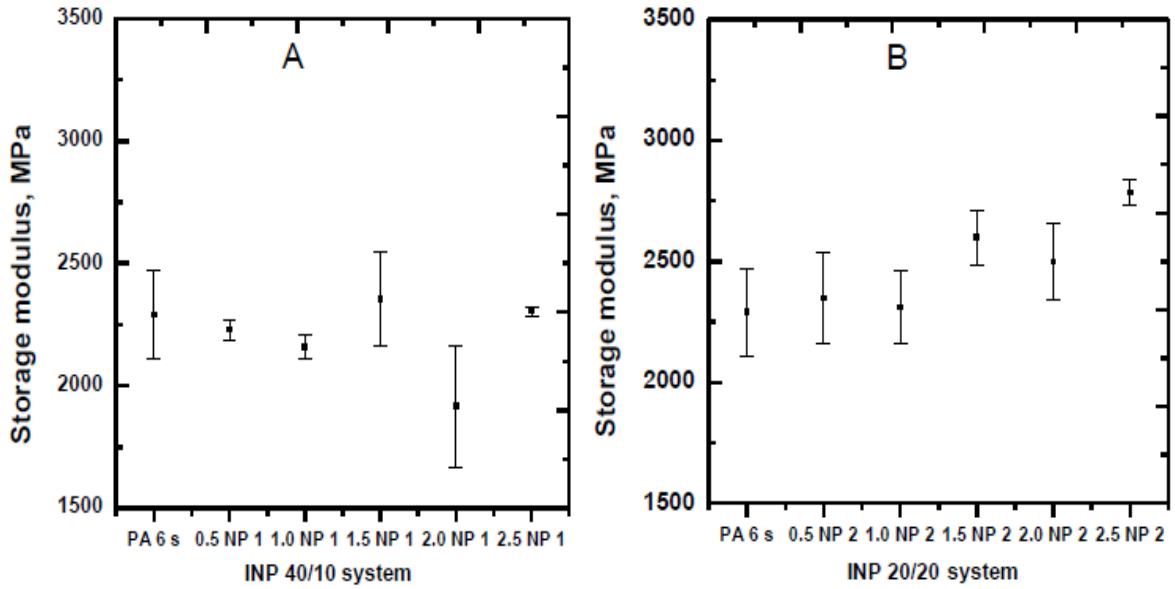


**Figure 3:** Room temperature storage modulus in (a) INP 40/10 and (b) INP 20/20 systems. INP 40/10 indicates 40% amplitude of sonication for 10 min and INP 20/20 indicates 20% amplitude for 10 min

*3.4. Room temperature storage moduli (E25) of the INP 200/3 and INP 100/6 systems*

Figure 4 presents the E25 of the PA6/GNP melt extruded systems. Unlike in the synthesized system, in both systems the standard deviation bars from 2.0NP wt. % loading do not overlap with the two unfilled PA6 matrices. In Figure 4a for INP 200/3 system, with the exception of 0.5 GNP wt. % loading, all other loadings show higher average modulus compared to unfilled PA6. This probably indicates that the rigour associated with the 200/3 processing regime causes GNP to fragment as suggested by (Fukushima *et al*., 2006). A response which coincides somewhat with the expected reinforcing effect of GNP is depicted in Figure 4b for the INP 100/6 system. This puts into context the

effect of processing with these two melt extrusion regimes of the same magnitude in strain history. Literature has shown the capability of GNP as a heterogeneous improver of matrix properties as reviewed in these works (Ramanathan *et al*., 2007; Wang *et al*., 2010; Vadukumpully *et al*., 2011; Kim *et al*., 2010). Here the effective moduli of GNP obtained are 13.8GPa in NP 200/3 system and 17.3GPa in NP 100/6 system. A difference of 3.5GPa reflecting the superiority in maintaining the aspect ratio of GNP in NP 100/6 the processing regime where a lesser GNP crumbling rigour is applied. These two GNP effective moduli values fall below that obtained in the INP 20/20 system, which is 22.4GPa. Thus, upholding superior interaction and dispersion ability of the GNP in the *in situ* polymerisation system with higher reaction rates and a lesser sonication power, which has a lesser fragmenting effect. The moduli values obtained in present study are normalised relative to their respective matrix and compared with those of polymer/GNP-15 nanocomposites from other studies (Ramanathan *et al*., 2007; Biswas *et al*., 2011) and is presented in Figure 5a and 5b.

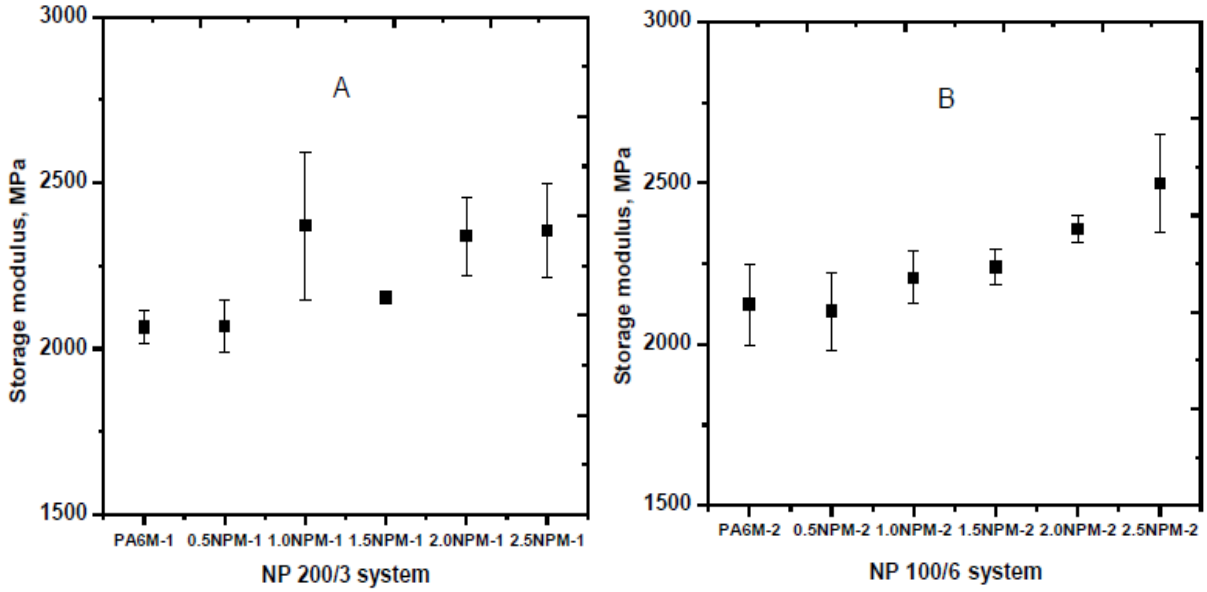


**Figure 4:** Room temperature storage modulus for (a) NP 200/3 (screw speed of 200 rpm for 3 min) and (b) NP 100/6 (screw speed of 100 rpm for 6 min) systems

In Figure 5a, the data for the INP 40/10 and INP 20/20 systems show that while modulus fluctuates with GNP loading in the former, in the latter the fluctuations are minimal. While the fluctuations may be ascribed to the reaction inhibiting effect of the GNP, which causes the ratio of catalysing species to be increased, it remains more likely to impact the INP 40/10 system because of the higher number of particle breakages imposed by harsh sonication conditions, which makes more surfaces available (Li *et al*., 2007). The end result points to an increase towards the tendency of carbon fillers to inhibit reaction (Horský *et al*., 2001; Penu *et al*., 2010; Horský *et al*., 2003; Horský *et al*., 1999). On all levels of comparison, the relative modulus values of the INP 20/20 system are higher than those of the 40/10 system, which reflects retention or even improvement in the aspect ratio of the GNP (due to less intensive sonication). Some E25 values from literature are higher than those of the present study, principally due to the difference in processing. With regards to Figure 5a, the work of Ramanathan *et al*. (2007) and Biswas *et al*. (2011) both used solution mixing which provides a good interfacial contact and retention of the GNP morphology. Ramanathan *et al*. (2007) showed that GNP, like other nano-carbon particulate fillers, can improve polymer mechanical properties at low loading fractions if good interfacial contact occurs. Biswas *et al*. (2011) using a liquid crystalline polymer (LCP) also found relatively higher E25 compared to an INP 20/20 system, although at 2.5 GNP wt. % loading. The authors ascribed the E25 enhancement to both good dispersion and to processing, using a doctor blade to distribute and align the GNP particles thereby leading to better reinforcement. Comparison with higher GNP loading is restricted since even the loading level of 2.5GNP wt. % was only achieved in the present study by increasing the mole % of the catalysing species.

In Figure 5b, the melt extruded systems; (NP 200/3 and NP 100/6) are compared with the same system as in Figure 5a. Ramanathan *et al*. (2007) PMMA based system again excelled in relative modulus improvement while comparatively both NP 200/3 and NP 100/6 systems are similar to

Biswas *et al*. (2011) study. Increases in relative modulus values are common upon filling polymers with particulate carbons. Krupta *et al*. (2001) studied expanded graphite (EG) composites with HDPE and LDPE and obtained more than 5 fold modulus increase at 0.5 wt. % of EG. Chandrasekaran *et al*. (2013) showed the relative modulus of an epoxy/GNP composite increased to the highest modulus ratio of 1.16 at 0.5 wt. %. However, at 1 and 2 GNP wt. % loading, the modulus ratios were only 1.09, and 1.14, respectively. This behaviour was suggested to occur due to percolation of GNP at the lower (0.5GNP wt. %) loading level, which also led to a reduced tan δ peak value and indicated additional constraint relative to the higher loading levels. It was also observed that the modulus value corresponding to $T_g$ also dropped compared to other nanocomposites.

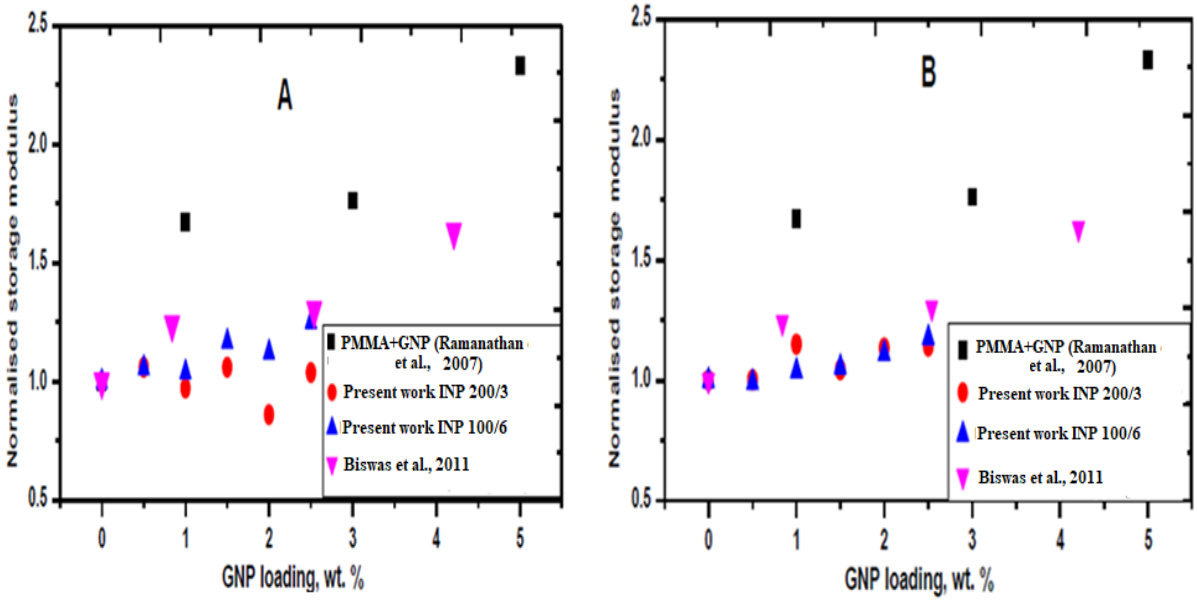


**Figure 5:** Comparison of storage moduli of (a) INP 40/10 and INP 20/20 (where 40/10 indicate 40% amplitude of sonication for 10 min and 20% amplitude for 10 min) and (b) G 200/3 and G 100/6 (where G 200/3 indicates screw speed of 200 rpm for 3 min and G 100/6 screw speed of 100 rpm for 6 min ), both of which are compared with storage moduli from literature (Ramanathan *et al*., 2007; Biswas *et al*., 2011)

## 4.0. Conclusion

PA6 fibres reinforced GNP nano-composites were successfully prepared by *in situ* polymerisation and melt extrusion methods. The storage moduli of the nano-composites were evaluated at 25°C (E25) and 80°C (E80). For INP 200/3 system, with the exception of 0.5 GNP wt. % loading, all other loadings show higher average modulus compared to unfilled PA6. An indication that the rigour associated with the 200/3 processing regime causes GNP to fragment. The effective moduli of GNP obtained are 13.8GPa in NP 200/3 system and 17.3GPa in NP 100/6 system. A difference of 3.5GPa reflecting the superiority in maintaining the aspect ratio of GNP in NP 100/6, the processing regime where a lesser GNP crumbling rigour is applied. These two GNP effective moduli fall below that obtained in the INP 20/20 system, which is 22.4GPa. Thus, upholding superior interaction and dispersion ability of the GNP in the *in situ* polymerisation system with higher reaction rates and a lesser sonication power, which has a lesser fragmenting effect. There was fluctuation in moduli with GNP loading for the INP 40/10 but minimal for INP 20/20 systems. While the fluctuations may be ascribed to the reaction inhibiting effect of the GNP, which causes the ratio of catalysing species to be increased, it is more likely to impact the INP 40/10 system because of the higher number of particle breakages imposed by harsh sonication conditions, which makes more surfaces available. On all levels of assessment, the relative modulus of the INP 20/20 system are higher than those of the 40/10 system, a reflection of the retention or improvement in the aspect ratio of the GNP.

## References

Biswas, S., Fukushima, H. and Drzal, L. T. (2011). Mechanical and electrical property enhancement in exfoliated graphene nanoplatelet/liquid crystalline polymer nanocomposites. *Composites Part A: Applied Science and Manufacturing*, 42(4), pp. 371-375.

Chandrasekaran, S., Seidel, C. and Schulte, K. (2013). Preparation and characterization of graphite nano-platelet (GNP)/epoxy nano-composite: Mechanical, electrical and thermal properties. *European Polymer Journal*, 49(12), pp. 3878-3888.

Celzard, A., Mareche, J. and Furdin, G. (2005). Modelling of exfoliated graphite. *Progress in Materials Science*, 50(1), pp. 93-179.

Clingerman, M. L. (2001). Development and modelling of electrically conductive composite materials: Michigan Technological University.

Clingerman, M. L., Weber, E. H., King, J. A. and Schulz, K. H. Synergistic effect of carbon fillers in electrically conductive nylon 6, 6 and polycarbonate based resins. *Polymer Composites*, 23(5), pp. 911-924.

Debelak, B. and Lafdi, K. (2007). Use of exfoliated graphite filler to enhance polymer physical properties. *Carbon*, 45(9), pp. 1727-3174.

Dikin, D. A., Stankovich, S., Zimney, E. J., Piner, R. D., Dommett, G. H., Evmenenko, G., *et al*. (2007). Preparation and characterization of graphene oxide paper. *Nature*, 448(7152), pp. 457-460.

Fukushima, H., Drzal, L., Rook, B. and Rich, M. (2006). Thermal conductivity of exfoliated graphite nanocomposites. *Journal of Thermal Analysis and Calorimetry*, 85(1), pp. 235-238.

Gao, J., Zhao, B., Itkis, M. E., Bekyarova, E., Hu, H., Kranak, V., *et al*. (2006). Chemical Engineering of the Single-Walled Carbon Nanotube−Nylon 6 Interface. *Journal of the American Chemical Society*, 128(23), pp. 7492-7496.

Geim, A. K. and Novoselov, K. S. (2007). The rise of graphene. *Nature Materials*, 6(3), pp. 183-191.

Hielscher, T. (2005). Ultrasonic production of nana-size dispersions and emulsion. ENS'05, Paris, France.

Howe, J. P. (1952). Properties of Graphite. *Journal of the American Ceramic Society*, 35(11), pp. 275-283.

Horský, J., Kolařík, J. and Fambri, L. (2003). One-Step Synthesis of Hybrid Composites of Poly (6-hexanelactam) Combining Solid Tribological Additives and Reinforcing Components. *Macromolecular Materials and Engineering*, 288(5), pp. 421-431.

Horský, J., Kolařík, J. and Fambri, L. (1999). Composites of alkaline poly (6-hexanelactam) with solid lubricants: one-step synthesis, structure, and mechanical properties. *Die Angewandte Makromolekulare Chemie*, 271(1), pp. 75-83.

Horský, J., Kolařík, J. and Fambri, L. (2001). Gradient Composites of Alkaline Poly (6-hexanelactam) with Graphite: One-Step Synthesis, Structure, and Mechanical Properties. *Macromolecular Materials and Engineering*, 286(4), pp. 216-224.

Heiser, J. A., King, J. A., Konell, J. P., Miskioglu, I. and Sutter, L. L. (2004). Tensile and impact properties of carbon filled nylon-6,6 based resins. *Journal of Applied Polymer Science*, 91(5), pp. 2881-2893.

Hussain, F., Hojjati, M., Okamoto, M. and Gorga, R. E. (2006). Polymer-matrix nanocomposites, processing, manufacturing, and application: an overview. *Journal of Composite Materials*, 40(17), pp. 1511-1575.

Kang, S-C. and Chung, D-W. (2003). Improvement of frictional properties and abrasive wear resistance of nylon/graphite composite by oil impregnation. *Wear*, 254(1), pp. 103-110.

Keledi, G., Hári, J. and Pukánszky, B. (2012). Polymer nanocomposites: structure, interaction, and functionality. *Nanoscale*, 4(6), pp. 1919-1938.

Kalaitzidou, K., Fukushima, H. and Drzal, L. T. (2007). Multifunctional polypropylene composites produced by incorporation of exfoliated graphite nanoplatelets. *Carbon*, 45(7), pp. 1446-1452.

Kim, S., Seo, J. and Drzal, L. T. (2010). Improvement of electric conductivity of LLDPE based nanocomposite by paraffin coating on exfoliated graphite nanoplatelets. *Composites Part A: Applied Science and Manufacturing*, 41(5), pp. 581-587.

Krupa, I. and Chodák, I. (2001). Physical properties of thermoplastic/graphite composites. *European Polymer Journal*, 37(11), pp. 2159-2168.

King, J. A., Klimek, D. R., Miskioglu, I. and Odegard, G. M. (2013). Mechanical properties of graphene nanoplatelet/epoxy composites. *Journal of Applied Polymer Science*, 128(6), pp. 4217-4223.

Li, J., Sham, M. L., Kim, J-K. and Marom, G. (2007). Morphology and properties of UV/ozone treated graphite nanoplatelet/epoxy nanocomposites. *Composites Science and Technology*, 67(2), pp. 296-305.

Li, B. and Zhong, W-H. (2011). Review on polymer/graphite nanoplatelet nanocomposites. *Journal of Materials Science*, 46(17), pp. 5595-5614.

Miller, M. G., Keith, J. M., King, J. A., Hauser, R. A. and Moran, A. M. (2006). Comparison of the guarded-heat-flow and transient-plane-source methods for carbon-filled nylon 6, 6 composites: Experiments and modeling. *Journal of Applied Polymer Science*, 99(5), pp. 2144-2151.

Pan, Y. X., Yu, Z. Z., Ou, Y. C. and Hu, G. H. (2000). A new process of fabricating electrically conducting nylon 6/graphite nanocomposites via intercalation polymerization. *Journal of Polymer Science Part B: Polymer Physics*, 38(12), pp. 1626-1633.

Penu, C., Hu, G. H., Fonteix, C., Marchal, P. and Choplin, L. (2010). Effects of carbon nanotubes and their state of dispersion on the anionic polymerization of ϵ-caprolactam: 1. Calorimetry. *Polymer Engineering & Science*, 50(12), pp. 2287-2297.

Ramanathan, T., Stankovich, S., Dikin, D., Liu, H., Shen, H., Nguyen, S., *et al*. (2007). Graphitic nanofillers in PMMA nanocomposites—an investigation of particle size and dispersion and their influence on nanocomposite properties. *Journal of Polymer Science Part B: Polymer Physics*, 45(15), pp. 2097-2112.

Sadasivuni, K. K., Ponnamma, D., Thomas, S. and Grohens, Y. (2014). Evolution from graphite to graphene elastomer composites. *Progress in Polymer Science*, 39(4), pp. 749-780.

Sengupta, R., Bhattacharya, M., Bandyopadhyay, S. and Bhowmick, A. K. (2011). A review on the mechanical and electrical properties of graphite and modified graphite reinforced polymer composites. *Progress in Polymer Science*, 36(5), pp. 638-670.

Supova, M., Martynkova, G. S. and Barabaszova, K. (2011). Effect of nanofillers dispersion in polymer matrices: a review. *Science of Advanced Materials*, 3(1), pp. 1-25.

Tung, J., Gupta, R., Simon, G., Edward, G. and Bhattacharya, S. (2005). Rheological and mechanical comparative study of in situ polymerized and melt-blended nylon 6 nanocomposites. *Polymer*, 46(23), pp. 10405-10418.

Tüzün, F. N. (2008). Effect of the Activator Type and Catalyst/Activator Ratio on Physical and Mechanical Properties of Cast PA-6. *Polym Plast Technol Eng.*, 47(5), pp. 532-5341.

Umar, M., Ofem, M. I., Anwar, A. S. and Salisu, A. G. (2020). Thermo gravimetric analysis (TGA) of PA6/G and PA6/GNP composites using two processing streams. *Journal of King Saud University - Engineering Sciences*, doi.org/10.1016/j.jksues.2020.09.003 (in the press).

Vadukumpully, S., Paul, J., Mahanta, N. and Valiyaveettil, S. (2011). Flexible conductive graphene/poly (vinyl chloride) composite thin films with high mechanical strength and thermal stability. *Carbon*, 49(1), pp. 198-205.

Van Rijswijk, K., Bersee, H., Beukers, A., Picken, S. and Van Geenen, A. (2006). Optimisation of anionic polyamide-6 for vacuum infusion of thermoplastic composites: Influence of polymerisation temperature on matrix properties. *Polymer Testing*, 25(3), pp. 392-404.

Van Rijswijk, K., Bersee, H., Jager, W. and Picken, S. Optimisation of anionic polyamide-6 for vacuum infusion of thermoplastic composites: choice of activator and initiator. *Composites Part A: Applied Science and Manufacturing*, 37(6), pp. 949-956.

Viculis, L. M., Mack, J. J., Mayer, O. M., Hahn, H. T. and Kaner, R. B. Intercalation and exfoliation routes to graphite nanoplatelets. *Journal of Materials Chemistry*, 15(9), pp. 974-978.

Wang, L., Hong, J. and Chen, G. (2010). Comparison study of graphite nanosheets and carbon black as fillers for high density polyethylene. *Polymer Engineering & Science*, 50(11), pp. 2176-2181.

Weber, E. H., Clingerman, M. L. and King, J. A. (2003). Thermally conductive nylon 6,6 and polycarbonate based resins. I. Synergistic effects of carbon fillers. *Journal of Applied Polymer Science*, 88(1), pp. 112-122.

Wissler, M. (2006). Graphite and carbon powders for electrochemical applications. *Journal of Power Sources*, 156(2), pp. 142-150.

**Cite this article as:**
Umar M., Ofem M. I., Anwar A. S. and Makama A. B. 2021. Storage Moduli of *in situ* Polymerised and Melt Extruded PA6 Graphite (G) Composites. *Nigerian Journal of Environmental Sciences and Technology*, 5(1), pp. 91-101. https://doi.org/10.36263/nijest.2021.01.0252

Nigerian Journal of Environmental Sciences and Technology (NIJEST)

www.nijest.com

ISSN (Print): 2734-259X | ISSN (electronic): 2734-2603

Vol 5, No. 1 March 2021, pp 102 - 109

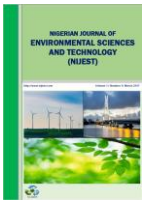

# An Assessment of Degradation of Soil Properties in Kabba College of Agriculture, Kogi State, Nigeria

Babalola T. S.[1,*], Ogunleye K. S.[2], Lawal J. A.[1] and Ilori A. O. A.[2]

[1]Kabba College of Agriculture, Division of Agricultural Colleges, Ahmadu Bello University, Kabba, Kogi State, Nigeria

[2]Department of Soil Science and Land Management, Federal University Oye-Ekiti, Ikole Campus, Ekiti State, Nigeria

Corresponding Author: *drbabalolatemitopeseun@gmail.com

https://doi.org/10.36263/nijest.2021.01.0240

## ABSTRACT

*Some soils in Kabba College of Agriculture, Kogi State, southern guinea savannah zone of Nigeria, were assessed to ascertain the levels of degradation of soil properties. The rigid grid soil survey method was used to identify seven soil units. Soils were sampled at 0-20 cm and 20-40 cm soil depth and analyzed for physical and chemical properties using standard methods. Levels of degradation were obtained by comparing laboratory data with the standard land/soil requirement (indicators/criteria) for grouping lands into different degradation classes of 1 to 4 (non to slightly, moderately, highly, and very highly degraded). Results showed that units D (soghum) and E (citrus) were very highly degraded (Class 4) of exchangeable potassium; units C (yam), D and E were highly degraded (Class 3) of organic matter. Other units were moderately degraded (Class 2) of base saturation, bulk density and total nitrogen. There was no degradation of available phosphorus and exchangeable sodium percentage in all the units. Physical and chemical degradation took place in the study area with respect to bulk density, base saturation, total nitrogen, potassium, and organic matter. Sustainable management practices that will promote good bulk density and organic matter accumulation should be encouraged.*

**Keywords:** Degradation, Assessments, Chemical, Physical, Indicators

## 1.0. Introduction

The threats to land by soil degradation have been the subject for intensive debate in the literature (Baumhardt *et al.*, 2015). In Africa, an estimated 500 million hectares of land have been affected by soil degradation including agricultural land (Wynants *et al.*, 2019). It's devastating effects have subjected local communities to high risks of loss of lives, properties and land resource that supports their livelihood.

In the world, there is practically no extensive area of land without limitation of one sort or another (Ibrahim and Idogba, 2013). Indiscriminate forest cleaning and burning, inappropriate land cultivation, over grazing, improper irrigation practice, urban development and high population density have no doubt contributed to changes in the landscape. More than 75 percent of Earth's land areas are substantially degraded, undermining the well-being of 3.2 billion people, according to the world's first comprehensive, evidence-based assessment (Leahy, 2018).

According to Idoga *et al.* (2007) land degradation is a universal set while soil degradation is derived from land degradation since soil is the most stable and most manipulated feature of the land. The major human activity that contributes to soil degradation is agriculture (Food and Agriculture Organization-FAO, 2005). Continuous and inappropriate land use systems have severely impaired the soil. It has been reported that every land use partly destroys the soil structure and reduces soil fertility (Altieri and Nicholis, 2003).

There have been many reports on implication of different land uses on soil properties and fertility, (Yusuf *et al.*, 2019; Yusuf *et al.*, 2015; Malgwi and Abu, 2011; Cobo *et al.*, 2010; Martensson, 2009) and other works on soil degradation assessment that examines the actual level, nature and forms in different agroecological zones of Nigeria (Adewuyi *et al.*, 2019; Senjobi *et al.*, 2013; Ibrahim and Idogba, 2013; Sotona, *et al*. 2013; Adewuyi 2011; Isirimah, 2005; Igwe, 2003). In Kabba College of Agriculture, Kabba, Kogi State the major land utilization type is agriculture involving intensive, continuous cropping and mechanization but there are no studies on soil degradation. Available report is on soil quality in relation to crop yield along toposequence (Babalola *et al.*, 2012); therefore, the need for this study arises. The objective of this study is to identify and document the actual level, nature and forms of soil degradation in the study area.

## 2.0. Methodology

### *2.1. Description of the study area*

Kabba is located in Kogi State, Kabba/Bunu Local Government Area in the Southern Guinea Savannah Agro-ecological zone of Nigeria. Kabba College of Agriculture is located on latitude $7^0$51'N and longitude $6^0$04'E. It has climate that is typical of humid tropics with rainfall that spans the month of May to October. The dry season extends from November to April. The vegetation of the area is dominated by tall grasses and shrubs. Also, human activities have influenced the vegetation in the area (Babalola *et al.*, 2012). The area belongs to the basement complex geology of Nigeria (Obaje, 2009).

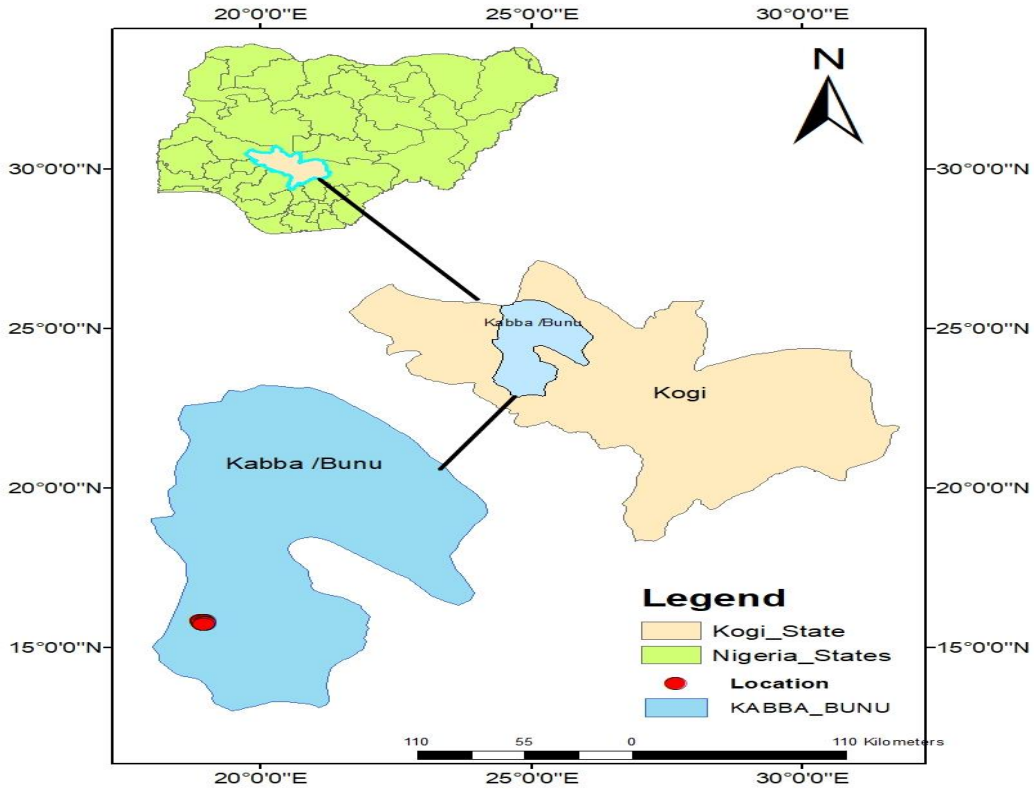


**Figure 1:** Map showing the location of the study within, Nigeria, Kogi State and Kabba/Bunu Local Government

### *2.2. Land use*

The major land use type in the area is arable crop land involving cultivation of crops such as maize, sorghum, rice, cassava, yam, pepper and dry season vegetable production in the wetland portion of the area. Also, tree crops such as oil palm, banana, pineapple and citrus are cultivated in some part of the area. Tillage practices in the area involved the use of simple implements while ploughing, harrowing, and ridging is practiced in some part.

*2.3 Field work and sampling*

The rigid grid soil survey method following the guidelines of Soil Survey Staff, (2014) was used to sample the soils. Soils were probed at 100m within traverse and the colour, texture, consistence, and structure were determined. Areas with similar characteristics were identified as soil units and were labelled with the prominent agricultural land use within the unit (Figure 2) as follows: Cassava-A, Oil palm- B, Yam- C, Sorghum- D, Citrus- E, Maize- F and Pasture- G. Within each soil unit a representative area was selected and soil samples were collected at 0-20 cm and 20-40 cm soil depth using auger. Core sample were also collected for the determination of bulk density and saturated hydraulic conductivity.

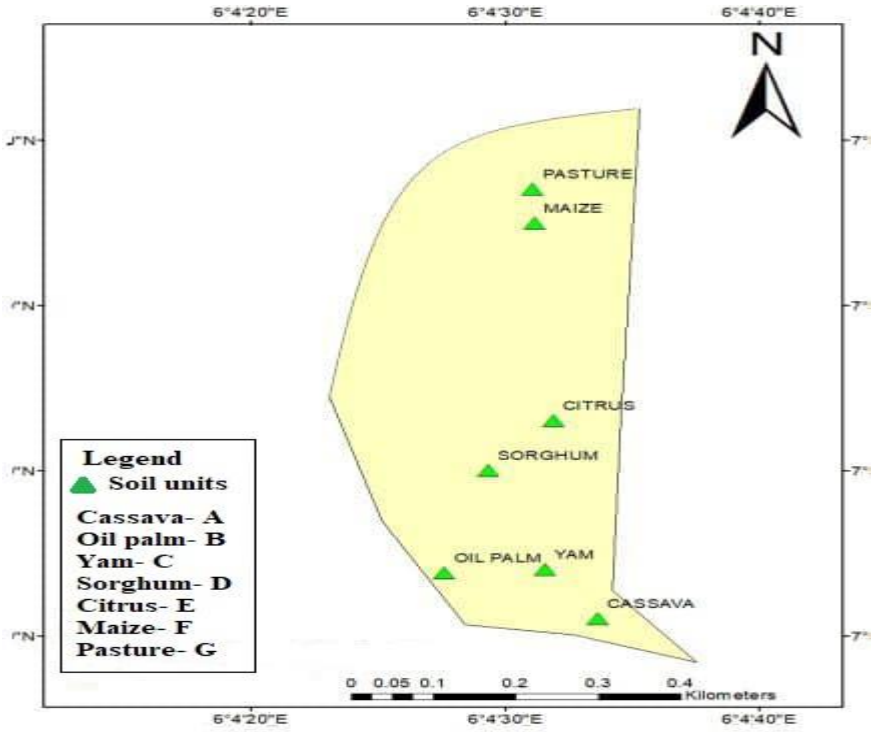


**Figure 2:** Map of the location showing the sampling points and agricultural land use of soil units

*2.4. Soil analysis*

The bulk samples were air dried, gently crushed and passed through a 2 mm sieve. Core samples were trimmed to the height of the core sampler for bulk density determination. Particle size distribution, pH, organic carbon, total nitrogen, available phosphorus, exchangeable bases, and exchangeable acidity were determined following the International Institute for Tropical Agriculture IITA, (1979) guidelines. The effective cation exchanges capacity, base saturation, and exchange sodium percentages were calculated.

*2.5 Land degradation assessment*

The levels of degradation of the soil were assessed using the standard indicator and criteria for degradation assessment (Tables 1 – 3) (FAO, 1979; Snakin *et al.*, 1996; Senjobi *et al*., 2013).
Analytical data from each sample were placed in a degradation class by matching the soil characteristics with the land degradation indicator. The estimates of the degree of degradation were based on the measured physical and chemical parameters.

**Table 1:** Indicators and criteria of physical degradation of soil

| Indicator | *Degree of degradation (%) | | | | |
|---|---|---|---|---|---|
| | Initial Level | 1 | 2 | 3 | 4 |
| Soil bulk density (g/cm$^3$) | 1.25 – 1.4 | < 1.5 | 1.5 – 2.5 | 2.5 – 5 | > 5 |
| Permeability (cm/hr) | 5 – 10 | < 1.25 | 1.25 – 5 | 5– 10 | > 20 |

*Sources:* FAO (1979), Snakin *et al.* (1996), Senjobi *et al*. (2013)
**Where 1. Non to slightly degraded soil where productivity ranges from 75-100%*
*2. Moderately degraded soil where productivity ranges from 50 -75%*
*3. Highly degraded soil where productivity ranges from 25-50%*
*4. Very high degraded soil where productivity ranges from 0-25%*

**Table 2:** Indicators and criteria of chemical degradation of soil

| Indicator | *Degree of degradation (%) | | | |
|---|---|---|---|---|
| | 1 | 2 | 3 | 4 |
| Content of Nitrogen Element (Multiple decrease) N (%) | > 0.13 | 0.10 – 0.13 | 0.08 – 0.10 | < 0.08 |
| Content of Phosphorus Element (mg/kg) | > 8 | 7 – 8 | 6 – 7 | < 6 |
| Content of Potassium Element (cmol/kg) | > 0.16 | 0.14 – 0. 16 | 0.12 – 0. 14 | < 0.12 |
| Content of Exchangeable Sodium Percentage (ESP) (Increase by 1% of CEC) | < 10 | 10 – 25 | 25 – 50 | > 50 |
| Base Saturation (decrease of saturation in more than 50%) | < 2.5% | 2.5 – 5% | 5 – 10% | > 10% |
| Excess salt (Salinization) (Increase in conductivity (mmho/cm/yr) | < 2 | 2 – 3 | 3 – 5 | > 5 |
| Content of organic matter in soil (% | > 2.5 | 2 – 2.5 | 1.0 – 2 | < 1.0 |

*Modified from:* FAO (1979), Snakin *et al.* (1996), Senjobi *et al*. (2013)

**Where 1. Non to slightly degraded soil where productivity ranges from 75-100%*

*2. Moderately degraded soil where productivity ranges from 50 -75%*

*3. Highly degraded soil where productivity ranges from 25-50%*

*4. Very high degraded soil where productivity ranges from 0-25%*

## 3.0. Results and Discussion

### *3.1. Soil properties*

The physical and chemical properties of surface (0 – 20 cm) and subsurface (20 – 40 cm) of the studied area are presented in Table 3 and 4, respectively. All the seven (7) soil units show differences in the surface and subsurface horizons. Bulk density values were higher in units A, C, E, F, and G in the subsurface horizons (1.60, 1.65, 1.75, 1.67 and 1.50 g/cm$^3$ respectively) than the surface horizons (1.58, 1.49, 1.50, 1.55 and 1.39 g/cm$^3$ respectively) while the opposite exists for units B and D (1.55 and 1.49 g/cm$^3$, 1.40 and 1.48 g/cm$^3$ respectively). The trend of distribution of bulk density between the soils studied can be attributed to differences in clay and soil organic matter (Ibrahim and Idogba, 2013). Idoga *et al.* (2007) state that soil organic matter is light and tends to lower bulk density when present in high amount in the soil. The result of the total porosity mostly follows the same pattern as bulk density. Particle size analysis shows decrease in sand content and increase in clay content in most of the units from the surface to subsurface horizons; this is typical of soils developed on basement complex areas in Nigeria and in agreement with reports of Babalola *et al.* (2012) for some soils in Kabba, Kogi State.

There are differences between the surface and subsurface horizons of chemical properties of soils. Soil pH, organic carbon, total nitrogen, available phosphorus, exchangeable cations, and Cation Exchange Capacity (CEC) are higher in the surface horizon of the soil units studied. These differences may be attributed to the production of humus in the surface horizon and cultivation practices.

**Table 3:** Physical properties of the soil units

| Soil Unit/Land use | Depth (cm) | Bulk Density (g/cm$^3$) | Total Porosity | Permeability (K Sat) (Cm/hr) | Sand % | Silt % | Clay% | Textural Class |
|---|---|---|---|---|---|---|---|---|
| A (Cassava) | 0 – 20 | 1.58 | 56 | 0.71 | 70 | 11 | 19 | Sandy Loam |
| | 20 – 40 | 1.60 | 45 | 0.65 | 71 | 09 | 20 | Sandy Loam |
| B (Oil palm) | 0 – 20 | 1.59 | 59 | 0.64 | 77 | 03 | 20 | Sandy Loam |
| | 20 – 40 | 1.55 | 50 | 0.52 | 71 | 13 | 16 | Sandy Loam |
| C (Yam) | 0 – 20 | 1.49 | 68 | 0.97 | 79 | 02 | 19 | Sandy Loam |
| | 20 – 40 | 1.65 | 51 | 1.01 | 39 | 08 | 53 | Sandy Clay |
| D (Sorghum) | 0 – 20 | 1.48 | 50 | 0.86 | 75 | 06 | 19 | Sandy Loam |
| | 20 – 40 | 1.40 | 35 | 3.09 | 62 | 08 | 30 | Clay Loam |
| E (Citrus) | 0 – 20 | 1.50 | 49 | 1.81 | 73 | 13 | 14 | Sandy Loam |
| | 20 - 40 | 1.75 | 37 | 1.71 | 60 | 08 | 32 | Sandy Clay Loam |
| F (Maize) | 0 – 20 | 1.55 | 65 | 2.71 | 35 | 26 | 39 | Clay Loam |
| | 20 – 40 | 1.67 | 55 | 1.91 | 46 | 19 | 35 | Sandy Clay Loam |
| G (Pasture) | 0 – 20 | 1.39 | 60 | 0.95 | 48 | 25 | 27 | Loam |
| | 20 – 40 | 1.50 | 41 | 0.88 | 57 | 21 | 22 | Sandy Loam |

**Table 4:** Chemical properties of the soil units

| Soil Properties | Soil Units | | | | | | | |
|---|---|---|---|---|---|---|---|---|
| | Soil Depth (cm) | A | B | C | D | E | F | G |
| pH ($H_2O$) | 0 – 20 | 5.95 | 6.14 | 5.67 | 5.51 | 6.22 | 5.97 | 4.97 |
| | 20-40 | 5.85 | 6.11 | 5.65 | 4.82 | 5.98 | 5.83 | 4.81 |
| Organic Carbon (%) | 0 – 20 | 1.68 | 1.85 | 1.12 | 1.24 | 0.89 | 2.53 | 2.70 |
| | 20-40 | 1.44 | 1.70 | 0.96 | 1.01 | 0.84 | 1.98 | 2.09 |
| Organic Matter (%) | 0 – 20 | 2.89 | 3.18 | 1.93 | 2.13 | 1.53 | 4.35 | 4.64 |
| | 20-40 | 2.48 | 2.92 | 1.65 | 1.74 | 1.45 | 3.41 | 3.60 |
| Total Nitrogen (%) | 0 – 20 | 0.121 | 0.114 | 0.116 | 0.170 | 0.162 | 0.180 | 0.179 |
| | 20-40 | 0.103 | 0.088 | 0.109 | 0.110 | 0.157 | 0.165 | 0.161 |
| Available Phosphorus (mg/kg) | 0 – 20 | 49.75 | 22.26 | 41.92 | 9.19 | 10.40 | 32.41 | 18.97 |
| | 20-40 | 40.18 | 19.15 | 39.11 | 7.82 | 9.69 | 30.97 | 17.65 |
| Exchangeable Sodium (cmol/kg) | 0–20 | 0.201 | 0.235 | 0.190 | 0.190 | 0.231 | 0.180 | 0.210 |
| | 20-40 | 0.196 | 0.213 | 0.189 | 0.169 | 0.207 | 0.179 | 0.198 |
| Exchangeable Potassium | 0 – 20 | 0.229 | 0.180 | 0.235 | 0.073 | 0.102 | 0.258 | 0.201 |
| (cmol/kg) | 20-40 | 0.229 | 0.175 | 0.221 | 0.064 | 0.097 | 0.237 | 0.199 |
| Exchangeable Calcium (cmol/kg) | 0 – 20 | 3.76 | 2.80 | 4.32 | 2.90 | 6.56 | 2.72 | 3.04 |
| | 20-40 | 3.28 | 2.72 | 4.16 | 2.86 | 6.40 | 2.56 | 2.98 |
| Exchangeable Aluminum | 0 – 20 | 0.01 | 0.01 | 0.01 | 0.02 | 0.01 | 0.02 | 0.01 |
| (cmol/kg) | 20-40 | 0.01 | 0.01 | 0.01 | 0.01 | 0.01 | 0.02 | 0.01 |
| Exchangeable Hydrogen | 0–20 | 0.15 | 0.15 | 0.12 | 0.13 | 0.14 | 0.13 | 0.11 |
| (cmol/kg) | 20-40 | 0.13 | 0.14 | 0.12 | 0.11 | 0.12 | 0.13 | 0.11 |
| Exchangeable Bases (cmol/kg) | 0 – 20 | 5.830 | 5.005 | 6.115 | 5.083 | 7.693 | 4.118 | 5.761 |
| | 20-40 | 4.845 | 4.768 | 5.770 | 4.903 | 7.424 | 3.856 | 5.347 |
| Cation Exchange Capacity | 0 – 20 | 5.990 | 5.165 | 6.245 | 5.233 | 7.843 | 4.268 | 5.881 |
| (cmol/kg) | 20-40 | 4.985 | 4.918 | 5.900 | 5.023 | 7.554 | 4.006 | 5.467 |
| Base Saturation (%) | 0 – 20 | 97.33 | 96.90 | 97.92 | 97.13 | 98.09 | 96.49 | 97.96 |
| | 20-40 | 97.19 | 96.95 | 97.80 | 97.61 | 98.28 | 96.26 | 97.81 |
| Exchangeable Sodium Percentage | 0 – 20 | 3.45 | 4.70 | 3.11 | 3.74 | 3.00 | 4.37 | 3.65 |
| (%) | 20-40 | 4.05 | 4.47 | 3.28 | 3.45 | 2.79 | 4.64 | 3.70 |

*3.2. Land degradation assessment*

The land/soil requirement (indicators and criteria i.e. land qualities/soil properties) for grouping lands into different degradation classes are given in Table 1-2. The matching of the soil indicators/criteria are given in Table 5.

The land degradation assessment results show that in terms of bulk density, only unit D was none degraded at both horizons, units C and G are none degraded at the surface and moderately degraded at the subsurface. Units A, B, E, and F are all moderately degraded at both horizons.
With respect to permeability, at the surface horizon, units A, B, C, E, and G are none degraded, unit D is highly degraded while unit F is moderately degraded.

Result of chemical properties showed that base saturation is moderately degraded in all the units; base saturation is an indicator of level of leaching, therefore this result signifies that the soils are moderately leached of their exchangeable bases.

Degradation assessment for total nitrogen shows that units E, F, and G are none degraded; Units A and C are moderately degraded at both horizons. Unit B is moderately degraded at the surface horizon and highly degraded at the subsurface. Unit D is non-degraded at the surface and moderately degraded at the subsurface.

Assessment for available phosphorus showed that all the soil units are non-degraded.
With respect to exchangeable Potassium; units A, B, C, F, and G are non-degraded while units D and E are very highly degraded at both horizons.

In terms of Exchangeable Sodium Percentage; all the units are non-degraded, indicating that the soils are not sodic.

With respect to organic matter contents; units B, F, and G are non-degraded at the surface and subsurface. Unit A is non-degraded at the surface and moderately degraded at the subsurface. Unit D is moderately degraded at the surface and highly degraded at the subsurface. Units C and E are highly degraded in both horizons.

Physical and chemical degradation took place in the study area. Chemical degradation is as a result of loss of fertility from leaching and low organic matter. This might have occurred as a result of land use practices such as continuous cropping, improper handling of plant residues and bush burning. The soils can be ameliorated through improved and proper nutrient management practices (Eswaran and Dumanski, 1998; Senjobi *et al*., 2013). Physical degradation of soil could be as a result of tillage practices and improper soil management and it requires a long time to meliorate (Hulugalle, 1994; Senjobi *et al*., 2013).

**Table 5:** Land qualities/soil properties of the soil units

| Soil Unit/Land use | Depth (cm) | Bulk Density ($g/cm^3$) | Permeability (cm/hr) | Base Saturation (%) | Total N (%) | Available P (ppm) | ExchK (cmol/kg) | ESP (%) | Organic Matter (%) |
|---|---|---|---|---|---|---|---|---|---|
| A (Cassava) | 0-20 | 2 | 1 | 2 | 2 | 1 | 1 | 1 | 1 |
| | 20-40 | 2 | 1 | 2 | 2 | 1 | 1 | 1 | 2 |
| B (Oil palm) | 0-20 | 2 | 1 | 2 | 2 | 1 | 1 | 1 | 1 |
| | 20-40 | 2 | 1 | 2 | 3 | 1 | 1 | 1 | 1 |
| C (Yam) | 0-20 | 1 | 1 | 2 | 2 | 1 | 1 | 1 | 3 |
| | 20-40 | 2 | 1 | 2 | 2 | 1 | 1 | 1 | 3 |
| D (Sorghum) | 0-20 | 1 | 1 | 2 | 1 | 1 | 4 | 1 | 2 |
| | 20-40 | 1 | 3 | 2 | 2 | 1 | 4 | 1 | 3 |
| E (Citrus) | 0-20 | 2 | 1 | 2 | 1 | 1 | 4 | 1 | 3 |
| | 20-40 | 2 | 1 | 2 | 1 | 1 | 4 | 1 | 3 |
| F (Maize) | 0-20 | 2 | 2 | 2 | 1 | 1 | 1 | 1 | 1 |
| | 20-40 | 2 | 1 | 2 | 1 | 1 | 1 | 1 | 1 |
| G (Pasture) | 0-20 | 1 | 1 | 2 | 1 | 1 | 1 | 1 | 1 |
| | 20-40 | 2 | 1 | 2 | 1 | 1 | 1 | 1 | 1 |

*N- Nitrogen, Exch. K- Exchange potassium, ESP- Exchangeable Sodium Percentage*
**Where 1. Non to slightly degraded soil where productivity ranges from 75-100%*
*2. Moderately degraded soil where productivity ranges from 50 -75%*
*3. Highly degraded soil where productivity ranges from 25-50%*
*4. Very high degraded soil where productivity ranges from 0-25%*

## 4.0. Conclusion

It is concluded that physical and chemical degradation took place in the study area with respect to bulk density, base saturation, total nitrogen, potassium, and organic matter. This study is considered as a preliminary project for the quality soil degradation assessment to develop sustainable practices to support the reclamation process and to develop a soil health program for the study area. Sustainable management practices that will promote good bulk density and organic matter accumulation should be adopted.

## References

Adewuyi, T. O, Daful, M. G. and Olofin, E. A. (2019). Characterization of land degraded sites for restoration Along Kaduna-Abuja expressway, Chikun L.G.A. of Kaduna State Nigeria. *Journal of Geography*, 11(1), pp. 58 – 71.

Adewuyi, T. O. (2011). Land Degradation in the peri-urban area: The case of Kaduna Metropolis, Nigeria. Lambert Academy Publishing, Germany. ISSN: 13 – 978-3847302490 158 pp.

Altieri, M. A. and Nicholis, C. (2003). Soil fertility and insect pests: Harmonizing soil and plant health in agro ecosystem. *Soil and Tillage Research*, 72, pp. 203-211.

Babalola, T. S., Oloniruha, J. A., Kadiri, W. O. J., Ogundare, S. K. and Tunku, P. (2012). Relationship between soil properties and yield of Amranthusvidris at two topo –locations within Kabba, Nigeria. *A.B.U Journal of Vocational Studies*, 6, pp. 178-180.

Baumhardt, R. L., Stewart, B. A. and Sainju, U. M. (2015). North American soil degradation: processes, practices and mitigating strategies. *Sustainability*, 7, pp. 2936-2960.

Cobo, J. G., Dercon, G. and Cadisch, G. (2010). Nutrient balances in African land use systems across different spatial scales: A review of approaches, challenges and progress. *Agriculture, Ecosystems & Environment*, 136(1–2), pp.1-15.

Eswaran, H. and Dumanski, J. (1998). Land degradation and sustainable agriculture: A global perspective. Proceedings of 8th ISCO Conference New Delhi India. pp 208-225.

Food and Agriculture Organization (FAO) (2005). Agro-Ecological Zoning and GIS application in Asia with special emphasis on land degradation assessment in drylands (LADA). *Proceedings of a Regional Workshop, Bangkok, Thailand10 14 November 2003*. FAO. Accessed August 7, 2019, available on ftp://ftp.fao.org/agl/agll/docs/misc38e.pdf.

Food and Agriculture Organization (FAO) (1979). A provisional methodology for land degradation assessment. FAO. Rome.

Hulugalle, N. R. (1994). Long-term effect of land clearing methods, tillage systems and cropping system on surface soil properties of a tropical Alfisol in S. W. Nigeria. *Soil use and Management*, 10, pp. 25-80.

Ibrahim, M. M. and Idoga, S. (2013). Soil degradation assessment of the University of Agriculture, Makurdi students' industrial work experience scheme (SIWES) farm, Makurdi, Benue State. *Pat. Journal*. 9(2), pp. 126-135.

Idoga, S., Ibanga, I. J. and Malgwi, W. B. (2007).Variation in soil morphological and physical properties and their management implications on a toposequence in savanna Nigeria. In: Uyovbisere, E.O., Raji, B.A., Yusuf, A.A., Ogunwole, J.O., Aliyu, L. and Ojeniyi, S.O. editors. Soil and Water Management for Poverty Alleviation and Sustainable Environment. Proceedings of the 31st Annual Conference of the Soil Science Society of Nigeria held at Ahmadu Bello University, Samaru Zaria. pp. 19-25.

Igwe, C. A. (2003). Soil degradation response to soil factors in central eastern Nigeria. In: Proceedings of the 28th Annual Conference of Soil Science Society of Nigeria held at National Root Crops Research Institute, Umudike, pp. 228-234.

Isirimah, N. O. (2005). Land degradation, pollution and rehabilitation. In: Salako, F. K., Adetunji, M. T., Ojanuga, A. G., Arowolo, T. A. and Ojeniyi, S. O. editors. Managing soil resources for food security and sustainable environment. Proceeding of the 29th Annual conference of the soil Science Society of Nigeria held at the University of Agriculture, Abeokuta, pp. 35-37.

IITA (1979). *Selected methods for soil and plant analysis*. 2nd Ed., International Institute for Tropical Agriculture, Ibadan Oyo State, Nigeria. 70.

Leahy, S. (2018). land-degradation-environmental-damage-report. https://www.nationalgeographic.com/news/2018/03/ipbes-land-degradation-environmental-damage-report-spd/

Malgwi, W. B. and Abu, S. T. (2011). Variation in some physical properties of soils form on a hilly terrain under different land use types in Nigeria savanna. *International Journal of Soil Science*, 6(3), pp.150-163.

Martensson, U. (2009). Extract from Assessment of Soil Degradation in Nigeria. SSC Satellitbild, SWECO International, and Niger Surveys and Consultants. Kiruna.

Obaje, N.G. (2009). *Geology and mineral resources of Nigeria*. Springer Dordrecht Heidelberg London New York. 219p.

Senjobi, B. A., Ande, O. T. and Ogunkunle, A. O. (2013). Land degradation assessment under different uses: Implications on soil productivity and food security. *Agronomski Glasnik.* 1, pp. 3-21.

Soil Survey Staff (2014). *Keys to soil taxonomy*, 12th ed. USDA-Natural Resources Conservation Service, Washington, DC.

Sotona, T., Salako, F. K. and Adesodun, J. K. (2013). Soil physical properties of selected soil series in relation to compaction and erosion on farmers' fields at Abeokuta, southwestern Nigeria. *Archives of Agronomy and Soil Science*, 60(6), pp. 841-857.

Sankin, V. V., Krechetor, P. P., Kuzovnikova, T. A., Alyabina, I. O., Gurov, A. F. and Steoichev, A. V. (1996). The system of assessment of soil degradation. *Soil Technology*. 8, pp. 331-343.

Wynants, M., Kelly, C., Mtei, K., Munishi, L., Patrick, A *et al*. (2019). Drivers of increased soil erosion in East Africa's agro-pastoral systems: Changing interactions between the social, economic and natural domains. *Regional Environmental Change*, https://doi.org/10.1007/s10113-019-01520-9

Yusuf, M. B., Abba, U. J and Isa, M. S. (2019). Assessment of soil degradation under agricultural land use sites: Emerging evidence from the savanna region of north east Nigeria. *Ghana Journal of Geography*, 11(2), pp. 243-263.

Yusuf, M. B., Firuza B. M. and Khairulmaini, O.S . (2015). Survey of rill erosion characteristics of small-scale farmers' crop fields in the northern art of Taraba State, Nigeria. *International Journal of Tropical Agriculture*, 33(4), pp. 3305-3313.

**Cite this article as:**
Babalola, T. S., Ogunleye, K. S., Lawal, J. A. and Ilori, A. O. A, 2021. An Assessment of Degradation of Soil Properties in Kabba College of Agriculture, Kogi State, Nigeria. *Nigerian Journal of Environmental Sciences and Technology*, 5(1), pp. 102-109. https://doi.org/10.36263/nijest.2021.01.0240

Nigerian Journal of Environmental Sciences and Technology (NIJEST)

www.nijest.com

ISSN (Print): 2734-259X | ISSN (electronic): 2734-2603

Vol 5, No. 1 March 2021, pp 110 - 119

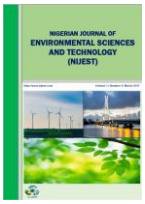

# Impact of Seasonal Variations on the Colonial Populations of Bacteria and Fungi in Soil and on Buried Plant Stems

Nwokoro O.[1] and Ekwem O. H.[2,*]

[1]Department of Microbiology, University of Nigeria, Nsukka, Nigeria

[2]South East Zonal Biotechnology Centre, University of Nigeria, Nsukka, Nigeria

Corresponding Author: ogechi.ekwem@unn.edu.ng

https://doi.org/10.36263/nijest.2021.01.0242

## ABSTRACT

*Forest soils and stems buried in them usually have varying degrees of colonization and abundance of bacteria and fungi. This study was undertaken to determine the effects of seasonal variations on the population of bacteria and fungi isolated from forest soil and on plant stems buried in the soil. Soil sampling and stem burial studies were conducted over a 12-month period in 2019. Serially diluted soil samples were plated on suitable media for bacterial and fungal growth and thereafter counted after incubation. Buried stems were removed from the soil, rinsed and placed in flasks containing suitable media for fungal and bacterial cultivation. Colonial growth was counted after incubation. Soil moisture was highest during the wet season months of July (27.7%), August (23.5 %), September 26.1 %) and October (29 %) whereas the average soil moisture content was lowest in the dry season. Seasonal pH did not significantly affect microbial population levels in the various months. Colony counts for Pseudomonas spp. during the dry season months (January, February, March and April) were very low. Growth of the bacterium showed peaks in the May through October during which counts reached $10^9$ cells per gram of soil except in August with counts of $10^8$ cells per gram of soil. Micrococcus spp. and Bacillus spp. also showed similar trends in colony counts with little variations. Fungi were generally fewer in number than bacteria and only one peak which reached $10^7$ cells/g soil was obtained for Fusarium spp. and Rhizopus spp. in September and October respectively. The density of Trichoderma spp. per gram of soil peaked at $10^6$ cells in June, July, September and October. Counts for Aspergillus spp. was negligible in January, February, March and April but reached $10^6$ cells per gram of soil in June, July and August. The colonization of Pseudomonas spp. on buried plant stem varied between 62% in June to 76% in October while Micrococcus spp. had levels which varied from 65% in May to 84% in June and 72% in October. Fusarium species were found most frequently on the stem every month except in February, March and April. Low colonization of Aspergillus spp. on stems occurred in January, February, March, November and December. Highest numbers of this organism was found in August, September and October. Rhizopus spp. was observed in 85 and 80% of the stem in September and October respectively but lower percentages of colonization occurred in January, February, March and April. In all the dry season months (January-April), all bacterial and fungal populations had low densities but their counts increased in the rainy season. Fungi were generally fewer in number than bacteria in both soil and stem burial experiments.*

**Keywords:** Microbial population, Soil sampling, Stem burial, Forest soil, Colonization rate

## 1.0. Introduction

Forest represents one of the largest and most important ecosystems on earth covering more than 40 million km$^2$ representing 30% of the global land and forest ecosystems are found in most of earth's biomes and harbour a large population of global diversity (Liado *et al*., 2007). Soil microorganisms constitute nearly 1% of the soil mass and they have a major impact on soil properties and processes (Cenciani *et al*., 2009). Nutrient cycles and functioning of the ecosystem are influenced by seasonal changes of soil microbial biomass (Lipson and Schmidt, 2004). Many biological activities which influence the growth of plants, animals and microbial populations occur in the soil. Microorganisms found in forest soil have been shown to perform various beneficial roles such as decomposition of soil

organic matter, nitrogen cycling and increase of soil fertility (Symochko *et al*., 2015). The activities and numbers of soil microorganisms determine soil fertility and its environmental status in the ecosystems as reflected on the level of soil biological activities (Cenciani *et al*., 2009). Microbial diversity in the forest soil occupying a particular location within the soil or on forest ground have been discovered to be affected by various environmental and climatic conditions. The soil microbial inhabitants could be referred to as the dominant organisms in contrast to transient organisms which do not occur most frequently throughout the months. The determination of the impact of environmental change on soil microbial function requires an understanding of how environmental factors shape microbial community and composition in the soil.

Determinations of numbers of microorganisms in soil as well as their isolations, morphological and physiological characteristics are important because soil is a huge reservoir of many biologically active agents. An active microorganism is capable of colonizing and growing on substrates and should be present in large numbers as to alter its environment. The existence of microorganisms in a particular environment including humid or warm environment usually develops through the ability of that organism to grow and multiply on the nutrients available in that locality or which have been transmitted to that locality.

Forest soil clearly represents the most important habitat for soil microorganisms especially fungi and bacteria with their activities being supported by the decomposition of organic matter, dead plant and animal remains. Microorganisms are responsible for the decomposition of soil organic matter thereby releasing nutrients that are absorbed by plants. These microorganisms are of importance in maintaining the fertility of the soil and factors which alter the rate of microbial processes in the soil are of importance for the functioning of the forest ecosystem. Although fungi are known to be the most dominant in forest soil but some bacteria are also abundant in most forest soils and results from recent studies have demonstrated an active role of bacteria in litter transformation (Liado *et al*., 2007).

Temperature of the tropical forest soil is always warm and moisture is abundant in the wet season and the relative humidity is high. Plants occasionally shed their leaves and provide organic matter on which microorganisms grow on and derive their energy. The spatial heterogeneity of forest top soils determines the composition of microbial communities mainly through two sets of drivers which include soil and litter chemistry which affect both bacteria and fungal population and diversities, although to variable degrees (Baldrian, 2017). Leaves of living plants provide shade for protection of microorganisms from direct sunlight. This makes biological activity intense and results in the abundance of different microbial forms in the forest soil. Dead plant biomass including fallen leaves and deadwood are the sources of most carbon compounds for forest microorganisms. Tons of fallen leaf matter which accumulate yearly on forest floor surface and their transformations is of great importance for the cycling of carbon and other nutrients. Litter habitat is composed of a diverse group of fungi and bacteria which play important roles in decomposition and transformation of forest soil organic matter.

Woody biomass of trees is a large resource in forest ecosystem which is reach in nutrients. Many and diverse species of microorganisms are well adapted to living on woods (Blanchette and Shaw, 1978). Fungi and bacteria are important in the soil ecosystem because they function in the decomposition mineralization and help in the movement of soil mineral elements to plant roots (Widawati and Suliash 2001). Species of fungi are important components of biodiversity in tropical forest soils and fungi perform some activities on which larger organisms including humans depend. Reported values of soil fungal diversity and population are a reflection of the sampling methods which differ from one organism to the other (Brock, 1987). Saprotrophic basidiophytes and white-rot wood-decomposing fungi often act as major litter decomposers together with ascomycetous fungi (Eichlerova *et al*., 2015). Deadwoods are also a source of carbon compounds in the forest. Decomposition of dead woods is influenced by diversities and types of fungi and bacterial species and also on the environmental conditions prevalent in that habitat (Gessner, 2010). Microorganisms produce a wide range of extracellular enzymes, which allows them to effectively degrade recalcitrant fractions of dead plant biomass (Eichlerova *et al*., 2015). Bacterial strains are among the dominant group of organisms in the forest soil. The ability of bacteria to survive ecological conditions includes the formation of endospores which have thick strong walls which make it easy for them to survive in extremes of environmental conditions (Kundu *et al*., 2009). Forests provide a wide range of habitats

for bacteria and they are abundant on forest soils and litter. Forest ecosystem provides a broad range of habitats for bacteria, including soil and plant roots but bacteria seems to be especially abundant on the forest floor, in soil and litter. Soil bacteria are the primary drivers of these ecological habitats (Bardgett and Leemas, 1995). Currently, bacteria community composition is an important determinant of ecosystem process rates, and identifying bacteria community composition has become an essential component for predicting ecosystem responses to environmental changes (Baldrian *et al*., 2012). However, before we can predict the ecosystem response to environmental change, we must first understand how the environment shapes bacteria community composition. For example, soil moisture can influence bacterial composition along topographic gradients as well as in multiple forest ecosystems (Brockett *et al*., 2012).

Forests represent a highly productive ecosystem that act as carbon sinks where soil organic matter is formed from residues after biomass decomposition as well as from rhizodeposited carbon (Baldrian, 2017). And factors such as pH, organic matter content, nutrient availability, climate conditions and biotic interactions affect the composition of bacterial communities in the soil is one of the important components and microbial activities and diversities in the soil help drive ecological and physicochemical reactions that occur in soil microenvironment. The determination of the impact of environmental change on soil microbial function requires an understanding of how environmental factors shape microbial composition (Allison *et al*., 2010). Microbial community composition is an important determinant of ecosystem process rates (Reed and Martiny, 2007), and identifying microbial community composition has become an essential component for predicting ecosystem responses to environmental change (Baldrian, *et al*., 2012). Climatic change alters the relative abundance and function of soil communities because soil community members differ in their physiology, temperature sensitivity, and growth rates (Castro *et al*., 2010; Gray *et al*., 2011). The direct effects of climatic change on microbial composition and activities have been well studied (Castro *et al*., 2010).

Soil temperature is an important physical property that regulates most of the physical, chemical, and biological processes of the soil, and the physiological processes of soil organisms and forest plants (Zogg *et al*., 1997). Soil temperature has tremendous ecological impacts through evaporation, transpiration, organic matter decomposition, $CO_2$ emission due to soil respiration. In forest ecosystems, soil temperature regulates microbial transformations of nitrogen sulphur and other nutrients and controls decomposition of organic matter and formation of humus. Temperature is one of the most important factors influencing soil organic matter decomposition and microbial communities. Temperature, together with moisture content is among the most important environmental factors affecting microbial growth and activity in soils. The role of elevated temperature on microbial metabolism has received considerable recent attention (Bradford *et al*., 2008; Karhu, 2014).

Soil moisture is one the most important environmental factors influencing soil organic matter decomposition and production of greenhouse gases in terrestrial environments (Kirschboum, 2006). Soil water content is important in regulating oxygen diffusion, with maximum aerobic microbial activity occurring at moisture levels between 50% and 70% of water-holding capacity (WHC) (Linn and Doran, 1984). Seasonal changes in soil water content influence function–structure relationships of microbial communities and enzyme activities (Brockett *et al*., 2012). Soil moisture content, by altering conditions for soil microbiota, causes changes in the structural diversity and activity of microorganisms (Kim *et al*., 2008). Excess of water in the soil environment due to flooding or periodically heavy rainfalls is particularly threatening to aerobic bacteria (Walker *et al*., 2003). For soil microbiologist, it is important to determine the optimum moisture content of soil because it is the soil microbiota that is responsible for the rate of organic matter transformations in the soil microenvironment.

Soil pH is considered as one of the important factors that controls microbial community structure (Fierer and Jackson, 2006; Lauber *et al*., 2009). pH influences abiotic factors, such as carbon availability, nutrient availability, and the solubility of metals etc. (Cho *et al*., 2016). In addition, soil pH also controls biotic factors, such as the biomass composition of microorganisms in both forest and agricultural soils (Rousk *et al*., 2010). This work is aimed to study the effects of seasonal variations

on bacterial and fungal populations in forest soils and how these variations affect the colonization of buried plant stems over a 12-month examination period.

## 2.0. Methodology

### *2.1. Study area and sampling*

The topography of the study area is characterized by mean maximum and minimum temperatures which lie between 30-3°C and 20-25°C respectively. Rainy season in the area lasts for about 8 months from April to early November, with peaks in July, September and October. The dry season commences from mid-November to March. Soil samples were collected from 1-5cm of top soil and after passing the sample through sieve clothe, soil moisture was determined by placing soil in aluminium foil and the weights of the samples were measured. The soil was oven dried at 105°C for 24h to achieve a constant weight. Soil moisture was determined gravimetrically by weight deference and the values were converted to percentages.

Soil pHs were determined twice a month by placing 20g of air dried soil in glass beaker. Distilled water was added into the beaker and shaken. Soil pH was then determined with hand held pH meter (Hannah instrument).

### *2.2. Isolation and culturing*

The experimental plot located in a forest in Uzo-Uwani, Nsukka measured 10 x 5m and was mapped with wire gauze to avoid disturbance. Soil samples were collected twice per month from January to December 2019 from the surface (0 – 5cm). The samples were gently collected into sterile conical flasks containing either Nutrient broth for bacterial cultivation or Potato Dextrose broth and shaken at 50 x g in Gallenkamp shaker for 5h. The samples were serially diluted using normal saline solution and plated onto Nutrient agar for bacterial enumeration and Potato Dextrose agar (PDA) plates for the enumeration of fungi. Control uninoculated plates were separately prepared. Nutrient agar plates were incubated at 35°C in an incubator for 24h. The PDA plates were placed on the laboratory bench for 48 h at an approximate temperature of 30±2°C. Colony counts were obtained from the plates after the incubation periods. Pure bacterial cultures were obtained by streaking on fresh agar plates. Only plates containing 30 and less than 300 colonies were considered valid. Otherwise, they were not recorded (NR).

### *2.3. Stem burial studies*

Sterile banana stems each measuring 10 x 3cm were placed inside the soil at a depth of about 12cm. Eight such stems were buried on the first day of every month. Soil was added to completely burn the stems. Two buried stems were each removed for either bacterial or fungal examination after 14th and 28th day of burial. Each stem was aseptically rinsed in sterile distilled water and placed in conical flasks containing Nutrient broth for bacterial cultivation or Potato Dextrose broth for fungal cultivation; then shaken at 50 x g in Gallenkamp shaker for 5h. The samples were serially diluted using normal saline solution and plated onto Nutrient agar for bacterial enumeration and Potato Dextrose agar (PDA) plates for the enumeration of fungi. Nutrient agar plates were incubated at 35°C in an incubator for 24h. The PDA plates were placed on the laboratory bench for 48h at an approximate temperature of 30±2°C. Pure bacterial cultures were obtained by streaking on fresh agar plates. Only plates containing 30 and less than 300 colonies were considered valid. Otherwise, they were not recorded (NR).

### *2.4. Identification of the isolates*

Bacteria were identified based on their morphological, physiological and biochemical characteristics as described in Bergey's Manual of Determinative Bacteriology (Holt *et al*., 1994). Fungal isolates were identified based on their morphological and cultural characteristics as outlined by Pitt and Hocking (1997).

## 3.0. Results and Discussion

Bacteria and fungi showed differences in their rates of occurrence in both the soil experiment and the stem burial studies. Four bacterial genera namely, *Bacillus* spp., *Pseudomonas* spp. and *Micrococcus* spp. were recovered from the soil in high numbers and they also showed best stem colonization. Fungal strains namely *Aspergillus* spp., *Fusarium* spp, *Rhizopus* spp., and *Trichoderma* spp. were dominant in the soil samples and were isolated in high numbers but only three of these fungi namely *Aspergillus* spp., *Fusarium* spp, and *Rhizopus* spp. displayed best colonization of the buried plant stems.

Results in Figure 1 show the mean soil moisture contents of the study area. It is evident that soil moisture was highest during the wet season months of July, (27.7%); August, (23.5 %); September, 26.1 % and October (29 %) whereas the average soil moisture contents were lowest in January, (6.4%); February, (5.6 %); March, (3.1%); April, (17.6 %). Data in Figure 2 shows the average soil pH values for the various months and these changes did not give any significantly positive growth responses to microbial population levels.

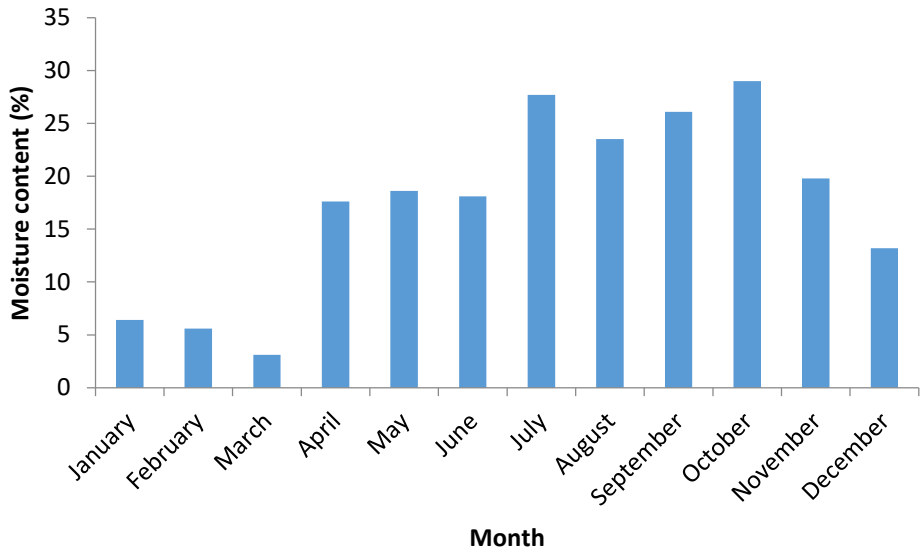


**Figure 1:** Moisture contents of soil at the study location

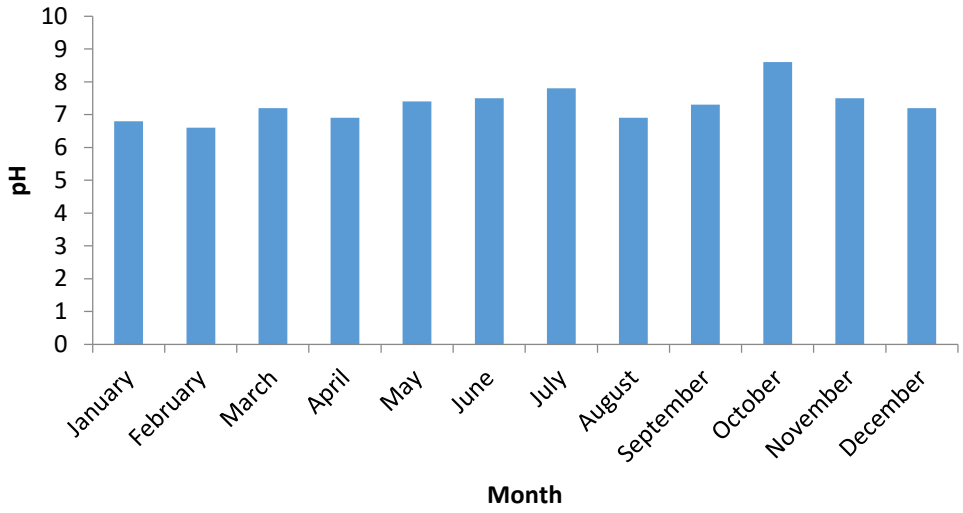


**Figure 2:** Soil pH at the study location

For *Pseudomonas* spp., colony counts during the dry season months (January, February, March and April) were very low (Table 1). Colonial growth showed peaks in May, June, July, September and October during which counts reached $10^9$ cells per gram of soil. This level fell in November and

December. *Bacillus* spp. and *Micrococcus* spp. counts also showed similar trends with little variations (Table 1). In all the dry season months (January-April), all bacterial populations did not reach densities of $10^6$ cells/gram of soil (Table 1).

**Table 1:** Relative frequency of bacteria per gram forest soil measured over a 12-month period

| Month | Number of organisms | | |
|---|---|---|---|
| | *Pseudomonas* spp. | *Bacillus* spp. | *Micrococcus* spp. |
| January | NR | NR | NR |
| February | NR | $2.6x10^2$ | NR |
| March | $6.3x10^2$ | $3.1x10^2$ | NR |
| April | $6.5x10^3$ | $3.4x10^3$ | $3.2x10^3$ |
| May | $8.2x10^9$ | $6.2x10^8$ | $4.9x10^4$ |
| June | $7.4x10^9$ | $6.5x10^9$ | $6.9x10^8$ |
| July | $7.9x10^9$ | $7.3x10^9$ | $8.8x10^8$ |
| August | $8.1x10^8$ | $8.1x10^9$ | $7.4x10^9$ |
| September | $7.8x10^9$ | $7.4x10^9$ | $7.9x10^9$ |
| October | $6.5x10^9$ | $8.6x10^8$ | $4.9x10^9$ |
| November | $5.1x10^8$ | $5.4x10^7$ | $8.2x10^7$ |
| December | $4.8x10^3$ | $5.2x10^5$ | $2.1x10^2$ |

NR: Not recorded

During the months of January, February, March, April and December 2019, there was very little rainfall and the numbers of fungi were very low (Table 2). Fungi were fewer in number than bacteria and only one peak which reached $10^7$ cells/g soil was obtained for *Fusarium* spp. in September and for *Rhizopus* spp. in October. The density of *Trichoderma* spp. per gram of soil started to increase from April and peaked at $10^6$ cells in June, July, September and October. Colony counts for *Aspergillus* spp. was negligible in January, February, March and April but reached $10^6$ cells per gram of soil in June, July and August. Colony counts of *Aspergillus* spp. reduced in September and October with further reductions in November and December (Table 2).

**Table 2:** Relative frequency of fungi per gram forest soil measured over a 12-month period

| Month | Number of organisms | | | |
|---|---|---|---|---|
| | *Aspergillus* spp. | *Fusarium* spp. | *Rhizopus* spp. | *Trichoderma* spp. |
| January | $6.2x10^2$ | $2.8x10^3$ | NR | NR |
| February | $2.8x10^2$ | NR | NR | NR |
| March | NR | NR | NR | NR |
| April | $1.0x10^4$ | $4.0x10^3$ | $3.9x10^3$ | $5.1x10^5$ |
| May | $2.1x10^5$ | $6.4x10^5$ | $3.6x10^5$ | $1.6x10^5$ |
| June | $6.5x10^6$ | $5.5x10^5$ | $4.4x10^7$ | $3.9x10^6$ |
| July | $5.3x10^6$ | $4.9x10^6$ | $5.9x10^7$ | $4.1x10^6$ |
| August | $4.9x10^6$ | $4.2x10^6$ | $5.8x10^6$ | $4.0x10^5$ |
| September | $6.9x10^5$ | $4.1x10^7$ | $4.2x10^6$ | $6.6x10^6$ |
| October | $9.2x10^5$ | $8.5x10^6$ | $2.6x10^7$ | $7.5x10^6$ |
| November | $9.5x10^3$ | $7.4x10^5$ | $7.5x10^5$ | $4.9x10^5$ |
| December | $6.6x10^2$ | $3.8x10^4$ | $4.3x10^5$ | NC |

NR: Not recorded

A number of previous studies have explored the influence of multiple environmental factors on the distribution of soil moisture (Nyberg, 1996; Crave and Gascuel-Odoux, 1997). Marked seasonal changes in vegetative cover were also thought partially to explain differences in soil moisture variability observed on different sampling dates (Reynolds, 1970). Reynolds (1970) examined the relationship between soil moisture variability, amount of rainfall and insolation received in the week preceding the sampling, and the moisture content and vegetation cover at the time of sampling. Although no attempt was made to infer the relative influence of each of these factors, trends were identified that were consistent with the notion that soil moisture variability increases with increasing mean moisture content. Specifically, it was noted that low variance was associated with dry periods i.e. low mean moisture content; and that high variance was associated with wet periods.

Bacteria grew in small colonies from the stems with percent colonization higher than the fungi (Table 3). The highest colonization for all three bacteria occurred between the months of May through October. The occurrence of *Pseudomonas* varied between 62% in June to 76% in October while *Micrococcus* spp. had levels which varied from 65% in May to 84% in June and 72% in October. *Bacillus* spp. had highest colonization rates in May with percent colonization at 61%. Highest

reductions in the percent colonization of stems for all three bacteria occurred in the dry season months such that in January, February and March almost all the stems had very low percent colonization rates (Table 3).

**Table 3:** Colonization of buried stem by bacteria measured over a 12-month period

| Month | Percent colonization | | |
|---|---|---|---|
| | *Pseudomonas spp.* | *Bacillus spp.* | *Micrococcus spp.* |
| January | NR | 30 | NR |
| February | NR | NR | NR |
| March | NR | NR | NR |
| April | 40 | 45 | NR |
| May | 50 | 61 | 65 |
| June | 62 | 49 | 80 |
| July | 77 | 36 | 84 |
| August | 72 | 40 | 79 |
| September | 79 | 46 | 80 |
| October | 76 | 48 | 72 |
| November | 49 | 45 | 39 |
| December | 35 | 31 | 31 |

NR: Not recorded

The numbers of fungi were examined as they grew and colonized the buried sterile banana stems. Colony totals of fungi which grew from the buried stems are summarized in Table 4. Only three fungal species namely *Aspergillus, Fusarium, Rhizopus* were predominant during the stem burial studies. The stem burial experiment showed a similar pattern as the soil experiment for instance, during the dry season months, there were generally low microbial counts as compared to counts obtained in wet season months (Table 4). *Fusarium* species were found most frequently on the stem every month except in February, March and April. Representative members of this genus appeared most frequently and more consistently than the other fungi especially from May to November and its occurrence varied between 75% in June and July; 81% in August and 73 and 79% in September and October respectively. Variations were found in January, February, March and April. Suppression of *Aspergillus* spp. occurred in January, February, March, November and December. Highest numbers of this organism was found in August, September and October. *Rhizopus* spp. was observed in 85 and 80% of the stem in September and October respectively but lower percentages of colonization was recorded in January, February, March and April. All fungi were more prevalent in August, September and October and decreased in January, February, March, April and December. Changes in soil nutrient content and some other environmental conditions more especially the availability of rainfall must have played a role in the pattern of microbial composition in soil and stem as reported in this work.

**Table 4:** Colonization of buried stem by fungi measured over a 12-month period

| Month | Percent colonization | | |
|---|---|---|---|
| | *Aspergillus* spp. | *Fusarium* spp. | *Rhizopus* spp. |
| January | 30 | 32 | NR |
| February | NR | NR | NR |
| March | NR | NR | NR |
| April | 44 | NR | NR |
| May | 69 | 64 | 62 |
| June | 52 | 75 | 71 |
| July | 50 | 75 | 69 |
| August | 62 | 81 | 77 |
| September | 68 | 73 | 85 |
| October | 72 | 79 | 80 |
| November | 38 | 53 | 60 |
| December | 32 | 39 | 53 |

NR: Not recorded

Numbers of both fungi and bacteria varied from time to time and from month to month. This tends to confirm that some elements of the microenvironment influence the types and numbers of microorganisms in the forest soil microenvironment (Girvan, 2003). It was reported that species of microorganisms must reach at least $10^6$ cells /g of soil to be of ecological importance in the soil (Symochko *et al*., 2015), but findings from this work revealed that for both soil experiment and stem burial studies, this level was not attained in the dry season months. The soil pH did not significantly influence microbial population levels as reported in this work. Cho *et al*. (2016) stated that soil pH

was critical to microbial community diversities and growth and these responses differed between a naturally acidic conifer forest soil with low pH and a sub urban forest soil with neutral pH but was loaded with several contaminants. Soil characteristics such as moisture, composition and diversity of substrates positively affected microbial population in the soil (Loeppmann *et al*., 2016). In the forest environment, large amounts of litter fall in the dry season and microorganisms derive energy by the metabolism of these organic matters, but this increased addition of organic matter did not result to increased fungal and bacterial densities observed in this study. Highest reductions in percent microbial colonization of the stem occurred in dry season months especially in January, February, March and April contrary to high percent colonization observed in the rainy season. It is evident from this work that soil water content optimally determined microbial population and Zogg *et al*. (1997) suggested that free water connecting soil particles optimally influenced microbial population and diversity patterns by controlling nutrient availability and cell movement while Brockett *et al*. (2012) reported that soil moisture was the major factor that influenced microbial community structure and enzyme activities across seven biogeoclimatic zones in western Canada.

## 4.0. Conclusion

This investigation was conducted to observe the populations of bacteria and fungi in forest soil determined over a 12-month period. Microbial colonization of buried straw was also evaluated with a view to finding how seasonal variations affect the rates of plant stem colonization by the organisms. Different levels of growth responses in terms of bacterial and fungal populations occurred due to changes in some environmental conditions like moisture and pH. Microbial population was highest during the wet season and the lowest fungal and bacterial populations occurred in the dry season. Positive growth responses of the organisms were largely dependent on the soil moisture but did not significantly depend on soil pH.

## References

Allison, S. D., Wallenstein, M. D. and Bradford, M. A. (2010). Soil-carbon response to warming dependent on microbial physiology. *Nature Geoscience*, 3, pp. 336–340.

Baldrian, P., Kolarik, M., Stursova, M., Kopecky, J., Valaskova, V., Vetrovsky, *et al*. (2012). Active and total microbial communities in forest soil are largely different and highly stratified during decomposition. *The ISME Journal*, 6, pp. 248–258.

Baldrian, P. (2017). Forest microbiome: diversity complexity and dynamics. *FEMS Microbiology Review*, 41, pp. 109-130.

Bardgett, R. D. and Leemas, D. K. (1995). The short-term effects of cessation of fertilizer applications, limiting and grazing on microbial biomass and activity in a reseeded upland grassland soil. *Biology and Fertility of Soils*, 19, pp. 148 – 154.

Blanchette, R. and Shaw, C. (1978). Associations among bacteria, yeasts and basidiomycetes during wood decay. *Phytopathology*, 63, pp.1-7.

Bradford, M. A., Davies, C. A., Frey, S. D., Maddox, T. R., Melillo, J. M., Mohan, J. E., *et al*. (2008). Thermal adaptation of soil microbial respiration to elevated temperature. *Ecology Letters*, 11, pp. 1316–1327.

Brock, T. D. (1987). The study of microorganisms in situ: Progress and Problems. *Symposium of the Society of General Microbiology*, 41, pp. 1 – 17.

Brockett, B. F. T., Prescott, C. E. and Grayston, S. J. (2012). Soil moisture is the major factor influencing microbial community structure and enzyme activities across seven biogeoclimatic zones in western Canada. *Soil Biology and Biochemistry*, 44, pp. 9–20.

Castro, H. F., Classen, A. T., Austin, E. E., Norby, R. J. and Schadt, C. W. (2010). Soil microbial community responses to multiple experimental climate change drivers. *Applied and Environmental Microbiology*, 76, pp. 999–1007.

Cenciani, K., Lambias, M. R., Cerri, C. C., Basilio den Azevedo, L. C. and Feigl, B. J. (2009). Bactria diversity and microbial biomass in forest, pasture and fallow soils in the Southwestern Amazon basin. *Revista Brasileira de Ciencia do Solo*, 33, pp. 907- 916.

Cho, S., Kim, M. and Lee, Y. (2016). Effect of pH on soil bacterial diversity. *Journal of Ecology and Environment*, 40, pp. 10

Crave, A. and Gascuel-Odoux, C. (1997). The influence of topography on time and space distribution of soil surface water content. *Hydrological Processes*, 11, pp. 203–210.

Eichlerova, I., Homolka, L., Zifcakova, L., Lisa, L., Dobiasova, P., and Baldrain, P. (2015). Enzymatic systems involved in decomposition reflects the ecology and taxonomy of saprotrophic fungi. *Fungal Ecoogy*, 13, pp. 10 – 22.

Fierer, N. and Jackson, R. B. (2006). The diversity and biogeography of soil bacterial communities. *Proceediings of the National Academy of Sciences*, 103, pp. 626–63.

Gessner, M. O. (2010). Diversity meets decomposition. *Trends in Ecological Evolution*, 25, pp. 372–380.

Girvan, M. S., Bullimore, J., Pretty, J. N., Osborn, A. M. and Ball, A. S. (2003). Soil type is the primary determinant of the composition of the total and active bacterial communities in arable soils. *Applied Environmental Microbiology*, 69, pp. 1800-1809.

Gray, S. B., Classen, A. T., Kardol, P., Yermakov, Z. and Miller, R. M. (2011). Multiple climate change factors interact to alter soil microbial community structure in an old-field ecosystem. *Soil Science Society of America Journal*, 75, pp. 2217–2226.

Holt, J. G., Krieg, N. R., Sneath, P. H. A., Staley, J. T. and Williams, S. T. (1994). Bergey's Manual of Determinative Bacteriology. 9th Ed. Baltimore, USA: Williams and Wilkins.

Karhu, K. (2014). Temperature sensitivity of soil respiration rates enhanced by microbial community response. *Nature*, 513, pp. 81–84.

Kim S.-Y., Lee S.-H., Freeman C., Fenner, N. and Kang, H. (2008). Comparative analysis of soil microbial communities and their responses to the short-term drought in bog, fen, and riparian wetlands. *Soil Biology and Biochemistry*, 40, pp. 2874–2880.

Kirschboum, M.U. (2006). The temperature dependence of organic-matter decomposition – still a topic of debate. *Soil Biology and Biochemistry*, 38, pp. 2510–2518.

Kundu, B. S., Nehra, K., Yadav, R. and Tomar, M. (2009). Biodiversity of phosphate solubilizing bacteria in rhizosphere of chickpea mustard and wheat grown in different regions of Haryana. *Industrial Journal of Microbiology*, 49, pp. 120 – 127.

Lauber, C. L., Hamady, M., Knight, R., and Fierer, N. (2009). Pyroseguencing- based assessment of soil pH as a predictor of soil bacterial community structure at the continental scale. *Applied and Environmental Microbiology*, 75, pp. 5111-5120.

Liado, S., Lopez – Mondejar, R. and Baldrian, P. (2017). Forest soil bacteria: Diversity, involvement in Ecosystem processes and response to global change. *Microbial Molecular Biology Review*, 81(2).

Linn, D. M. and Doran, J. W. (1984). Effect of water filled pore space on carbon dioxide and nitrous oxide production in tilled and non-tilled soils. *Soil Science Society American Journal*, 48, pp. 1267–1272.

Lipson, D. A. and Schmidt, S. K. (2004). Seasonal changes in an Alpine soil bacterial community in the Colorado Rocky Mountains. *Applied and Environmental Microbiology*, 70, pp. 2867 – 2879.

Loeppmann, S., Blagodatskaya, E., Pausch, J. and Kuzyakov, Y. (2016). Substrate quality affects kinetics and catalytic efficiency of exo-enzymes in rhizosphere and detritusphere. *Soil Biology and Biochemistry*, *92*, pp. 111–118.

Nyberg, L. (1996). Spatial variability of water content in the covered catchment at Gardsjon, Sweden, *Hydrological Processes*, 10, pp. 89–103.

Pitt, J. and Hocking, A. D. (1997). Fungi and food spoilage. London, United Kingdom: Blackie Academic and Professional.

Reynolds, S. G. (1970). The gravimetric method of soil moisture determination, III: An examination of factors influencing soil moisture variability. *Journal of Hydrology*, 11, pp. 288–300.

Rousk, J., Baath, E., Brookes, P. C., Lauber, C. L., Lozupone, C., Caporaso, J. G. *et al*. (2010). Soil bacterial and fungal communities across a pH gradient in an arable soil. *The ISME Journal*, 4, pp 1340 – 1351.

Symochko, L., Patyka, V., Symochko, V. and Kalinichenko, A. (2015). Soil microbial activity and functional diversity in Primeval Beech forests. *Journal of Earth Science and Engineering*, 5, pp. 363-371.

Widawati, S. and Suliasih (2001). The population of nitrogen fixing bacteria and phosphate solubilizing bacteria in the rhizosphere from Gunung Halimum National Park, Edisi Khusus Biodiversittas Taman National Gunung Halimum. *Berita Biologi*, 5, pp. 691 – 695.

Walker, T. S., Bais, H. P., Grotewold, E. and Vivanco, J. M. (2003). Root exudation and rhizosphere biology. *Plant Physiology*, 132, pp. 44–51.

Zogg, G. P., Zak, D. R., Ringelberg, D. B., MacDonald, N.W., Pregitzer, K. S. and White, D. C. (1997). Compositional and functional shifts in microbial communities due to soil warming. *Soil Science Society of America Journal*, 61, pp. 475–481.

**Cite this article as:**
Nwokoro O. and Ekwem O. H. 2021. Impact of Seasonal Variations on the Colonial Populations of Bacteria and Fungi in Soil and on Buried Plant Stems. *Nigerian Journal of Environmental Sciences and Technology*, 5(1), pp. 110-119. https://doi.org/10.36263/nijest.2021.01.0242

Nigerian Journal of Environmental Sciences and Technology (NIJEST)

www.nijest.com

ISSN (Print): 2734-259X | ISSN (electronic): 2734-2603

Vol 5, No. 1 March 2021, pp 120 - 139

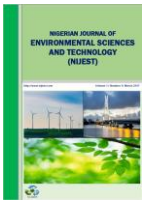

# Assessing the Impact of Urbanization on Outdoor Thermal Comfort in Selected Local Government Areas in Ogun State, Nigeria

Akinbobola A.[1,*] and Fafure T.[2]

[1,2]Department of Meteorology and Climate Science, School of Earth and Mineral Sciences, Federal University of Technology, Akure, Ondo State, Nigeria

Corresponding Author: *aakinbobola@futa.edu.ng

https://doi.org/10.36263/nijest.2021.01.0243

## ABSTRACT

*This study seeks to assess the land use land cover (LULC) and spatial-temporal trends of six outdoor thermal comfort indices in four Local Government Areas (LGAs) of Ogun state, Southwestern, Nigeria. Data used for this study are air temperature, relative humidity, cloud cover and wind speed which span from 1982 to 2018. These data were obtained from ERA-INTERIM archive. The 1986, 2000 and 2018 used for the analysis of the LULC were from the satellite imagery hosted by the United States Geological Survey (USGS). Landsat Thematic Mapper, Landsat 7 and Landsat 8 Operational Land Imager data of 1986, 2000 and 2018 to assess the changes that have taken place between these periods. Thermal comfort indices such as Effective Temperature (ET), Temperature Humidity Index (THI), Mean radiant temperature (MRT) and Relative Strain Index (RSI) were used. Rayman model was used for the computation of the three thermal comfort indices (MRT, PET, PMV). The results show decrease in vegetation, forest, and an increase in percentage of built-up areas between 1986–2000, and 2000–2018. A rapid increase in built-up areas in the three (Abeokuta South, Ifo, Shagamu,) of the four LGAs, while one (Ijebu East) has a slow increase in the built-up areas. The trend in the thermal comfort indices also shows that thermal discomfort had been on increase for the past 37 years and it was observed that the level of comfort has deteriorated more in the last decade compared to the previous decade especially in the built-up areas. This work suggests a framework for evaluating the relationship between the quantitative and qualitative parameters linking the microclimatic environment with subjective thermal assessment. This will contribute to the development of thermal comfort standards for outdoor urban settings. Also, the study will help urban planners in their decision making, and in heat forecast.*

**Keywords:** Thermal comfort, Urbanization, Temperature, Urban space, Trends

## 1.0. Introduction

Urbanization in Nigeria, as in most developing countries, has been rapid, and the explosion of urban population has not been matched by a change in social, economic and technological development (United Nations Population Fund, 2007; WHO, 2011). Public infrastructure, social and health services have been neglected, and urban planning and zoning have been very slow or even stagnant in many cases (Eludoyin *et al.*, 2013). Due to little or no climate responsive guidelines, sustaining outdoor life has been a serious issue in the tropics as urbanization increases rapidly (Ahmad, 2003). Also, the increasing urbanization of the subtropics is producing expanding urban areas with high density and a growing number of tall buildings (Ng, 2012). Comfort is more paramount to man, and that has brought about the study of thermal comfort over the years. The belief of thermal comfort came from the desire of man to be comfortable despite the climate (Eludoyin *et al*., 2013). Outside comfort zone lies the thermal stress (Ogunsote and Prucnal-Ogunsote, 2007). Studies have been made on thermal comfort since the 20th centuries, and it has brought improvements in which buildings are constructed, and also discoveries of air conditioning systems which aids comfortability in indoors even during the hottest and coldest climates. Outdoor thermal comfort is mainly about the physiology and also the heat balance of human body, which is commonly referred to as thermo-physiology (Höppe, 2002).

The outdoor thermal comfort assessment focuses on estimating people's thermal sensation in outdoor environment by considering meteorological factors and individual activities. The results can be used to identify the high-risk area suffering from thermal stress in urban area and the valuable measures to mitigate harmful environment. Yang *et al.* (2019) concluded that urban land use and anthropogenic heat (AH) emission can considerably influence the human thermal comfort during extreme heat events. In this study, a spatially heterogeneous AH emission data and updated urban land use data were integrated into the Weather Research and Forecasting model to simulate the physical processes of urban warming during summer. Simulations conducted in the Yangtze River Delta (YRD) of east China suggest that the mean urban heat island intensity reaches 1.49℃ in urbanized areas during summer, with AH emission making a considerable contribution. The warming effect due to urban land use is intensified during extremely hot days, but in contrast, the AH effects are slightly reduced. Urban development increases the total thermal discomfort hours by 27% in the urban areas of YRD, with AH and urban land use contributing nearly equal amount. By limiting the daytime latent heat release, urban land use reduces the daily maximum heat stress particularly during extremely hot days; however, such alleviations can be offset by the AH emission. Strategies for mitigation of urban heat island effect and heat stress in cities should therefore include measures to reduce AH emission. Massetti *et al.* (2019) observed that more than half of the world population lives nowadays in urban areas and that's the reason why the quality of the urban environment has become a key issue for human health. In this context, it is important to estimate and document any action that contributes to improving thermal comfort and air quality.

Simulated results in Quang-Van *et al.* (2016) show that the increase in the surface air temperature is approximately 0.22 ℃ in the preexisting urbanized area and approximately 0.41℃ in new highly urbanized areas. The rapid increase in global temperature has made outdoor thermal comfort an urgent topic (IPCC, 2007). It has been observed that there is a higher temperature in the urban growing areas compared to the rural areas, and that has made the assessment of thermal comfort in the urban areas more essential regarding the human health quality (Polydoros and Cartalis, 2014) for both indoor and outdoor environs. Galony (1996) revealed that temperature is non uniform across the perimeter of a city and it's largely dependent on land cover, location and the geometry of the city which are classified as local variables. Eludoyin *et al.* (2013) studied relative humidity, air temperature, thermal comfort and climate regionalization of Nigeria. The thermal comfort indices used such as THI, RSI, and effective temperature showed a contrasting result of thermal comfort for Nigeria due to variation in climate. Moreover, there was an observed increase in thermal stress from 2000 at most stations mostly in the north and south-western region.

This work seeks to assess the impact of urbanization on outdoor thermal comfort in selected Local Government Areas in Ogun state, by comparing trends in landuse/landcover with trends in temperature humidity index (THI), relative strain index (RSI), effective temperature index (ET), physiologically equivalent temperature (PET), and predicted mean vote (PMV).

## 2.0. Methodology

### *2.1. Study area*

The study areas as shown in Figure 1 are four selected local government areas in Ogun state, namely: Abeokuta South, Ifo, Shagamu, Ijebu East. Ogun State is considered to be one of the most developing areas in the southwest region of Nigeria because it shares boundary with Lagos State which is the main hub of activities. As a result of these developments, the four local government were selected, Abeokuta south, Ifo, and Shagamu local government areas plays a large part in this development while Ijebu east is known to be a rural area.

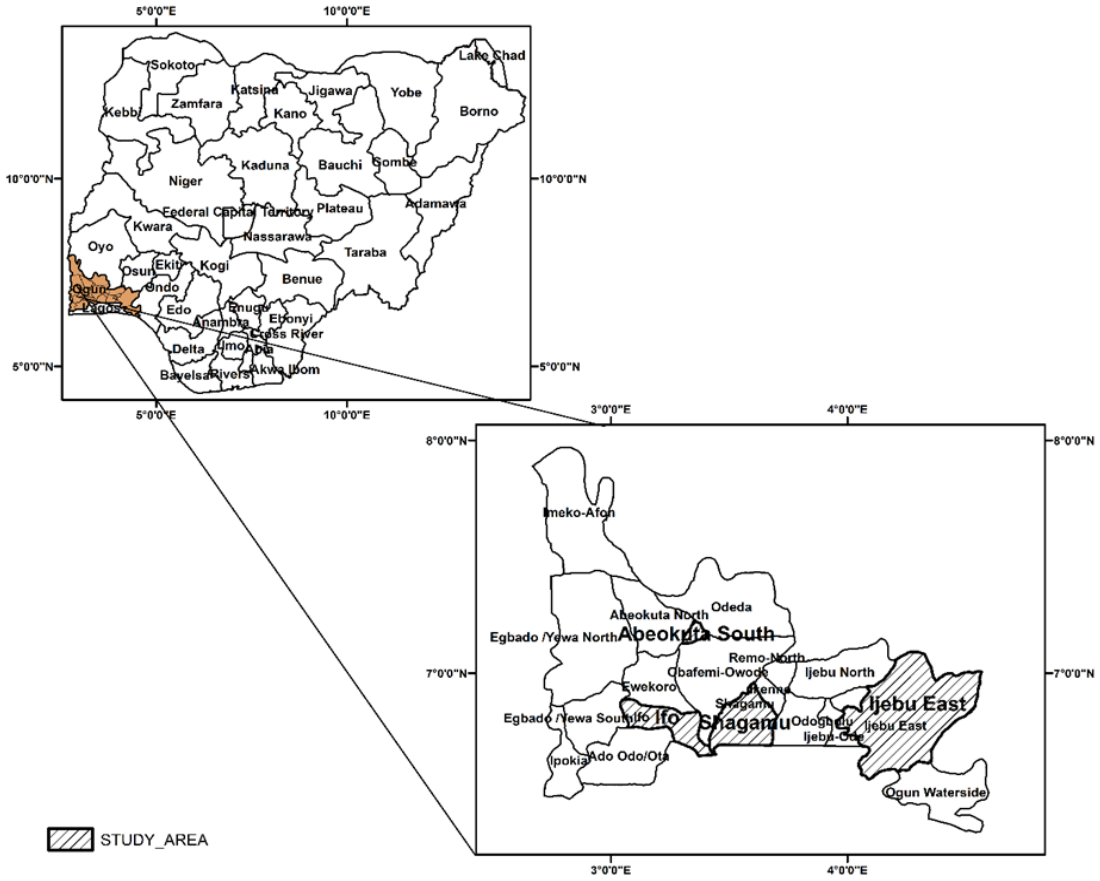


**Figure 1:** Maps showing location of the study area

2.1.1. Data acquisition

The research work used a gridded mean monthly data archived by ERA-INTERIM from the year 1982 to 2018 and this dataset includes the meteorological parameters needed for outdoor thermal comfort studies such as; relative humidity, air temperature, wind speed and cloud cover. Four LGAs (Abeokuta south, Ijebu east, Shagamu, Ifo) would be focused on in the study area. The LGAs can be classified under two categories; rural and urban. Ijebu east as rural, Abeokuta south, Ifo and Shagamu urban areas. What influenced the decision to use these four LGA classified into two, is for the comparison between the rural and urban area.

Rayman model was used in computing thermal comfort indices such as physiological equivalent temperature (PET), predicted mean vote (PMV) while effective temperature, relative strain index, and temperature humidity index were computed using a generally accepted formula for tropical regions. Outdoor thermal comfort indices like physiological equivalent temperature (PET) and predicted mean vote (PMV) asses thermal comfort in a thermo-physiological way, while Effective temperature (ET), relative strain index (RSI), and temperature humidity index (THI) does not. Figure 2 is the flowchart showing the procedure used in obtaining the data and methods used.

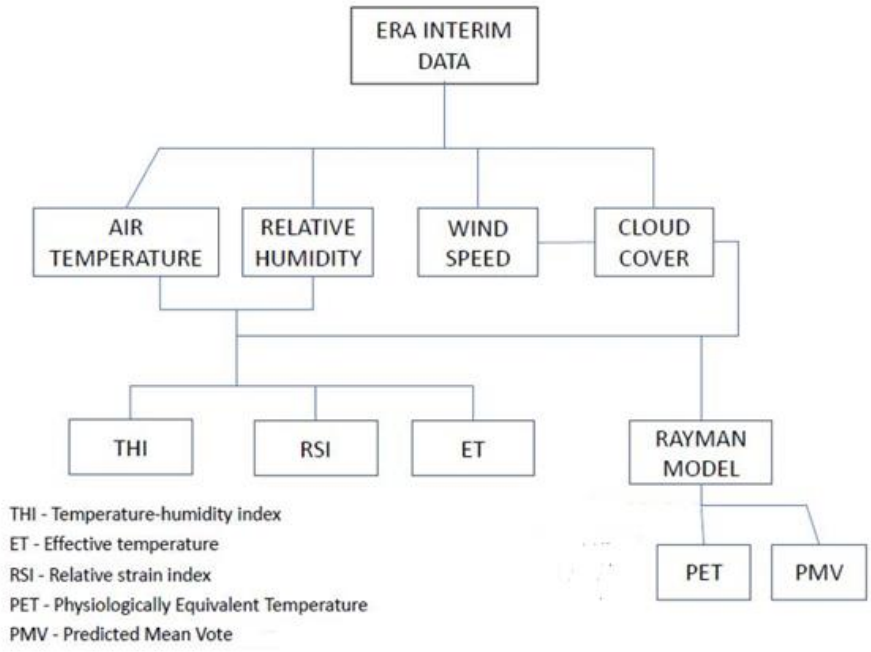


**Figure 2:** Flow chart showing how the data of each index were obtained

The formulae used in computing ET, THI, and RSI have been used by various researchers (Ayoade, 1978; Olaniran, 1982; Unger, 1999), and found to be valid and accepted for use in Nigeria and also in the tropics.

*2.2. Methods*

2.2.1. Estimation of THI
THI was estimated with the algorithm modified by (Nieuwolt, 1977) which is;

$$THI = 0.8T + \frac{RH \times T}{500} \quad (1)$$

where; THI – is Temperature Humidity Index, T – is air temperature, RH – is Relative Humidity
The categories of THI classification is given in Table 1.

**Table 1:** Thermal sensations with corresponding THI scale for Nigeria

| Thermal sensation | THI scale for Nigeria (°C) |
|---|---|
| Very cold | <14 |
| Cold | 14–17 |
| Cool | 18 – 19.5 |
| Slightly Cool | 20–22 |
| Neutral | 23 – 24.6 |
| Slightly warm | 24.7 – 27 |
| Warm | 28–30 |

Source: (Ogunsote, 2003; Olaniran, 1982; Ayoade, 1978; Markus and Morris, 1980; Omonijo and Matzarakis, 2011).

2.2.2. Estimation of RSI
RSI was estimated with the algorithm;

$$RSI = \frac{[10.74 + 0.74 + (T - 35)]}{44 - 0.0075\,(RH.es)} \quad (2)$$

where RH – Is Relative Humidity, T – Is the Air Temperature, es – saturated vapour pressure.

The classification of RSI developed by (Kyle, 1992) is presented in Table 2.

**Table 2:** RSI classification

| RSI | Proportion of persons unstressed/distressed (%) |
|---|---|
| 0.10 | 100 unstressed |
| 0.20 | 75 unstressed |
| 0.30 | 0 unstressed |
| 0.40 | 75 stressed |
| 0.50 | 100 stressed |

Source: (Kyle, 1992)

2.2.3. Estimation of ET

ET was estimated using the equation shown below:

$$ET = T - 0.4(T - 10)\left(1 - \frac{RH}{100}\right) \quad (3)$$

where T – Is the Air Temperature, RH – Is the Relative Humidity.

Table 3 shows the effective temperature scale which gives the ranges of temperature for thermal sensation.

**Table 3:** Thermal sensations with corresponding ET scale

| ET scale (◦C) | Thermal sensation |
|---|---|
| <18.9 | Cold Stress |
| 18.9 – 25.6 | Comfortable |
| 25.6 | Heat Stress |

Source: (Eludoyin *et al.,* 2013).

2.2.4. Estimation of PET and PMV

Matzarakis *et al*. (2007) developed Rayman model, an urban climate model which has been used for several studies on urban climate. This model was used in estimating PET and PMV. The comfort scale is presented in Table 4.

**Table 4:** PMV comfort scale

| PMV values | Human sensations |
|---|---|
| -3 | Cold |
| -2 | Cool |
| -1 | Slightly cool |
| 0 | Neutral (comfort) |
| +1 | Slightly warm |
| +2 | Warm |
| +3 | Hot |

Source: Given by the American Society of heating, refrigerating, and air conditioning engineers, Inc (ASHRAE).

The PET comfort scale is presented in Table 5.

**Table 5:** PET comfort scale

| Thermal sensation | PET range for Nigeria (◦C) |
|---|---|
| Very cold | <11 |
| Cold | 11-15 |
| Cool | 16-19 |
| Slightly cool | 20-23 |
| Neutral | 24-27 |
| Slightly warm | 28-31 |
| Warm | 32-36 |
| Hot | 37-42 |
| Very hot | >42 |

Source: Given by the American Society of heating, refrigerating, and air conditioning engineers, Inc (ASHRAE).

2.2.5. Land use change

The satellite imagery for 1982, 2001 and 2018 were used. This selection was made considering the availability of a cloud free imagery in the study between 1982 and 1999 and other factors like scar line error found in Landsat 7, otherwise the interval would have been regular.

Imagery for the selected years were classified into urban areas (this includes industrial, commercial, residential and non-vegetated area), forest, vegetation's (Thick bushes, farm lands, non-forest), and water bodies (lakes, rivers and ponds) using supervised method of classification.

Field calculator was used in calculating the counts of the classified divisions into hectares.

$$Hectares = \frac{(Count \times Square\ of\ Cell\ size\ of\ classified\ image)}{10000} \quad (4)$$

## 3.0. Results and Discussion

### *3.1. Land use*

Figures 3(a-d), 4(a-d) and 5(a-d) show the land use trend in Abeokuta south, Ifo, Shagamu, and Ijebu east in 1986, 2000 and 2018 respectively. In these figures, it was observed that there is a significant deterioration of vegetation and forests from 1986 to 2018, while the urban areas keep expanding.
This Figure 3(a-d) revealed the percentage covered by different classes of LULC in 1986. In 1986 LULC of Abeokuta south shows that 55% of the land area was covered with vegetation, while 39% of the land area was urban and the remaining 6% were areas covered with forest. That of Ifo showed that 68% of land area was covered with forest, while built-up areas and vegetation takes 7% and 25% respectively. Shagamu LULC revealed that forest covered up to 22% of the land, while vegetation took up to 73%; the built-up area covered just 5% of the land area. Ijebu east has little or no water body, 74% of Ijebu east land area was covered with forest, vegetation takes 25% and built-up areas covered 1% of the area.

LULC of the four LGAs in 2000 is represented in Figure 4(a-d). It was observed in the figure that Abeokuta south had a slight decrease in the percentage of vegetation that covers the land area (vegetation – 54%), built-up area and forest still maintains 39% and 6% respectively. There was a notable addition of water body, which might have been covered by vegetation in Figure 3(a) representing 1986 LULC. Water body takes 1% of the land area.

Ifo in 2000 as shown in Figure 4(a-d) has a 2% reduction from 1986 LULC in the amount of vegetation that covered the area (vegetation 66%). Built-up areas increased to 12% from 7% while forest reduced to 22% from 25%. Shagamu has 0% of vegetation, forest covered 92% of the land and remaining 8% were fuilt-up areas. No notable change in the LULC of Ijebu east from 1986 to 2000. Forest maintains 74%, vegetation 25%, and built-up areas 1%.

In Figure 5(a-d) there was a drastic change in LULC for most of the LGAs when compared to 1986 and 2000 LULC. Abeokuta south land area in the figure was observed to be covered by 93% built-up areas, 1% forest and 6% vegetation. Ifo land area increased in number of built-up areas to 37%, the amount of forest reduced to 45%, and the amount of vegetation in the area also decreased to 18%
LULC of Shagamu in 2018, showed the amount of forest in the area increased to 58% from 22% in year 2000. Vegetation also reduced drastically to 17%, while 25% of built-up area was observed, which is a large increase from the 5% it was in 2000. Ijebu east LULC shows a noticeable increase in the amount of forest covering the area (forest – 85%), 14% of the area were covered by vegetation, while 1% of built-up area was still maintained.

The increase in built up areas and deterioration in other classes such as (vegetation, forest and water bodies) shows that there is an increase in the level of urbanization in the four LGAs and Njoroge *et al.* (2011) already showed that land use related to human activities such as built areas increased to the detriment of wetland and vegetated areas, which signifies the city's growth. A rapid increase in built-up areas were observed in Ifo and Abeokuta south LGAs, while Ijebu east LGA has a slow increase in the built-up areas. A rapid increase in urbanization was however expected in Abeokuta south which is the capital of Ogun state.

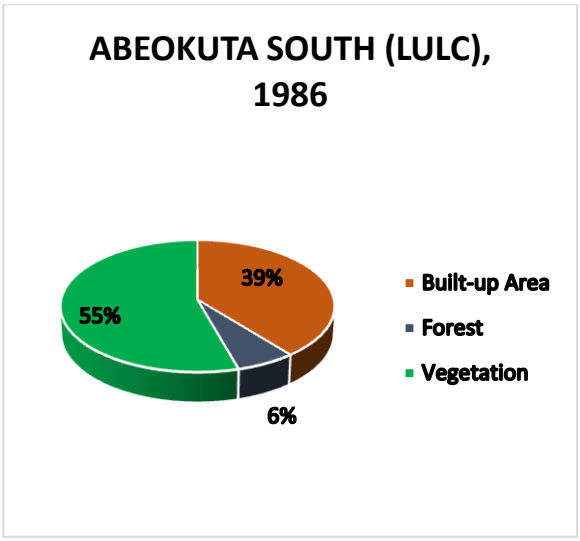


(a)

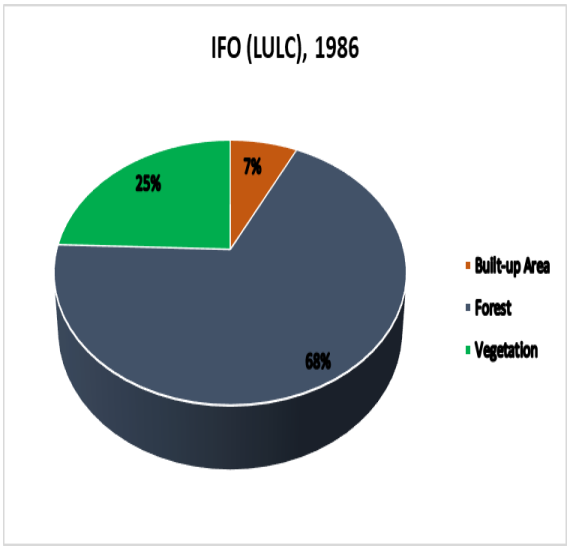


(b)

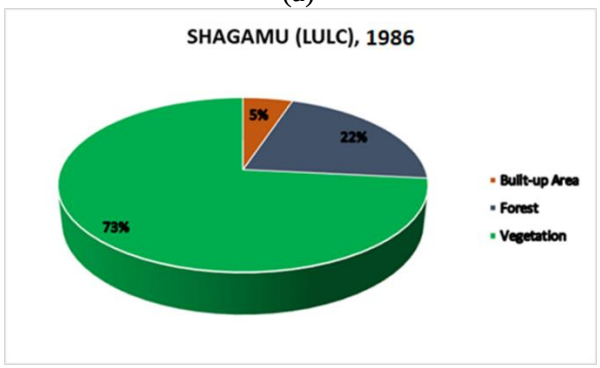


(c)

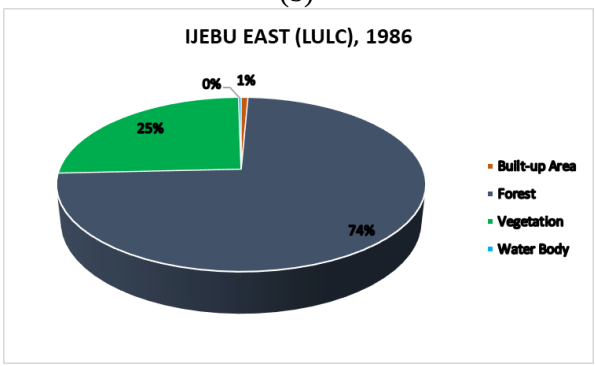


(d)

**Figure 3(a-d):** Pie chart showing the percentage covered by different class of LULC in 1986

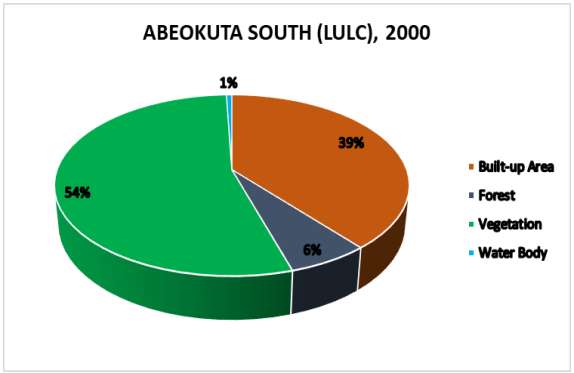


(a)

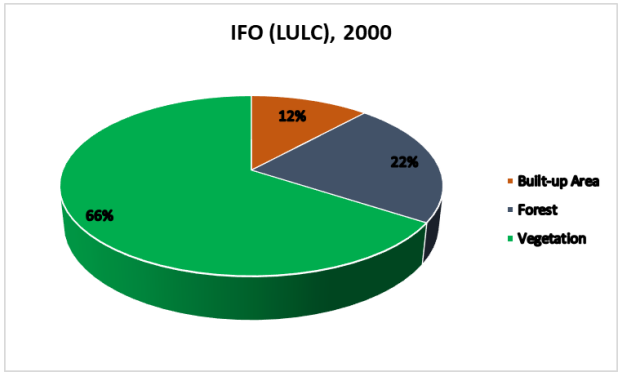


(b)

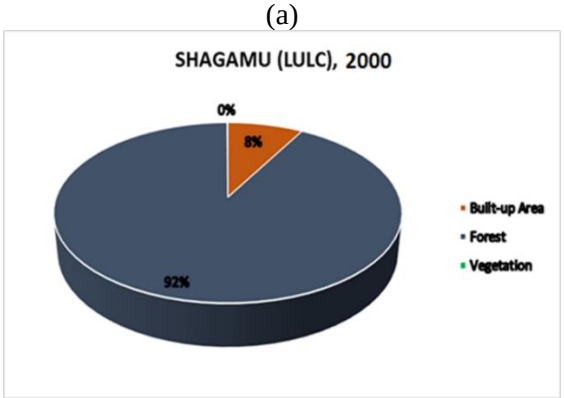


(c)

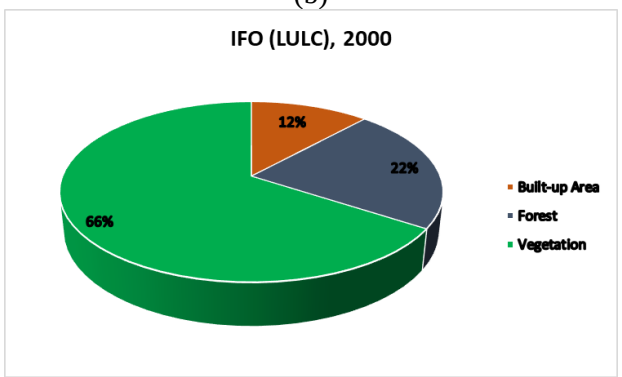


(d)

**Figure 4(a-d):** Pie chart showing the percentage covered by different class of LULC in 2000

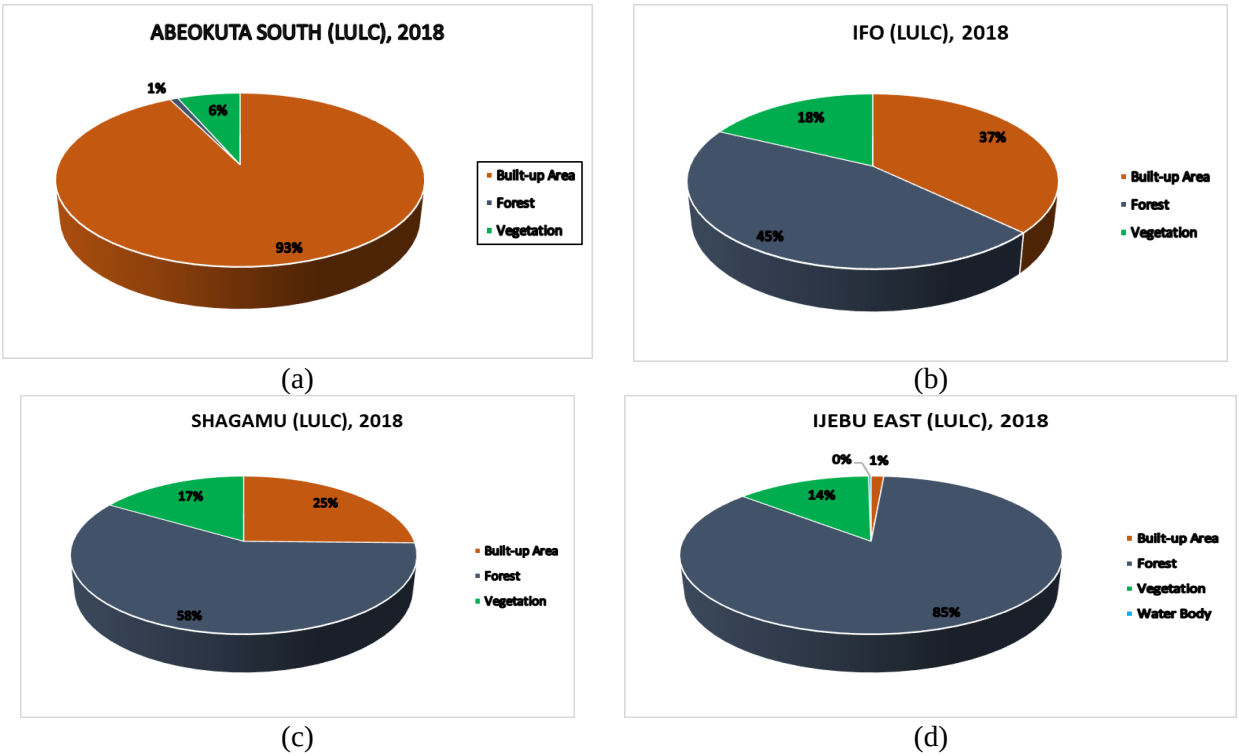


**Figure 5(a-d):** Pie chart showing the percentage covered by different class of LULC in 2018

*3.2. Annual trends of estimated thermal conditions*

Figure 6(a-e) shows the annual trends of AT, THI, PET, ET, RSI, PMV. Figure 6a shows the annual trends of estimated THI values, it can be observed that the highest value for THI in Abeokuta South, Ifo, Ijebu east were seen in 2010 (26.51, 26.65, 26.28 respectively) and Shagamu had its highest value both in 2010 and 2016 (26.58), while the lowest THI occurred in 1992 (Ifo 25.24, Ijebu East 24.69, Shagamu 25.07) except for Abeokuta South that has its lowest in 1989 which is 25. The figure showed increase in the trend of THI from 1982 to 2018 in all the LGAs; study from (Eludoyin *et al.*, 2013) shows that there was an increase in the value of THI in the tropical rain forest in region of Nigeria, which means an increase in the level of discomfort.

According to the THI classification used by (Omonijo and Matzarakis, 2011), the THI estimated values in the areas studied can be observed to be comfortable from 1982, and the level of discomfort significantly increased over the years. Despite the increase in the discomfort level THI value hasn't gone beyond the slightly warm THI classification level, however, some very close values to the upper limit of slightly warm level were noted.

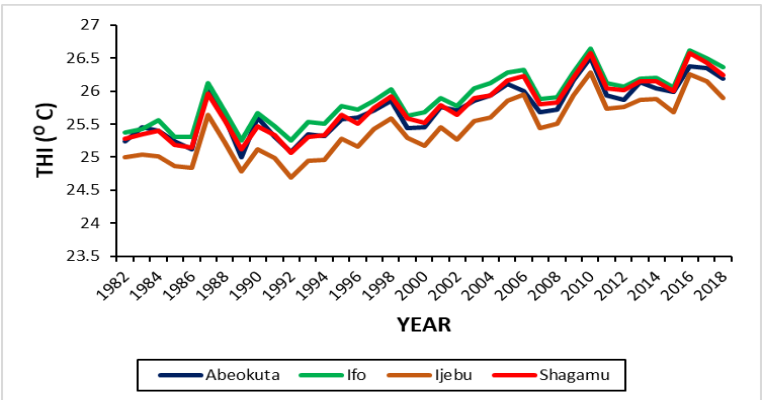


**Figure 6a:** Annual trends of estimated THI values from 1982 – 2018

Figure 6b shows the trends of RSI values in the stations; the RSI values from 1982 to 2018 drastically increased, which means the level of thermal discomfort are on the rise in these areas. Abeokuta South and Shagamu have their least RSI values in 1989 (0.089 and 0.091 respectively) while Ifo and Ijebu

east had the least RSI values in 1992 (0.099 and 0.073 respectively). The peak RSI values for all the areas were in 2010 (Abeokuta South – 0.157, Ifo – 0.164, Ijebu east – 0.146, Shagamu – 0.160). The Kyle RSI classification (1992) shows that above 75% of people in the study area feels unstressed.

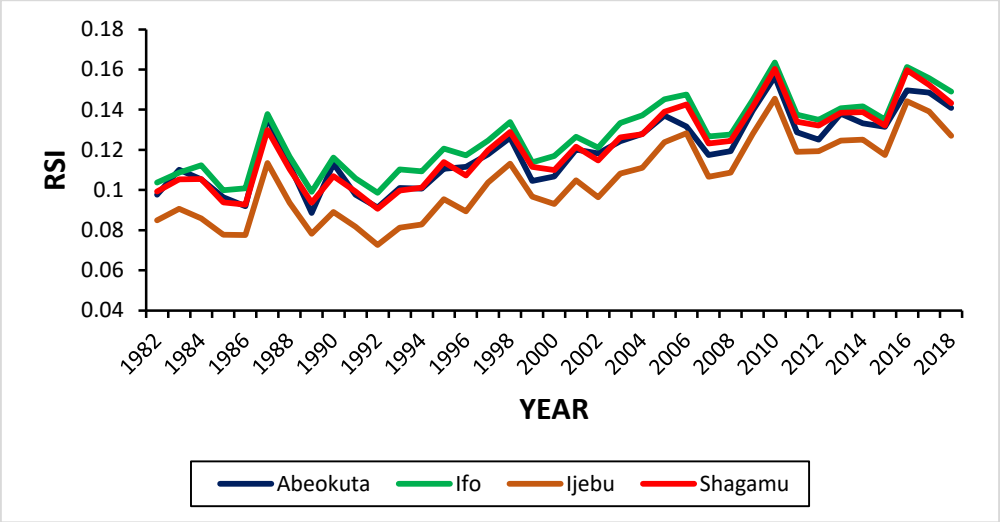


**Figure 6b:** Annual trends of estimated RSI values from 1982 – 2018

From the annual trends of PMV values in Figure 6c, it can be observed that there is an increase in thermal discomfort over the years. Based on PMV classification Ifo LGA exceeded the neutral (comfort) level all through the years (1982 – 2018), Abeokuta south and Shagamu had in one occasion recorded a PMV value at neutral level, while Ijebu east recorded PMV at neutral level in several occasions.

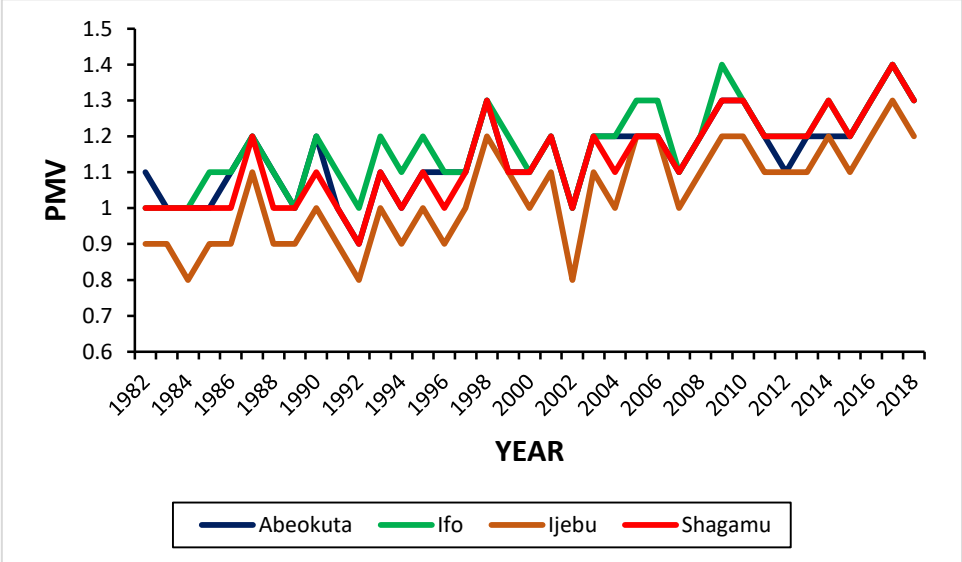


**Figure 6c:** Annual trends of estimated PMV values from 1982 – 2018

The annual trends of the PET value in the study area are shown in Figure 6d. The PET values of these areas can be categorized under slightly cool and neutral based on PET classification given by the American Society of heating, refrigerating, and air conditioning engineers, Inc (ASHRAE). Ijebu east PET values range from slight cool to neutral thermal conditions, while neutral conditions dominate all through (1982 – 2018) in Abeokuta south, Ifo, and Shagamu.

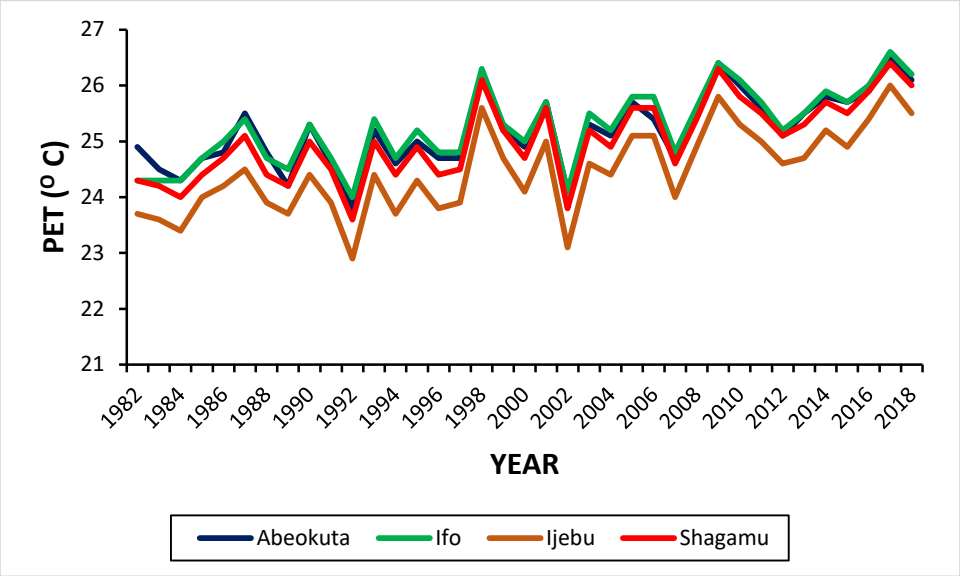


**Figure 6d:** Annual trends of estimated PET values from 1982 – 2018

The annual trend of effective temperature (ET) is shown in Figure 6e. The four LGAs all have their peak in 2010 (Abeokuta south – 26.29, Ifo – 26.43, Ijebu – 26.11, Shagamu – 26.37), while the least values of ET were found in 1992, except for Abeokuta south that has it's least ET value in 1989; Abeokuta south – 24.80, Ifo – 25.04, Ijebu – 24.53, Shagamu – 24.87. Using the ET classification by (Eludoyin *et al.*, 2013), it can be deduced that the comfortability state of the four LGAs in the first decade has deteriorated, and the heat stress of this areas are on the rise.

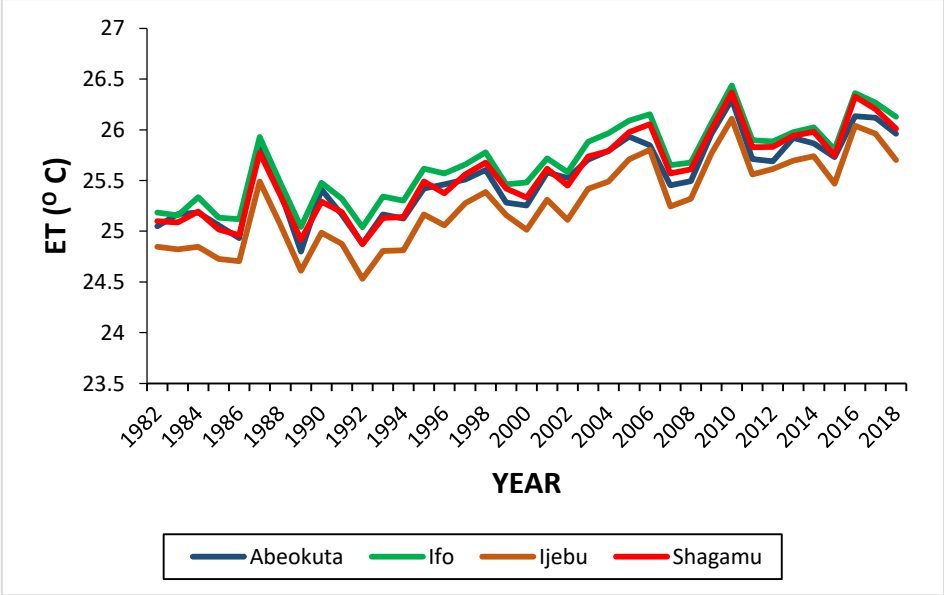


**Figure 6e:** Annual trends of estimated ET values from 1982 – 2018

The coefficient of determination for THI, ET, RSI in the four local government is above 50% and it implies that there is a high chance for the increase trend to continue with time. Coefficient of determination for PMV and PET values in Ifo, Shagamu, and Ijebu east are above 50%, thus a higher chance for continuous increase in the trend; Abeokuta South PMV and PET value is slightly below 50%. Coefficient of determination for MRT in the four LGAs is considerably low compared to the other five thermal comfort indices. Five out of the six thermal comfort indices in the four local government areas shows the rate at which thermal discomfort is increasing with time.

From the plots (Figure 6a-e), similar trend patterns were observed. The annual trends depict that thermal discomfort had been on the increase for the past 37 years and it could be observed that the level of thermal comfort has deteriorated more in the last decade compared to the previous decades.

Ifo LGA appears to be the most thermally discomfort in all the four LGAs, while Ijebu East LGA is the most thermally comfortable.

### *3.3. Spatial variations of estimated thermal conditions*

The spatial variations of the estimated mean of different thermal conditions (THI, RSI, PMV, PET, ET) from 1982 – 2018 are shown in the Figure 7(a-f).

Figure 7a shows the spatial variation of THI mean value from 1982 – 2018. From the figure, the four LGAs thermal condition can be categorized under slightly warm condition based on THI classification (Omonijo and Matzarakis, 2011). Discomfort condition was more pronounced in Ifo while Ijebu east has the lowest level of thermal discomfort. Figure 7b which is the estimated RSI mean values shows that the study areas fall within RSI categories of 100% of persons who feel unstressed and 75% of persons who feel unstressed. The level of thermal discomfort was also noticed to be higher in Ifo and lesser in Ijebu east.

Figure 7c represents the estimated PMV mean values; it also shows similar observations classifying the areas under slightly warm categories. With Ijebu east having a less thermal discomfort condition compared to the other LGA and Ifo has the highest discomfort level. Abeokuta south appear to be in a higher level of discomfort than Shagamu.

From Figure 7d showing the PET mean value, it can be observed that the four LGAs falls under the neutral category. The estimated effective temperature mean value from 1982 – 2018 presented in Figure 7e shows that Ifo and Shagamu can be classified under the heat stress level based on the ET classification by (Eludoyin *et al.*, 2013), while Ijebu East and Abeokuta South seats at the upper limit of the comfortability level of ET.

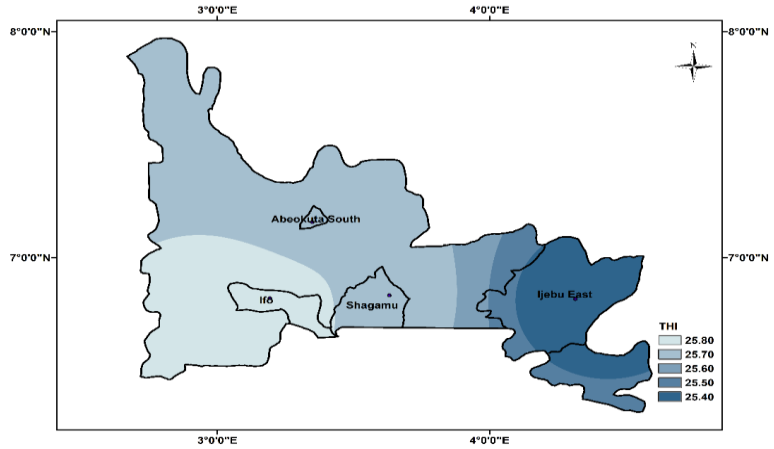


**Figure 7a:** Spatial variation of estimated THI mean value for the period 1982 – 2018

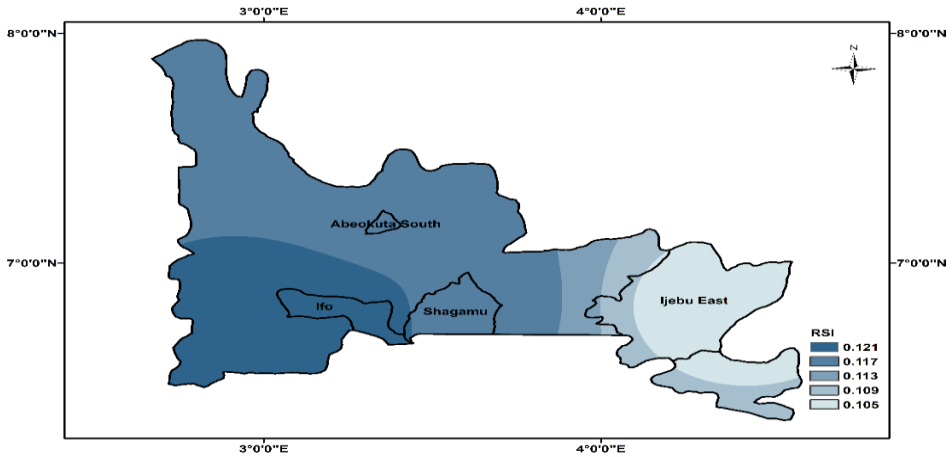


**Figure 7b:** Spatial variation of estimated RSI mean value for the period 1982 – 2018

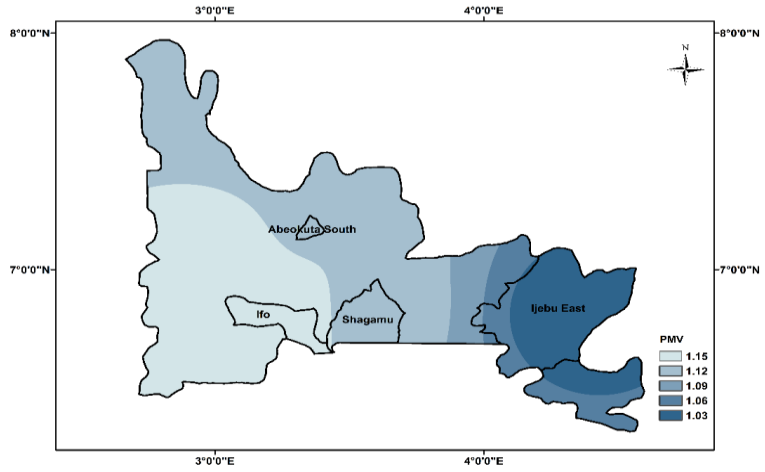


**Figure 7c:** Spatial variation of estimated PMV mean value for the period 1982 – 2018

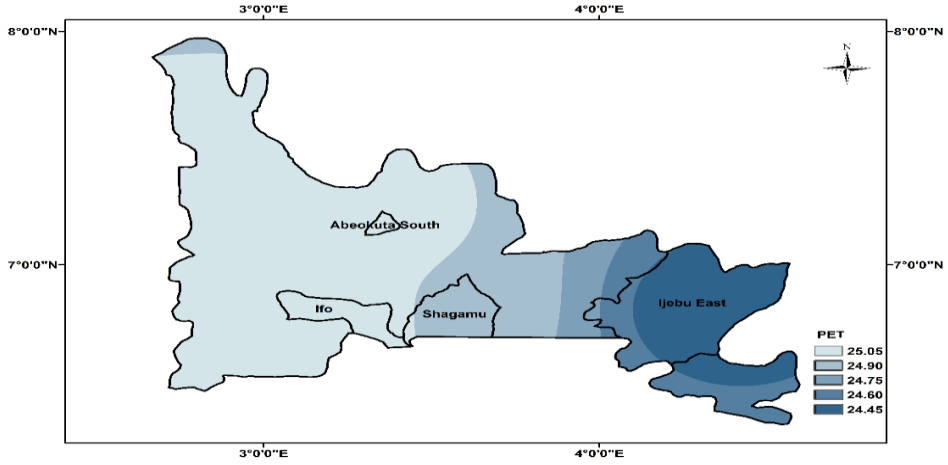


**Figure 7d:** Spatial variation of estimated PET mean value for the period 1982 – 2018

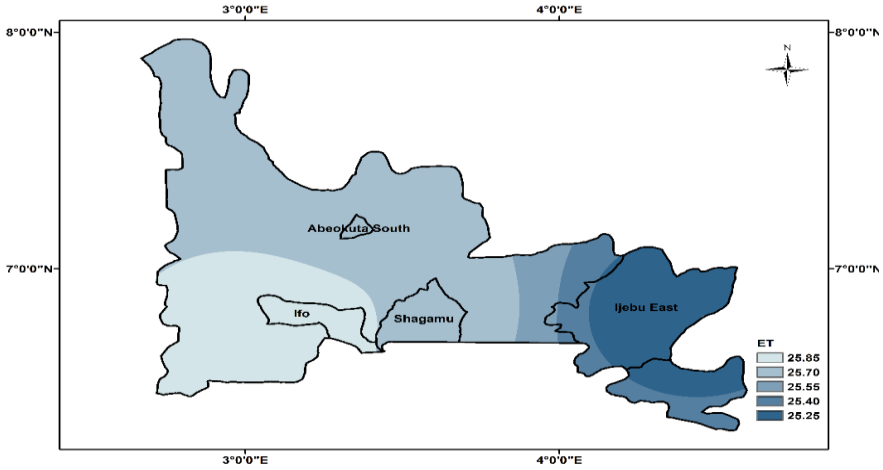


**Figure 7e:** Spatial variation of estimated ET mean value for the period 1982 – 2018

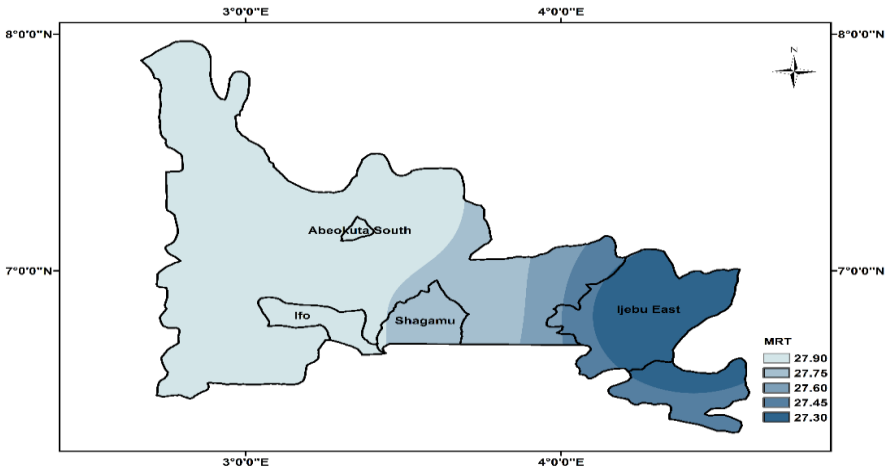


**Figure 7f:** Spatial variation of estimated MRT mean value for the period 1982 – 2018

*3.3. Thermal comfort and Land Use/Land Cover*

Figure (8a-p) show the trends of Air temperature and thermal indices along with the built-up areas within 1986 to 2018 in each LGAs, while Table 6 to 11 showed the percentage change of the built-up areas within 1986 to 2000 and 2000 to 2018. The built-up areas in Abeokuta south took as much as 2785 hectares in 1986; it later increased with 37.4% to 3826 hectares, and by 2018 it expanded by 72% to 6579 hectares. In 1986, built-up areas covered 3801 hectares in Ifo and by 2000 it increased by 62% to 6156 hectares; the built-up areas expanded drastically in 2018 by 214.3% (19351 hectares in 2018). Shagamu built-up areas increased by 60.9% from 3157 hectares in 1986 to 5079 hectares in 2000, and then further increased by 206.2% to 15554 hectares in 2018. Ijebu east recorded 1579 hectares covered with built-up areas in 1986, with 62% change from 1986 to 2000 it expanded to 2724 hectares and by 2018 it has expanded to 2843, which is only 4.4% increase from 2000.

It can be observed also from the figures that air temperature and the estimated thermal indices increases along with increase in Built-up areas from 1986 to 2018. Similar studies show that urbanization or more impervious surfaces have result to rising temperature in urban areas. (Silva *et al.*, 2018) found that rapid urbanization in Paçodo Lumiar County, Brazil had a significant impact on its surface temperature, which result to 5.3°C increase in urban surface temperature within 1988 and 2014 (a warming trend of 2.03°C/ decade), due to the result of the increase in the areas of impervious surfaces. Xiong *et al.* (2012) studied the urbanization impact in the urban climate of Guangzhou, South China showed that the highest increase in temperature anomalies was strongly associated with built-up areas. There were some exception; MRT in the four LGAs, had a lesser value in year 2000 compared to that of year 1986, but then, it increases to a higher value in 2018. Abeokuta south and Ifo LGAs maintained the same value of PMV in 1986 and 2000.

It can also be observed that among the four LGAs Ijebu east has the lowest urban development rate and it appears to be the area with the least thermal discomfort, while Ifo appears to be the highest both in urban development rate and thermal discomfort level. However, environmental development as studied by (Unger, 1999); can cause disruption of wind flow and air turbulence by built-up areas, alteration of natural radiation balance, upset of water vapour balance due to change of moist surfaces and the emission of artificial heat, water vapour through combustion processes. There has being an increase in commerce and industry with the human population, and the impacts on local climate cannot be overemphasized with 'heat islands' in many of the towns (Omogbai, 1985; Aina, 1989; Oniarah, 1990; Adebayo, 1991; Efe, 2004; Adelekan, 2005; Akinbode *et al.*, 2008). Robaa (2011) investigated the effect of urbanization on outdoor thermal human comfort in greater Cairo region. The study showed that urbanization plays a major role in the increase of human hot uncomfortable feeling, which limits human activities in the urban area, whereas the rural conditions lead to optimum weather comfort for further and more human activities.

**Table 6:** Built-up areas in Abeokuta south and Ifo and its percentage change within 1986 to 2018

| Year | Built-up Areas in Abeokuta South (hectares) | Percentage Change (%) | Built-up Areas in Ifo (hectares) | Percentage Change (%) |
|---|---|---|---|---|
| 1986 | 2785 | 37.4 | 3801 | 62 |
| 2000 | 3826 | 72 | 6156 | 214.3 |
| 2018 | 6579 | | 19351 | |

**Table 7:** Built-up areas in Shagamu and Ijebu East (°C) and its percentage change within 1986 to 2018

| Year | Built-up Areas in Shagamu (hectares) | Percentage Change (%) | Built-up Areas in Ijebu East (hectares) | Percentage Change (%) |
|---|---|---|---|---|
| 1986 | 3157 | 60.9 | 1579 | 72.5 |
| 2000 | 5079 | 206.2 | 2724 | 4.4 |
| 2018 | 15554 | | 2843 | |

**Table 8:** Trends in built-up areas, greenspace, and selected thermal comfort indices in Abeokuta South

| Year | Built-up area (Ha) | Greenspace (Ha) | THI (°C) | ET (°C) | PET (°C) | RSI | PMV |
|---|---|---|---|---|---|---|---|
| 1986 | 2785 | 4315 | 25.116 | 24.932 | 24.9 | 0.0919 | 1.1 |
| 2000 | 3826 | 3232 | 25.454 | 25.255 | 24.9 | 0.107 | 1.1 |
| 2018 | 6579 | 301 | 26.192 | 25.961 | 26.1 | 0.141 | 1.3 |

**Table 9:** Trends in built-up areas, greenspace, and selected thermal comfort indices Ifo

| Year | Built-up area (Ha) | Greenspace (Ha) | THI (°C) | ET (°C) | PET (°C) | RSI | PMV |
|---|---|---|---|---|---|---|---|
| 1986 | 3801 | 48299 | 25.313 | 25.118 | 25 | 0.101 | 1.1 |
| 2000 | 6156 | 45944 | 25.682 | 25.482 | 25 | 0.117 | 1.1 |
| 2018 | 19351 | 32749 | 26.363 | 26.127 | 26.2 | 0.149 | 1.3 |

**Table 10:** Trends in built-up areas, greenspace, and selected thermal comfort indices in Shagamu

| Year | Built-up area (Ha) | Greenspace (Ha) | THI (°C) | ET (°C) | PET (°C) | RSI | PMV |
|---|---|---|---|---|---|---|---|
| 1986 | 3157 | 58243 | 25.140 | 24.959 | 24.7 | 0.093 | 1 |
| 2000 | 5079 | 56,321 | 25.526 | 25.332 | 24.7 | 0.110 | 1.1 |
| 2018 | 15554 | 45846 | 26.242 | 26.010 | 26 | 0.143 | 1.3 |

**Table 11:** Trends in built-up areas, greenspace, and selected thermal comfort indices in Ijebu East

| Year | Built-up area (Ha) | Greenspace (Ha) | THI (°C) | ET (°C) | PET (°C) | RSI | PMV |
|---|---|---|---|---|---|---|---|
| 1986 | 1579 | 221216 | 24.843 | 24.703 | 24.2 | 0.078 | 0.9 |
| 2000 | 2724 | 220081 | 25.174 | 25.015 | 24.1 | 0.093 | 1 |
| 2018 | 2843 | 220019 | 25.901 | 25.702 | 25.5 | 0.127 | 1.2 |

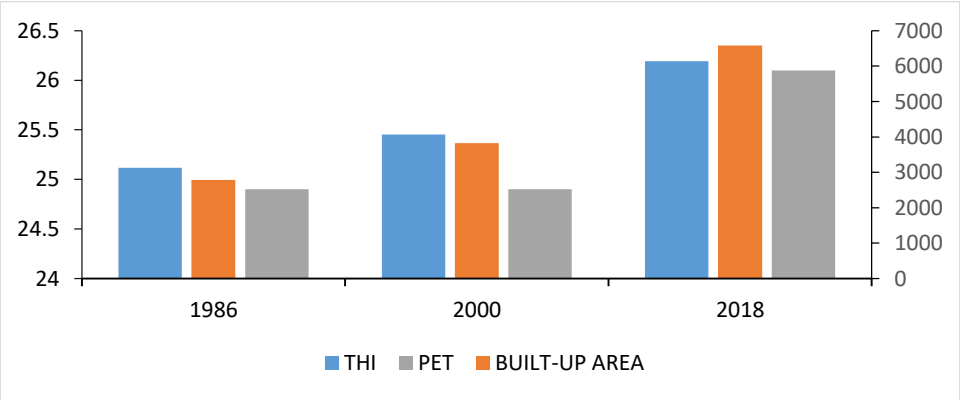


**Figure 8a:** Trends of THI, PET, and built-up areas in Abeokuta South

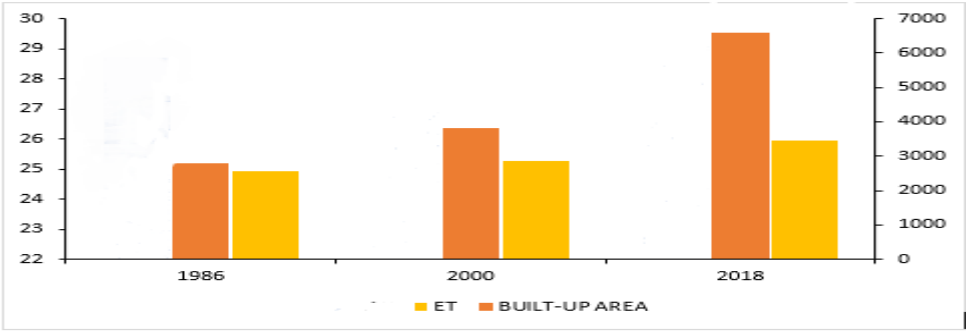


**Figure 8b:** Trends of ET and built-up areas in Abeokuta South

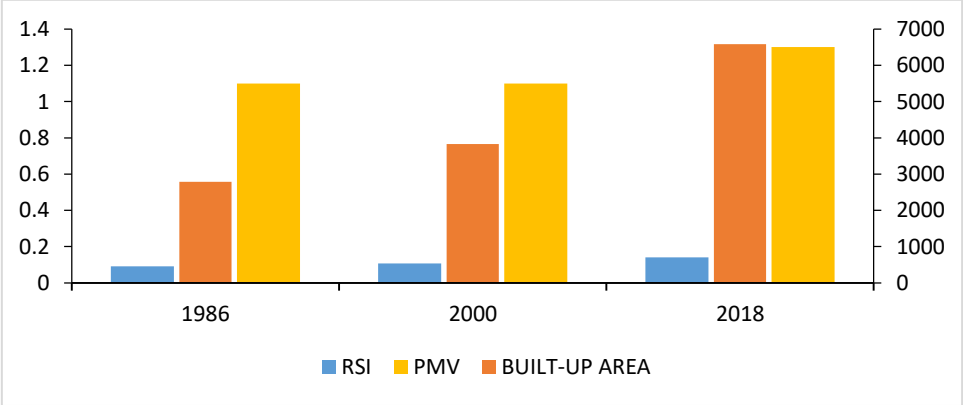


**Figure 8c:** Trends of RSI, PMV, and built-up areas in Abeokuta South

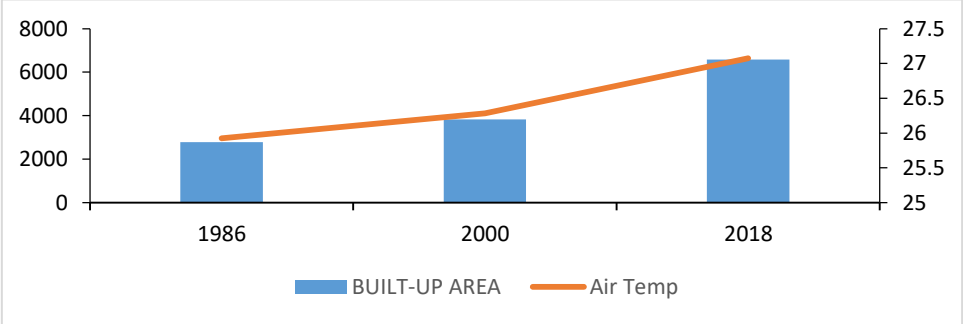


**Figure 8d:** Trends of air temperature and built-up areas in Abeokuta South

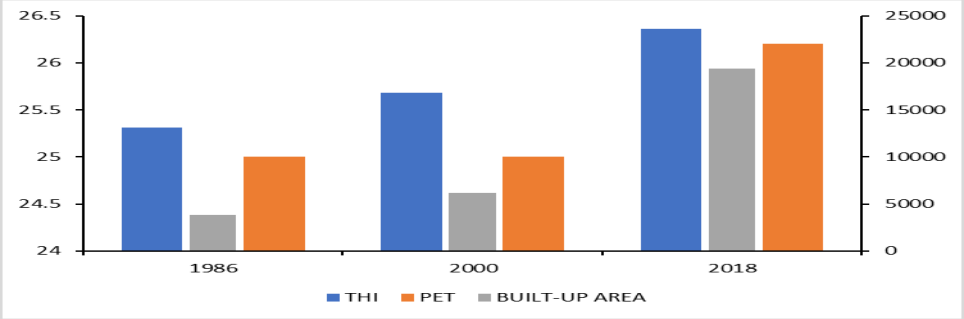


**Figure 8e:** Trends of THI, PET, and built-up area in Ifo

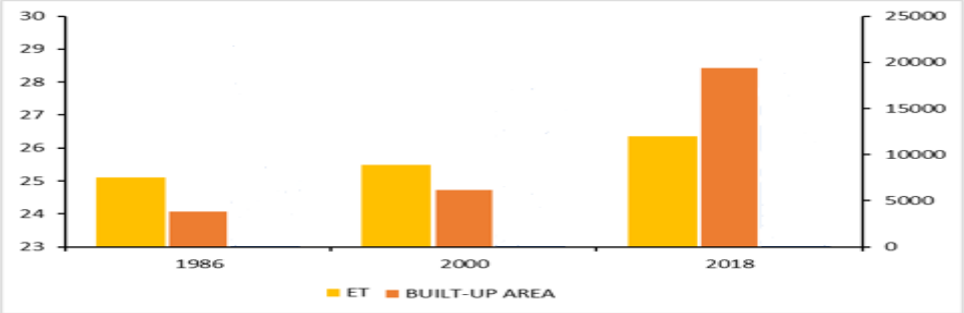


**Figure 8f:** Trends of ET and built-up areas in Ifo

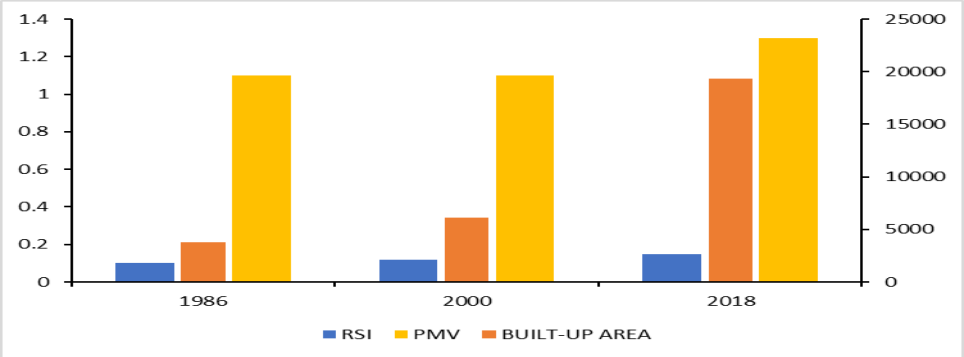


**Figure 8g:** Trends of RSI, PMV, and built-up areas in Ifo

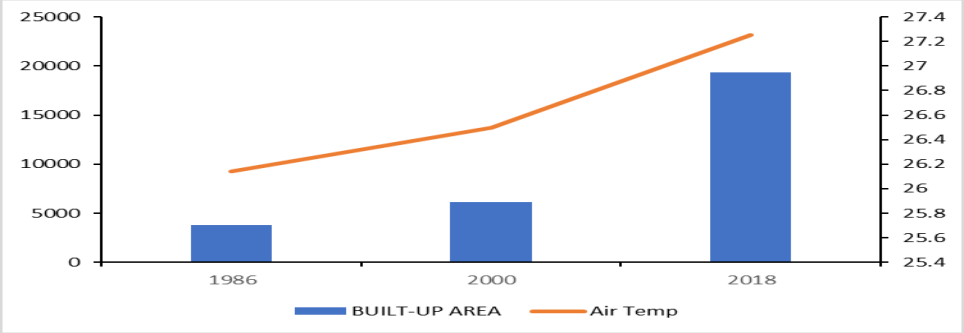


**Figure 8h:** Trends of air temperature and built-up areas in Ifo

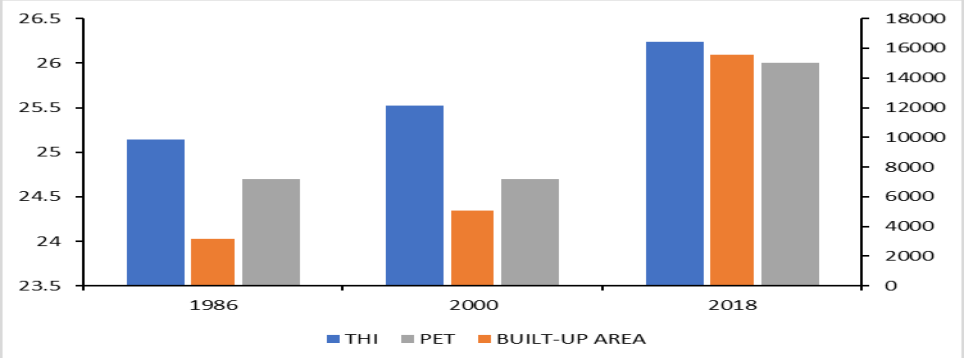


**Figure 8i:** Chart showing the trends of THI, PET, and built-up area in Shagamu

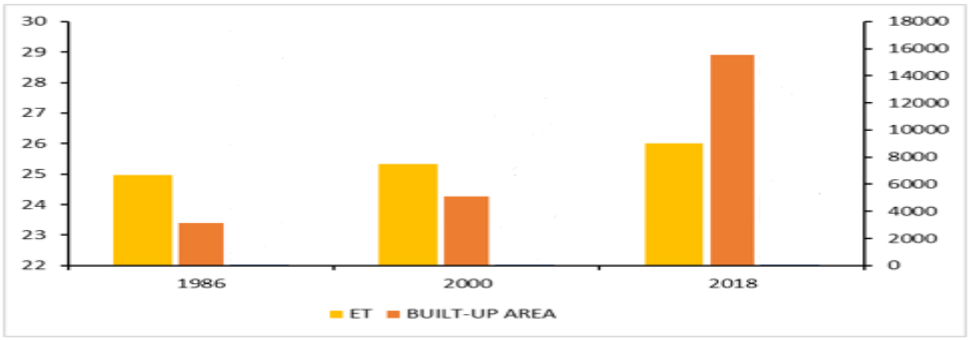


**Figure 8j:** Trends of ET and built-up areas in Shagamu

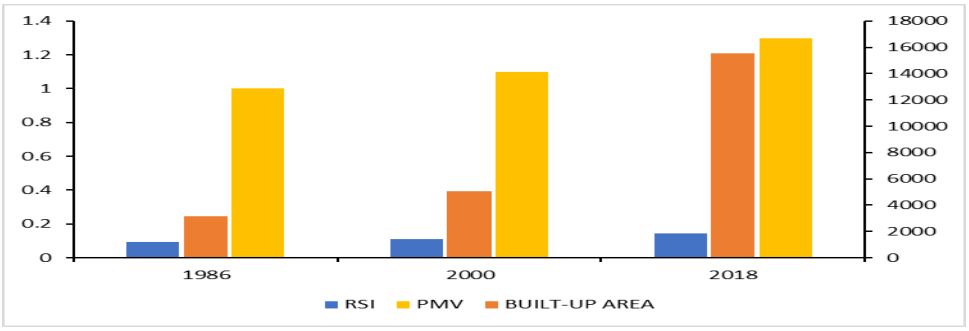


**Figure 8k:** Trends of RSI, PMV, and built-up areas in Shagamu

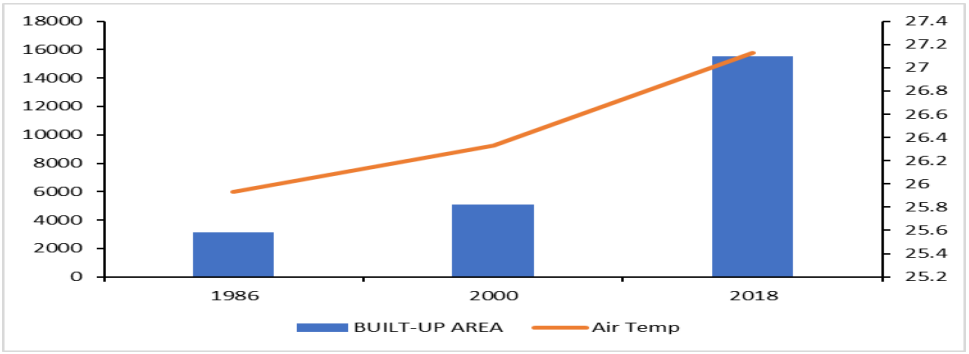


**Figure 8l:** Trends of air temperature and built-up areas in Shagamu

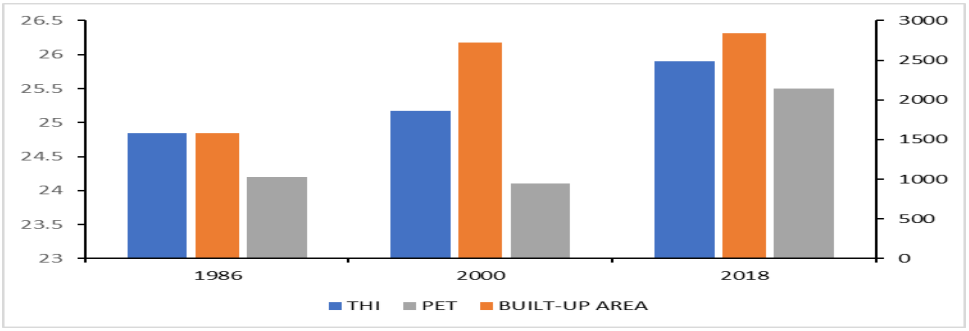


**Figure 8m:** Trends of THI, PET, and built-up areas in Ijebu East

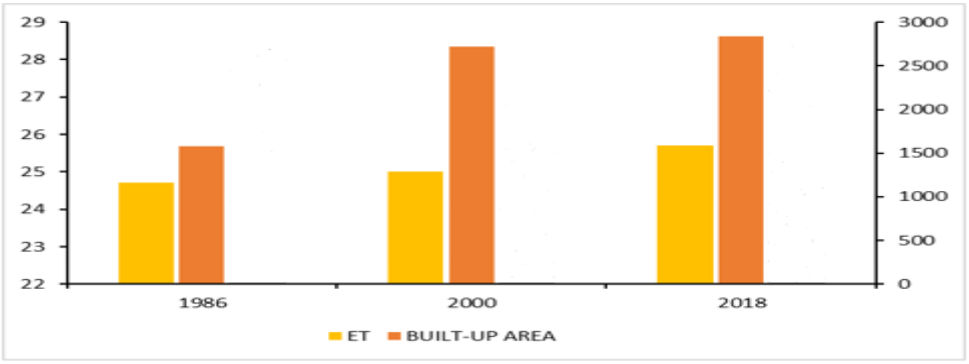


**Figure 8n:** Trends of ET and built-up areas in Ijebu East

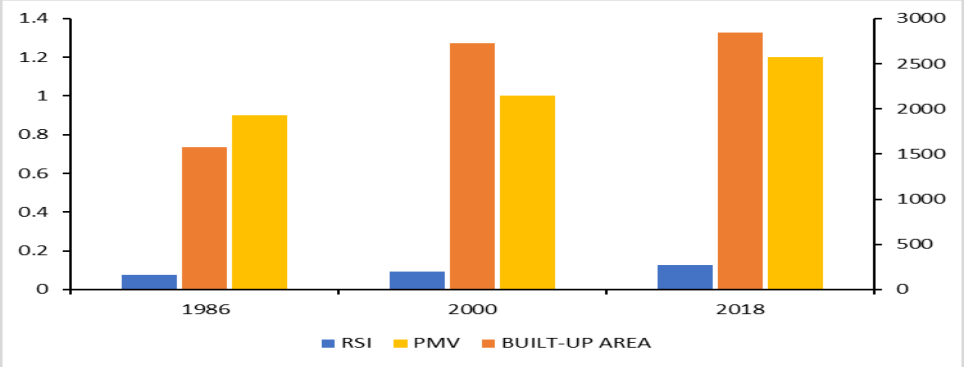


**Figure 8o:** Trends of RSI, PMV, and built-up areas in Ijebu East

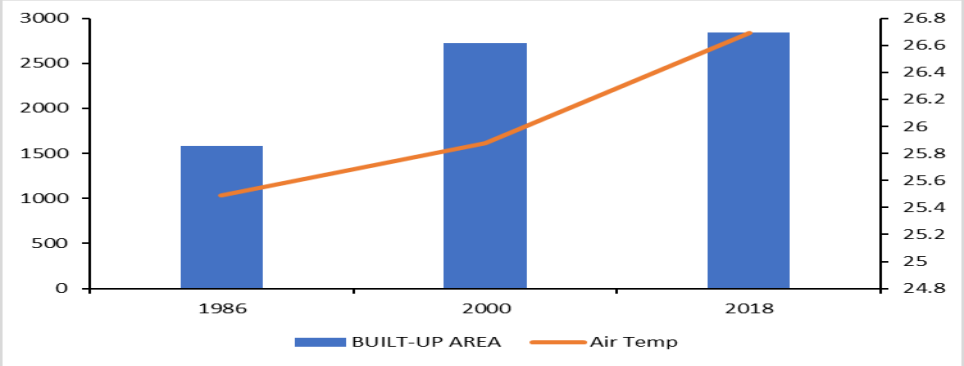


**Figure 8p:** Trends of air temperature and built-up areas in Ijebu East

## 4.0. Conclusion

This study assessed the impact of urbanization on the outdoor thermal conditions in Abeokuta South, Ifo, Shagamu, Ijebu East. The thermal condition of the four selected local government areas has deteriorated progressively along with increase in built-up areas. The area that's least developed (Ijebu East) was found to be more comfortable than others, while the area with the highest rate of development (Abeokuta south and Ifo LGAs) has the highest level of thermal discomfort.

Heat stress is known to have influence in the mental and physical efficiency of man. In tropical areas like Nigeria, illnesses resulting from extremely high temperatures and excess heat leading to heat stroke, and heat cramps are very common. Hence, the reason why thermal comfortability deserves some close study.

## References

Adebayo, Y. (1991). Day-time effects of urbanization on relative humidity and vapour pressure in tropical city. *Theor. Appl. Climatol.* 43, pp. 17-30.

Adelekan, I. O. (2005). Urban climate research in Nigeria. Country Report. *Newslett. Int. Assoc. Urban Clim.* 13, pp. 8–10.

Ahmed, K.S. (2003). Comfort in urban spaces: Defining the boundaries of outdoor thermal comfort for the tropical urban environments. *Energy and Buildings*, 35(1), pp. 103-110. doi: 10.1016/S0378-7788(02)00085-3

Aina, S. A. (1989). Aspects of the Urban Climate of Oshogbo. Unpublished M.Sc Dissertation, University of Ibadan, Nigeria.

Akinbode, O. M., Eludoyin, A. O. and Fashae, O. A. (2008). Temperature and relative humidity distributions in a medium–size administrative town in southwest Nigeria. *J. Environ. Manage.* 87, pp. 95–105.

ASHRAE, (2010). Thermal environmental conditions for human occupancy. ASHRAE standard; American Society of Heating, Refrigerating and Air-Conditioning Engineers. Atlanta: ASHRAE.

Ayoade, J. (1978). Spatial and seasonal patterns of physiologic comfort in Nigeria. *Theor. Appl. Climatol.* 26, pp. 319–337.

Efe, S. I. (2004). Urban Effects on Precipitation Amount and Rainwater Quality in Warri Metropolis, Unpublished PhD thesis, Delta University, Abraka, Nigeria.

Eludoyin, O.M., Adelekan, I.O., Webster, R. and Eludoyin, A.O. (2013). Air temperature, relative humidity, climate regionalization and thermal comfort of Nigeria. *Int. J. Climatol.*, 34, pp. 2000-2018.

Galony, G. S. (1996). Urban design morphology and thermal performance. *Atmospheric Environment*, 30(3), pp. 455-465.

Höppe, P. (2002). Different aspects of assessing indoor and outdoor thermal comfort. *Energy & Buildings*, 34(6), pp. 661-665.

IPCC, (2007). Solomon S, Qin D, Manning M, Chen, Z, Marquis M, Averyt K, Tignor M, Miller H, 2007. IPCC fourth assessment report (AR4). Climate change.

Kyle, W. J. (1992). Summer and winter patterns of human thermal stress in Hong Kong

Markus, T. A. and Morris, E. N. (1980). Buildings, climate and energy. London: Pitman

Massetti, L., Petralli, M. and Brandani, G. (2019). Modelling the effect of urban design on thermal comfort and air quality: The SMART Urban Project. *Build. Simul.* 12, pp. 169–175.

Matzarakis, A., Rutz, F. and Mayer, H. (2007). Modelling radiation fluxes in simple & complex environments – application of the Rayman model. *Int. J. Biometeorol*. 51, pp. 323-334.

Ng, E. (2012). Towards planning and practical understanding of the need for meteorological and climatic information in the design of high-density cities: A case-based study of Hong Kong. *Int. J. Climatol*. 32, pp. 582–598.

Nieuwolt S. Tropical climatology. London: Wiley; 1977.

Njoroge, J.B.M., Nda'Nganga, K., Wariara, K. and Maina, M.G. (2011). Characterising changes in urban landscape of Nairobi city, Kenya. *Acta Horticulturae*, 911, pp. 537–543.

Ogunsote, O. O. and Ogunsote, B. P. (2003). Choice of a thermal index for architectural design with climate in Nigeria. *Habitat International*, 27, pp. 63-81.

Ogunsote, O. O. and Prucnal-Ogunsote, B. (2007). Extreme Weather and Climate Events: Implications for Urban Planning, Architecture and Tourism Infrastructure in Nigeria. Federal University of Technology, Akure.

Olaniran, O. J. (1982). The Physiological Climate of Ilorin, Nigeria. *Arch. Met. Geoph. Biokl. Ser. B*, 31, pp. 287-299.

Omogbai, B.E. (1985). Aspects of Urban Climate of Benin City. Unpublished M.Sc. Dissertation, University of Ibadan, Nigeria.

Omonijo, A. G. and Matzarakis, A. (2011). Climate and bioclimate analysis of Ondo State. *Meteorologische Zeitschrift*, 20(5), pp. 531-539.

Oniarah, A. (1990). Aspects of urban Climate of Benin City. Unpublished M.Sc Dissertation University of Ibadan, Nigeria.

Polydoros, T. and Cartalis, C. (2014). Assessing Thermal Risk in Urban Areas - an Application for the Urban Agglomeration of Athens. *Advances in Building Energy Research,* 8(1), pp. 74-83.

Quang-Van Doan, Hiroyuki Kusaka, and Quoc-Bang Ho, (2016). Impact of future urbanization on temperature and thermal comfort index in a developing tropical city: Ho Chi Minh City. *Urban Climate,* 17, pp. 20-31.

Robaa (2011). Effect of Urbanization and Industrialization Processes on Outdoor Thermal Human Comfort in Egypt. *Atmospheric and Climate Sciences*, 1, pp. 100-112. doi:10.4236/acs.2011.13012

Unger, J. (1999). Comparisons of urban & rural bioclimatological conditions in the case of a Central-European city. *Int. J. Biometeorol* 43, 139. doi: 10.1007/s004840050129.

United Nations Population Division (2012), World Urbanization Prospects: The 2011 Revision, POP/DB/WUP/Rev.2007, United Nations Department of Economic and Social Affairs, New York.

Xiong, Y., Huang, S., Chen, F., Ye, H., Wang, C. and Zhu, C. (2012). The Impacts of Rapid Urbanization on the Thermal Environment: A Remote Sensing Study of Guangzhou, South China. *Remote Sens.* 4, pp. 2033-2056. doi:10.3390/rs4072033

Yang, B., Yang, X., Leung, L. R., Zhong, S., Qian, Y., Zhao, C., *et al*. (2019). Modelling the impacts of urbanization on summer thermal comfort: the role of urban land use and anthropogenic heat. *J. Geophys. Res. Atmos.* 124, pp. 6681–6697.

**Cite this article as:**
Akinbobola A. and Fafure T. 2021. Assessing the Impact of Urbanization on Outdoor Thermal Comfort in Selected Local Government Areas in Ogun State, Nigeria. *Nigerian Journal of Environmental Sciences and Technology,* 5(1), pp. 120-139. https://doi.org/10.36263/nijest.2021.01.0243

Nigerian Journal of Environmental Sciences and Technology (NIJEST)

www.nijest.com

ISSN (Print): 2734-259X | ISSN (electronic): 2734-2603

Vol 5, No. 1 March 2021, pp 140 - 151

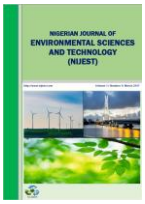

# Models for Estimating the Hearing Threshold of Quarry Workers at High Frequencies

Akanbi O. G.[1], Oriolowo K. T.[2], Oladejo K. A.[3]*, Abu R.[4], Mogbojuri A. O.[5] and Ogunlana R.[6]

[1,2]Department of Industrial and Production Engineering, University of Ibadan, Nigeria

[3]Department of Mechanical Engineering, Obafemi Awolowo University, Ile Ife, Nigeria

[4]Department of Mechanical Engineering, University of Ibadan, Nigeria

[5]Department of Mechanical Engineering, Yaba College of Technology, Yaba, Nigeria

[6]Department of Mechanical Engineering, Adeseun Ogundoyin Polytechnic, Eruwa, Nigeria

Corresponding Author: *wolesteady@yahoo.com

https://doi.org/10.36263/nijest.2021.01.0254

## ABSTRACT

*It is widely known that quarry industry has great importance in developing countries, such as Nigeria. There is paucity of information regarding effects of noise experienced by quarry workers during their working time. Therefore, this study investigated the influence of age of workers, years of exposure of workers and noise level of the machine used in quarry on hearing threshold. A factorial design of experiment was employed for the investigation. Two hundred and four quarry workers volunteered for this study from four quarries in South western Nigeria. Emitted noise, which quarry workers were exposed to during machinery operation, was measured with a digital sound level meter and workers hearing threshold was measured in an audiogram sound proofing testing booth at standard conditions. Predicted models were established from experimental design to determine main and interactions effects towards the response (hearing threshold). These were statistically analysed using analysis of variance (ANOVA). All terms of the models were significant at $p<0.05$. The best fitted model was at 4kHz ($R^2 = 0.639$, $p<0.05$). The magnitudes of the main effect of the factors are in ascending order of noise level >years of exposure>age. The analysis of the experimental response indicated that there is no interaction of any factors on the hearing threshold. It can be concluded that age, years of exposure and noise level have main effects at various capacities at different frequency to predict the hearing threshold of the quarry workers. This work determined the factors and the predicted model to spell out safe hearing threshold of quarry workers that fitted for the job at a particular noisy workstation as well as ensuring comfortable, safe and effective workstation design.*

**Keywords:** Factorial design, Safe hearing threshold, Quarry workers, Noise level, High frequency

## 1.0. Introduction

In the industrial sense, noise usually means excessive sound or harmful sound (Al-Maghrabi *et al.*, 2013). Sound is generally understood as a pressure wave in the atmosphere. Human sense of hearing can detect both of these characteristics. Pressure intensity is sensed as loudness, whereas pressure frequency is sensed as pitch. For human being hearing perception, low frequency noise is 250 Hertz (Hz) and below. High frequency noise is 2000Hz and above. Mid-frequency noise falls between 250 and 2000Hz.The formal recording of an individual's hearing forms the basis of the audiogram. Auditory sensitivity is usually assessed by means of Pure Tone Audiometry, which measures the lowest detectable sound levels at different frequencies. This measurement may reflect the loss of sensitivity to weak sounds (Lobarinas *et al.*, 2013) an individual's threshold hearing to pure tones at different frequencies (250-8000Hz) is performed.

The workers exposure time weighted average for high noise level working environment, requires the wearing of earplugs and earmuffs all together. Proper insertion of earplugs in the ears is the only guarantee to efficacy of the earplugs. Earmuffs have higher noise reduction rating than earplugs (Abe

*et al*., 2009).The most important factor in selecting a type of noise protection is probably effectiveness in reducing decibel level of noise exposure. The workers' comfort factor goes beyond the simple goal of promoting worker satisfaction. If workers find a type of ear protection uncomfortable or awkward to wear they will use every excuse not to wear it, which results in loss of protection. Due to ever increasing level of industrialization, industrial noise is an ever growing problem. It is very important to be able to quantify and control this noise and thus its effects on man and its environment. This can be better achieved if planning ahead of an envisaged potential danger which may be caused eventually if not controlled. Although normally, individual noise is one of the less prevalent community noise problems, neighbours of noisy manufacturing plants can be disturbed by sources such as fans, motors, compressors etc. mounted on the outside building (Ojolo and Ismail, 2011).

The prevalence of hearing loss increases with age (Akeroyd, 2014). Excessive sound is one of the most common causes of hearing loss. The hazardous effects of noise on hearing have been studied for over a century. Over the past few decades, considerable attention has been given to the mechanisms and features of noise induced hearing loss (Solanki *et al.*, 2012). The sound levels in urban communities are apparently rising, and the nuisance value of unwanted sound is greatly increased (Karvana *et al.*, 2012). The most serious pathological effect of noise on man is hearing loss leading to complete deafness. The victim is generally unaware of it at the early stages. It is unfortunate that workers failed to realize that the repeated and continuous exposure to noise above 90dBA may result in permanent hearing loss. Noise Induced Hearing Loss (NIHL) initially affects the frequencies of 6, 4, or 3kHz, and with the progression of the loss, it can reach the regions of 8, 2, 1kHz, 500 and 250Hz. Moreover, the individual can have tinnitus and discomfort related to intense sounds, and once the noise exposure ends, there is no more hearing loss progression (Hong *et al.*, 2013; England and Larsen, 2014; Biassoni *et al.*, 2014). Noise induced damages amount to approximately 4 million dollars per day (McBride, 2004; Williams *et al.*, 2004). Tinnitus can be defined as an auditory illusion, or sound sensation unrelated to the external source of stimulation. This is frequently related to hearing loss, but it is also known to be presented in individuals without apparent hearing loss (Ibraheemm and Hassaan, 2016).When susceptible, unprotected ears are exposed to loud noise potentially injurious to hearing, the inner ear seems to react in one of three ways: by adapting to the noise (i.e. the inner ear seems to "toughens" in some individuals), by developing a Transient Threshold Shift (TTS) or a Permanent Threshold Shift (PTS) (England and Larsen, 2014). TTS refer to a transient sensorineural hearing loss lasting hours to a few days. Hearing thresholds are depressed until the metabolic activity in the cochlear recovers. For this reason, workers ideally should be out of noise for at least 24hours if not 48hours prior to audiometric testing to avoid the effects of TTS on hearing. PTS refers to a permanent loss of sensorineural hearing which is the direct result of irreparable injury to the organ of Corti. Noise induced deafness generally affects hearing between 3000-6000Hz with maximal injury centring around 4000Hz initially, an important point to remember.

As age affects sensitivity to the high frequencies of noise is lost first and the loss is irreversible. In audiometry, such loss is described as a permanent threshold shift. Audiometric testing consists of determination of the minimum intensity (the threshold) at which a person can detect sound at a particular frequencies is lost as a result of age or damage, the intensity at which a stimulus can be detected increases. It is in this sense that hearing loss can be described as a threshold shift. Studies have shown age decrements in performance of sustained attention tasks. Onder *et al.*, (2012) studied NIHL in mines at Turkey. They had applied statistical analysis (hierarchical log-linear) of the data. Data were collected from a quarry and stone crushing screening plant. According to their study, the risky occupation job group of the places surveyed was the drivers and this job group had high possibility of exposure to 70 - 79dBA noise levels. The drivers, especially of the 46 – 54 years age group, had experienced NIHL. When the important interactions in the analyses were evaluated, it was found out that 4-11 years experienced crusher workers working in the stone crushing - screening plants had high probability of NIHL because of high exposure to 90 - 99dBA noise level. Bouloiz *et al*., (2013) presented an analysis, by a combination of dynamic systems and fuzzy logic, of the work environment of human factor. This environment contains a set of factors (variables) that influence human behaviour in the context of industrial safety. Fuzzy logic is used to account the qualitative and uncertain nature of variables value resulting from the phenomenon of perception. The fuzzy logic was used for modelling the safe behaviour of human factor.

Ojolo and Ismail (2011) modelled the effects of noise on machine operators. Major hearing losses were traced to noise generated by machinery. The results showed that hearing loss increases with increase in frequency and age; and is influenced by the loudness level and sound intensity. Fourth order Newton difference scheme was used in modelling; the result was simulated using MATLAB program with the operator's age as the major factor. Other effects are indirect health, psychosocial and economic effects which can lead to social isolation and reduced quality of life (Bainbridge and Wallhagen, 2014; Mick *et al*., 2014; Kamil and Lin, 2015). Older persons with hearing loss are prone to hospitalization (Genther *et al.,* 2013), death (Contrera *et al.,* 2015; Fisher *et al.,* 2014), as well as higher rates of dementia (Lin *et al.*, 2011; Gallacher *et al.*, 2012), and depression (Li *et al.*, 2014; Mener *et al.,* 2013), even when known risks for these abnormality are considered. (Lin *et al.*, 2011; Allen and Eddins, 2010) stated that annual health care costs for middle-age United States of America adults with hearing loss are significantly higher than the costs of care for those without hearing loss. Person with hearing loss achieve lower level of education and cognition than those with normal hearing, higher unemployment level or underemployment which may results to lower income level than those with normal hearing (Starr and Rance, 2015).

There are two major methods used for analysing the variables: classical and statistical. The former method is a conventional method approach, involves varying one independent variable at a time, (OVAT), or one-factor-at-a-time, (OFAT) has been found to be useful to observe the individual effects on certain components and process conditions. It is however, lacking in predicting the interaction and interrelationship between the various components influencing the realization of a particular response(s). But found to be full of bias, tiring, and time consuming by having too much experimental runs. This is further argued by the fact that variable cannot be studied by varying one factor at a time, as it often does not allow determination of actual optimum level of different components, as well as identification of vital factors affecting a system or process (Ridzuan and Yacoub, 2016). The latter methods which include factorial experiments, provides an alternative approach through screening of a particular process by considering individual or linear and mutual interactions among the variables and give an estimate of the combined effect of these variables on the final results.

Though many research work has been done in the area of the factors affecting hearing threshold (age, years of exposure and noise level), but this work is yet to come across the degree of contributions of each independent variable factors to the dependent factors. In lieu of this observation, this work will analyze the contributions of age, years of exposure and noise level to the hearing threshold at each frequency by applying factorial experimental statistical design to screen the main and interactions effects of the independent variables on the dependent variables. Following are the objectives of this study:

- To estimate the amount of noise emitted by various heavy earth moving machineries which workers are exposed to during working hours in a stone quarry
- To develop a predictive model of occupational noise impact on quarry workers.
- To determine contribution of each of independent variables (age of workers, years of exposure and noise level) on the dependent variable (hearing threshold) as well as their interactive effects.

## 2.0. Methodology

### *2.1. Subject selection*

Four quarry sites were selected for this study. Two hundred and four workers volunteered for this study for the first research arrangement in the month of June – July, 2017. The permission of the quarry management was obtained prior to the start of the study. Participants from different sections in each quarry were selected and were notified several days before the commencement of the study, given consent form to sign and questionnaire answered before data collection began. All tools and equipment used in this study were evaluated using standard procedures, pretested and revised to ensure their validity and reliability to ensure uniformity in the administration of the data from the study. The workers in this study had completely rested for 48 hours or more after their day shift in order to prevent transient hearing loss.

### *2.2. Noise measurement*

This study considered the operators that are exposed directly to the following noise emitted equipment: Primary Crushers, Secondary Crushers, Dumpers, Payloader, Wagon drilling machine, Lathe, Drilling Machine and Excavator. Their operations were used in categorizing the workers into seven groups: Primary Crusher, Secondary Crusher, Compressor, Dumper, Wagon Drilling, Pay loader, Lathe, Drilling Machine and Excavator operators and Administrative staffs. Digital Sound Level Meter (TESTO 815) with sound calibrator (TESTO 0554.0452) which was used to calibrate the sound level meter to the appropriate level, in conformity to the American National Standard Institute, ANSI, and Standard SI. 4 – 2006 was used for the noise emitted by the machine in the quarry. It consists of a microphone that converts sound pressure variations into electrical signals, a frequency selective amplifier, a level range control, frequency weighting to shape the frequency response of the instrument, and an indicator. The reading was then compared with the calibrator's value. The sound level meter was adjusted when required to bring it into calibration. For each particular application, the measurement technique was carefully chosen and controlled to obtain valid and consistent results. A-weighted frequency scales with fast response setting; Type 1 Sound Level Meter was used in this work since it measures how noise fluctuates over time rather than noise exposure.

### *2.3. Audiometric testing*

Audiometric test was conducted in an audiogram sound proofing testing booth (TRIVENI TAM -10 5100B) (Howard *et al*., 2017), on each subject at the hospital in Ibadan by a specialist. Ambient noise met the American National Standards Institute S3.1 standards for maximum permissible ambient noise levels. Audiometric air conduction tests were performed by pre-setting a pure tone at the frequencies of 250, 500, 1000, 2000, 3000, 4000, 6000 and 8000Hz at 5dBA intervals to the ear of the participant through an earphone. These are the conventional sound frequencies related to the human auditory system. The hearing threshold (dB) was recorded at the frequency at which a particular lowest tone was perceived and the participants respond. Hearing was considered normal if the threshold level was less than or equal to 25dBA at a frequency (Gallacher *et al*., 2012; Fisher *et al*., Kamil and Lin, 2015; Ibraheemm and Hassan, 2016; Howard *et al*., 2017). The intensity of the stimuli was increased beyond 25dBA at any frequency until a response was obtained. Intervals of 5 seconds duration were maintained between the tones. The duration of the pre-set tone was 1 – 3 seconds. The total time used to perform the audiometric test on a subject was 3 – 5 minutes.

### *2.4. Factorial design for screening parameters affecting hearing threshold*

In this study, three factors: age, years of exposure, and noise level were selected and screened for their effect on hearing threshold using a multilevel 1^3^4^5 full factorial design. Selection of the factors was based on previous research from several articles based on one factor at a time (OFAT). Table 1, 2 and 3 shows the coded value of independent variables. The factorial design of Experimental Design SPSS 23.0 was used to design and analyse the experimental data. Each variable effects and interactions on the hearing threshold was statistically determined. A first-order polynomial model that can estimate the main effects of the experimental factors as well as interactive effects is appropriate for modelling (Onsekizoglu *et al*., 2010). The first-order model with interaction terms proposed for each response variable Y was based on the multiple linear regression method. A p-value for a given factor less than 0.05 (95% confidence interval) was considered as significant. For three factors system, a polynomial equation model was used to predict the response of hearing threshold to the selected variables:

$$Y = \beta_0 + \beta_1 x_1 + \beta_2 x_2 + \beta_3 x_3 + \beta_{12} x_1 x_2 + \beta_{13} x_1 x_3 + \beta_{23} x_2 x_3 \quad (1)$$

where,

$\beta_0$ was the constant term, $\beta_1$, $\beta_2$, $\beta_3$are the main effects, $\beta_{12}$, $\beta_{13}$, $\beta_{23}$ are the interaction effects, and statistically non-significant terms were eliminated by stepwise deletion. Regression analyses of the residual values, analysis of variances, normal probability plot were used to evaluate the goodness of fit of the models and significance of each regression coefficient. F-test was used to test for the statistical significance.

**Table 1**: Codes, ranges and age classifications

| Code | Levels of age (years) | Classification |
|---|---|---|
| 1 | 15 – 30 | Young age |
| 2 | 31 – 50 | Middle age |
| 3 | 51 – 70 | Senior age |

**Table 2**: Codes, ranges and years of exposure classifications

| Code | Levels of years of exposure | Classification |
|---|---|---|
| 1 | 0 – 10 | Short term |
| 2 | 11 – 20 | Medium term |
| 3 | 21 – 30 | Long term |
| 4 | 30+ | Very long term |

**Table 3**: Codes, ranges and noise levels classifications

| Code | Levels of noise level | Classification |
|---|---|---|
| 1 | 25 – 45 | Low |
| 2 | 46 – 65 | Medium |
| 3 | 66 – 85 | High |
| 4 | 86 – 105 | Very high |
| 5 | 105+ | Extremely high |

## 3.0. Results and Discussion

### *3.1. Noise measurement at various facilities under study*

The four understudied quarries had different production units with more or less of the same type of machinery. The noise measurement values were in the range of 87.3dBA to 116.98dBA, which implies that the noise levels produced exceed the limiting threshold level of 85dBA except in administrative block.

### *3.2. Mean hearing threshold level of respondent*

The mean hearing threshold among all workers in the quarry was 27.9dBA and 105 respondents (51.7%) had hearing threshold higher than 25dBA. The differences between the mean values of hearing threshold level of the respondent of the four quarries are not significant (one-way ANOVA). Thus, the respondents at all the quarries were subjected to about the same working conditions and environmental noise levels.

### *3.3. Effect of factors of age, years of exposure and noise level on hearing threshold at frequency 3 kHz*

Table 5 shows that main effect of Years of exposure F- value ($F_{VE}$) = 3.608, p = 0.015 and Noise level F- value ($F_{NL}$) = 3.553, p = 0.008, are significant ($R^2$ = 0.448, $p < 0.05$) with large effects that accounted for 52.8% of the variability in hearing threshold at 3kHz. Years of exposure has the highest contribution of 29.9% as shown in Table 6. None of the factors interactions are significant. The normal probability curve of residual is considerably linear, which suggested the adequacy of the model.

The model equation:

$$HT = 3.70 + 0.0551VE + 0.233NL \quad (2)$$

where,
HT is the Hearing Threshold.

The model is appropriate for the data as the normal probability plot of residual is approximately linear as shown in Figure 1.

**Table 5:** Analysis of Variance (ANOVA) of the independent variables at frequency 3kHz

| Source | Sum of square | df | Mean square | F | P value |
|---|---|---|---|---|---|
| Corrected Model | 7233.342 | 22 | 328.788 | 6.189 | .000* |
| Intercept | 63632.906 | 1 | 63632.906 | 1197.826 | .000* |
| VE | 755.058 | 3 | 251.686 | 3.608 | .015* |
| NL | 574.951 | 4 | 143.738 | 3.553 | .008* |
| VA | 262.920 | 2 | 131.460 | 2.475 | .087 |
| VE*NL | 704.385 | 7 | 100.626 | 1.894 | .073 |
| VE*VA | 23.834 | 2 | 11.917 | .224 | .799 |
| NL*VA | 197.282 | 3 | 65.761 | 1.238 | .298 |
| VE*NL*VA | .000 | 0 | | | |
| Error | 8924.773 | 168 | | 53.124 | |
| Total | 494959.000 | 191 | | | |
| Corrected Total | 16158.115 | 190 | | | |

R Squared = .448

*P < 0.005

VA, VE and NL are independent variables of age, years of exposure and noise levels respectively

**Table 6:** Factor effect estimates and sums of squares for the independent variables at frequency 3kHz

| Factor | Regression coefficient | Effect estimate | Sum of square | % contribution |
|---|---|---|---|---|
| VE | 0.551 | 1.102 | 755.058 | 29.98 |
| NL | 0.233 | 0.466 | 574.951 | 22.83 |
| VA | 0.057 | 0.114 | 262.920 | 10.44 |
| VE*NL | -0.002 | -0.004 | 704.385 | 27.97 |
| VE*VA | 0.002 | 0.004 | 23.834 | 0.95 |
| VE*NL*VA | -1.05E-5 | -2.11E-5 | 0.000 | 0.00 |

VA, VE and NL are independent variables of age, years of exposure and noise levels respectively

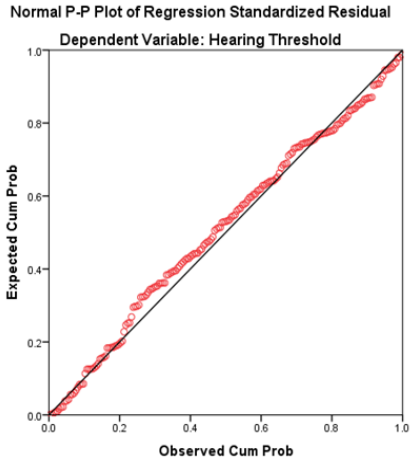


**Figure 1:** Normal probability plot of standardized residual dependent variable at frequency 3kHz

*3.4. Effect of factors of age, years of exposure and noise level on hearing threshold at frequency 4kHz*

Table 7 shows that Age F- value $F_{VA}$= 6.135, p = 0.003, $F_{VE}$= 9.108, p = 0.000 and $F_{NL}$ = 8.464, p = 0.000, have main effects on the hearing threshold and are significant ($R^2$ = 0.639, p < 0.05). Table 8 shows 79.7% of the variability of the factors in hearing threshold at 4kHz. Years of exposure have the highest contribution of 36.73% followed by Noise level with 29.64%. None of the factors interactions are significant. The model equation:

$$HT = 20.579 - 0.418VA + 0.383VE + 0.197NL \quad (3)$$

where,
HT is the Hearing Threshold.

**Table 7:** Analysis of Variance (ANOVA) of the independent variables at frequency 4kHz

| Source | Sum of square | df | Mean square | F | P value |
|---|---|---|---|---|---|
| Corrected Model | 23718.432 | 22 | 1078.111 | 13.504 | 0.000* |
| Intercept | 98141.058 | 1 | 98141.058 | 1229.277 | 0.000* |
| VE | 2702.947 | 3 | 900.982 | 9.108 | 0.000* |
| NL | 2181.511 | 4 | 545.378 | 8.464 | 0.000* |
| VA | 979.573 | 2 | 489.786 | 6.135 | 0.003* |
| VE*NL | 1104.957 | 7 | 157.851 | 1.977 | 0.061 |
| VE*VA | 93.197 | 2 | 46.599 | 0.584 | 0.599 |
| NL*VA | 297.497 | 3 | 99.166 | 1.242 | 0.296 |
| VE*NL*VA | .000 | 0 | | | |
| Error | 13412.521 | 168 | 79.836 | | |
| Total | 844496.000 | 191 | | | |
| Corrected Total | 37130.953 | 190 | | | |

R Squared = .639

*P < 0.05

VA, VE and NL are independent variables of age, years of exposure and noise levels respectively

**Table 8:** Factor effects estimates and sums of squares for the frequency 4kHz

| Factor | Regression coefficient | Effect estimate | Sum of square | % contribution |
|---|---|---|---|---|
| VE | 0.383 | 0.766 | 2702.947 | 36.73 |
| NL | 0.197 | 0.3094 | 2181.511 | 29.64 |
| VA | -0.418 | -0.836 | 979.573 | 13.31 |
| VE*NL | 0.000 | 0.000 | 1104.957 | 15.01 |
| VE*VA | 0.019 | 0.038 | 93.197 | 1.27 |
| NL*VA | 0.008 | 0.016 | 297.497 | 4.04 |
| VE*NL*VA | 0.000 | 0.000 | 0.000 | 0.00 |

VA, VE and NL are independent variables of age, years of exposure and noise levels respectively

The normal probability plot of residual of has minimal negligible extensions away from linearity; the model fits the data (Figure 2).

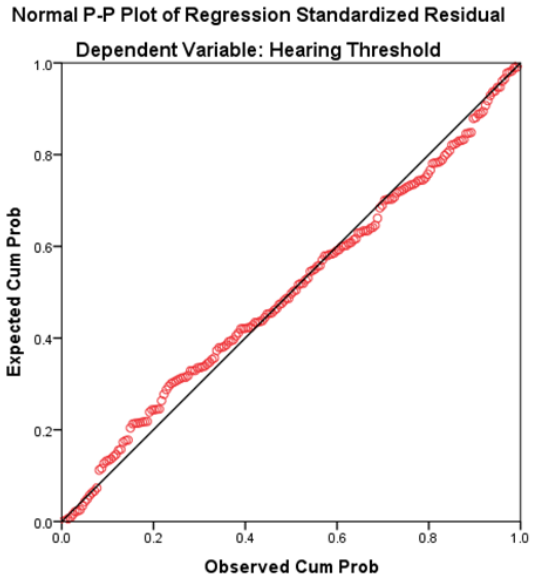


**Figure 2:** Normal probability plot of standardized residual dependent variable at 4kHz

*3.5. Effect of factors of age, years of exposure and noise level on hearing threshold at frequency 6kHz*

Table 9 shows that only $F_{NL}$=7.026, p < 0.05 is significant with 51.2% contribution of the variability in hearing threshold (Table 10). None of these factor interactions are significant. The normal probability plot of standardized residual dependent variable proves that the model is good for the data. The value of $R^2$ = 0.229, p<0.05 obtained at this frequency is too small, this situation calls for further studies. The model equation:

$$HT = -23.072 + 0.809NL \quad (4)$$

where,
HT is the Hearing Threshold.

**Table 9:** Analysis of Variance (ANOVA) of the independent variables at frequency 6kHz

| Source | Sum of square | df | Mean square | F | P value |
|---|---|---|---|---|---|
| Corrected Model | 6922.589 | 22 | 314.663 | 2.270 | .002* |
| Intercept | 559997.767 | 1 | 559997.670 | 403.973 | .000* |
| VE | 386.766 | 3 | 128.922 | .930 | .428 |
| NL | 3895.971 | 4 | 973.993 | 7.026 | .000* |
| VA | 392.388 | 2 | 196.194 | 1.415 | .246 |
| VE*NL | 1538.404 | 7 | 219.772 | 1.585 | .143 |
| VE*VA | 821.660 | 2 | 410.830 | 2.964 | .054 |
| NL*VA | 577.814 | 3 | 192.605 | 1.389 | .248 |
| VE*NL*VA | .000 | 0 | | | |
| Error | 23287.777 | 168 | 138.618 | | |
| Total | 433355.000 | 191 | | | |
| Corrected Total | 30210.366 | 190 | | | |

R squared = .229,
*P < 0.05
VA, VE and NL are independent variables of age, years of exposure and noise levels respectively

**Table 10:** Factor effect estimates and sums of squares for the independent variables at frequency 6kHz

| Factor | Regression coefficient | Effect estimate | Sum of square | % contribution |
|---|---|---|---|---|
| VE | -5.942 | 11.884 | 386.766 | 5.08 |
| NL | 0.809 | 1.618 | 3895.971 | 51.18 |
| VA | -0.819 | 1.638 | 392.388 | 5.15 |
| VE*NL | -0.074 | -0.148 | 1538.404 | 20.21 |
| VE*VA | -0.016 | -0.232 | 821.660 | 10.79 |
| NL*VA | -0.010 | -0.020 | 577.814 | 7.59 |
| VE*NL*VA | 0.001 | 0.002 | 0.000 | 0.00 |

VA, VE and NL are independent variables of age, years of exposure and noise levels respectively

### *3.6. Effect of factors of age, years of exposure and noise level on hearing threshold at frequency 8kHz*

Table 11 presents the ANOVA test of Between-Subject Effect. $F_{VE}$= 7.873, p = 0.000, $F_{NL}$ = 6.075, p = 0.000 and $F_{VA}$ = 3.293, p = 0.040 are significant ($R^2$ = 0.467, p < 0.05) with large effects that together account for 77.1% of the variability in hearing threshold at 8kHz (Table 12); as years of exposure has the highest contribution of 34.36% followed by Noise level with 33.39%. None of the factor interaction is significant. The normal probability curve of residual is approximately linear, which indicates the adequacy of the model. The model equation:

$$HT = 39.489 - 0.799VA + 0.511VE - 0.022NL \quad (5)$$

where,
HT is the Hearing Threshold.

The normal probability plot of residual is a little skewed on one side; just as other normal probability plots of residual under previous frequencies; there are no outliers. The model is still good for the data (Figure 3).

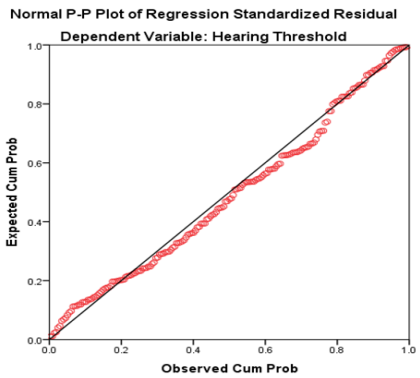


**Figure 3:** Normal probability plot of standardized residual dependent variable at 6kHz

**Table 11:** Analysis of Variance (ANOVA) for the independent variables at frequency 8kHz

| Source | Sum of square | df | Mean square | F | P value |
|---|---|---|---|---|---|
| Corrected Model | 13076.375 | 22 | 594.381 | 6.693 | .000* |
| Intercept | 53333.103 | 1 | 53333.103 | 600.537 | .000* |
| VE | 2158.156 | 3 | 719.385 | 7.873 | .000* |
| NL | 2097.679 | 4 | 524.419 | 6.075 | .000* |
| VA | 584.971 | 2 | 292.485 | 3.293 | .040* |
| VE*NL | 796.617 | 7 | 113.802 | 1.281 | .262 |
| VE*VA | 395.532 | 2 | 197.766 | 2.227 | .111 |
| NL*VA | 248.509 | 3 | 82.836 | .933 | .426 |
| VE*NL*VA | .000 | 0 | | | |
| Error | 14919.918 | 168 | 88.809 | | |
| Total | 481408.00 | 191 | | | |
| Corrected Total | 27996.293 | 190 | | | |

R Square = .467

*P < 0.05

VA, VE and NL are independent variables of age, years of exposure and noise levels respectively

**Table 12:** Factor effect estimates and sums of square for the independent variables at frequency 8kHz

| Factor | Regression coefficient | Effect estimate | Sum of square | % contribution |
|---|---|---|---|---|
| VE | 0.511 | 1.022 | 2158.156 | 34.36 |
| NL | 0.022 | 0.044 | 2097.679 | 33.39 |
| VA | -0.799 | -1.598 | 584.971 | 9.31 |
| VE*NL | -0.006 | -0.012 | 796.617 | 12.68 |
| VE*VA | 0.022 | 0.044 | 395.532 | 6.30 |
| NL*VA | 0.013 | 0.026 | 248.509 | 3.96 |
| VE*NL*VA | 0.000 | 0.000 | 0.000 | 0.00 |

VA, VE and NL are independent variables of age, years of exposure and noise levels respectively

The model is appropriate for the data as the normal probability plot of residual is approximately linear (Figure 4). The present study investigated the physiological response of quarry workers working in noisy environment. Amount of noise emitted by various equipment which workers were exposed to during work in selected quarries were estimated. The noise measurement values in this study were in the range of 28.4dBA in the administrative section to 116.98dBA in the production section. The mean hearing threshold among all workers in the quarry was 27.9dBA, 51.7% had hearing threshold level higher than 25dBA. The differences between the mean values of hearing threshold level of the respondents of the four quarries are not significant (F=1.068, P=0.364) which indicated that all the quarries were subjected to about the same working conditions and environmental noise. There is a stronger linear relationship between the average hearing loss over the frequencies 3kHz through 8kHz, and the age of workers, years of exposure and noise level. Seventy percent of the variation in hearing threshold is sought in and explained by the factors variables. Therefore 30% variation in hearing loss is explained by variable not figured in the model. The maximum association between hearing loss and age, years of exposure and workstation at 4kHz indicates a dip notch at the characteristic frequency. This is in agreement with Akanbi and Oriolowo (2016). It can be concluded that a number of the respondent may have been exposed to areas with high noise levels in the 4kHz frequency. There was also a relationship between hearing loss, and age at all workstations with the degree of association between 0.6 and 0.9; also with years of exposure between 0.5 and 0.9.

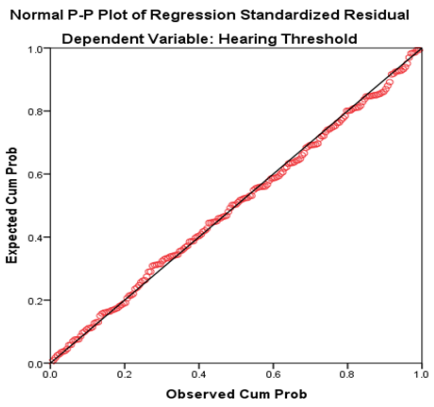


**Figure 4:** Normal Probability plot of standardized Residual Dependent variable at 8kHz

## 4.0. Conclusion

It can be concluded that most of the machines used in quarry operation produces noise level in the range of 87.3 - 116.9dBA which is greater than the acceptable threshold sound level; except in the administrative section where the noise level is 28.4dBA which is lesser than the acceptable threshold of 85dBA. The discrepancies between the noise level in the administrative block and quarry section also indicates the proneness of the workers at quarry section to the higher hearing threshold than the administrative workers. This study has established statistically that all respondents' at all four different quarries were subjected to about the same working conditions and environmental noise level. The study further revealed the impacts of the age, years of exposure and noise level on the hearing threshold across some frequency which is used in modelling formulation. The contributions of each independent variable and their interactive effects on the dependent variables were spelt out at the various frequencies. At frequency 4kHz and 8kHz, there is only main effect contribution of age, years of exposure and noise level with no interactive effect indicating that the 3 factors mentioned can independently predict the hearing threshold of the workers. Only main effects of years of exposure and noise level are the determining factors on the hearing threshold of workers at frequency 3kHz; while only the noise level as main variables at the frequency 6kHz can determine the hearing threshold of the workers. Conclusively, the degree of predictors and contribution of Noise level > Years of exposure > Age to the hearing threshold at 3, 4, 6 and 8kHz. These finding are of concern to the researcher in order to have the independent variables data before embarking on recruiting workers to be working in noisy environment in order to protect their hearing status.

**Acknowledgement**
The authors are grateful to the Management of the Quarries used for the conduct of this research: Ladson Quarry, Alleluyah Quarry, MPC Quarry and Ilugun Quarry; and Engr. Busari of Human Factor Engineering Laboratory of Industrial and Production Engineering Department, University of Ibadan.

**References**

Abe, T., Soer, M. and Abiodun, K. (2009). Effect of use of personal hearing protective devices among oil Depot Industrial Workers in Lagos, Nigeria. *Nigerian Journal of Medical Rehabilitation (NJMR)*, 14(1), pp. 22 – 32.

Akanbi, O. G. and Oriolowo, K. T. (2016). Modeling the Prevention of Transformation of Pressbycusis to Noise Induced Hearing Loss. *Journal of Nigerian Institute of Industrial Engineers (NIIE)*, 6, pp. 47-58.

Akeroyd, M.A., Foreman, K., and Holman, J. A. (2014). Estimates of the number of adults in England, Wales and Scotland with a hearing loss. *International Journal of Audiology*, 53(1), pp. 60 - 67.

Allen, P. D. and Eddins, D. A. (2010). Presbycusis phenotypes form a heterogeneous continuum when ordered by degree and configuration of hearing loss. *Hear Res*, 264, pp. 10-20.

Al-Magharabi, M.N., Shewakh, W. M. and Halem, A. (2013). Degradation of Industrial Performance due to environmental factors: Impacts of Noise on Mining and Manufacturing workers. *International Journal of Mechanical and Production Engineering Research and Development (IJMPERD)*, 3(2), pp. 147 - 154.

Bainbridge, K. E., and Wallhagen, M. I. (2014). Hearing Loss in an aging America population: extent, impact and management. *Annu Rev Public Health*, 35, pp. 139-152.

Biassoni, E. C., Serra, M. R., Hinalaf, M., Abraham, M., Paylik., M. and Villalobo, J. P. (2014). Hearing and loud music exposure in a group of adolescent at the ages of 14-15 and retested at 17 – 18. *Noise Health*, 16(72), pp. 331-341.

Bouloiz, H., Garbolino, E., and Tkiouat, M. (2013). Modeling of an Organizational Environment by System Dynamics and Fuzzy Logic. *Open Journal of Safety Science and Technology,* 3, pp. 96-104. http://dx.doi.org/10.4236/ojsst.2013.34012.

Contrera, K.J., Bertz, J., Genther, D.J. and Lin, F.R. (2015). Association of hearing impairment and mortality in the National Health and Nutrition Examination Survey.*JAMA Otolaryngol Head Neck Surg,* 141, pp. 944 - 946.

Durakovic, B. (2017). Design of Experiments Application, Concepts, Examples: State of Art. *Periodicals of Engineering and Natural Sciences*, 5(3), pp. 421– 439.

England, B., and Larsen, J.B. (2014). Noise Levels among Spectators at an intercollegiate sporting event.*Am J Audiol,* 23(1), pp. 71-78.

Fisher, D., Li, C.M., and Chiu, M.S. (2014). Impairments in hearing and vision impact on mortality in older people: the AGES-Reykjavik Study. *Age Ageing,* 43, pp. 69 - 76.

Gallacher, J., Ilubaera, V., and Ben-Shlomo, Y. (2012). Auditory Threshold, phonologic demand, and incident dementia. *Neurology,* 79, pp. 1583-1590.

Genther, D. J., Frick, K.D., Chen, D., Betz, J., and Lin, F.R. (2013). Association of hearing loss with hospitalization and burden of disease in older adults. *JAMA*, 309, pp. 2322-2324.

Hong, O., Kerr, M. J. Poling, G. L., and Dhar, S. (2013). Understanding and Preventing Noise Induced Hearing Loss. *Dis Mon,* 59(4), pp. 110-118.

Howard, J. H., Robert, A. D., Katalin, G. L., Christa, L., Themann, M. A., and Gregory, A. F. (2017). Declining Prevalence of Hearing Loss in US Adults Aged 20 to 69 years. *JAMA Otolaryngol Head Neck Surg,* 143(3), pp. 274-285.

Ibraheemm, O. A. and Hassaan, M. R. (2016). Psychoacoustic characteristics of tinnitus versus temporal resolution in subjects with normal hearing sensitivity. *Int Arch Otorhinolarryngol.20. https://doi.org/10.1055/s-0036-1583526.*

Kamil, R. J. and Lin, F.R. (2015). The effects of hearing impairment in older adults on communication partners: a systematic review. *J Am AcadAudiol,* 26, pp. 155-182.

Karvana, G., Venkatappa, V. S., and NachalAnnamalia, M.S. (2012). Assessment of Knowledge, Attitude and Practices of Traffic Policemen regarding the auditory effects of Noise. *Indian J. Physiolpharmacol,* 56(1), pp. 69-73.

Lobarinas, E., Salvi, R. and Ding, D. (2013). Insensitivity of the audiogram to carbon plating induced inner hair cells loss in Chinchillas.*Hear Res,* 302, pp. 113-120.

Li, C. M., Zhang, X., Hoffman, H. J., Cotch, M. F., Themann, C. L. and Wilson, M. R. (2014). Hearing Impairment associated with depression in US adults, National Health and Nutrition Examination Survey 2005-2010. *JAMA Otolaryngol Head Neck Surg,* 140, pp. 293-302.

Lin, F.R., Metter, E.J., O'Brien R. J.,Resnick, S.M., Zonderman, A.B. and Ferrucci, L. (2011): "Hearing Loss and incident dementia. *Arch Neurol,* 68, pp. 214-220.

McBride, D.I. (2004). Noise Induced Hearing Conversation in Mining.*Occup Med (Long),* 54(5), pp. 290-296.

Mener, D.J., Bertz, J., Genther, D.J., Chen D. and Lin, F.R. (2013). Hearing loss and depression in older adults. *J Am GeriatrSoc,* 61, pp. 1627-1629.

Mick, P., Kawachi, I. and Lin, F.R. (2014). The association between hearing loss and social isolation in older adults. *Otolaryngol Head Neck Surg*., 150, pp. 378-384.

Montgometry, D.C. (2013). Design and Analysis of Experiments. John Wiley & Sons, Inc., 8$^{th}$ed.

Ojolo, S.J. and Ismail, S.O. (2011). Mathematical Modeling of effects of Noise on Machine Operators. *Proceeding of International Conference on Innovation in Engineering and Technology*, pp.78 – 90.

Onder, M., Onder S. and Mutlu, A. (2012). Determination of Noise Induced Hearing Loss in Mining: an application of Hierarchical log linear Modelling. *Environ Monitoring Assessment*, Springer, 184, pp. 2443-2451.

Onsekizoglu, P., Bahceci, K.S. and Acar, J. (2010). The use of factorial design for modelling membrane distillation. *Journal of Membrane science*, 349, pp. 225 – 230.

Ridzuan, N., Adam, F. and Yaacob, Z. (2016). Screening of factor influencing wax deposition using full factorial experimental design. *Petroleum Science and Technology,* 34(1), pp. 84-90.

Solanki, J. D., Mehta, H. B., Shah, C. J. and Gokhale, P. A. (2012). Occupational Noise Induced Hearing Loss and Hearing Threshold Profile at High Frequencies. *Indian Journal of Otology,* 18(3), pp. 125 – 128.

Starr, A., and Rance, G. (2015). Auditory Neuropathy. *HandbClinNeurol*, 129, pp. 495-508.

Williams, W., Purdy, S., Murray, N., Lepage, E., and Challinor, K. (2004). Hearing Loss and Protection of Noise in the workplace among Rural Australians. *Aus. Rural Health*, 12(3), pp. 115-119.

**Cite this article as:**
Akanbi, O. G., Oriolowo, K. T., Oladejo, K. A., Abu, R., Mogbojuri, A. O. and Ogunlana, R. 2021. Models for Estimating the Hearing Threshold of Quarry Workers at High Frequencies. *Nigerian Journal of Environmental Sciences and Technology*, 5(1), pp. 140-151. https://doi.org/10.36263/nijest.2021.01.0254

Nigerian Journal of Environmental Sciences and Technology (NIJEST)

www.nijest.com

ISSN (Print): 2734-259X | ISSN (electronic): 2734-2603

Vol 5, No. 1 March 2021, pp 152 - 164

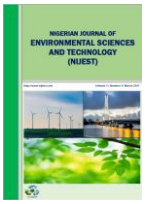

# Modelling of Input Parameters for Power Generation using Regression Models

Agbondinmwin U.[1] and Ebhojiaye R. S.[2,*]

[1,2]Department of Production Engineering, University of Benin, Benin City, Nigeria

Corresponding Author: *raphael.ebhojiaye@uniben.edu

https://doi.org/10.36263/nijest.2021.01.0241

## ABSTRACT

*In this study, multiple linear regression models were employed in the correlation of gas supply and power generation using a gas Power Plant in Niger Delta, Nigeria as a Case study. From the analysis based on outlier detection, reliability analysis and test of homogeneity, it was observed that the independent variable data such as ambient temperature, gas pressure and compressed temperature failed normality test. Therefore, the use of any linear model for either analysis or modelling of the data was not acceptable. Data used for reliability analysis of the gas pressure and compressed temperature difference were positively correlated with power generation, having a covariance value of 0.639 and 113.148. The ambient temperature was negatively correlated with power generation, having a covariance value of 14.564. The positive value showed that both dimensions exclusively increased and decreased together with respect to the output while the negative value showed that increment in value of one variable led to decrease in the value of the other, and vice versa.*

**Keywords:** Natural gas, Power generation, Regression models, Power plant, Ambient temperature

## 1.0. Introduction

Nigeria's natural gas reserves, estimated at about 188 trillion standard cubic feet is the largest in Africa and known to be substantially larger than its oil resources (Nwokeji, 2007; Izuwan, 2017). According to Oyedepo (2012), the largest single consumer of natural gas in Nigeria (before its privatization in November 2013) was the Power Holding Company of Nigeria (PHCN), it accounted for over 70% used in operating electricity-generating gas plant in the country. Given the current reserves and rate of exploitation (about 900mmscfd) for power generation, the expected life span of Nigerian natural gas is over 1000 years, thus making it a good means for power generation. As a result, the gas produced in Nigeria is used mostly in the power sector for power generation and for export as liquefied Petroleum Gas (LPG) (Sambo et al., 2010). Electricity plays a vital role in economic growth and social welfare, thus it is essential to have accessible and reliable electricity at safe conditions (Luis *et al*., 2019).

Rapu *et al*. (2015) put the average generation capacity of electricity in Nigeria to be fluctuating within the range of 2,623.1 MW/hr in 2007 and 3,485.5 MW/hr in 2014 as against the estimated demand of 10,000MW per day. Enete and Alabi (2011) estimated the distribution of household final energy consumption by types in Nigeria to be 4% electricity, 13% kerosene, 1% LPG and 82% wood and others. Currently, over 70% of Nigeria power generation is from natural gas utilization in power plants. There are over 15 power stations in Nigeria with total generation capacity of over 15,000MW that are currently generating about 7000MW (Onochie *et al*., 2015). The problem is attributed to various factors that include gas supply, transmission, grid capacity, plant ambient temperature and operating conditions (such as gas pressure and compressed temperature difference), etc. Orogun (2015) in his work discussed the challenge of gas pipeline vandalisation as one of the major challenge militating against the Federal Government of Nigeria efforts to utilize Nigeria's natural gas sustainably for power generation. This challenge is also compounded due to the inadequacy of natural gas transmission and distribution infrastructure. The power station situated in Benin City, Edo state is

incorporated with a simple cycle gas turbine with over 450MW capacity and has the following coordinates: 6°24'20"N 5°41'00"E, with Escravos-Lagos pipeline system as the source of gas supply.

Although some studies such as Oricha and Olarinoye (2012) and Iwuamadi and Dike (2012) have shown that poor plant maintenance, operational policies and power transmission issues are factors that also affect adequate power generation in Nigeria, however, the veracity of these militating factors has been tested on the field assessment in some gas power plants and results show less impact on both plant capacity performance and economic viability when compared to the effect of gas supply to the plants. This paper therefore, attempts to correlate the gas supply and power generation based on statistical regression models.

## 2.0. Methodology

Questionnaires were designed from the data obtained from the National Integrated Power Project (NIPP) power stations and some relevant literature. Forty-three (43) variables were considered in the questionnaires which was scaled with five (5) point Resits Likert's attitudinal scale and administered to 150 respondents. Respondents' responses were transposed into metric variables. Gas pressure, ambient temperature, compressed temperature difference (CTD) and power generation have been identified as variable (Oyedepo *et al*., 2015) and were used as research parameters in this study. The correlation of gas supply and power generation of gas power plant was done using the multiple linear regression models to assess the data quality, normality of data and the diagnostic analysis of data.

### *2.1. Assessment of data quality*

To assess the quality of the data, three important tests were conducted which includes: outlier detection; data fitness using reliability analysis; and test of homogeneity.

#### 2.1.1. Detection of outliers using the labelling rule

In this study, the labelling rule method was employed to detect the presence of outliers. The labelling rule is the statistical method of detecting the presence of outliers in data sets using the 25th percentile (lower bound) and the 75th percentile (upper bound). The underlying mathematical equation based on the lower and the upper bound is presented as follows:

$$\text{Lower Bound } Q_1 - [2.2 \times (Q_3 - Q_1)] \quad (1)$$

$$\text{Upper Bound } Q_3 + [2.2 \times (Q_3 - Q_1)] \quad (2)$$

At 0.05 degree of freedom, any data lower than $Q_1$ or greater than $Q_3$ was considered an outlier and need to be removed before analysis (Levi *et al*., 2009).

#### 2.1.2. Data fitness using reliability analysis

Reliability analysis of the data was done to ascertain the fitness of the data for the selected analysis. Descriptive analysis of the reliability test was based on the data scale (measured in terms of weight and order of distribution). The summary statistics was done to compute the data means, variance, covariance and correlations using the intra class correlation coefficient.

#### 2.1.3. Test of homogeneity

Homogeneity test was carried out to establish the fact that the data used (i.e. gas pressure, ambient temperature, CTD and power generation) for the analysis were from the same power plant (same population). Homogeneity test is based on the cumulative deviation from the mean as expressed using the mathematical equation below (Raes *et al*., 2006).

$$S_k = \sum_{i=1}^{k} \left( X_i - \bar{X} \right) \quad k = 1, \ldots n \quad (3)$$

where, $X_i$ = the record for the series $X_1$ $X_2$, … $X_n$,

$\bar{X}$ = the mean,

$S_{ks}$ = the residual mass curve.

For a homogeneous record, one may expect that the $S_{ks}$ fluctuate around the zero-centre line in the residual mass curve since there is no systematic pattern in the deviation $X_i$'s from the average values $\bar{X}$. To perform the homogeneity test, a software package for analysing time series data known as Rainbow (Raes *et al*., 2006) was used.

*2.2 Assessment of normality*

In the study the Jarque-Bera (JB) test for normality was employed because the sample size was large (i.e. >1000). Mathematically, the JB test is defined (Bowman and Shenton, 1975) as follows:

$$JB = n[(\sqrt{b_1})^2/6 + (b_2 - 3)^2/24] \quad (4)$$

where, n = sample size,
$\sqrt{b_1}$ = sample skewness, and
$b_2$ = kurtosis coefficient.

The hypothesis for the JB test is:
$H_0$ = Data follows a normally distribution
$H_1$ = Data do not follow a normal distribution

In general, a large JB value indicates that the residuals are not normally distributed. A value of JB greater than 10 means that the null hypothesis has been rejected at the 5% significance level. In other words, the data do not come from a normal distribution. JB value of between (0-10) indicates that the data is normally distributed (Das and Imon, 2016).

*2.3 Diagnostic analysis of data*

Diagnostic statistics were conducted to verify the statistical properties of the overall regression model. The selected diagnostic statistics include:

i. Heteroskedasticity test using Breusch-Pagan Godfrey
ii. Serial Correlation test using Breusch Godfrey
iii. Variance Inflation Factor (VIF)

**3.0. Results and Discussion**

*3.1 Data quality assessment results*

The results of outlier detection test; data fitness test using reliability analysis; and test of homogeneity are discussed below.

3.1.1 Data fitness test result using the labelling rule
Results of the computed percentiles for both the dependent and independent variable are presented in Table 1.

**Table 1:** Computed percentile for both dependent and independent variables

| | | Percentiles | | | | | | |
|---|---|---|---|---|---|---|---|---|
| | | 5 | 10 | 25 | 50 | 75 | 90 | 95 |
| Weighted Average (Definition 1) | Gas Pressure (FPG2) | 20.300 | 20.300 | 20.600 | 21.400 | 21.500 | 21.500 | 21.700 |
| | Ambient Temp. (INLET) | 25.300 | 25.900 | 27.000 | 28.200 | 29.300 | 30.700 | 31.600 |
| | Compressed Temp. Diff. (CTD) | 328.400 | 331.400 | 335.650 | 340.100 | 350.750 | 359.700 | 364.530 |
| | Power Generation (MWATTS) | 76.200 | 81.500 | 86.400 | 91.900 | 101.150 | 107.700 | 109.430 |
| Tukey's Hinges | Gas Pressure (FPG2) | | | 20.600 | 21.400 | 21.500 | | |
| | Ambient Temp. (INLET) | | | 27.000 | 28.200 | 29.300 | | |
| | Compressed Temp. Diff. (CTD) | | | 335.700 | 340.100 | 350.700 | | |
| | Power Generation (MWATTS) | | | 86.400 | 91.900 | 101.100 | | |

Using the weighted average shown in Table 1, the 25th percentile ($Q_1$) for gas pressure was observed to be 20.600 while the 75th percentile ($Q_3$) was observed to be 21.500. Substituting into Eqn. (1) and Eqn. (2), the lower and upper bound statistics were computed to be 18.62 and 23.58 respectively.

Table 2 shows the highest gas pressure extreme value statistic to be 33.2 and 29.4. These values are higher than the calculated upper bound value of 23.58. Likewise the lowest gas pressure are seen to be 19.4 and 19.5, these are greater than the calculated lower bound of 18.62. It was observed that gas pressure values indicated by case number 587, 87, 226, 327 and 351 contained values that are greater than the calculated upper bound, hence, they were declared outliers and were removed (Levi *et al*., 2009).

From Table 1, the 25th percentile ($Q_1$) for ambient temperature was observed to be 27.000 while the 75th percentile ($Q_3$) was observed to be 29.300. Using eqns. (1) and (2) the lower and upper bound statistics were computed as 21.94 and 34.36 respectively. Table 3 shows the extreme value statistics of ambient temperature for the highest and lowest ambient temperature. The highest ambient temperature values are 344.3, 330.5 and 185.8, these are higher than the calculated upper bound of 34.36. The lowest ambient temperature values are 21.0, 21.5, 22.3, 22.8 and 23.5 some of which were greater than the calculated lower bound of 21.94. In this case, it was observed that ambient temperature values indicated by case number 242, 542, 151, 470 and 1113 contained values that are greater than the calculated upper bound, and case number 669 and 739 contained values that are lower than the calculated lower bound, hence, they are considered as outliers and removed.

**Table 2:** Extreme value statistics for gas pressure

| | | | Case Number | Value |
|---|---|---|---|---|
| Gas Pressure (FPG2) | Highest | 1 | 587 | 33.2 |
| | | 2 | 87 | 29.4 |
| | | 3 | 226 | 29.4 |
| | | 4 | 327 | 29.4 |
| | | 5 | 351 | 29.4[a] |
| | Lowest | 1 | 954 | 19.4 |
| | | 2 | 264 | 19.4 |
| | | 3 | 496 | 19.5 |
| | | 4 | 486 | 19.5 |
| | | 5 | 455 | 19.5[b] |

**Table 3:** Extreme value statistics for ambient temperature

| | | | | |
|---|---|---|---|---|
| Ambient Temp. (INLET) | Highest | 1 | 242 | 344.3 |
| | | 2 | 542 | 344.3 |
| | | 3 | 151 | 330.5 |
| | | 4 | 470 | 330.5 |
| | | 5 | 1113 | 185.8 |
| | Lowest | 1 | 669 | 21.0 |
| | | 2 | 739 | 21.5 |
| | | 3 | 652 | 22.3 |
| | | 4 | 44 | 22.8 |
| | | 5 | 631 | 23.5 |

The extreme value statistics of CTD is shown in Table 4. The 25th percentile ($Q_1$) for CTD was seen to be 335.650 while the 75th percentile ($Q_3$) was seen to be 350.750. The lower and upper bound statistics were computed as 302.43 and 383.97 using eqns. (1) and (2) respectively. From Table 4, the highest CTD values were 625.1, 582.2 and 470.6. These values are higher than the calculated upper bound of 383.97. The lowest CTD values were observed to be 21.4, 97.5, 100.7 and 123.4. These are lower than the calculated lower bound of 302.43. It was observed that CTD values indicated by case number 300, 986, 511, 378, 1055 contained values that are greater than the calculated upper bound and case number 949, 259, 2, 21 and 15 contained values that are lower than the calculated lower bound hence, they were declared outliers and were removed.

Table 5 shows the extreme value statistics of power generation. From Table 1, the 25th percentile ($Q_1$) for power generation was observed to be 86.40 while the 75th percentile ($Q_3$) was observed to be 101.15. Using Eqns. (1) and (2), the lower and upper bound statistics were computed as 53.95 and 133.60 respectively. From Table 5, the highest power generation values are 161.7, 159.6, 153.8, 152.5 and 138.9. These are higher than the calculated upper bound of 133.60. The lowest power generation values are 21.4 and 28.7. These values are lower than the calculated lower bound of 53.95. It was observed that power generation values indicated by case numbers 622, 658, 46, 604 and 275 contained power generation values that are greater than the calculated upper bound. Also, case numbers 949, 259, 948, 257 and 196 contained power generation values that are lower than the calculated lower bound, hence, removed as outliers.

**Table 4:** Extreme value statistics for CTD

| | | | | |
|---|---|---|---|---|
| Compressed Temp. Diff. (CTD) | Highest | 1 | 300 | 625.1 |
| | | 2 | 986 | 625.1 |
| | | 3 | 511 | 582.2 |
| | | 4 | 378 | 470.6 |
| | | 5 | 1055 | 470.6 |
| | Lowest | 1 | 949 | 21.4 |
| | | 2 | 259 | 21.4 |
| | | 3 | 2 | 97.5 |
| | | 4 | 21 | 100.7 |
| | | 5 | 15 | 123.4 |

**Table 5:** Extreme value statistics for power generation

| | | | | |
|---|---|---|---|---|
| Power Generation (MWATTS) | Highest | 1 | 622 | 161.7 |
| | | 2 | 658 | 159.6 |
| | | 3 | 46 | 153.8 |
| | | 4 | 604 | 152.5 |
| | | 5 | 275 | 138.9 |
| | Lowest | 1 | 949 | 21.4 |
| | | 2 | 259 | 21.4 |
| | | 3 | 948 | 28.7 |
| | | 4 | 257 | 28.7 |
| | | 5 | 196 | 28.7[a] |

3.1.2. Results of data reliability analysis

Table 6 shows the summary statistics of data means, variance, covariance and correlations using the intra-class correlation coefficient.

**Table 6:** Result of summary item statistics

| | Mean | Minimum | Maximum | Range | Maximum / Minimum | Variance | N of Items |
|---|---|---|---|---|---|---|---|
| Item Means | 121.436 | 21.250 | 341.688 | 320.438 | 16.079 | 2.260E4 | 4 |
| Item Variances | 349.277 | 1.054 | 886.707 | 885.653 | 840.947 | 1.501E5 | 4 |
| Inter-Item Covariances | 15.937 | -14.564 | 113.148 | 127.711 | -7.769 | 2.101E3 | 4 |
| Inter-Item Correlations | .068 | -.063 | .311 | .374 | -4.952 | .016 | 4 |

The two-way mixed model with confidence interval of 95% (i.e. p-value of 0.05) and initial test value of zero was used. The reliability hypothesis was as follows:

$H_0$: Data are reliable
$H_1$: Data are not reliable

The Fisher's probability test (F-test) was used for the analysis and result obtained are presented in Table 7.

**Table 7:** Inter-item correlation and covariance statistics

| | Gas Pressure (FPG2) | Ambient Temp. (INLET) | Compressed Temp. Diff. (CTD) | Power Generation (MWATTS) |
|---|---|---|---|---|
| Gas Pressure (FPG2) | 1.000 | .011 | .112 | .051 |
| Ambient Temp. (INLET) | .011 | 1.000 | -.013 | -.063 |
| Compressed Temp. Diff. (CTD) | .112 | -.013 | 1.000 | .311 |
| Power Generation (MWATTS) | .051 | -.063 | .311 | 1.000 |

**Inter-Item Covariance Matrix**

| | Gas Pressure (FPG2) | Ambient Temp. (INLET) | Compressed Temp. Diff. (CTD) | Power Generation (MWATTS) |
|---|---|---|---|---|
| Gas Pressure (FPG2) | 1.054 | .220 | 3.435 | .639 |
| Ambient Temp. (INLET) | .220 | 360.238 | -7.257 | -14.564 |
| Compressed Temp. Diff. (CTD) | 3.435 | -7.257 | 886.707 | 113.148 |
| Power Generation (MWATTS) | .639 | -14.564 | 113.148 | 149.109 |

Table 7 shows that the gas pressure and compressed temperature difference were positively correlated with power generation and have a covariance value of 0.639 and 113.148 respectively. The large covariance value of compressed temperature difference indicates that the variable has an overriding influence on power generation compare to gas pressure and ambient temperature. These are seen to be negatively correlated with power generation. The computed coefficient of correlations of 0.051 for gas pressure, -0.063 for ambient temperature, and 0.311 for compressed temperature difference were observed to be relatively weak, which is indicative of the absence of co-linearity problem in the regression variables. The highest coefficient of (+0.311) which is between compressed temperature

difference and power generation still did not pose any challenge of multi-collinearity. Hence, we can conclude that there is no issue of multicollinearity and that the regression variables are clearly correlated with the dependent variable. This is evident in the intra-class correlation coefficient presented in Table 8.

**Table 8:** Computed intra-class correlation coefficients

| | Intraclass Correlation[a] | 95% Confidence Interval | | F Test with True Value 0 | | | |
|---|---|---|---|---|---|---|---|
| | | Lower Bound | Upper Bound | Value | df1 | df2 | Sig |
| Single Measures | .046[b] | .021 | .072 | 1.191 | 1152 | 3456 | .000 |
| Average Measures | .161[c] | .079 | .237 | 1.191 | 1152 | 3456 | .000 |

Again, we observed from the result of Table 8 that the single and average measure intra-class correlation coefficients are relatively weak (0.046 and 0.161) which is indicative of the absence of multicollinearity. To ascertain the reliability of the data, one-way analysis of variance (ANOVA) was generated and presented in Table 9. At 0.05 degree of freedom (df), with a computed p-value of 0.000 as observed in Table 9, the null hypothesis was accepted and it was concluded that the data are good and can be employed for further analysis.

**Table 9:** Analysis of variance table

| | | Sum of Squares | df | Mean Square | F | Sig |
|---|---|---|---|---|---|---|
| Between People | | 457445.219 | 1152 | 397.088 | | |
| Within People | Between Items | 7.816E7 | 3 | 2.605E7 | 7.816E4 | .000 |
| | Residual | 1152024.163 | 3456 | 333.340 | | |
| | Total | 7.931E7 | 3459 | 22928.352 | | |
| Total | | 7.977E7 | 4611 | 17299.201 | | |

3.1.3. Homogeneity test results

Raes *et al*. (2006) described homogeneity test as one based on the cumulative deviation from the mean. The homogeneity test hypothesis of gas pressure is defined as:

$H_0$: Data are statistically homogeneous.
$H_1$: Data are not homogeneous.

The null and alternate hypotheses were tested at 90%, 95% and 99% confidence interval (i.e. 0.1, 0.05 and 0.01) df as shown in Figure 1.

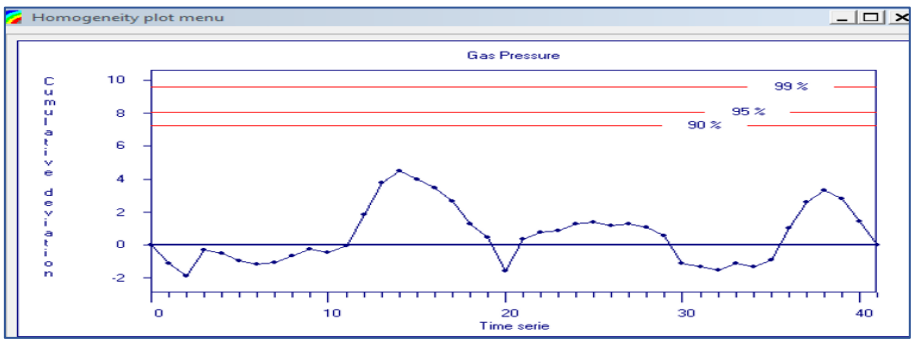


**Figure 1:** Homogeneity test of gas pressure data

The gas presure data is seen to fluctuated around the zero-center line of the residual mass curve in Figure 1, an indication that the data were statistically homogeneous. A further test of homogeneity was done using the homogeneity statistics to check the strength of the null hypothesis over the alternate hypothesis. Based on the result obtained, the null hypothesis ($H_0$) was accepted, and we concluded that the gas pressure data were statistically homogeneous at 90%, 95% and 99% confidence interval.

The homogeneity test hypothesis for ambient temperature is as follows:

$H_0$: Data are statistically homogeneous.
$H_1$: Data are not homogeneous.

The null and alternate hypotheses were tested at 90%, 95% and 99% confidence interval (i.e. 0.1, 0.05 and 0.01) df as shown in Figure 2.

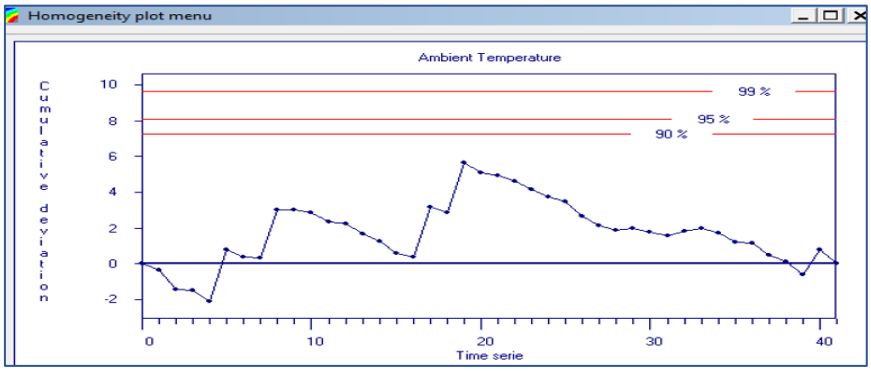


**Figure 2:** Homogeneity test of ambient temperature data

The ambient temperature data (Figure 2) fluctuated around the zero-center line of the residual mass curve, an indication that the data were statistically homogeneous. The homogeneity statistics was used to check the strength of the null hypothesis over the alternate hypothesis. Based on the result obtained, the null hypothesis ($H_0$) was accepted, and it was concluded that the ambient temperature data were statistically homogeneous at 90%, 95% and 99% confidence interval.

The hypothesis of homogeneity test of compressed temperature difference data is:

$H_0$: Data are statistically homogeneous.
$H_1$: Data are not homogeneous.

The null and alternate hypothesis were tested at 90%, 95% and 99% confidence interval (i.e. 0.1, 0.05 and 0.01) df as shown in Figure 3.

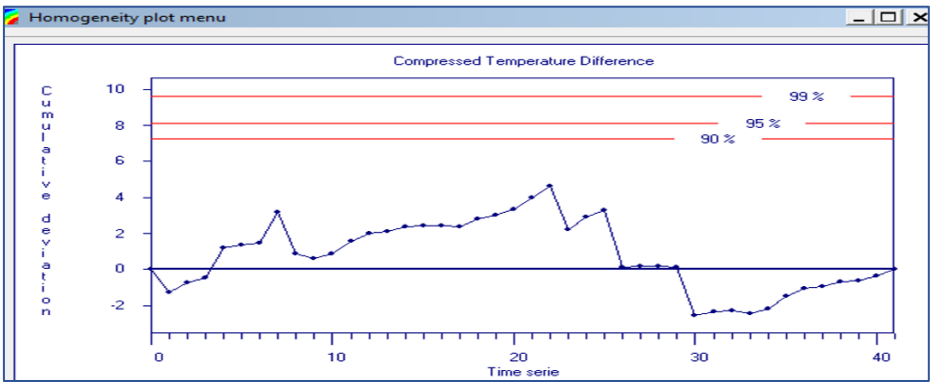


**Figure 3:** Homogeneity test of compresses temperature difference data

From Figure 3, the compressed temperature difference data fluctuated around the zero-center line of the residual mass curve, an indication that the data were statistically homogeneous. The homogeneity statistics was used to check the strength of the null hypothesis over the alternate hypothesis. Based on the result obtained, the null hypothesis ($H_0$) was accepted, and it was concluded that the compressed temperature difference data were statistically homogeneous at 90%, 95% and 99% confidence interval.

The hypothesis of homogeneity test of power generation data is:

$H_0$: Data are statistically homogeneous.
$H_1$: Data are not homogeneous.

The null and alternate hypothesis were tested at 90%, 95% and 99% confidence interval (i.e. 0.1, 0.05 and 0.01) df as shown in Figure 4.

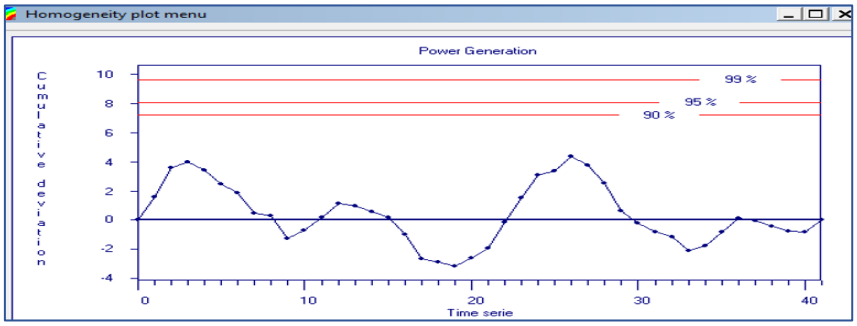


**Figure 4:** Homogeneity test of power generation data

Figure 4 showed that the power generation data fluctuated around the zero-center line of the residual mass curve, an indication that the data are statistically homogeneous. The homogeneity statistics was used to check the strength of the null hypothesis over the alternate hypothesis. Based on the result obtained, the null hypothesis ($H_0$) was accepted, and it was concluded that the power generation data were statistically homogeneous at 90%, 95% and 99% confidence interval.

*3.2. Normality test results*

The normality test was done for the one independent and three dependent variables using the JB test for normality statistical software. Figure 5 shows the results of the normality test of gas pressure.

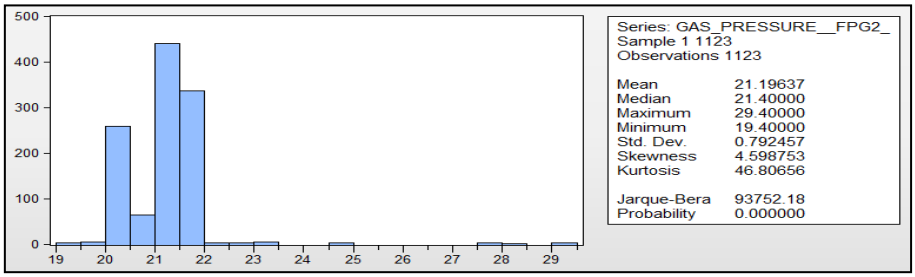


**Figure 5:** Normality test of gas pressure data

A skewness coefficient of 4.598753 and kurtosis value of 46.80656 shown in Figure 5 indicate that the gas pressure data is not normally distributed. For normality, the skewness coefficient should not be greater than 1 and the kurtosis should not be greater than 3 (Bai and Ng, 2005). JB value of 93752.18 and a probability (p-value) of 0.00% observed in Figure 5 indicates that the gas pressure data is not normally distributed. JB value >10 means that the null hypothesis is rejected at that level of significance (Das and Imon, 2016), meaning, the data did not come from a normal distribution. Since the JB test value is greater than 10 and the (p-value) is less than the 5% significant value, the null hypothesis was rejected and it was concluded that the data is not from a normal distribution.

The normality test result of ambient temperature is shown in Figure 6.

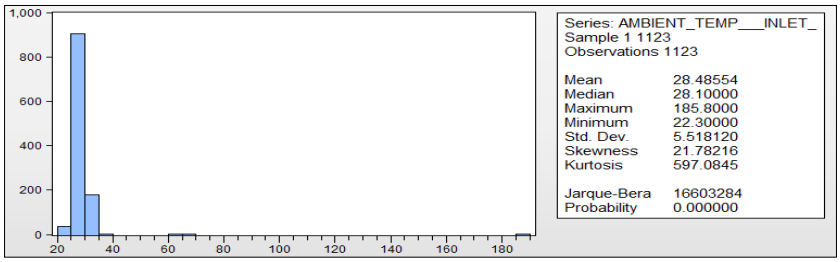


**Figure 6:** Normality test of ambient temperature data

A skewness coefficient of 21.78216 and a kurtosis value of 597.0845 observed in Figure 6 indicate that the ambient temperature data is not normally distributed. JB value of 16603284 and a probability

(p-value) of 0.00% observed in Figure 6 indicates that the ambient temperature data is not normally distributed. Since the JB test value is greater than 10 and the p-value is less than the 5% significant value, the null hypothesis was rejected and it was concluded that the data is not from a normal distribution.

Figure 7 shows result of the normality test of compressed temperature difference.

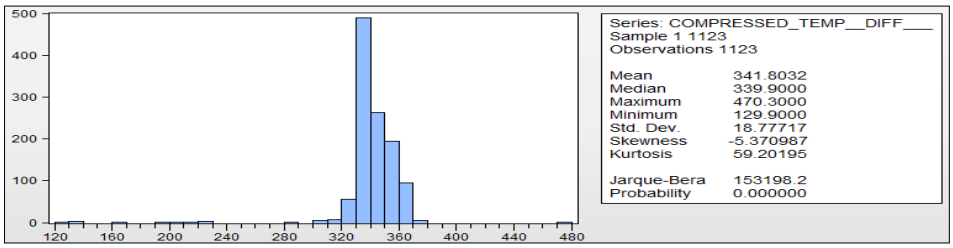


**Figure 7:** Normality test of compressed temperature difference data

A skewness coefficient of -5.370987 shows that the data is negatively skewed an indication that the data is not normally distributed. Kurtosis value of 59.20195 observed in Figure 7 is also an indication that the data is not from a normal population distribution. JB value of 153198.2 and a probability (p-value) of 0.00% also indicated that the compressed temperature difference data was not normally distributed. Since the JB test value is greater than 10 and the p-value is less than the 5% significant value, the null hypothesis was rejected and it was concluded that the data is not from a normal distribution.

Figure 8 shows result of the normality test of power generation data.

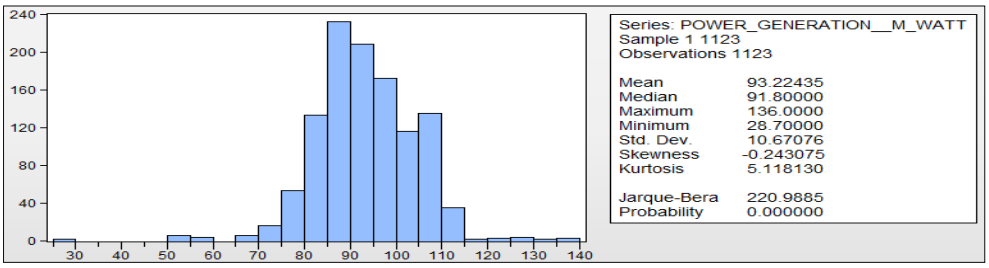


**Figure 8:** Normality test of power generation data

A skewness coefficient of -0.243075 shows that the data is negatively skewed an indication that the data is not normally distributed. Kurtosis value of 5.118130 observed in Figure 8 is also an indication that the data is not from a normal population distribution. JB value of 220.9885 and a probability (p-value) of 0.00% as observed in Figure 8 also indicates that the power generation data is not normally distributed Since the JB test value is greater than 10 and the p-value is less than the 5% significant value, the null hypothesis was rejected and it was concluded that the data is not from a normal distribution.

### *3.3. Results of the Diagnostic Analysis of Data*

The diagnostic statistical analyses done in this study include: Heteroskedasticity test using Breusch-Pagan Godfrey; Serial Correlation test using Breusch Godfrey; and Variance Inflation Factor (VIF).

#### 3.3.1. Heteroskedasticity test

Result of heteroskedasticity test using Breusch-Pagan Godfrey method showed that (i) the calculated (p-value) based on the F-statistics is 0.0000; (ii) the calculated p-value based on Lagrange multiplier (LM) is 0.0000. Since the computed p-value based on F-statistics and Lagrange multiplier is less than 0.05 ($P < 0.05$), we rejected the null hypothesis of homoskedasticity and conclude that there is no heteroskedasticity in the data (Astivia and Zumbo, 2019).

#### 3.3.2. Serial correlation test result

The result of serial correlation LM test using Breusch Godfrey method indicated that (i) the calculated p-value based on the F-statistics is 0.0000; and (ii) the calculated p-value based on LM is 0.0000.

Since the computed p-value based on F-statistics and LM is less than 0.05 ($P < 0.05$), we rejected the null hypothesis of serial correlation and concluded that there is the presence of serial correlation in the data.

3.3.3. The Variance Inflation Factor (VIF) result

The result of the calculated VIF for the selected variables was observed to be less than 10. Since the computed variance inflation factors (centred VIF) for the selected independent variables were less than 10, it was concluded that the variables were well correlated with the dependent variable, hence absence of multicollinearity (Montgomery, 2005). The Output of regression analysis is presented in Table 10. Finally, the reliance of the dependent variable on the selected independent variables was evaluated using the coded least square regression equation as shown in Eqn. (5).

$$(M/watts)C\ FPG2\ INLET\ CTD \quad (5)$$

**Table 10**: Output of regression analysis

View | Proc | Object | Print | Name | Freeze | Estimate | Forecast | Stats | Resids

Dependent Variable: POWER_GENERATION__M_WATT
Method: Least Squares
Date: 01/01/20 Time: 14:43
Sample: 1 1123
Included observations: 1123

| Variable | Coefficient | Std. Error | t-Statistic | Prob. |
|---|---|---|---|---|
| C | 29.61506 | 9.196908 | 3.220111 | 0.0013 |
| GAS_PRESSURE__FPG2_ | 0.197497 | 0.377239 | 0.523532 | 0.6007 |
| AMBIENT_TEMP___INLET_ | -0.247932 | 0.053707 | -4.616362 | 0.0000 |
| COMPRESSED_TEMP__DIFF___ | 0.194514 | 0.015927 | 12.21311 | 0.0000 |

| | | | |
|---|---|---|---|
| R-squared | 0.137577 | Mean dependent var | 93.22435 |
| Adjusted R-squared | 0.135265 | S.D. dependent var | 10.67076 |
| S.E. of regression | 9.922863 | Akaike info criterion | 7.431115 |
| Sum squared resid | 110180.3 | Schwarz criterion | 7.449010 |
| Log likelihood | -4168.571 | Hannan-Quinn criter. | 7.437878 |
| F-statistic | 59.50232 | Durbin-Watson stat | 0.928874 |
| Prob(F-statistic) | 0.000000 | | |

From the result of Table 10, with a regression p-value of 0.0013, it was concluded that the regression analysis was significant at 0.05 df. The Independent variables, namely; (INLET and CTD) were observed to have a very strong influence on the dependent variable when compared to FPG2. The poor regression terms such as coefficient of determination and adjusted coefficient of determination was apparently due to the presence of serial correlation in the used data. The overall regression equation was then generated as:

$$(M/watts) = 21.61506 + 0.197497(FGP2) - 0.247932(INLET) + 0.194514(CTD) \quad (6)$$

*3.4. Model development*

Table 11 shows the estimated regression parameters of eqn. (2).

**Table 11:** Estimated Regression Parameters

| S/N | Regression parameters | Estimated values |
|---|---|---|
| 1 | Coefficient of determination (R- Squared) | 0.137577 |
| 2 | Adjusted Coefficient of determination (Adjusted R-Squared) | 0.135265 |
| 3 | Sum of Error of Regression (S.E. of Regression) | 9.922863 |
| 4 | Residual Sum of Square | 110180.3 |

From Table 11, the estimated values of regression parameters were very poor. An indication that the exact relationship between the dependent variable (power generation) and the selected independent variables (gas pressure, ambient temperature and compressed temperature difference) cannot be determined using linear regression model. Hence, non-linear model equations method (power function; quantile regression; robust regression; inverse function based on gamma distribution; and log function based on negative binomial distribution) were developed to determine the exact relationship between the dependent variable and the selected independent variables. Statistical software was used to develop the model equations.

3.4.1. Power function model
The model equation developed using the power function model is shown in Table 12.

**Table 12:** Result of power function model

**ANOVA[b]**

| Model | | Sum of Squares | df | Mean Square | F | Sig. |
|---|---|---|---|---|---|---|
| 1 | Regression | 2.196 | 3 | .732 | 57.436 | .000[a] |
| | Residual | 14.262 | 1119 | .013 | | |
| | Total | 16.458 | 1122 | | | |

a. Predictors: (Constant), Compressed Temp. Diff. (CTD), Ambient Temp. (INLET), Gas Pressure (FPG2)

b. Dependent Variable: Power Generation (M/WATTS)

**Coefficients[a]**

| Model | | Unstandardized Coefficients | | Standardized Coefficients | t | Sig. |
|---|---|---|---|---|---|---|
| | | B | Std. Error | Beta | | |
| 1 | (Constant) | 3.101 | .399 | | 7.763 | .000 |
| | Gas Pressure (FPG2) | .107 | .097 | .031 | 1.095 | .274 |
| | Ambient Temp. (INLET) | -.339 | .034 | -.278 | -9.980 | .000 |
| | Compressed Temp. Diff. (CTD) | .383 | .049 | .222 | 7.883 | .000 |

a. Dependent Variable: Power Generation (M/WATTS)

Results of the power function method as shown in Table 2 using ANOVA showed that the power function model is significant at 0.05df. Using the unstandardized coefficients, the power function equation was developed as:

$$(M/watts) = 22.22 \times (FPG2)^{0.107}(INLET)^{-0.339}(CTD)^{0.383} \quad (7)$$

3.4.2. Quantile regression method
The ANOVA result shown in Table 12 showed that the quantile regression model is significant at 0.05df. Using the unstandardized coefficients, the quantile regression equation is:

$$(M/watts) = -106.4318 + 0.096263(FPG2) - 1.560389(INLET) + 0.703719(CTD) \quad (8)$$

3.4.3. Robust regression method
Table 12 shows the ANOVA results which indicated that the robust regression model is significant at 0.05df. Using the unstandardized coefficients, the robust regression equation was developed as:

$$(M/watts) = -117.8962 + 0.123039(FPG2) - 1.776864(INLET) + 0.752693(CTD) \quad (9)$$

3.4.4. Inverse function method
From the ANOVA results in Table 12, the inverse function model is significant at 0.05df. Using the unstandardized coefficients, the inverse function equation developed is:

$$Z = 0.019253 - 2.48E(-05)(FPG2) + 3.86E(-05)(INLET) - 2.66E(-05)(CTD) \quad (10)$$

$$(M/watts) = {}^{1}/_{Z} \quad (11)$$

3.4.5. Log function method
The ANOVA analysis in Table 12 indicated that the log function model is significant at 0.05df. Using the unstandardized coefficients, the log function equation was developed as:

$$Z = 3.963366 + 0.002036(FPG2) - 0.002265(INLET) + 0.001733(CTD) \quad (12)$$

$$(M/watts) = Exp\,(Z) \quad (13)$$

The summary of the developed mathematical models are shown in Table 13, and can be used to predict the power generation.

**Table 13:** Summary of developed mathematical equations (models)

| S/N | Method | Developed mathematical equation |
|---|---|---|
| 1 | Linear Regression | $(M/watts) = 21.61506 + 0.197497(FGP2) - 0.247932(INLET) + 0.194514(CTD)$ |
| 2 | Robust Regression | $(M/watts) = -117.8962 + 0.123039(FPG2) - 1.776864(INLET) + 0.752693(CTD)$ |
| 3 | Quantile Regression | $(M/watts) = -106.4318 + 0.096263(FPG2) - 1.560389(INLET) + 0.703719(CTD)$ |
| 4 | Power Function | $(M/watts) = 22.22 \times (FPG2)^{0.107}(INLET)^{-0.339}(CTD)^{0.383}$ |
| 5 | Inverse Function | $Z = 0.019253 - 2.48E(-05)(FPG2) + 3.86E(-05)(INLET) - 2.66E(-05)(CTD)$ $(M/watts) = {}^{1}/_{Z}$ |
| 6 | Log Function | $Z = 3.963366 + 0.002036(FPG2) - 0.002265(INLET) + 0.001733(CTD)$ $(M/watts) = Exp\,(Z)$ |

## 4.0. Conclusion

The relationship between the output of gas power plant and the quantitative variables were not linearly related, but could be best described by a non-linear regression model. The study provided a veritable and laudable process to systematically identify factors that are capable of influencing the generation of power in gas power plants. One dependent (power generation) and three independent variables (Gas Pressure, Ambient Temperature, Compressed Temperature) were used for this analysis. The three critical numeric variables were observed to play a key role in assessing the relationship between input and output parameters in gas power plant. The study also showed that the ambient temperature and compressed temperature difference had very strong influence on the dependent variable when compared to the gas pressure variable.

## References

Astivia, O. L. O. and Zumbo, B. D. (2019). Heteroskedasticity in Multiple Regression Analysis: What it is, How to detect it and How to solve it with Application in R and SPSS. *Practical Assessment, Research, and Evaluation*, 24(1), pp. 1 – 17.

Bai, J. and Ng, S. (2005). Tests for Skewness, Kurtosis, and Normality for Time Series Data. *American Statistical Association Journal of Business & Economic Statistics*, 23(1), pp. 49 – 60.

Bowman, K. O. and Shenton, B. R. (1975). Omnibus test contours for departures from normality based on $\sqrt{b_1}$ and $b_2$. *Biometrika*, 64, pp. 243- 450.

Das, K. R. and Imon, A. H. M. R. (2016). A Brief Review of Tests for Normality. *American Journal of Theoretical and Applied Statistics*, 5(1), pp. 5 - 12.

Enete, C. I. and Alabi, M. O. (2011). Potential Impacts of Global Climate Change on Power and Energy Generation. *Journal of Knowledge Management, Economics and Information Technology*, 6, pp. 1-14.

Iwuamadi, O. C., and Dike, D. O. (2012). Empirical Analysis of Productivity of Nigerian Power Sector. *IOSR Journal of Electrical and Electronics Engineering (IOSR-JEEE)*, 3(4), pp. 24 – 38.

Izuwan, N. C. (2017). Improving Natural Gas Distribution and Management in Nigeria. *International Journal of Scientific and Engineering Research*, 8(7), pp. 330 - 344.

Levi, D. B., Julie, E. K., Olsen, J. R., Pulwarty, R. S., Raff, D.A., Turnipseed, D. P., Webb, R. S and Kathleen D. W. (2009). Climate Change and Water Resources Management: A Federal Perspective. *Circular*, 1331, pp. 1-72.

Luis, R., Bolonio, D., Mazadiego, L. F. and Valencia-Chapi, R. (2019). Long-Term Electricity Supply and Demand Forecast (2018–2040): A LEAP Model Application towards a Sustainable Power Generation System in Ecuador. *Sustainability*, 11(5316), pp. 2-19.

Montgomery, D. C. (2005). *Design and Analysis of Experiments*. 6th Edition, New York, John Wiley and Sons, Inc. USA.

Nwokeji, G. U. (2007). The Nigerian National Petroleum Cooperation and the Development of the Nigerian Oil and Gas Industry: History, Strategies and Current Directions. Baker Institute and Japan Petroleum Energy Centre.

Onochie, U. P., Obanor, A. and Aliu, S. A. (2015). Electricity Crisis in Nigeria: The Way Forward. *American Journal of Renewable and Sustainable Energy*, 1(4), pp. 180-186.

Oricha, J.Y. and Olarinoye, G.A. (2012). Analysis of Interrelated Factors Affecting Efficiency and Stability of Power Supply in Nigeria. *International Journal of Energy Engineering*, 2(1), pp. 1 – 8.

Orogun, B. O. (2015). Natural Gas to Power in Nigeria, the Practices and the Way Forward for Sustainable Development. *Sustainable Development and National Resources*, University of Manitoba.

Oyedepo, S. O. (2012). Efficient Energy Utilization as a tool for Sustainable Development in Nigeria. *International Journal of Energy and Environmental Engineering*, 3(11), pp. 1-12.

Oyedepo, S.O., Fagbenle, R. O. and Adefila, S. S. (2015). *Assessment of Performance Indices of Selected Gas Turbine Power Plants in Nigeria*. Energy Science & Engineering, Society of Chemical Industry and John Wiley & Sons Ltd., U. S. A.

Raes, D., Willens, P. and Gbaguidi (2006). Rainbow-A Software Package for Analyzing Data and Testing the Homogeneity of Historical Data Sets, 1, pp. 1-15.

Rapu, C. S., Adenuga, A. O., Kanya, W. J., Abeng, M. O., Golit, P. D., Hilili, M. J., et al. (2015). Analysis of Energy Market Conditions in Nigeria. *Occasional Paper*, No. 55, Central Bank of Nigeria, Garki, Abuja, Nigeria.

Sambo, A. S., Garba, B., Zarma, I. H. and Gaji, M. M. (2010). Electricity Generation and the Present Challenges in the Nigerian Power Sector. Energy Commission of Nigeria, Abuja-Nigeria.

**Cite this article as:**
Agbondinmwin U. and Ebhojiaye R. S. 2021. Modelling of Input Parameters for Power Generation using Regression Models. *Nigerian Journal of Environmental Sciences and Technology*, 5(1), pp. 152-164. https://doi.org/10.36263/nijest.2021.01.0241

Nigerian Journal of Environmental Sciences and Technology (NIJEST)

www.nijest.com

ISSN (Print): 2734-259X | ISSN (electronic): 2734-2603

Vol 5, No. 1 March 2021, pp 165 - 172

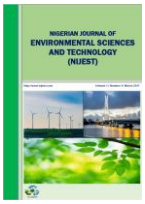

# Exposure to Atrazine Impairs Behaviour and Growth Performance in African Catfish, *Clarias gariepinus* (Burchell, 1822) Juveniles

Opute P. A.[1,*] and Oboh I. P.[2]

[1,2]Department of Animal and Environmental Biology, University of Benin, Benin City, Edo State, Nigeria

Corresponding Author: *ashibudike.opute@uniben.edu

https://doi.org/10.36263/nijest.2021.01.0263

## ABSTRACT

*Clarias gariepinus juveniles of average weight, 17.57±1.95 g and an average length of 14.26±0.39 cm were exposed to environmentally relevant concentrations of 0 (control), 2.5, 25, 250, and 500 µg $L^{-1}$ atrazine in a quality-controlled 28-day bioassay. Growth performance was assessed bi-weekly and fish samples were taken from different tanks to determine the relative growth rate, specific growth rate, feed conversion ratio, condition factor and behaviour. At the end of two weeks of exposure, the relative growth rate and the specific growth rate among exposed fish groups was found to reduce significantly ($p<0.05$) compared to the control, an indication of poor growth performance. The average specific growth rates (SGR) of control fish is 3.86±0.02 %/w at the end of the exposure duration while recording -0.64±0.09 in the 500 µg $L^{-1}$ group. Feed conversion ratio increased significantly from control to the group with highest atrazine concentration. Condition factor (K) of fish among treatment groups showed significant decrease in values with increasing concentration of atrazine in a dose-dependent pattern. Atrazine exposure resulted in behavioural anomalies including erratic swimming, clinging to the water surface, loss of equilibrium, lethargy, and discolouration. The behavioural responses were found to be concentration-dependent. The length-weight relationships for both control and atrazine exposed fish exhibited positive allometric growth and significant relationships as depicted by the value of $R^2$ (coefficient of determination) except in the fish group exposed to 500 µg $L^{-1}$ atrazine which exhibited negative allometric growth. Findings from this study indicate interference with normal behaviour and growth performance of C. gariepinus juveniles with ecological implications in water bodies exposed to atrazine even at reduced concentrations.*

**Keywords:** *Clarias gariepinus*, Atrazine, Behaviour, Growth, Condition factor

## 1.0. Introduction

Increased industrialization and agricultural production, as evident in Nigeria in recent years, has exacerbated environmental contamination by the introduction of anthropogenic compounds that are alien to living systems. The quest for food security has raised several concerns about how to feed the growing population of over 200 million people. Since the adoption of the Millennium Development Goals (MDGs) at the beginning of the twenty-first century, this has been a major topic in government circles (Ashe, 2019). The government has no choice but to encourage intensified agriculture beyond subsistence scale to adequately feed the country's teeming population. However, the use of pesticides and other agricultural chemicals to promote and enhance the quantity and quality of farm produce cannot be divorced from agricultural mechanization. Thus, pesticides have become an indispensable tool in large-scale agricultural development in Nigeria (Opute and Oboh, 2021). Despite the overwhelming benefits of pesticide use, warnings of significant health risks for humans and the environment have been reported. The potential risks to human health from both occupational and non-occupational exposures, the death of farm animals, and the alteration of the local environment are all part of the health implications. Immunologic, teratogenic, carcinogenic, reproductive, and neurological issues are among the other side effects (Lushchaka, *et al*., 2018). Because of these health risks, most pesticide classes have been banned in developed and some developing countries.

Fish are presumably the best-understood species in the aquatic environment and are also important to man as a source of animal protein, thus, they have become the most common choice as a test organism for toxicological studies. Also, because of their significance as a protein source, aquatic pollution influences humans indirectly through the ingestion of contaminated fish following the bioaccumulation of toxicants in their bodies. It is therefore important to evaluate the impact of pollution on fish for both environmental and socio-economic reasons. *Clarias gariepinus* is a commercially important freshwater fish whose production is rapidly growing around the world. Besides its economic value, *C. gariepinus* has been used in fundamental and ecotoxicological studies, and it is currently a model test species for environmental research (Opute *et al*., 2021).

Farmers in Nigeria use atrazine, a class III herbicide from the triazine family, as one of their most popular pesticides (Olatoye *et al*., 2021). It is a registered and approved herbicide for use in Nigeria by the National Agency for Food and Drug Administration and Control (NAFDAC). However, registration criteria often overlook the pesticides' subtle effects on non-target organisms, which can only be determined by comprehensive descriptive and mechanistic toxicological studies. Atrazine is one of the most commonly detected pesticides in streams, rivers, ponds, lakes, and ground waters, and it is rated moderately harmful to aquatic organisms. Despite considerable usefulness, there is a lack of knowledge on the fate and consequences of these chemicals after they have been applied to crop fields in areas where farmers are unaware of healthy practices and the threats they pose to their health (Opute and Oboh, 2021). Herbicides are still being found in water sources, indicating that regulatory strategies have flaws and are ineffective in ensuring end-user and environmental protection. In November 1989, Nigeria's then-president unveiled the country's national environmental policy (Kankara, 2013). The policy aimed to achieve sustainable development in Nigeria, including, among other things, ensuring a quality environment suitable for the health and well-being of all Nigerians, as well as conserving and using the environment and natural resources for the benefit of present and future generations. Environmental conservation programs, on the other hand, are only effective if the environment to be protected is well understood. The ecosystem should not be over-protected or under-protected in any way. Standards should, ideally, be focused on environmental baseline data collected across the country. Unfortunately, such data are scarce in Nigeria, and even when they are, they are vastly underutilized. Understanding the extent of potential adverse effects of atrazine on the behavioural and growth performance of *C. gariepinus*, a Pan-African and widespread food fish in most African countries, including Nigeria, would be an invaluable tool in assessing the environmental risks posed by this widely used pesticide to our immediate environment.

## 2.0. Methodology

### *2.1. Materials*

Atrazine with CAS No:1912-24-9; technical grade, and of 99.5% purity, purchased from AccuStandard Incorporated (New Haven, CT, USA) was used as test chemical. Three hundred (300) four-week-old *C. gariepinus* juveniles were procured from the aquaculture section of the department of fisheries and aquaculture, faculty of agriculture, university of Benin, and were kept in the animal house of the department of animal and environmental biology. Twenty (20) juvenile fish were assigned at random to each treatment and control tank. The juvenile fish weighed an average of 17.57 ± 1.95 g and measured 14.26 ± 0.39 cm in length.

### *2.2. Test chemical and water analysis*

Atrazine with CAS No:1912-24-9; technical grade, and of 99.5% purity was purchased from AccuStandard Incorporated (New Haven, CT, USA). In distilled water, a 25 mg $L^{-1}$ atrazine stock solution was prepared (Milli-Q). The mixture was sonicated and warmed to 50 ° C for no more than 15 minutes to dissolve the atrazine (Zaya, 2011). Final exposure solutions were made by diluting the stock solution with nominal atrazine concentrations of 0 (Control), 2.5, 25, 250, and 500 µg $L^{-1}$ in exposure water. Three replicates were prepared for each concentration. Throughout the 28-day exposure period, the concentrations of atrazine in all tanks were monitored weekly using enzyme-linked immunosorbent assay (ELISA) kits (Abraxis, Warminster, PA) with n=12 (4 samples per replicate). The method detection limit (MDL) of the atrazine ELISA procedure was 0.05 µg $L^{-1}$ of water. A confirmatory test was performed on atrazine stock solutions and selected tank water samples using gas chromatography (Jimenez *et al*., 1997). Water was obtained using methylene chloride, then

dried with sodium sulfate and filtered through glass fibres. After that, the volume was reduced to 0.1 mL in methyl tertiary butyl ether (MtBE). Triphenylphosphate (Chem Service Inc., 500 ng $mL^{-1}$ in MtBE) was used as an instrumental internal standard. A GC/NPD (Gas Chromatographic/Nitrogen Phosphorus Detector) and PerkinElmers' TotalChromTM workstation chromatography data software was used to analyze the extracts. Samples for the GC/NPD analysis were obtained on three of the five days that water was collected. In each of the sample groups, triplicate water samples from each of the treatments (0, 2.5, 25, 250, and 500 µg $L^{-1}$) were used. Each sample set included atrazine-spiked water, water-blank matrix (tap), and a blank procedural as quality control samples.

*2.3. Experimental design and treatment*

The research was conducted with the approval of the University of Benin's College Research Ethics Committee and under the institutional guidelines, laws, and regulations of the Federal Republic of Nigeria's National Code of Health Research Ethics; REC approval number: CMS/REC/2017/026. Three hundred (300) four-week-old *C. gariepinus* juveniles were procured from the aquaculture section of the department of fisheries and aquaculture, faculty of agriculture, university of Benin, and were kept in the animal house of the department of animal and environmental biology. Twenty (20) juvenile fish were assigned at random to each treatment and control tank. The juvenile fish weighed an average of 17.57 ± 1.95 g and measured 14.26 ± 0.39 cm in length. The fish were then allowed to acclimate for seven days before being fed commercial fish feed at 8 hourly intervals once daily (Aller aqua, Allervej 130, 6070 Christiansfeld, Denmark). For 28 days, the fish were exposed to four concentrations of atrazine (2.5, 25, 250, and 500 µg $L^{-1}$) and control (0 µg $L^{-1}$) in a static renewal bioassay. The experimental tanks, which measured 670mm x 450mm x 355mm, were all correctly labelled as $AT_1$, $AT_2$, $AT_3$, $AT_4$, and C, representing 2.5, 25, 250, and 500 µg $L^{-1}$ of atrazine concentrations and control (0 µg $L^{-1}$), respectively. Three replicates of each concentration of test solutions were applied in a static-renewal exposure regime. Every 7 days, test solutions were renewed by 50% replacement to allow for maximum survival and to reduce stress on the fish caused by a sudden change in the water chemistry of the test media (Okomoda *et al*., 2016). A 12 h light:12 h dark photoperiod was used throughout the study period. Growth parameters were taken weekly throughout the four-week exposure duration.

*2.4. Measurement of growth performance*

Weight gain WG (g), specific growth rate (SGR, % d-1) was calculated as the following formulae:

$$WG = (W_t - W_o) \quad (1)$$

$$SGR = 100 \times [\ln(W_t) - \ln(W_o)]/days \quad (2)$$

where $W_o$ and $W_t$ were initial body weight and body weights of fish at time $t$ (g).

Feed conversion ratio (FCR): The feed conversation ratio was calculated using the formula below:

$$FCR = Feed\ intake/WG \quad (3)$$

Fulton's condition factor ($K$): Fulton's condition factor ($K$) was calculated using the formula given below:

$$K = \frac{W \times 100}{L^3} \quad (4)$$

where, $W$ = weight of fish (g), $L$ = Length of fish (cm).

*2.5. Physicochemical analysis of treatment water*

The physicochemical parameters of the various treatment water samples, including pH, Temperature, Conductivity, Total Dissolved Solids (TDS), and Dissolved Oxygen (DO), were measured throughout the study using standard methods (APHA, 2005).

### *2.6. Data analysis*

All the data were analyzed using the statistical package for social sciences (SPSS version 21). Data are presented as treatment means ± standard deviation of the mean (SD). Data were analysed by one-way Analysis of Variance (ANOVA) to test significance among exposure chemical and concentrations with significance at $P < 0.05$. Tukey's posthoc test was performed to compare the means of all treatments. Regression analysis was used to test for linear relationships between standard length (SL) and body weight (BW).

## 3.0. Results and Discussion

### *3.1. Concentration of atrazine in exposure tanks*

Throughout the experiment, the concentration of atrazine in the exposure tanks remained relatively stable (Table 1). Mean atrazine concentrations in tank water were <MDL, 2.50 ± 0.13, 25.08 ± 1.82, 250.81 ± 2.45, and 500.14 ± 4.57 in the control, $AT_1$, $AT_2$, $AT_3$, and $AT_4$ groups, respectively.

**Table 1:** Atrazine concentrations in water ($gL^{-1}$) in *Clarias gariepinus* exposure tanks. The mean and standard deviation of atrazine ELISA determinations from each exposure tank ($n$ = 12) are presented

| Water treatment ($\mu gL^{-1}$) | Exposure Days | | | | | |
|---|---|---|---|---|---|---|
| | Day 0 | Day 7 | Day 14 | Day 21 | Day 28 | Mean Conc. |
| Control | <MDL | <MDL | <MDL | <MDL | <MDL | <MDL |
| $AT_1$ | 2.60 ± 0.13 | 2.49 ± 0.12 | 2.47 ± 0.08 | 2.46 ± 0.11 | 2.50 ± 0.13 | 2.50 ± 0.13 |
| $AT_2$ | 25.64± 1.61 | 24.91 ± 1.28 | 24.53 ± 1.50 | 25.02 ± 2.32 | 25.30 ± 2.41 | 25.08 ± 1.82 |
| $AT_3$ | 251.70 ± 1.90 | 250.02 ± 2.02 | 250.15 ± 2.41 | 251.03 ± 3.11 | 251.15 ± 2.81 | 250.81 ± 2.45 |
| $AT_4$ | 499.81± 3.12 | 500.53 ± 4.33 | 498.55 ± 4.80 | 501.22 ± 4.11 | 500.59 ± 6.48 | 500.14 ± 4.57 |

*MDL: The method detection limit.

### *3.2. Behavioural performance of juveniles*

Sub-lethal atrazine exposure of *Clarias gariepinus* juveniles resulted in different responses and tolerance to different atrazine treatment concentrations (Table 2). Anomalies observed included erratic swimming, clinging to the water surface, loss of equilibrium or balance, lethargy, and discolouration. The behavioural responses were found to be concentration-dependent, with increasing concentration resulting in the intensity of the behavioural responses. The bioassay results revealed that exposed juveniles showed signs of stress, such as slow and uncoordinated movement. Abnormalities increased as atrazine concentrations increased. Our findings are similar to the report of Marzouk *et al*. (2012) on female *Clarias gariepinus*. They observed that the effects of both acute and chronic exposures revealed clinical abnormalities which were manifested by loss of appetite, sluggish or restlessness, rapid opercular movements and abnormal skin pigmentation in the form of faded skin. Xing et al. (2012b) reported an abnormal response on behaviour and feeding. The authors reported that fish exposed to atrazine at 428 $\mu gL^{-1}$ showed abnormal behaviour, including decreased intake of food, slower swimming speed, and unresponsiveness to outside stimuli. In the present study, increase in the respiratory movements was observed during entire period of the bioassay, while fishes became inactive and almost non-motile with clinical signs of fading of body colour, erosion of scales, lesions, and hemorrhagic patches all over the body especially on the ventral side. Similar changes were observed by Elias *et al*. (2018). They reported several distinct unusual swimming behaviour and increased deformities in fish exposed to sub-lethal concentration of thiobencarb. These behaviours include lack of balance, agitated or jerky swimming, air gulping, sudden quick movement, and excessive secretion of mucus. Moreover, the colour of fish skin was changed from normal darkly pigmentation in the dorsal and lateral parts to very light pigmentation in the dorsal and lateral part, as well as peeling of the skin was observed. Hyperactivity in *C. gariepinus* exposed to atrazine was reported by Mekkawy *et al*. (2013), which was characterized by rapid and irregular swimming or darting, partial loss of equilibrium, rapid pectoral fins and opercular movements, reduction in feeding activity. A possible explanation for this, as well as other unusual behaviours, is likely a nervous system failure caused by pesticide poisoning, which affects physiological and biochemical activities.

**Table 2:** Behavioural observations of *Clarias gariepinus* juveniles after 28day exposure to varying concentrations of atrazine

| Behaviour | Control | $AT_1$ | $AT_2$ | $AT_3$ | $AT_4$ |
|---|---|---|---|---|---|
| Erratic swimming | - | - | + | + | + |
| Loss of Balance | - | + | + | ++ | +++ |
| Discolouration | - | + | + | +++ | +++ |
| Lethargy | - | + | + | ++ | +++ |
| Hanging on water Surface | - | + | ++ | ++ | +++ |

(+) indicates increasing response; (-) indicates no response

*3.2. Growth performance of Juveniles*

Atrazine was found to significantly affect the growth of the juveniles (Table 3). The total length and body weight showed significant decrease with increasing concentration of atrazine during the four weeks of exposure. At the end of two weeks of exposure, the standard length ranged from 15.02 to 16.01cm in the control group and 13.10 to 14.87cm in the 500µg$L^{-1}$ treatment group. Similar trend was observed in body weight which ranged from 32.75-32.99g in the control group and 22.62 to 22.67g in the 500µg$L^{-1}$ treatment group. The decrease in growth observed followed the same dose dependent pattern even in the last two weeks of exposure (Table 4). The final average specific growth rates (SGR) of control fish ranged from 4.45 to 4.50%/w in the first two weeks. Similarly, during the first 2 weeks of exposure, fish from all the treatment groups displayed significantly ($p<0.05$) lower SGR than in control groups (Table 4). Again, in the 2nd week of exposure, the SGR of all the atrazine-exposed fish further decreased with concentration toward the termination of the test while the values increased in the control. Results of the condition factor (*K*) of both control and treated groups are presented in Table 3. The results showed significant decrease in the values of *K* with increasing concentration of atrazine in a dose dependent pattern. The condition factor of the treatment groups significantly declined from the control (0.97±0.36) except for the 250µg$L^{-1}$ treatment group (0.95±0.39) in the first two weeks. After the first two weeks of exposure, the mean feed conversion ratio (FCR) in the control group was 0.07±0.02 while 0.21±0.09 was recorded for the highest treatment concentration, indicating a significant ($p<0.05$) increase in FCR with increasing concentration of atrazine. However, the next two weeks of continuous exposure did not reveal any pattern in the FCR (Table 4).

**Table 3:** Summary of growth performance of *C. gariepinus* juveniles exposed to varying concentrations of atrazine (Week 2)

| Parameters | Control | AT1 | AT2 | AT3 | AT4 | P-value | Significance |
|---|---|---|---|---|---|---|---|
| ISL (cm) | 14.26±0.39 | 14.26±0.39 | 14.26±0.39 | 14.26±0.39 | 14.26±0.39 | 1.000 | *p > 0.05* |
| FSL (cm) | 15.02±0.27 | 14.78±0.29 | 14.64±0.90 | 14.45±0.22 | 14.33±0.56 | 0.000 | *p < 0.05* |
| IW (g) | 17.57±1.95 | 17.57±1.95 | 17.57±1.95 | 17.57±1.95 | 17.57±1.95 | 1.000 | *p > 0.05* |
| FW (g) | 32.82±1.78 | 28.78±5.95 | 27.64±3.09 | 25.89±1.20 | 22.64±3.31 | 0.000 | *p < 0.05* |
| SGR (%/w) | 4.46±0.00 | 3.52±0.01 | 3.24±0.00 | 2.77±0.00 | 1.81±0.00 | 0.000 | *p < 0.05* |
| RGR (%/w) | 108.96±34.46 | 80.06±25.32 | 71.96±22.76 | 59.44±18.79 | 36.24±11.46 | 0.000 | *p < 0.05* |
| FCR | 0.07±0.02 | 0.09±0.04 | 0.10±0.04 | 0.13±0.05 | 0.21±0.09 | 0.000 | *p < 0.05* |
| K | 0.97±0.36 | 0.89±0.36 | 0.88±0.35 | 0.95±0.39 | 0.89±0.36 | 0.000 | *p < 0.05* |

Data are presented as mean ± SD. Different letters indicate significant differences between treatments. IL-Initial length; FL-Final length; IW-Initial weight; RGR-Relative growth rate; FCR-Feed conversion ratio; K-Condition factor. P-value of 1.000 indicates no significance

**Table 4:** Summary of growth performance of *C. gariepinus* juveniles exposed to varying concentrations of atrazine (Week 4)

| Parameters | Control | AT1 | AT2 | AT3 | AT4 | P-value | Significance |
|---|---|---|---|---|---|---|---|
| ISL (cm) | 15.02±0.27 | 14.78±0.29 | 14.64±0.90 | 14.45±0.22 | 14.33±0.56 | 0.000 | *p < 0.05* |
| FSL (cm) | 18.14±0.75 | 16.62±0.62 | 15.68±0.43 | 14.96±0.16 | 14.81±0.61 | 0.000 | *p < 0.05* |
| IW (g) | 32.82±1.78 | 28.78±5.95 | 27.64±3.09 | 25.89±1.20 | 22.64±3.31 | 0.000 | *p < 0.05* |
| FW (g) | 56.31±6.17 | 42.37±9.07 | 35.35±4.07 | 23.98±2.58 | 20.10±2.63 | 0.000 | *p < 0.05* |
| SGR (%/w) | 3.86±0.02 | 2.76±0.03 | 1.76±0.02 | -0.55±0.06 | -0.64±0.09 | 0.000 | *p < 0.05* |
| RGR (%/w) | 167.75±0.97 | 97.09±1.07 | 55.07±0.60 | -13.64±1.35 | -18.21±1.21 | 0.000 | *p < 0.05* |
| FCR | 0.04±0.02 | 0.07±0.02 | 0.14±0.06 | -0.55±0.22 | -0.41±0.17 | 0.000 | *p < 0.05* |
| K | 0.94±0.38 | 0.92±0.38 | 0.91±0.38 | 0.71±0.29 | 0.70±0.29 | 0.000 | *p < 0.05* |

Data are presented as mean ± SD. Different letters indicate significant differences between treatments. IL-Initial length; FL-Final length; IW-Initial weight; RGR-Relative growth rate; FCR-Feed conversion ratio; K-Condition factor

Several factors such as the difference in feed intake or the difference in the food metabolism (Lal *et al*., 2013) could explain the retardation observed in growth of the exposed fish. Another important factor that may be responsible for the reduction in growth rate could be the transformation into energy of a portion of nutrients from digestion of food consumed to cope with chemical stress as a result of exposure to atrazine. This may explain the observed increase in feed conversion ratio of exposed fish with increasing treatment concentration.

Toxicants inhibit fish growth, with the severity of this effect being dose dependent (Opute and Oboh, 2021). Toxicants can influence growth directly or indirectly by its effects on feeding because these processes are intertwined. Reduced physical activity can have an indirect effect on feeding and, as a consequence, growth. Fish, for example, appear to increase their metabolic activities toward toxicant excretion, thereby freeing up more energy for homeostatic maintenance rather than storing it for growth (Elias *et al*., 2018). Also, Lal *et al.* (2013) reported a significant decline in plasma levels of growth hormone (GH) and insulin-like growth factor (IGF-I) in malathion exposed Asian stinging catfish, *Heteropneutes fossilis*. They showed that this decline was related to reduction in fish growth, and also due to low food intake and influence of the pesticide on metabolization of feed into somatic growth. Similar findings of weight reduction have been reported in Australian catfish, *Tandanus tandanus* exposed to 2-10 $mgL^{-1}$ of chlorpyrifos (Huynh and Nugegoda, 2012). Heavy metal pollution has also been implicated with reduced growth rate caused by high metabolic cost (Xie *et al*., 2014). They reported that reduced feed conversion rate in marine organisms at sub-lethal levels of heavy metals might be due to the tissue burden of heavy metals, which in turn could cause increase in metabolic cost. The retarded growth observed in the exposed juveniles of *C. gariepinus* could be attributed to the inhibition of acetylcholinesterase as reported by Lecomte *et al*. (2018). Acetylcholinesterase is an enzyme normally responsible for inactivation of the neurotransmitter, acetylcholine, at synaptic and neuro-effector endings of cholinergic motor and secreto-motor neurons in the enteric nervous system. Inhibition of enzyme activity allows accumulation of acetylcholine leading to increased motor activity in the gastrointestinal tract caused by stimulation of smooth muscle M3 muscarinic receptors. The accumulated acetylcholine also acts at M1 and M3 muscarinic receptors to increase salivary, gastric, pancreatic, and intestinal secretions. Extensive inhibition of acetylcholinesterase leads to the secretion of large volumes of fluid and electrolytes into the lumen of the intestine, which results in profuse, watery diarrhoea (Haschek *et al.,* 2010). In this study, inhibition of acetylcholinesterase in exposed fish may have resulted to serious decline in the efficient use of the dietary proteins in fish feeds resulting in growth retardation.

The length-weight relationship (LWR) of the exposed juveniles was also estimated. The length-weight relationships for both control and atrazine exposed fish exhibited positive allometric growth and significant relationships as depicted by the value of $R^2$ (Coefficient of determination) with b values of 4.31, 5.14, 6.60 and 4.73 for control, $AT_1$, $AT_2$ and $AT_3$, respectively (Table 5). However, fish in tank $AT_4$ exhibited negative allometric growth with 'b' value of 0.95. This observation indicates that although atrazine had significant effect on the growth rate and condition factor, it however did not affect the pattern of growth. Length-weight relationships are commonly used in fisheries biology to convert length measurements into weight and to ascertain the growth characteristics related to those variables. On the other hand, length-weight relationships are also used for estimating fish condition factor and these values are used for comparing the condition (fatness or well-being) of fish (Jisr *et al*., 2018). The condition factor could reflect the physiological state of a fish, which is influenced by both intrinsic (gonadal development, organic reserves, presence or absence of food in the gut) and extrinsic (food availability, environmental variability) factors (Flura *et al*., 2015). The decrease in fish weight gain and specific growth rate observed with increasing atrazine concentrations in this study is attributed to energy being directed toward homeostatic processes and tissue damage repair to offset the toxicant's impact, rather than storage and growth.

**Table 5:** Final length-weight relationship of *C. gariepinus* juveniles exposed to varying concentrations of atrazine for 28days

| TANK | FAW (g) | FSGR (%/) | Logarithm Equation Log | 'R' | '$R^2$' | 'FAK' | 'b' |
|---|---|---|---|---|---|---|---|
| Cont. | 44.57±5.25 | 4.16±0.13 | Log W=Log -3.651 + 4.308 Log L | 0.9359 | 0.876 | 0.96 | 4.308 |
| $AT_1$ | 35.58±3.04 | 3.14±0.17 | Log W=Log -4.627 + 5.138 Log L | 0.9327 | 0.870 | 0.91 | 5.138 |
| $AT_2$ | 31.49±1.72 | 2.50±0.33 | Log W=Log -6.324 + 6.602 Log L | 0.9121 | 0.832 | 0.89 | 6.602 |
| $AT_3$ | 24.94±0.43 | 1.11±0.74 | Log W=Log -4.153 + 4.729 Log L | 0.5701 | 0.325 | 0.83 | 4.729 |
| $AT_4$ | 21.37±0.57 | 0.59±0.55 | Log W=Log 0.199 + 0.948 Log L | 0.1517 | 0.023 | 0.79 | 0.948 |

FAW-Final average weight; FSGR-Final average specific growth rate; R-Correlation coefficient; $R^2$- Coefficient of determination; FAK-Final average condition factor; b-Slope

## 4.0. Conclusion

This study found that exposing *Clarias gariepinus* juveniles to very low concentrations of atrazine interfered with their normal behaviour and growth performance. More energy was directed toward the detoxification process in exposed fish juveniles, resulting in a higher feed conversion ratio and less energy for growth. This suggests that atrazine exposure slowed the growth of *C. gariepinus*, particularly during the juvenile stage. Furthermore, given the detected effects of atrazine in *C. gariepinus* even at reduced concentrations, it is safe to conclude that the unregulated use of atrazine as a herbicide in Nigerian may result in increased atrazine accumulation in fish via aerosol or runoff, leaving a residue in aquatic animals. Pesticide usage regulation will promote food safety and public health across the country by proper legislation, routine pesticide monitoring of fish and fish products, and corrective steps to decrease residue occurrence with suitable sanctions for noncompliance.

## References

APHA (2005). Standard methods for the examination of water and wastewater, 21st edition. American Public Health Association, Washington, DC.

Ashe, M. O. (2019). International Agencies and the Quest for Food Security in Nigeria, 1970-2015. *Journal of Conflict and Social Transformation*. Special issue, pp. 251-274

Elias, N.S., Abouelghar, G.E., Sobhy, H.M., El Miniawy, H.M. and Elsaiedy E.G. (2018). Sublethal effects of the herbicide thiobencarb on fecundity, histopathological and biochemical changes in the African catfish (*Clarias gariepinus*). *Iranian Journal of Fisheries Sciences*, 19(3), pp. 1589-1614.

Flura, Zaher, M., B.M. Rahman, S., Rahman, A., Alam, M. A. and Pramanik, M. H. (2015). Length-weight relationship and GSI of hilsa, *Tenualosa ilisha* (hamilton, 1822) fishes in Meghna river, Bangladesh. *International Journal of Natural and Social Sciences*, 2, pp. 82-88.

Haschek, W. M., Rousseaux, C. G. and Wallig, M.A. (2010). *Gastrointestinal tract. In Fundamentals of Toxicologic Pathology* (Haschek, W.M., Rousseaux, and C.G., Wallig, M.A., eds.), 2nd ed., pp. 163–96. Elsevier, London, UK.

Huynh, H.P.V. and Nugegoda, D. (2012). Effects of Chlorpyrifos exposure on growth and food utilization in Australian catfish, *Tandanus tandanus. Bulletin of Environmental Contamination and Toxicology*, 88, pp. 25–29.

Jimenez, J. J., Bernal, J. L., del Nozal, M. J. and Rivera, J. M. (1997). Determination of pesticide residues in water from small loughs by solid-phase extraction and combined use of gas chromatography with electron capture and nitrogen–phosphorous detection and high-performance liquid chromatography with diode array detection. *The Journal of Chromatography A*, 778, pp. 289–30.

Jisr, N., Younes, G., Sukhn, C. and El-Dakdouki, M. H. (2018). Length-weight relationships and relative condition factor of fish inhabiting the marine area of the Eastern Mediterranean city, Tripoli-Lebanon. *Egyptian Journal of Aquatic Research*, 44, pp. 299–305.

Kankara, A. I. (2013). Examining Environmental Policies and Laws in Nigeria. *International Journal of Environmental Engineering and Management*, 4(3), pp. 165-170.

Lal, B., Sarang, M. K. and Kumar, P. (2013). Malathion exposure induces the endocrine disruption and growth retardation in the catfish, *Clarias batrachus* (Linn). *General and Comparative Endocrinology*, 181, pp. 139–145.

Lecomte, M., Bertolus, C., Ramanantsoa, N., Saurini, F., Callebert, J., Namaud-Beaufort, C. S., *et al*. (2018). Acetylcholine Modulates the Hormones of the Growth Hormone/Insulin-like Growth Factor-1 Axis During Development in Mice. *Endocrinology*, 159(4), pp. 1844–1859.

Lushchaka, V. I., Matviishyna, T. M., Husaka, V. V., Storeyb, J. M. and Storey, K. B. (2018). Pesticide Toxicity: A Mechanistic Approach. *EXCLI Journal*, 17, pp. 1101-1136.

Marzouk, M. S., Kadry, S. M., Amer, A.M., Hanna, M.I., Azmy, I.H. and Hamed, H. S. (2012). Effect of Atrazine Exposure on Behavioral, Haematological and Biochemical Aspects of Female African Catfish (*Clarias gariepinus*). *Journal of Scientific Research in Science*, 29, pp. 110-130.

Mekkawy, I. A. A., Mahmoud, U. M. and Mohammed, R. H. (2013). Protective effects of tomato paste and Vitamin E on atrazine-induced hematological and biochemical characteristics of Clarias gariepinus (Bürchell, 1822). *Global Advanced Research Journal of Environmental Science and Toxicology*, 2(1), pp. 11- 21.

Okomoda, V. T., Tiamiyu, L. O. and Iortim, M. (2016): The effect of water renewal on growth of *Clarias gariepinus* fingerlings. *Croatian Journal of Fisheries*, 74, pp. 25-29.

Olatoye, I. O., Okocha, R. C., Oridupa, O. A., Nwishienyi, C. N., Tiamiyu, A. M. and Adedeji, O. B. (2021). Atrazine in fish feed and african catfish (*Clarias gariepinus*) from aquaculture farms in Southwestern Nigeria. *Heliyon*,7, e06076.

Opute, P. A. and Oboh, I. P. (2021). Effects of Sub-Lethal Atrazine Concentrations on Embryogenesis, Larval Survival and Growth of African catfish, *Clarias gariepinus* (Burchell, 1822). *Aquaculture Studies*, 21, pp. 143-152

Opute, P. A., Udoko, A. O., Oboh, I. P. and Mbajiorgu, F. E. (2021) Changes induced by atrazine in *Clarias gariepinus* provide insight into alterations in ovarian histoarchitecture and direct effects on oogenesis, *Journal of Environmental Science and Health, Part B*, 56 (1), pp. 30-40

Xie, Y., Hu, L., Du1, Z., Sun, X., Amombo, E., Fan, J., Fu, J. (2014). Effects of Cadmium Exposure on Growth and Metabolic Profile of Bermudagrass [*Cynodon dactylon* (L.) Pers.]. *PLoS ONE*, 9(12), e115279

Xing, H., Li, S., Wang, Z., Gao, X., Xu, S.,Wang, X. (2012b). Oxidative stress response and histopathological changes due to atrazine and chlorpyrifos exposure in common carp. *Pestic Biochem Physiol*, 103, pp. 74–80.

Zaya, R. M. (2011). Molecular, cellular and systemic effects of atrazine on the xenopus laevis tadpole. dissertations, Western Michigan University. 488. https://scholarworks.wmich.edu/dissertations/488

**Cite this article as:**
Opute P. A. and Oboh I. P. 2021. Exposure to Atrazine Impairs Behaviour and Growth Performance in African Catfish, *Clarias gariepinus* (Burchell, 1822) Juveniles. *Nigerian Journal of Environmental Sciences and Technology*, 5(1), pp. 165-172. https://doi.org/10.36263/nijest.2021.01.0263

Nigerian Journal of Environmental Sciences and Technology (NIJEST)

www.nijest.com

ISSN (Print): 2734-259X | ISSN (electronic): 2734-2603

Vol 5, No. 1 March 2021, pp 173 - 190

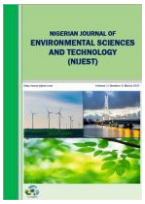

# Validating Gauge-based Spatial Surface Atmospheric Temperature Datasets for Upper Benue River Basin, Nigeria

Salaudeen A.[1,2,]*, Ismail A.[3], Adeogun B. K.[4] and Ajibike M. A.[5]

[1,3,4,5]Department of Water Resources and Environmental Engineering, Ahmadu Bello University Zaria, Nigeria

[2]Department of Civil Engineering, Abubakar Tafawa Balewa University, Bauchi, Nigeria

Corresponding Author: *asalaudeen@atbu.edu.ng

https://doi.org/10.36263/nijest.2021.01.0259

## ABSTRACT

*Like most other countries of Africa, one of the main problems threatening effective impact modelling in Nigeria including Upper Benue river basin, dwells in lack of high-quality in-situ observation datasets at appropriate spatiotemporal scales. Gridded meteorological variables can serve as promising alternatives to in-situ measurements in data sparse regions, but then, require validations to assess quantitatively their level of accuracies and reliabilities. As a consequence, this study makes comparative analysis of two gauge-based, spatially interpolated surface atmospheric temperature datasets with in-situ measurements in seven distinct meteorological stations covering the period of 1982-2006. Correspondingly, spatial analysis and statistical measures were used to assess the performances of the gridded datasets from the Climate Research Unit (CRU) and the Climate Prediction Centre (CPC). Results from spatial distributions depict 8, 11 and 10 °C as observed minimum temperatures and 33, 36, 42 °C as observed maximum temperatures over the Cameroon highland (Gembu), the Jos plateau and at the northern fringes of the basin respectively. Consequently, both the CRU and CPC datasets captured remarkably well the observed temperature gradients along the varying topography, though with differing margins. The interannual variabilities indicate CRU dataset to better capture the signs and magnitudes of the observed anomalies as compared to the CPC data. Moreover, the CRU data was noted to be more outstanding in representing the observed features in seasonal temperature variations over most stations. Also, the shapes of the probability density function (PDF) for both datasets in minimum and maximum temperatures measured closely the shapes of the observed PDF. Trend analysis suggests CRU datasets to better represent the warming and the cooling trends than the CPC. Overall, the CRU datasets are the most outstanding in this study and is therefore preferred for water resource application over the study area.*

**Keywords:** Assessment, Upper Benue river basin, temperature, CRU, CPC

## 1.0. Introduction

The variations of near-surface air temperature are influential on agriculture, hydrology, energy and ecosystems; as it is one of the key elements, which represent the state of the atmosphere (Adeniyi and Dilau, 2015; Chen *et al*., 2014). Thus, understanding the climate systems of a region and their impacts on the environment depends largely on accurate meteorological observations (Chen *et al*., 2014; Akinsanola and Ogunjobi, 2014). The significant input from Africa continent to the global climate system is well documented in literatures, yet, ground observation networks are non-existence in most remote areas (Hassan *et al*., 2020), where they are needed for analysis. Even where they exist, the datasets are usually characterized with gaps, limited and restricted accessibility and inadequate spatiotemporal continuity and distributions (Piyoosh and Ghosh, 2016). This is particularly true for most developing countries. This scenario is more poignant in Upper Benue river basin in the northeast of Nigeria, considering the few number of gauging stations for the entire basin. Nevertheless, advancement in computational technologies in recent decades has aided the availability of climate datasets in digital forms over the entire globe (Daly, 2006), which serve as key input data for computer models, particularly in water resource and environmental managements as well hydro-climatological impact assessments.

The climate datasets have however, witnessed heavy usage within the scientific community, most especially in data sparse regions. Though, the gridded datasets undergo rigorous quality control checks before interpolations. Anyway, errors in datasets are functions of spatial variability of the gauging stations. Therefore, river basins with insufficient meteorological stations and low spatial variability are prone to large interpolation errors (Tanarhte *et al*., 2012). This explains the sole reason why there is striking regional difference in the datasets, despite their correspondence in geographical distributions and temporal trends (Chen *et al*., 2014; Burton *et al*., 2018; Hassan *et al*., 2020). It is therefore imperative to validate them against ground reference observations, to ascertain their level of accuracies and reliabilities, to avoid drawing erroneous scientific conclusions and defective decisions, which may arise due to poor quality data.

Minimum and maximum temperatures and rainfall datasets are the most common meteorological variables provided by most of the world's meteorological organizations, owing to their dominant influence on hydrology, meteorology and agrometeorology. In any case, precipitation datasets have remained the most studied meteorological variable in recent literature, with less attentions being paid to validation of the temperature products. Consequently, this study presents the inter-comparison of the near-surface atmospheric temperature datasets (Collins, 2011) developed by the Climate Research Unit (CRU) at the University of East Anglia and the Climate Prediction Centre (CPC)-Global Unified Gauge-based Analysis with in-situ measurements to assess their skills in simulating changes in the present climate systems (Fu *et al*., 2013).

Of the three available gridded datasets namely, gauge-based observations, reanalysis datasets and satellite estimates; gauge-based observations provide relatively accurate and reliable measurements (Hassan *et al*., 2020). This premised on the fact that they are products of geospatial interpolation of ground-based measurements (Kanda *et al*., 2020). This accounts for the sole reason why it has been widely used recently, as the basis for drawing scientific conclusions and management decisions. Although the reanalysis products combine irregular measurements of climate data and models to produce a synthesized estimate with uniform spatial distribution and temporal continuity (Sun *et al*., 2018). They are however, widely used by scientists, but are considered non-observation data. The satellite estimates are well known for adequate spatiotemporal scales, but contain random errors and non-negligible biases (Kanda *et al*., 2020; Hassan *et al*., 2020). The fact that the land surface temperatures are derived from satellite estimates through retrieval algorithms from the measured radiant emitted from earth back into the space (Hooker *et al*., 2018; Kanda *et al*., 2020), exacerbates the uncertainties.

Nonetheless, gauge-based temperature datasets have been validated in recent literature to suggest probably the most credible datasets for a particular region. For example, Tang *et al*. (2010) inter-compare a number of temperature datasets over China for 100 years period including CRU. Findings from their study showed CRU to be in good concurrence with the Northern Hemisphere, Chinese and Global series. Tanarhte *et al*. (2012) evaluated the performances of global and regional precipitation and temperature datasets relative to ground observational data over the Middle East and Mediterranean, and remarked that the global temperature datasets including CRU and CPC have good skills in representing the observed pattern over all the sub-regions. In a similar study over Dehradun, India, Piyoosh and Ghosh (2016) noted good correlation between CRU temperature dataset and in-situ observations for different periods between 1901 and 2012. They further opined that the CRU captured well the trends of the observed pattern both in magnitude and direction. Also, Nashwan *et al*. (2019) examined the capabilities of three gauge-based observations including, CRU, CPC and Udel in replicating the observed temperature patterns for the purpose of developing high-resolution temperature datasets for the north central part of Egypt, and showed CPC-global to be most outstanding of all. However, Kanda *et al*. (2020) compared seven gridded climate datasets with ground observations over northwest Himalaya; they found out that interpolated temperature estimates better represent the observed pattern than their corresponding precipitation datasets over the mountainous region. The findings revealed CRU, ERA-I, PGF and Udel to outperform APHRODITE at all zones. Furthermore, Hassan *et al*. (2020) analysed the annual cycle of three gridded climate products such as; CRU, PGF and CFRS in terms of correlation and errors over Niger Delta region of Nigeria for the common period of 1980-2005. Findings from their study recommended CRU data for hydrological applications over the region owing to its least error and highest degree of correspondence with the ground reference observational data.

Studies on atmospheric temperature in Upper Benue river basin is very limited despite its importance, but over the larger Nigeria. Abatan *et al*. (2016) studied the trends in extreme daily temperatures (Tmin and Tmax) for 21 stations distributed over the whole Nigeria. Adebayo and Yahya (2015) assessed trends in mean monthly temperature in Savannah Sugar Plantation. Akinsanola and Ogunjobi (2014) investigated variabilities in temperature and precipitation using records from 25 synoptic stations over the whole country. Eludoyin *et al*. (2014) studied the changes in thermal conditions over the entire Country through temperature and relative humidity. Weli *et al*. (2017) carried out statistical analysis on minimum and maximum temperatures in Port Harcourt metropolis. Hassan *et al*. (2020) inter-compared basic meteorological dataset including minimum and maximum temperatures and precipitation in the Niger Delta with ground observational dataset for water resources management. The whole of these studies focused on trend analysis and variability, except Hassan *et al*. (2020) who evaluated the performances of the temperature data relative to ground observational dataset. However, the study domain lies in the Niger Delta region. It is therefore clear that despite the potentials of the Upper Benue river basin, studies to evaluate gridded temperature data in the basin does not exists, which create significant research vacuum to be filled. The focus of this study therefore dwells on validating gauge-based spatial interpolated atmospheric temperature dataset including; CRU and CPC-global for the common period of 1982 -2006 over Upper Benue river basin for possible water resource applications.

## 2.0. Methodology

### *2.1. The study area*

The Upper Benue river basin lies between the tropical rain forests of the southern Nigeria and the Savannah of the north, comprising of four states in the northeast including; Adamawa, Bauchi, Gombe and Taraba states as shown in Figure 1. Though, the basin cut across some other states, notably; the Jos plateau, Yobe and Borno states. It is one of the twelve River Basin Development Authorities (RBDA), with its administrative headquarters in Yola, Adamawa state; and at the same time the hydrological area 3 (HA-3) out of the eight designated hydrological areas in Nigeria. The basin encompasses an area of approximately 156,546 km$^2$. The Jos plateau, the Cameroon highlands and the Biu plateau, which form the western, the southern and the north-eastern boundaries, greatly influence the basin's micro-climate, owing to its varying topography.

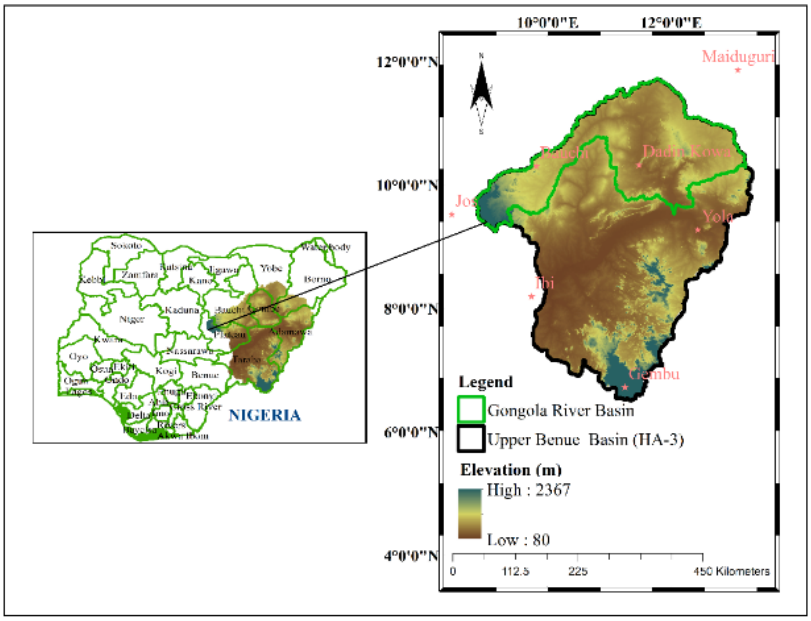


**Figure 1:** The study area

Three categories of climate are identified with the study area as; the northern Guinea savannah, the Sudan savannah and the montane or highland climates. The northern Guinea savannah extents from the Jos plateau to the southern region of the basin in Taraba state, and over an isolated portion of the Biu plateau. The central and the northern fringes of the basin exhibit Sudan savannah climate. Consequently, the montane climate is experienced over the Cameroun highlands (Eludoyin *et al*.,

2014), which lies at the southernmost part. Annual rainfall over the basin ranges from 700 mm to over 1800 mm (Federal Government of Nigeria, 2012), which contributes over 60.2 billion $m^3$ to the total annual flow of river Benue (Japan International Cooperation Agency (JICA), 2014). Essentially, through the two major river systems; the Gongola, which lies on the right arm of Benue; and the Donga, which is situated on the left arm. These two major tributaries are well known for the annual runoff volumes they contribute to the Benue. They are rated as the largest and the second largest from each arm respectively. The annual temperature of the basin is 26 °C, though it is lower on the plateaus (Federal Government of Nigeria, 2012). The dry season extents from December to March which is usually dry, with prevailing harmattan winds. The dwellers rely mainly on rain-fed agriculture. Thus, agro as well as hydroclimatic studies for the region are crucial for sustainable agriculture and water resource managements. In spite of these potentials, spatiotemporal distribution and continuity of in-situ observational datasets is limited; and therefore, appeal for alternative sources of accurate and reliable datasets, which can only be obtained through proper validations.

### *2.2. Datasets*

The monthly minimum and maximum near-surface air temperature datasets consisting of seven stations in and around Upper Benue river basin with 24 years records, covering the period of 1982-2006, were procured from the Nigerian Meteorological Agency (NiMET), Abuja; although, the datasets of Dadin Kowa, Gembu and Yola were obtained from the archive of the Upper Benue River Basin Development Authority (UBRBDA), Yola. These serve as reference observations for the evaluations. The geographical distributions of these stations are sparse and uneven over the basin (Figure 1), owing to the few number of stations maintained by the agency in each state; although, meteorological data are measured by some other organisations e.g. UBRBDA and some higher institutions of learning. However, the datasets are in most cases characterised with gaps, which often render them unsuitable for hydro-climatological impact assessments. Nonetheless, the stations are sited at key locations over the basin, where measurements are most critical.

The Climate Research Unit (CRU TS3.10) datasets were developed at the University of East Anglia, with major contribution from World Meteorological Organization. The data derived its sources mainly from the Global Historical Climatology Network (GHCN-v2), monthly climate bulletin (CLIMAT) (Tanarhte *et al*., 2012), Monthly Climate Data for the World (MCDW) and World Weather Records (WWR) consisting of over 4000 stations globally (Akinsanola *et al*., 2016). They consist of gridded climatological variables (Tmin, Tmax and prec) at 0.5° spatial resolutions at monthly scales covering the entire global land surface from 1901-2014 (Harris *et al*., 2014; New *et al*., 2000). However, the daily datasets of the CRU are available globally for the period 1970-2006, downloadable from www.2w2e.com (Vaghefi *et al*., 2017). The dataset underwent stringent quality control checks through an automated method (New *et al*., 2000). Anomalies are interpolated rather than the absolute values of the data, which consequently produces high-quality estimates, with fewer biases (New *et al*., 1999; Tanarhte *et al*., 2012). In any case, errors in datasets are functions of spatial variability of the gauging station. Incidentally, regions with poor station coverage and high spatial variability are prone to large interpolation errors (Tanarhte *et al*., 2012), which are noted to be prevalent in cold, dry and mountainous areas. Nonetheless, temperature data produce estimates with better quality than their corresponding precipitation datasets. The summary of the gridded datasets are shown in Table 1.

**Table 1:** Summary of selected global, spatially interpolated datasets

| Dataset & Source | Product | Spatial Resolution | Geographical Coverage | Temporal Resolution/Coverage | Reference |
|---|---|---|---|---|---|
| Climate Research Unit (CRU) at the University of East Anglia | CRU TS 3.10 | $0.5^0$ x $0.5^0$ | Global land | Daily (1970-2006) | (Vaghefi *et al*., 2017) |
| Climate Prediction Centre (CPC)-Global unified gauge-based analysis of daily minimum and maximum temperature | CPC-Global | $0.5^0$ x $0.5^0$ | Global land | Daily (1979-Present) | (NOAA/OAR/ESRL PSL) |

The Climate Prediction Centre gauge-based analysis of global daily minimum and maximum temperature and precipitation product was initiated by the National Oceanic and Atmospheric Administration (NOAA) Climate Prediction Centre. The product is freely available on 0.5° latitude/longitude grids over the entire global land areas from 1979-present. The mandate is to construct a set of unified climate datasets with improved quality and inter-product consistency to suite a wide range of applications. In formulating the CPC-Global datasets, gauge reports from over 30,000 stations worldwide including Global Telecommunication System (GTS), Cooperative Observer Network (COOP) and other national and international agencies, consisting of in-situ measurements and satellite estimates were utilised (NOAA/OAR/ESRL PSL).

*2.3 Methods*

The minimum and maximum air temperature climatology of two spatially interpolated datasets including CRU and CPC were evaluated in this study relative to observed meteorological measurements for 24 years period, covering 1982-2006 over the study domain. The study quantifies the degree of pattern correspondence between the gridded datasets and ground reference observations through temporal and geographical distributions and various parametric and nonparametric statistical indices. They include: Probability density function (PDF) overlap, annual long-term temperature anomaly, t', Mann-Kendall test, MK, correlation coefficient, r, refined index of agreement ($d_{ref}$), mean absolute error, MAE, and mean bias error, MBE.

The temporal distributions of the minimum and maximum temperature examine the annual cycle of monthly climatology in all the stations. While, the geographical distributions compare each of the gridded minimum and maximum temperature data over the entire basin with ground observations using spatial description. The PDFs for the gridded observations and in-situ measurements were computed for monthly minimum and maximum temperature in all the seven stations to determine the probability of occurrence of any given data as demonstrated by (Perkins *et al*., 2007) through MATLAB distribution fitting. The PDF has been widely used by earlier researchers to compare between two climate datasets e.g. Maxino *et al*. (2008), Anandhi *et al*. (2019) and Kabela and Carbone (2015). To quantify the area of overlap, which may reveal the degree of correspondence of the two datasets, Perkins *et al*. (2007) proposed a metric known as Skill Score. This computes the cumulative minimum value of the two distributions of each binned value defined as:

$$S_{score} = \sum_{1}^{n} minimum(P_m, P_o) \quad (1)$$

where $P_m$ and $P_o$ are the modelled and observed probabilities in a given bin, and n is the number of bins used in computing the PDF. Consequently, a bin size of 0.5° was chosen for both the minimum and maximum temperature for these assessments.

A comparison of the spatially interpolated and the ground observation datasets was done through long-term temperature anomaly, defined as:

$$T_a = \frac{T - \bar{T}}{\bar{T}} \quad (2)$$

where $T$ is the mean annual temperature of a given year and $\bar{T}$ is the long-term average temperature, with positive and negative anomalies indicating warmer and cooler conditions than the baseline period respectively.

Also, Mann-Kendall test [Eq. 3a-3d)] was employed to examine trends in monthly time series of the temperature datasets. This is a nonparametric statistic that has been used in earlier studies for trend analysis in climate time series data due to its robustness (Akinsanola *et al*., 2017; Abatan *et al*., 2016; Agyekum *et al*., 2018; Shiru *et al*., 2018; Jia *et al*., 2019; Mondal *et al*., 2018; Fu *et al*., 2013; Akande *et al*., 2017). The method was therefore utilized in this study to assess the trends and the magnitude of monthly time series data at 5 % significant level ($\alpha$). The test statistic $S_m$ is given as:

$$S_m = \sum_{i=1}^{n-1} \sum_{j=i+1}^{n} sign(x_j - x_i) \quad (3a)$$

where $x$ is the temperature variables and $n$ is the number of observations. If $x_j - x_i = \varphi$, it then follows that:

$$sign(\varphi) = \begin{cases} 1 & if\ \varphi > 1 \\ 0 & if\ \varphi = 0 \\ -1 & if\ \varphi < 1 \end{cases} \quad (3b)$$

The standardized $S_m$ is computed by equation of the form:

$$Z_{Sm} = \begin{cases} \dfrac{S_m - 1}{\sqrt{Var(S_m)}} & if\ S_m > 1 \\ 0 & if\ S_m = 0 \\ \dfrac{S_m + 1}{\sqrt{Var(S_m)}} & if\ S_m < 1 \end{cases} \quad (3c)$$

Reports have shown that for $n \geq 25$, the distribution of $S_m$ statistic is assumed to be normally distributed. This implies that the mean, $\mu_{sm} = 0$, and the variance is defined as:

$$Var(S_m) = \frac{n(n-1)(2n+5) - \sum_t t(t-1)(2t+5)}{18} \quad (3d)$$

$t$ is the number of ties.

Basically, the null hypothesis is rejected, should $Z_{Sm}$ yields result less or equal to the $p$-value.

In addition to the aforementioned, the correlation coefficient $r$ (Eq. 4a-4b) was applied to quantify the strength of association between the data distributions. This assesses the observed co-variation, and generally lies in the intervals, $-1 \leq r \leq 1$, where -1 shows negative association, +1 signifies positive relationship, and 0 means no relationship of any kind between the two datasets.

$$r = \frac{1}{n-1} \sum_{i=1}^{n} \left[ \left( \frac{X_m - \bar{X}_m}{\sigma_m} \right) \left( \frac{X_o - \bar{X}_o}{\sigma_o} \right) \right] \quad (4a)$$

$$\sigma_{m,o} = \sqrt{\frac{1}{n} \sum_{i=1}^{n} (X_{m,o} - \bar{X}_{m,o})^2} \quad (4b)$$

The refined index of agreement $(d_{ref})$ weights errors and differences, which in turn prevents exaggeration of squared values. It is given as (Willmott *et al*., 2012):

$$d_{ref} = \begin{cases} 1 - \dfrac{\sum_{i=1}^{n} |X_m - X_o|}{2 \sum_{i=1}^{n} |X_o - \bar{X}_o|}, when \\ \sum_{i=1}^{n} |X_m - X_o| \leq c \sum_{i=1}^{n} |X_o - \bar{X}_o| \\ \dfrac{\sum_{i=1}^{n} |X_m - X_o|}{2 \sum_{i=1}^{n} |X_o - \bar{X}_o|} - 1, when \\ \sum_{i=1}^{n} |X_m - X_o| > 2 \sum_{i=1}^{n} |X_o - \bar{X}_o| \end{cases} \quad (5)$$

Consequently, the commonly used error statistics such as; MAE (Eq. 6) and MBE (Eq. 7) were further utilized to quantitatively measure the errors between the observed and the gridded datasets. The MAE presents the magnitude of the mean difference between the measured and interpolated datasets, and varies between 0 and $+\infty$. In any case, 0 value signifies a better score. The MBE demonstrates the degree of under- or overestimation of a model from observed values. It ranges between $-\infty$ and $+\infty$, with 0 value representing a perfect score.

$$MAE = \frac{1}{n}\sum_{i=1}^{n}|X_o - X_m| \quad (6)$$

$$MBE = \frac{1}{n}\sum_{i=1}^{n}(X_m - X_o) \quad (7)$$

In Eqs. (4)-(7), $X_m$ and $X_o$ refer to modelled and observed data; $\bar{X}_m$ and $\bar{X}_o$ are the mean values of modelled and observed data; $\sigma_m$ and $\sigma_o$ define the standard deviation of the modelled and observed data; and n is number of observations.

In $d_{ref}$ the 95 % confidence interval of each index value was calculated through bootstrap approach as contained in (Pereira *et al*., 2018).

Finally, it is to be noted that the point-pixel comparison between the datasets were undertaken in this study to avert errors which may arise as a result of gridding of the observed data (Wang *et al*., 2019).

## 3.0. Results and Discussion

Two selected gridded, gauge-based, minimum and maximum temperature datasets namely; CRU and CPC are validated in this study relative to reference observation data for Upper Benue river basin between 1982 and 2006. These are presented on the annual and monthly timescales as the case may be.

### *3.1. Spatial distribution*

The spatial representations of the minimum annual minimum temperature and maximum annual maximum temperature for the 25 years period over Upper Benue river basin are shown in Figure 2 for the reference observational data, CRU and CPC. From the Figure (top row), it is clear that the observed minimum temperature is about 8°C over the Cameroon highland (Gembu),11°C over the Jos plateau and 10 °C at the northern fringes of the basin. Consequently, all the datasets captured remarkably well the observed temperature gradient along the varying topography, though with slight overestimation. However, in terms of magnitude, the CPC gives estimates which are closer to the observed values than the CRU dataset. It is to be noted that each of the two main seasons of the year vis-à-vis; dry and rainy seasons has its peculiar low temperatures, which are mainly controlled by (i) the dust-laden wind (the harmattan) driven by the tropical continental (cT) airmass from the Sahara Desert and, (ii) the tropical maritime (mT) airmass from the Atlantic Ocean which is associated with cloudiness and moist convection (Eludoyin *et al*., 2014; Abatan *et al*., 2016). While the high elevations of the eastern and north-central highlands are the driving factors for the low temperatures over the Mambila and the Jos plateaus, incidentally, the low temperature in the northern axis of the basin is induced by the harmattan wind, owing to its proximity to the Sahara Desert. Thus, this explains the sole reason why low temperature is recorded in this region.

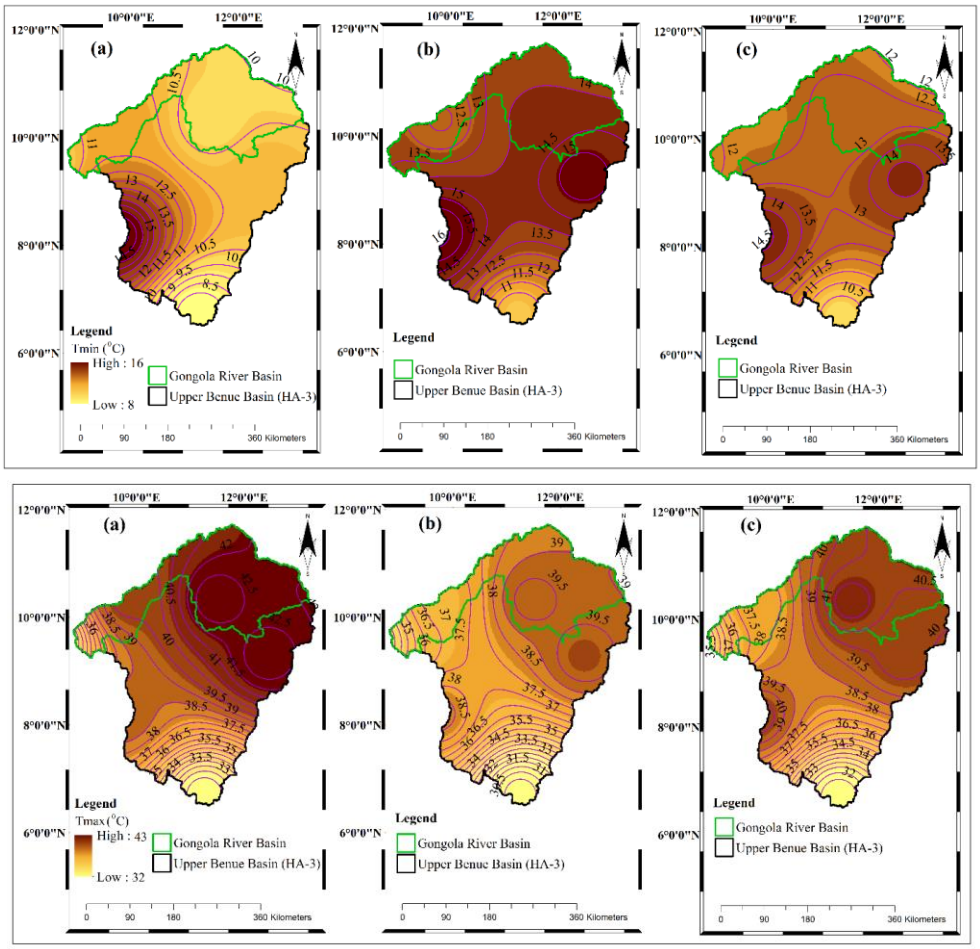


**Figure 2:** Geographical distribution of temporal temperature datasets covering the period of 1982-2006 with the top row illustrating the annual minimum temperature, and the bottom row representing the annual maximum temperature for (a) Observed (b) CRU and, (c) CPC.

The observed variations in the maximum annual maximum temperatures (Figure 2, bottom row) over the study domain show a general increasing trend from south to north with marked peak values of 33, 36 and 42 °C respectively over Gembu, the Jos plateau and the northern fringes of the basin. The gridded datasets have good representations of the observed trends, though with differing margins. However, the CPC dataset captured reasonably well the observed pattern than the CRU in this regard. The influence of inter-tropical discontinuity (ITD) on the microclimate of the basin is significant, as it controls the spatial variability of climate over Nigeria as a whole, and even the West African subregion. This is a region of trade-wind confluence which generates weak horizontal pressure gradients as a result of contact between the cT and mT with consequent, weak wind at the surface. Though, the Saharan heat-low (SHL) dominates the seasonal progression of air temperature over the study domain. In any case, the seasonal evolution of the ITD aligns with the seasonal cycle of the SHL. This accounts for high temperatures being experienced over this region, particularly, during the month of April, as a result of low humidity, occasioned by dry continental air mass associated with SHL.

### *3.2. Air temperature anomalies*

The inter-comparison of the anomalies of surface air temperature across the seven meteorological stations over the basin from 1982 to 2006 is shown in Figures 3 and 4 respectively. Figure 3 presents the anomalies for minimum temperature, while Figure 4 indicates the maximum temperature anomalies. Essentially, temperature anomaly measures the inter-annual variability in temperature and allows assessments of the magnitude of deviation of gridded datasets from the observation. Consequently, positive anomalies signify warmer conditions, while negative values depict cooler conditions. The observed anomalies in minimum temperature show increasing trends in all the stations except over Gembu where a decreasing trend was noticed. These conditions are well replicated by the gridded datasets, although, they failed to capture the unique cooling condition over

Mambila plateau. Interestingly, the gridded datasets represent well the exceptional cooling conditions of 1989 over all the stations, though, with varying magnitudes. Nevertheless, none of the datasets systematically performed best over all the stations. The CRU dataset has improved skill in representing the anomalies over Ibi, Jos and Maiduguri, while CPC dataset better reproduces the anomalies over Bauchi and Yola. In any case, the gridded datasets have worst performance records around Dadin Kowa and Mambila plateau.

The ability of the gridded datasets to skilfully replicate the inter-annual anomalies of the maximum temperature are evaluated similar to the minimum temperature as represented in Figure 4. Here, the CRU dataset better captures the signs and magnitudes of the observed anomalies as compared to the CPC dataset. However, the CPC data reproduces the cooling trends in maximum temperature over Mambila plateau to a very large extent. They signify a cooling trend in almost all the stations rather than the warming trend noticeable in the reference observation data, thus, this is alien to the warming trend reported in literature over West Africa including the Upper Benue river basin. It is therefore evident that CRU outperformed CPC in this regard and better represents the observed anomalies.

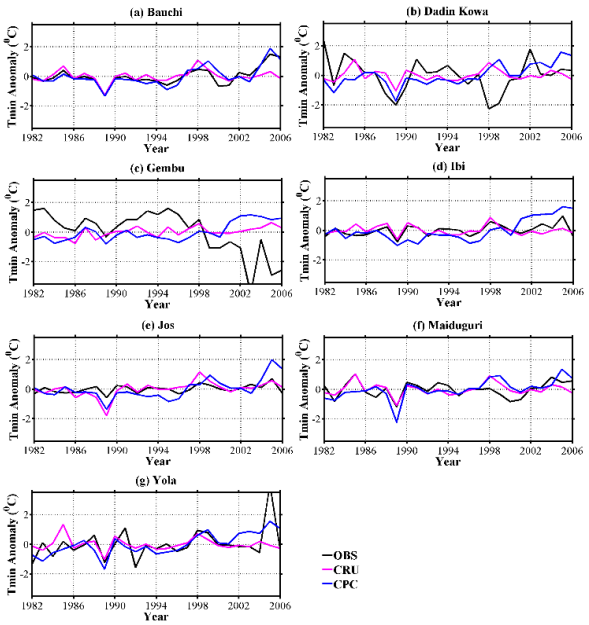


**Figure 3:** Interannual variability of minimum air temperature anomalies of the reference observation data and CRU and CPC datasets over UBRB between 1982 and 2006

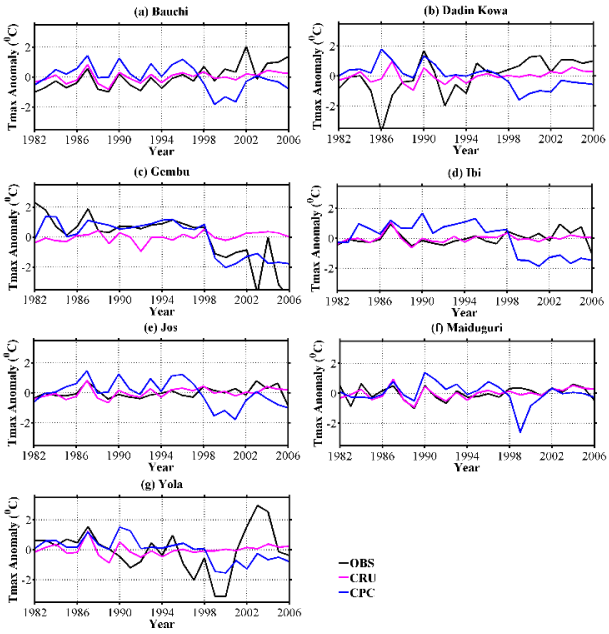


**Figure 4:** Interannual variability of maximum air temperature anomalies of the reference observation data and CRU and CPC datasets over UBRB between 1982 and 2006

*3.3. Mean monthly annual cycle of surface air temperature climatology*

The results of the evaluation of annual cycle of mean monthly climatology of air temperature are shown in Figures 5 and 6 respectively, covering a 25 years' period (1982-2006) over the study domain for in-situ measurements and gridded temperature datasets. This presents the capability of the gridded datasets to replicate the seasonal distribution and to demonstrate their skills in capturing the amplitudes and phases of the observed minimum and maximum temperatures. The variations in mean annual cycle of temperature exhibit a bimodal pattern with primary and secondary peak values occurring in the months of April and October respectively everywhere in the basin, except over Mambila plateau where the peak occurred much earlier in February due to early onset of rainy season. This is influenced by the montane climate identified with this region. Consequently, the month of August has a noticeable lowest day and night time temperature values. In any case, the maximum nocturnal temperatures (Figure 5) are 24 °C in Bauchi, 25 °C around Dadin Kowa, Ibi and Maiduguri, while Gembu and Jos have unique values of 16 and 18 °C respectively and 21 °C in Yola. The highest daytime temperature values (Figure 6) are observed to be in consonant with the night temperatures over the stations, thus, the temperature values at these stations are characterised by diurnal variation with maximum ranging from 28 to 42 °C.

These observed features in seasonal temperature variations everywhere in the basin are well replicated to a large extent by the gridded datasets, though with noticeable over- and underestimations. It is worthy of note that the gridded datasets grossly overestimate the observed pattern over Gembu and Yola which appear to be more in CPC dataset, suggesting CRU dataset to be more outstanding in this regard.

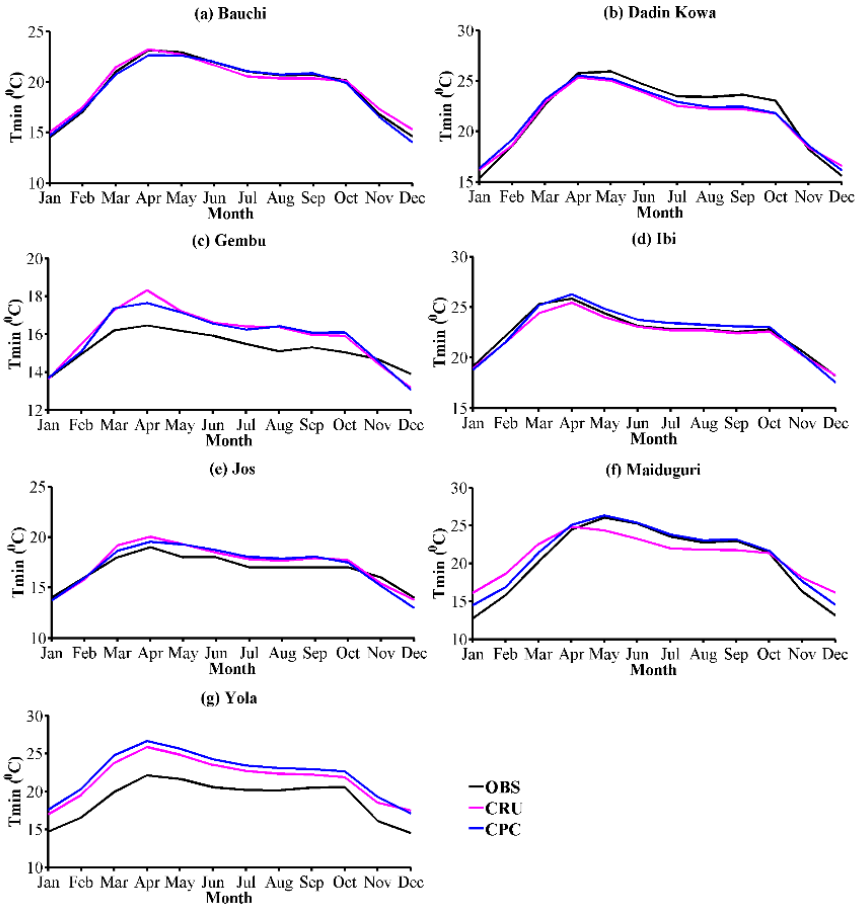


**Figure 5:** Mean monthly annual cycle of minimum temperature between 1982 and 2006

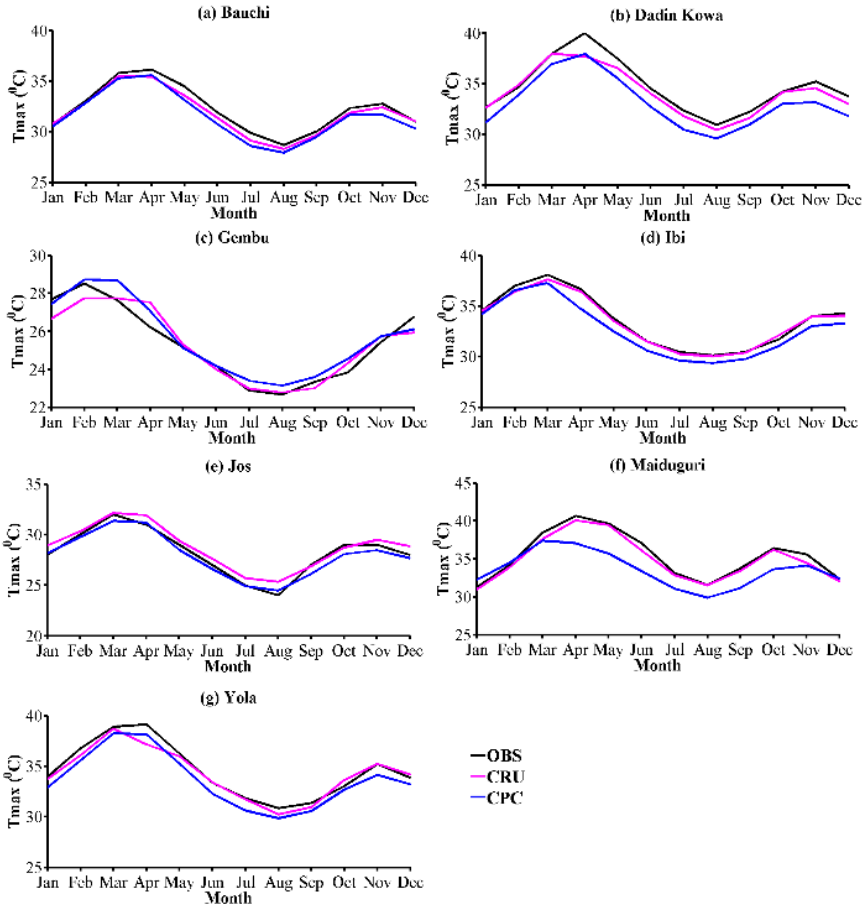


**Figure 6:** Mean monthly annual cycle of maximum temperature between 1982 and 2006

*3.4. Analysis of PDFs for minimum and maximum temperatures*

The capabilities of the spatially interpolated temperature datasets to measure closely the distributions of the observed minimum and maximum temperature data over the basin was evaluated using PDF metric along with Perkin's skill score. Figures 7 and 8 show comparison of observed and spatially interpolated PDFs for minimum and maximum temperatures respectively; while, Figures 9(a) and (b) indicate their corresponding PDF-based skill scores. The shapes of the gridded data's PDFs for both minimum and maximum temperatures measured closely the shape of the observed PDF, similar to the findings reported by Perkins *et al*. (2007), Fu *et al*. (2013), and Anandhi *et al*. (2019). Although, the deviations of the gridded datasets from observed data are substantial in Gembu and Yola for minimum temperature, but have improved skill in replicating the observed maximum temperature. The CPC PDFs closely match the observed PDFs over Bauchi and Maiduguri for minimum temperature, while the CRU produced the best replica over Bauchi, Ibi and Jos plateau for maximum temperature.

The skill score in Figure 9(a) and (b) reveal the strength and weakness of the gridded datasets in representing the observed PDFs. This generally varies from 0.6 to 0.9 for minimum temperature, while the range in maximum temperature is between 0.5 and 0.9. The results from the skill score agree with those obtained from the PDFs. Apparently, the CPC data skill scores are higher for minimum temperature, while the CRU shows better performance for maximum temperature. In any case, the CPC dataset is found to have best skill score and therefore appears to be most agreeable with the reference observational data, hence it is considered to be most outstanding in representing the distribution of the observed temperature over the entire study domain.

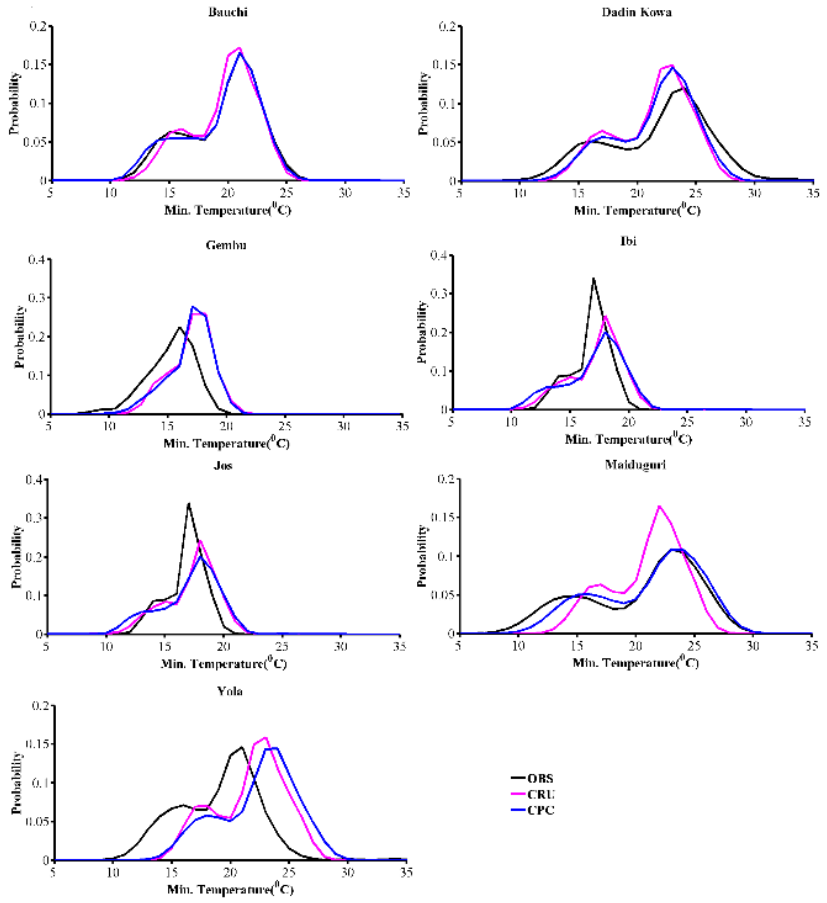


**Figure 7:** Probability density function for observed and gridded minimum temperature dataset

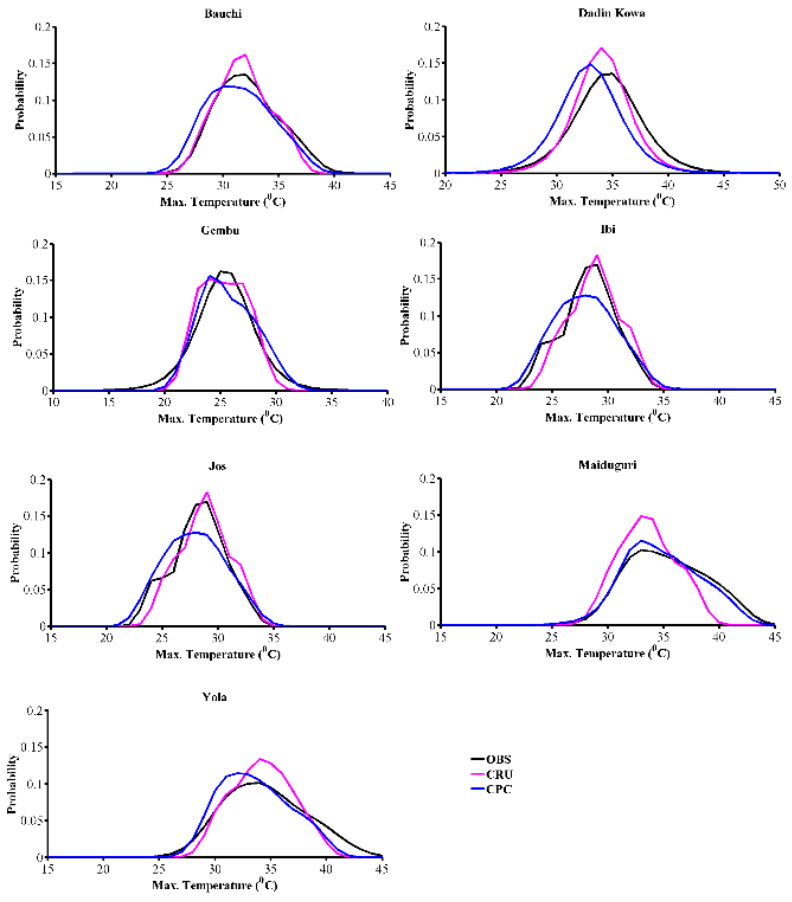


**Figure 8:** Probability density function for observed and gridded maximum temperature dataset

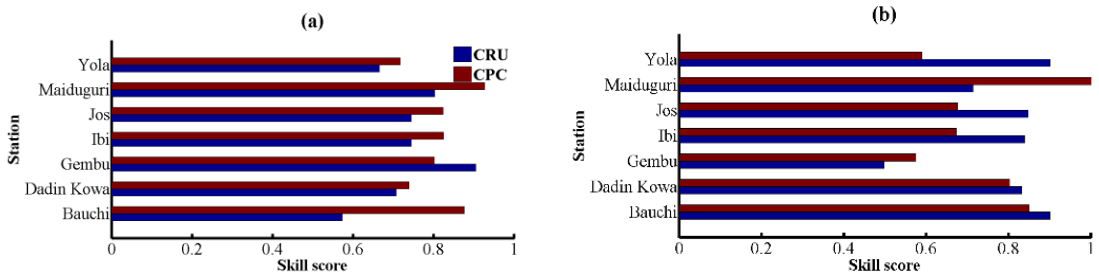


**Figure 9:** PDF- based skill score for (a) minimum temperature (b) maximum temperature

*3.5. Analysis of Statistical Indices*

In this section, the results from different statistical methods applied to the monthly minimum and maximum temperature are presented for the seven weather stations in Upper Benue river basin to further understand the performance of the gridded datasets. Figures 10 (a) and (b) present the MBE for the minimum and maximum temperature respectively; while the MAE are shown in Figures 11 (a) and (b) indicating the quantitative measure of the dataset. Likewise, the root mean square error, RMSE, coefficient of correlation, *r* and, refined index of agreement, $d_{ref}$ for the datasets are presented in Table 2 and 3. MBE indicates the degree of over- or under-prediction of observation; while MAE and RMSE are pointers to the overall performance of the gridded datasets; a high MAE signifies a poor replica of observation, while a low MAE depicts good performance. This is also true for RMSE. The *r* and $d_{ref}$ measure the degree of correspondence between the modelled and observed data. The use of $d_{ref}$ for the evaluation in conjunction with *r* was primarily to strengthen the outputs, since the results from $d_{ref}$ are not influenced by the presence of outliers in datasets. In the main, the two datasets are noted to have similar biases, though with varying magnitudes: positive bias for the minimum temperature, while the maximum temperature has negative bias, with exception of few stations. On the whole, the warm bias is most prevalent over Yola than other stations suggesting overestimation of the observed minimum temperature. The magnitudes are more in CPC than the CRU datasets. Conversely, the CRU dataset grossly underestimates the observed maximum temperature in Maiduguri station, but nevertheless, the underestimations are more in CPC dataset than in CRU, suggesting a better representation of the observed temperature values.

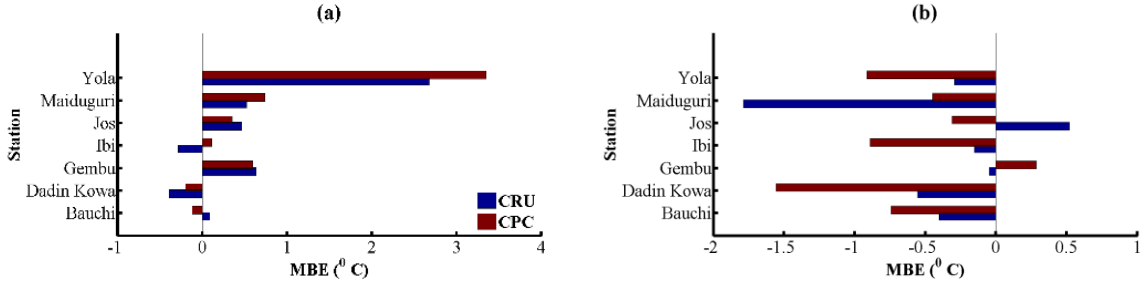


**Figure 10:** Mean bias error for (a) minimum temperature (b) maximum temperature

Further assessment using MAE and RSME indices demonstrate similar magnitudes of errors to those obtained from MBE between the reference ground observation dataset and the gauge-based data. Consequently, the CRU dataset records the lowest MAE and RMSE in most of the stations with the exceptions of Bauchi, Gembu and Maiduguri for both minimum and maximum temperature, though with narrow margins. However, Yola weather station depicts the highest MAE and RMSE and turnout to be the worst of all stations for both datasets. Nevertheless, the CRU dataset appears to be substantially better than the CPC owing its low error statistics.

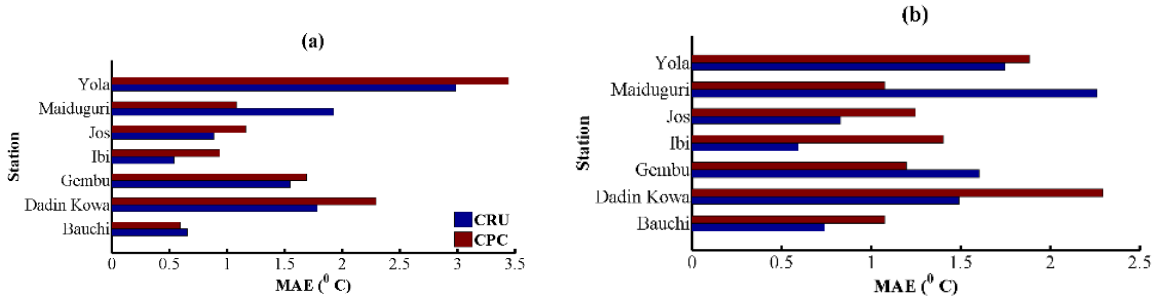


**Figure 11:** Mean absolute error for (a) minimum temperature (b) maximum temperature

The $d_{ref}$ proposed by Willmott *et al*. (2012) and demonstrated by Pereira *et al*. (2018) was used to test the level of agreement of the datasets relative to the reference observations over the study domain. The results obtained from the $d_{ref}$ are similar to those from *r*. However, the range of values obtained using $d_{ref}$ are generally lower but yet credible enough to reveal the accuracy of the datasets. For instance, the CRU and CPC datasets have *r* values that vary from 0.72 to 0.97 for minimum temperature, and 0.61 to 0.92 for maximum temperature. Correspondingly, the $d_{ref}$ generally range between 0.50 and 0.89 for the gridded datasets for both minimum and maximum temperatures. However, Yola station recorded exceptionally low $d_{ref}$ of 0.46 and 0.37 respectively for CRU and CPC. This range of values concurs with those obtained from *r* and therefore reveals the strengths of the temperature products across the basin. Based on level of agreement with the ground reference observations in terms of correspondence and low error value, CRU was found to be more reliable than CPC.

The ability of the monthly gridded temperature datasets to measure closely the observed trends was evaluated over Upper Benue river basin using Mann-Kendal rank statistics, $\tau$. These are shown in Tables 2 and 3 for the minimum and maximum temperatures respectively. During 1982-2006, the observed temperatures in the basin depict statistically significant and nonsignificant warming trends at 5 % significance level over the stations. Nevertheless, over a significant cooling trend were recorded for both minimum and maximum temperatures over Gembu. Separate reports indicating decreasing trend in temperature over the montane climate zones in Nigeria are substantially available in literature (e.g. Akinsanola and Ogunjobi, 2014; Abatan *et al*., 2016; Yusuf *et al*., 2017). However, Dadin Kowa and Yola stations show decreasing trends for minimum and maximum temperatures respectively. The warming trend is well replicated over most stations by the datasets. Nevertheless, CRU failed to capture the warming trend over Ibi, Maiduguri and Yola for minimum temperature; while, CPC lacks skill in depicting the warming trend over majority of the stations for maximum temperature. To a large extent, the degrees of warming and cooling trends are in some cases over- and under-predicted by the datasets. The findings on warming trend of temperature data over the study domain are well supported by earlier studies (e.g. Eludoyin *et al*., 2014; Abatan *et al*., 2016; Ilori and Ajayi, 2020) who separately reported statistically significant increasing trend in both minimum and maximum temperature over most part of Nigeria.

**Table 2:** Mann-Kendall rank statistic, τ, coefficient of correlation, r, refined index of agreement, $d_{ref}$ and, root mean square error, RMSE for minimum temperature (°C)

| Station | OBS | CRU | CPC | CRU | CPC | CRU | CPC | CRU | CPC |
|---|---|---|---|---|---|---|---|---|---|
| | τ | | | r | | $d_{ref}$ | | RMSE | |
| Bauchi | 0.220** | 0.073** | 0.233** | 0.959 | 0.964 | 0.874 | 0.886 | 0.917 | 0.858 |
| Dadin Kowa | -0.084** | 0.007** | 0.500 | 0.832 | 0.683 | 0.749 | 0.677 | 2.418 | 3.126 |
| Gembu | -0.450** | 0.387 | 0.433 | 0.721 | 0.774 | 0.517 | 0.621 | 2.213 | 2.450 |
| Ibi | 0.220** | -0.040** | 0.367** | 0.950 | 0.901 | 0.846 | 0.733 | 0.787 | 1.227 |
| Jos | 0.067** | 0.048** | 0.113 | 0.912 | 0.843 | 0.644 | 0.533 | 1.080 | 1.447 |
| Maiduguri | 0.007** | -0.017** | 0.064** | 0.920 | 0.969 | 0.765 | 0.868 | 2.313 | 1.417 |
| Yola | 0.070** | -0.023** | 0.121 | 0.746 | 0.719 | 0.458 | 0.374 | 3.506 | 3.991 |

** significant at 95 % confidence interval

**Table 3:** Mann-Kendall rank statistic, τ, coefficient of correlation, r, refined index of agreement, $d_{ref}$ and, root mean square error, RMSE for maximum temperature (°C)

| | OBS | CRU | CPC | CRU | CPC | CRU | CPC | CRU | CPC |
|---|---|---|---|---|---|---|---|---|---|
| Station | τ | | | r | | $d_{ref}$ | | RMSE | |
| Bauchi | 0.533 | 0.327 | -0.253** | 0.911 | 0.838 | 0.832 | 0.756 | 1.196 | 1.734 |
| Dadin Kowa | 0.487 | 0.360 | -0.507 | 0.809 | 0.710 | 0.703 | 0.544 | 1.976 | 2.810 |
| Gembu | -0.494 | 0.280** | -0.440 | 0.607 | 0.789 | 0.624 | 0.717 | 2.156 | 1.690 |
| Ibi | 0.019** | 0.004** | -0.176 | 0.961 | 0.840 | 0.466 | 0.707 | 0.784 | 1.840 |
| Jos | 0.019** | 0.037** | -0.107 | 0.919 | 0.804 | 0.777 | 0.665 | 1.052 | 1.603 |
| Maiduguri | 0.005** | 0.021** | -0.039** | 0.806 | 0.907 | 0.601 | 0.810 | 2.692 | 1.503 |
| Yola | -0.043** | 0.004** | -0.128 | 0.757 | 0.763 | 0.693 | 0.669 | 2.283 | 2.441 |

** significant at 95 % confidence interval

## 4.0. Conclusion

Adequate meteorological variables such as; temperature datasets needed for impact models are lacking over Upper Benue river basin due to inadequate spatiotemporal continuity and distributions of gauging stations as well as limited and restricted accessibility. Accordingly, we present in this study the inter-comparison of two global, gauge-based gridded temperature datasets (CRU, CPC) with ground-based reference observations to assess their skills in representing the present-day observed temperature climatology. Results from spatial distributions of both minimum and maximum temperatures show the gridded datasets to represent reasonably well the observed patterns. There are markedly low temperatures over the Jos plateau and the Cameroon highland in the western and southern peripheries of the basin due to high altitudes. Temperature increases exponentially as one move towards the northern fringes of the basin. However, an exceptionally low temperature around the northern axis during the harmattan period is well documented owing to its proximity to Sahara Desert. By the way, the CPC dataset showed improved skill in replicating these observed features.
The interannual variability in both minimum and maximum temperatures show positive anomalies, which signify warming trends in almost all the stations; except over Gembu, where a cooling trend was noticed. The gridded datasets measured closely these observed conditions. However, CRU datasets are noted to outperform the CPC data in this regard. Also, the annual cycle of mean monthly temperature exhibits a bimodal pattern, with primary and secondary peaks occurring in the months of April and October everywhere in the basin except over Gembu. In any case, the nocturnal temperature variations range from 13 to 25 °C, while the diurnal temperature varies between 23 and 42 °C. Overall, temperatures are lower over the Jos plateau and Cameroon highland with Maiduguri recording the highest maximum temperature. Interestingly, the gridded temperature products show good skills in capturing the observed amplitudes and phases, though with varying margins.

Results from PDF analysis reveal the shapes of the PDFs for the spatial interpolated datasets to capture remarkably well those of the observed PDFs everywhere in the basin, although, substantial difference exists over Gembu and Yola in minimum temperature. In any case, the dispersity was noted to be higher in CPC than in CRU dataset. These findings were further corroborated by Perkin's skill scores for the PDFs which indicate good performance of the gridded datasets in the range of 0.6 to 0.9 and 0.5 to 0.9 for minimum and maximum temperatures respectively.

Further assessments indicate CRU to be substantial in this study as compared to CPC owing to its lowest error magnitudes and higher degrees of pattern correspondence using statistical indicators as MAE, MBE, RMSE, *r* and $d_{ref}$. Also, results from Mann-Kendall statistics suggest significant warming trend for both minimum and maximum temperatures, except over the Cameroon highland where a significant cooling trend was obvious. The CRU datasets reproduced these observed trends with some degrees of accuracies, whereas CPC was dubious in replicating the observed warming trends for maximum temperature over the entire study domain. In spite of the improved performance of CRU over CPC in most stations, CPC was as well noted to outperform CRU in some stations. Based on improved performance of CRU datasets over the study site, it is therefore deemed suitable for impact models.

**Acknowledgements**

The financial support to the first author by the Federal Government of Nigeria through Tertiary Education Trust Fund for Academic Staff Training and Development is greatly acknowledged. The authors are grateful to the services that have operated the CRU and CPC.

**References**

Abatan, A.A., Abiodun, B.J., Lawal, K.A. and Gutowski, W.J. (2016). Trends in Extreme Temperature over Nigeria from Percentile-based Threshold Indices. *Int. J. Climatol.* 36(6), pp. 2527-2540.

Adebayo, A.A. and Yahya, A.S. (2015). Assessment of Climate Change in the Savannah Sugar Project Area, Adamawa State, Nigeria. *15th International Academic Conference*. Rome, pp. 19-28.

Adeniyi, M.O. and Dilau, K.A. (2015). Seasonal Prediction of Precipitation over Nigeria. *J. Sci. Tech (Ghana).* 35(1), pp. 103-113.

Agyekum, J., Annor, T., Lamptey, B., Quansah, E. and Agyeman, R.Y.K. (2018). Evaluation of CMIP5 Global Climate Models over the Volta Basin: Precipitation. *Adv Meteorol.* 2018, pp. 1-24.

Akande, A., Costa, A.C., Mateu, J. and Henriques, R. (2017). Geospatial Analysis of Extreme Weather Events in Nigeria (1985–2015) using Self-organizing Maps. *Adv. Meteorol.* 2017, pp. 1-11.

Akinsanola, A.A., Ajayi, V.O., Adejare, A.T., Adeyeri, O.E., Gbode, I.E., Ogunjobi, K.O., Nikulin, G. and Abolude, A.T. (2017). Evaluation of Rainfall Simulations over West Africa in Dynamically Downscaled CMIP5 Global Circulation Models. *Theor Appl Climatol.* 132(1-2), pp. 437-450.

Akinsanola, A.A. and Ogunjobi, K.O. (2014). Analysis of Rainfall and Temperature Variability Over Nigeria. *Global Journal of Human-Social Science: B Geography, Geo-Sciences, Environmental Disaster Management*, 13(3), pp. 1-19.

Akinsanola, A.A., Ogunjobi, K.O., Ajayi, V.O., Adefisan, E.A., Omotosho, J.A. and Sanogo, S. (2016). Comparison of Five Gridded Precipitation Products at Climatological Scales over West Africa. *Meteorol Atmos Phys.* 129(6), pp. 669-689.

Anandhi, A., Pierson, D.C. and Frei, A. (2019). Evaluation of Climate Model Performance for Water Supply Studies: Case Study for New York City. *J. Water Resour. Plann. Manage.* 145(8), pp. 3302-3311.

Burton, C., Rifai, S. and Malhi, Y. (2018). Inter-comparison and Assessment of Gridded Climate Products over Tropical Forests during the 2015/2016 El Nino. *Philos Trans R Soc Lond B Biol Sci.* 373(1760), pp. 1-10.

Chen, U.K.O.W., Chineke, C. and Nwofor, O. (2014). Comparative Analysis of Gridded Datasets and Gauge Measurements of Rainfall in the Niger Delta Region. *Res. J. Environ. Sci.* 88(7), pp. 373-390.

Collins, J.M. (2011). Temperature Variability over Africa. *J. Clim.* 24(14), pp. 3649-3666.

Daly, C. (2006). Guidelines for Assessing the Suitability of Spatial Climate Data sets. *Int. J. Climatol.* 26(6), pp. 707-721.

Eludoyin, O.M., Adelekan, I.O., Webster, R. and Eludoyin, A.O. (2014). Air Temperature, Relative Humidity, Climate Regionalization and Thermal Comfort of Nigeria. *Int. J. Climatol.* 34(6), pp. 2000-2018.

Federal Government of Nigeria (2012). Annual Abstract of Statistics. National Bureau of Statistics Abuja: www.nigerianstat.gov.ng.

Fu, G., Liu, Z., Charles, S.P., Xu, Z. and Yao, Z. (2013). A Score-based Method for Assessing the Performance of GCMs: A Case Study of Southeastern Australia. *J. Geophys. Res. Atmos.* 118(10), pp. 4154-4167.

Harris, I., Jones, P.D., Osborn, T.J. and Lister, D.H. (2014). Updated High-resolution Grids of Monthly Climatic Observations - the CRU TS3.10 Dataset. *Int. J. Climatol.* 34(3), pp. 623-642.

Hassan, I., Kalin, R.M., White, C.J. and Aladejana, J.A. (2020). Evaluation of Daily Gridded Meteorological Datasets over the Niger Delta Region of Nigeria and Implication to Water Resources Management. *Atmos Clim Sci.* 10(01), pp. 21-39.

Hooker, J., Duveiller, G. and Cescatti, A. (2018). A Global Dataset of Air Temperature Derived from Satellite Remote Sensing and Weather Stations. *Sci Data.* 5, pp. 1-11.

Ilori, O.W. and Ajayi, V.O. (2020). Change Detection and Trend Analysis of Future Temperature and Rainfall over West Africa. *Earth Syst. Environ.* 4(3), pp. 493-512.

Japan International Cooperation Agency (JICA) (2014). National Water Rresources Master Plan 2013. Federal Ministry of Water Resources (ed.) *Volume 4.* Abuja: Federal Government of Nigeria.

Jia, K., Ruan, Y., Yang, Y. and Zhang, C. (2019). Assessing the Performance of CMIP5 Global Climate Models for Simulating Future Precipitation Change in the Tibetan Plateau. *Water.* 11(9), pp. 1771.

Kabela, E.D. and Carbone, G.J. (2015). NARCCAP Model Skill and Bias for the Southeast United States. *Am. J. Clim. Change.* 04(01), pp. 94-114.

Kanda, N., Negi, H.S., Rishi, M.S. and Kumar, A. (2020). Performance of Various Gridded Temperature and Precipitation Datasets over Northwest Himalayan Region. *Environ. Res. Commun.* 2(8), pp. 1-20.

Maxino, C.C., Mcavaney, B.J., Pitman, A.J. and Perkins, S.E. (2008). Ranking the AR4 Climate Models over the Murray-Darling Basin using Simulated Maximum Temperature, Minimum Temperature and Precipitation. *Int. J. Climatol.* 28, pp. 1097–1112.

Mondal, A., Lakshmi, V. and Hashemi, H. (2018). Intercomparison of Trend Analysis of Multisatellite Monthly Precipitation Products and Gauge Measurements for River Basins of India. *J. Hydrol.* 565, pp. 779-790.

Nashwan, M.S., Shahid, S. and Chung, E.S. (2019). Development of High-resolution Daily Gridded Temperature Datasets for the Central North Region of Egypt. *Sci Data.* 6(1), pp. 1-13.

New, M., Hulme, M. and Jones, P. (1999). Representing Twentieth-Century Space–Time Climate Variability. Part I: Development of a 1961–90 Mean Monthly Terrestrial Climatology. *J. Clim.* . 12, pp. 829–856.

New, M., Hulme, M. and Jones, P. (2000). Representing Twentieth-Century Space–Time Climate Variability. Part II: Development of 1901–96 Monthly Grids of Terrestrial Surface Climate. *J. Clim.* 13, pp. 2217–2238.

NOAA/OAR/ESRL PSL CPC Global Unified Precipitation data. From their Website at https://PSL.NOAA.Gov/. Boulder, Colorado, USA.

Pereira, H.R., Meschiatti, M.C., Pires, R.C.D.M. and Blain, G.C. (2018). On the Performance of Three Indices of Agreement: An Easy-to-use R-code for Calculating the Willmott Indices. *Bragantia.* 77(2), pp. 394-403.

Perkins, S.E., Pitman, A.J., Holbrook, N.J. and Mcaneney, J. (2007). Evaluation of the AR4 Climate Models' Simulated Daily Maximum Temperature, Minimum Temperature, and Precipitation over Australia Using Probability Density Functions. *J. Clim.* 20, pp. 4356-4376.

Piyoosh, A.K. and Ghosh, S.K. (2016). A Comparative Assessment of Temperature Data from Different Sources for Dehradun, Uttarakhand, India. *J. Meteor. Res.* 30(6), pp. 1019–1032.

Shiru, M.S., Shahid, S., Alias, N. and Chung, E.-S. (2018). Trend Analysis of Droughts during Crop Growing Seasons of Nigeria. *Sustainability.* 10(871), pp. 1-13.

Sun, Q., Miao, C., Duan, Q., Ashouri, H., Sorooshian, S. and Hsu, K.-L. (2018). A Review of Global Precipitation Data Sets: Data Sources, Estimation, and Intercomparisons. *Rev Geophys.* 56, pp. 79-107.

Tanarhte, M., Hadjinicolaou, P. and Lelieveld, J. (2012). Intercomparison of temperature and precipitation data sets based on observations in the Mediterranean and the Middle East. *J. Geophy Res. Atmos.* 117(D12), pp. 1-24.

Tang, G., Ding, Y., Wang, S., Ren, G., Liu, H. and Zhang, L. (2010). Comparative Analysis of China Surface Air Temperature Series for the Past 100 Years. *Adv. Clim. Chang. Res.* 1(1), pp. 11-19.

Vaghefi, S.A., Abbaspour, N., Kamali, B. and Abbaspour, K.C. (2017). A Toolkit for Climate Change Analysis and Pattern Recognition for Extreme Weather Conditions-Case Study: California-Baja California Peninsula. *Environ. Model. Softw.* 96, pp. 181-198.

Wang, G., Zhang, X. and Zhang, S. (2019). Performance of Three Reanalysis Precipitation Datasets over the Qinling-Daba Mountains, Eastern Fringe of Tibetan Plateau, China. *Adv. Meteorol.* 2019, pp.1-16.

Weli, V.E., Nwagbara, M.O. and Ozabor, F. (2017). The Minimum and Maximum Temperature Forecast Using Statistical Downscaling Techniques for Port-Harcourt Metropolis, Nigeria. *Atmo. Clim. Sci.* 07(04), pp. 424-435.

Willmott, C.J., Robeson, S.M. and Matsuura, K. (2012). A Refined Index of Model Performance. *Int. J. Climatol.* 32(13), pp. 2088-2094.

Yusuf, N., Okoh, D., Musa, I., Adedoja, S. and Said, R. (2017). A Study of the Surface Air Temperature Variations in Nigeria. *Open Atmospheric Sci. J.* 11(1), pp. 54-70.

**Cite this article as:**
Salaudeen A., Ismail A., Adeogun B. K. and Ajibike M. A. 2021. Validating Gauge-based Spatial Surface Atmospheric Temperature Datasets for Upper Benue River Basin, Nigeria. *Nigerian Journal of Environmental Sciences and Technology*, 5(1), pp. 173-190. https://doi.org/10.36263/nijest.2021.01.0259

Nigerian Journal of Environmental Sciences and Technology (NIJEST)

www.nijest.com

ISSN (Print): 2734-259X | ISSN (electronic): 2734-2603

Vol 5, No. 1 March 2021, pp 191 - 196

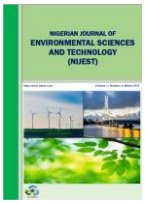

# Seismic Waves Response Characteristics of Niger Delta Soils

Okovido J. O.[1] and Kennedy C.[2]

[1,2]Department of Civil Engineering, University of Benin, Benin City, Nigeria

Corresponding Author: *johnokovido@uniben.edu

https://doi.org/10.36263/nijest.2021.01.0255

## ABSTRACT

*The study investigated the dynamic soil properties of States in Niger Delta region of Nigeria as a function of seismic activities. The down-hole seismic test was used to determine the response of the soils. The results of soil samples collected up to 30m depth, showed that the average young modulus increases with increase in depth, which ranged from 115.77±1.74 to 3231.17±1.01 kPa across the States. Also, shear wave velocity generally increases with increase in depth. The average shear wave velocity across the States ranged from 126.00±1.86 to 288.00±2.63m/s. Also, the average P-wave velocity increases with depth, with values across the States ranging from 310.60±3.51 to 656.00±3.69m/s. On the other hand, the void ratio was observed to be constant at certain range of depth, and in most with values across the States ranging from 0.651±.093 to 0.860±.067. Unlike void ratio, Poisson's ratio fluctuates with depth, with values across the States ranging from 0.23±2.27 to 0.36±1.18. Based on the results, the Niger Delta region may be resistant to earthquake, but as an oil hub of Nigeria, it is also susceptible to earthquake that could be triggered by stress due to heavy load and seismic activities.*

**Keywords:** Seismic activities, Soil dynamic response, Niger Delta region

## 1.0. Introduction

Globally, natural disasters have become a great challenge to humans. These disasters ranged from the failures of embankments, natural slopes, earth structures and foundations; and they have been attributed to the liquefaction of sands, landslides and slope instability (Ige *et al*., 2016). However, these natural disasters are a result of seismic effects and only occur in a geographical area with distinct characteristics. The geotechnical seismic response is a function of intense motion due to the stress-strain response of soils. The parameters of soil mechanical properties of damping ratio (D), shear modulus (G), shear wave velocity (Vs) and Poisson's ratio are those connected with dynamic loading.

The wave generated due to earthquakes developed vibrations in the ground and create severe natural disasters which are functions of regional seismicity, nature of the source of mechanism, geology, and local soil conditions. Seismic activities of a natural or induced earthquake or earth tremor, tsunami, flood, cyclone liquefaction, and landslide cause extensive damages to the environments, roads, buildings, bridges, ports, life-line, oil and gas infrastructures and loss of life. Earthquake or earth tremor is the trembling or shaking of the ground resulting from the unexpected or startling release of energy within the earth. Its activities result from accumulated stresses within the outer 700 Km shell of the earth (Osagie, 2008).

Historical and notable earthquakes or earth tremors in Nigeria were compiled and documented from journals, personal communications with the natives of the associated areas and newspapers written from 1933 - 2016. These developments in the nations' geological history bring to the question of age-long belief that Nigeria is seismically safe and not prone to earthquakes. The possible mechanisms for these intraplate tremors could be due to the regional stress created by the West African Craton (Adepelumi *et al*., 2008). In homogeneities and zones of weakness in the crust created by the various episodes of magmatic intrusions and other tectonic activities also were considered as sources of seismicity in Nigeria. Two assumptions and theories were considered as the possible basis of the seismicity in the country, the possible faults systems were inferred based on the spatial distribution of

the earth tremors in Yola- Dambata, Akka-Jushi, and Warri – Ijebu Remo systems (Afegbua, 2011). Most of these fault systems are trending northwest-southeast. The second was affirmed that earlier theory revealed that the tremors occurred in the inland extension of the northeast- southwest originating from the Atlantic Ocean and that possibly causes the activities along the Ijebu-Ode and Ibadan axis which is inferred to be associated with the Ifewara- Zungeru fracture systems (Adepelumi *et al*., 2008).

Some earth tremor reviewed and documented in Nigeria is of southern origin, (Osagie, 2008; Akpan and Yakubu, 2010). The areas which have experienced ground motion include Lagos, Ibadan and Ile-Ife on 22nd June 1939. On the same day, the event was recorded in Accra (Ananaba, 1991); Ijebu-Ode on 21st December, 1963 (Ajakaiye *et al*., 1987); Ibadan, Ijebu-Ode, Shagamu and Abeokuta on 28th July and 2nd August, 1984 (Ajakaiye *et al*., 1987); Ibadan and Ijebu-Ode on 27th June, 1990 (Ananaba, 1991; Ojo, 1995 and Osagie, 2008); Okitipupa in 1997 (Odeyemi, 2006), Okitipupa, Ibadan, Ijebu-Ode, Akure, Shagamu, Abeokuta and Oyo on 7th March, 2000 (Elueze, 2003; Odeyemi, 2006; Akpan and Yakubu, 2010). Tremors were also felt in other parts of the country, Gembu and Jalingo on 16th October 1982, Yola on 8th December 1984 and March 2005 (Akpan and Yakubu, 2010), Kombani Yaya in present-day Gombe State between 18th to 19th June 1985 (Ugodulunwa *et al.,* 1986; Ajakaiye *et al*., 1988). Dan Gulbi near Gusau in Zamfara State on November 7, 1994, witness some ground motion caused by an earthquake of local magnitude 4.2 (Akpan and Yakubu, 2010). Lupma near Minna in Niger State also experienced ground motion on 25th March 2006 (Akpan and Yakubu, 2010). Historical earthquakes or earth tremors in Nigeria were compiled from journals, personal communications with the natives of the associated areas and newspapers written from 1933 -2016. The intensities of these events ranged from III to VI based on the Modified Mercalli Intensity Scale. Therefore, this study investigates the dynamic soil properties of Niger Delta region of Nigeria as a function of seismic parameters.

## 2.0. Methodology

### *2.1. Sample location*

The soil samples were collected from four (4) States of the Niger Delta Region of Nigeria. The sampling locations are in Rivers State (Akinima and Mbiama Towns in Ahoada West Local Government, Ogbogu Town in Ogba/Egbema/Ndoni Local Government Area, Tombia Town in Degema Local Government Area and Bori Town in Khana Local Government Area; Bayelsa State (Igbogene and Agudama Towns in Yenagoa Local Government Area, Otuasega Town in Ogbia Local Government Area and Nembe Town in Nembe Local Government Area), Akwa-Ibom State (Ikot Abasi Town in Ikot Abasi Local Government Area, Ibagwa Town in Abak Local Government Area and Ibiaku Offot Town in Uyo Local Government Area) and Delta State (Aboh Town and Afor Ogbodigbo Town in Ndokwa East Local Government Area).

### *2.2. Soil sample collection*

All soil samples were collected by subsurface exploration activities at the sites which included drilling and deep boring by standard penetration test (SPT). In-situ field test and laboratory test were adopted in this research work. The tests were conducted to estimate the dynamic soil properties. The soil samples were dried, crushed and sieved on sieve No. 4 (4.75mm) with standard and known weights taken, mixed with amount water which represented natural water content state. Soil samples were remolded to field density and natural moisture content stage. Samples were prepared with specimen standard measurements of 20mm height and 70mm diameter, placed in membrane of rubber, mounted on bottom plate of cyclic direct simple shear machine of confined rings of control lateral deformation at consolidation stages.

### *2.3. Seismic bore-hole test*

This test enables characterization of lithologic and ground water flow conditions than cuttings, split spoon samples, or core samples alone in a more detailed manner. The borehole technique has an advantage in that it can describe subsurface conditions in greater detail than surface-based methods. By the cross-hole seismic (CS) measurements, the dynamic elastic moduli including shear modulus, Young's modulus, and Poisson's ratio can be determined. This is a field test in which bore holes are installed and instrumented to measure the wave propagation velocity.

The shear wave velocity and *p*-wave velocity were determined using the down-hole seismic **(**DS) test method, which uses a hammer source at the surface to impact a wood plank and then generate shear and compressing waves. This is typically accomplished by coupling a plank to the ground near the borehole and then impacting the plank in the vertical and horizontal directions. The energy from these impacts is then received by a pair of matching three component geophone receivers, which have been lowered in the down hole and are spaced at 1.5 m to 3 m apart.

## 3.0. Results and Discussion

The seismic down-hole dynamic soil properties of the various locations in Niger Delta region of Nigeria was studied based on young modulus, shear wave velocity, *p*-wave velocity, void ratio and Poisson's ratio.

### *3.1. Variation of Young modulus*

The Young modulus, as an important material property essential for the evaluation of soil dynamic response, was studied and compared across the five States of the Niger Delta region represented in Figure 1. Thus, the average young modulus increased with increase in the sampling depth. Though, the behavior of young modulus in sites located in Rivers State showed high fluctuating characteristics compared to sites in the other States. However, from analysis, the numerical values of the average young modulus obtained from sites located in Rivers State ranged from 156.96±2.18-3231.17±1.01 kPa, while others ranged from 118.17±3.37-2809.21±2.51 kPa for Bayelsa State, 119.81±1.13-2769.53±0.46 kPa for Akwa Ibom State and 115.77±1.74-2900.25±2.09 kPa for Delta State. Although, at initial and final soil depth of 30m, the values of young modulus recorded across the soil layers as depth increases was highest in Bayelsa State followed by Akwa-Ibom, Delta and Rivers State. Despite the variations, the average young modulus across the States is not significantly different. Therefore, it can be said that the soil dynamic response of States in the Niger Delta region of Nigeria, based on the young modulus analysis, are interwoven.

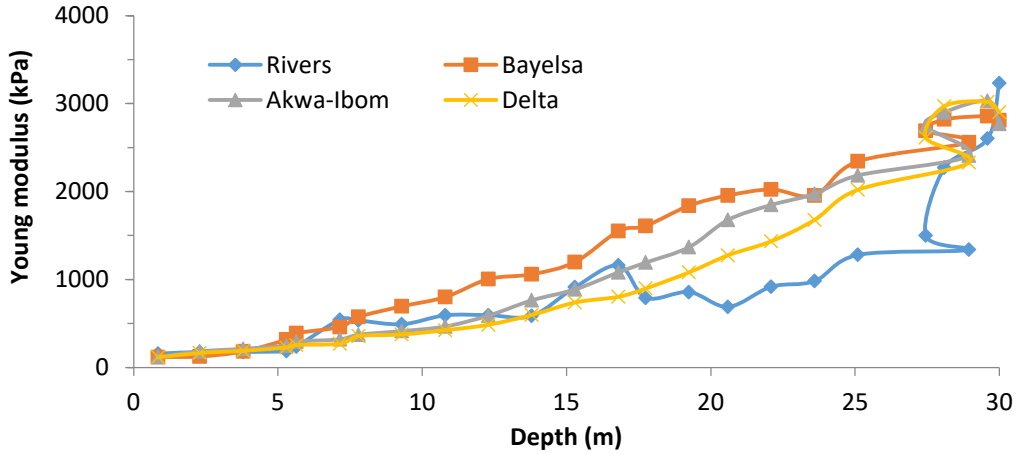


**Figure 1:** Variation of young modulus across the States

### *3.2. Variation of shear wave velocity*

Figure 2 shows the profiles of the variability in shear wave velocity in Niger Delta soils. This property is important for characterization of vibration effect that often resulted in earthquake or tremor. Although this situation, especially earthquake, has not been recorded in this region, but there is potential for its occurrence in the future due to the continuous exploitation of crude oil and gas. The determination of shear wave velocity in soil makes the measurement of soil stiffness easy to determine (Viggiani and Atkinson, 1995). Hence, the soils' analysis revealed that shear wave velocity generally increase with increase in soil depth. The average shear wave velocity results obtained from the sites across the State ranged from 128.30±1.78 to 288.00±2.63m/s, 130.00±0.56 to 253.67±1.09m/s, 136.67± to 264.00±3.01m/s and 126.00±1.86 to 275.00±1.42m/s Rivers, Bayelsa, Akwa Ibom and Delta States respectively. Again, the ranges of shear wave velocity recorded across the Niger Delta States show no much variation. Hence, the shear wave velocity results have further shown that the Niger Delta region of Nigeria shares a similar soil dynamic response.

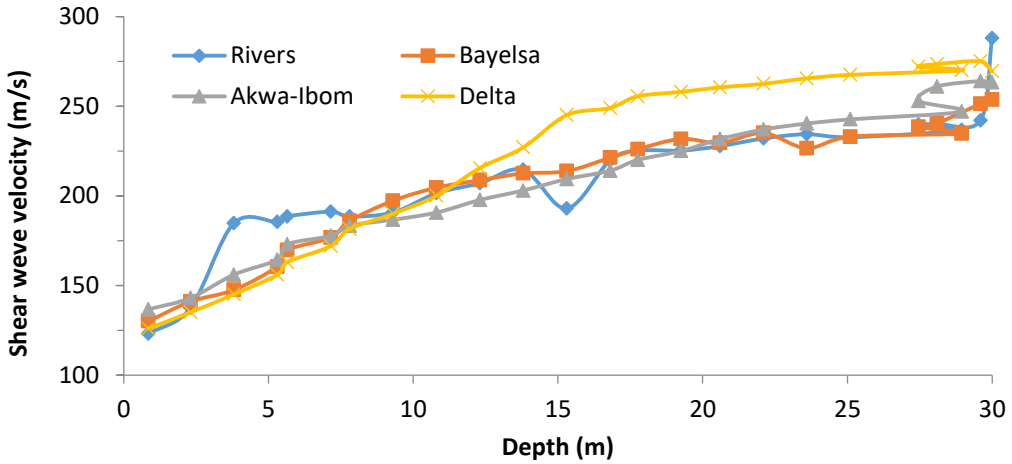


**Figure 2:** Variation of shear wave velocity across the States

*3.3. Variation of P-wave velocity*

Figure 3 showed the profiles of *p*-wave velocity investigated between 0.85 to 30m soil depth across site locations. Like the shear wave velocity, *p*-wave velocity generally increases with increase in soil depth in all the investigated sites. Meanwhile, the magnitude of *p*-wave velocity recorded is over twice the values of shear wave. However, as shown in Figure 3, the average *p*-wave velocity recorded in Delta is slightly higher than those obtained from other States, especially beyond 15 meters depth, with values ranging from 325.50±3.02-649.50±1.32m/s, while the average values of *p*-wave velocity recorded in the other States ranged from 310.60±3.51-595.00±0.77m/s, 327.25±2.10-579.25±3.04m/s and 345.67±2.11-656.00±3.69m/s respectively. Like shear wave velocity, the average *p*-wave velocity in the Niger Delta States is not significantly different.

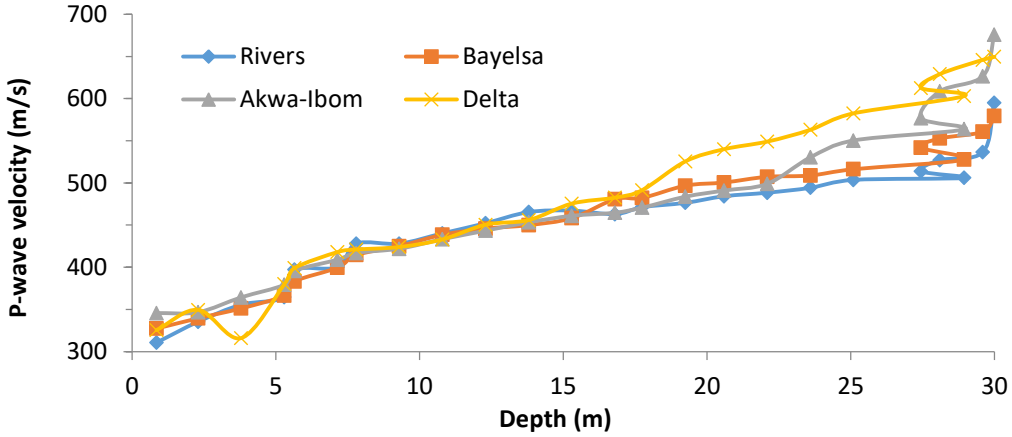


**Figure 3:** Variation of *p*-wave velocity across the States

*3.4. Variation of void ratio*

Figure 4 shows the profiles of the average void ratio of the respective States obtained across site locations. The void ratio was observed to be constant at certain range of depth in the soil strata, and in most cases, it does not increase correspondingly with depth. These circumstances arose due to soil characteristics, primarily due to particles size distribution across the soil strata. The ranges of average void ratio results obtained from the States are recorded as 0.672±1.001 - 0.860±.067, 0.651±0.093 - 0.751±0.115, 0.700±2.134 - 0.804±1.071 and 0.670±1.404 - 0.801±0.833 for Rivers, Bayelsa, Akwa-Ibom and Delta States respectively. Again, there is high proximity of void ratio values of soils in the different States, which at some sites, it cannot be vividly differentiated.

It has been established that larger void ratio may reduce the dynamic shear modulus and shear wave velocity of soil, and as well, the natural frequency (vibration) of soil due to earthquake load (Panuska and Frankovska, 2016; Munirwansyah *et al*., 2020). Therefore, it can be inferred from the range of void ratio recorded that Niger Delta soil may be resistant to earthquake.

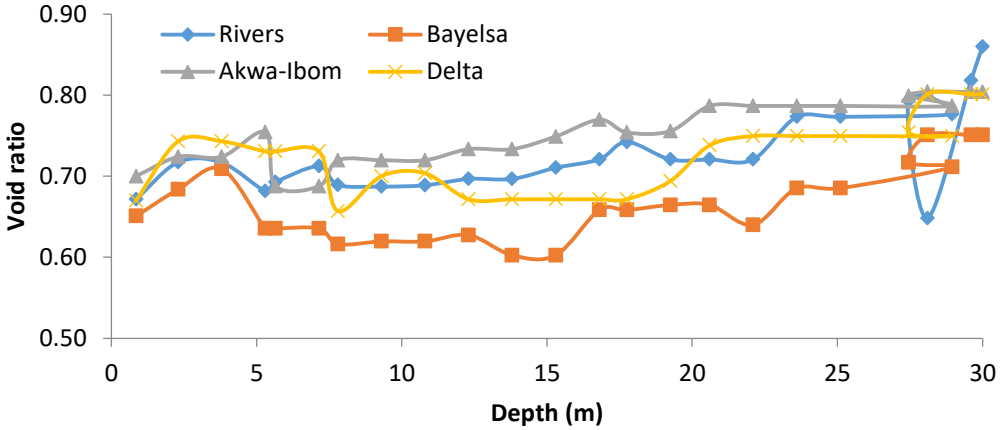


**Figure 4:** Variation of void ratio across the States

*3.5. Variation of Poisson's ratio*

Figure 5 showed the profiles of average Poisson's ratio obtained from the sites locations in the various States. Unlike void ratio, Poisson's ratio was observed to be highly fluctuating with depth. The fluctuations can be attributed to soil characteristics properties. From the figure, it can be seen that Bayelsa State recorded the least average Poisson's ratio, while it was relatively highest in Delta State at some soil depth. The average Poisson's ratio obtained from sites located across the States ranged from 0.25±1.04 - 0.35±2.09 for Rivers State, 0.23±2.27 - 0.33±1.14 for Bayelsa State, 0.27±0.92 - 0.35±2.20 for Akwa Ibom State, and 0.25±1.48 - 0.36±1.18 for Delta State.

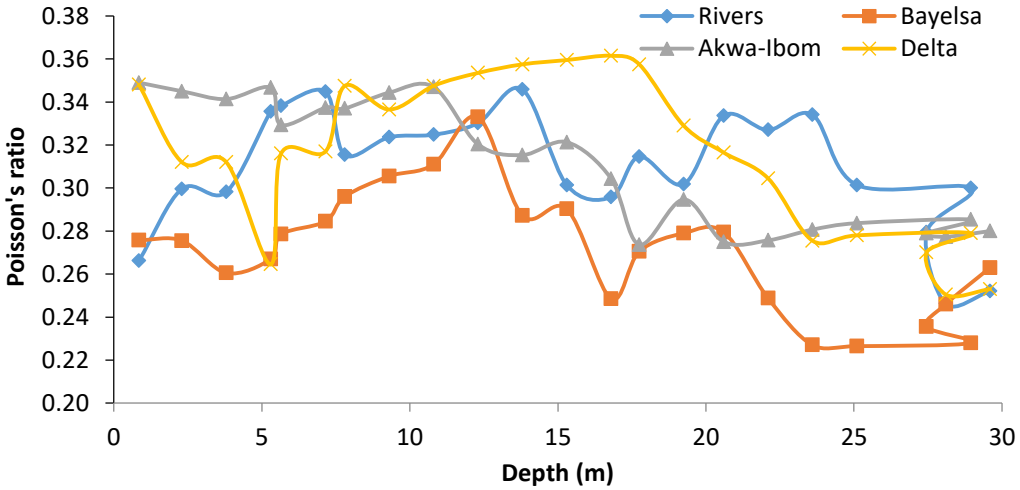


**Figure 5:** Variation of Poisson's ratio across the States

## 4.0. Conclusion

The seismic dynamic soil properties of the various sites across the States of Niger Delta region based on analysis of young modulus, shear wave velocity, *p*-wave velocity, void ratio and Poisson's ratio showed no significant different in the soil dynamic properties within the region. In addition, the young modulus, shear wave velocity and *p*-wave velocity, generally increased with soil depth, while the void ratio was constant at certain range in the soil layers. These circumstances were due to particles size distribution across the soil strata. Also, there was high fluctuation in Poisson's ratio as soil depth was increased. However, based on results of some of the dynamic soil properties, it can be concluded that the Niger Delta region may be resistant to earthquake, but as an oil hub of Nigeria, it is also susceptible to earthquake that could be triggered with time if over stressed by heavy load and seismic activities.

**References**

Adepelumi, A. A., Ako, B. D., Ajayi, T. R., Olorunfemi, A.O., Awoyemi, M. O. and Falebita, D. E. (2008). Integrated geophysical mapping of the Ifewara transcurrent fault system, Nigeria. *Journal of African Earth Sciences*, 52(4-5), pp. 161-166.

Ajakaiye, D. E., Daniyan, M. A., Ojo, S. B. and Onuoha, K. M. (1987). The July 28, 1984 southwestern Nigeria evolution of Nigeria. *Journal of Geodynamics*, 7, pp. 205-214.

Ajakaiye, D. E., Hall D. H., Millar, T. W., Verheijen, P. J., Awad, M. B. and Ojo, S. B. (1988). Aeromagnetic Anomalies Trough, Nigeria. *Nature*, 319, pp. 582-584.

Akpan, O. U. and Yakubu, A. Y. (2010). Earthquake Science, 23, pp. 289-294.

Ananaba, S. E. (1991). Dam sites and crustal mega lineaments in Nigeria. *ITC J.*, 1, pp. 26-29.

Elueze, A. A. (2003). Evaluation of the 7 March 2000 earth tremor in Ibadan area, southwestern Nigeria. *Jour. of Min. and Geol.*, 39(2), pp. 79-83.

Ige, O.O., Oyeleke, T. A., Baiyegunhi, C. and Oloniniyi, T. L. (2016). Liquefaction, Landslide and Slope Stability Analyses of Soils: A Case Study of Soils from Part of Kwara, Kogi and Anambra States of Nigeria, Natural Hazards Earth System Science Discussions. Available at: http://www.doi:10.5194/nhess-2016-297, July 24, 2018.

Munirwansyah, M., Munirwan, R.P., Listia, V., Munirwan H. and Melinda, Z. (2020). Void ratio effect on dynamic shear modulus and shear wave velocity for soil stiffness in Banda Aceh and Aceh Besar, *Journal of Physics: Conference Series*. Retrieved from: https://doi:10.1088/1742-6596/1572/1/012090

Odeyemi, I. B. (2006). The Ifewara fault in Southwestern Nigeria: Its relationship with fracture zones along the Nigerian Coast. Lecture delivered at the Centre for Geodesy and Geodynamics, Toro, Bauchi State. 13p.

Ojo, O. M. (1995). Survey of occurrences in Nigeria of natural and man-made hazards related to geological processes. In: Onuoha K M and Offodile M E (eds.), Proceedings of the International workshop on natural and man-made hazards in Africa, Awka, Nigeria, pp. 10- 14.

Osagie, E.O. (2008). Seismic activity in Nigeria, *Pacific Journal of Science Tech*., 9(2), pp. 1-6.

Panuska, J. and Frankovska, J. (2016). Effect of void ratio on the small strain shear modulus for coarse-grained soils. *Procedia Engineering*, 161, pp. 1235-1238.

Ugodulunwa, F. X. O., Ajakaiye, D. E., Guiraud, M. and Hossan, M. T. (1986). The Pindiga and Obi fractures-possible earthquake sites in Nigeria. In: Proceedings of the 3rd International Conference on current research in geophysics and geophysical research in Africa, Jos, Nigeria, 6p.

Viggiani, G. and Atkinson, J. H. (1995). Interpretation of Bender Element Tests. *Geotechnique*, 45(1), pp. 149-154.

**Cite this article as:**
Okovido, J. O. and Kennedy, C. 2021. Seismic Waves Response Characteristics of Niger Delta Soils. *Nigerian Journal of Environmental Sciences and Technology*, 5(1), pp. 191-196.
https://doi.org/10.36263/nijest.2021.01.0255

Nigerian Journal of Environmental Sciences and Technology (NIJEST)

www.nijest.com

ISSN (Print): 2734-259X | ISSN (electronic): 2734-2603

Vol 5, No. 1 March 2021, pp 197 - 221

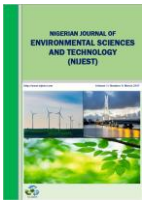

# Analysis of Soil Quality Status and Accumulation of Potentially Toxic Element in Food Crops Growing at Fecal Sludge Dumpsite in Ubakala, Nigeria

Ogbonna P.C.[1,*], Okezie I.P.[2], Onyeizu U.R.[3], Biose E.[4], Nwankwo O.U.[5] and Osuagwu E.C.[6]

[1,2,3,5,6]Department of Environmental Management and Toxicology, Michael Okpara University of Agriculture, Umudike, Abia State, Nigeria

[4]Department of Environmental Management and Toxicology, University of Benin, Edo State, Nigeria

Corresponding Author: *ogbonna_princewill@yahoo.com

https://doi.org/10.36263/nijest.2021.01.0273

## ABSTRACT

*This study investigated the magnitude of potentially toxic element (PTE) in fecal sludge and the level of contamination of soil and food crops at Ubakala, Abia State, Nigeria. Soil samples were collected in four cardinal points at north (N), south (S), east (E) and west (W) of 1 m, 5 m, 15 m and 30 m from the edge of the fecal sludge dumpsite and standards (2 ppm, 4 ppm and 6 ppm) were prepared from 1000 ppm stock solution of the metals and used to plot the calibration curve with Atomic Absorption Spectrometer. Commonly consumed Carica papaya, Telfairia occidentalis and Manihot esculenta leaf samples were collected and analyzed to measure the concentrations of PTEs such as Cd, Zn Cr, Mn, Pb and Cu. The concentrations of Zn (12.41±0.30 mg/kg), Cd (0.07±0.00 mg/kg), Cr (4.47±0.34 mg/kg), Cu (2.12±0.03 mg/kg), Mn (8.13±0.03 mg/kg) and Pb (0.01±0.00 mg/kg) in dried fecal sludge are below the permitted limits of European Union. Concentrations of PTEs in soil and plants were Zn (13.40±1.20 to 100.80±1.40 and 1.24±0.06 to 56.02±5.02 mg/kg), Cd (0.07±0.01 to 0.92±0.02 and 0.0000±0.000 to 0.085±0.01 mg/kg), Cu (6.27±0.31 to 31.39±1.04 and 0.002±0.001 to 10.80±2.01 mg/kg), Mn (36.00±1.56 to 188.57±2.25 and 0.11±0.00 to 17.21±2.01 mg/kg), Cr (2.40±0.40 to 21.03±1.43 and 0.000±0.00 to 9.60±1.13 mg/kg) and Pb (0.09±0.02 to 0.35±0.03 and <0.00001±0.00 to 0.008±0.00 mg/kg), respectively. Zinc in soil is higher than FAO/WHO permissible limit while Cd in soil is higher than FAO/WHO limit and Dutch criteria for soil. Zinc and Cr in food crops are higher than FAO/WHO permissible limit. Strong positive relationship exist between Zn in soil and food crops ($r = 0.616$, $p<0.05$). Based on the findings, it is recommended that the fecal sludge should be treated with lime to precipitate PTE content of sludge and lowering the corresponding environmental risks.*

**Keywords:** Fecal sludge, Soil quality, Food crops, Toxic elements, Ubakala

## 1.0. Introduction

Urban development in the last 30 to 40 years seems to have culminated to an increase in rural-urban migration in Nigeria, thus, increasing the population of people in urban areas. Urban development brings about an overall increase in the number of buildings by Landlords that are mostly occupied by tenants as well as some Landlords. The concomitant effect of sharp increase in number of tenants may result to an exponential inversely proportion on the generation of waste since people (i.e. the tenants) consume foods ranging from staples (garri, rice, yam etc.), fruits and vegetables (oranges, cucumber, carrots, pawpaw, spinach, bitter leaf, fluted pumpkin, waterleaf etc.) to can foods and takeaway. The foods eaten by the tenants digest in their alimentary system, and supply the body with the required nutrients while the rest are passed out from the body as feces. The fecal wastes are passed out into on-site sanitation system. An on-site sanitation system is defined as a system of sanitation where the means of storage are contained within the plot occupied by the dwelling and its immediate surroundings (WHO, 2006). In Sub-Saharan Africa, 65 to 100 % of sanitation access in urban areas is provided through onsite technologies (Strauss *et al*., 2000). The on-site sanitation system gets filled

up with feces over a period of years and are emptied into tankers (trucks) without treatment, transported and discharged into open drains, irrigation fields, open lands, or surface waters. According to Bassan *et al*. (2014), a 5 $m^3$ truck load of fecal sludge dumped into the environment is the equivalent of 5,000 people practicing open defecation. The amount of untreated fecal sludge discharged into the open environment poses a serious financial and public health risk. For example, the World Bank estimates that poor sanitation costs the world 260 billion USD annually and contributes to 1.5 million child deaths from diarrhea each year. Fecal sludge contains various heavy metals and microorganisms which have potential ecological, biological and health impacts (Hashem, 2000).

Since Ubakala is located in South east Nigeria which experience heavy rainfall during the wet season, the fecal sludge may be leached into water bodies with its concomitant challenges. For instance, the United Nations reported that about 1.8 billion people globally use source of drinking water that is contaminated with feces (Zziwa *et al*., 2016). Currently one in five children die from diarrheal related diseases, which is more than that of HIV Aids, malaria, and measles combined (UNICEF and WHO, 2009) and chronic diarrhea hinder child development by impeding the absorption of essential nutrients that are critical to the development of the mind, body, and immune system (Strande *et al*., 2014). In furtherance of this, some proportion of the fecal sludge may contain heavy metals which is of great concern in the world. The accumulation of dissolved heavy metals in water is hazardous to water bodies and human health when their values are higher than the corresponding threshold (Pape *et al*., 2012; Varol *et al*., 2013; Bu *et al*., 2015; Ogbonna *et al*., 2020a).

Poor planning and ineffective implementation of laws and regulations for waste collection, treatment and disposal at various levels of Governance in Nigeria may have resulted to indiscriminate dumping of fecal sludge on terrestrial and aquatic ecosystems. As urbanization continues to take place, the management of fecal sludge is becoming a serious public health and environmental concern particularly in South east Nigeria. Fecal sludge from the on-site sanitation systems does not undergo treatment because there is no fecal sludge treatment plant in South east Nigeria. The technologies or technical options applied for fecal sludge treatment are categorized into established fecal sludge treatment technologies (co-composting, co-treatment in waste stabilization ponds, deep row entrenchment), transferred sludge treatment technologies (anaerobic digestion, lime addition, sludge incineration, mechanical sludge treatment) and innovative technologies (vermicomposting, black soldier fly, ammonia treatment) for fecal sludge treatment (Strande *et al*., 2014; Ackah, 2016). Poor fecal sludge management may have far reaching adverse impacts on the chemical characteristics of soil since the contents of fecal sludge may have the capacity to influence soil quality and possible accumulation of contaminants in plants. For instance, heavy metal is part of the constituents of fecal sludge (Hashem, 2000).

Plants growing on potentially toxic element (PTE) contaminated soil tend to absorb PTE such as heavy metals from soil solution via the roots and translocate it to the stems and the leaves (Ogbonna *et al*., 2018a; 2020a). The chemical form of potentially toxic element in soil can strongly influence their uptake by plants as mobile ions present in the soil solution through the roots resulting in bioaccumulation of the elements in plants tissues (Pitchell and Anderson, 1997; Davies, 1983; Amusan *et al*., 2005). The harvest of such plants at maturity, their sales at the farms or in the markets and subsequent consumption by man (including animals) may result to accumulation of heavy metals in the body. Some potentially toxic element such as copper Cu, nickel (Ni), and zinc (Zn) are essential at trace amount while lead (Pb), cadmium (Cd) and mercury (Hg) are non-essential to living organisms. Consequently, the investigation of PTE in fluted pumpkin (*Telfairia occidentalis* Hook f.), pawpaw (*Carica papaya* Linn) and cassava (*Manihot esculenta* Crantz) growing at fecal sludge dumpsite is vital since these foodstuffs are important components of human diet. For instance, vegetables are rich in vitamins such as beta carotene, ascorbic acid, riboflavin, folic acid as well as minerals like iron, calcium, phosphorus, bioactive non-nutritive health promoting factors as antioxidants, phyto-chemicals, essential fatty acids and dietary fibre which are essential dietary constituents required for growth, development and reproduction (Gupta *etal*., 2008; Okonwu *et al*., 2018). It (vegetables) also supply alkaline substance in the body to maintain acid-base balance (Funke, 2011), serve as medicine to reducing the risk of chronic diseases (Gosslau and Chen, 2004; Lee *et al*., 2008) cancer, blood pressure and high cholesterol (Antonious *et al*., 2009). *Carica papaya* contains enzymes, minerals (Santana *et al*., 2019), phytochemicals such as polyphenols, phenols,

flavonoids, carotenoid, Lycopene, betacarotinoid, benzylisothyocynate, betacryptoxanthin, benzylglucosinolate, chlorogenic acid, caffeic acid, protocatachuic acid, Quercetin and traditional antioxidant vitamins such as vitamin C and E (Pinnamaneni, 2017). It (pawpaw) also contain hymopapain and papain which are widely used for digestive disorders (Huet *et al*., 2006), antihelminthic and anti-amoebic (Okeniyi *et al*., 2007), while leaf decoction is administered as a purgative for horses and used for the treatment of genito-urinary system (Pinnamaneni, 2017). Cassava root is rich in carbohydrate, calcium, iron, potassium, magnesium, copper, zinc, and manganese comparable to many legumes (Montagnac *et al*., 2009).

This study aimed to determine the distribution of potentially toxic element (PTE) in soil and accumulation in food crops at fecal sludge dumpsite in Umuahia, Abia State, Nigeria and the result obtained were compared to permissible limits set by International Organizations and National Standards of some countries to ascertain the status of the fecal sludge as organic material and possible health implications of consuming food crops growing on the site.

## 2.0. Methodology

### *2.1. Study area*

The study was carried out in Ubakala in Umuahia South Local Government Area of Abia State, Nigeria (Figures 1 and 2). Ubakala is located in the lowland rainforest zone of Nigeria (Keay, 1959) and lies on latitude 5°26' to 5°34' N and longitude 7°22' to 7°33' E. It experience two seasons viz the wet season that is characterized with heavy rainfall between April to November and short dry season from December to early March. The mean annual rainfall is 1,122 mm, and annual relative humidity is over 65 % while the mean annual temperature exceeds 27 °C.

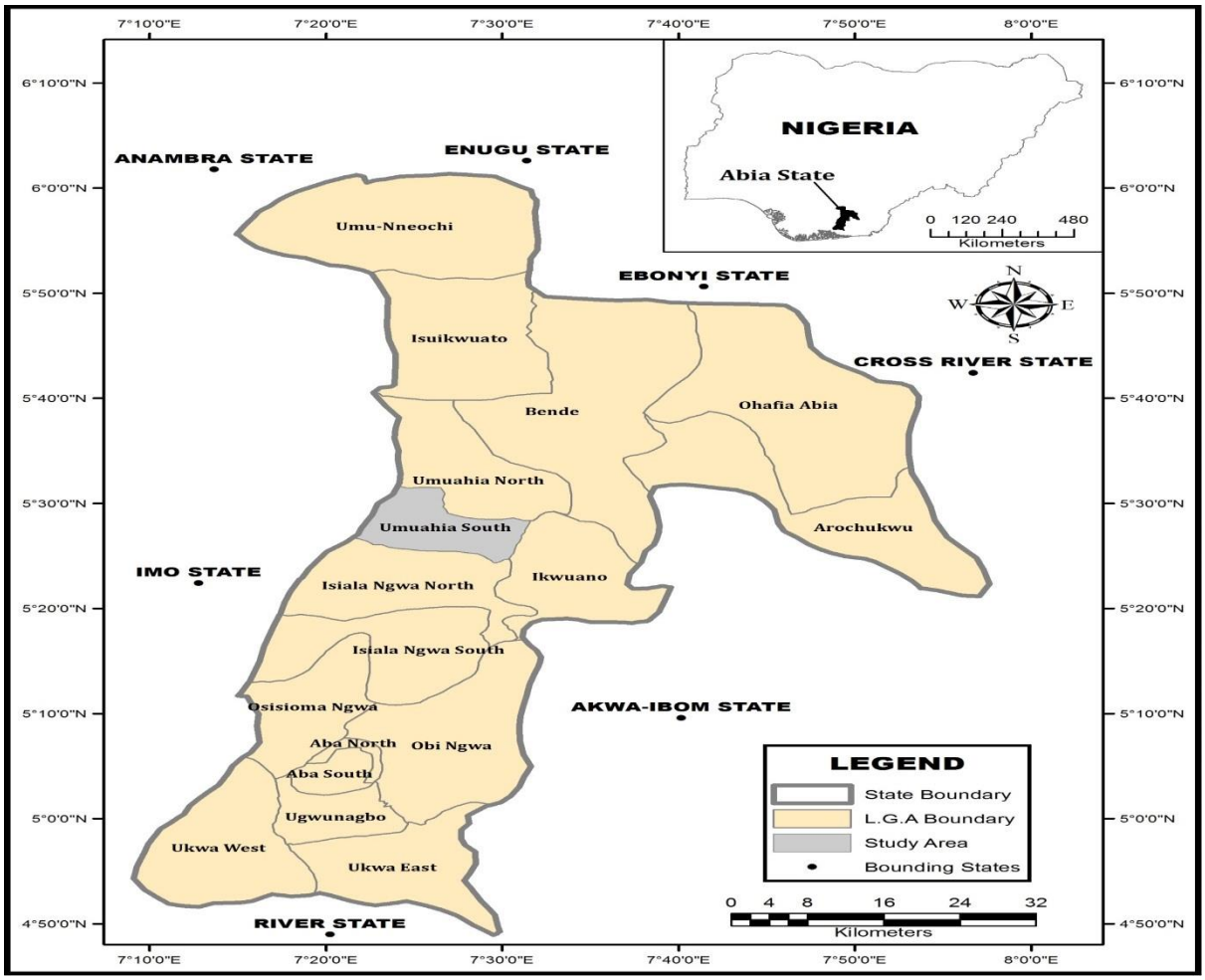


**Figure 1:** Abia State showing Umuahia South
*Source: Ogbonna et al. (2020a)*

The surface elevation is about 120 m and the area has low-lying to moderately high plain topography. It is drained by Imo River and its tributaries are perennial, resulting in secondary rainforest vegetation along the river banks. Agriculture is well practiced by the people and crops commonly grown include cassava, maize, fluted pumpkin, yam, okra, groundnut, pawpaw, oil palm trees, cola nuts, cocoa while animals such as poultry birds, pigs, goats, snails are raised.

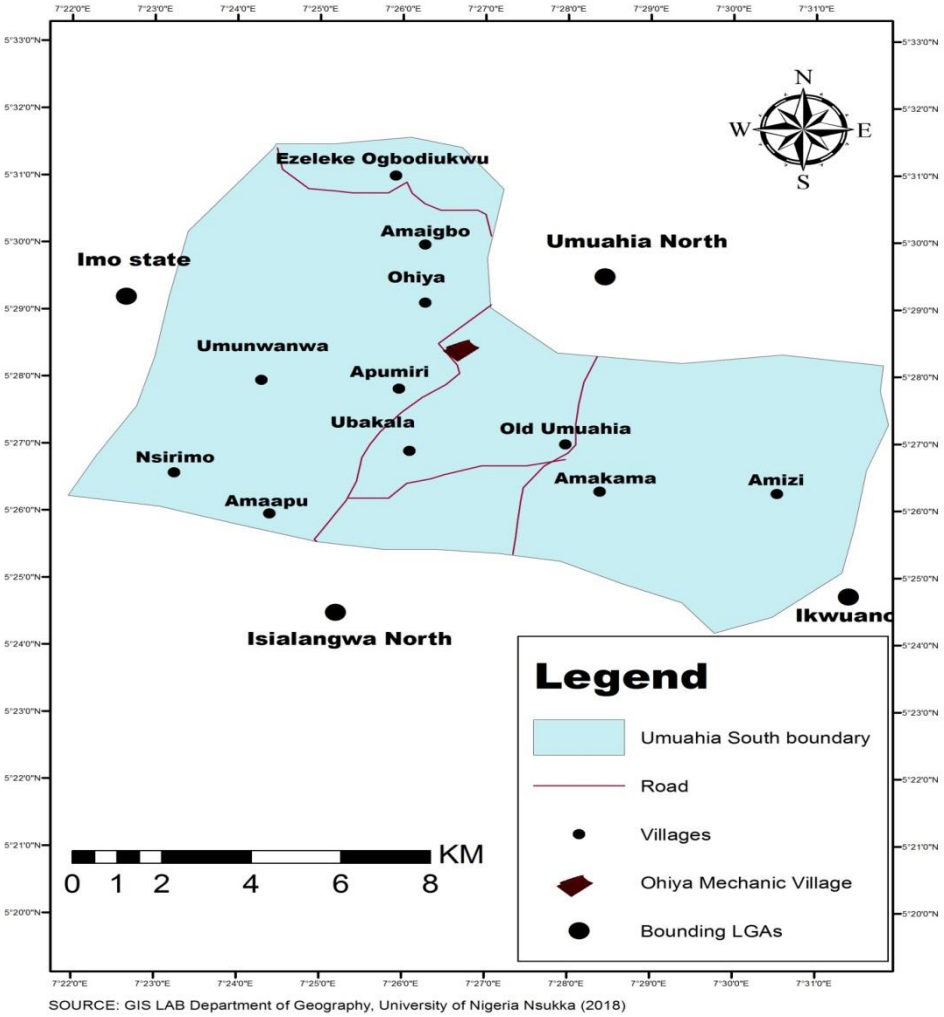


**Figure 2:** Map of study area

*2.2. Sample collection*

2.2.1. Collection of fecal sludge samples

The experiment was preceded by a visit to the fecal sludge dumpsite area. The purpose of the visit was to learn the history of the fecal sludge dumpsite, identify the food crops that were common in the study site, the various distances the food crops were growing at the four cardinal points from the edge of the fecal sludge dumpsite as well as the terrain of the site (which is table in nature). Fecal samples were collected with steel core sampler to the depth of 1 m from ten (10) different sampling points in four cardinal points (i.e. two sampling points each at north (N), south (S), east (E), west (W), and at the center (C) of the fecal sludge dumpsite. The steel core sampler was cleaned with deionized water for each individual sample collection to avoid cross-contamination. The samples from N, S, E, W and C were bulked together to form a composite sample and placed (about 160 g) in large ASEPA polythene bags, well-sealed, labeled, placed in a wooden box and covered to avoid contamination from external sources. The samples in the wooden box were transferred to the laboratory for pre-treatment and analysis. The fecal samples were air-dried at room temperature until all moisture was completely eliminated. The sample was subjected to crushing and grinding and then homogenized using a porcelain pestle and mortar. The homogenized fecal samples were sieved (0.2 mm) and stored in refrigerator prior to digestion. The sample were analyzed for pH, organic matter, nitrogen (N),

phosphorus (P), potassium (K), calcium (Ca), sodium (Na), magnesium (Mg), and potentially toxic elements chromium (Cr), copper (Cu), cadmium (Cd), zinc (Zn), lead (Pb), and manganese (Mn) using standard laboratory methods.

2.2.2. Collection of soil samples

Surface soil (0-20 cm) samples were collected from eight (8) different points with thoroughly cleaned Dutch soil auger in four cardinal points (i.e. two sampling points each at north (N), south (S), east (E) and west (W) of 1 m, 5 m, 15 m and 30 m from the edge of the fecal sludge dumpsite in September 2019. The Dutch soil auger was cleaned with deionized water for each individual sample collection to avoid cross-contamination. The control sample was collected in a 2 year upland bush fallow about 1 km from the dumpsite where there was no visible source of contamination. Soil samples from the same distance (e.g. 0-20 cm depth from 1 m at N, S, E and W) were bulked together to form a composite sample and placed in large polythene bags (about 80 g), well-sealed, labeled, placed in a wooden box and covered to avoid contamination from external sources. The samples in the wooden box were transferred to the laboratory for pre-treatment and analysis. Each bulked soil sample was freed from roots, stones, and seeds and air-dried at room temperature until all moisture was completely eliminated. The samples were crushed, ground to increase the surface area for chemical reactions and homogenized using a porcelain pestle and mortar. The homogenized soil samples were sieved (< 2 mm) and analyzed for pH, organic matter, electrical conductivity (EC) and potentially toxic elements (Cr, Cu, Cd, Zn, Pb and Mn) using standard laboratory methods.

2.2.3. Collection of plants samples

Fresh leaves were sampled from eight stands each of *Carica papaya* Linn. (pawpaw, Caricaceae), *Telfairia occidentalis* Hook f. (fluted pumpkin, Cucurbitaceae) and *Manihot esculenta* Crantz (cassava or manioc, Euphorbiaceae) at each particular distance. For example, two (2) stands of pawpaw were collected each at N, S, E and W). The leaves were randomly collected in September 2019 from different parts of each plant species using thoroughly cleaned secateurs. These three plant species were sampled because they were common among all sampling distance, thus, the plants were growing around the points where soil samples were collected from the fecal sludge dumpsite. Samples from each plant species was placed separately in large envelopes, labeled well and sealed, placed in a wooden box and covered to avoid contamination from external sources. The samples in the wooden box were transferred to the laboratory for pre-treatment and analysis.

2.2.4. Analysis of potentially toxic element in plant samples

The leaves were thoroughly rinsed with deionized water to remove adhered soil, dust and pollen particles and placed in large crucibles and oven dried at 60°C for 96 hours. The dried leaves samples was milled to fine powder (< 1 mm) using a cyclone sample mill (model 3010-019). The analysis was carried out using the procedure of Yeketetu (2017). About 0.5 g of each of the plant samples were weighed separately into a digestion flask and digested in furnace at 500 °C for four hours, and then 10 ml of 6 M HCl were added, covered and heated on a steam bath for 15 minute in fume hood. Another 1 ml of $HNO_3$ was added and evaporated to dryness by continuous heating for one hour to dehydrate silica and completely digest organic compounds. Finally, 5 ml of 6 M HCl and 10 ml of water were added and the mixture was heated on a steam bath to complete dissolution. The mixture was cooled, filtered into a 50 mL volumetric flask and made up to the mark with distilled water (Singh *et al*., 2010). Then the samples were analyzed for potentially toxic element (Cr, Cu, Cd, Zn, Pb and Mn) using Atomic Absorption Spectrometer (model AA-7000 Shimadzu, Japan).

2.2.5. Analysis of exchangeable bases, organic matter, EC in fecal samples and potentially toxic element in soil and fecal sludge

The procedures of Adeyeye (2005) and Bhowmick *et al*. (2013) was adopted with modifications. One (1) g of the sieved samples were weighed into digestion flask and 30 $cm^3$ of aqua regia was added and digested in a fume-cupboard until clear solution was obtained, which was cooled, filtered and then made up to 50 ml mark in a standard volumetric flask with de-ionized water. A blank sample was prepared to zero the instrument before running other series of samples. Standards (2 ppm, 4 ppm and 6 ppm) were prepared from 1000 ppm stock solution of the metals and used to plot the calibration curve. The curve was plotted automatically by the instrument. Exactly 0.2 g was pipette from 1000

ppm, pour into 100 ml flask and made to the mark with deionized water. This procedure was used in the preparation of 4 ppm and 6 ppm, respectively. High temperature was produced in the ignition chamber and provided enhanced reducing settings for the atomization of the respective metals/minerals. Each standard was aspirated by nebulizer, converted into an aerosol, mixed with the gases and converted into atomic form. All the standard solutions were analyzed and the calibration curve was plotted automatically for the metals/minerals of interest. Each metal/mineral (Pb, Mn, Zn, Cr, Cu, Cd, K, Na, Ca and Mg) were analyzed using its respective wavelength after which its concentration was generated from the standard graph by the instrument (Atomic Absorption Spectrometer, model AA-7000 Shimadzu, Japan). Triplicate digestion of each sample was carried out together with blank digest without the sample. The measuring conditions of Pb, Mn, Zn, Cr, Cu, Cd, K, Na, Ca and Mg ions are as follows:

**Pb**: Burner height: 8.0 mm; Wave length: 283.3 nm; Burner angle: 0 degree; Slit width: 0.7 nm; Fuel gas flow rate: 2.3 L/min; Lighting mode: BGC-D2; Flame type: air-$C_2H_2$. A five point's calibration curve is made with 0, 0.1 ppm, 0.2 ppm, 0.4 ppm, 0.6 ppm standard solutions prepared from certified 1000 ppm standard solution.

**Mn**: Burner height: 7.0 mm; wave length: 279.5 nm; Burner angle: 0 degree; Slit width: 0.2 nm; Fuel gas flow rate: 2.0 L/min; Lighting mode: BGC-D2; Flame type: air-$C_2H_2$. A five point's calibration curve is also made with 0, 0.1 ppm, 0.2 ppm, 0.3 ppm, 0.4 ppm standard solutions prepared from certified 1000 ppm standard solution.

**Zn**: Burner height: 7.0 mm; Wave length: 213.9 nm; Burner angle: 0 degree; Slit width: 0.7 nm; Fuel gas flow rate: 2.0 L/min; Lighting mode: BGC-D2; Flame type: air-$C_2H_2$. A five point's calibration curve is also made with 0, 0.1 ppm, 0.2 ppm, 0.4 ppm, 0.8 ppm standard solutions prepared from certified 1000 ppm standard solution.

**Cr**: Burner height: 7 mm; Wave length: 766.5 nm; Burner angle: 0 degree; Slit width: 0.5 nm; Fuel gas flow rate: 2.0 L/min; Lighting mode: BGC-D2; Flame type: air-$C_2H_2$. A five point's calibration curve is also made with 0, 0.1 ppm, 0.2 ppm, 0.4 ppm, 0.8 ppm standard solutions prepared from certified 1000 ppm standard solution. Moreover, same volume of 0.1 to 0.2% cesium chloride is added to the standard and unknown sample to prevent the ionization of potassium.

**Cu**: Burner height: 7 mm; Wave length: 766.5 nm; Burner angle: 0 degree; Slit width: 0.5 nm; Fuel gas flow rate: 2.0 l/min; Lighting mode: BGC-D2; Flame type: air-$C_2H_2$. A five point's calibration curve is also made with 0, 0.1 ppm, 0.2 ppm, 0.4 ppm, 0.8 ppm standard solutions prepared from certified 1000 ppm standard solution. Moreover, same volume of 0.1 to 0.2% cesium chloride is added to the standard and unknown sample to prevent the ionization of potassium.

**Cd**: Burner height: 7 mm; Wave length: 766.5 nm; Burner angle: 0 degree; Slit width: 0.5 nm; Fuel gas flow rate: 2.0 l/min; Lighting mode: BGC-D2; Flame type: air-$C_2H_2$. A five point's calibration curve is also made with 0, 0.1 ppm, 0.2 ppm, 0.4 ppm, 0.8 ppm standard solutions prepared from certified 1000 ppm standard solution. Moreover, same volume of 0.1 to 0.2% cesium chloride is added to the standard and unknown sample to prevent the ionization of potassium.

**K**: Burner height: 7.0 mm; Wave length: 766.5 nm; Burner angle: 0 degree; Slit width: 0.7 nm; Fuel gas flow rate: 2.0 L/min; Lighting mode: NON-BGC; Flame type: air-$C_2H_2$. A five point's calibration curve is also made with 0, 0.1 ppm, 0.2 ppm, 0.4 ppm, 0.8 ppm standard solutions prepared from certified 1000 ppm standard solution. Moreover, same volume of 0.1 to 0.2% cesium chloride is added to the standard and unknown sample to prevent the ionization of potassium.

**Na**: Burner height: 7.0 mm; wave length: 589.0 nm; Burner angle: 0 degree; Slit width: 0.2 nm; Fuel gas flow rate: 1.8 L/min; lighting mode: NON-BGC; Flame type: air-$C_2H_2$. A five point's calibration curve is also made with 0, 0.1 ppm, 0.2 ppm, 0.3 ppm, 0.4 ppm standard solutions prepared from certified 1000 ppm standard solution.

**Ca**: Burner height: 17 mm; Wave length: 422.7 nm; Burner angle: 0 degree; Slit width: 0.7 nm; Fuel gas flow rate: 2.0 L/min; Lighting mode: BGC-D2; Flame type: air-$C_2H_2$. A five point's calibration

curve is made with 0, 0.1 ppm, 0.2 ppm, 0.4 ppm, 0.6 ppm standard solutions prepared from certified 1000 ppm standard solution. However, it is ionized and 0.1 to 0.2% potassium chloride is added to the standard and unknown sample with same extent.

**Mg**: Burner height: 7 mm; Wave length: 285.2 nm; Burner angle: 0 degree; Slit width: 0.7 nm; Fuel gas flow rate: 1.8 L/min; Lighting mode: BGC-D2; Flame type: air-$C_2H_2$. A five point's calibration curve is also made with 0, 0.1 ppm, 0.2 ppm, 0.4 ppm, 0.8 ppm standard solutions prepared from certified 1000 ppm standard solution.

2.2.6. Determination of nitrogen

Nitrogen was determined by the micro-Kjedahl method as described in Pearson (1976). The 1 g of the ground samples was weighed into the 500 ml Kjedahl digestion flask (Barloworld UK, model Fk 500/3l). The 1 g of catalyst mixture (20 g potassium sulphate, 1 g copper sulphate and 0.1 g selenium powder) was weighed and added into the flask, and 15 ml of conc. $H_2SO_4$ was also added. Heating was carried out cautiously on a digestion rack in a fume cupboard until a greenish clear solution appeared. The digest was allowed to clear for about 30 minute and allowed to cool. Ten (10) ml of distilled water was added to avoid caking. Then the digest was transferred with several washings into a 100 ml volumetric flask and made up to the mark with distilled water. A 10 ml aliquot was collected from the digest and placed in the flask. A 100 ml receiver flask containing 5 ml boric acid indicator solution was placed under the condenser of the distillation apparatus so that the tip was 2 cm inside the indicator. Ten (10) ml of 40 % NaOH solution was added to the digested sample through a funnel stop cork. The distillation commenced by closing the system jet arm of the distillation apparatus. The distillate was collected in the receiver flask (35 ml). Titration was carried out with 0.01M standard HCl to first pink colour. Triplicate digestion of each sample was carried out together with blank digest without the sample.

$$\%\ \text{Nitrogen wt. of sample} = \frac{\text{Titration vol.} \times 0.014 \times M \times 100 \times 50}{10} \quad (1)$$

where $M$ = molarity of std. HCl

2.2.7 Determination of phosphorus

Phosphorus (P) was determined by the Vanodo-molybdate spectrophotometric method using Shimadzu UV-Visible Spectrophotometer UV1800, Japan. About 3.0 to 3.2 g of samples to the nearest 0.001 g were weighed into vijcor crucible. A 0.5 g zinc oxide was added and the mixture was heated slowly on hot plate until the sample thickens, then the heating was slowly increased until the mass is completely charred. The crucibles were placed in muffle furnace at 550-600 °C and held for 2 hours before it was removed and cooled to room temperature. The 5 ml each of distilled water and hydrochloric acid were added to the ash and the crucibles were covered with watch glasses and heated to gentle boiling for 5 minute and the solution were filtered into 100 ml volumetric flasks. The inside of the watch glass and the sides of the crucibles were washed with 5 ml of hot distilled water using wash bottle with fine jet. The crucibles and the filter papers were washed with four additional 5 ml portions of hot distilled water and the solution was cooled to room temperature and neutralize to a faint turbidity by drop-wise addition of 50 % potassium hydroxide solution. A 0.5N hydrochloric acid was added drop-wise until the zinc oxide precipitate is dissolved. Then 2 additional drops was added and diluted to volume with distilled water and thoroughly mixed. About 10 ml of the solution was pipette into clean dry 50 ml volumetric flask and 8.0 ml of hydrazine sulphate solution and 2.0 ml of sodium molybdate solution were added. The flask was stopper and inverted 2 to 3 times, thereafter the stopper was loosen and heat for 10-15 minute in a vigorous boiling water bath. The bath was removed and cools to 25±5 °C in water bath and the volume was diluted with distilled water and thoroughly mixed. The solution was transferred to clean, dry cuvette and the transmittance was measured at 650 ml with the instrument adjusted to read 100 % transmittance for a cuvette containing water. Reagent blanks were prepared using the procedure described with no samples. The phosphorus content of the samples and blanks were read from the transmittance graph.

$$\text{Phosphorus} = \frac{10(A - B)}{W_v} \quad (2)$$

where:
A = phosphorus content of the sample aliquot
B = phosphorus content of the blank aliquot
W = weight of sample
V = volume of aliquot

2.2.8. Determination of pH

The term pH is used to measure the amount of hydrogen ion concentration ($H^+$) of a solution. It is, therefore, described as a measure of the acidity or alkalinity of the solution. The pH meter (Jenway pH meter, model 3510 USA) was standardized with pH 4, 7 and 10 buffer solutions. It was then washed with distilled water, wiped and immersed in the samples (soil and fecal) and retained for a short while until the readings stabilized. The readings were then recorded from the display. The readings were taken in triplicates.

2.2.9. Determination of organic matter

Organic matter levels in the sieved soil and fecal samples were estimated indirectly from organic carbon (C) using the Walkley and Black procedure (Walkley and Black, 1934). Exactly 1 g of the finely ground samples were weighed separately into 500 ml conical flasks. A 10 ml of 1M potassium dichromate was poured inside the flasks and the mixture was swirled. Then 20 ml of conc. $H_2SO_4$ was added and the flasks were swirled again for 1 minute in a fume cupboard. The mixture were allowed to cool for 30 minutes after which 200 ml of distilled water, 1 g NaF and 1 ml of diphenylamine indicator were added. The mixtures were swirled and titrated with ferrous ammonium sulphate. The blanks were also treated in the same way. Triplicate digestion of each sample was carried out together with blank digest without the sample.

$$\% \text{ Carbon} = \frac{(B - T) \times M \times 1.33 \times 0.003 \times 100}{g} \quad (3)$$

where:
B = Titration volume (Blank)
T = Titration volume (Sample)
M = Molarity of Fe solution
Organic matter = Organic carbon x 1.724

2.2.10. Quality assurance

Triplicate digestion of each sample was carried out and blanks were prepared from only reagents without sample to check for background contamination by the reagents. Appropriate quality assurance procedures and precautions were taken to ensure the reliability of the results in all fecal sludge, soil and plant sample test. Samples were carefully handled to avoid cross-contamination. All Glass wares used were soaked into 3 M $HNO_3$ overnight and washed with deionized water to reduce the chances of interferences, and reagents used were of analytical grades. Distilled and deionized water were used throughout the study.

The comparison and interpretation of the results of analyzed fecal sludge, soils and food crops is based on the control values, permissible limits established by Codex Alimentarius Commission (WHO/FAO), National standards of different countries and related studies.

## 3.0. Results and Discussion

### *3.1. Potentially toxic element in dried fecal sludge*

The concentration of potentially toxic element in dried fecal sludge is summarized in Table 1. The result indicate that the six (6) potentially toxic element tested in this study were present in the fecal sludge. The concentrations of PTE in the dried fecal matter were Zn (12.41±0.30 mg/kg), Cd (0.07±0.00 mg/kg), Cr (4.47±0.34 mg/kg), Cu (2.12±0.03 mg/kg), Mn (8.13±0.03 mg/kg) and Pb (0.01±0.00 mg/kg). The concentration of Zn in the dried fecal sample was Zn is 12.41±0.30 mg/kg, which is well below the accepted limits of 500 and 1200 mg/kg (Zn) set by China (GB 4284-1984 and

GB 4284-2018), respectively, 2500-4000 mg/kg (Zn) by the European Union (Directive 86/278/EEC) and 800 mg/kg (Zn) in Sweden (Chen *et al*., 2003) (Table 2). The concentration of Zn (12.41±0.30 mg/kg) from fecal sludge dumpsite at Ubakala, Nigeria is higher than 0.058 to 0.094 mg/kg in fecal sludge at Accra region of Ghana (Ahmed *et al*., 2019). The concentration of Cd in the dried fecal sample was 0.07±0.00 mg/kg, which is well below the accepted limits of 5 mg/kg and 3 mg/kg set by China (GB 4284-1984 and GB 4284-2018), respectively, 20-40 mg/kg (Cd) by the European Union (Directive 86/278/EEC) and 2 mg/kg (Cd) in Sweden (Chen *et al*., 2003) (Table 2). The concentration of Cd (0.07±0.00 mg/kg) in fecal sludge dumpsite at Ubakala, Nigeria is well below 0.90 to 112.03 mg/kg in sludge from municipal and industrial wastewater treatment plants in China (Wang and Mulligan, 2005), 0.8 to 7.3 mg/kg in dried sewage sludge in Greece (Spanos *et al*., 2016), 1.17±0.19 to 1.71±0.29 µg/g in sludge from wastewater treatment plants of Sparta and Kavala, Greece (Angelidis and Aloupi, 1999).

**Table 1:** Heavy metal concentration in dried fecal matter

| Potentially toxic element | Concentration |
|---|---|
| pH | 8.90±3.10 |
| Organic matter (OM) | 7.41±2.01 % |
| N | 0.06±0.02 |
| P | 0.02±0.00 mg/kg |
| K | 0.47±0.01 cmol/kg |
| Ca | 0.03±0.00 cmol/kg |
| Mg | 0.05±0.00 cmol/kg |
| Na | 0.78±0.01 cmol/kg |
| Cd | 0.07±0.00 mg/kg |
| Zn | 12.41±0.30 mg/kg |
| Cr | 4.47±0.34 mg/kg |
| Cu | 2.12±0.03 mg/kg |
| Mn | 8.13±0.03 mg/kg |
| Pb | 0.01±0.00 mg/kg |

*Values are mean ± standard deviation of 3 replicates*

The concentration of Cu in the dried fecal sample was Cu is 2.12±0.03 mg/kg, which is well below the accepted limits of 500 mg/kg (Cu) in China (GB 4284-2018), 1000-1750 mg/kg (Cu) by the European Union (Directive 86/278/EEC) and 600 mg/kg in Sweden (Chen *et al*., 2003) (Table 2). The concentration of Cu (2.12±0.03 mg/kg) in fecal sludge dumpsite at Ubakala, Nigeria is well below 120.31 to 2051.26 mg/kg (Wang and Mulligan, 2005), 51.0 to 198 mg/kg (Spanos *et al*., 2016), 78.7±6.5 to 141.7±6.6 µg/g (Angelidis and Aloupi, 1999) but higher than 0.018 to 0.030 mg/kg (Ahmed *et al*., 2019).

The concentration of Mn in the dried fecal sludge was 8.13±0.03 mg/kg, which is below 122.2±82.0 to 251.0±115.6 mg/kg in pilot-scale sludge drying reed beds (Stefanakis and Tsihrintzis, 2012). The level of Mn in the fecal sludge suggests that its application in soil will enhance Mn in soil and subsequent assimilation in plants. The concentration of Cr in the dried fecal sample was 4.47±0.34 mg/kg which is wellbelow the permitted limits of 600 mg/kg (GB 4284-1984) and 500 mg/kg (GB 4284-2018) (Cr) established by China and 100 mg/kg (Cr) in Sweden (Chen *et al*., 2003) (Table 2).

**Table 2:** Limit values for heavy-metal concentrations in sludge for use in agriculture (mg/kg of dry matter)

| Standard by country | pH | Cd | Cu | Pb | Cr | Zn | Mn |
|---|---|---|---|---|---|---|---|
| GB 4284-1984 (China) | pH＜6.5 | 5 | 250 | 300 | 600 | 500 | NA |
| | pH≥6.5 | 20 | 500 | 1000 | 1000 | 1000 | NA |
| | Grade A | 3 | 500 | 300 | 500 | 1200 | NA |
| GB 4284-2018 (China) | Grade B | 15 | 1500 | 1000 | 1000 | 3000 | NA |
| 40 CFR Part 503 (US) | | 85 | 4300 | 840 | NA | 7500 | NA |
| Directive 86/278/EEC (EU 1986) | | 20-40 | 1000-1750 | 750-1200 | NA | 2500-4000 | NA |
| (Sweden) (Chen *et al*., 2003) | | 2 | 600 | 100 | 100 | 800 | NA |
| AbfKlaeV (Germany) | | 10 | 800 | 900 | 900 | 2500 | NA |
| EU 3rd Draft (2000) | | 10 | 1000 | 750 | 1000 | 2500 | NA |
| Greek Legislation 80568/4225/91 (1991) | | 20-40 | 1000-1750 | 750-1200 | *510 | 2500-4000 | NA |

*NA = Not available, *Cr (total) = (Cr (III) + Cr (VI)], - not specified*

The concentration of Cr (4.47±0.34 mg/kg) in samples of fecal sludge dumpsite in Ubakala, Nigeria is higher than 0.00 to <0.01 mg/kg in Accra region of Ghana (Ahmed *et al*., 2019).

The concentration of Pb in the dried fecal sludge was 0.01±0.00 mg/kg, which is well below the permitted limits of 300 mg/kg (Pb) set by China (GB 4384-2018), 750-1200 mg/kg (Pb) by the European Union (Directive 86/278/EEC) and 100 mg/kg (Pb) in Sweden (Chen *et al*., 2003). The concentration of Pb (0.01±0.00 mg/kg) in samples of fecal sludge dumpsite in Ubakala, Nigeria is higher than 0.002 to 0.010 mg/kg (Ahmed *et al*., 2019). The concentrations of PTE in the dried fecal matter were below the permissible limits established by European Union, China and Sweden. The low concentration of PTEs in fecal sludge at Ubakala, Nigeria may be attributed to inadequate manufacturing of agricultural input (e.g. inorganic fertilizer, pesticides among others) for crop production in Nigeria unlike the developed countries. Thus, reducing the level of soil contamination by PTEs and uptake by food crops consumed by the people. Thus, the fecal sludge could be harnessed by farmers as organic material to boost crop yield. Consequently, there is need for periodic monitoring of PTE in soil to ascertain their (PTE) status in line with permitted limits set by countries in Europe, China, USA as well as International and National Organizations. Generally, the order of abundance of the potentially toxic element in the dried fecal matter from the fecal sludge dumpsite at Ubakala, Nigeria is: Zn>Mn>Cr>Cu>Cd>Pb.

### *3.2. Chemical properties in soil*

The values of some selected chemical properties such as pH, organic matter and electric conductivity in soil at the fecal sludge dumpsite in Ubakala, Nigeria is presented in Table 3. The results indicate that the highest and lowest values of soil pH, electric conductivity and organic matter were observed at the fecal sludge dumpsite and control site, respectively. The high pH values in soil from the fecal sludge dumpsite may be attributed to the buffering effect of fecal matter as well as soil organic matter against pH change, in addition to release of high basic cations during decomposition of organic material. High basic cations are released during organic matter decomposition and this increases soil pH (Oyedele *et al*., 2008; Awotoye *et al*., 2011; Ogbonna *et al*., 2018b). The pH of soils from the fecal sludge dumpsite increased from 4.80±0.10 to 6.60±0.03 which is higher than 4.80±0.10 recorded in soils from the control site. Thus, the soils from the fecal sludge dumpsite were less acidic unlike the soils from the control site. Soil pH is influenced by the use of chemicals such as fertilizers, sludge and liquid manures, and pesticides (Smith and Doran, 1996). Olness and Archer (2005) observed an increase in soil pH from 4.9 to 6.3 following the application of animal waste compost. The lower acidic nature of soils from the fecal sludge dumpsite can be attributed to the organic nature of the fecal sludge. Study in the composition of feces reported that majority (84%) of the solid matter in feces is organic in nature (Lopez Zavala, 2002). The low acidic nature of soils at the fecal sludge dumpsite will facilitate the decomposition of fecal sludge by soil microorganisms' vis-à-vis the release of macronutrients and potentially toxic element in the fecal sludge dumpsite. In contrast, the strong acidic nature of soils at the control site might have hindered the effectiveness of microorganisms to decomposing organic materials since pH influence the inactivation of pathogen in fecal sludge (Appiah-Effah *et al*., 2014).

**Table 3:** Some chemical properties in soil

| Distance (m) | pH | Organic Matter (%) | EC (μScm-$^{1}$) |
|---|---|---|---|
| 1 | $6.60^{a}$ ± 0.03 | $24.11^{a}$ ± 0.01 | $33.27^{a}$ ± 0.83 |
| 5 | $5.75^{b}$ ± 0.05 | $13.95^{b}$ ± 0.05 | $20.03^{b}$ ± 1.05 |
| 15 | $5.12^{c}$ ± 0.10 | $7.75^{c}$ ± 1.49 | $15.93^{c}$ ± 1.17 |
| 30 | $4.80^{d}$ ± 0.10 | $2.22^{d}$ ± 0.02 | $9.79^{d}$ ± 0.58 |
| Control | $4.80^{d}$ ± 0.10 | $2.14^{d}$ ± 0.03 | $8.40^{d}$ ± 1.11 |

*Values are mean ± standard deviation of 3 replicates*

$^{abc}$ *Means in a column with different superscripts are significantly different (P<0.05)*

The highest level of organic matter in this study was observed to apex within 1 m (24.11±0.01) followed by its (organic matter) values at the distance of 5 m (13.95±0.05), 15 m (7.75±1.49) and 30 m (2.22±0.02) while the control site (2.14±0.03) had the lowest level of organic matter. The level of organic matter in soil indicates that the values of organic matter in soil samples were decreasing with increasing distance from the fecal sludge dumpsite. The magnitude of decline in organic matter content with distance in this study varied amongst sampling distance but the rate of decline were higher at 30 m, followed by 15 m and lastly 5 m. The high value of organic matter at 1 m may be

linked with its proximity to the fecal sludge dumpsite while the low organic matter content in soil at the control site may be attributed to low quantity of organic materials unlike the fecal sludge dumpsite area that provided sustained supply of organic matter to the soils at various distance. The level of organic matter at 1 m (24.11±0.01) was 1.73, 3.11, 10.86 and 11.27 folds higher than its value at 5 m, 15 m, 30 m and control, respectively. The organic matter content in soil from the fecal sludge dumpsite at Ubakala, Nigeria increased from 2.22±0.02 to 24.11±0.01, which is lower than 62.49±1.63 to 70.36±0.88 % in sewage sludge in Greece (Angelidis and Aloupi, 1999) but higher than 1.5 to 1.9 (Bozym, 2019) (Table 4), 5.12±0.02 to 6.59±0.07 % in waste dump soil (Obasi *et al*., 2013), 3.81 to 7.94 % in municipal landfilled soil (Fonge *et al*., 2017) and 1.74±0.04 to 3.88±0.08 % in soil amended with sewage sludge (Elloumi *et al*., 2016). Soil organic matter content is an important soil quality indicator (Larson and Pierce, 1991) since it influences soil biological, physical and chemical characteristics. It (soil organic matter) is a sink and source for plant nutrients and very crucial in sustaining soil fertility, reducing erosion, influencing aggregation, and improving water infiltration and retention (Sikora and Stott, 1996; Doran *et al*., 1996), buffering capacity and microbial activity/diversity (Arshad and Coen, 1992).

**Table 4:** Comparison of concentration of some chemical properties and PTE in soils with related studies and EU standard

| Parameters | This study | Related studies | EU Standards |
|---|---|---|---|
| pH | 4.80-6.60 | 7.09-7.60 Amos-Tautua *et al*. (2014), 8.0-8.3 Bozym (2019), 7.56-8.65 Anhwange and Kaana (2013) | NA |
| Organic matter | 2.22-24.11 | 1.03-4.71 Amos-Tautua *et al*. (2014), 1.5-1.9 Bozym (2019. | NA |
| Electrical conductivity | 9.79-33.27 | | NA |
| Cr | 2.40-21.03 | 11.40-18.34 Ajah *et al*. (2015), 12.0-355 Spanos *et al*. (2016), 39.67-48.08 Vongdala *et al*. (2019), 53.5-134.5 Shamuyarira & Gumbo (2014), 0.10-536.5 Esakku *et al*. (2005), 29.21-32.41 Ayari *et al*. (2010) | 150 |
| Cu | 6.27-31.39 | 51.0-198.0, Spanos *et al*. (2016), 54.06-66.82 Vongdala *et al*. (2019), 25.17-87.77 Ajah*et al*. (2015), 263.7-626 Shamuyarira (2013), Ideriah *et al*. (2010), 2.18-1005 Esakku*et al*. (2005), 45.0-48.23 Ayari *et al*. (2010) | 140 |
| Pb | 0.09-0.35 | 35.6-172.9 Shamuyarira (2013), 9.10-271.9 Esakku *et al*. (2005), 52.45-56.12 Ayari *et al*. (2010), 125.72-138.48 Ajah *et al*. (2015), 67.99-80.17 Vongdala *et al*. (2019), 12.0-102 Spanos *et al*. (2016) | 300 |
| Zn | 13.40-100.80 | 52.48-77.46 Vongdala *et al*. (2019), 86.95-98.25 Ayari *et al*. (2010), 856.0-1880 Spanos *et al*. (2016), 43.37-76.37 Ajah *et al*. (2015), 5.52-777.9 Esakku *et al*. (2005), 951.0-1732 Shamuyarira (2013) | |
| Mn | 36-188.57 | 263-1348 Shamuyarira (2013), 6.44-12.28 Ajah *et al*. (2015), 8.36-383.1 Esakku *et al*. (2005) | |
| Cd | 0.07-0.92 | 0.8-7.3 Spanos *et al*. (2016), 0.82-3.11 Shamuyarira (2013), 3.73-3.76 Vongdala *et al*. (2019), BDL-3.80 Esakku *et al*. (2005), 0.88-1.10 Ayari *et al*. (2010) | 3 |

NA = Not available

The highest value of electrical conductivity was obtained at the distance of 1 m (33.27±0.83 mS/cm) and the value is significantly ($P<0.05$) higher than values observed at 5 m (20.03±1.05 mS/cm), 15 m (15.93±1.17 mS/cm), 30 m (9.79±0.58 mS/cm) and control (8.40±1.11 mS/cm). The values of electrical conductivity in soil were decreasing with increasing distance from the fecal sludge dumpsite. The high values of EC in soil at the fecal sludge dumpsite may be attributed to presence of soluble salt in the fecal sludge. For instance, winery sludge (Saviozzi*et al*., 1994) and brewery sludge (Alayu and Leta, 2020) were found to increase soil salinity, which exerts severe stress on non-salt-tolerant plants and inhibits the plant growth (Mtshali*et al*. 2014). However, the value of soil salinity in this study was not at a level that could restrict plant growth rate and yield of crops because the EC value meets the tolerable salinity limit of most plants that ranges from 3 to 4 mS/cm (Abdullah *et al*. 2016. The level of EC at 1 m (33.27±0.83 mS/cm) is 1.66, 2.09, 3.40 and 3.96 fold higher than its values at 5 m, 15 m, 30 m and control, respectively. The values of EC in soil from the fecal sludge (FS) dumpsite in Ubakala, Nigeria increased from 9.79±0.58 to 33.27±0.83 mS/cm, which is higher than 1.53±0.01 to 2.46±0.02 mS/cm in waste dump soil (Obasi *et al*., 2013), 0.03 to 0.04 mS/cm in municipal landfilled soil (Fonge *et al*., 2017) and 0.58±0.07 to 0.80±0.08 dS/m in soil amended with sewage sludge (Elloumi *et al*., 2016) (Table 4). Electrical conductivity (EC) is a measure of soil

salinity (Rhoades, 1996) and it significantly impacts microbial respiration, decomposition and other processes involved in nitrogen cycling (Smith and Doran, 1996).

### *3.3. Horizontal distribution of potentially toxic element in soil*

The distribution of potentially toxic element in soil samples collected at various distance from the fecal sludge dumpsite and control site is summarized in Table 5. The results show that significant differences exist among the PTE at the various distance from the fecal sludge dumpsite. The results also indicate that highest and lowest concentrations of the PTE were observed at the fecal sludge dumpsite and control area, respectively. The high PTE in soils from the study site may be attributed to the fecal sludge dumpsite since the PTE were present in the samples of dried fecal matter analyzed in this study (Table 1) as well as the high content of organic matter in soil (Table 3). Organic matter in soils immobilizes heavy metals at strongly acidic conditions and mobilizes metals at weakly acidic to alkaline reactions by forming insoluble or soluble organic metal complexes, respectively (Brümmer and Herms, 1982). More so, the pH values in soils (4.80±0.10 to 6.60±0.03) of the fecal sludge dumpsite is also implicated for the high PTE values. At low pH some metallic elements are overly abundant and highly mobile (Brady and Weil, 2000). Notwithstanding this, studies have shown that sites adjoined to source of pollution are subjected to high concentration of PTE such as heavy metals unlike the control site (Ogbonna *et al*., 2013, 2018c, 2020b) The concentration of six (6) PTE tested in the soil was observed to climax within 1 m followed by their (PTE) values at the distance of 5 m, 15 m, 30 m while the control site had the lowest concentration of the PTE. The pattern of migration of the PTE in soil suggests that the concentration of PTE in soil sample were decreasing with increasing distance from the fecal sludge dumpsite. Similar pattern in distribution of PTE (Pb, Cd, As, Ni, Fe and Zn) with highest concentration at 1 m and decreased with distance has been reported in a related study at Ngwogwo in Ebonyi State, Nigeria (Ogbonna *et al*., 2020b).

The highest concentrations of Zn (100.80±1.40 mg/kg), Cd (0.92±0.02 mg/kg), Cu (31.39±1.04 mg/kg), Mn (188.57±2.25 mg/kg), Cr (21.03±1.43 mg/kg) and Pb (0.35±0.03 mg/kg) were recorded in soil at a distance of 1 m from the fecal sludge dumpsite. The values of Zn, Cd, Cu, Mn, Cr and Pb at 1 m are significantly ($P<0.05$) higher than their values at 5 m (87.30±2.75, 0.62±0.02, 19.13±0.15, 119.90±0.95, 10.07±1.10 and 0.28±0.01 mg/kg) and 15 m (37.33±0.99, 0.11±0.01, 13.63±0.47, 94.07±1.01, 6.00±0.20 and 0.16±0.00 mg/kg). Similarly, the values of PTE at 1 m is significantly ($P<0.05$) higher than their values at 30 m (13.40±1.20, 0.07±0.01, 6.27±0.31, 36.00±1.56, 2.40±0.40 and 0.09±0.02 mg/kg) as well as the control (2.10±0.02, 0.00±0.00, 0.45±0.03, 9.36±1.50, 0.01±0.00 and 0.00±0.00 mg/kg) for Zn, Cd, Cu, Mn, Cr and Pb, respectively. The PTE in the large volume of fecal sludge dumpsite may have provided a source for continued leaching and migration via runoff and have culminated to various level of contamination of Zn, Cd, Cu, Mn, Cr and Pb at the various distance of 1, 5, 15 and 30 m. Potentially toxic element like heavy metals are part of the composition of fecal sludge (Hashem, 2000).

**Table 5:** Heavy metal concentration in soils at various distances from fecal sludge dumpsite

| Distance (m) | Zn | Cd | Cu | Mn | Cr | Pb |
|---|---|---|---|---|---|---|
| 1 | $100.80^{a} \pm 1.40$ | $0.92^{a} \pm 0.02$ | $31.39^{a} \pm 1.04$ | $188.57^{a} \pm 2.25$ | $21.03^{a} \pm 1.43$ | $0.35^{a} \pm 0.03$ |
| 5 | $87.30^{b} \pm 2.75$ | $0.62^{b} \pm 0.02$ | $19.13^{b} \pm 0.15$ | $119.90^{b} \pm 0.95$ | $10.07^{b} \pm 1.10$ | $0.28^{b} \pm 0.01$ |
| 15 | $37.33^{c} \pm 0.99$ | $0.11^{c} \pm 0.01$ | $13.63^{c} \pm 0.47$ | $94.07^{c} \pm 1.01$ | $6.00^{c} \pm 0.20$ | $0.16^{c} \pm 0.00$ |
| 30 | $13.40^{d} \pm 1.20$ | $0.07^{d} \pm 0.01$ | $6.27^{d} \pm 0.31$ | $36.00^{d} \pm 1.56$ | $2.40^{d} \pm 0.40$ | $0.09^{d} \pm 0.02$ |
| Control | $2.10^{e} \pm 0.02$ | $0.00^{e} \pm 0.00$ | $0.45^{e} \pm 0.03$ | $9.36^{e} \pm 1.50$ | $0.01^{e} \pm 0.00$ | $0.00^{e} \pm 0.00$ |

*Values are mean ± standard deviation of 3 replicates*

$^{abc}$ *Means in a column with different superscripts are significantly different ($P<0.05$)*

The concentration of Zn in soil at the fecal sludge dumpsite was 13.40±1.20 to 100.80±1.40 mg/kg, which is below the Environmental Quality Standard of 421 mg/kg (Zn) set by National Environmental Standards and Regulations Enforcement Agency, NESREA (NESREA, 2011) of Nigeria, the accepted limit (i.e. target value) of 140 mg/kg (Zn) as described by Dutch criteria for soil (Ogbonna *et al*., 2020b) but higher than 60 mg/kg (Zn) established by Codex Alimentarius Commission (FAO/WHO, 2001) (Table 6). The concentration of Zn (100.80±1.40 mg/kg) at 1 m is 1.15, 2.70, 7.52 and 48 times higher than its values at 5 m, 15 m, 30 m from the fecal sludge dumpsite and control, respectively. The concentration of Zn (13.40±1.20 to 100.80±1.40 mg/kg) in soils at the various distance from the

fecal sludge dumpsite is lower than 122.92±0.06 to 235.75±0.04 mg/kg in soil at waste dumpsite in Uyo, Akwa Ibom State, Nigeria (Nkop *et al*., 2016) but higher than 43.37 to 76.37 mg/kg in soil at MSW dumpsite in Enugu State, Nigeria (Ajah *et al*., 2015), 13.82 to 17.26 mg/kg in soil at MSW dumpsite in Benue State, Nigeria (Anhwange and Kaana, 2013). The differences in the concentrations of PTE in soil from the fecal sludge area and municipal solid waste dumpsites may be attributed to source of wastes, composition and length of time the wastes has lasted at the dumpsites. Zinc is an essential nutrient in soil for the growth and development of plants.

The concentration of Cd in soil at the fecal sludge dumpsite was 0.07±0.01 to 0.92±0.02 mg/kg, which is higher than the maximum permitted level of 0.1 mg/kg (Cd) established by the Codex Alimentarius Commission (FAO/WHO, 2001), the accepted limit of 0.8 mg/kg (Cd) as described by Dutch criteria for soil (Ogbonna *et al*., 2020b) but lower than 50 mg/kg (Cd) set by National Environmental Standards and Regulations Enforcement Agency, NESREA (NESREA, 2011) of Nigeria. The concentration of Cd (0.92±0.02 mg/kg) at 1 m is 1.48, 8.36, 13.14 and 92 times higher than its values at 5 m, 15 m, 30 m from the fecal sludge dumpsite and control, respectively. The concentration of Cd (0.07±0.01 to 0.92±0.02 mg/kg) in soils at the various distances from the fecal sludge dumpsite is lower than 219 to 330 mg/kg in soil at waste dumpsite (Awokunmi *et al*., 2010).

**Table 6:** Comparison of concentration of heavy metals in soils with international and national standards (*ECDGE, 2010); Ogbonna *et al*. (2020a)

| Heavy metals | This study | NESREA 2011 | FEPA 1991 | FAO/WHO 2001, 2006, 2007 | Dutch criteria (target value) | Dutch criteria (intervention value) | *Sweden | *France | *UK | *Austria | *Germany | *USA |
|---|---|---|---|---|---|---|---|---|---|---|---|---|
| Cr | 2.40-21.03 | 100 | NA | 100 | 100 | 380 | 60 | 150 | 400 | 100 | 60 | NA |
| Cu | 6.27-31.39 | 100 | 70-80 | 100 | 36 | 190 | 40 | 100 | 135 | 60-100 | 40 | 75 |
| Pb | 0.09-0.35 | 164 | 1.6 | 50 | 85 | 530 | 40 | 100 | 300 | 100 | 70 | 15 |
| Zn | 13.40-100.80 | 421 | 300-400 | 60 | 140 | 720 | NA | NA | NA | NA | NA | 140 |
| Mn | 36-188.57 | NA | NA | NA | NA | NA | NA | NA | NA | NA | NA | NA |
| Cd | 0.07-0.92 | 3 | 0.01 | 0.1 | 0.8 | 12 | 0.4 | 2 | 3 | 1-2 | 1 | 1.9 |

NA = Not available

The concentrations of Cu and Mn in soil at the fecal sludge dumpsite in Ubakala, Nigeria were 6.27±0.31 to 31.39±1.04 and 36.00±1.56 to 188.57±2.25 mg/kg, respectively for Cu and Mn. The values of Cu in soil at the fecal sludge dumpsite at Ubakala, Nigeria was 6.27±0.31 to 31.39±1.04 mg/kg, which is lower than the maximum permitted level of 100 mg/kg (Cu) established by Codex Alimentarius Commission (FAO/WHO, 2001), the accepted limit of 36 mg/kg (Cu) as described by Dutch criteria for soil (Ogbonna *et al*., 2018a), 100 mg/kg (Cu) set by National Environmental Standards and Regulations Enforcement Agency, NESREA (NESREA, 2011) and 70-80 mg/kg (Cu) set by Federal Ministry of Environment (FMEnv, 2002) of Nigeria. The concentration of Cu (31.39±1.04 mg/kg) at 1 m is 1.64, 2.30, 5.01 and 69.76 times higher than its values at 5 m, 15 m, 30 m from the fecal sludge dumpsite and control, respectively. The concentration of Cu (6.27±0.31 to 31.39±1.04 mg/kg) in soils at the various distance from the fecal sludge dumpsite is lower than 2.18±0.1 to 1005.2±6.0 mg/kg in soil (Esakku *et al*., 2005) but higher than 6.68 to 11.4 mg/kg in soil (Anhwange and Kaana, 2013).

The concentration of Mn (188.57±2.25 mg/kg) at 1 m is 1.57, 2.00, 5.24 and 20.15 times higher than its values at 5 m, 15 m, 30 m from the fecal sludge dumpsite and control, respectively. The concentration of Mn (36.00±1.56 to 188.57±2.25 mg/kg) in soils at the various distance from the fecal sludge dumpsite is lower than 2000 mg/kg (Mn) in soil (FAO/WHO, 1984) but higher than 6.44 to 12.28 mg/kg in soil at MSW dumpsite in Enugu State, Nigeria (Ajah *et al*., 2015).

The concentrations of Cr and Pb in soil at the fecal sludge dumpsite were 2.40±0.40 to 21.03±1.43 and 0.09±0.02 to 0.35±0.03 mg/kg, respectively. The values of Cr (2.40±0.40 to 21.03±1.43 mg/kg) is well below the accepted limit of 100 mg/kg (Cr) as described by Dutch criteria for soil (Ogbonna *et al*., 2020a), the 100 mg/kg (Cr) established by Codex Alimentarius Commission (FAO/WHO, 2001),

the 100 mg/kg (Cr) set by National Environmental Standards and Regulations Enforcement Agency, NESREA of Nigeria (NESREA, 2011), 50 mg/kg (Cr) set by Ministry of Agriculture, Fisheries and Food, MAFF (MAFF, 1992) and 50 mg/kg (Cr) set by the European Commission, EC (EC, 1986). The concentration of Cr (21.03±1.43 mg/kg) at 1 m is 2.09, 3.51, 8.76 and 2,103 times higher than its values at 5 m, 15 m, 30 m from the fecal sludge dumpsite and control, respectively. The concentration of Cr (2.40±0.40 to 21.03±1.43 mg/kg) in soils at the various distances from the fecal sludge dumpsite is lower than 239.00±120 to 677.00±232 mg/kg in soil of landfilled foundry site in Poland (Bozym, 2019).

The concentration of Pb in soil at the fecal sludge dumpsite was 0.09±0.02 to 0.35±0.03 mg/kg, which is well below 164 mg/kg (Pb) set by National Environmental Standards and Regulations Enforcement Agency, NESREA (NESREA, 2011) of Nigeria, the accepted limit of 85 mg/kg (Pb) described by Dutch criteria for soil (Ogbonna *et al*., 2020a) and the maximum permitted level of 50 mg/kg (Pb) established by Codex Alimentarius Commission (FAO/WHO, 2001) (Table 6). The concentration of Pb (0.35±0.03 mg/kg) at 1 m is 1.25, 2.19, 3.89 and 35 times higher than its values at 5 m, 15 m, 30 m from the fecal sludge dumpsite and control, respectively. The concentration of Pb (0.09±0.02 to 0.35±0.03 mg/kg) in soils at the various distances from the fecal sludge dumpsite is lower than 9.10±0.1 to 271.9±22 mg/kg in soil (Esakku *et al*., 2005) and 125.72 to 138.48 mg/kg in soil (Ajah *et al*., 2015). Generally, the concentration of the potentially toxic element in soil followed a decreasing order: Mn>Zn>Cu>Cr>Cd>Pb. The purpose of ranking the PTEs is to show their level of distribution in soil in order of concentrations.

### *3.4. Potentially toxic element in food crops*

Table 7 shows the concentrations of Cd, Cu, Pb, Mn, Cr and Zn in leaves of *Carica papaya* L, *Telfairia occidentalis* Hook f. and *Manihot esculenta* Crantz sampled at the fecal sludge dumpsite area and control site of Ubakala, Nigeria. The results showed that the leaf concentrations of potentially toxic element in the contaminated site were significantly higher than that of the control site in all plant species. The result also indicates significant differences among the plant species sampled from the study site (i.e. fecal sludge dumpsite area). The disparity in concentrations of potentially toxic element in plant species tested in this study may be attributed to their dissimilarity in inherent ability to uptake potentially toxic element from soil (Ogbonna *et al*., 2018a). From the results, the highest concentrations of Zn (56.02±5.02 mg/kg), Cd (0.085±0.01 mg/kg), Cr (9.60±1.13 mg/kg) and Pb (0.008±0.00 mg/kg) were assimilated in the *Carica papaya* leaves and the values are significantly ($P<0.05$) different from their (Zn, Cd, Cr and Pb) values in *Telfairia occidentalis* and *Manihot esculenta* as well as some values of *Carica papaya* at various distance from the fecal sludge dumpsite (Table 7). The high concentrations of Zn, Cd, Cr and Pb in *Carica papaya* leaves may be attributed to its network of fibrous root that offered large surface area at the surface soil (0-15 cm) and beyond the surface soil (16-50 cm) as well as horizontal spread of its roots in soil. The papaya root is predominately a non-axial, fibrous system, composed of one or two 0.5–1.0 m long tap roots, and secondary roots that branch profusely (Marler and Discekici, 1997; Carneiro and Cruz, 2009).

The concentration of Zn increased from 1.24±0.06 to 56.02±5.02 mg/kg, which is higher than 22.09 to 45.71 mg/kg in tomato growing on soil amended with applied sewage sludge (Elloumi *et al*., 2016), 5.96±0.02 to 28.85±0.04 mg/kg in *Amaranthus hibridus*, *Talinum triangulare*, *Carica papaya*, *Ipomea batatas* and *Luffa aegyptiaca* at waste dump site (Obasi *et al*., 2013), 0.02 to 0.40 mg/kg in *Zea mays*, *Hibiscus sabdarifa*, *Abelmuschus esculentus*, *Amaranthus dubius* and *Arachis hypogea* at municipal waste dumpsite in Nasarawa State, Nigeria (Opaluwa *et al*., 2012). The concentration of Zn (1.24±0.06 to 56.02±5.02 mg/kg) in this study is relatively higher than the permissible limit of 50 mg/kg (Zn) established by the Codex Alimentarius Commission (FAO/WHO, 2006) (Table 8). Zinc is an essential element for healthy growth and development of plants, animal and man but will be harmful to flora and fauna when thethreshold limit is exceeded. High level of Zn is known to inhibit copper absorption, resulting to Cu deficiency symptoms (Tothert *et al*., 2016). Its (Zn) deficiency in flora and fauna may result to stunted growth and impair cell division.

**Table 7:** Heavy metal concentration in plants at various distances from the fecal waste dumpsite

| Distance (m) | Plant species | Zn | Cd | Cu | Cr | Pb | Mn |
|---|---|---|---|---|---|---|---|
| 1 | *Telfairia occidentalis* | $26.14^{c}$±2.10 | $0.007^{c}$±0.00 | $10.80^{a}$±2.01 | $4.01^{b}$±0.02 | $0.001^{b}$±0.00 | $17.21^{a}$±2.01 |
| | *Carica papaya* | $56.02^{a}$±5.02 | $0.085^{a}$±0.01 | $5.10^{b}$±0.03 | $9.60^{a}$±1.13 | $0.008^{a}$±0.00 | $8.60^{b}$±1.03 |
| | *Manihot esculenta* | $37.60^{b}$±3.28 | $0.011^{c}$±0.01 | $2.94^{c}$±0.06 | $2.06^{b}$±0.04 | $0.001^{b}$±0.00 | $4.91^{c}$±0.10 |
| 5 | *Telfairia occidentalis* | $14.20^{d}$±1.20 | $0.005^{d}$±0.00 | $1.84^{cd}$±0.01 | $0.60^{c}$±0.01 | $0.0001^{c}$±0.00 | $3.20^{c}$±0.13 |
| | *Carica papaya* | $24.11^{c}$±2.82 | $0.010^{c}$±0.01 | $1.04^{d}$±0.02 | $0.82^{c}$±0.02 | $0.0003^{c}$±0.01 | $1.60^{d}$±0.01 |
| | *Manihot esculenta* | $16.23^{d}$±2.04 | $0.009^{c}$±0.02 | $0.88^{d}$±0.04 | $0.63^{c}$±0.01 | $0.0002^{c}$±0.00 | $1.00^{d}$±0.03 |
| 15 | *Telfairia occidentalis* | $5.12^{e}$±0.12 | $0.001^{d}$±0.00 | $0.28^{e}$±0.01 | $0.04^{d}$±0.00 | $0.00001^{d}$±0.00 | $0.72^{e}$±0.01 |
| | *Carica papaya* | $7.00^{e}$±0.14 | $0.008^{c}$±0.00 | $0.64^{de}$±0.02 | $0.07^{d}$±0.00 | $0.00002^{d}$±0.01 | $0.31^{e}$±0.02 |
| | *Manihot esculenta* | $6.01^{e}$±0.04 | $0.003^{d}$±0.001 | $1.03^{d}$±0.03 | $0.02^{d}$±0.00 | $0.00001^{d}$±0.01 | $0.28^{e}$±0.00 |
| 30 | *Telfairia occidentalis* | $1.24^{f}$±0.06 | $0.0000^{e}$±0.000 | $0.002^{f}$±0.001 | $0.000^{e}$±0.00 | $<0.00001^{e}$±0.00 | $0.20^{e}$±0.00 |
| | *Carica papaya* | $2.01^{f}$±0.00 | $0.0000^{e}$±0.000 | $0.008^{f}$±0.001 | $0.001^{e}$±0.00 | $<0.00001^{e}$±0.00 | $0.18^{e}$±0.01 |
| | *Manihot esculenta* | $1.68^{f}$±0.03 | $0.0000^{e}$±0.000 | $0.009^{f}$±0.002 | $0.000^{e}$±0.00 | $<0.00001^{e}$±0.00 | $0.11^{e}$±0.00 |
| Control | *Telfairia occidentalis* | $0.22^{g}$±0.00 | BDL | $<0.0001^{g}$±0.00 | BDL | BDL | $0.06^{f}$±0.00 |
| | *Carica papaya* | $0.70^{g}$±0.01 | BDL | $<0.0001^{g}$±0.00 | BDL | BDL | $0.04^{f}$±0.00 |
| | *Manihot esculenta* | $0.31^{g}$±0.00 | BDL | $<0.0001^{g}$±0.00 | BDL | BDL | $0.01^{f}$±0.00 |

*Values are mean ± standard deviation of 3 replicates*

$^{abc}$ *Means in a column with different superscripts are significantly different (P<0.05)*

The concentration of Cd in the food crops increased from 0.0000±0.000 to 0.085±0.01 mg/kg, which is lower than 0.05 to 1.55 mg/kg in *Xanthosomasagittifolium*, *Telfairia occidentalis* and *Amaranthus hybridus* at municipal solid waste dumpsite in Awka, Nigeria (Nduka *et al*., 2008). The concentration of Cd (0.0000±0.000 to 0.085±0.01 mg/kg) in food crops is lower than the permissible limit of 0.2 mg/kg (Cd) established by the Codex Alimentarius Commission (FAO/WHO, 2006) (Table 8). Cadmium is a non-essential element in plant metabolism and has no nutritional benefits in human body (Ogbonna *et al*., 2020b). It (Cd) can be toxic even at low concentrations (Jain *et al*., 2007; Ogbonna *et al*., 2020a) as it replaces Zn biochemically and cause kidney damage (Feng *et al*., 2011).
The concentration of Pb in this study increased from <0.00001±0.00 to 0.008±0.00 mg/kg, which is lower than 1.95±0.04 to 16.75±0.04 mg/kg in *A. hybridus*, *T. triangulare*, *C. papaya*, *I. batatas* and *L. aegyptiaca* (Obasi *et al*., 2013) and 0.10 to 1.74 mg/kg in *X. sagittifolium*, *T. occidentals* and *A. hybridus* (Nduka *et al*., 2008). The concentration of Pb (<0.00001±0.00 to 0.008±0.00 mg/kg) in food crops is lower than the permissible limit of 0.30 mg/kg (Cd) established by the Codex Alimentarius Commission (FAO/WHO, 2007). Lead (Pb) is a non-essential element in plant metabolism and has no nutritional benefit in human body. Lead (Pb) exposure can impair brain and nervous system, cause chronic kidney disease even at relatively low blood Pb levels (ATSDR, 2007; IARC, 2006).

The concentration of Cr in plant leaves increased from 0.000±0.00 to 9.60±1.13 mg/kg, which is lower than 0.12 to 25.0 mg/kg in tomato (Elloumi *et al*., 2016). The concentration of Cr (0.000±0.00 to 9.60±1.13 mg/kg) in plant leaves is higher than the permissible limit of 2.30 mg/kg (Cr) established by Codex Alimentarius Commission (FAO/WHO, 2006). The fecal sludge with 4.47±0.34 mg/kg (Cr) and high concentration of Cr (21.03±1.43 mg/kg) in soil are implicated for the high values of Cr above the permissible limit of FAO/WHO in plant leaves. Chromium is essential for carbohydrate metabolism in animals (Tucker *et al*., 2005) but its (Cr) concentration in food crops tested in this study pose serious health risk to man and animals that depend on *C. papaya* leaves for food and

medicine in South east Nigeria. For instance, the leaves of *C. papaya* are a viable forage for West African dwarf (WAD) goats while infusion of the leaves is used therapeutically for treatment of malaria, headache and wound-healing. Besides the effects on hepatic and renal toxicity, *C. papaya* displays anti-malaria actions (Bhat and Surolia, 2001; Udoh *et al*., 2005; Imaga and Adepoju, 2010; Aravind *et al*., 2013), antitumor, wound-healing and free radical scavenging activity (Basalingappa *et al*., 2018), antimicrobial (Olagunju *et al*., 2009) and immunomodulatory activity on peripheral human blood mononuclear cells (Otsuki *et al*., 2010). Exposure to Cr could lead to allergic dermatitis in human, bleeding of the gastrointestinal tract, cancer of the respiratory tract and ulcers of the skin (Bhagure and Mirgane, 2010; Al Hagibi *et al*., 2018).

**Table 8:** Comparison of concentration of heavy metals in plants with international and national standards

| Heavy metals | This study | Related studies | NESREA | FAO/WHO 2001, 2006, 2007 | FEPA | DPR |
|---|---|---|---|---|---|---|
| Zn | 1.24±0.06 to 56.02±5.02 | 0.30-212.7 Onyedikachi *et al*. (2018) | NA | 0.3 | NA | NA |
| Cd | 0.0000±0.000 to 0.085±0.01 | 55.4-136.7 Raimi *et al*. (2019) | NA | 1.63 | NA | NA |
| Cu | 0.002±0.001 to 10.80±2.01 | 40.4-720.6 Al-Farraj and Al-Wabel, 2007 | NA | 50 | NA | NA |
| Cr | 0.000±0.00 to 9.60±1.13 | 49-7,521 González-Chávez *et al*. (2015) | NA | 0.2 | NA | NA |
| Pb | <0.00001±0.00 to 0.008±0.00 | 54.1-134.3 Raimi *et al*. (2019) | NA | 0.2 | NA | NA |
| Mn | 0.11±0.00 to 17.21±2.01 | 205-9,432 Olufemi *et al*. (2014)<br>196.5-2,925 Raimi *et al*. (2019)<br>31.95-2,654.11 Onyedikachi *et al*. (2018) | NA | 425 | NA | NA |

The highest concentrations of Cu (10.80±2.01 mg/kg) and Mn (17.21±2.01 mg/kg) are recorded in *Telfairia occidentalis* leaves and the values are significantly ($P<0.05$) higher than their (Cu and Mn) highest values in *C. papaya* and *M. esculenta* leaves. The concentration of Cu increased from 0.002±0.001 to 10.80±2.01 mg/kg, which is lower than 7.15 to 32.34 mg/kg in tomato (Elloumi *et al*., 2016) and 1.37±0.01 to 28.90±0.01 mg/kg in *A. hybridus, T. triangulare, C. papaya, I. batatas* and *L. aegyptiaca* (Obasi *et al*., 2013). The concentration of Cu (0.002±0.001 to 10.80±2.01 mg/kg) is below the permissible limit of 73.0 mg/kg (Cu) set by Codex Alimentarius Commission (FAO/WHO, 2001). The Recommended Dietary Allowance (RDA) of Cu for proper growth and human health of an adult ranges from 1.5 to 3 mg/day (Samira and Tawner, 2013). Copper is one of the essential micronutrients in plant metabolism. It (Cu) is part of enzymes involved in specific metabolic processes (Tothert *et al*., 2016) but it could cause damage to immune system, reproductive ability, liver, neurological system and gastrointestinal tract (ATSDR, 2004).

The concentration of Mn in plant leaves increased from 0.11±0.00 to 17.21±2.01 mg/kg, which is relatively lower than 0.10 to 20.57 mg/kg in *X. sagittifolium, T. occidentals* and *A. hybridus* (Nduka *et al*., 2008) but relatively higher than 1.95±0.02 to 15.36±0.02 mg/kg in *A. hybridus, T. triangulare, C. papaya, I. batatas* and *L. aegyptiaca* (Obasi *et al*., 2013). The concentration of Mn (0.11±0.00 to 17.21±2.01 mg/kg) is well below the permissible limit of 500 mg/kg (Mn) set by Codex Alimentarius Commission (FAO/WHO, 2001) (Table 8). The Recommended Dietary Allowance (RDA) of Mn for proper growth and human health of an adult ranges from 2 to 5 mg/day (Samira and Tawner, 2013). Manganese is essential element in plant metabolism and has nutritional benefit in human body. For instance, Mn play key role in photosynthetic processes in plants (Lei *et al*., 2007). Exposure to high dose of Mn affects the respiratory tract and brain of human and the symptoms include hallucinations, forgetfulness and nerve damage (Prashanth *et al*., 2015). The sequence of potentially toxic element in plant leaves at the fecal sludge dumpsite area was found in the order of Pb<Cd<Cr<Cu<Mn<Zn. The purpose of ranking the PTEs is to show their level of accumulation in food crops in order of concentrations.

### *3.5. Pearson correlation between PTE in soil and food crops*

The result of the Pearson correlation analysis of potentially toxic elements in soil and food crops is summarized in Table 9. The result show strong positive relationship between PTE in soil and food

crops; very strong positive relationship between PTE in soil. Emphatically, strong positive relationship exist between Zn in soil and food crops (r = 0.616, p<0.05) and Cu in soil and food crops (r = 0.544, p<0.05), which suggest that increase in Zn and Cu in soil culminated in their (Zn and Cu) increase in food crops. In addition, strong positive relationship exist between Zn in food crops and Pb in soil (r = 0.571, p<0.05). More so, strong relationship occur between Cu in food crops and Mn in soil (r = 0.6000, p<0.05) and Cu in food crops and Pb in soil (r = 0.560, p<0.05). Furthermore, very strong positive relationship occur between Zn and Cd in food crops (r = 0.601, p<0.01), Zn and Cu in food crops (r = 0.813, p<0.01), Zn and Mn in food crops (r = 0.770, p<0.01), Zn and Cr in food crops (r = 0.854, p<0.01), Zn and Pb in food crops (r = 0.661, p<0.01). In furtherance of this, very strong positive relationship exist between Cu and Mn in food crops (r = 0.959, p<0.01), Cu and Cr in food crops (r = 0.897, p<0.01), Cu and Pb in food crops (r = 0.890, p<0.01), Mn and Cr in food crops (r = 0.961, p<0.01), Mn and Pb in food crops (r = 0.886, p<0.01) and Cr and Pb in food crops (r = 0.813, p<0.01). Similarly, very strong positive relationship occur between Zn and Cd in soil (r = 0.966, p<0.01), Zn and Cu in soil (r = 0.955, p<0.01), Zn and Mn in soil (r = 0.955, p<0.01), Zn and Cr in soil (r = 0.923, p<0.01). In addition to this, very strong positive relationship exist between Zn and Pb (r = 0.981, p<0.01), Cd and Cu in soil (r = 0.942, p<0.01), Cd and Mn in soil (r = 0.929, p<0.01), Cd and Cr in soil (r = 0.953, p<0.01), Cd and Pb in soil (r = 0.942, p<0.01). Lastly, very strong positive relationship occur between Cu and Mn in soil (r = 0.996, p<0.01), Cu and Cr in soil (r = 0.982, p<0.01), Cu and Pb in soil (r = 0.976, p<0.01), Mn and Cr in soil (r = 0.971, p<0.01), Mn and Pb in soil (r = 0.975, p<0.01) as well as Cr and Pb in soil (r = 0.942, p<0.01).

**Table 9:** Correlation between heavy metals in soil and plants

| | Zn (soil) | Cd (soil) | Cu (soil) | Mn (soil) | Cr (soil) | Pb (soil) | Zn (plant) | Cd (plant) | Cu (plant) | Mn (plant) | Cr (plant) | Pb (plant) |
|---|---|---|---|---|---|---|---|---|---|---|---|---|
| Zn (soil) | 1 | | | | | | | | | | | |
| Cd (soil) | 0.966** | 1 | | | | | | | | | | |
| Cu (soil) | 0.955** | 0.942** | 1 | | | | | | | | | |
| Mn (soil) | 0.955** | 0.929** | 0.996** | 1 | | | | | | | | |
| Cr (soil) | 0.923** | 0.953** | 0.982** | 0.971** | 1 | | | | | | | |
| Pb (soil) | 0.981** | 0.942** | 0.976** | 0.975** | 0.942** | 1 | | | | | | |
| Zn (plant) | 0.616* | 0.414 | 0.456 | 0.500 | 0.328 | 0.571* | 1 | | | | | |
| Cd (plant) | 0.345 | 0.283 | 0.213 | 0.225 | 0.188 | 0.301 | 0.601** | 1 | | | | |
| Cu (plant) | 0.521* | 0.320 | 0.544* | 0.600* | 0.425 | 0.560* | 0.813** | 0.319 | 1 | | | |
| Mn (plant) | 0.287 | 0.061 | 0.299 | 0.364 | 0.167 | 0.325 | 0.770** | 0.288 | 0.959** | 1 | | |
| Cr (plant) | 0.231 | -0.015 | 0.170 | 0.232 | 0.021 | 0.246 | 0.854** | 0.412 | 0.897** | 0.961** | 1 | |
| Pb (plant) | 0.313 | 0.111 | 0.360 | 0.406 | 0.232 | 0.353 | 0.661** | 0.094 | 0.890** | 0.886** | 0.813** | 1 |

**. Correlation is significant at 5% (P<0.05).*
***. Correlation is significant at 1% (P<0.01).*

## 4.0. Conclusion

The study shows that potentially toxic element (Cd, Zn, Pb, Cu, Cr and Mn) were present in the fecal sludge at Ubakala, Nigeria. The PTE were distributed in soil at various concentrations and assimilated at varying levels in *C.papaya*, *T. occidentalis* and *M. esculenta* leaves. The concentrations of the PTEs tested in dried fecal sludge were below the permitted limits established by European Union, China and Sweden. Zinc (Zn) concentration in soil is higher than the permissible limit established by Codex Alimentarius Commission while Cd is higher than both FAO/WHO limit and Dutch criteria for soil. The concentration of Zn and Cr in food crops is higher than the permissible limit established by the Codex Alimentarius Commission. Thus, prolong utilization of the food crops by human and animals might have serious deleterious effects on them. Strong positive relationship exist between Zn in soil and food crops (r = 0.616, p<0.05) and Cu in soil and food crops (r = 0.544, p<0.05). Very

strong positive relationship occur between Zn and Cd in food crops ($r = 0.601$, $p<0.01$), Zn and Cu in food crops ($r = 0.813$, $p<0.01$) while very strong positive relationship occur between Zn and Cd in soil ($r = 0.966$, $p<0.01$) and Zn and Cu in soil ($r = 0.955$, $p<0.01$). Considering the level of Zn and Cd in soil, we recommend that the fecal sludge should be treated with lime to precipitate PTE content of sludge and lowering the corresponding environmental risks.

**Conflict of interest**

There is no conflict of interest.

**References**

Abdullah, N.H., Mohamed, N., Sulaiman, L.H., Zakaria, T.A. and Rahim, D.A. (2016). Potential health impacts of bauxite mining in Kuantan. *Malaysian Journal of Medical Sciences*, 23(3), pp. 1–8.

Ackah, E.K. (2016). Assessment of the suitability of sludge from Dompoase faecal sludge treatment plant as a building material. A Thesis report submitted to the Department of Civil Engineering, Kwame Nkrumah University of Science and Technology for the award of degree of Master of Science (M.Sc.) in Water Supply and Environmental Sanitation, pp. 87.

Adeyeye, E.I. (2005). Distribution of major elements (Na, K, Ca, Mg) in the various anatomical parts of FADAMA crops in Ekiti State, Nigeria. *Bulletin of the Chemical Society of Ethiopia*, 19(2), 175-183.

Agency for Toxic Substances and Disease Registry, ATSDR (2007). Toxicological Profile for Lead. U.S. Department of Health and Human Services, p. 582.

Agency for Toxic Substances and Disease Registry, ATSDR (2004). Toxicological Profile for Copper. U.S. Department of Health and Human Services, p. 272.

Ahmed, I., Ofori-Amanfo, D., Awuah, E. and Cobbold, F. (2019). A comprehensive study on the physicochemical characteristics of faecal sludge in greater Accra Region and analysis of its potential use as feedstock for green energy. *Journal of Renewable Energy*, 2019, pp. 1-11.

Ajah, K.C., Ademiluyi, J. and Nnaji, C.C. (2015). Spatiality, seasonality and ecological risks of heavy metals in the vicinity of a degenerate municipal central dumpsite in Enugu, Nigeria. *Journal of Environmental Health Science and Engineering*, 13, pp. 15-28.

Alayu, E. and Leta, S. (2020). Brewery sludge quality, agronomic importance and its short‐term residual effect on soil properties. *International Journal of Environmental Science and Technology*, 17, pp. 2337–2348.

Al-Farraj, A.S., and Al-Wabel, M.I. (2007). Heavy metals accumulation of some plants species grown on mining area at Mahad AD'Dahab, Saudi Arabia. Journal of Applied Sciences 7: 1170–1175.

Al Hagibi, H.A., Al-Selwi, K.M., Nagi, H.M. and Al-Shwafi, N.A. (2018). Study of heavy metals contamination in mangrove sediments of the Red Sea coast of Yemen from Al-Salif to Bab-el-Mandeb Strait. *Journal of Ecology and Natural Resources*, 2(1), pp. 121-138.

Amos-Tautua, B.M.W., Onigbinde, A.O. and Ere, D. (2014). Assessment of some heavy metals and physicochemical properties in surface soils of municipal open waste dumpsite in Yenagoa, Nigeria. *African Journal of Environmental Science and Technology*, 8(1), pp. 41-47.

Amusan, A.A., Ige, D.V. and Olawale, R. (2005). Characteristics of soils and crops uptake of metals in municipal waste dumpsites in Nigeria. *Journal of Human Ecology*, 17(3), pp. 167-171.

Angelidis, M.O. and Aloupi, M. (1999). Assessment of sewage sludge quality in Greece. *Toxicological and Environmental Chemistry*, 68(1-2), pp. 133-139.

Anhwange, B.A. and Kaana, A. (2013). Evaluation of heavy metals in waste dumpsites. IAP Lambert Academic Publishing, Heinrich-Bocking Str. 6-8, 66121 Saarbrucken, Deutschland/Germany, pp. 1-54.

Antonious, G., Lobel, L., Kochhar, T., Berke, T. and Jarret, R.L. (2009). Antioxidants in *C. chinense*: variation among Countries Origin. *Journal of Environmental Science and Health*, Part B, 44 (6), pp. 621-666.

Appiah-Effah, E., Nyarko, K.B., Gyasi, S.F. and Awuah, E. (2014). Faecal sludge management in low income areas: a case study of three districts in the Ashanti Region of Ghana. *Journal of Water, Sanitation and Hygiene Development*, 4, pp. 189–199.

Aravind. G, Debjit, B., Duraivel, S. and Harish, G. (2013). Traditional and Medicinal Uses of *Carica papaya*. *Journal of Medicinal Plants Studies*, 1(1), pp. 7-15.

Arshad, M.A. and Coen, G.M. (1992). Characterization of soil quality: Physical and chemical criteria. American *Journal of Alternative Agriculture*, 7, pp. 25-31.

Awokunmi, E.E, Asaolu, S.S. and Ipinmoroti, K.O. (2010). Effect of leaching on heavy metals concentration of soil in some dumpsites. *African Journal of Environmental Science and Technology*, 4, pp. 495-499.

Awotoye, O.O., Ogunkunle, C.O. and Adeniyi, S.A. (2011). Assessment of soil quality under various land use practices in a humid agro-ecological zone of Nigeria. *African Journal of Plant Science*, 5(10), pp. 565-569.

Ayari, F., Hamdi, H.,Jedidi, N., Gharbi, N. and Kossai, R. (2010). Heavy metal distribution in soil and plant in municipal solid waste compost amended plots. *International Journal of Environmental Science and Technology*, 7(3), pp. 465-472.

Basalingappa, K.M., Anitha, B., Raghu, N., Gopenath, T.S., Karthikeyan, M., *et al*. (2018). Medicinal uses of *Carica papaya*. *Journal of Natural and Ayurvedic Medicine*, 2(6), pp. 144-154.

Bassan, M., Brdjanovic, D., Dangol, B., Dodane, P., Hooijmans, C.M., *et al*. (2014). Faecal sludge management systems approach for implementation and operation. Editors L. Strande, M. Ronteltap, and D. Brdjanovic. IWA PublishingAlliance House, 12 Caxton Street London SW1H 0QS, UK, pp. 1-427.

Bhagure, G.R. and Mirgane, S.R. (2010). Heavy metals contaminations in groundwater and soils of Thane Region of Maharashtra, India. *Environmental Monitoring and Assessment*, 173(1-4), pp. 643-652.

Bhat, G.P. and Surolia, N. (2001). In vitro antimalarial activity of extracts of three plants used in the traditional medicine of India. *American Journal of Tropical Medicine and Hygiene*, 65, 304–308.

Bhowmick, A.C., Salma, U., Siddiquee, T.A., Russel, M. and Bhoumik, N.C. (2013). Effect of temperature on the uptake of Na+, K+, Ca2+and Mg2+ by the various anatomical parts of the vegetable *Amaranth gangeticus*. *IOSR Journal of Environmental Science, Toxicology and Food Technology*, 3(6), pp. 20-31.

Bożym, M. (2019). Assessment of leaching of heavy metals from landfilled foundry waste during exploitation of the heaps. *Polish Journal of Environmental Studies*, 28(6), pp. 4117-4126.

Brady, N.C. and Weil, R.R. (2000). The Nature and property of soils. Prentice Hall, Inc. pp. 123-127 and 506-511.

Brummer, G. and Herms, U. (1982). Effects of accumulation of Air pollutants in Forest ecosystems, Reidel Publishing Company, pp. 233 -243.

Bu, H., Wang, W., Song, X. and Zhang, Q. (2015). Characteristics and source apportionment of dissolved trace elements in the Jinshui River of the South Qinling Mts., China. *Environmental Science and Pollution Research*, 22(18), pp. 14248-14257.

Carneiro, C.E. and Cruz, J.L. (2009). Caracterizaçãoanatômica de órgãosvegetativos do mamoeiro. Ciênc Rural 39(3), pp. 918–921.

Chen, T., Huang, Q.F., Gao, D., Zheng, Y.Q. Wu, J.F. (2003) Heavy metal concentrations and their decreasing trends in sewage sludges of China. *Acta Scientiae Circumstantiae*, 23, pp. 561-569.

Davies, B.E., (1983). A graphical estimation of the normal lead content of some British soils. *Geoderma*, 29, pp. 67-75.

Doran, J.W., Sarantonio, M. and Leibig, M. (1996). Soil health and sustainability. *Advances in Agronomy*, 56, pp. 1-54.

Elloumi, N., Belhaj, D., Jerbi, B., Zouari, M. and Kallel, M. (2016). Effects of sewage sludge on bio-accumulation of heavy metals in tomato seedlings. *Spanish Journal of Agricultural Research*, 14(4), pp. 1-13.

Esakku, S., Selvam, A., Joseph, K. and Palanivelu, K. (2005) Assessment of heavy metal species in decomposed municipal solid waste. *Chemical Speciation and Bioavailability*, 17(3), pp. 95-102.

European Community (1986). Commission Directive No. 278. *Official Journal of the European Communities*, 181, pp. 5-12.

European Commission, EC (2000). DG Environment, Working Document on Sludge, 3rd Draft, Brussels. Available from: http://ec.europa.eu/environment/waste/sludge/pdf/sludge en.pdf.

European Commission Director General Environment, ECDGE (2010). Heavy Metals and Organic Compounds from Wastes Used as Organic Fertilizers. Final Rep., July. WPA Consulting Engineers Inc. Ref. Nr. TEND/AML/2001/07/20, pp. 73-74. http://ec.europa.eu/environment/waste/compost/pdf/hm_finalreport.pdf.

FAO/WHO (1984). List of maximum levels recommended for contaminants by the Joint FAO/WHO Codex Alimentarius Commission (3rdSeries), CAC/FAL, Rome, 3, pp. 1-8.

FAO/WHO (2001). Food additives and contaminants. Joint FAO/WHO Food Standards Program, ALINORM 01/12A, 1-289.

FAO/WHO (2006). Guidelines for assessing Quality of Herbal Medicines with Reference to Contaminants and Residues, World Health Organization, Geneva, Switzerland.

FAO/WHO (2007). Joint FAO/WHO Food Standard Programme Codex Alimentarius Commission 13th Session. Report of the Thirty Eight Session of the Codex Committee on Food Hygiene. Houston, TX, ALINORM 07/30/13.

Federal Ministry of Environment, FMEnvi Report (2002) Studies on the construction of industrial effluent treatment facilities in Kaduna.

Feng, H., Jiang, H.Y., Gao, W.S., Weinstein, M.P., Zhang, Q.F., *et al*. (2011). Metal contamination in sediments of the western Bohai Bay and adjacent estuaries, China. *Journal of Environmental Management*, 92(4), pp. 1185-1197.

Fonge, B.A., Nkoleka, E.N., Asong, F.Z., Ajonina, S.A. and Che, V.B. (2017). Heavy metal contamination in soils from a municipal landfill, surrounded by banana plantation in the eastern flank of Mount Cameroon. *African Journal of Biotechnology*, 16(25), pp. 1301-1399

Funke, O.M. (2011). Evaluation of nutrient contents of Amaranth leaves prepared using different cooking methods. *Food and Nutrition Sciences*, 2(4), pp. 249-252.

González-Chávez, M.A., Sánchez-López, A.S. and González, R.C. (2015). Arsenic concentration in wild plants growing on two mine tailings. *Pharmacognosy Communications*, 5(3), pp. 197-206.

Gosslau, A. and Chen, K.Y. (2004). Nuetraceuticals, apoptosis and disease prevention. *Nutrition*, 20(1), pp. 95-102.

Greek legislation 80568/4225/91of 22 March 1991 on methods, specifications and requirements for the use in agriculture of the sludge originating from household and urban waste treatment, harmonized from European Council Directive 86/278/EEC.

Gupta, S., Lakshmi, J. and Prakash, J. (2008). Effect of different blanching treatments on ascorbic acid retention in green leafy vegetables, *Natural Product Radiance*, 7(2), pp. 111-116.

Hashem, A. R. (2000). Microbial and mineral content of sewage sludge from Riyadh and Yanbu, Saudi Arabia. *Emirates Journal of Agricultural Sciences*, 12, pp. 33–41.

Huet, J., Kristin, B., Vincent, R. and Yvan, L. (2006). Structural characterization of the papaya cysteine proteinases at low pH. *Biochemical and Biophysical Research Communications*, 341(2), pp. 620-626.

Ideriah, J.K.T., Harry, F.O., Stanley, H.O. and Igbara, J.K. (2010). Heavy metal contamination of soils and vegetation around solid waste dumps in Port Harcourt, Nigeria. *Journal of Applied Sciences and Environmental Management*, 14(1), pp. 101-109.

International Agency for Research on Cancer, IARC (2006). Monographs on the evaluation of carcinogenic risks to humans, Inorganic and organic lead compounds, Lyon, France, vol. 87, p. 519.

Imaga, N.A. and Adepoju, O.A. (2010). Analyses of anti-sickling potency of *Carica papaya* dried leaf extract and fractions. *Journal of Pharmacognosy Phytotherapy*, 2(7), pp. 97-102.

Jain, M., Pal, M., Gupta, P. and Gadre, R. (2007). Effect of cadmium on chlorophyll biosynthesis and enzymes of nitrogen assimilation in greening maize leaf segments: role of 2-oxoglutarate. *Indian Journal of Experimental Biology*, 45(4), pp. 385-389.

Keay, R.W.J. (1959). An outlines of Nigeria vegetation. 3rd ed. Government Printer, Lagos, Nigeria.

Larson, W.E. and Pierce, F.J. (1991). Conservation and enhancement of soil quality. Evaluation for sustainable land management in the developing world, vol. 2. IBSRAM Proceedings 12, 2 Technical Papers, International Board for Soil Research and Management, Bangkok, Thailand, pp. 175-203.

Lee, Y, Lee, H.J., Lee, H.S., Jang, Y.A. and Kim, C. (2008). Analytical dietary fiber database for the National Health and Nutrition Survey in Korea. *Journal of Food Composition and Analysis*, 21, pp. 35-42.

Lei, Y., Korpelainen, H. and Li, C. (2007).Physiological and biochemical responses to high Mn concentrations in two contrasting *Populuscathayana*populations. *Chemosphere*, 68, pp. 686-694.

Lopez Zavala, M.A. (2002). Characterization of feces for describing the aerobic biodegradation of feces. *Journal of. Environ Syst. and Engineering*, 720(VII-25), pp. 99-105.

MAFF (Ministry of Agriculture, Fisheries and Food) and Welch Office Agriculture Department (1992). Code of Good Agriculture Practice for the Protection of Soil. Draft Consultation Document, MAFF, London.

Marler, T.E. and Discekici, H.M. (1997). Root development of 'Red Lady' papaya plants grown on a hillside. *Plant Soil*, 195(1), pp. 37–42.

Ministerial Decision Greek legislation (1991). 80568/4225/91 of 22 March 1991 on methods, specifications and requirements for the use in agriculture of the sludge originating from household and urban waste treatment, harmonized from European Council Directive 86/278/EEC, 1991.

Mtshali, J.S., Tiruneh, A.T. and Fadiran, A.O. (2014). Assessment of mobility and bioavailability of heavy metals in sewage sludge from Swaziland through speciation analysis. *Resources and Environment*, 4(4), pp. 190–199.

Montagnac, J.A., Davis, C.R. and Tanumihardjo, S.A. (2009). Nutritional value of cassava for use as a staple food and recent advances for improvement. *Comprehensive Reviews in Food Science and Food Safety*, 8, pp. 181-194.

Nduka, J.K.C., Orisakwe, O.E., Ezenweke, L.O., Chendo, M.N. and Ezenwa, T.E., *et al*. (2008). Heavy metal contamination of foods by refuse dump sites in Awka, Southeastern Nigeria. *The Scientific World Journal*, 8, pp. 941–948.

NESREA (2011). "1st Eleven Gazetted Regulations Federal Republic of Nigeria Official Gazette".

Nkop, E.J., Ogunmolasuyi, A.M., Osezua, K.O. and Wahab, N.O. (2016). Comparative study of heavy metals in the soil around waste dump sites within University of Uyo. *Archives of Applied Science Research*, 8(3), pp. 11-15.

Obasi, N.A. Akubugwo, E.I., Kalu, K.M. and Ugbogu, O.C. (2013). Speciation of heavy metals and phyto-accumulation potentials of selected plants on major dumpsites in Umuahia, Abia State, Nigeria. *International Journal of Current Biochemistry Research*, 1(4), pp. 16-28.

Ogbonna, P.C., Odukaesieme, C. and Teixeira da Silva, J.A. (2013). Distribution of heavy metals in soil and accumulation in plants at an agricultural area of Umudike, Nigeria. *Chemistry and Ecology*, 29(7), pp. 595-603.

Ogbonna, P.C., Kalu, E.N. and Nwankwo, O.U. (2018a). Determination of heavy metals in sawdust particles, distribution in soil and accumulation in plants at Ahiaeke timber market. *Nigerian Journal of Environmental Sciences and Technology*, 2(2), pp. 160-170.

Ogbonna, P.C., Nzegbule, E.C. and Okorie, P.E. (2018b). Soil chemical characteristics in wet and dry season at Iva long wall underground mined site, Nigeria. *Nigerian Journal of Environmental Sciences and Technology*, 2(1), pp. 96-107.

Ogbonna, P.C., Nzegbule, E.C., Obasi, K.O. and Kalu, H. (2018c). Heavy metals in soil and accumulation in medicinal plants at an industrial area in Enyimba city, Abia State, Nigeria. *Nigerian Journal of Environmental Sciences and Technology*, 2(1), pp. 89-95.

Ogbonna, P.C., Osim, O.O. and Biose, E. (2020a). Determination of heavy metal contamination in soil and accumulation in Cassava (*Manihot esculenta*) in automobile waste dumpsite at Ohiya mechanic village. *Nigerian Journal of Environmental Sciences and Technology*, 4(1), pp. 54-69.

Ogbonna, P.C., Ukpai, N.P., Obasi, K.O. and Umezuruike, S.O. (2020b). Monitoring the distribution of potentially toxic elements in soil and accumulation in fodder and medicinal plant species at a quarry site in Ebonyi State, Nigeria. *Nigerian Research Journal of Engineering and Environmental Sciences*, 5(2) 2020 pp. 535-553.

Okeniyi, J.A.O., Ogunlesi, T.A., Oyelami, O.A. and Adeyemi, LA. (2007). Effectiveness of dried *Carica papaya* against human intestinal parasitosis: A pilot study. *Journal of Medicine and Food,* 10(1), pp. 194-196.

Okonwu, K., Akonye, L.A. and Mensah, S.I. (2018). Nutritional composition of *Telfairia occidentalis* leaf grown in hydroponic and geoponic Media. *Journal of Applied Sciences and Environmental Management*, 22(2), pp. 259–265.

Olagunju, J., Adeneye, A., Fagbohunka, B., Bisuga, N., Ketiku, A., *et al*. (2009). Nephroprotective activities of the aqueous seed extract of Carica papaya Linn. In carbon tetrachloride induced renal injured Wistar rats: a dose-and time-dependent study. *Biology and Medicine*, 1, pp. 11–19.

Olness, A. and Archer, D. (2005). Effect of organic carbon on available water in soil. *Soil Science*, 170, pp. 90–101.

Olufemi, J.A., Olubunmi, S.S. and Temitope, B. (2014). Heavy metal pollution assessment of granite quarrying operations at Ikole-Ekiti, Nigeria. *International Journal of Environmental Monitoring and Analysis.* 2(6), pp. 333-339.

Onyedikachi, U.B., Belonwu, D.C. and Wegwu, M.O. (2018). Human health risk assessment of heavy metals in soils and commonly consumed food crops from quarry sites located at Isiagwu, Ebonyi State. *Ovidius University Annals of Chemistry*, 29(1), pp. 8-24.

Opaluwa, O. D., Aremu, M. O., Ogbo, L. O., Abiola, K. A., Odiba, I. E. (2012). Heavy metal concentrations in soils, plant leaves and crops grown around dump sites in Lafia Metropolis, Nasarawa State, Nigeria. *Advances in Applied Science Research*, 3 (2), pp. 780-784.

Otsuki, N., Dang, N.H., Kumagai, E., Kondo, A., Iwata, S. (2010). Aqueous extract of *Caricapapaya* leaves exhibits anti-tumor activity and immunemodulatory effects. *Journal of Ethnopharmacology*, 127, pp. 760–767.

Oyedele, D.J., Gasu, M.B., Awotoye, O.O. (2008). Changes in soil properties and plant uptake of heavy metals on selected municipal solid waste dump sites in Ile-Ife, Nigeria. *African Journal of Environmental Science and Technology*, 3(5), pp. 107-115.

Pape, P., Ayrault, S. and Cecile, Q. (2012). Trace element behavior and partition versus urbanization gradient in an urban river (Orge River, France). *Journal of Hydrology*, 99, pp. 472-473.

Pearson, D. (1976) Chemical Analysis of Foods. 7th Edition, Churchhill Livingstone, London.

Pitchell, J. and Anderson, M., (1997). Trace metal bioavailability in municipal solid waste and sewage sludge composts. *Bioresource Technology*, 60, pp. 223-229.

Pinnamaneni, R. (2017). Nutritional and medicinal value of Papaya (Carica papaya Linn). *World Journal of Pharmacy and Pharmaceutical Sciences*, 6(8), pp. 2559-2578.

Prashanth, L., Kattapagari, K.K., Chitturi, R.T., Baddam, V.R.R. and Prasad, L.K., *et al*. (2015). A review on role of essential trace elements in health and disease. *Journal of NTR University of Health Sciences*, 4, pp. 75-85.

Raimi, I.O., Komolafe, B.F., Agboola, O.O., Mugivhisa, L.L. and Olowoyo, J.O. (2019). Influence of wind direction on the level of trace metals in plants collected around a quarry site in South Africa. *Polish Journal of Environmental Studies*, 28(5), pp. 3385-3393.

Rhoades, J.D. (1996). Salinity: Electrical conductivity and total dissolved solids. In Methods of Soil Analysis: Chemical Methods. Part 3. D.L. Sparks, editor. Soil Sci. Soc. of Am., Madison WI.

Samira, I.K. and Tawner, H.M.M. (2013), "Evaluation of heavy metals content in dietary supplements in Lebanon". *Chemistry Central Journal*, 7, pp. 1-12.

Santana, L.F., Inada, A.C., Santo, B.L.S.E., Filiú, W.F.O., Pott, A., *et al*. (2019). Nutraceutical potential of *Carica papaya* in metabolic syndrome. *Nutrients*, 11, pp. 1608-1626.

Saviozzi, A., Riffaldi, R. andCardelli, R. (1994). Suitability of a winery—sludge as soil amendment. *Bioresources Technology*, 49, pp. 173–178.

Shamuyarira, K.K. and Gumbo, J.R. (2014). Assessment of Heavy Metals in Municipal Sewage Sludge: A Case Study of Limpopo Province, South Africa. *International Journal of Environmental Research and Public Health***,** 11, pp. 2569–2579.

Sikora, L. and Stott, D. (1996). Soil organic carbon and nitrogen. In: Doran W and Jones A (eds) Methods for Assessing Soil Quality, vol. 49, pp. 157–167. SSSA, Madison, WI.

Singh, A., *et al*. (2010). Risk assessment of heavy metal toxicity through contaminated vegetables from wastewater irrigated areas in Varanasi, India. *Journal of Tropical Ecology*, 51(2), pp. 375-387.

Smith, J. L. and Doran, J. W. (1996). Measurement and use of pH and electrical conductivity for soil quality analysis. In J. W. Doran and A. J. Jones (Eds.), Methods for assessing soil quality, pp. 169–185). Madison, WI: SSSA.

Spanos, T., Ene, A., Patronidou, C.S. and Xatzixristou, C. (2016). Temporal variability of sewage sludge heavy metal content from Greek wastewater treatment plants. *Ecological Chemistry and Engineering*, 23(2), pp. 271-283.

Stefanakis, A.I. and Tsihrintzis, V.A. (2012). Heavy metal fate in pilot-scale sludge drying reed beds under various design and operation conditions. *Journal of Hazardous Materials*, 213-214, pp. 393-405.

Strande, L., Ronteltap, M. and Brdjanovic, D. (2014). Faecal sludge management: systems approach for implementation and operation, IWA Publishing. *IWA Publishing*, Alliance House 12 Caxton Street, London SW1H 0QS, UK.

Strauss, M., Heinss, U. and Montangero, A. (2000). On-Site Sanitation: When the pits are full – Planning for esource protection in faecal sludge management. In: Proceedings, International Conference, Bad Elster, 20–24 Nov. 1998. Schriftenreihe des Vereins fuer Wasser-, Boden und Lufthygiene, 2000;105:353-60: Water, Sanitation and Health – Resolving Conflicts between Drinking Water Demands and Pressures from Society's Wastes (I. Chorus, U. Ringelband, G. Schlag, and O. Schmoll, eds.). IWA Publishing House and WHO Water Series.

Tóthert, G., Hermann, T., Da Silva, M.R. and Montanarella, L. (2016). Heavy metals in agricultural soils of the European Union with implications for food safety. *Environment International*, 88, pp. 299-309.

Tucker M R, Hardy D H and Stokes C E. (2005) Heavy metals in North Carolina soils: occurrence and significance. North Carolina Department of Agriculture and Consumer Services, pp. 1-2.

Udoh P, Essien I. and Udoh F. (2005). Effect of *Carica papaya* (paw paw) seeds extract on the morphology of pituitary-gonadal axis of male Wistar rats. *Phytotherapy Research*, 19, pp. 1065–1068.

UNICEF and WHO (2009). Diarrhoea: Why children are still dying and what can be done.

Varol, M., Gakot, B. and Bekleyen, A. (2013). Dissolved heavy metals in the Tigris River (Turkey): spatial and temporal variations. *Environmental Science and Pollution Research*, 20, pp. 6096-6108.

Vongdala, N., Tran, H., Xuan, T.D.,Teschke, R. and Khanh, T.D. (2019). Heavy metal accumulation in water, soil, and plants of municipal solid waste landfill in Vientiane, Laos. *Environmental Research and Public Health*, 16(22), pp. 1-12.

Walkley, A. and Black, I.A. (1934). An examination of the Degtajareff method for soil organic matter determination and a proposed modification of the chronic acid titration. *Soil Science*, 37, pp. 29-38.

Wang, S. and Mulligan, C.N. (2005). Occurrence of Arsenic contamination in Canada: Sources behavior and distribution. *Science of the total Environment*, 366, pp. 701-721.

WHO (2006). Guidelines for the safe use of wastewater, excreta and greywater. Volume 4. Excreta and greywater use in agriculture. ISBN 92 4 1546859.

Yeketetu, B.A. (2017). Toxic heavy metal and Salinity assessment In: Water, soil and vegetables around Meki irrigation farms. *International Journal of Scientific and Technology Research*, 6(9), pp. 5-10.

Zziwa, A., Nabulime, M.N., Kiggundu, N., Kambugu, R., Katimbo, A. *et al*. (2016). A critical analysis of physiochemical properties influencing pit latrine emptying and feacal sludge disposal in Kampala Slums, Uganda. *African Journal of Environmental Science and Technology*, 10(10), PP. 316-328.

**Cite this article as:**
Ogbonna P. C., Okezie I. P., Onyeizu U. R., Biose E., Nwankwo O. U. and Osuagwu E. M. 2021. Analysis of Soil Quality Status and Accumulation of Potentially Toxic Element in Food Crops Growing at Fecal Sludge Dumpsite in Ubakala, Nigeria.*Nigerian Journal of Environmental Sciences and Technology*, 5(1), pp. 197-221. https://doi.org/10.36263/nijest.2021.01.0273

Nigerian Journal of Environmental Sciences and Technology (NIJEST)

www.nijest.com

ISSN (Print): 2734-259X | ISSN (electronic): 2734-2603

Vol 5, No. 1 March 2021, pp 222 - 233

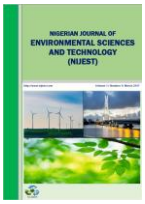

# Evaluating the Main Challenges to a Sustainable Physical Environment in Benin City

Onwuanyi N.[1,*] and Ojo E. P.[2]

[1]Department of Estate Management, University of Benin, Benin City, Nigeria

[2]Department of Geomatics, University of Benin, Benin City, Nigeria

Corresponding Author: *ndubisi.onwuanyi@uniben.edu

https://doi.org/10.36263/nijest.2021.01.0268

## ABSTRACT

*In the shaping of cities as physical environments, planning governance is a principal factor which has sustainability implications for the entire urban system. This suggests that planning governance is a factor which has the potential to contribute to the occurrence of environmental challenges as well their resolution. Nigeria's cities are facing many environmental challenges which constitute threats to sustainable development. This paper examines the main challenges to the development of a sustainable physical environment in Benin City, Nigeria's ninth largest urban centre by population. Relying on archival records and observation, the study evaluates the city's major physical environmental problems and their connection with planning governance; and thereafter, undertakes a comparison of planning governance features in the city with practice in the now sustainable, but once unsustainable environment of London City. The findings are that planning governance exerts a critical influence on the sustainable urban physical environment as in London City; that Benin City's weak planning governance (as manifested by the absence of a master plan, inadequate personnel and equipment, a low public awareness of planning laws, a low level of compliance and a general lack of enforcement) is contributory to the emergence and subsistence of its environmental challenges. The conclusion is that the subsisting environmental challenges of Benin City are rooted in planning governance which, as presently run, lacks the capacity to achieve a sustainable physical environment. It is recommended that the city be re-directed to a trajectory of sustainable physical development through sweeping changes in planning governance and public enlightenment.*

**Keywords:** Benin City, Environmental challenges, Physical planning, Sustainable development

## 1.0. Introduction

Human settlements are physical spaces which have been adapted from their natural state. According to Williams (2014) the "urban form is the physical characteristics that make up built-up areas, including the shape, size, density and configuration of settlements". This form is produced by a process which involves changes to terrain and morphology. The urban physical form is created for the provision of space for living, working and recreation (Lohmann, 2006) for which purposes all urban land needs must be accommodated as a cardinal principle of planning design(Keeble,1982). These needs are arranged to achieve complementarity, the separation of incompatible land uses and allowances made for the effect of topography and ecology on the urban form (Keeble, 1982). Urban infrastructure constitutes the physical and related structures needed for functioning of the urban area. It energises the urban form, provides the means of movement of people, information and goods and services. According to Onwuanyi (2020), a city's infrastructure usually comes in two broad forms: the grey (or built) and the green (or planted). Onwuanyi (2020) further states that the former mainly constitute constructed facilities whilst the latter consists of trees, gardens, parks, urban forests and the like. The physical structure of a city, which can be perceived from its layout, reveals the composition of land uses, the space provision for various needs, the pattern of arrangement of land uses, accessibility, aesthetics and physical and ecological constraints imposed on the urban form (Keeble, 1982). The land use pattern particularly influences the quality of the physical environment and its capacity to sustain human activities which, if uncontrolled or unmonitored tend to produce

environmental stresses. These problems come in dimensions which can be seen, heard, felt, and perceived.

Human activities, according to the United Nations (2015), have the potential to impact negatively upon the environment by reducing its quality and depleting resources. Undoubtedly, human activities create challenging situations in the sense of difficulties for those who occupy and use the environment. According to Massachusetts Institute of Technology (2000), these difficulties come in the form of damage to the physical environment, mostly caused by other people, and usually with harmful consequences for human welfare, either now or in the future. MIT (2000) further argues that some of these difficulties have the potential to extend beyond the present to future occupiers and users of the environment. Environmental challenges may be defined either in broad or narrow terms, depending on intention and focus. A broad definition of may include virtually all issues which impact both people and environment in an urban area.

Damage to the physical environment mostly comes through anthropogenic activities. These produce nuisance, pollution of the air and water bodies, resource depletion, poor sanitation and waste disposal challenges which are common to Nigeria's urban environments. These are threats to present or future human well-being of humans.

As the world's populations increasingly settle in cities, sustainable urban living has become a topical issue. Sustainable urbanism is an environmental, livelihood and urban concept. It envisions cities which are designed, managed and governed to function on a long-term basis as human habitats. This would necessitate their serving as living, working and recreational spaces where the environment is protected, social development promoted and livelihoods and resources sustained to deliver long-term value for the present and in the future. According to Sharifi (2016), sustainable urbanism is the application of sustainability and resilient principles to the design, planning, and administration/operation of cities. This is tantamount to the application of sustainable development principles to urban environments, that is, development (which) seeks to meet the needs and aspirations of the present without compromising the ability to meet those of the future. UN World Commission on Environment and Development (1987). Fundamental to a sustainable urban environment is sustainable physical planning. This is essentially because sustainable environments are sustainably planned, managed and effectively governed. The importance of sustainable environments is emphasised by the UN Sustainable Development Goals (Global Goals) policy 2015 to 2030.This policy which involves 17 goals and 169 targets dedicates Goal 11 and its 10 targets towards the creation of sustainable cities and communities across the world.

Published research and public commentary suggest that Nigeria's cities, including Benin City, are challenged by physical environmental issues. These findings and observations further suggest the existence of challenges to achieving a sustainable physical environment which is necessary for sustainable urban living, development and management. If Nigeria's rapidly urbanising cities are not developing on a trajectory of sustainable development, it is necessary and important to identify the nature of the challenges; ascertain the prerequisites for a sustainable physical environment; and then consider how these measures may be effectively deployed in the study area. It is argued that cities are governed physical spaces and that their challenges of environment cannot be distanced from governance, particularly planning governance, which has the potential to exert a great influence on the condition and quality of the physical environment. Thus, an enquiry into urban environmental challenges necessarily requires an examination of planning governance standards and performance. It is in these regard that this paper evaluates planning governance in Benin City.

The study identifies the nature and manifestations of extant challenges of the physical environment in Benin City. The state of planning governance in the city is compared with practice in the established and sustainable physical environment of London City. The aim is to find out Benin City's areas of conformance with, or divergence from, the path of sustainable physical development. This is done with the intention of drawing lessons which would advise the best approach to the attainment of a sustainable physical environment in Benin City.

## 2.0. Methodology

This study relies upon archival records and observation to argue its premise that a nexus exists between planning governance and a sustainable physical environment. These data sources are used to identify the nature and manifestations of environmental challenges in Benin City. Furthermore, the challenges are evaluated in terms of their origins. Thereafter, relevant issues of physical planning in the city are evaluated in order to identify their connection with planning governance. Subsequently, the study further stresses the connection between planning governance and a sustainable physical environment by comparing the study area with London City, using the latter as an example of an environment once characterised by unsustainable development, but which now has a sustainable physical environment.

## 3.0. Results

### *3.1. Urban environmental problems of Benin City*

Environmental problems are noticeable by the impacts which they produce. These impacts announce their presence or emergence and the nature of the challenge which they pose or can pose. According to Abdallah (2017) "environmental impacts are changes in the natural or built environment, resulting directly from an activity that can have adverse effects on the air, land, water, fish and wildlife or the inhabitants of the ecosystem". This is mostly the case with the main environmental problems of Benin City as collated from the archives and observation and displayed in Table 1. These environmental issues are described and classified either as managerial or cultural.

**Table 1:** Existing urban challenges in Benin City

| | Environmental Problem | Managerial | Cultural |
|---|---|---|---|
| 1. | Biodiversity (parks, gardens, street trees, open spaces) | Planning governance/ personnel | Public Awareness |
| 2. | Waste Dumping(conventional household, industrial and commercial solid waste, electronic and hazardous waste | Operational Equipment/Facilities | Public Compliance |
| 3. | Refuse Burning(release of chemical pollutants) | Enforcement Capacity | |
| 4. | Erosion(Soil & Gully) (absent/inadequate/silted drainage channels, deforestation) | Public Education | |
| 5. | Air &Noise Pollution(generator noise, incompatible land uses) | Enforcement Capacity | |

*Authors' Compilation, 2020*

The table shows that the lack of open and green spaces is a managerial (decision-making) issue of the planning process, but it is also cultural in the sense of a lack of public awareness of the benefits (Onwuanyi, 2020), giving rise to indifference. The lack of enforcement and monitoring is associated with poor waste management and refuse-burning. Erosion and flooding are associated with improper waste disposal and the cultural issue of poor construction practices involving an increasing use of paved surfaces which prevent rainwater infiltration, and therefore, exacerbate the problem, particularly where storm water drainage is either absent or inadequate (Effiong and Uzoezie, 2017).

Clearly, these listed problems of the Benin City environment typically arise from anthropogenic behaviour and activities. Thus, the solutions must be sought in the alteration of behaviour and practices. Indeed, at one end, humans are responsible for urban governance whilst at the other humans also are responsible for the how the environment is used. A lack of good policies and a failure to adopt good practices both have the potential to impact the environment. Environmental policies and practices are usually subjected to human control by urban planning, a tool for planned development and urban management which shows concern for health and maintaining well-being through averting diseases and illnesses associated with overcrowding, poor sanitation, and exposure to environmental pollution (Hphp, 2015). The suggestion is that the challenges of the urban physical environment as well as their solutions have a common ground in urban planning. The paper, therefore, proceeds to consider the situation of urban physical planning in Benin City by an evaluation of the urban planning function. This is done by reference to archival records and physical observation.

### *3.2. Situation of urban physical planning in Benin City*

Further evaluations were undertaken in regard to the status of physical planning in Benin City. In Table 2, pertinent issues which relate to the urban planning function are listed. For each of these issues an assessment is made of the present status as revealed by archival records and observation.

**Table 2:** Evaluation of physical planning administration in Benin City

| Physical Planning Issues | Situation | Evidence/Evaluation |
|---|---|---|
| Planning Administration | Planning was transferred from Town/City council to state Authority in 1968 | Planning administration was until 2016 subsumed under the Ministry of Lands; confirmed by enquiry (2020) |
| Urban Governance | City Governance was under local authority, but now under four, plus the state authority | 4 local governments exist in the city (Constitution of the Federal Republic of Nigeria (1999, as amended) |
| Existence of an Urban Masterplan | Not Available | Braimah (1984); Confirmed by enquiry |
| Existence of a Planning Agency | Available | A fact confirmed by enquiry (2020) |
| Accessibility of the Planning Agency | Not very Accessible due to a low public awareness | Omuta (1988); Omorotionmwan (2012); Adamolekun *et al*. (2017) |
| Resources of the Planning Agency | Limited(human/equipment) | Braimah(1984);Confirmed by enquiry (2020) |
| Public awareness of essence of building approvals | Low | Adamolekun *et al.* ( 2017) |
| Public compliance with building Laws | Low | Ogeah and Omofonmwan (2013); Omuta (1988) Adamolekun *et al.* (2017); Omorotionmwan (2012); confirmed by observation (2020) |
| Effective Enforcement | Poor | Ogeah and Omofonmwan (2013); Adamolekun *et al.* (2017); Evbuomwan as reported by Eweka (2017); Omorotiomwan(2012) |

*Authors' Compilation, 2020*

The most important issues in the table are that the city has no masterplan to guide its physical development. Thus there are no structure plans. There is a planning agency, but this is not adequately staffed and properly equipped. It is, therefore, unable to make an impact on monitoring, enforcement and in educating the public on planning laws. These assessments form the basis of the findings which are treated in the discussion section.

### *3.3. Sustainable physical environments*

It was considered relevant to this study to undertake evaluations of the factors which have enabled the development of sustainable physical environments in other jurisdictions and the extent to which these factors feature in Benin City. Ever since the report of the UN World Commission on Environment and Development (1987) known otherwise as the Brundtland Report, the sustainable development discourse has permeated all aspects of human endeavour, but the environment remains the most critical aspect of the concept because it is base of human activities. Has planning been a factor in achieving a sustainable physical environment in other climes? As expressed by Keeble (1984), town planning ideally involves deciding what a city should look like before it is built. However, because most cities have grown of their own accord, planning usually concerns itself with deciding in which ways a city should remain as it is and in which ways it should be changed for the better. The nature of change required is not solely decided by the planner, but by society through the political process and the instrumentality of governance (Roberts, 1999) with the planner placing his expertise at the service of society. Through the planner and the planning process may decide the most appropriate choices for society and in the process restrain, constrain or coerce the individual in the interest of others (Roberts, 1999). The objective is to provide for urban dwellers the best possible standard for living and working by applying a process of continual improvement (Lohmann, 2006).Society's desires and expressed preferences are, therefore, critical to achieving a sustainable physical environment. A sustainable urban physical environment comes through environmentally responsible governance which creates a liveable space (New Zealand Ministry of the Environment, 2016). It is founded upon commitment: political commitment on the side of government, and social commitment or "buy-in", by the governed. This enables the creation of what is desired and the management of what is actually created.

### *3.4. Physical planning in Benin City and the City of London*

From the preceding, it should be clear that the fundamental issue in the development of a sustainable physical environment is planning governance which is supported by appropriate laws and equipped and empowered for performance. There are jurisdictions which have attained sustainable conditions by overcoming challenges such as faced by Benin City. An example is London City in the United Kingdom which has a history of "apparently unsuitable development, some very like those being experienced in today's most rapidly growing 'new' cities (Clark, 2015) having had a multi-century struggle for sustainable development (Clark, 2015). For these additional reasons, Benin City is compared with London City in terms of planning practice. First, London is an example of an environment where modern urban planning has been practiced for many decades. Secondly, it is chosen because it is an environmentally responsible city. Thirdly, although Benin has ancient origins, it is a relatively new city compared with London, considering that ancient Benin was burned down in 1897 and started its renaissance as a 1920 colonial township. London, on the other hand has evolved for over hundreds of years. British urban planning legislation and practice as well as research (Williams, 2014; Callies, n.d.) reveal some factors which are relevant to the sustainable development of cities These factors are listed in Table 3 as constituting the main requirements which make for effective physical planning. The items are seven in number starting from the availability of a plan. The other requirements relate to the implementation of the plan through appropriate laws made by society which presumably has a consensus on the desirability of planned development and the need to comply with the laws which drive the process.

**Table 3:** Instruments of physical planning: Benin City and London City

| Prerequisites for effective and sustainable physical planning | Benin City | City of London | Evidence |
|---|---|---|---|
| An urban plan | None available | Available | London is a leading world city shaped by the British system of land use planning and control system which is among the world's most sophisticated and complex; has been experimenting with comprehensive planning laws since at least 1909; permission for all private development requires local government permission (Callies, n.d.); Much of the London's urban form (in terms of settlement patterns, street layouts and so on) has been in place for hundreds of years (Williams,2014); citizens are compliant because planning laws are understood and enforcement effective. However, has challenges of air quality & social cohesion (Clark, 2015) |
| An urban management structure | Available, but weak | Firmly established | |
| An urban management team | Poorly established and ineffective/Poor staffing by professionals | Firmly established and effectively managed by professionals | |
| Work equipment for planning administration | Poorly equipped | Well-equipped and professional | |
| Appropriate legislation | Yes | Yes | |
| Societal support | Weak as evidenced by illegal development | Strong | |
| Political consensus on planned development/planning policy/ planning process | Arguable. Existence of a consensus is not reflected in the state of the environment/compliance with planning laws | Yes, long established and widely accepted | |
| A highly enlightened citizenry | Low, as evidenced by low awareness and compliance | High, as evidenced by high compliance with planning laws | |

*Authors' Compilation, 2020*

Table 3 shows that Benin City lacks effectiveness in many areas where London is fully established. The issues raised in this table form a part of the findings and come up in the discussion.

### *3.5. Summary of findings*

The findings come from Table 1 which lists and classifies the urban physical problems Benin City; Table 2 which outlines and explains the state of physical planning in Benin City; and Table 3 which compares Benin City and London City in regard to the availability of the instruments of physical planning necessary for creating a sustainable environment. The results are as follows:

(1) Benin City lacks an urban masterplan.
(2) There is a low public awareness of the planning function in the city.
(3) The planning function is in a weak state, lacking the capacity for effective administration and enforcement. Planning was transferred from the town/city council to state authority in 1968.

(4)There is now a fragmentation of urban governance between the state, on the one hand, and the four local government jurisdictions, on the other. This is a departure from the colonial practice of governance under a single authority.
(5) When compared with the City of London using the perquisites for effective and sustainable physical planning, Benin City suffers many deficiencies.
These findings are interwoven and they are considered in the discussion below.

## 4.0 Discussion

The lack of a master plan is unarguably a major challenge According to Braimah (1984), "the planning authorities, have failed in initiating master plans for urban centres in the state. So far, no urban centre in the State has a prepared and adopted master plan to serve as a guide to development control" (Braimah, 1984). This situation did not follow the promise represented by the British preparation of a survey plan for Benin Township. The designed township covered the present day Government Reservation Area (GRA) and the central part of the city. The GRA consisted of a residential area of 54 residential plots, set out in a grid-iron pattern crisscrossed by roads and an administrative area consisting of the High Courts, Prisons, Central Hospital, the Palace and Ring Road as well as the various roads which lead off this central point in a radial pattern (Aihie, 2015). This was evidence of physical planning in its original sense of deciding in advance what is to be built before it is built. Further evidence of planning is seen in the city's radial road network from the centre, the various quarters, Urubi, Oliha, Ogidan, Uselu and Eyaen and markets, and the establishment of three public cemeteries in different areas. There is also evidence of planning in the location of the aerodrome at the outskirts of town; the golf course; and planted trees along the township streets. The later establishment of a town council (later renamed city council to approve and monitor building development is also evidence of urban planning administration. The town was subject to the various colonial legislation on building lines, public sanitation and orderly development. There were three main legislations of the era – first the Nigerian Town and Country Planning Law of 1948 which provided "a legal, administrative and financial framework for physical planning schemes and the control of development" (Braimah, 1984); second, the Western Nigeria Planning law of 1969 which emphasised zoning and third, the Building Adoptive By-laws of 1960 for building control. It is correct to say that at independence in 1960, there had been established in the city a tradition of orderly physical development and public sanitation. The system was managed by town council engineers and sanitary inspectors. In 1959, the 1948 law was adopted for use in the Western Nigeria region of which Benin City was then a part. By the adoption of this law, three principles were emphasised: first, to make it possible for all land to be subjected to planning control by the planning authority; second, zoning for the separation of incompatible uses; and third, the allocation of future land use.

The absence of a master plan suggests that sub-optimal land use decisions have been taken over the years usually by private interests in pursuit of their own agenda. Uncontrolled, *laissez faire* spatial expansion at the periphery leads to a continuing loss of land cover as agricultural land is privately sub-divided and converted into development land without the input of the planner. As the environments thus created usually consist of only residential, commercial and industrial land uses, it has not been possible to have a land use pattern which reflects all urban land needs. This development of a non-rational pattern of land use (Aluko, 2011) is a characteristic of Nigeria's cities which has led Agboola and Agboola (1997) to assert that these spaces have grown in spite of the planning laws further leading to deficiencies in urban land management (Ikejiofor, 2009). Additionally, in the absence of a master plan, extant laws of planning such as zoning and development control have not been effectively managed. Omuta (1988) identifies weaknesses in administration and managerial capacity coupled with unplanned land use and uncontrolled physical development as being principally responsible for the state of city. Likewise, research by Ogeah and Omofonmwan (2013) also mention the role of poor planning enforcement capacity in the lack of separation amongst incompatible land uses and the congested nature of residential areas. Poor capacity in this case extends not only to the availability of equipment and personnel, but also, the effective implementation of the laws. This lack of capacity cuts across all aspects of planning.

Regarding zoning, residential, commercial and industrial areas were separated up till the 1970s. For instance, industrial activity such as sawmilling was not allowed in residential areas. This is not the case today. In these earlier years, physical development generally adhered to setbacks, but this is

rarely the case today. Ogeah and Omofonmwan (2013) observe that the city had a relatively good environmental order up to the mid-1980s but the turn in the economy led to a deterioration as straitened circumstances led residential property owners to carry out conversions to non-residential (basically) commercial use. Such changes included the erection of kiosks, use of open spaces around buildings for workshops, building extensions and, in many cases, complete demolition and rebuilding with the common objective of either supplementing income or to create a new means of livelihood in the case of those who had lost theirs. Ogeah and Omofonmwan (2013) ascribe blame for these unpermitted changes to government, the defaulters, but also, the planning authority for not acting according to the 1992 law which provides for building plan approval before development can be done. Because the authors' survey revealed that only 36% of respondents were aware of the planning law, the planning authorities were found to be remiss in not educating the public aright.

Furthermore, since a master plan attempts to provide adequate space for all urban land needs, its absence implies that absence of a land use balance. A particular land use which is inadequately provided for in the present physical environment is open space (inclusive of green space and street trees). Research by Onwuanyi and Ndinwa (2017) established that there is a great dearth of open spaces in the city. There is a poor provision for green infrastructure, particularly street trees (Onwuanyi, 2020). A modern master plan is a *sine qua non* for planning, as a tool of urban management. Aspects of this plan may be reviewed periodically as required. The absence of a masterplan is compounded in Benin City by the absence of a practice of reviewing urban growth patterns and directing or redirecting them in the best interest of even development (Braimah, 1984).

Again, the poor situation of planning is also reflected in the level of compliance amongst the residents of the city. This has implications for the quality of the physical environment. Adamolekun *et al*. (2017) reveal that there is a low awareness of planning laws amongst the populace on setbacks, site coverage, zoning, parking and more. The authors attributing the finding to "a high level of poverty amongst the residents, a lack of awareness of regulatory standards and poor implementation on the part of the regulatory agency" (Adamolekun *et al*., 2017). In their Benin City study, Ogeah and Omofonmwan 2013) found that only 36% of respondents had an awareness of the planning laws. This is a challenge to compliance which compounds, and is compounded by, the challenge of official capacity. The effect is that enforcement cannot really be effective. In spite of the subsisting Edo State Urban Development Regulations of 2014, there have been chaotic developments such as "roof eaves-extensions, structures erected on the right of way of roads/streets, the moat, river banks, under high tension cables of the electricity transmission company, attachments on wall fences, caravans, kiosks and wooden sheds which are scattered all over" (Omobude, 2019). This is because the machinery for administration and enforcement (professional planners, planning assistants, technical officers, organisational spread and equipment) are still inadequate. Furthermore, a senior government official, Dania, is reported by Eweka (2017), as admitting to a "problem of political interference" and a "lack of capacity in terms of adequate manpower and equipment", suggesting as solution "the political will to do the right thing".

Yet again, the transfer of the planning function from the town/city councils as it was before the 1970s to the state authority cannot really be seen as serving to make planning more effective. When Benin City became the capital of Mid-West region in 1963 following a plebiscite, the Benin City Council took charge of city administration and saw to physical development and environmental issues, using the structures and standards set in colonial times. This established system which was run by elected officials was interrupted by the 1966 political crisis which led to military rule starting in 1966 and subsisting until 1979 in the first instance. This was a precursor of change in governance and urban management. The 1967 military-induced geo-political restructuring of Nigeria led to the Mid-West *region* being re-designated as one of Nigeria's twelve new *states.* The change involved a shift of power at regional (now state) and federal levels from elected representatives to appointed military governors who operated outside the constitution. This also implied a shift in accountability. Rather than being from electorate to citizen, it shifted to the military and its high command. The 1976 second re-naming of the Mid-West State by military fiat as "Bendel" state was a reflection of the new ethos. In 1968, important environmental management functions of the Benin City Council were taken over by a new, military-created body known as the Bendel Development and Property Authority (BDPA). Thus, the Benin City Council ceased to be a planning authority. Being a state-wide agency, other town councils in the state such as Warri Township Council also ceased to function as planning authorities.

Thus, urban planning and management for Benin City and the entire state became the sole responsibility of the agency. In this period, the city's population was far less than 400,000 persons. This view is supported by Doxiades Associates 1972 city population estimate of 201,000 (Doxiades Associates, 1972) and Sada's 1976 estimate of 314, 219 (Sada, 1976). Ikhuoria (1984) reveals that the city's spatial extent as at 1972 was 30 $km^2$ or 3000 hectares whilst Odjugo *et al*. (2015) give an estimate of 359 $km^2$ (35,900 hectares) as at 2013. This means that in the intervening years, the city had expanded over ten times in spatial extent. This was a good reason to evaluate the growth pattern of the city and its implications for orderly development in the years to come. However, the system in place was unable to discharge this responsibility.

The transfer of responsibility from council to state authority did not take into account the fact planning is a local activity. The effect of this reform was to centralise a function which was previously localised in the city councils. This might have made monitoring less effective, and therefore, increased the numbers of unplanned, unapproved and non-conforming development. The fact that the BDPA became defunct at a time and its functions taken over by the Military Governor's Office could have been contributed to the weakening of planning. It is important to recall that despite the existence of the Bendel Development and Planning Authority (BDPA) Order 1977 which was designed to be managed by the BDPA, planning functions were still being performed by the office of the military governor. In this connection Braimah (1987) states that: "since 1978, the Town Planning Division, currently part of the Military Governor's Office, has been entrusted the powers of the now defunct Bendel Development and Planning Authority, to control developments in the state. In addition, it possesses power to prepare land-use layouts and master plans, for declared planning areas" (Braimah, 1987). Thus, planning which should be a local activity was centrally managed in a top-bottom manner. For instance, between 1967 and 1975, the military governor's office reconstructed and widened the city's major streets such as Mission Road, Forestry Road and Akpakpava Street and also established the BDPA and Aduwawa housing estates and built a stadium (1968) and university (1970). These important decisions were able to be taken by the governor's office because of the absence of elected officials. *De jure* and *de facto*, therefore, both city and state governance were responsibilities of the governor. Thus, the city's trajectory of growth and the quality of its management from the 1970 to 1990s were effectively set by successive unelected (military) officials who administered the state and the city and controlled all available resources. Then, as now, the case until that the state chief executive (the governor of Edo state) greatly influences the direction of the city's environmental policies and the pace at which they are implemented. Indeed, a parliament is in place, but it is a strong feature of the military-crafted 1999 constitution (now partially amended) that much power is placed in the office of the governor. This is evidenced by the 1979 Land Use Act (also a part of the constitution, which vests all land in urban areas in the office of the governor. The import of this provision can be appreciated from the essentiality of land to sustainable environmental development. The governor's exercise of his many powers tends to be the source of confrontations between the executive and legislature (Fatile, 2017). The situation is not helped by the apparent reluctance of state legislative assembles to exert their independence and perform oversight duties (Nwagwu, 2014).

The present fragmentation of city management into four local jurisdictions may not aid the effective development and management of the physical environment. Whilst physical planning is now a state responsibility, the local governments, as grassroots entities, need to be co-opted and involved in environmental management. This is particularly important since Area Planning Offices tend to be inadequate both in numbers and personnel (Braimah, 1988), giving room to haphazard land sub-division (Omuta, 1988). The existence of four local jurisdictions has the tendency to create an overlap not only between these four authorities, but between them and the state government which, as the constitutionally appointed supervisor of the former, is *de facto* and *de jure* manager of the city. UN (2012) emphasises thus: "urban governance is the hardware which enables the urban software to function ... to enable the local government response to the needs of citizens". This suggests that the capacity of cities to perform their developmental function and grow in a sustainable way depends on how well they are governed.

Lastly, a comparison of Benin City with the established jurisdiction of London City reveals that the former is deficient in many respects. Of course, the difference is that London has been exposed to modern planning interventions for a far longer time being the capital city of the UK where the Garden

Cities Movement originated. London's poor environmental conditions in many decades past have been transformed. The city authority's commitment to doing better is expressed in the London Plan which presents a vision for sustainable development up to 2031.The aim is to make the city excel amongst global cities by achieving the highest environmental standards and quality of life whilst tackling urban challenges of the 21st century, particularly climate change(Greater London Authority, 2011).The indicative features of sustainable physical development which are available in London City constitute lessons for Benin City if it desires also to achieve sustainable physical development.

In sum, the weak state of the planning function is a great threat to having a sustainable physical environment, particularly in the absence of a masterplan. This situation sustains the reign of *laissez faire* urban development, particularly at the periphery where most new development is taking place and where control is most needed. The direct causes of the present state of the physical environment are the lack of monitoring due to inadequate personnel and equipment; a failure to educate the public; to achieve a "buy in" to planning; and to implement sanctions, where necessary. Benin City is not truly characterised by modern practices in urban planning substantially because the urban physical form which was developed decades earlier when the population was far lower has not been reviewed to accommodate the changes made inevitable by population growth and urban sprawl. An inadequate response to the increase in the human and vehicular populations by expanding the road network, has brought about traffic congestions, rising air pollution from vehicular carbon emissions (Verere *et al*., 2015), sanitation and waste disposal challenges (Isah and Okojie, 2007), and of course, increased erosion and flooding events (Iyalomhe and Cirella, 2018). All of these affect sustainability of the physical environment.

## 5.0. Conclusion

This paper set out to evaluate the main challenges to achieving a sustainable physical environment in the modernising and urbanising space of Benin City. The study relied upon archival records and observation to identify and classify these challenges, outline and explain the state of physical planning in the city and evaluate the adequacy of the city's instruments of physical planning in relation to London which is established as a sustainable physical environment. The conclusion is that the weak state of planning governance in Benin City is a great threat to achieving a sustainable physical environment which is a requisite for sustainable development.

The findings are that Benin City lacks an urban masterplan. In addition, there is a low public awareness of the planning function. Furthermore, the planning function is in a weak state, lacking the capacity for administration and enforcement. Again, the planning function was transferred from the then sole city authority to the state government in 1968, but this has not manifestly strengthened it. Yet again, the city's governance was once under a single local authority, but is now fragmented amongst four and the state government. Lastly, a comparison of planning governance in Benin City with the established and sustainable City of London, reveals many important deficiencies on the part of the former which constitute barriers to achieving a sustainable physical environment.

The findings suggest that planning governance as currently constituted and practiced is not equipped to tackle the city's environmental challenges and deliver a sustainable physical environment. The present system may also create overlaps between the state government and the four city local governments on the one hand; and between the local governments, on the other. These may create ineffectiveness. Furthermore, the absence of a master plan is an indication that modern urban planning is not being practised in Benin City and this diminishes its capacity to respond to the demands of sound physical planning and management of the environment.

The study recommends production of a masterplan to guide the future development of the city. Furthermore, a stakeholder consensus built upon environmental responsibility is required, together with appropriate laws and empowerment of the planning function for good governance. Additionally, the engagement of numerically adequate planning personnel who must be well-trained and equipped for performance. Lastly, the commitment of officials at state and local levels to redirecting the city onto a trajectory of full compliance with the law and promotion of the ideals of sustainable development.

**References**

Abdallah, T. (2017).Sustainable mass transit: Challenges and opportunities in urban public transportation. [online] Available at https://doi.org/10.1016/B978-012-811299-1.00001-0 Science Direct 1-14 [Accessed 17 March, 2021]

Adamolekun, M.O., Isiwele, A.J. and Akhimien, N.G. (2017).An assessment of the level of compliance with development control standards and housing policy in Nigeria: a case study of Esan West local government area of Edo State. https://openlearning.aauekpoma.edu.ng

Agboola, T. and Agboola, E.O. (1997). The development of urban and regional planning legislation and their impact on the morphology of Nigerian cities. *The Nigerian Journal of Economic and Social Studies*, 39(1) pp.123-144.

Aihie, E. (2015). *The Benin City Pilgrimage Stations*. Benin City: Aisien Publishers.

Aluko, O.E. (2011). Urbanization and effective town planning in Nigeria. *African Research Review*, 5(2) pp. 126-139.

Braimah, A.A. (1984). Town and country planning machinery in Bendel State, Nigeria. *Third World Planning Review*, 6(3) pp.255-261.

Braimah, A. A. (1987). Planning practice in Bendel State, Nigeria. *Habitat International*, 2(2), pp.19-31.

Callies, D.I. (n.d.) Town and country planning in the United Kingdom. Environmental laws and their enforcement. Vol II *Encyclopedia of Life Support Systems* (EOLSS).http:// www.eolss.net/Eolss-sampleAllChapter.aspx.

Clark, W.C. (2015).London: A multi-century struggle for sustainable development in an urban environment. HKS Faculty Research Working Paper Series RWP15-047John F. Kennedy school of Government, Harvard University.

Doxiades Associates (1972). *Nigeria: development problems and future needs of major urban centres*, Doxiades Associates, Benin City.

Effiong, J. E. and Uzoezie, A.D. (2017). Increased paved surfaces as major factor of urban flooding in humid tropics: An example from Calabar, Cross River State, Nigeria. Presented at The 1st Geography and Environmental Science World Environmental Day Conference, University of Calabar on the 1st of June 2017.

Eweka, R. (2017, May19). Edo government holds workshop on urban and regional planning. *Nigerian Observer*. [online] Available at: www.nigerianobservernews.com (Accessed October 20, 2019).

Fatile, J.O. (2017). Legislative-executive relations and public policy formulation and implementation in Lagos state, Nigeria. *OIDA International Journal of Sustainable Development*, 10(6), pp. 1-12.

Greater London Authority (2011).The London plan: Spatial development strategy for Greater London, July 2011.Greater London Authority.

Healthy Parks Healthy People (2015).Urban planning and the importance of green space in cities to human and environmental health.www.hphpcentral.com.

Ikejiofor, U.C. (2009).Planning within the context of informality: issues and trends in land delivery in Enugu, Nigeria. Case study prepared for revisiting urban planning: Global Report on Human Settlements 2009.1-22 Available from http//www.unhabitat.org/grhs/2009. (Accessed 2 February, 2019).

Ikhuoria, I.A. (1984). Rapid urban growth and urban land use patterns in Benin City, Nigeria. University of Benin, Nigeria (Mimeo).

Isah, E.C. and Okojie, O.H. (2007). Environmental sanitation in an urban community in Benin City. *The Nigeria Postgraduate Medical College Journal*, 14(1), pp. 12-15.

Iyalomhe, F. and Cirella, G.T. (2018). Flooding in Benin City, Nigeria. Krakow, Poland 2nd International Conference on Sustainability, Human Geography and Environment 2018 (ICSHGE18).

Keeble, L. (1982). *Town Planning Made Plain*. Construction Press, London

Lohmann, K.B. (2006). *Principles of City Planning*. McGraw Hill, New York

MIT (2000).What are key urban environmental problems? Understanding Issues [online] Extracted from DANIDA Workshop Papers: Improving the Urban Environment and Reducing Poverty, December 5, 2000, Copenhagen, Denmark. Available at http://web.mit.edu/urban_upgrading/urban environment/issues/key-UE-issues.html. [Accessed 19 March, 2021].

New Zealand Ministry for the Environment (2016). Attributes of successful towns and cities [online] Available at: http://www.mfe.govt.nz/publications/towns-and-cities [Accessed 17 July, 2019].

Nwagwu, E.J. (2014).Legislative oversight in Nigeria: A watch dog or a hunting Dog? *Journal of Law, Policy and Globalisation.* 22. www.iiste.org

Odjugo, P.A.O., Enarubve, G.O. and Isibor, H.O. (2015).Geo-spatial approach to spatio-temporal pattern of urban growth in Benin City, *African Journal of Environmental Science and Technology*, 9(3), pp.166-175.

Ogeah, F.N. and Omofonmwan, S.I. (2013).Creation and demolition of illegal structures in Nigerian cities. *Jorind* 11(1) pp. 270-270., Available at: www.transcampus.org (Accessed October 27, 2019).

Omobude, T. (2019, April 9).Edo government to demolish illegal structures in Benin City. [online] *Factsreportersng*. Available at http://www.factsreportersng.blogspot.com [Accessed October 20, 2019].

Omorotiomwan, J. (2012, December 27). We were asleep while they built. *Vanguard* [online] Available at: http://www.vanguardnews.com (Accessed July 17, 2018).

Omuta, G.E.D. (1988).Environmental planning, administration and management in Nigerian cities: The example of Benin City, Bendel State. *Public Administration and Development*, 8(1), pp. 1-14.

Onwuanyi, N. and Ndinwa, C.E (2017). Remaking Nigeria's urbanism: Assessing and redressing the dearth of open spaces in Benin City. *International Journal of Built Environment and Sustainability*, 4(2), pp.121-130.

Onwuanyi, N. (2020).Deficiency of street trees in Benin City: A survey of residents' perceptions, pp. 1-14 in *Land Use Management and Environmental Sustainability in Nigeria* edited by V. Umoren and & J. Aster (Eds.), University of Uyo, Nigeria. ISBN: 978-978-57832-0-9.

Roberts, M. (1999). *An Introduction to Town Planning Techniques*. UCL Press. London

Sada, P.O**.** (1984). *Urbanisation and living conditions in Nigerian cities*. Research Triangle Institute, North Carolina.

Sharifi, A. (2016). From garden city to eco-urbanism: the quest for sustainable neighborhood development. *Sustainable Cities and Society*, 20, pp. 1–16 [Accessed 1 June, 2018]

Report of the UN world commission on environment and development (1987). *Our Common Future*, www.un-document.net.our-common-future.

UN (2012).Governance [online]. Available at: http://unhabitat.org/governance. [Accessed 23 February, 2021].
United Nations (2015).Sustainable development goals.

Verere, S.B., Oluwagbenga, O., and Orimoogunje, I. (2015).Geo-spatial mapping of air pollution in Benin City, Nigeria. *Journal of Geography, Environment and Earth Science International*, 3, pp. 1-17 [Accessed 30 September, 2016].

Williams, K. (2014). Urban form and infrastructure: A morphological review. Government Office for Science. The UK Government's Foresight Future of Cities Project.

**Cite this article as:**
Onwuanyi N. and Ojo E. P. 2021. Evaluating the Main Challenges to a Sustainable Physical Environment in Benin City. *Nigerian Journal of Environmental Sciences and Technology*, 5(1), pp. 222-233. https://doi.org/10.36263/nijest.2021.01.0268

Nigerian Journal of Environmental Sciences and Technology (NIJEST)

www.nijest.com

ISSN (Print): 2734-259X | ISSN (electronic): 2734-2603

Vol 5, No. 1 March 2021, pp 234 - 239

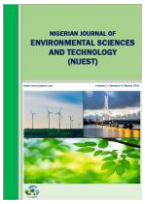

# Bacteriological Assessment of Palms of Students of Delta State University, Abraka

Jemikalajah D. J.[1], Enwa F. O.[2,*] and Etaoghene A. D.[2]

[1]Department of Microbiology, Faculty of Science, Delta State University, Abraka, Nigeria

[2]Department of Pharmaceutical Microbiology & Biotechnology, Faculty of Pharmacy, Delta State University, Abraka, Nigeria

Corresponding Author: *felixenwa@delsu.edu.ng

https://doi.org/10.36263/nijest.2021.01.0276

## ABSTRACT

*The bacteriological assessment of palms of students of Delta state University Abraka, was undertaken. A total of hundred samples were collected using a sterile swab sticks. Streak plate method was used and also biochemical test carried out following standard procedures. Results showed growth on ninety-three (93) cultured plates (93%). Bacteria isolates identified were Staphylococcus aureus, Escherichia coli, Proteus sp., Streptococcus sp, Bacillus sp., Salmonella sp. and Klebsiella. Staphylococcus aureus had the highest prevalence of 41% while, Salmonella sp (1%) was the least prevalent. Results also showed that female students had a higher incidence of bacterial load (58%) compared to the male students (42%), There is therefore a need to create awareness among students on good hand hygiene practices since the hand is a major reservoir of pathogenic organisms.*

**Keywords:** Bacteria, Palms, hygiene, *Staphylococcus aureus, Escherichia coli,* Abraka

## 1.0. Introduction

The hand is the extremity of the superior limb, hence, serves as a medium for the transfer of microorganisms from one location to the other and from one person to another (Hammond *et al.*, 2000). ‘‘According to the US Centre for Disease Control and Prevention and the Association for Professionals in Infection Control and Epidemiology, simple hand washing is the single most important and effective method of preventing the spread of transmissible disease’’ (Burton *et al.*, 2011). Human hands usually harbour microorganisms both as part of normal micro flora and microorganisms contacted from the environment. These normal microfloras such as *Staphylococcusaureus* resident in the human skin and can therefore be passed from one individual to another. Other pathogen that may be present on the hand as transient types includes *Salmonella* spp., *Shigella* spp., *Escherichiacoli* (Curtis and Cairncross, 2003). The high incidence of diarrheal diseases and other communicable disease among students are actually due to poor knowledge and practice of personal and environmental hygiene (Strina *et al.,* 2002). Poor knowledge and practice of, and attitudes to personal hygiene, such as hand washing, has negative consequences for a child’s long term overall development. Good hand washing practice is therefore a prerequisite to a child’s survival (Lopez-Quintero *et al.*, 2009). Infectious transmission through contaminated hands among students is a common pattern seen in higher institutions and failure to perform appropriate hand hygiene practices has been recognized as a significant contributor to outbreaks of infectious diseases by the world health organization (WHO, 2009). Hand washing is critical in this era of covid-19 where human to human transmission is mainly through respiratory droplets from infected individuals, contact with contaminated objects and surfaces, social activities like hand-shaking, hugging and kissing (Imai *et al.*, 2020; Majumdar and Mandl, 2020).This study is thus designed to determine the bacterial load on the palms of university students to assess whether they carry pathogenic bacteria that could cause an infection to these students and the level of adherence of students to proper hygiene especially hand washing.

## 2.0. Methodology

### *2.1. Study area*

This research was carried out among students in different faculties in campus 3 of Delta State University Abraka. Abraka is lies on longitude $5.7917^0$N and latitude $6.0987^0$E with a student population of 22,000 (undergraduate) located in the South-South geopolitical zone of Nigeria (Figure 1). It is an urban town with the major occupation of farming, trading, civil servants and students (DELSU, 2019/2020).

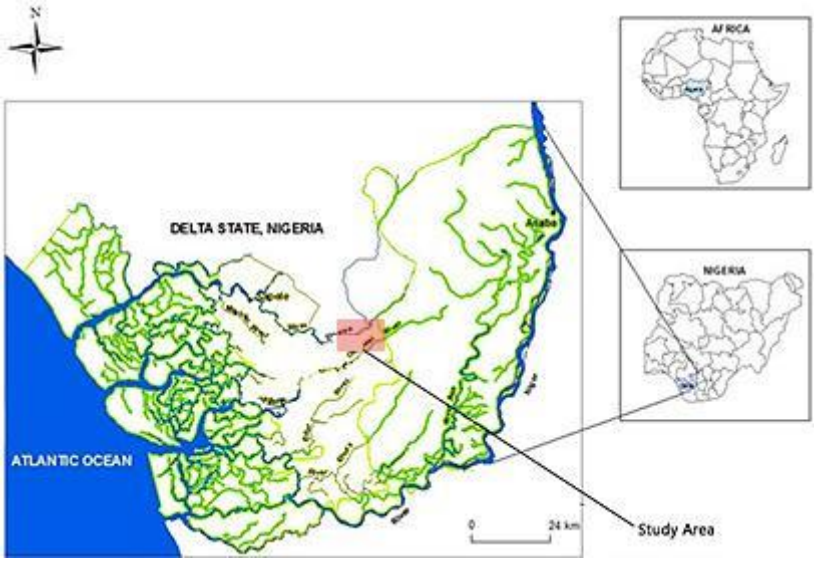


**Figure 1:** Map of Delta State Nigeria showing location of study area
Source: Irwin and Oghenevwede (2014)

### *2.2. Study population*

This study enrolled a total of 100 students made up of 50 males and 50 females. Ten (10) students each were randomly selected from each of the faculties on campus 3.

### *2.3. Sample collection*

With the aid of sterile swab sticks, Hundred (100) samples were collected from students. Each swab stick was introduced into 2-3mls of peptone water in sterile sample bottles. The hand swabs were properly closed and transported to the Microbiology Laboratory Delta State University, Abraka for analysis.

### *2.4. Media preparation and culture*

The media used were MacConkey agar and Nutrient agar which was weighed according to manufacturer's instruction and was sterilized at 121°C by autoclaving for 15 minutes. Blood agar was prepared by removing 50mls of molten nutrient agar and replaced with 50mls of sheep blood to give 5% blood agar. Samples were culture by streak plate method and incubated at $37^0$C for 24 hours.

### *2.5. Biochemical identification of isolates*

Isolated microbes were characterized and identified based on colony morphology, cultural appearance and biochemical tests (Cowan and Steel, 1974; Cruishank *et al.*, 1975; Sanders, 1994).

### *2.6. Gram staining*

The developed bacteria colonies after 24 hours of incubation was Gram stained and examined for Gram positive and negative bacteria.

*2.7. Catalase test*

This test was done to differentiate Staphylococcus and streptococcus. Few drops of hydrogen peroxide solution were placed on a glass slide and an applicator stick was used to emulsify the suspected colonies of the test organism and observed for bubbles. Staphylococcus was positive and streptococcus negative.

*2.8. Motility test*

Motility was performed on all isolated bacteria. Semi-solid agar was prepared and stabbed with the isolates to the bottom of the tube and incubated at $37^0$c for 24 hours. The swarming of bacteria in the medium is positive for motile bacteria.

*2.9. Oxidase test*

Three drops of oxidase reagent (tetra-methyl-p-phenylenediaminedihydrochloride) was added on a filter paper. Colony of the test organism was picked, smeared on the filter paper and observed for development of a blue purple colour within 10 seconds. The formation of purple color indicates a positive result.

*2.10. Indole test*

Indole test demonstrate the ability of certain bacteria to decompose the amino acid called tryptophan to indole that accumulate in the medium (tryptone water). The test organism was inoculated in the medium and incubated at 37°C for 24 hours. Then 0.5 ml of Kovac's reagent was added and gently shaken formation of pink to red ring color on top of the medium indicates a positive results.

*2.11. Citrate test*

Some Gram negative bacteria utilize citrate and change Simmon's Citrate Agar medium to blue. The slants agar were streaked with a suspension of the test organisms and incubated at 37 $^0$C for 24 hours. Blue colouration indicates positive.

*2.12. Urease test*

The test demonstrate the ability of some Gram negative bacteria that produces the enzyme urease which breakdown urea. Urea agar was prepared according to manufacturer's instruction and 2mls was dispensed into bijou bottles to form a slant. It was inoculated with isolated colonies, incubated at 37°C for 12 hours. A colour change from light orange to pink indicates the production of urease enzyme (positive). No colour change indicates negative.

*2.13. Coagulase test*

This test differentiates coagulase positive bacteria like *Staphylococcus aureus* from coagulase negative *Staphylococcus epidermidis* when human citrated plasma was tested with isolated colonies. The enzyme coagulase produced by *Staphylococcus aureus react* with the plasma and form clot.

## 3.0. Results and Discussion

Our result shows that out of the 100 samples examined, a total of ninety-three (93) isolates were obtained. Eight (8) different bacterial species were identified from the total number of samples investigated. Among the bacterial species identified after biochemical characterization includes *Staphyloccocusaureus*, *Escherichia coli*, *Proteus* sp, *Streptoccocus* sp, *Bacillus* sp, *Salmonella* sp, and *Klebsiella* sp (Table 1).

The bacterial species observed in this study such as, *Staphyloccocus aureus*, *Bacillus* sp., *Klebsiella* sp., and *Escherichia coli* were however similar to the findings of Bellissimo-Rodrigues *et al.* (2017). *Staphyloccocus aureus* was seen to have the highest prevalence. The findings of these bacteria are in agreement with the work of Bellissimo-Rodrigues *et al.* (2017). This may be attributed to the presence of some pathogenic bacteria that are spread by contaminated hands especially the carriers of *Staphyloccocus aureus* in their nostrils and faecal contamination of palms with enterobacteriaceae. These bacteria are passed to other students by hand shake, hugging and eating together as earlier

opined by Lax and Smith (2014) and Mathieu *et al*. (2013). Washing of hand has great impact on reducing the burden of infections in the developing world. In this study, the practice of hand washing among the students is very poor with respect to reported studies from other countries.

**Table 1:** Biochemical identification of bacterial isolates

| Gram stain | Shape | Catalase | Coagulase | Motility | Indole | Urease | Citrate | Bacteria |
|---|---|---|---|---|---|---|---|---|
| + | Cocci | + | + | - | - | - | + | *Staphylococcus aureus.* |
| - | Bacilli | - | - | + | + | - | - | *Escherichi* coli |
| - | Bacilli | - | - | + | - | + | + | *Proteus* sp. |
| + | Cocci | - | - | - | - | - | + | *Streptococcus* sp. |
| + | Bacilli | + | - | + | - | - | + | *Bacillus* sp. |
| - | Bacilli | + | - | + | - | - | - | *Salmonella* sp. |
| - | Bacilli | + | - | - | - | + | - | *Klebsiella* sp. |

Table 2 shows the prevalence of bacterial isolates from the sample examined. *Staphylococcus aureus* had the highest prevalence rate of 44.1 % followed by *Escherichia coli* 15.1% and the least Salmonella sp. 1.1%. This is not alarming because these organisms are predominant as carriers in humans and causes harm only when the infectious dose is high enough to induce an infection. In spite of this, effective hand washing is important in infection control. Appropriate hand washing is the most vital way to reducing the spread of communicable diseases and an intervention that can break the chain of food poisoning and respiratory infection such as covid-19 as observed by Uneke *et al*. (2014).

**Table 2:** Bacterial isolates from palm of students

| Bacterial isolates | No.of samples | No. (%) positive for palm isolates | No. (%) negative for palm isolates | % Prevalence |
|---|---|---|---|---|
| *Staphylococcus aureus* | 100 | 41(0.41) | 52(0.52) | 44.1 |
| *Escherichia coli* | 100 | 14(0.14) | 79(0.79) | 15.1 |
| *Bacillus sp.* | 100 | 19(0.19) | 74(0.74) | 11.1 |
| *Proteus sp.* | 100 | 7(0.7) | 86(0.86) | 7.5 |
| *Streptococcus sp.* | 100 | 6(0.6) | 87(0.87) | 8.0 |
| *Salmonella sp.* | 100 | 1(0.1) | 92(0.92) | 1.1 |
| *Klebsiella sp.* | 100 | 5(0.5) | 88(0.88) | 5.4 |
| Total | | 93 | | 100 |

Table 3 shows the percentage prevalence rate of bacterial isolates that occurred in both male and female students. It was observed that females had more bacteria load of about 54% when compared to the males having about 39% bacterial load. Out of the bacteria species identified *Staphylococcus aureus* were the most predominant and highest in females with relatively low prevalence rate of about 15% in males. There was thus an increase in the prevalence rate of *Bacillus* species of about 11% when compared to females (8%).

The human hands naturally harbors microorganisms both as part of a person's normal microbial flora as well as transient microbes acquired from the environment (Curtis *et al*., 2009). This study shows that over 93% of all students hands were contaminated with bacteria pathogens. This agrees with the findings of Kenneth *et al*., (2018) who reported that about 95% of bacterial load from hands of pupils in their study. This could be an indication of poor personal hygiene practices particularly to maintaining good hand washing practices as stated in a health report by the WHO, (2009). This work further shows that bacterial palm carriage was 58% higher in the female students than 42% recorded among the male students. This differs from the findings of Vishwanath *et al*. (2019) who reported a higher prevalence in male than in female in their study. This could be as a result of age differences and the subjects recruited into current work since their research was carried out among primary school pupils and ours was among university students. However, the high percentage prevalence obtained among female and male students may due to poor hygiene in the school environment because most higher institutions in the developing countries lacks hand washing facilities and where available, they

may be poorly located, no hand washing materials and in accessibility to students even in this era of covid-19 where hand washing practices is key to reducing transmission of the virus.

**Table 3:** Bacteria isolates from male and female palm

| Bacterial isolates | No. (%) positive for palm isolates (male) | No. (%) negative for palm isolates (male) | No. (%) positive for palm isolates (Female) | No. (%) negative for palm isolates (Female) |
|---|---|---|---|---|
| *Staphylococcus aureus* | 15(0.15) | 78(0.78) | 26(0.26) | 67(0.67) |
| *Escherichia coli* | 8(0.8) | 85(0.85) | 7(0.7) | 86(0.86) |
| *Bacillus sp.* | 11(0.11) | 82(0.82) | 8(0.8) | 85(0.85) |
| *Proteus sp.* | 2(0.2) | 91(0.91) | 5(0.5) | 88(0.88) |
| *Streptococcus sp.* | 0(0.0) | 93(0.93) | 6(0.6) | 87(0.87) |
| *Salmonella sp.* | 1(0.1) | 92(0.92) | 0(0.0) | 93(0.93) |
| *Klebsiella sp.* | 3(0.3) | 90(0.90) | 2(0.20) | 91(0.91) |
| Total | 39 | | 54 | 93 |

## 4.0. Conclusion

The present study shows that the palms of university students harbor a variety of pathogenic organisms which could cause serious infectious diseases like gastro-intestinal infection which are possibly fatal if not attended to. Lack of proper hand washing model, basic hand washing material like soap and water, and the presence of hand sinks at various locations within the university premises were among the reasons for failures of students to adhere to hand washing practices. Provision of these materials can bridge the gap between proper hand washing techniques and the spread of diseases.

## Conflict of interest

All authors declares no conflict of interest

## References

Bellissimo-Rodrigues, F., Pires, D., Soule, H., Gayet-Ageron, A., Pittet, D., (2017). Assessing the likelihood of hand-to-hand cross-transmission of bacteria: an experimental study. *Infection Control Hospital Epidemiology,* 38, pp. 553–558.

Burton, M., Cobb, E., Donachie, P., Judah, G., Curtis, V. and Schmidt, W.P. (2011). The effect of handwashing with water or soap on bacterial contamination of hands. *International Journal of Environmental Research and Public Health,* 8(1), pp. 97-104.

Cowan, S.T. and Steel, K.J. (1974). Identification of Medical Bacterial 2nd edition, Cambridge University Press, (London). pp.46-81.

Cruishank, R., Duguid, J.P. and Mamion, B.P. (1975). Medical Microbiology. Vol.2 12th edition, Churchill Livingstone, pp. 428-434.

Curtis, V. and Cairncross, S. (2003) Effect of washing hands with soap on diarrhea risk in the community: A systematic review. *Lancet Infection Disinfection,* 3, pp. 275-281.

Curtis, V., Danquah, L. O. and Aunger, R. V. (2009). Planned, motivated and habitual hygiene behaviour: An eleven country review. *Health Education Research,* 24(4), pp. 655-673.

Delta State University (2019/2020). Delta State University,Abraka, Nigeria. History. https//www.delsu.edu.ng> history. Retreived.

Hammond, B., Ali, Y., Fendler, E., Dolan, M. and Donovan, S. (2000). Effect of hand sanitizer use on elementary school absenteeism. *American Journal of Infection Control,* 28, pp. 340-346.

Imai, N., Cori, A. and Dorigatti, I. (2020). Transmissibility of 2019nCoV. https:www.imperial.ac.uk/mrcglobal-infectious-diseaseanalysis/news—wuhancronavirus/last (Accessed 2020)

Irwin, A. A. and Oghenevwede, E. (2014) *International Journal of Water Resources and Environmental Engineering*. 6(1), pp. 19-31.

Kenneth, A., Hamady, M., Lauber, C.L. and Knight, R. 2018. The influence of sex, handedness, and washing on the diversity of hand surface bacteria. *Proceedings of National Academic Science United State of America*, 105, pp. 17994–17999.

Lax, S. and Smith, P. (2014). Longitudinal analysis of microbial interaction between humans and the environment. *Science magazine*, 345, p. 1048

Lopez-Quintero, C., Freeman, P. and Neumark, Y. (2009). Hand washing among school children in Bogata, Colombia. *American Journal of Public Health*, 99(1), pp. 94-101. https://doi.org/10.2105/AJPH.2007.129759

Majumdar, M. and Mandl, K. (2020). Early transmissibility assessment of a novel coronavirus in Wuhan, China. Preprint. https://papers.ssrn.com/soI3/papers.cfm?abstract_id3524675. Last accessed 2020

Mathieu, A., Delmont, T. and Voget, T. (2013). Life on human surfaces: Skin metagenomics. *Public Library of science* 8(6), e65288.

Sanders, C.C. (1994). Identification of medically important bacteria.Clinical microbiology. Miles, Inc; 3rd edition, pp. 17-18.

Strina, A. S., Cairncross, M. L., Larrea, C. B. and Prado, M. S. (2002). Childhood diarrhoea and observed hygiene behaviour in Salvodor, Brazil. *American Journal of Epidemiology*, 157, pp. 1032-1038.

Uneke, C.I., Ndukwe, C.D. and Oyibo, P.G. (2014). Promotion of hand hygiene strengthening initiative in a Nigeria teaching hospital: Implication for improved patient safety in low income health facilities. *The Brazillian Journal infections Diseases*, 18(1), pp. 21-27.

Vishwanath, R., Selvabai, A.P. and Shanmugam, P. (2019). Detection of bacterial pathogens in the hands of rural school children across different age groups and emphasizing the importance of hand wash. *Journal of prevalence medical hygiene*, 60(2), pp. 103-108.

World Health Organization, (2009). WHO Guidelines on Hand Hygiene in Health Care. World Health Organization, Geneva, Switzerland.

**Cite this article as:**
Jemikalajah D. J., Enwa F. O. and Etaoghene A. D. 2021. Bacteriological Assessment of Palms of Students of Delta State University, Abraka. *Nigerian Journal of Environmental Sciences and Technology*, 5(1), pp. 234-239. https://doi.org/10.36263/nijest.2021.01.0276

Nigerian Journal of Environmental Sciences and Technology (NIJEST)

www.nijest.com

ISSN (Print): 2734-259X | ISSN (electronic): 2734-2603

Vol 5, No. 1 March 2021, pp 240 - 257

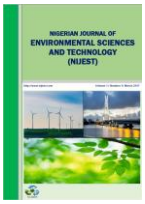

# Weighted Linear Combination Procedures with GIS and Remote Sensing in Flood Vulnerability Analysis of Abeokuta Metropolis in Nigeria

Oyedepo J. A.[1,*], Adegboyega J.[2], Oluyege D. E.[3], and Babajide, E. I.[4]

[1,3,4]Institute of Food Security, Environmental Resources and Agricultural Research, Federal University of Agriculture, Abeokuta, Nigeria

[2]Department of Environmental Management and Toxicology, College of Environmental Resources Management, Federal University of Agriculture, Abeokuta, Nigeria

Corresponding Author: *oyedepoja@fuaab.edu.ng

https://doi.org/10.36263/nijest.2021.01.0260

## ABSTRACT

*The study offered the opportunity for an evaluation of the role of Remote Sensing and Geospatial techniques in flood disaster risk management and development of spatial decision support system for flood risk assessment and management in Abeokuta metropolis. Datasets used includes cloud free high resolution satellite images and Shuttle Radar Topographic Mission (SRTM) data downloaded from earth explorer site. Soil data used was obtained from Food and Agriculture Organization (FAO's) Harmonised World Soil Database, while rainfall data was obtained from the Climate Hazards Group InfraRed Precipitation Station. Maps of flood enhancing factors namely: soil types, rainfall intensity, drainage density and topography were created in Geographic Information Systems using same scale of 1: 50,000 and Geographic coordinate system (WGS 1984). All maps were produced in raster format with the same cell grid cell size of 0.0028 mm. They were then subjected to weighting by ranking and Multi-Criteria Analysis (MCA) using the Weighted Linear Combination. The study identified topography and land use as key factors contributing to flooding within Abeokuta metropolis. Obstruction of natural drainage channels by buildings aggravates disasters from flash flood events.*

**Keywords:** Flash flooding, Flood Vulnerability, GIS-Remote sensing model, Weighted Linear combination, Multi-Criteria Evaluation, Abeokuta Metropolis

## 1.0. Introduction

Inundations from runoffs and river overflows have become a frequent occurrence in many urban areas of the world (Tanoue *et al*., 2016; Egbinola *et al*., 2017; Cirella and Iyalomhe, 2018; Zorn, 2018; Rubinato *et al*., 2019). Floods have affected more than 2.8 billion people in the world and caused more than 200,000 deaths in the last thirty years (BBC News, 2018; Olanrewaju *et al*., 2019). Greater percentages of recent global fatalities in cities have been associated with flood-induced events (Hong *et al*., 2018; Hu *et al*., 2018; Špitalar *et al*., 2020). This supports the claim that flooding accounts for 47% of weather-related disasters world-wide (UNISDR, 2015).

Available records in Nigeria indicate devastating urban flood events in several cities in the two decades (Olawuni *et al*., 2015). Floodlist (2020) documented close to four dozens of flood incidents that have occurred across Nigeria in the last thirty-five years. These events include Ibadan floods of years 1985, 1987, 1990, and 2011; Osogbo floods of years 1992, 1996, 2002, and 2010; Yobe flood of year 2000 and Akure flood of years 1996, 2000, 2002, 2004 and 2006. For other locations such as Lagos, Abeokuta, Benin, Port Harcourt, Calabar, Uyo and Warri to list a few, authors like Ogbonna *et al*., (2011), Aderogba (2012), Efobi (2013), Ogundele and Ubaekwe (2019) and Echendu (2020) reported flooding as a disaster of immense ecological and socio-economic impacts. Abeokuta metropolis for instance witnessed flash floods that swept people and properties off at specific locations in the years 2012, 2016, 2018, and 2020. Ogunaike (2020) reported flood disasters within the metropolis in places like Igbore, Gbangba, Abiola way, Ijaye, Oke-Ejigbo, Isale Abese Obantoko

and Opako Oke Lantoro, Iyana-Amolaso, Lafenwa, Ijaiye, Totoro, Kuto and Kobiti. The city flash flood of year 2020 was particularly recounted to destroy public and private buildings in many areas in the metropolis.

As efforts to reduce the frequency of occurrence and lessen impacts of flood disasters in many susceptible areas intensify, more methods of flood vulnerability and flood risks assessments have emerged over the decades (Perera *et al*., 2019; Martinez *et al*., 2021). Flood risk evaluation or vulnerability assessment has been described as the proactive steps for preventing flood disasters and to provide guidance for mitigation decisions (MRC, 2016; Tascón-González *et al*., 2020). According to Wang *et al*. (2011), there are two broad categories of methodologies for flood risk assessments namely; quantitative and qualitative approaches. The quantitative method estimates the magnitude of expected losses to flood with existing numerical data, while qualitative procedures examines a combination factors can influence the chances of occurrence of flood. The qualitative technics invariably combines flood risk indicators using ranking and weighting to determine relative levels of vulnerabilities of a given area to flooding (Dewan, 2013; Nkeki *et al*., 2013; Umaru and Adedokun, 2020). Nasiri *et al.* (2016) further separated the two broad methods into four most frequently used methods of flood risk analysis which includes; vulnerability index system, vulnerability curve, disaster loss data and computer models. According to Wang *et al*. (2011), vulnerability curve and disaster loss data qualify as quantitative methods; since they rely on availability of previous flood statistics, while vulnerability index systems and computer modelling can be grouped as qualitative techniques.

The demerits and merits of these methods are often considered before adopting any of them for particular flood risk assessment case. Quantitative methods of flood vulnerability assessment could sometimes give superior results where there are accurate and reliable data and statistics of previous flood events. This also implies that the method is limited by data availability and accuracy. Vulnerability curve method for instance, can be used to relate the flood risk and the elements at risk through realistic damage curves (Nasiri *et al*., 2019). This is however; greatly dependent on reliable empirical cases, the limitation of the method is greatly highlighted with paucity of numerical and comprehensive morphological data (Halgamuge and Nirmalathas, 2017). More frequently, actual damage survey is required and this is not only time and resource consuming, but its reliability is less than others because the data is location specific and cannot be applied for other geographic locations. Similarly, Disaster-loss method is premised on data obtained from real flood hazard, although it is a relatively very simple approach and can be used to predict imminent flood events, but its major demerit is in its inaccuracy due to disproportionately chronicled data (Nazeer and Bork, 2019). Its results are usually taken with great caution.

Modeling methods however include the combination of a number of factors that can influence flooding to create vulnerability scenarios (Djimesah *et al*., 2018; Komolafe *et al.*, 2020). Often computer programming is employed in modelling of flood vulnerability. A very common example of flood vulnerability modelling includes the use of multi-criteria evaluation (MCE) or convolutional neural network (CNN) analysis within a Geographical Information System (GIS) and satellite remote sensing environment (Wang *et al*., 2011; Wang *et al*., 2019). When factors like channel parameters, flood velocity, terrain and relief (elevations and depression) and hydrologic data of an area are combined in GIS environment to create flood scenarios, the model is described as multi-criteria evaluation (Tzioutzios and Kastridis, 2020). Various multi-criteria evaluation (MCE) techniques have been used for flood susceptibility and vulnerability analysis and risk mapping with very good accuracy levels (Elsheikh *et al.*, 2015; Fernandez *et al*., 2016; Rimba *et al*., 2017). A mode of MCE is the weighted linear combination procedures (WLC) in a GIS environment (Morales and de Vries, 2021). The weighted linear combination (WLC) procedure is one of the widely used multi-criteria decision-making tools. One great merit of WLC procedure above other methods is its provision of spatial decision-support tool in analyzing environmental problems such as flood (Siddayao *et al*., 2014). The method can rank multiple alternatives, on the basis of several criteria that may have different units and evaluate their respective consequences (Mahmoody and Jelokhani-Niaraki, 2021). The method also does not depend on availability of previous or actual flood data. It is a much cheaper and faster method of vulnerability analysis since it relies on environmental parameters such as soil types, rainfall intensities, relief (topographical data) which are readily available (Wang *et al*., 2011; Chen *et al*., 2014). Beyond these, WLC procedures is quite simple to

implement and interpret, it is also capable in handling poor quality can be efficiently applied in any region since it is not limited by geographical locations.

In this paper, combination of weighted linear procedures with GIS and remote sensing was employed to combine heterogeneous flood inducing environmental factors and spatial data to determine the relative susceptibility of different parts of Abeokuta city to flooding.

## 2.0 Methodology

### *2.1. The study area*

Abeokuta metropolis; one of the capital cities in Southwest Nigeria with a population of 593,140 spread over 125,600 hectares of land (Population Stat, 2020). The city lies between Latitudes, $7^0$5'N and $7^0$20'E and between Longitudes, $3^0$17'E and $7^0$27'E. The geology is crystalline pre-Cambrian basement complex with outcrops of igneous and metamorphic rocks visible in different parts of the conurbation. The city has a mesh of streams all draining into the Ogun River. The yearly annual releases from the Oyan and Ikere gorge Dams makes the inland valleys of the river which has been encroached by residential buildings to become heavily flooded at the peak of the rains (Sobowale and Oyedepo, 2013). Abeokuta portrays the geology of an underlying basement complex of Precambrian origin which predisposes it to poor water percolations (Akinse and Gbadebo, 2016). The city metropolis also has a convoluted drainage networks made up of dendrite rivulets; all draining into one long tortuous Ogun River that runs into Lagos lagoon. These unique peculiarities of the Abeokuta city make it vulnerable to flooding at the in-land valleys and flood plains of the rivulets which incidentally are been encroached by residential buildings.

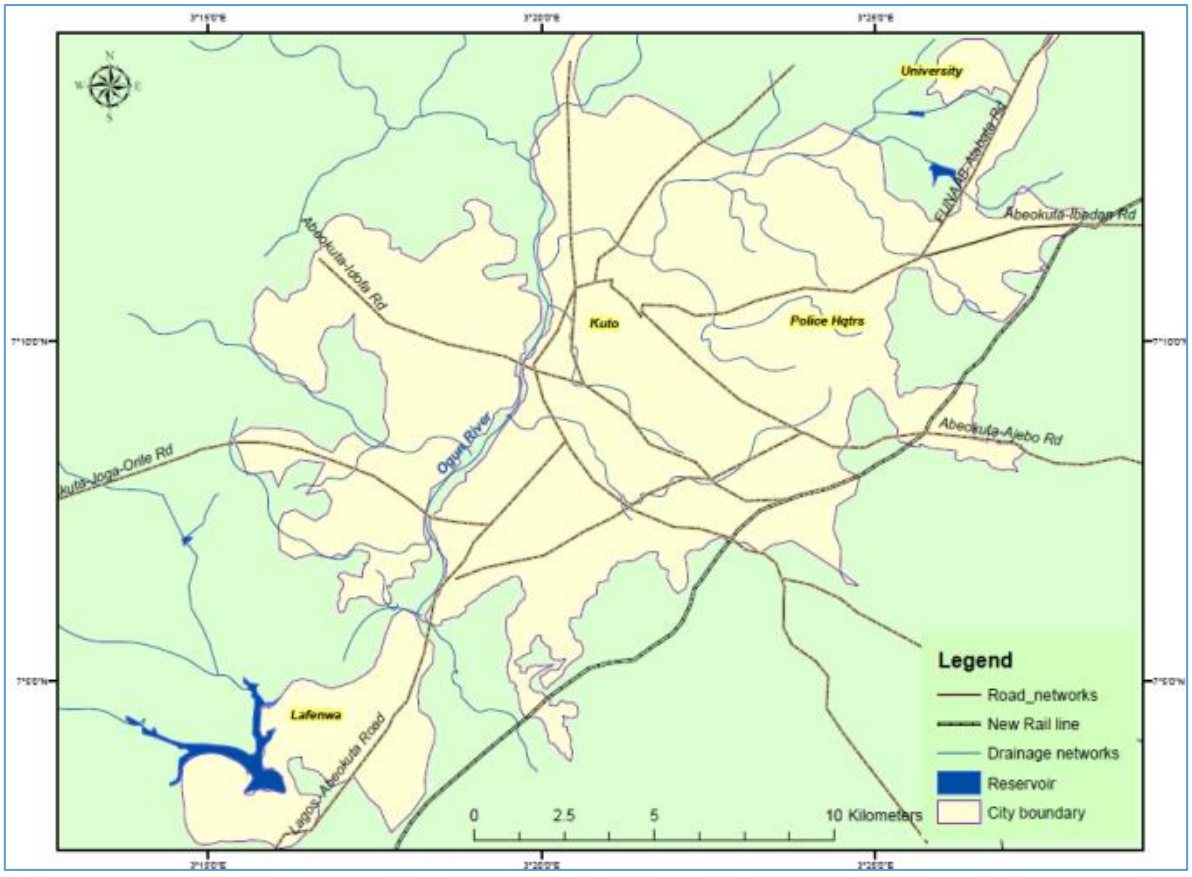


**Figure 1**: Map of Abeokuta Metropolis

### *2.2. Data collection and data analysis*

Data from both primary and secondary sources were used for the study. The primary data include field measurements such as river channel width and depth and stream flow rate (velocity). Stream flow rate and channel metrics (width and depth) were taken from 3 main points namely: Ita Eko River, Ogun River and Arakanga River. The lengths of the various streams from the satellite image were

determined in a GIS environment. The other points were from rivulets and tributary to Ogun River namely: Apete, Ole and Apakila. Secondary data includes: soil types obtained from Harmonized World Soil Data Base (HWSD), Satellite image of drainage networks of the city, the land use/ land cover data, Digital Elevation Model obtained from Shuttle Radar Topographic Missions (SRTM) and rainfall data obtained from Climate Hazards Group InfraRed Precipitation with Station data (CHIRPS).

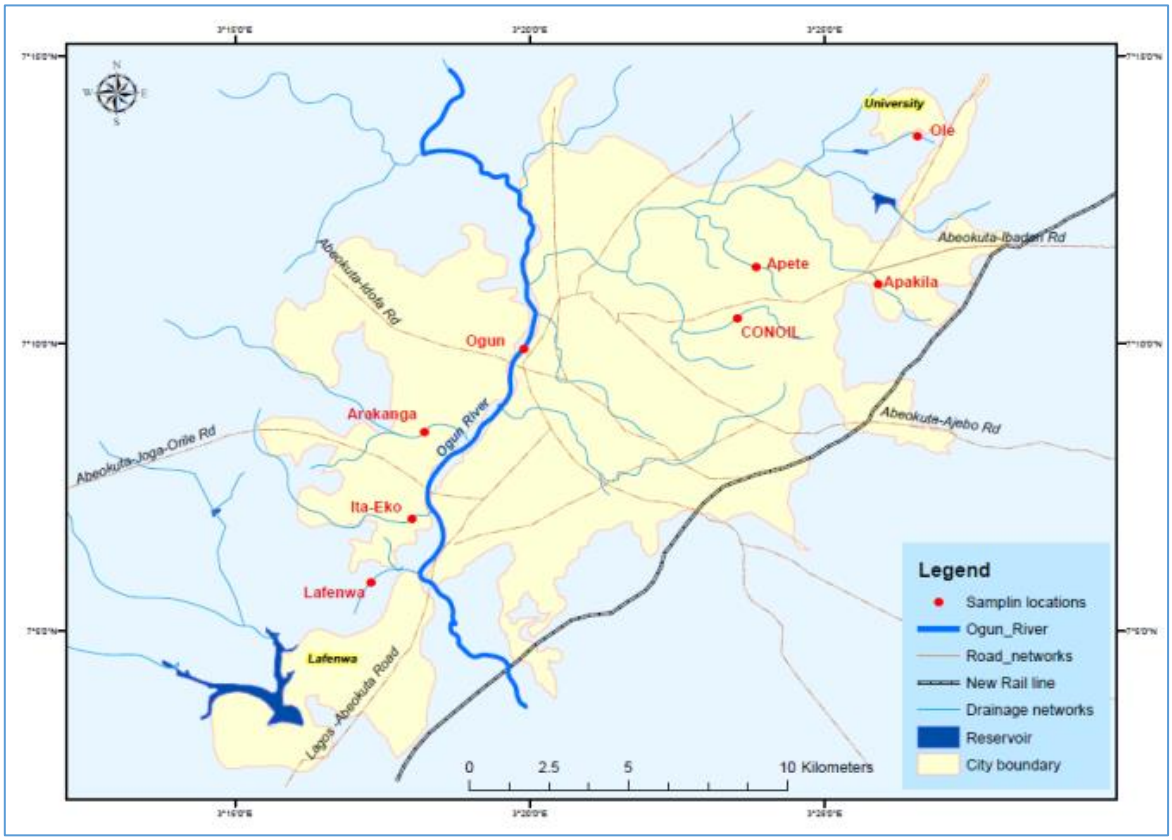


**Figure 2:** Map showing sampling locations

The reliability of satellite-derived meteorological data has been tested in very recent past with very positive outcomes. Akinyemi *et al*. (2020) compared satellite-derived rainfall records namely; CHIRPS, TRIMM and RFE data for six locations in South-west Nigeria with records from NIMET ground stations in order to ascertain the reliability of satellite derived data. The authors reported very high positive correlation values as presented in Table 1.

**Table 1**: Correlation values ($R^2$) of NIMET, with TRMM, CHIRPS and RFE data

| Locations | TRMM/NIMET | CHIRPS/NIMET | RFE/NIMET |
|---|---|---|---|
| Abeokuta | 0.985 | 0.961 | 0.897 |
| Ado-Ekiti | 0.821 | 0.775 | 0.892 |
| Akure | 0.979 | 0.995 | 0.894 |
| Ikeja | 0.782 | 0.85 | 0.844 |
| Oshogbo | 0.98 | 0.979 | 0.927 |
| Ibadan | 0.801 | 0.807 | 0.854 |

Source: Akinyemi *et al.* (2020)

The data set used by the authors in Table 1 namely; Tropical Rainfall Measuring Mission (TRMM), Climate Hazards Group Infrared Precipitation with Stations (CHIRPS) and African Rainfall Estimation (RFE 2.0), which were obtained from the archives of the NOAA Climate Prediction Centre while the ground meteorological data were obtained from the Nigerian Meteorological Agency (NIMET), Oshodi in Lagos.

The high positive correlation value of 0.985 in comparison of CHIRPS with NIMET ascertains the reliability of the data for this study.

Landsat TM 8 acquired in year 2019 downloaded from United State Geological Survey USGS geo-portal (Earth explorer) was georeferenced and the drainage networks of the city were digitized from it. Soil data was also acquired from Food and Agriculture Organization FAO Harmonized World Soil Data base. The Shuttle Radar Topographic Mission was used to produce the Digital Elevation Model (DEM) from which terrain modelling and hydrological analysis of the area was done.

### *2.3. Data processing, integration and spatial analysis*

The primary data collected from the field (soil type, flow rate, channel metrics) were all collated and analysed using the Statistical Package for Social Scientists (SPSS). Maps of all contributing factors to flash flood namely: soil types, meteorology, drainage density and topography were created in ArcMap using same scale of 1: 50,000 and Geographic coordinate system (WGS 1984). All maps were ensured to be in raster format with the same cell grid cell size of 0.0028 mm. They were then subjected to weighting by ranking and Multi-Criteria Analysis (MCA) using the "Weighted Linear Combination" (WLC) method (Moeinaddini *et al*., 2010; Al-Hanbali *et al*., 2011).

For the weighting by ranking to be performed, each data was reclassified into five groups of 1 to 5 as shown in the Table 2.

**Table 2:** Ranking for factors of flooding

| |
|---|
| Not vulnerable |
| Less vulnerable |
| Moderately vulnerable |
| More vulnerable |
| Most vulnerable |

(Class 1 is not vulnerable while 5 is most vulnerable)

In order to find the percentage influence of each contributing factors, weighting factors were attached to each layer of raster data as shown in the Table 3.

**Table 3:** Weighting of each factor associated with flooding

| Criteria | Percentage of influence |
|---|---|
| Landuse | 20% |
| Rainfall | 25% |
| Elevation | 10% |
| Slope degree | 15% |
| Soil drainage | 20% |
| Drainage Density | 10% |
| Total | 100% |

The contributing factor with the highest influence to flash flooding is rainfall with a score of 25%. Table 4 presents the weighting and ranking of all contributing factors to flash flooding.

## 3.0. Results and Discussion

### *3.1. Contributing factors to flood vulnerability in Abeokuta*

Increased run-offs which is a direct effect of rainfall intensity often leads to channel overflow and the persistence of any overflow in an environment is a function of its topographical characteristics and soil permeability. The volume of the run offs and severity of flood also depends on drainage intensity, land use pattern.

In this study, a simple linear combination of the various factors of flooding namely; rainfall intensity, soil types, topography, natural drainage density and land use pattern was done and their relative contributions are ranked by attaching some weighting factors as described in Multi-Criteria Analysis procedures. Since spatial technologies particularly GIS is employed as an analytical tool, most of the results are presented graphically in map form.

*a. Flood vulnerability by rainfall intensity*

The map shown in Figure 3 is the mean rainfall from March to October over Abeokuta region which has been spatially range into five categories namely; (a) 170 to 176 mm, (b) 177 to 181 mm, (c) 182 to 186 mm (d) 187 and 191mm and (e) areas with rainfall above 192 to 199 mm.

**Table 4:** Weighting and ranking of all factors associated with flood vulnerability

| Criteria | Class | Ranking | Weight |
|---|---|---|---|
| Soil | Dystric Nitosols (Well drained) | 1 (Not vulnerable) | 20% |
| | Lithosols (Moderately drained) | 3 (Moderately vulnerable) | |
| | Ferric Luvisols (Imperfectly drained) | 4 (More vulnerable) | |
| | Pellic Vertisols (Poorly drained) | 5 (Most vulnerable) | |
| Elevation | <50 | 5 (Most vulnerable) | 10% |
| | 50 – 130 | 4 (More vulnerable) | |
| | 130 – 217 | 3 (Moderately vulnerable) | |
| | 217-331 | 2 (Less Vulnerable) | |
| | >331 | 1 (Not vulnerable) | |
| Slope degree | 0 – 1 | 5 (Most vulnerable) | 15% |
| | 2 – 3 | 4 (More vulnerable) | |
| | 4 – 4 | 3 (Moderately vulnerable) | |
| | 5 – 7 | 2 (Less Vulnerable) | |
| | 8 -19 | 1 (Not vulnerable) | |
| Drainage Density | < 0.002 | 1 (Not vulnerable) | 10% |
| | 0.003 - 0.003 | 2 (Less Vulnerable) | |
| | 0.004 - 0.005 | 3 (Moderately vulnerable) | |
| | 0.006 - 0.007 | 4 (More vulnerable) | |
| | 0.008 - 0.008 | 5 (Most vulnerable) | |
| Mean Rainfall | 170 – 176 | 1 (Not vulnerable) | 25% |
| | 177 – 181 | 2 (Less Vulnerable) | |
| | 182 – 186 | 3 (Moderately vulnerable) | |
| | 187 – 191 | 4 (More vulnerable) | |
| | 192 – 199 | 5 (Most vulnerable) | |
| Land use | Built up | 5 (Most vulnerable) | 20% |
| | Bare land | 4 (More vulnerable) | |
| | Grassland | 3 (Moderately vulnerable) | |
| | Intensive row crop rain-fed agriculture | 2 (Less Vulnerable) | |
| Total | | | 100% |

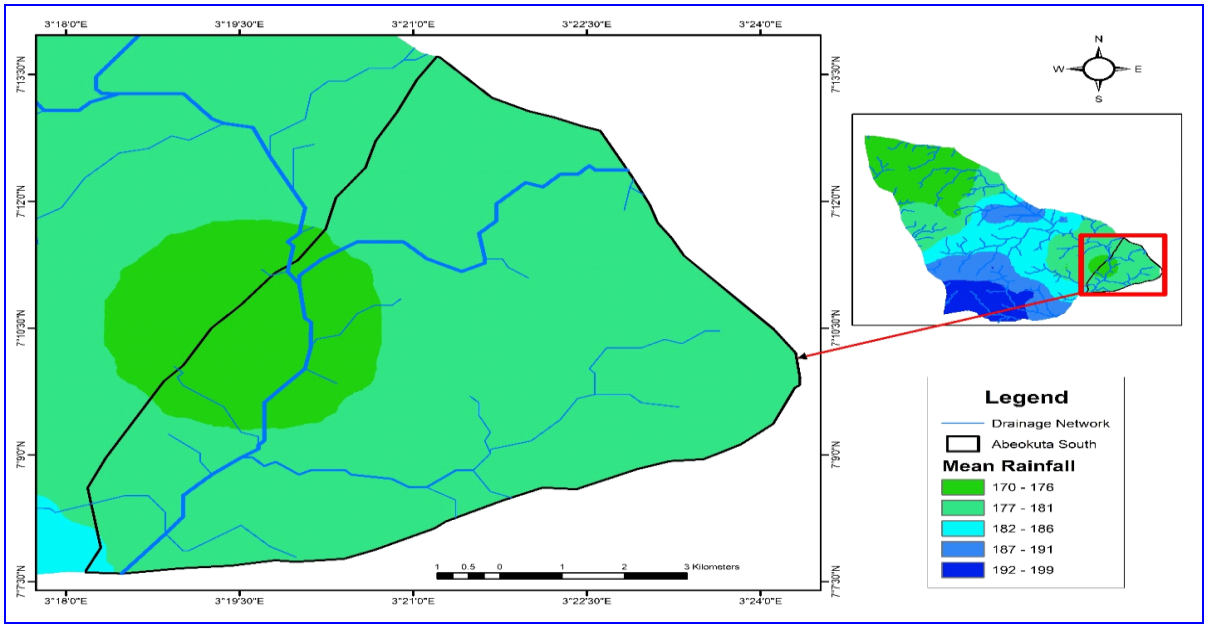


**Figure 3:** Mean rainfall over Abeokuta metropolis (inset: Abeokuta region).

The area occupied by the metropolis (left inset) has rainfall range of 170 to 181 mm which is the lowest mean annual rainfall. This implies that relative influence of rainfall intensity on area occupied by the metropolis with regards to flooding is lowest in the region. However, ranking the map in figure 4 by assigning weights and Multi-Criteria Analysis gives better insights to flood vulnerability by rainfall intensity as shown in Figure 4.

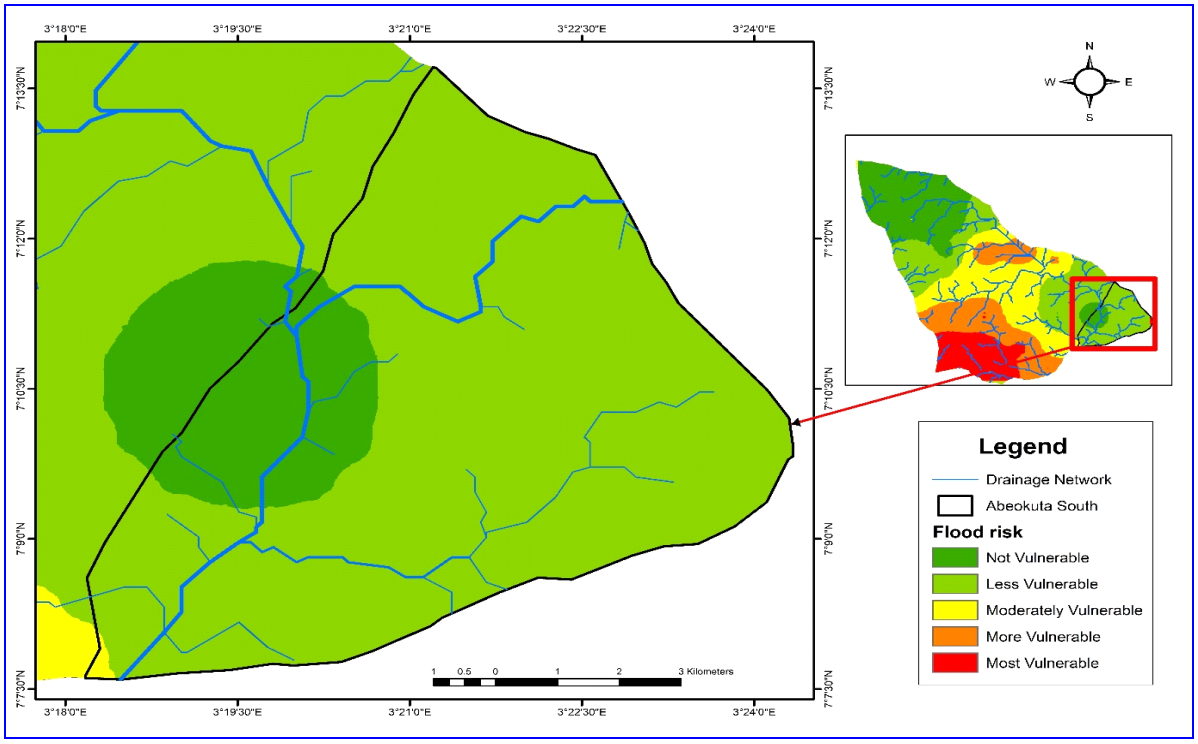


**Figure 4:** Vulnerability ranking of the study area by rainfall intensity

The map reveals the south western parts of Abeokuta region as the most susceptible to flooding using rainfall as a sole factor in flood vulnerability ranking as shown (red to orange). The populated areas of the region (left) are the least vulnerable. This is however does not exempt the metropolis from flooding particularly when other factors such as soil type, land use and drainage intensities are combined.

*b. Flood vulnerability by soil types*

According to FAO classification, Abeokuta city has four soil types namely: Lithosols, Districc Nitosols, Pellic Vertisols and Ferric Luvisols. Districc Nitosols and Ferric Luvisols are the two dominant soil types for Abeokuta-metropolis. While, Districc Nitosols is well drained, Lithosols is moderately drained, Ferric Luvisols is perfectly drained and Pellic Vertisols is poorly drained as presented in Table 5.

**Table 5:** Area occupied by soil classes in Abeokuta region

| Soil type | Area ($km^2$) | Drainage |
|---|---|---|
| Lithosols | 259.5 | Moderate |
| Districc Nitosols | 437.7 | Well |
| Pellic Vertisols | 0.2 | Poor |
| Ferric Luvisols | 169.7 | Imperfectly |

Using soil type alone, the northern part of Abeokuta region will be the most susceptible to flooding being the most poorly drained. The persistence of a flooding is determined by soil type (Ponting *et al*., 2021).

Incidentally, the distribution of the two dominant soil types in Figure 5 reveals the imperfectly drained Ferric Luvisol covering a larger portion of the area occupied by the city metropolis is as shown. With weighting and reclassification, the soil map reveals relative vulnerabilities as shown in Figure 6.

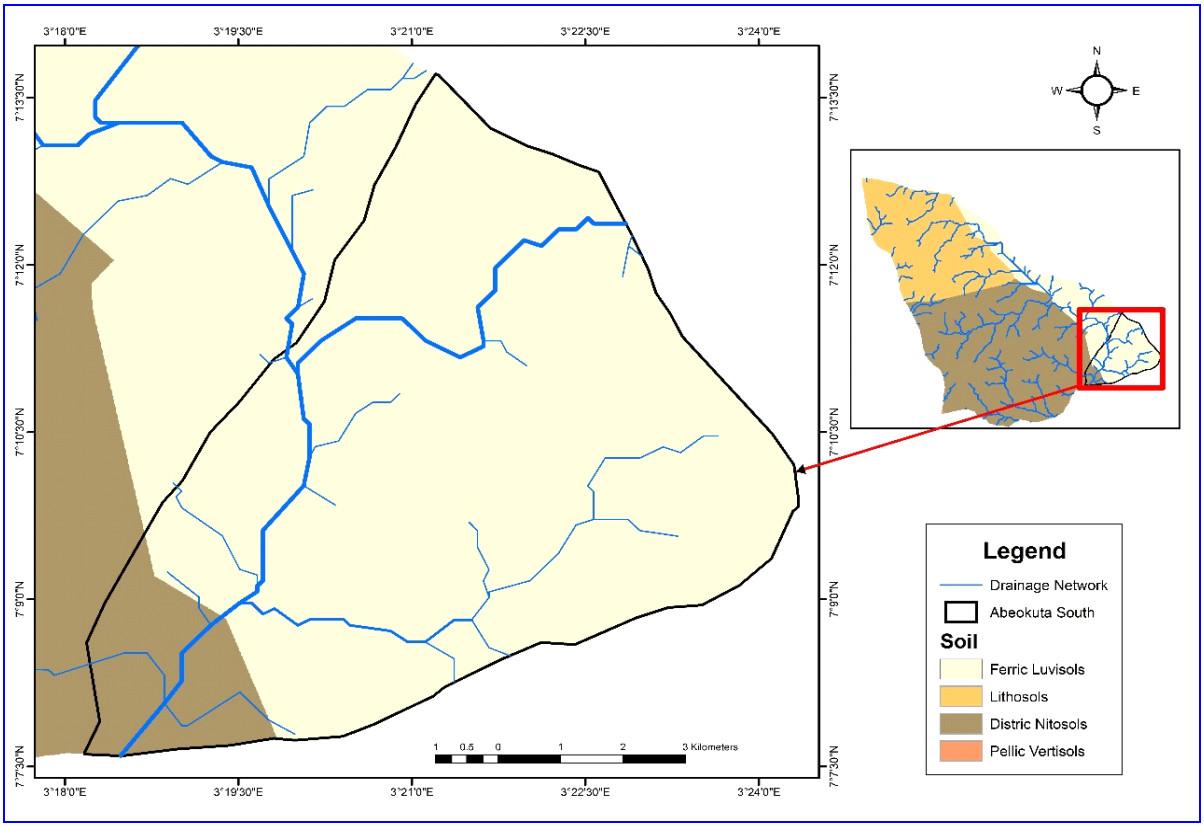


**Figure 5:** Dominant soils of the study area

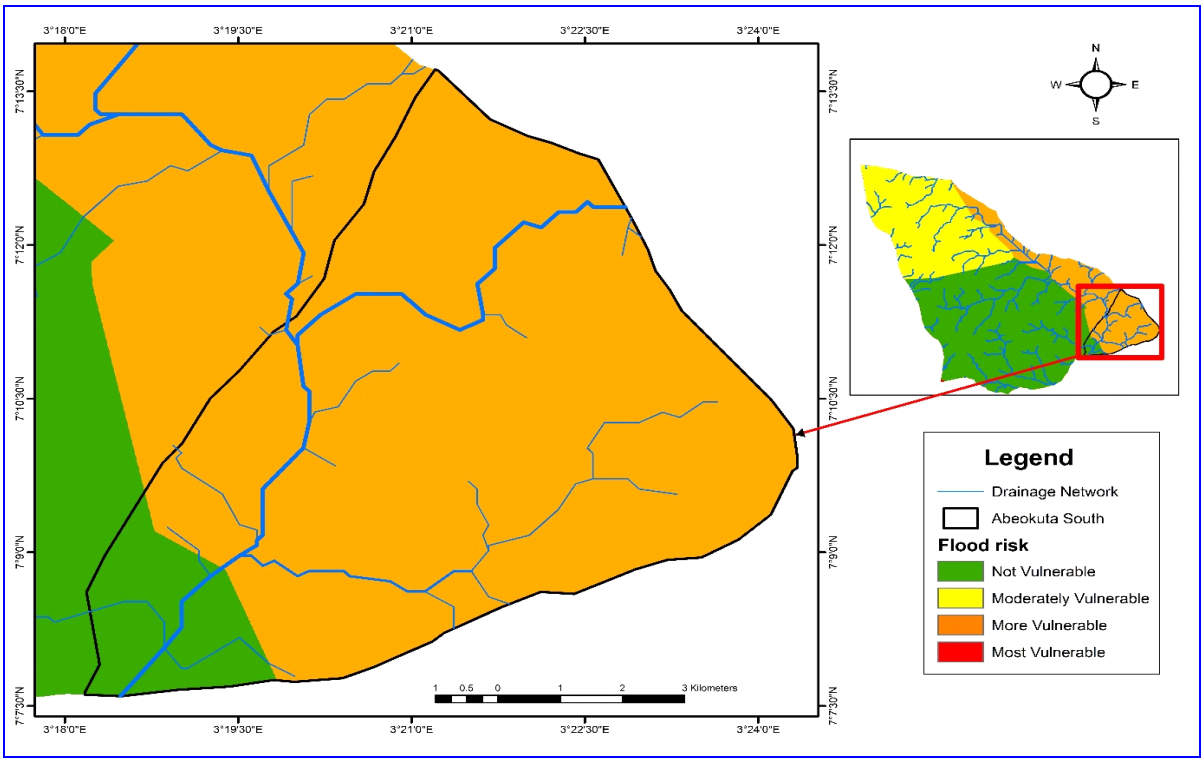


**Figure 6:** Vulnerability ranking of the study area by soil types

The orange portion of the map portrays most parts of the city as more vulnerable to flooding based on soil characteristics. The most vulnerable portion of the region is occupied by the metropolis as shown.

*c. Flood vulnerability by topography*

The relief of Abeokuta-South is a mixture of high, low and undulating terrain as shown by the Digital Terrain Model (DTM) in Figure 7.

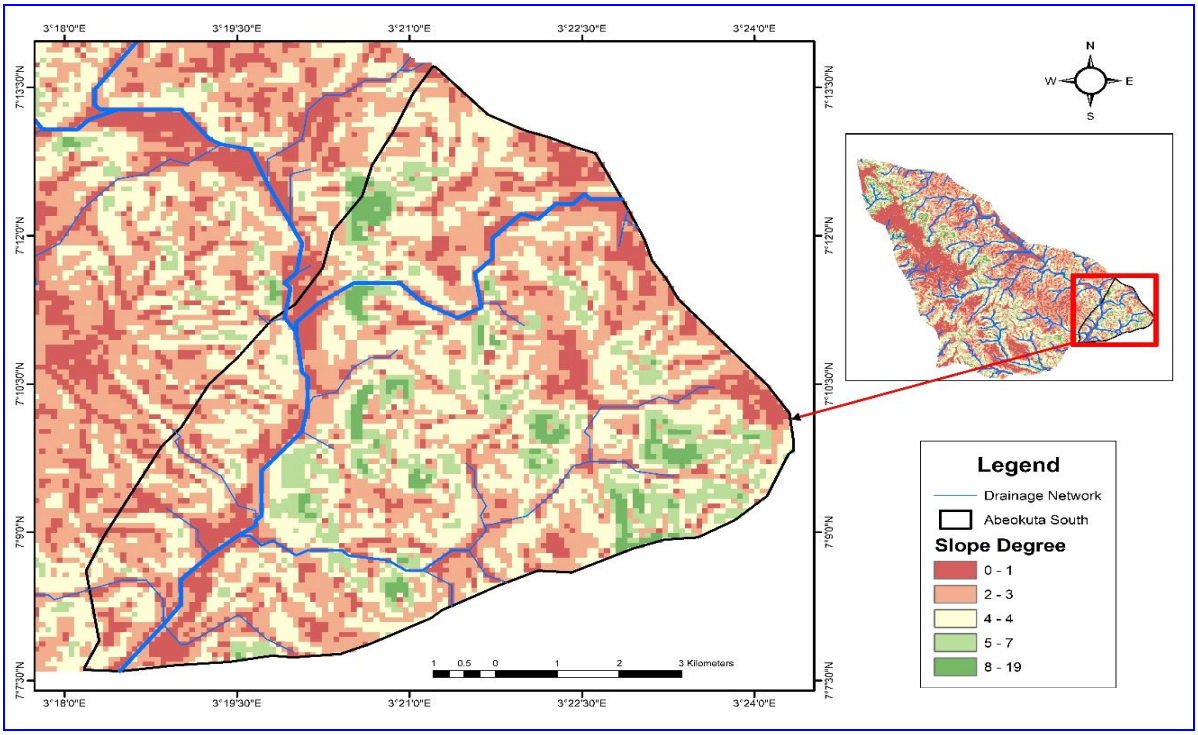


**Figure 7:** Digital Terrain Model of Abeokuta

The map reveals areas with the steepest slopes (deep to light green) and those with gentle to flat slopes (deep brown to light brown). The areas with almost imperceptible slopes retain more water as the run-off velocities is considerable reduced along the channels and flood plains. The weighted relief presents 5 categories of vulnerability to flooding as shown in Figure 8.

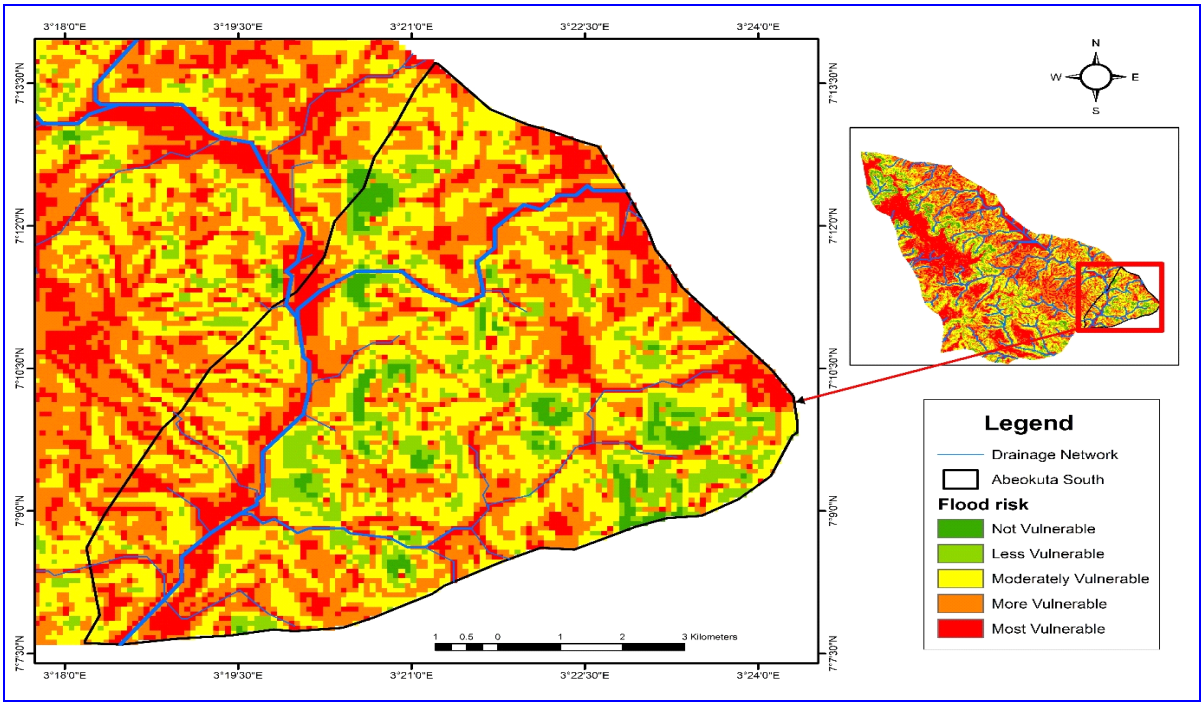


**Figure 8:** Vulnerability ranking of the study area by topography

The most vulnerable areas (in red) are located along the flood plains of streams and rivers. The areas in yellow are of moderate susceptibility to flooding. A good percentage of the city ranks from more to most vulnerable as shown. Most of the areas coded orange and yellow in the map are actually inland valleys which witness flash flooding annually. Ordinarily, the red-brown zones are natural buffers to the rivers and streams, but they have almost all been built-up. At present they have become locations where the flash flood persists in the city. A recent example is in Plate 1.

**Plate 1 (a-d):** Flooding in different parts of Abeokuta Metropolis in April 2020

*d. Hydrological Modelling*

The hydrological modelling of the map in Figure 9 reveals that about 48% of the metropolis is more or highly vulnerable to flooding. This implies that based on topography almost all parts of the metropolis can be flooded as shown.

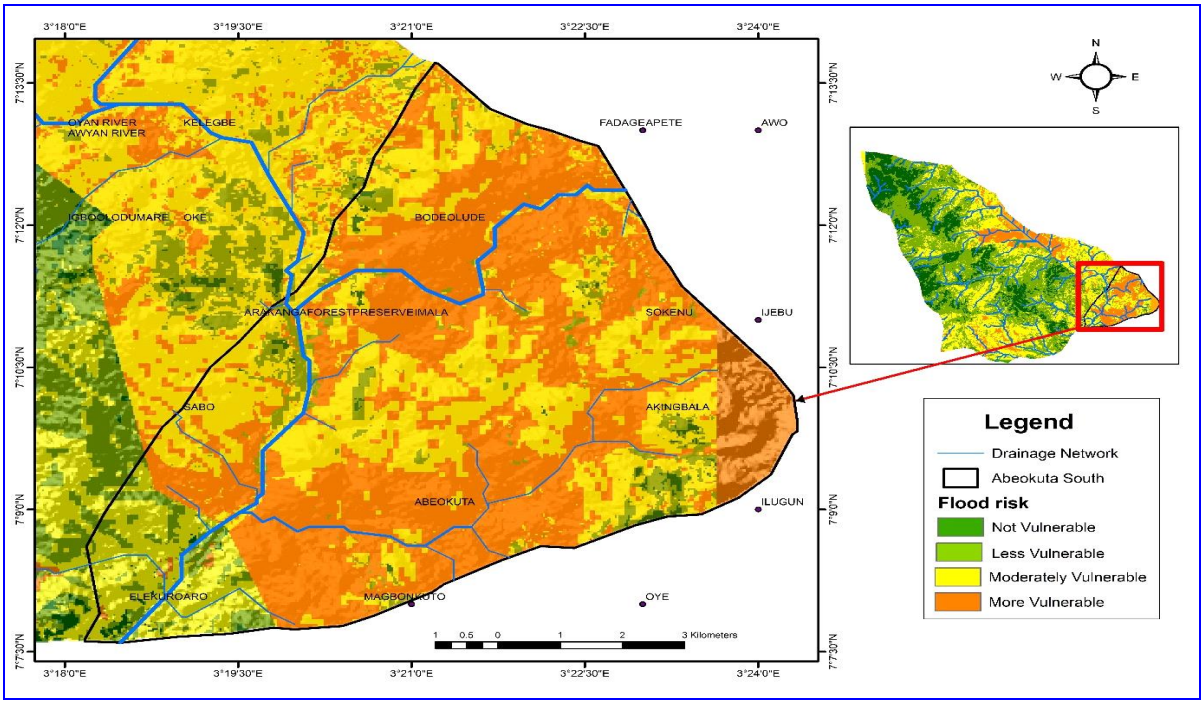


**Figure 9:** Overall map of vulnerability based on combination of the multiple criteria

*e. Flood vulnerability by drainage density*

Drainage density is also a very crucial factor in flooding events. The higher the value of drainage density in an area, the less persistent the flash flood in the area. Drainage density (DD) is given by the equation: DD = L/A in which L is the total length of drainage channel in km and A is the Total area of watershed in $km^2$. The map in Figure 10 shows the GIS computation of drainage density of Abeokuta metropolis.

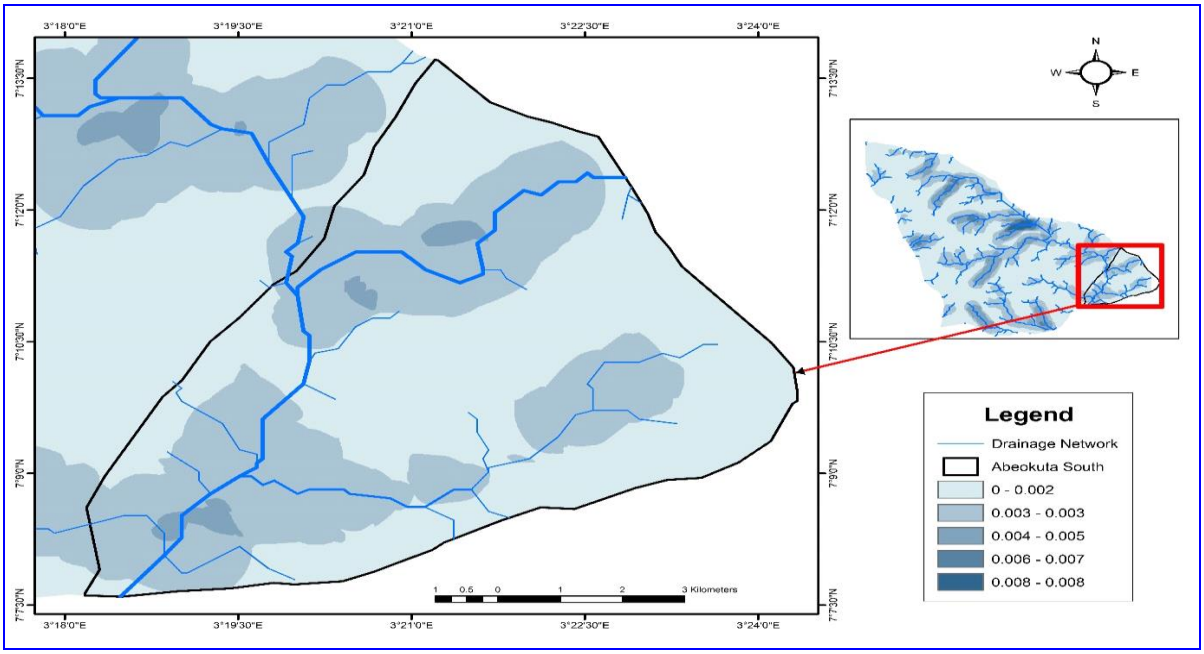


**Figure 10:** Drainage density of Abeokuta Metropolis (Inset is Abeokuta region)

The darker tone colour tone depicts higher drainage density. The more the density the more susceptible the area is to flooding. Ogun river; the main river in the metropolis has a lot of tributaries. The weighting of the drainage density produced four categories of vulnerability as shown in Figure 11.

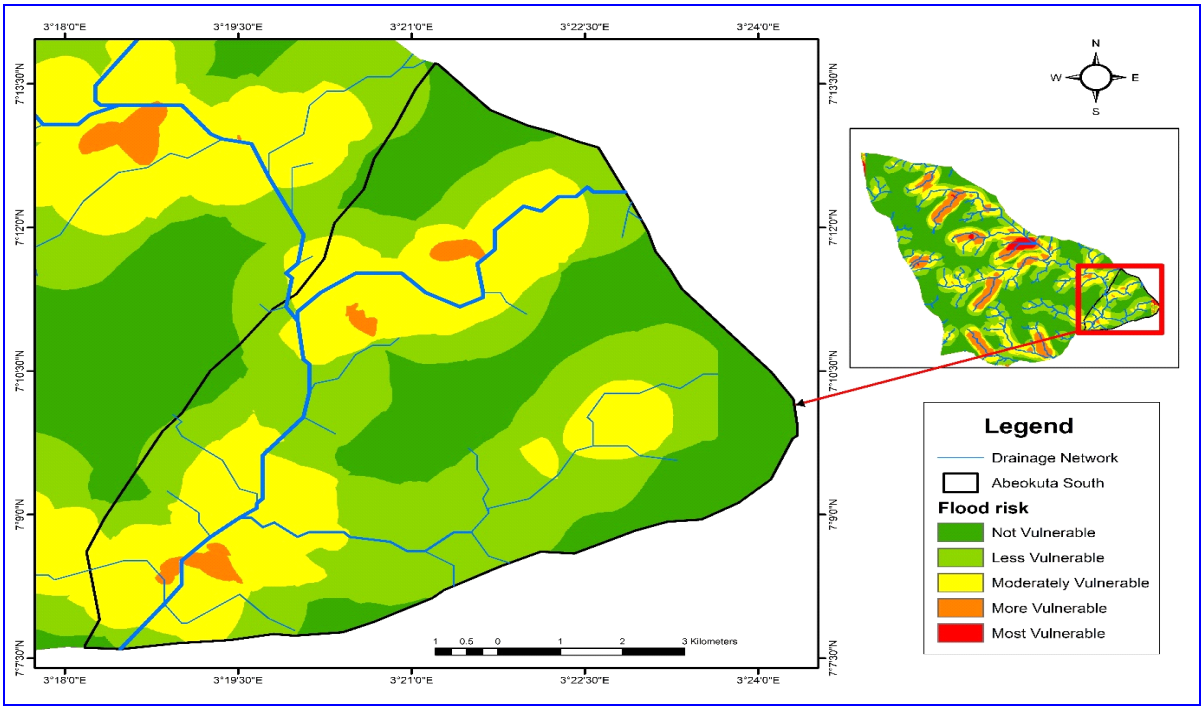


**Figure 11:** Vulnerability ranking of the study area by drainage density

The most vulnerable areas are around the inland valleys which are often encroached by human buildings as earlier mentioned and depicted in Plate 2.

**Plate 2:** part of Abeokuta city on the flood plain of Ogun River (at the background)

*f. Flood vulnerability by land use patterns*

Poor urban planning and land use pattern is a huge predisposing factor to flood disasters. Where the houses are compact and a greater percentage of the grounds are concreted, the tendencies for generating high volume of run-offs are high. Meanwhile, with poor artificial drainage networks, congested areas are easily flooded.

Figure 12 is the land use map of Abeokuta region from which a very massive portion of Abeokuta metropolis (left) is shown as built (comprising of roofed areas and concretized grounds).

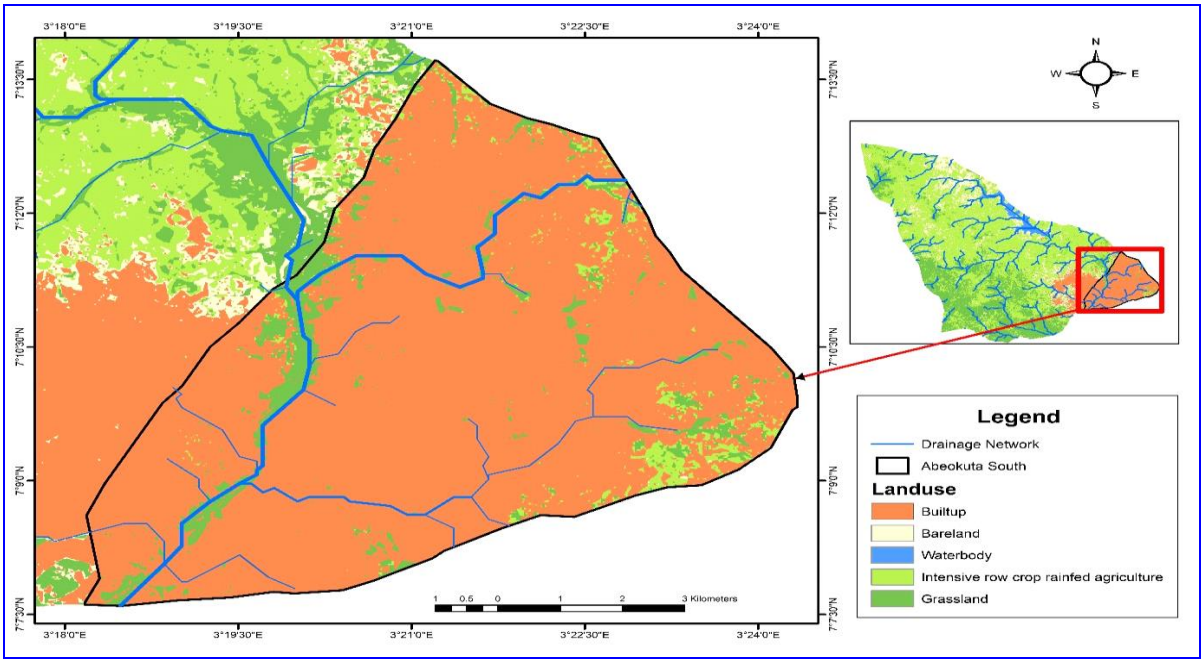


**Figure 12:** General Land use types of Abeokuta

The map shows very sparse portion of the area occupied by the metropolis as vegetated. Where the constructed channels are blocked by debris or have become too narrow to contain the high volume of run-off from the city, the flood appears in the inland valleys which incidentally have become occupied by residential and other human structures. Further to this is the fact that changes in land use associated with urbanization also contributes to flooding. For instance, construction of roads, schools or factories often remove vegetation, causing free flow of run-offs, soil erosion and creation of depressions on the land surface. When permeable soil is replaced by impermeable surface, reduction in water percolation and consequently flooding occurs.

The land use types of Abeokuta metropolis include: Built up, Water bodies, Grassland, rain-fed Agriculture and Bare-land. Assigning weights to the land use types shows five levels of susceptibility to flooding as shown in the vulnerability map in Figure 13.

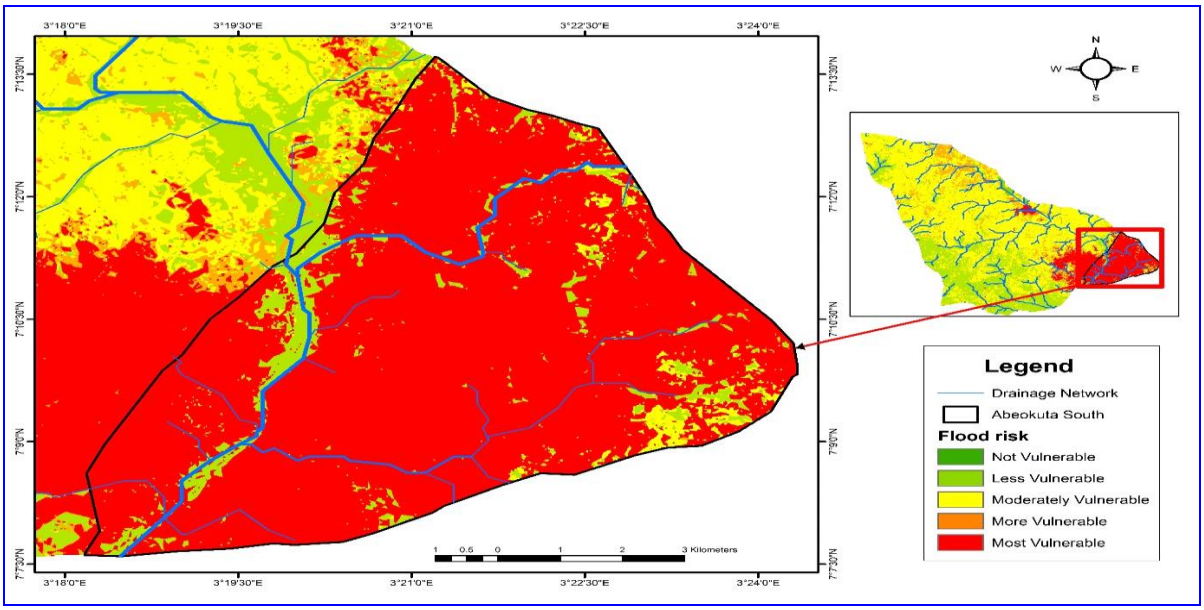


**Figure 13:** Vulnerability ranking of the study area by drainage density

With respect to land use types, most parts of the city (in red) are highly vulnerable since large part of the area is built up.

*g. Flood vulnerability by a combination of contributing factors*

It may be slightly difficult to take decision on the relative vulnerabilities of the various parts of the city by independent consideration of the respective factors of flooding considered in this study. A combination of the factors is always useful for spatial decision support.

In Figure 14 is the result of the combination of the multiple criteria.

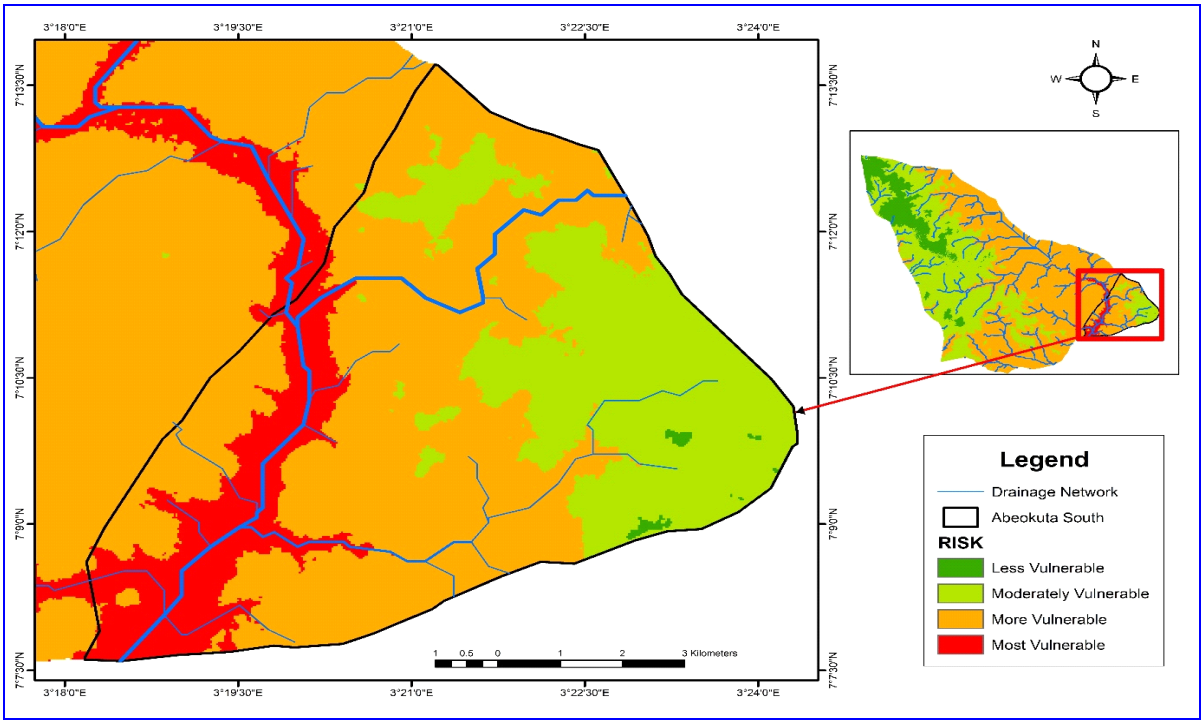


**Figure 14:** Overall map of vulnerability based on combination of the multiple criteria

The map shows the flood plains as the most vulnerable to flooding and next to it is a large portion all around the flood plains. Although no area upland is in the red zone but almost half of the metropolis are still highly vulnerable to flood events especially along streams and rivulets within the townships.

Figure 14 becomes a spatial decision support tool if the nearness to the sources of flooding is examined. For example, with a setback of 500 meters from the rivers and flood plains, it is possible to determine. The result shows areas that are more vulnerable to flooding are within a distance of 500 meters from the river. These areas are likely to be the mostly impacted in the event of flooding.

Figure 15 gives the picture of the 500 m zone of influence with regards to flash flood. All structures within these zones should be inspected and ensured that they would be safe in the event of flood.

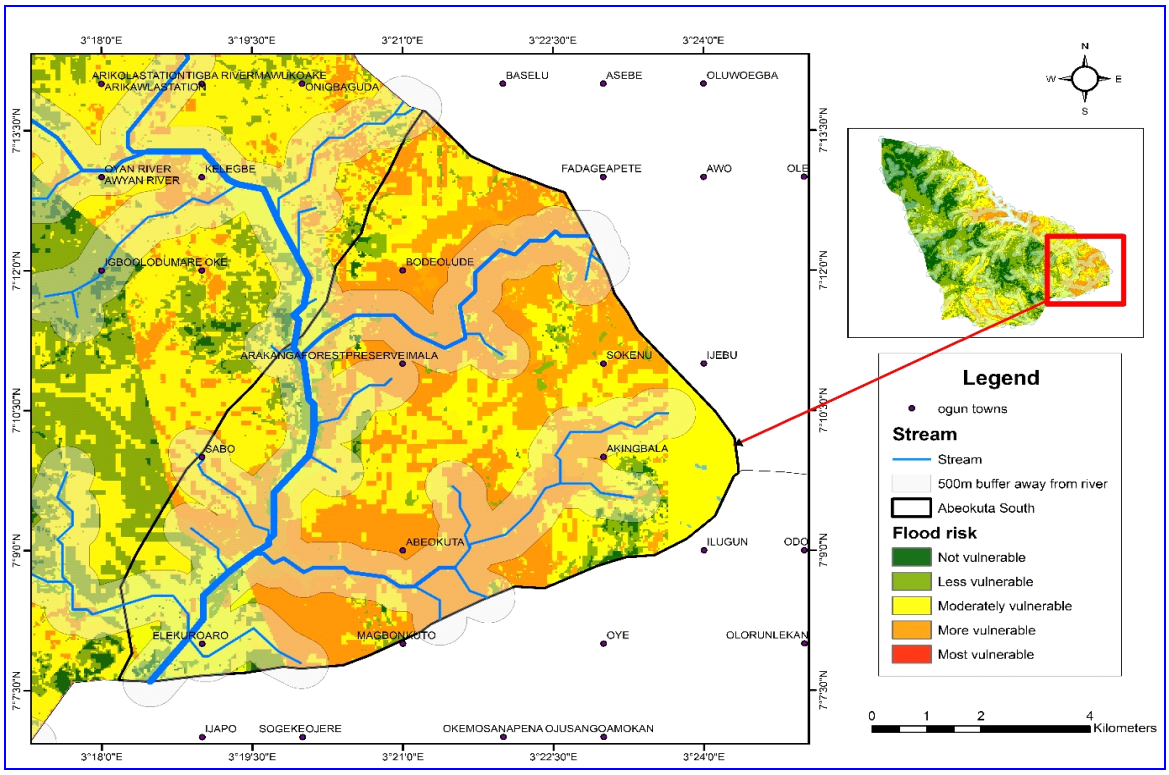


**Figure 15:** Map of flood risk zone

The various phases of analysis carried out have given an in-depth understanding of the areas that are vulnerable to flood within Abeokuta metropolis and the factor that has played the major role in predisposing the city to deluge. This insight pre-empts the recommendations of the study on how flood could be effectively controlled and managed. The key findings are documented in the conclusion.

## 4.0. Conclusion

Weighted linear combination procedures using remote sensing and Geospatial techniques was reliable in the determination of areas vulnerable to flooding across Abeokuta region. The city is less vulnerable with regards rainfall intensity, but the soil in most part of the city Ferric Luvisol; which are poorly drained and as such by soil type almost the entire metropolis is susceptible to flooding. The city relief also show a lot of inland valleys and high drainage density both factors influences flooding. Another predisposing factor is the compact nature of the settlement pattern; the city is compact and most building roofs and concreted premises contribute to the volume of run offs. Most importantly, several buildings are sited within the inland valleys. The overall result of the analysis shows that the flood plains and inland valleys are the most vulnerable to flooding and next to it is the large portion of the landscape surrounding the flood plains. Although no area upland is in the red zone but almost half of the metropolis are still highly vulnerable to flood events especially along streams and rivulets within the townships. The study identified topography and land use as key factors contributing to

flooding within Abeokuta metropolis. Obstructions of natural drainage channels by buildings can aggravate disasters from flash flood events.

**References**

Aderogba, K. A., Oredipe, M., Oderinde, S. and Afelumo, T. (2012). Challenges of poor drainage systems and floods in Lagos Metropolis, Nigeria. *International J. Soc. Sci. & Education*, 2(3), pp. 412–427.

Akinse, A. G. and Gbadebo, A. M. (2016). Geologic Mapping of Abeokuta Metropolis, Southwestern Nigeria. *International Journal of Scientific & Engineering Research*, 7(8), pp. 979-983.

Akinyemi, D. F., Ayanlade, O. S., Nwaezeigwe, J. O. and Ayanlade, A. (2020). A Comparison of the Accuracy of Multi-Satellite Precipitation Estimation and Ground Meteorological Records Over Southwestern Nigeria. *Remote Sens Earth Syst Sci*, 3, pp. 1–12.

Al-Hanbali, A. (2011). Using GIS-Based Weighted Linear Combination Analysis and Remote Sensing Techniques to Select Optimum Solid Waste Disposal Sites within Mafraq City, Jordan *Journal of Geographic Information System*, 3(04), pp. 267-278. DOI: 10.4236/jgis.2011.34023

BBC News (2018). Why does Nigeria keep flooding? Online news article available at https://www.bbc.com/news/world-africa-45599262 Reality Check team Published 26 September 2018, Retrieved 2 September 2020.

Chen, S., Liu, H., You, Y., Mullens, E., Hu, J,, Yuan, Y., Huang, M., He, L., Luo, Y., Zeng, X., Tang, Y., Hong, Y. et al. (2014) Evaluation of High-Resolution Precipitation Estimates from Satellites during July 2012 Beijing Flood Event Using Dense Rain Gauge Observations. PLoS ONE 9(4): e89681. doi:10.1371/journal.pone.0089681

Cirella, G. T. and Iyalomhe, F. O. (2018). Flooding Conceptual Review: Sustainability-Focalized Best Practices in Nigeria. *Appl. Sci.* 8, pp. 1558. https://doi.org/10.3390/app8091558

Dewan, A. M. (2013). Floods in a Megacity: Geospatial Techniques in Assessing Hazards, Risk and Vulnerability. Springer Publication, Netherlands. 199p http://dx.doi.org/10.1007/978-94-007-5875-9

Djimesah, I. E., Okine, A.N.D. and Mireku, K. K. (2018). Influential factors in creating warning systems towards flood disaster management in Ghana: An analysis of 2007 Northern flood. *International Journal of Disaster Risk Reduction*, 28, pp. 318–326.

Echendu, A. J. (2020). The impact of flooding on Nigeria's sustainable development goals (SDGs), Ecosystem. *Health and Sustainability*, 6(1), pp. 1-13. https://doi.org/10.1080/20964129.2020.1791735

Efobi, K. (2013). Urban Flooding and Vulnerability of Nigerian Cities: A Case Study of Awka and Onitsha in Anambra State, Nigeria. *Journal of Law, Policy and Globalization*, 19, pp. 58-64.

Egbinola, C. N., Olaniran, H. D. and Amanambu, A. C. (2017). Flood management in cities of developing countries: the example of Ibadan, Nigeria. *J. Flood risk management*, 10, pp. 546–554.

Elsheikh, R. F. A., Ouerghi, S. and Elhag, A. R. (2015). Flood Risk Map Based on GIS, and Multi Criteria Techniques (Case Study Terengganu Malaysia). *Journal of Geographic Information System*, 7, pp. 348-357.

Fernandez, P., Mourato, S. and Moreira, M. (2016). Social vulnerability assessment of flood risk using GIS-based multi-criteria decision analysis. A case study of Vila Nova de Gaia (Portugal). *Geomatics, Natural Hazards and Risk*, 7(4), pp. 1367-1389.

Floodlist (2020). Nigeria. Online flood news articles available at http://floodlist.com/tag/nigeria

Halgamuge, M. N. and Nirmalathas, A. (2017). Analysis of large flood events: Based on flood data during 1985–2016 in Australia and India. *International Journal of Disaster Risk Reduction*, 24, pp. 1-11.

Hong, M., Kim, J. and Jeong, S. (2018). Rainfall intensity-duration thresholds for landslide prediction in South Korea by considering the effects of antecedent rainfall. *Landslides*, 15, pp. 523–534.
Hu, P., Zhang, Q., Shi, P., Chen, B. and Fang, J. (2018). Flood-induced mortality across the globe: Spatiotemporal pattern and influencing factors. *Science of the Total Environment*, 643, pp. 171-182.

Komolafe, A. A., Awe, B. S., Olorunfemi, I. E. and Oguntunde, P. G. (2020). Modelling flood-prone area and vulnerability using integration of multi-criteria analysis and HAND model in the Ogun River Basin, Nigeria. *Hydrological Sciences Journal*, 65(10), pp. 1766-1783.

Mahmoody, V. N. and Jelokhani-Niaraki, M. (2021). The use of subjective–objective weights in GIS-based multi-criteria decision analysis for flood hazard assessment: a case study in Mazandaran, Iran. *GeoJournal*, 86, pp. 379–398. https://doi.org/10.1007/s10708-019-10075-5

Martinez, M., Bakheet, R. and Akib, S. (2021). Innovative Techniques in the Context of Actions for Flood Risk Management: A Review. *Eng*, 2, pp. 1– 11. https://dx.doi.org/10.3390/ eng2010001

Mekong River Commission (MRC, 2016). Manual on Flood Preparedness Program for Provincial and District Level Authorities in the Lower Mekong Basin Countries. 26p https://www.preventionweb.net/files/13076_Flood09.pdf

Moeinaddini, M., Khorasani, N., Danehkar, A., Darvishsefat, A. A., and Zienalyan, M. (2010). Siting MSW landfill using weighted linear combination and analytical hierarchy process (AHP) methodology in GIS environment (case study: Karaj). *Waste Management*, 30(5), pp. 912–920.

Morales, F. F. and de Vries, W. T. (2021). Establishment of Natural Hazards Mapping Criteria Using Analytic Hierarchy Process (AHP). *Front. Sustain*. 2, 667105p. doi: 10.3389/frsus.2021.667105

Nasiri, H., Mohd Yusof, M.J. and Mohammad Ali, T.A. (2016). An overview to flood vulnerability assessment methods. *Sustain. Water Resour. Manag.* 2, pp. 331–336. https://doi.org/10.1007/s40899-016-0051-x

Nasiri, H., Yusof, M. J. M. and Ali, T. A. M. (2019). District flood vulnerability index: urban decision-making tool. *Int. J. Environ. Sci. Technol*. 16, pp. 2249–2258.

Nazeer, M. and Bork, H. (2019). Flood Vulnerability Assessment through Different Methodological Approaches in the Context of North-West Khyber Pakhtunkhwa, Pakistan. *Sustainability*, 11, 6695p, doi:10.3390/su11236695 www.mdpi.com/journal/sustainability

Nkeki, F. N., Henah, P. J. and Ojeh, V. N. (2013). Geospatial Techniques for the Assessment and Analysis of Flood Risk along the Niger-Benue Basin in Nigeria. *Journal of Geographic Information System*, 5(2), pp. 123-135. DOI: 10.4236/jgis.2013.52013.

Ogbonna, D. N., Amangabara, G. T. and Itulua, P. A. (2011). Study of the nature of urban flood in Benin City, Edo State, Nigeria. *Global Journal of Pure and Applied Sciences*, 17(1), pp. 7-21.

Ogunaike, J. (2020). Flood destroys part of Obasanjo Library Fence. An article in Vanguard a Nigerian daily newspaper also available on line at https://www.vanguardngr.com/2020/07/photos-flood-destroys-part-of-obasanjo-library-fence/

Ogundele, O. M. and Ubaekwe, R. E. (2019). Early Warning System and Ecosystem-Based Adaptation to Prevent Flooding in Ibadan Metropolis, Nigeria. In: Leal Filho W. (eds) Handbook of Climate Change Resilience. Springer, Cham. https://doi.org/10.1007/978-3-319-71025-9_112-1

Olanrewaju, C. C., Chitakira, M., Olanrewaju, O. A. and Louw, E. (2019). Impacts of flood disasters in Nigeria: A critical evaluation of health implications and management. *Jamba (Potchefstroom, South Africa)*, 11(1), 557p. https://doi.org/10.4102/jamba.v11i1.557

Olawuni, O.P., Popoola, A.S., Bolukale, A.T., Eluyele, K. P. and Adegoke, J. O. (2015) An Assessment of the Factors Responsible for Flooding in Ibadan Metropolis, Nigeria. Journal of Environment and Earth Sciences, 5(21): 1-7.

Perera, D., Seidou, O., Agnihotri, J., Rasmy, M., Smakhtin, V., Coulibaly, P., *et al*. (2019). Flood Early Warning Systems: A Review of Benefits, Challenges and Prospects. *UNU-INWEH Report* Series, Issue 08. United Nations University Institute for Water, Environment and Health, Hamilton, Canada. http://inweh.unu.edu/publications/ ISBN: 978-92-808-6096-2

Ponting, J., Kelly, T. J., Verhoef, A., Watts, M. J. and Sizmur, T. (2021). The impact of increased flooding occurrence on the mobility of potentially toxic elements in floodplain soil. *Science of the Total Environment*, 754 (2021), 142040p. https://doi.org/10.1016/j.scitotenv.2020.142040

Population Stat (2020). Abeokuta, Nigeria, Population. https://populationstat.com/nigeria/abeokuta Accessed on October, 15th, 2020

Rimba, A. B., Setiawati, M. D., Sambah, A. B. and Miura, F. (2017). Physical Flood Vulnerability Mapping: Applying Geospatial Techniques in Okazaki City, Aichi Prefecture, Japan. *Urban Sci*. 2017(1), 7p. https://doi.org/10.3390/urbansci10100077

Rubinato, M., Nichols, A., Peng, Y., Zhang, J., Lashford, C., Cai, Y., *et al*. (2019). Urban and river flooding: Comparison of flood risk management approaches in the UK and China and an assessment of future knowledge needs. *Water Science and Engineering*, 12(4), pp. 274-283.

Sobowale, A. and Oyedepo, J. A. (2013). Status of flood vulnerability area in an ungauged basin, South-west Nigeria. *International Journal of Agricultural and Biological Engineering*, 6(2), pp. 28-36. DOI:10.3965/j.ijabe.20130602.004

Siddayao, G. P., Valdez, S. E., and Fernandez, P. L. (2014). Analytic Hierarchy Process (AHP) in Spatial Modeling for Floodplain Risk Assessment. *International Journal of Machine Learning and Computing*, 4(5), pp. 450-457. DOI: 10.7763/IJMLC.2014.V4.453

Špitalar, M., Brilly, M., Kos, D. and Žiberna, A. (2020). Analysis of Flood Fatalities–Slovenian Illustration. *Water*, 12(1), pp. 64-78,https://doi.org/10.3390/w12010064

Tanoue, M., Hirabayashi, Y. and Ikeuchi, H. (2016). Global-scale river flood vulnerability in the last 50 years. *Scientific reports*, 6, 36021p. https://doi.org/10.1038/srep36021

Tascón-González, L., Ferrer-Julià, M., Ruiz, M. and García-Meléndez, E. (2020). Social Vulnerability Assessment for Flood Risk Analysis. *Water*, 12, 558p, doi:10.3390/w12020558

Tzioutzios, C. and Kastridis, A. (2020). Multi-Criteria Evaluation (MCE) Method for the Management of Woodland Plantations in Floodplain Areas. *ISPRS Int. J. Geo-Inf.* 2020(9), 725p. https://doi.org/10.3390/ijgi9120725

United Nations Office for Disaster Risk Reduction (UNISDR, 2015) UNISDR annual report 2015. 75 p. https://www.undrr.org/publications

Umaru, E. T. and Adedokun, A. (2020). Geospatial Analysis of Flood Risk and Vulnerability Assessment along River Benue Basin of Kogi State. *Journal of Geographic Information System*, 12, pp. 1-14. DOI: 10.4236/jgis.2020.121001

Wang, Y., Fang, Z., Hong, H. and Peng, L. (2019). Flood susceptibility mapping using convolutional neural network frameworks. *Journal of Hydrology*, 124482p. doi:10.1016/j.jhydrol.2019.124482

Wang, Y., Li, Z., Tang, Z. and Zeng, G. (2011). A GIS-Based Spatial Multi-Criteria Approach for Flood Risk Assessment in the Dongting Lake Region, Hunan, Central China. *Water Resources Management, 25*(13), pp. 3465–3484. doi:10.1007/s11269-011-9866-2

Zorn, M. (2018). Natural Disasters and Less Developed Countries. In: Nature, Tourism and Ethnicity as Drivers of (De) Marginalization, Pelc, S. and Koderman, M. (Eds)., pp. 59–78. Springer international publishing

**Cite this article as:**
Oyedepo J. A., Adegboyega J., Oluyege D. E. and Babajide, E. I. 2021. Weighted linear combination procedures with GIS and remote sensing in Flood Vulnerability analysis of Abeokuta metropolis in Nigeria. *Nigerian Journal of Environmental Sciences and Technology*, 5(1), pp. 240-257. https://doi.org/10.36263/nijest.2021.01.0260

Nigerian Journal of Environmental Sciences and Technology (NIJEST)

www.nijest.com

ISSN (Print): 2734-259X | ISSN (electronic): 2734-2603

Vol 5, No. 1 March 2021, pp 258 - 270

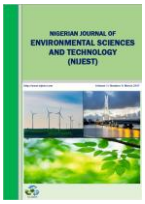

# Bio-monitoring of Environmental Toxicants using West African Dwarf Goats at Amawzari Mbano, Imo State, Nigeria

Ogbonna P. C.[1,]*, Dikeogu, E. C.[2], Nwankwo, O. U.[3], Kanu, K. C.[4] and Osuagwu E. C.[5]

[1,2,3,4,5]Department of Environmental Management and Toxicology, Michael Okpara University of Agriculture, Umudike, Abia State, Nigeria

Corresponding Author: *ogbonna_princewill@yahoo.com

https://doi.org/10.36263/nijest.2021.01.0279

## ABSTRACT

*Several health risks have been linked to exposure to environmental toxicants in food consume by man. This study aimed to determine the level of environmental toxicants in goats tended by rural farmers. Fur and blood samples were carefully collected from sixteen (16) goats in open range husbandry (ex situ) at four sites in Amawzari, Imo State, Nigeria. The samples were digested and analyzed separately to determine the concentrations of some environmental toxicants (heavy metals). The concentrations of Pb, Cr, Cd and Ni in blood were 0.01 to 0.05, 0.01 to 0.07, 0.00 to 0.01 and 0.05 to 0.12 mg/kg, while their concentration in fur were 0.02 to 0.03, 0.001 to 0.006, 0.00 to 0.00, and 0.04 to 0.05 mg/kg, respectively. Pearson correlation analysis show very strong positive relationship between Pb in blood and Pb in fur ($r = 0.855$, $p < 0.01$) and Ni in blood and Ni in fur ($r = 0.811$, $p < 0.01$). The order of abundance of the four heavy metals tested in goat fur and blood is Ni > Cr > Pb > Cd. Based on our findings, the concentrations of heavy metals in blood were higher than its corresponding values in fur. Thus, consumption of meat processed from these metal-contaminated goats and utilization of their blood to manufacture blood meal for pigs and poultry birds will result to bio-magnification of heavy metals in man and animals. Therefore, we recommend that rural farmers should be enlightened on health challenges associated with in situ form of animal husbandry.*

**Keywords:** Environmental toxicants, Blood, fur, West African dwarf goats, Amawzari

## 1.0. Introduction

The West African Dwarf (WAD) goat is the commonest and most important indigenous goat breed in the 18 countries of West and Central Africa (ILCA, 1987) but Nigeria hosts the largest WAD goat population with approximately 11 million in the humid zone of Eastern Nigeria (Chiejina and Behnke, 2011). It is estimated that at least 90% of these animals are owned by small-holder rural goat keepers, for whom goats represent an important asset (Jabbar, 1998). Goats provide their owners with a broad range of products and socio-economic services such as cash income (meat), security (milk), gifts (skin), and manure for crops (Chiejina and Behnke, 2011). Goats account for about 30% of Africa's ruminant livestock and produce about 17% and 12% of its meat and milk, respectively (Wilson, 2011). Goat is an excellent source of meat called chevron (that is meat from adult goat) which is composed mainly of proteins, fat and some important essential elements and is necessary for growth and maintenance of good health. The protein in goat meat is higher than most of other meats and the fat content is lower than beef or pork (FAO/WHO, 1985).

Goats not only play a vital role in ensuring food security of a household (often being the only asset possessed by a poor household), but when needed and in time of trouble (e.g. crop failure or family illness, school fees), goats may be sold to provide an important source of cash (Peacock, 2005). Any intervention aiming to improve goat productivity will therefore have an immediate socio-economic impact on rural communities, especially the poorest of these for whom goats represent the only livestock they can afford to raise (Chiejina and Behnke, 2011). For about a decade now, factors such as increase in human population, construction of more buildings to ameliorate the challenges of

accommodation, decline in soil fertility among others have resulted to serious short fallow period in South east Nigeria. The cut-and-carry fodder/foliage, which are important ingredients in the husbandry of goats in rural areas is taking tolls on the rural farmers because they spend quantum of time walking distances to collect forage or grasses for their goats that are domesticated in their various homes. This invariably affects other activities embarked by the farmers such as farming, selling of farm products at the market, fetching of water from streams, collection of fuel wood, preparation of food and time spent with their families. Consequently, most livestock farmers resulted to moving their goats to various locations where there are grasses and forage plants. This, however, may expose the domestic animals to the deposition of contaminants on their furs.

The environment is exposed to continuous contamination due to human activities such as industrial production, agricultural processes, mineral exploitation, food processing, commercial, social, and domestic activities (Ogbonna *et al*., 2018). These anthropogenic activities release potential toxic element such as heavy metals into the aquatic and terrestrial ecosystems. For instance, waste water runoff from industries/factories enters fallow/pasture lands as a result of lack of proper drainage system. Indiscriminate discharge of untreated industrial waste water enhances the concentrations of heavy metals in the environment. Particulate matter such as dust and vehicular exhaust smoke contains relative amount of heavy metals that might settle on grasses and fodder plants consume by livestock, thus, contaminating and bio-accumulating in the organs, tissues, and hair/furs of the livestock. Hairs contain sulfhydryl group that can bind toxic element for a long period of time resulting to forgetfulness, nerve damage, lung embolism and bronchitis due to manganese poisoning (Santamaria, 2008). Zinc, lead, aluminum and copper poisoning are implicated for gastrointestinal disorder, ataxia, vomiting, convulsion and paralysis (McCluggage, 1991).

Owing to close association and common environment shared with humans, domestic goats are exposed to similar pollutants and have been suggested as sentinels for biohazards from pollutants (Swarup *et al.*, 2000; Berny *et al.*, 1995). Since furs of domestic goats may accumulate trace elements or heavy metals for a longer period of time and are known to be metabolically inert, it (furs) will serve as an important indicator to determining the level of environmental exposure of goats to heavy metal. Hair tissues analysis has been found to be an excellent tool for monitoring general health and nutritional status for both animals and human (Manson and Zlotkin, 1985; Bhattacharya *et al.*, 2004).

Literature search showed that there is paucity of research carried out on the concentration of heavy metals in goats over the world. These studies are: heavy metals in selected tissues and organs of slaughtered goats from Akinyele Central Abattoir, Ibadan, Nigeria (Oladipo and Okareh, 2015), heavy metals and trace elements in the livers and kidneys of slaughtered cattle, sheep and goats from West of Iran (Bazargani-Gilani *et al*., 2016), survey of trace elements and some heavy metals in goats in Zaria and its environs, Kaduna State (Omoniwa *et al*., 2017). Furthermore, assessment of heavy metals in the blood and some selected entrails of cows, goat and pigs slaughtered at Wurukun abattoir, Makurdi, Nigeria (Ubwa *et al*., 2017), concentration of some heavy metals in the hair, kidney and liver of cattle and goats in the oil and non-oil producing areas of Ondo State, Nigeria (Egigba *et al*., 2018), assessment of heavy metals contents in goat and sheep organs from Ashaka Cements, Gombe State, Nigeria (Chadi and Abdulhameed, 2018) but none of these studies determined the concentrations of potential toxic element in fur and blood in WAD goats. This study, therefore, is aimed to determine the concentrations of heavy metals in fur and blood of WAD goats at open range husbandry (ex situ) in Amawzari Mbano in Imo State, Nigeria. The results of this study will provide baseline information on the level of heavy metals contamination in the WAD goats and possible health hazards associated with consumption of such meat in the area.

## 2.0. Methodology

### *2.1. Study area*

The study was carried out at Amawzari in Isiala Mbano Local Government Area of Imo State, Nigeria (Figures 1 and 2). The headquarters of Isiala Mbano LGA is Umuelemai, and it lies between latitude 5.71°N and longitude 7.18°E on the equator. It is located in the tropical rainforest zone of Nigeria (Keay, 1959). According to the National Population Commission (NPC, 2006) of Nigeria, Isiala Mbano had a population of 198,736.

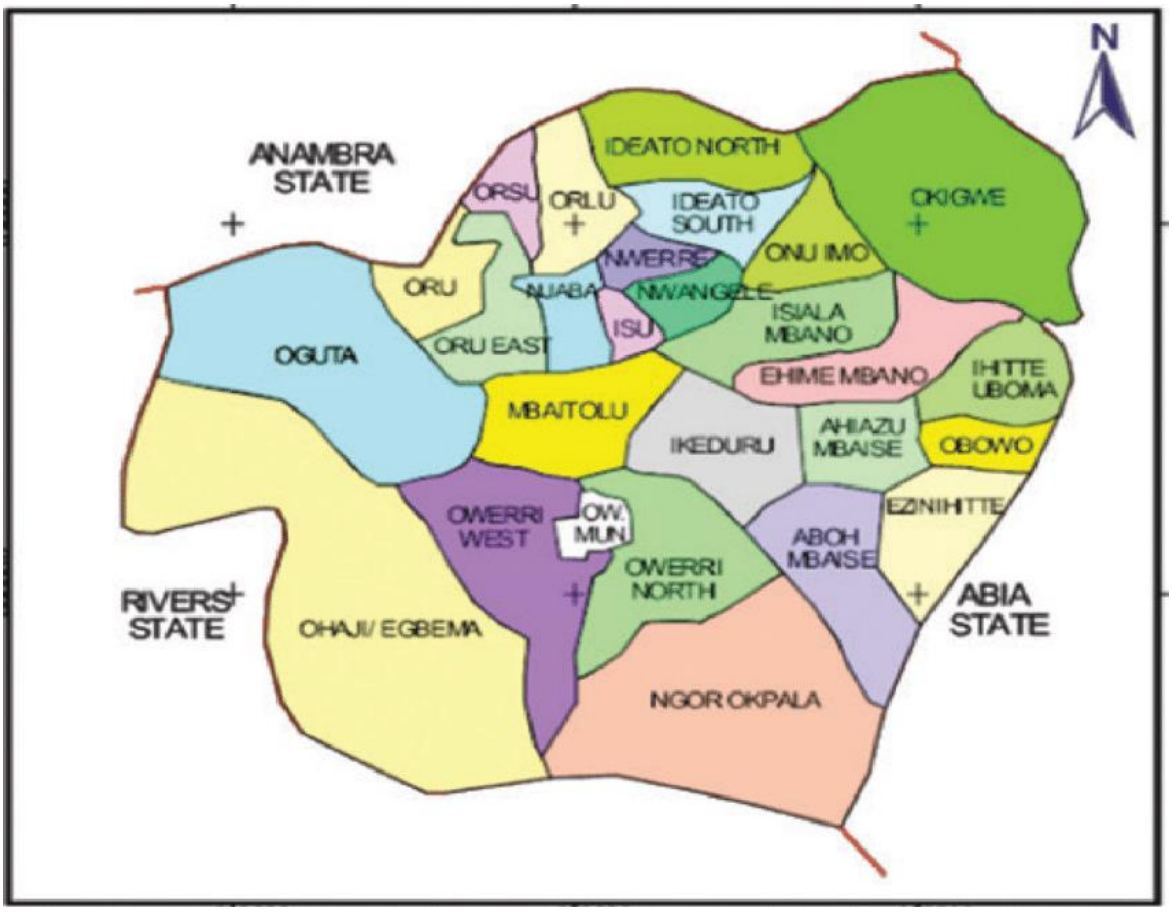


**Figure 1**: Map of Imo State showing Isiala Mbano LGA

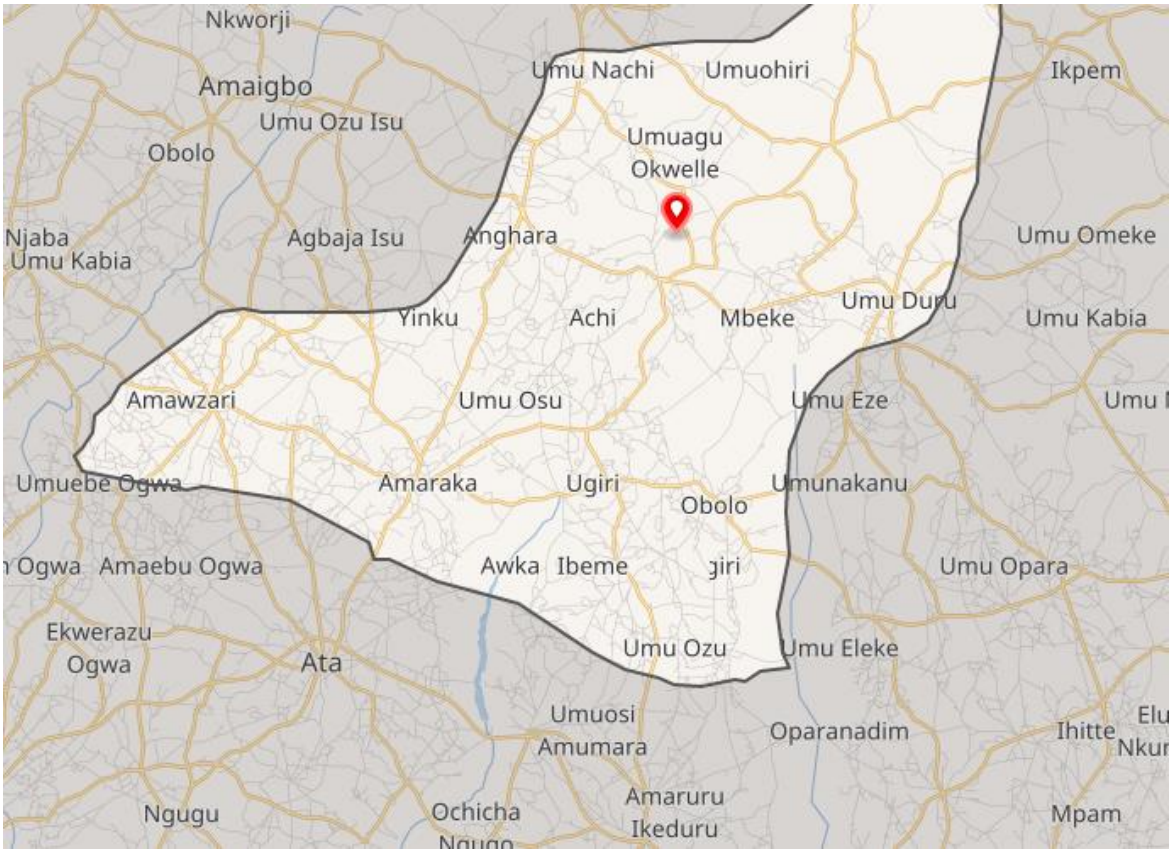


**Figure 2**: Map of Isiala Mbano showing Amawzari

It is bounded on the north by Onuimo Local Government Area and some parts of Nwangele Local Government Area, on the east by Isu and some parts of Nwangele Local Government Areas, on the

south by Ehime Mbano, Ahiazu Mbaise and Ikeduru Local Government Areas, while it has boundary on the west with Ihite Uboma and Obowo Local Government areas. It experience two distinct seasons viz the wet and dry seasons. The dry season begins in November and ends in March while the wet season commence in April and ends in October with peak in July and September. Though, there may be relative break in August, the average annual rainfall is between 1800mm and 2280mm (Warris, 2013). Over the course of the year, the temperature typically varies from 66°F to 87°F and is rarely below 59°F or above 90°F (https://weatherspark.com/y/54991/Average-Weather-in-Umuelemai-Nigeria-Year-Round). The local populace practice subsistence farming that include rearing of domestic livestock especially goats, cultivation of crops such as cassava, maize, yam, cocoyam, plantain, fluted pumpkin, okra, pepper, oil palm trees and fruit trees like *Dacryodes edulis*, *Treculia africana*, *Carica papaya* among others (Field visit).

### *2.2. Sample collection*

Prior to sample collection, reconnaissance survey was carried out to determine the various locations where the farmers tied their goats every morning for preceding three (3) years for foraging. In Amauzari, domestic goats are usually brought out and tied to pole-like stalks to feed in the morning and are taken home in the evenings.

### *2.3. Collection, digestion and analysis of blood sample*

Four (4) locations were used for the study and four goats were selected from each location for sample collection. Fresh blood samples were collected separately from each goat at each location via vein puncture using sterilized syringes. The blood sample from each goat was collected in 25 mL clean sterilized metal-free plastic bottles with gentle handling to prevent hemolysis (Ubwa *et al*., 2017). The sample was placed in icebox and transported to the laboratory. In order to prevent platelet disintegration, it was kept frozen at 4°C in the freezer until the time for pre-treatment and analysis of heavy metals. Samples from each location was thoroughly mixed and homogenized. Sub sample was taken from each homogenized samples for digestion. The wet digestion method of FAO (1990), Licata *et al*. (2004) and Ubwa *et al*. (2017) was adopted with minor modification. About 0.5 mL of the blood sample from each location was predigested with 10 mL 1:1 concentrated $HNO_3$ and $HCLO_4$ acids on a hot plate at 120°C until the liquor had finished undergoing oxidation. Then 5 mL $H_2O_2$ was added and temperature was maintained at 120°C for an hour and 30 minutes until the liquor got completely digested and showed a clear colour. The product of the digestion was allowed to slowly evaporate to near dryness and the digests (blood) was cooled and filtered through Whatman (No. 42) filter paper into 100 mL volumetric flask and made up to the mark with deionized water. Thereafter, determination of the amount of each heavy metal (Pb, Cd, Ni, and Cr) was carried out using Perkin-Elmer analyst 300 Atomic Absorption Spectrophotometer (AAS). The control samples were collected from goat reared indoors (in situ i.e. that are fed and restricted within a hut).

### *2.4. Collection, digestion and analysis of hair*

About 1.5 g hair were collected randomly and separately from different body parts (neck, tail, belly and back) of four (4) goats at each location using well cleaned stainless steel scissors and stored separately in well cleaned zip locks, labeled well and well-sealed, stored in a wooden box to avoid cross contamination from external sources and taken to the laboratory for pre-treatment and analysis. Hairs of goats from each location were bulked together and homogenized. The hair samples were washed briefly with acetone, deionized water, then again with acetone and oven dried at 105°C for 4 hours. Then 1 g of the hair was manually cut to small, homogenized pieces and treated with 10 ml of $HNO_3$, $HClO_4$ and $H_2SO_4$ acid mixture in a ratio of 8:1:1, which was heated to near dryness. The product of the digestion was allowed to slowly evaporate to near dryness. At the end of complete digestion, the digest (hair) was cooled and filtered (Ubwa *et al*., 2017) through Whatman (No. 42) filter paper into 100 ml volumetric flask and made up to mark with distilled water. The control samples were collected from goat reared indoors (i.e. that are fed and restricted within a hut).

### *2.5. Quality assurance and quality control*

For quality assurance and control measures, high purity reagents of analytical grades were obtained from British Drug Houses (BDH) Chemicals Ltd., UK. All plastic and glass containers were cleaned by soaking in dilute $HNO_3$, rinsed in distilled water six times, rinsed in deionized water three times,

oven dried (but for zip locks that were air dried) and cool before use. Reagent blanks and a series of standard solutions of 0.5, 1.0, 2.0, 5.0, 10.0 and 100 mg/l were prepared from the stock standard solution of each test heavy metal by diluting known volumes of the stock solution in 100 ml volumetric flasks using distilled water. The elements that were determined at their various wavelengths were Cr = 283.5, Ni = 221.6, Cu = 766.5, Pb = 220.3, Zn = 213.9, Cd = 228.8, Fe = 510 and Mn = 279.5 nm.

*2.6. Experimental design and statistical analysis*

A total of sixteen (16) goats were sampled from four (4) different locations in Amauzari (i.e. 4 from each location). The location serves as a block while the four goats from each location are the replicates. The experiment was carried out as a simple factorial in Randomized Complete Block Design (RCBD). The data generated from laboratory analysis were subjected to one-way analysis of variance (ANOVA) using Statistical Package for Social Sciences (SPSS), and means were separated with Duncan New Multiple Range Test, DNMRT (Steel and Torrie, 1980).

## 3.0. Results and Discussion

*3.1. Concentration of environmental contaminants in blood and fur*

The concentrations of environmental contaminants such as heavy metals assessed in the blood of goats are summarized in Table 1. The results indicate that highest and lowest concentrations of the metals were observed in goats at ex situ and in situ (control) sites, respectively. The concentration of Pb were statistically the same at Site 1 (0.05±0.01 mg/kg), Site 2 (0.04±0.01 mg/kg), Site 3 (0.05±0.01 mg/kg) and Site 4 (0.04±0.01 mg/kg) but the values are significantly ($p < 0.05$) higher than the control (0.01±0.00 mg/kg). The high concentration of Pb in goat blood at Sites 1, 2, 3 and 4 may be attributed to high deposition of contaminants (Pb, Cd, Cr and Ni) on grasses and fodders at these locations and subsequent consumption, digestion and assimilation of metals into their blood stream. Studies have shown that grasses, fodders and roughages grown in agricultural sites, industrial areas, and sewer water irrigation fields contain heavy metals (Mora *et al*., 2000; Dietz *et al*., 2001; Rozso *et al*., 2003). The place of animal rearing, dietary habits and exposure time are important factors in heavy metal contamination of livestock (Sabir *et al*., 2003). Inhalation is one of the major entries of heavy metals (Järup, 2003), thus, inhalation is another route of entry of metals into the body of goats in ex situ.

The values of Pb in the blood increased from 0.01 to 0.05 mg/kg which is lower than 0.068±0.0227 mg/l in goat blood at Turkey (Yazar *et al*., 2006), 0.56 mg/l in goat blood at Shagamu, Ogun State (Oluokun *et al*., 2007), 0.259±0.470 mg/l in goat blood at Kaduna State (Omoniwa *et al*., 2017), 5.0867±2.9326 to 7.755±7.4943 mg/kg in goat blood at Zamfara State (Orisakwe *et al*., 2017), 0.411±0.021 mg/kg in sheep blood in China (Shen *et al*., 2019) and 0.31±0.03 mg/kg in human blood at China (Shen *et al*., 2019). Pb has no positive biological function in the growth and development of man. Lead (Pb) is known to alter the hematological system by inhibiting the activities of several enzymes involved in heme-biosynthesis (Okiei *et al*., 2009). Exposure to Pb is considered to be detrimental and associated with behavioral abnormalities, hearing deficits, neuromuscular weakness, and impaired cognitive functions in humans and experimental animals (Flora *et al*., 2012; Assi *et al*., 2016). Acute and chronic lead poisoning contributes in vascular and cardiac damage as well as possible fatal consequences such as cardiovascular illnesses and hypertension (Navas-Acien *et al*., 2007).

The highest concentration of Cr in blood was recorded in goats at Site 1 and the value is significantly ($p < 0.05$) higher than values of Cr obtained in goat blood at Site 2 (0.02±0.01 mg/kg), site 3 (0.02±0.01 mg/kg), site 4 (0.01±0.00 mg/kg), and the control (0.00±0.00 mg/kg). The source of Cr in goat blood may be attributed consumption of fodders, grasses and water contaminated by Cr. Indeed, Imo State is an oil producing State and share boundaries with Rivers State, hence, gas flaring and other industrial activities in Rivers State may result to atmospheric deposition of metals on soil, grasses and water at the study site and subsequent uptake by the goats. The values of Cr in goat blood increased from 0.01 to 0.07 mg/kg which is lower than 0.009 to 0.092 mg/l (Pechova and Pavlata, 2007), 2.7683±0.5477 to 2.9219±1.1640 mg/kg (Orisakwe *et al*., 2017), 0.18 mg/l (Ubwa *et al*., 2017), and 0.072±0.064 mg/l (Omoniwa *et al*., 2017). Chromium cause ulceration and perforation of

the nasal system (Shekhawat *et al*., 2015), acute tubular necrosis, vomiting, abdominal pain, kidney failure and even death (Beaumont *et al*., 2008). Human liver, kidney, spleen and bone have more concentration of Cr in comparison to other organs (NTP, 2008).

**Table 1**: Heavy metals on blood of domestic goat

| Samples | Pb | Cr | Cd | Ni |
|---|---|---|---|---|
| Site 1 | $0.05^{a} \pm 0.01$ | $0.07^{a} \pm 0.02$ | $0.00^{b} \pm 0.00$ | $0.10^{a} \pm 0.01$ |
| Site 2 | $0.04^{a} \pm 0.01$ | $0.02^{b} \pm 0.01$ | $0.00^{b} \pm 0.00$ | $0.10^{a} \pm 0.02$ |
| Site 3 | $0.05^{a} \pm 0.01$ | $0.02^{bc} \pm 0.00$ | $0.00^{b} \pm 0.00$ | $0.10^{a} \pm 0.01$ |
| Site 4 | $0.04^{a} \pm 0.01$ | $0.01^{bc} \pm 0.00$ | $0.01^{a} \pm 0.00$ | $0.12^{a} \pm 0.01$ |
| Control | $0.01^{b} \pm 0.00$ | $0.00^{c} \pm 0.00$ | $0.00^{b} \pm 0.00$ | $0.05^{b} \pm 0.01$ |

*Values are mean ± standard deviation of 3 replicates*

$^{abc}$ *Means in a column with different superscripts are significantly different (P<0.05)*

The highest concentration of Cd in goat blood was obtained in goats at Site 4 (0.01±0.00 mg/kg) and the value is significantly ($p < 0.05$) higher than values obtained at Site 1 (0.00±0.00 mg/kg), Site 2 (0.00±0.00 mg/kg), Site 3 (0.00±0.00 mg/kg) and control (0.00±0.00 mg/kg). The values of Cd in goat blood increased from 0.00 to 0.01 mg/kg which is lower than 0.2433±0.1589 to 0.2835±0.1446 mg/kg (Orisakwe *et al*., 2017), 0.03 mg/l (Jubril *et al*., 2017) and 0.021 mg/l (Skalicka *et al*., 2002) but higher than 0.002 mg/l in goat blood (Or *et al*., 2005) and 0.006±0.004 mg/l in goat blood (Omoniwa *et al*., 2017). Cadmium is of no biological importance to human/animal growth and development. Cadmium causes reductions in both intestinal zinc absorption and hepatic zinc reserves in cattle, respectively, as a result of competition for the cation-binding sites of metallothionein (Orisakwe *et al*., 2017). Exposure to cadmium also affect the function of the nervous system (Vaziri, 2008; Lee *et al*., 2018), with symptoms including headache and vertigo, olfactory dysfunction, Parkinsonian-like symptoms, slowing of vasomotor functioning, peripheral neuropathy, decreased equilibrium, decreased ability to concentrate, and learning disabilities (Abdullahi, 2013). The risk of livestock getting contaminated with heavy metals is a subject of great concern for both food safety and human health because of the toxic nature of metals at relatively minute concentrations (Santhi *et al*., 2008).

The concentrations of Ni in goat blood were statistically ($p > 0.05$) the same in goats sampled from site 1 (0.10±0.01 mg/kg), Site 2 (0.10±0.02 mg/kg), Site 3 (0.10±0.01 mg/kg) and Site 4 (0.12±0.01 mg/kg) but the values are significantly ($p < 0.05$) higher than the value of Ni at the control (0.05±0.01 mg/kg). The values of Ni increased from 0.05 to 0.12 mg/kg which is lower than 0.25 mg/l in goat blood (Yazar *et al*., 2006) and 1.7869±1.6479 to 3.9583±3.0875 mg/kg in goat blood (Orisakwe *et al*., 2017) but higher than 0.03 mg/l (Miranda *et al*., 2005) and 0.05 mg/l (Bernard, 2008). Nickel (Ni) is needed at trace level for normal functioning of the goats. In animals, its deficiency result in depress growth, alterations in carbohydrate and lipid metabolism, delay gestation period, fewer offspring, anaemia, skin eruptions, reduce haemoglobin and hematocrit values, hematopoiesis and alterations in the content of iron, copper, and zinc in liver and reduce activity of several enzymes like hydrogenases, transaminases and α-amylase (Alexandrovn *et al*., 2006; Samal and Mishra, 2011). Notwithstanding this, the lung has been identified as the critical target of nickel toxicity. Nickel substitution for other essential elements may contribute to the adverse health effects of nickel (Al-Ghafari, 2019). The replacement of nickel for magnesium leads to a 40-fold increase in the formation of C3b, Bb enzyme, which amplifies activation of the complement pathway (Orisakwe *et al*., 2017). The order of abundance of the four heavy metals tested in goat blood in this study is as follows: Ni > Cr > Pb > Cd.

The concentrations of heavy metals on fur of goat are presented in Table 2. The results indicate higher concentrations of metals on goats fur at ex situ than that of in situ. The highest concentration of Pb (0.03±0.01 mg/kg) on goat fur was obtained at Site 1 and the value is significantly ($p < 0.05$) higher than values of Pb on goat fur at Site 2 (0.02±0.00 mg/kg), Site 3 (0.02±0.00 mg/kg), Site 4 (0.02±0.00 mg/kg) and control (0.00±0.00 mg/kg). The high value of Pb in goat fur at Site 1 may be as a result of high atmospheric deposition of contaminant (metals) on soil at Site 1 than other sites. The exposure of domestic goats via body contact with (contaminated) soil can be an important route of heavy metal entry (Sabir *et al*., 2003). The concentration of Pb in goat fur increased from 0.02 to 0.03 mg/kg which is lower than 3.76±0.21 reported in sheep wool at China (Shen *et al*., 2019), 0.543±0.062 to 0.649±0.048 mg/kg in fox hair at Poland (Filistowicz *et al*., 2012) and 2.71±0.33 mg/kg in human hair at China (Shen *et al*., 2019) but higher than 0.35±0.09 to 12.0±0.97 µg/g in goat at Egypt (Rasheed and Soltan, 2005).

The concentration of Cr in goat fur was highest in goats sampled at Site 4 (0.006±0.002 mg/kg) and the value is statistically the same ($p > 0.05$) with the concentrations of Pb in goat fur at Site 1 but significantly ($p < 0.05$) higher than values of Cr in goat fur at Site 2 (0.001±0.001 mg/kg), Site 3 (0.001±0.001 mg/kg) and control (0.001±0.001 mg/kg). The concentration of Cr in goat fur increased from 0.001 to 0.006 mg/kg which is relatively higher than 0.04 mg/l reported by Ubwa *et al*. (2017). The concentration of Cd in goat fur are statistically equal ($p > 0.05$) for all the sites (0.00±0.00 mg/kg). The values indicated that the level of Cd at the various sites were very low (Tables 1 and 2). The concentration of Cd on goat fur in this study is lower than 2.28±0.13 mg/kg in sheep wool at Egypt (Shen *et al*., 2019) and 1.88±0.12 in human hair at China (Shen *et al*., 2019).

**Table 2**: Heavy metals on fur of domestic goat

| Samples | Pb | Cr | Cd | Ni |
|---|---|---|---|---|
| Site 1 | $0.03^{a} \pm 0.01$ | $0.004^{ab} \pm 0.004$ | $0.00^{a} \pm 0.00$ | $0.04^{ab} \pm 0.01$ |
| Site 2 | $0.02^{b} \pm 0.00$ | $0.001^{b} \pm 0.001$ | $0.00^{a} \pm 0.00$ | $0.05^{a} \pm 0.03$ |
| Site 3 | $0.02^{b} \pm 0.00$ | $0.001^{b} \pm 0.001$ | $0.00^{a} \pm 0.00$ | $0.05^{a} \pm 0.02$ |
| Site 4 | $0.02^{b} \pm 0.00$ | $0.006^{a} \pm 0.002$ | $0.00^{a} \pm 0.00$ | $0.05^{a} \pm 0.01$ |
| Control | $0.00^{c} \pm 0.00$ | $0.001^{b} \pm 0.001$ | $0.00^{a} \pm 0.00$ | $0.02^{b} \pm 0.00$ |

*Values are mean ± standard deviation of 3 replicates*

$^{abc}$ *Means in a column with different superscripts are significantly different (P<0.05)*

The concentration of Ni in goat fur was highest in goats sampled from Site 2 (0.05±0.03 mg/kg), Site 3 (0.05±0.02 mg/kg), Site 4 (0.05±0.01 mg/kg) and Site 1 (0.04±0.01 mg/kg) but the values are significantly ($p < 0.05$) higher than the value observed at the control (0.02±0.00 mg/kg). The concentration of Ni in this study is lower than 0.410±0.264 to 0.560±0.362 mg/kg in fox hair in Poland (Filistowicz *et al*., 2012) but higher than 0.71±0.21 to 2.11±0.98 µg/g in goat hair at Egypt (Rasheed and Soltan, 2005). The order of abundance of the four (4) heavy metals tested in this study that may be causing contamination of fur on goats reared ex situ are as follows: Ni > Cr > Pb > Cd.

Comparatively, the values of heavy metals tested in this study were higher in blood than on fur of the goats at various sites. For instance, the concentrations of Pb, Cr, Cd and Ni were significantly ($p < 0.05$) higher in the blood than on the fur of the goats (Figure 1 to 4). Consequently, the use of such contaminated blood for formation of blood meal for chicken will lead to bio-magnification of these metals vis-à-vis serious health risk to man. Similarly, the consumption of metal-contaminated goat meat will be a route of entry of heavy metals in human alimentary system. The contribution of livestock to food supplies in developing countries is increasing at a higher rate than that of cereals (FAO, 1994).

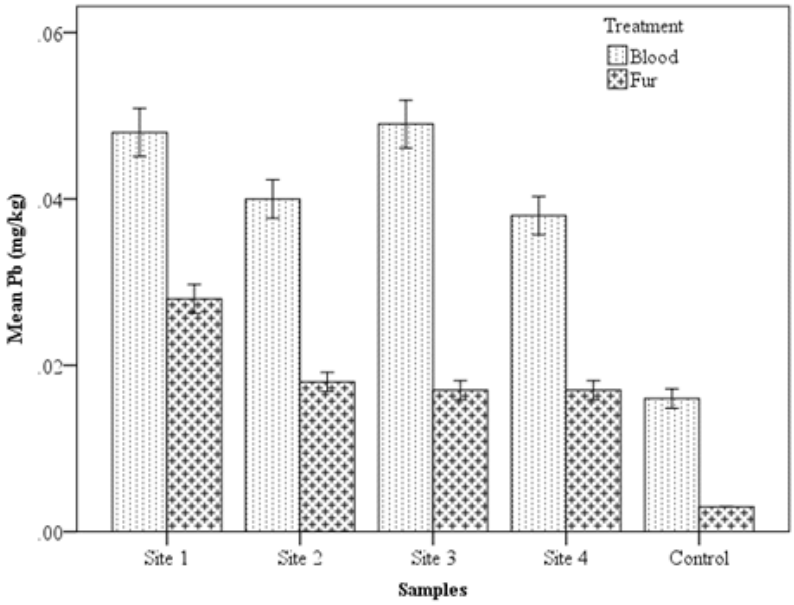


**Figure 1:** Mean concentration of Pb in blood and fur

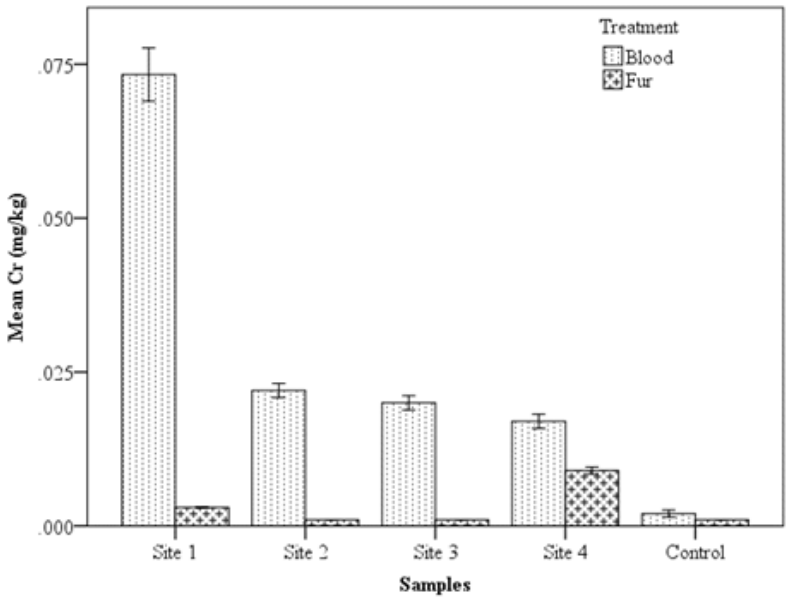


**Figure 2:** Mean concentration of Cr in blood and fur

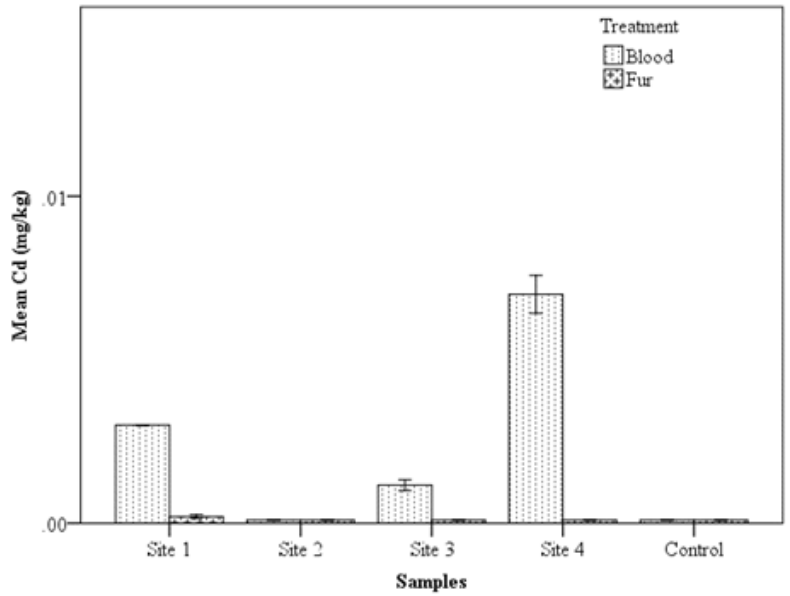


**Figure 3:** Mean concentration of Cd in blood and fur

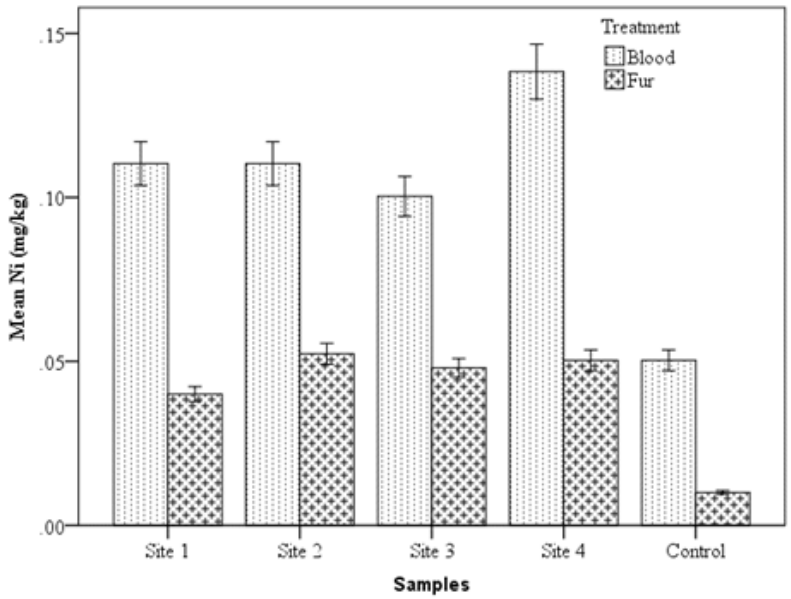


**Figure 4:** Mean concentration of Ni in blood and fur

*3.2. Pearson correlation coefficient of heavy metals in goat blood and fur*

The result of the Pearson correlation analysis of heavy metals in goat blood and fur is summarized in Table 3. The result show very strong positive relationship between heavy metals in blood and fur. For instance, very strong positive relationship exists between Pb in blood and Pb in fur ($r$ = 0.855, $p$ < 0.01) and Ni in blood and Ni in fur ($r$ = 0.811, $p$ < 0.01) which suggest that increase in Pb and Ni in blood might have resulted to their (Pb and Ni) increase in goat fur. Strong positive relationship exist between Pb in blood and Ni in fur ($r$ = 0.585, $p$ < 0.05). Positive relationship exist between Cr in blood and Cr in fur ($r$ = 0.336) and Cd in blood and Cd in fur ($r$ = 0.017). However, there were very strong positive relationship between Cr in blood with Pb in fur ($r$ = 0.685, $p$ < 0.01), Ni in blood with Pb in fur ($r$ = 0.651, $p$ < 0.01) and Cd in blood with Cr in fur ($r$ = 0.756, $p$ < 0.01) while negative relationship occurred between Cr in blood with Cd in fur ($r$ = -0.017), Cr in fur with Cd in fur ($r$ = -0.175) and Cd in fur with Ni in fur ($r$ = -0.145).

**Table 3:** Correlation between heavy metals in blood and fur

| | Pb (blood) | Cr (blood) | Cd (blood) | Ni (blood) | Pb (fur) | Cr (fur) | Cd (fur) | Ni (fur) |
|---|---|---|---|---|---|---|---|---|
| Pb (blood) | 1 | | | | | | | |
| Cr (blood) | 0.476 | 1 | | | | | | |
| Cd (blood) | 0.155 | -0.017 | 1 | | | | | |
| Ni (blood) | 0.741** | 0.226 | 0.480 | 1 | | | | |
| Pb (fur) | 0.855** | 0.685** | 0.066 | 0.651** | 1 | | | |
| Cr (fur) | 0.167 | 0.336 | 0.756** | 0.439 | 0.188 | 1 | | |
| Cd (fur) | 0.354 | 0.455 | 0.017 | 0.044 | 0.504 | -0.175 | 1 | |
| Ni (fur) | 0.585* | 0.000 | 0.200 | 0.811** | 0.413 | 0.150 | -0.145 | 1 |

** Correlation is significant at 5% (P<0.05)*

*** Correlation is significant at 1% (P<0.01)*

## 4.0 Conclusion

The results of the bio-monitoring survey showed that environmental contaminants such as heavy metals contaminated the blood and fur of goats that were fed ex situ than that of in situ. The order of abundance of heavy metals in blood is: Ni > Cr > Pb > Cd while that of fur is also Ni > Cr > Pb > Cd. The values of highest concentration of heavy metals (Cr, Cd, and Pb) occurred at Sites 1 and 4. The level of Pb and Cd in goat blood is a serious concern to man and animals' health. Continuous consumption of the goats raised ex situ in Amauzari will likely have adverse effects on the people of Mbano Local Government Area. Thus, we recommend periodic monitoring of environmental contaminants in Amauzari since the goats are being sold to hoteliers, used for preparation of stew and sauce during occasions such as chieftaincy titles, child dedications, new yam festival and burial ceremony. Therefore, it is recommended that rural farmers should be informed about the consequences of raising goats ex situ.

## Acknowledgement

The authors acknowledge the rural goat farmers for given us access to the goats at various sampling sites in this study. The services (statistical analysis of the data) of Mr. Emebu, Prosper Kome are also appreciated.

## Conflict of interest

There is no conflict of interest associated with this work.

## References

Abdullahi, M.S. (2013). Toxic effects of lead in humans: an overview. *Global Advanced Journal of Environmental Science and Toxicology*, 2(6), pp. 157-162.

Alexandrovn, R., Costisor, O. and Patron, I. (2006). Nickel. *Experimental Pathology and Parasitology*, 911, pp. 64-74.

Al-Ghafari, A., Elmorsy, E., Fikry, E., Alrowaili, M. and Carter, W.G. (2019). The heavy metals lead and cadmium are cytotoxic to human bone osteoblasts via induction of redox stress. *PLoSONE*, 14(11), pp. 1-18.

Assi, M.A., Hezmee, M.N.M., Haron, A.W., Sabri, M.Y. and Rajion, M.A. (2016). The detrimental effects of lead on human and animal health. *Veterinary World*, 9(6), pp. 660-671.

Bazargani-Gilani, B., Pajohi-Alamoti, M., Bahari, A. and Sari, A.A. (2016). Heavy metals and trace elements in the livers and kidneys of slaughtered cattle, sheep and goats. *Iranian Journal of Toxicology*, 10(6), pp. 7-13.

Beaumont, J.J., Sedman, R.M., Reynolds, S.D., Sherman, C.D., Li, L.H., Howd, R.A., et al. (2008). Cancer mortality in a Chinese population exposed to hexavalent chromium in drinking water. *Epidemiology*, 19(1), pp. 12- 23.

Bernard, A. (2008). Heavy metal and their adverse effects on human health. *Indian Journal of Medical Research*, 128(5), pp. 557-564.

Berny, P.J., Cote, L.M. and Buck, W.B. (1995). Can household pets be used as reliable monitors of lead exposure to humans? *Science of the Total. Environment*, 172(2-3), pp. 163-173.

Bhattacharya, M., Chatterjee, A., Kishore, R., Sudarsham, M. and Chakraborty, A. (2004). Elemental concentration in hair of domestic animals-a SEM-EDS study. Indian Journal of Veterinary Anatomy, 9, pp. 61-68.

Chadi, A.S. and Abdulhameed, A. (2018). Assessment of heavy metals contents in goat and sheep organs from Ashaka Cements, Gombe State, Nigeria. *Journal of Water Technology and Treatment Methods*, 1(4), pp. 117-121.

Chiejina, S.N. and Behnke, J.M. (2011). The unique resistance and resilience of the Nigerian West African Dwarf goat to gastrointestinal nematode infections. *Parasites and Vectors*, 4(1), pp.

Dietz, M.C., Ihrig, A., Wrazidlo, W., Bader, M., Jansen, O. and Triebig, G. (2001). Results of magnetic resonance imaging in long-term manganese dioxide-exposed workers. Environ. Res. 85(1), pp. 37–40.

Egigba, G.O., Odokuma, E.J., Ikhatua, U.J. and Bamikole, M.A. (2018). Concentration of some heavy metals in the hair, kidney and liver of cattle and goats in the oil and non-oil producing areas of Ondo State, Nigeria. *Nigerian Journal of Animal Production*, 44(3), pp. 49-55.

FAO/WHO (1985). Energy and Protein Requirements. Technical Report. Series 724 World Health Organization, Geneva.

Food and Agriculture Organization, FAO (1990). Manual on simple methods of meat preservation. Health Paper No. 79. FAO, Rome.

Food and Agriculture Organization, FAO (1994). Special Programme on food production for food security in low-income food deficit countries (LIFDCs), Rome.

Flora, G., Gupta, D. and Tiwari, A. (2012) Toxicity of lead: A review with recent updates. *Interdisciplinary Toxicology*, 5(2), pp. 47-58.

Filistowicz, A., Przysiecki, P., Nowicki, S., Filistowicz, A. and Durkalec, M. (2012). Contents of copper, chromium, nickel, lead and zinc in hair and skin of farm foxes. *Polish Journal of Environmental Studies*, 21(4), pp. 865-869.

ILCA, (1987). Annual Report of the International Livestock Centre for Africa, ILCA. 1987, Addis Ababa, Ethiopia.

Jabbar, M.A. (1998). Buyer preferences for sheep and goat in southern Nigeria: A hedonic price analysis. Agricultural Economics. 1998, 18: 21-30.

Järup, L. (2003). Hazards of heavy metal contamination. *British Medical Bulletin*, 68(1), pp. 167-182.

Keay, R.W.J. (1959). An outlines of Nigeria vegetation. 3rd ed. Government Printer, Lagos, Nigeria.

Jubril, A.J., Taiwo, V.O., Olopade, J.O. and Kabiru, M. (2017). Biological monitoring of heavy metals in goats exposed to environmental; contamination in Bagega, Zamfara State, Nigeria. *Advances in Environmental Biology*, 11(6), pp. 11-18.

Lee, M.J., Chou, M.C., Chou, W.J., Huang, C.W., Kuo, H.C., Lee, S.Y., et al. (2018). Heavy metals' effect on susceptibility to attention-deficit/hyperactivity disorder: implication of lead, cadmium, and antimony. *International Journal of Environmental Research and Public Health*, 15, pp. 1221-1232.

Licata, P., Trombetta, D., Cristani, M., Giofre, F., Martino, D., Calo M. and Naccari, F. (2004). Levels of ''toxic'' and ''essential'' metals in samples of meat and blood from various farm animals in Calabria, Italy. *Journal of Environment International*, 30 (1), pp. 1-6.

Manson, P. and Zlotkin, S. (1985). Hair analysis-a critical review. *Canadian Medical Association Journal*, 133, pp. 186-188.

McCluggage. D. (1991). *Heavy metals poisoning*, NCS Magazine. The Bird hospital Co.USA www.cockatiels.org/ariticle/diseases/metals.html.

Miranda, M., Lopez-Alonso, M., Castillo, C., Hernadez, J. and Benedito, J.L. (2005). Effects of moderate pollution on toxic and trace metal levels in calves from a polluted area in northern Spain. *Environmental International*, 31, pp. 543-548.

Mora, M.A., Laack, L.L., Lee, M.C., Sericano, J., Presly, R., Gardinali, P.R. and Gamble, L.R. (2000). Environmental contamination in blood, hair and tissues of Ocelots from the Lower Rio Grande Valley, Texas, 1986–1997. *Environ. Monit. Assess*. 64(2), pp. 477–492.

Navas-Acien, A., Guallar, E., Silbergeld, E.K. and Rothenberg, S.J. (2007). Lead exposure and cardiovascular disease - A systematic review. *Environmental Health Perspectives*, 115(3), pp. 472-482.

National Population Commission of Nigeria (NPC) (2006). Population and Housing Census Result. NPC, Lagos, Nigeria.

NTP (2008). Technical Report on the toxicology and carcinogenesis studies of sodium dichromate dihydrate (CAS No. 7789-12-0) in F344/N rats and B6C3F1 mice (drinking water studies) National Toxicology Program NIH Publication; 08-5587.

Ogbonna, P.C., Nzegbule, E.C. and Okorie, P.E. (2018). Soil chemical characteristics in wet and dry season at Iva long wall underground mined site, Nigeria. *Nigerian Journal of Environmental Sciences and Technology*, 2(1), pp. 96-107.

Okiei, W., Ogunlesi, M., Alabi, F., Osiughwu, B and Sojinrin, A. (2009). Determination of toxic metal concentrations in flame treated meat products, Ponmo. *African Journal of Biochemistry Research*, 3(10), pp. 332-339.

Oladipo, T.A. and Okareh, O.T. (2015). Heavy metals in selected tissues and organs of slaughtered goats from Akinyele Central Abattoir, Ibadan, Nigeria. *Journal of Biology, Agriculture and Healthcare*, 5(2), pp. 25-29.

Oluokun, J.A., Fajimi, A.K., Adebayo, A.O. and Ajayi, F.T. (2007). Lead and cadmium poisoning of goals raised in cement kiln dust polluted area. *Journal Food Agricultural Environment*, 1, pp. 382-384.

Omoniwa, O.D., Uchendu, C., Abdullahi, S.U., Bale, J.O.O. and Abdullahi, U.S. (2017). Survey of trace elements and some heavy metals in goats in Zaria and its environs, Kaduna State. *Nigerian Veterinary Journal*, 38(4), pp. 280-287.

Or, M.E., Kayar, A., Kizilier, A.R., Parkan, C., Gonal, R., Barutai, B. et al. (2005). Determination of levels of some essential and toxic metals in the blood as sheep and samples of water plants and soil in North Western Turkey. *Veterinarski Arhive*, 19(6), pp. 453 – 456.

Orisakwe, O.E., Oladipo, O.O., Ajaezi, G.C. and Udowelle, N.A. (2017). Horizontal and vertical distribution of heavy metals in farm produce and livestock around lead-contaminated goldmine in Dareta and Abare, Zamfara State, Northern Nigeria. *Journal of Environmental and Public Health*, 2017, pp. 1-12.

Peacock, C. (2005). Goats - a pathway out of poverty. *Small Ruminant Research*, 60, pp. 179-186.

Pechova, A. and Pavlata, L. (2007). Chromium as an essential nutrient: a review. *Veterinarni Medicine*, 1, pp. 1-18.

Rasheed, M.N. and Soltan, M.E. (2005). Animal hair as biological indicator for heavy metal pollution in urban and rural areas. *Environmental Monitoring and Assessment*, 110, pp.41–53.

Rozso, K., Varhegyi, J., Mocsenyi, A.R. and Fugli, K. (2003). Lead content of the forages and the effect of lead exposure on ruminants. *Veterinary Bulletin*, 73, pp. 510-510.

Sabir, S.M., Khan, S.W. and Hayat, I. (2003). Effect of environmental pollution on quality of meat in District Bagh, Azad Kashmir. *Pakistan Journal of Nutrition*, 2(2), 98-101.

Samal, L. and Mishra, C. (2011). Significance of nickel in livestock health and production. *International Journal for Agro Veterinary and Medical Sciences*, 5(3), pp. 349-361.

Santamaria, A.B. (2008). Manganese exposure, essentiality and toxicity. *Indian Journal of Medical Research*, 128, pp. 484-500.

Santhi, D., Balakrishnan, V., Kalaikannan, A., and Radhakrishnan, K.T. (2008). *Presence of heavy metals in pork* products in Chennai (India). *American Journal of Food Technology*, 3(3), pp. 192-199.

Shekhawat, K., Chatterjee, S. and Joshi, B. (2015). Chromium toxicity and its health hazards. *International Journal of Advanced Research*, 3(7), pp. 167-172.

Shen, X., Chi, Y. and Xiong, K. (2019). The effect of heavy metal contamination on humans and animals in the vicinity of a zinc smelting facility. *PLoS ONE*, 14(10), pp. 1-15.

Skalická, M., Koréneková, B., Nad, P. and Makoóvá, Z. (2002). Cadmium levels in pig meat. *Veterinarski Archive*, 72(1), pp. 11-17.

Steel, R.G.D. and Torrie, J.H. (1980). *Principles and procedures of statistics: A biometric approach*, McGraw-Hill, New York, p. 633.

Swarup, D., Patra, R.C., Naresh, R., Kumar, P., Shekhar, P. and Balgangadharthilaghar, M. (2006). Lowered blood copper and cobalt contents in goats reared around lead zinc smelter. *Small Ruminant Research*, 63, pp. 309-313.

Ubwa, S.T., Ejiga, R., Okoye, P.A.C. and Amua, Q.M. (2017).Assessment of heavy metals in the blood and some selected entrails of cows, goat and pigs slaughtered at Wurukun abattoir, Makurdi, Nigeria. *Advances in Analytical Chemistry*, 7(1), pp. 7-12.

Vaziri, N.D. (2008). Mechanisms of lead-induced hypertension and cardiovascular disease. *American Journal of Physiology-Heart and Circulatory Physiology*, 295, pp. 454–465.

Warris, P.D. (2013) Plant species colonizing abandoned farmlands less than 20 years in Isiala Mbano Local Government Area, Imo State, Nigeria. ARPN *Journal of Agriculture and Biological Science*, 7(2):117-120.

Wilson, T. (2011). Small ruminant production and the small ruminant genetic resource in tropical Africa. Rome: Food and Agriculture Organization (FAO) of the United Nations, (FAO Animal Production and Health Paper 88), 231 pp.

Yazar, E., Altunok, V. and Erogulu, T. (2006): Concentrations of some elements in the blood serums of Angora goats. *Medycena Weterynaryjna*, 11, pp. 1249-1251.

**Cite this article as:**
Ogbonna P. C., Dikeogu, E. C., Nwankwo, O. U., Kanu, K. C. and Osuagwu E. C. 2021. Bio-monitoring of environmental toxicants using West African dwarf goats at Amawzari Mbano, Imo State, Nigeria. *Nigerian Journal of Environmental Sciences and Technology*, 5(1), pp. 258-270. https://doi.org/10.36263/nijest.2021.01.0279

Nigerian Journal of Environmental Sciences and Technology (NIJEST)

www.nijest.com

ISSN (Print): 2734-259X | ISSN (electronic): 2734-2603

Vol 5, No. 1 March 2021, pp 271 - 280

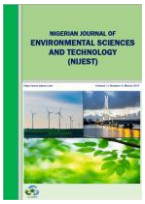

# A Qualitative Study of Time Overrun of Completed Road Projects Awarded by the Niger Delta Development Commission in the Niger Delta Region of Nigeria

Ogbeide F. N.[1,*], Ehiorobo J. O.[2], Izinyon O. C.[3] and Ilaboya I. R.[4]

[1]Utilities, Infrastructural Development & Waterways, NDDC Port Harcourt, Nigeria

[2,3,4]Department of Civil Engineering, University of Benin, Benin City, Edo State, Nigeria

Corresponding Author: *nosakhderick@yahoo.com

https://doi.org/10.36263/nijest.2021.01.0269

## ABSTRACT

*Time overrun of completed road projects awarded by the Niger Delta Development Commission (NDDC) in the Niger Delta Region of Nigeria from its inception in 2000 up to 2015 was studied. Out of 3315 roads awarded, only 1081 roads representing 31.65 percent were completed within the review period. The qualitative study was carried out on randomly selected completed 162 road projects for analysis, and a conceptual model of time series was developed. In developing the regression model, both dependent and independent variables were subjected to normality tests assessed by skewness coefficient, kurtosis value, Jarque-Bera test, residual probability plot, heteroscedasticity test and the variance inflation factor. Also, with knowledge of total road projects awarded by the Commission, it is now possible to predict proportions of roads experiencing schedule overruns.*

**Keywords:** Construction delays, Time overrun, Qualitative studies, Inflation factor

## 1.0. Introduction

Schedule control is the main key to a successful project (Pall *et al*., 2016). A construction project is acknowledged as successful when the aim of the project is achieved in terms of the predetermined objectives of the completed projects which include completing the projects on time, within budget and desired quality in accordance with the specifications, as well as to stakeholder's satisfaction (Owolabi *et al*., 2014; Khan, 2015). Time overruns give negative impressions on the project and all the involved construction parties. Ramli *et al*. (2018) asserted that when this happens, the overall project performance will decrease and competency of involved workers and professionals will be doubtful.

Delay is one of the numerous challenges of construction worldwide. The others include cost overrun, construction waste, poor safety, poor quality, excessive resource consumption and threat to environment (Memon *et al*., 2014). Although scientific and engineering tools have been applied to improve construction process, the complex nature of road construction projects still makes construction delays inevitable.

Fregenti and Cominios (2012) defined construction delay as time lag in completion of activities from its specified time in the contract but, Mohamad (2010) defined construction delay as an act or event that extend the time to complete or perform an act under the contract. Pickavance (2010) refers to construction delay as something happening at a late time than planned, expected, specified in a contract or beyond the date the parties agreed upon for the delivery of a project, Kolhe and Darade (2014) conceptualized delay to mean loss of revenue to the owner through lack of production facilities and rent-able space or a dependence on present facilities. While all above studies and many more theorize construction delay essentially in terms of time overruns that go beyond agreed date, Lo *et al*. (2006) however, introduced a different view of delay, in which the progress of work has not entirely stopped but has slowed down. The perception emphasises the slowing of progress, in contrast with the generally held view of postponement and stoppage of work. Another closely related concept of construction delay is construction disruption which Kikwasi (2012) defined as events that disturb the

construction programme and interferes with the flow of work in the project. Chai *et al*. (2015) also introduced the concept of sick projects defined as projects that results from delay with extensive critical delays, leading to abandonment. A simple pictorial illustration of the concept of construction delay as depicted by Chai *et al*. (2015) is shown in Figure 1.

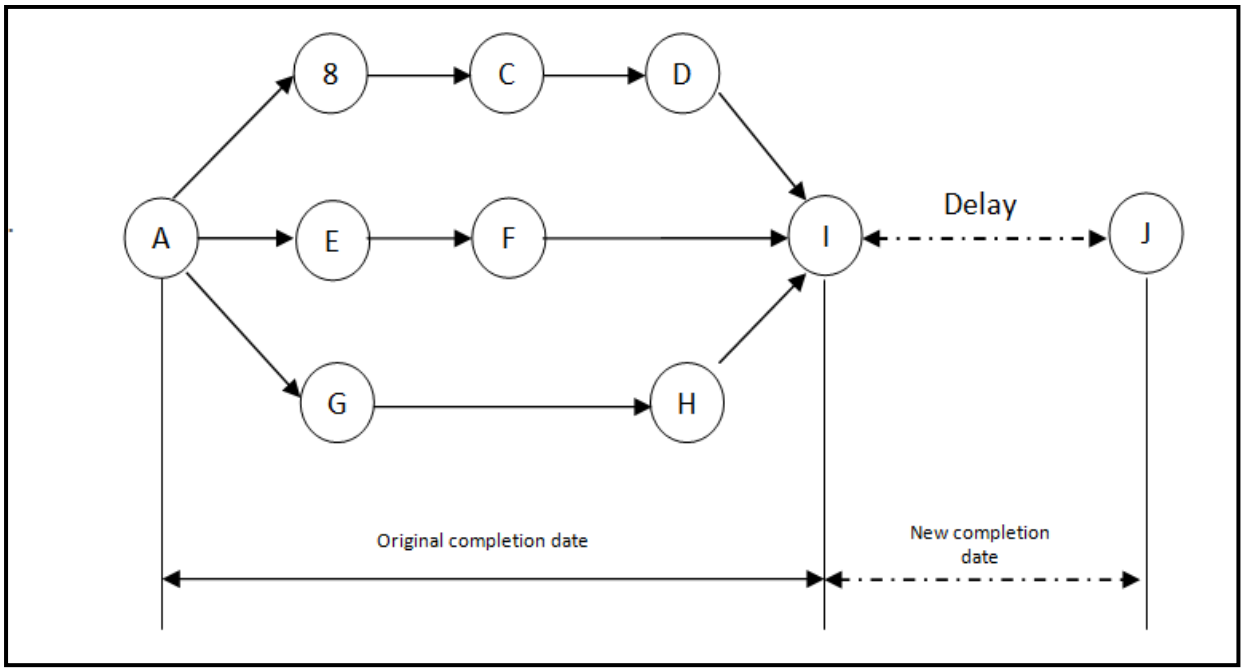


**Figure 1:** Philosophy of delay in the construction industry (Chai *et al*., 2015)

The major challenges when prescribing solutions of handling delay problems in construction processes have been magnitude and size, availability of fund, environment, organisational structure, etc. One of such scientific process introduced by Fregenti and Cominios (2012) rests on the cumulative aggregation of the principles of STEEPOL, GRC and MEDIC in achieving a strategically planned project:

| STEEPOL | GRC | MEDIC |
|---|---|---|
| S = Social | G = Governance, mandate, ethics | M = Maintain |
| T =Technology | R = Risk | E = Eliminate |
| E = Environmental | C = Compliance, standards, specifications | D = Decrease |
| E =Economic | | I = Increase |
| P = Political | | C = Create |
| O = Organisation | | |
| L = Legal | | |

Duerkop and Hurt (2017) also proposed a PESTLE (Political, Economic, Social, Technological, Legal and Environmental) model in assuring that critical infrastructure are delivered to time and cost. Fregenti and Comninos (2012) identified four variables as critical factorial determinants of a successful project as shown in Figure 2.

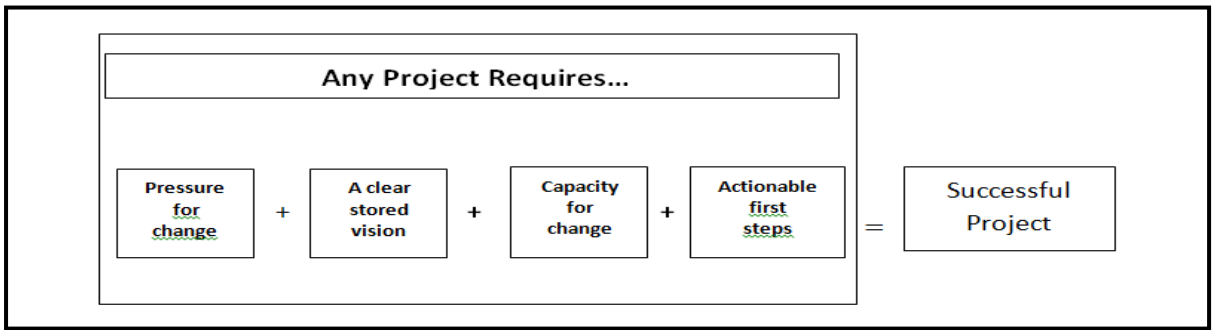


**Figure 2a:** Success factors for project implementation
*Source: Fregenti and Cominios (2012)*

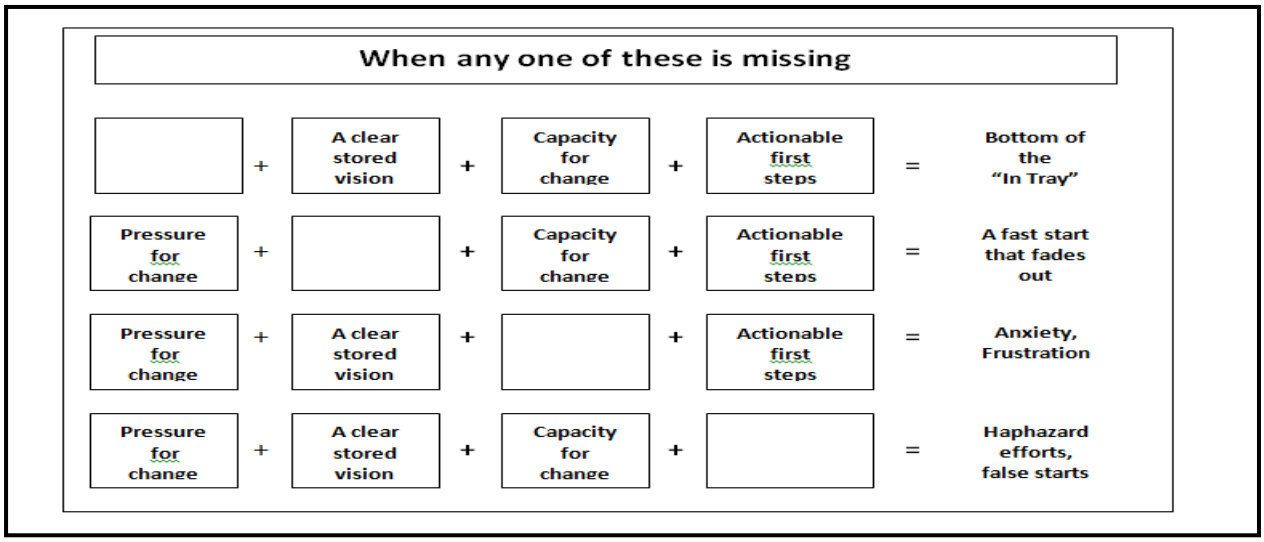


**Figure 2b:** Success factors for project implementation
*Source: Fregenti and Cominios (2012)*

In 2008, NDDC appointed ACCENTURE-Nigeria to carry out a Repositioning of the Commission. They were also to assist in building the Project Management Capacity of the Commission and assure timely delivery of high impact infrastructural projects. However, road projects awarded by the Commission afterwards still suffer from abandonment and time overrun.

As at 2016, NDDC had a total project portfolio of above 8,355 with roads/bridges projects accounting for over 3,300 (Ekere, 2017), and only about 30 percent of these roads projects are completed. There is also the perception that schedule overrun experienced on road projects awarded by NDDC results in expensive litigations. Omatsuli (2014) posited that the Commission as at 2014 had about 400 Legal cases instituted against it by aggrieved stakeholder in nine states of the Niger Delta Region with huge financial repercussion on the Commission.

## 2.0. Methodology

Physical visits to project sites and desk-top project file assessment were conducted on some completed road projects awarded by NDDC. Time-lag data of 162 data sets were analysed to enable the conduct of time-series and, the development of a regression model.

### *2.1. Data collection*

Data were collected on completed road projects awarded by NDDC in the Nine State making up the region. While a total of 340 completed road projects were studied only 162 of these projects were analysed for the following reasons: (i) many of the completed projects were not comprehensively documented (ii) states like Edo and Ondo have relatively small number of well documented completed projects of 10 and 6 respectively (iii) Cross River state has 20 well documented completed projects and approximately this number of projects were taken for the other six states; (iv) only completed projects valued above two hundred million Naira (N200m) was considered for this study so that small and *informal* completed "road" projects like grading of roads, foot bridges, minor rehabilitation works, etc. were excluded. Table 1 below shows the distribution of completed road projects used for the studies.

**Table 1:** Completed road projects awarded by NDDC in the Niger Delta Region of Nigeria

| S/N | State | Completed road projects | Completed road projects with complete documentation | Selected data sets |
|---|---|---|---|---|
| 1 | Abia | 73 | 33 | 21 |
| 2 | Akwa-Ibom | 109 | 42 | 21 |
| 3 | Bayelsa | 78 | 34 | 21 |
| 4 | Cross River | 46 | 20 | 20 |
| 5 | Delta | 219 | 51 | 21 |
| 6 | Edo | 46 | 10 | 10 |
| 7 | Imo | 96 | 40 | 21 |
| 8 | Ondo | 28 | 6 | 6 |
| 9 | Rivers | 374 | 104 | 21 |
| 10 | Regional | 12 | - | - |
| 11 | Total | 1081 | 340 | 162 |

## 3.0. Results and Discussion

### *3.1. Time overrun*

Tables 2 and 3 show results of qualitative studies of some completed road projects awarded by NDDC. Table 2 show the numerical time-lag in weeks and Table 3 show the percentage time-lag in weeks.

**Table 2:** Grouping of time overrun of completed NDDC roads (above N200 million Naira)

| State | Time lag (weeks) | | | | | | | | | |
|---|---|---|---|---|---|---|---|---|---|---|
| | 0 | Less than 26 | 27-52 | 53-104 | 105-156 | 157-208 | 209-260 | 261-312 | Above 312 | Projects |
| Abia | 5 | 2 | 4 | 6 | 3 | 0 | 0 | 0 | 1 | 21 |
| Akwa-Ibom | 8 | 4 | 1 | 2 | 2 | 0 | 1 | 1 | 2 | 21 |
| Bayelsa | 4 | 3 | 6 | 2 | 5 | 1 | 0 | 0 | 0 | 21 |
| Cross River | 5 | 3 | 3 | 3 | 4 | 2 | 0 | 0 | 0 | 20 |
| Delta | 5 | 5 | 2 | 4 | 4 | 0 | 0 | 0 | 1 | 21 |
| Edo | 2 | 1 | 3 | 2 | 0 | 2 | 0 | 0 | 0 | 10 |
| Imo | 10 | 0 | 3 | 4 | 3 | 1 | 0 | 0 | 0 | 21 |
| Ondo | 0 | 1 | 1 | 2 | 1 | 0 | 0 | 1 | 0 | 6 |
| Rivers | 8 | 2 | 1 | 5 | 4 | 0 | 0 | 1 | 0 | 21 |
| Total | 47 | 21 | 24 | 30 | 26 | 6 | 1 | 3 | 4 | 162 |

**Table 3:** Percentage of groups of time overrun of completed roads (above N200 million Naira)

| State | Time lag (%) | | | | | | | | | |
|---|---|---|---|---|---|---|---|---|---|---|
| | 0 % | Less than 26% | 27-52% | 53-104% | 105-156% | 157-208% | 209-260% | 261-312% | Above 312% | Projects |
| Abia | 23.80 | 9.52 | 19.05 | 28.57 | 14.29 | 0 | 0 | 0 | 4.76 | 21 |
| Akwa-Ibom | 38.10 | 19.05 | 4.76 | 9.52 | 9.52 | 0 | 4.76 | 4.76 | 9.52 | 21 |
| Bayelsa | 19.05 | 14.29 | 28.57 | 9.52 | 23.81 | 4.76 | 0 | 0 | 0 | 21 |
| Cross River | 25.00 | 15.00 | 15.00 | 15.00 | 20.00 | 10.00 | 0 | 0 | 0 | 20 |
| Delta | 23.81 | 23.81 | 9.52 | 19.05 | 19.05 | 0 | 0 | 0 | 4.76 | 21 |
| Edo | 20.00 | 10.00 | 30.00 | 20.00 | 0 | 20.00 | 0 | 0 | 0 | 10 |
| Imo | 47.62 | 0 | 14.29 | 19.05 | 14.29 | 4.76 | 0 | 0 | 0 | 21 |
| Ondo | 0 | 16.67 | 16.67 | 33.33 | 16.67 | 0 | 0 | 16.67 | 0 | 6 |
| Rivers | 38.10 | 9.52 | 4.76 | 23.81 | 19.05 | 0 | 0 | 4.76 | 0 | 21 |

Summary result based on a total of 162 completed road project is presented in Table 4.

**Table 4:** Summary results of projects delayed/not delayed

| No. of projects selected states | Delay Periods | No. of projects delayed | Percentage of projects delayed |
|---|---|---|---|
| 162 Awarded Projects | No Delay | 47 | 29.01 |
| | Less than 26 weeks | 21 | 12.96 |
| | 27-52 weeks | 24 | 14.81 |
| | 53-104 weeks | 31 | 19.14 |
| | 105-156 weeks | 26 | 16.15 |
| | 157-208 weeks | 6 | 3.72 |
| | 209-260 weeks | 1 | 0.62 |
| | 261-312 weeks | 3 | 1.85 |
| | Above 312 weeks | 4 | 2.47 |

*3.2. Regression analysis of time series*

One independent and nine dependent variables were employed for this analysis. The selected independent and dependent variables and their codes are presented in Table 5.

**Table 5:** Independent and dependent variables of time lag data

| S/N | Variables | Abbreviation |
|---|---|---|
| 1 | 0 | $X_1$ |
| 2 | <26 | $X_2$ |
| 3 | 27-52 | $X_3$ |
| 4 | 53-104 | $X_4$ |
| 5 | 105-156 | $X_5$ |
| 6 | 157-208 | $X_6$ |
| 7 | 209-260 | $X_7$ |
| 8 | 261-312 | $X_8$ |
| 9 | >312 | $X_9$ |
| 10 | Total Projects | Y |

To assess the dependence of the variables ($X_1$, $X_2$, $X_3$, $X_4$, $X_5$, $X_6$, $X_7$, $X_8$, $X_9$) on the independent variable (Y), regression analysis using the method of multiple regression was employed. An appropriate time series analysis of time overrun of completed NDDC roads is shown in Table 6.

**Table 6:** Time series analysis of time overrun of completed NDDC roads

| States | Y | $X_1$ | $X_2$ | $X_3$ | $X_4$ | $X_5$ | $X_6$ | $X_7$ | $X_8$ | $X_9$ |
|---|---|---|---|---|---|---|---|---|---|---|
| Abia | 21 | 5 | 2 | 4 | 6 | 3 | 0 | 0 | 0 | 1 |
| Akwa-Ibom | 21 | 8 | 4 | 1 | 2 | 2 | 0 | 1 | 1 | 2 |
| Bayelsa | 21 | 4 | 3 | 6 | 2 | 5 | 1 | 0 | 0 | 0 |
| Cross River | 20 | 5 | 3 | 3 | 3 | 4 | 2 | 0 | 0 | 0 |
| Delta | 21 | 5 | 5 | 2 | 4 | 4 | 0 | 0 | 0 | 1 |
| Edo | 10 | 2 | 1 | 3 | 2 | 0 | 2 | 0 | 0 | 0 |
| Imo | 21 | 10 | 0 | 3 | 4 | 3 | 1 | 0 | 0 | 0 |
| Ondo | 6 | 0 | 1 | 1 | 2 | 1 | 0 | 0 | 1 | 0 |
| Rivers | 21 | 8 | 2 | 1 | 5 | 4 | 0 | 0 | 1 | 0 |
| Total | 162 | 47 | 21 | 24 | 30 | 26 | 6 | 1 | 3 | 4 |

*3.3. Assessment of normality*

For regression analysis, it is expected that the individual variables (dependent and independent) be approximately normally distributed. To test whether the variables are statistically normally distributed, the Jarque-Bera test for normality was employed. Mathematically, the Jarque-Bera test is defined as follows:

$$JB = n\left[\frac{\left(\sqrt{b_1}\right)^2}{6} + \frac{(b_2 - 3)^2}{24}\right] \quad (1)$$

where:

$n$ sample size

$\sqrt{b_1}$ sample skewness and

$b_2$ kurtosis coefficient

The null hypothesis for the Jarque-Bera test is that the data is normally distributed while the alternate hypothesis is that the data does not come from a normal distribution. In which case;

$H_0$ = Data follows a normally distributed
$H_1$ = Data do not follow a normal distribution

In general, a large JB value indicates that the residuals are not normally distributed. A value of JB greater than 10 means that the null hypothesis has been rejected at the 5% significance level. In other words, the data do not come from a normal distribution. JB value of between (0-10) indicates that data is normally distributed. For normality, the skewness coefficient should not be greater than 1 and the kurtosis should not be greater than 3.4. Also, the Jarque-Bera test value less than 10 and the (p-value) is greater than the 5% significant value are indicative that the null hypothesis should be accepted, whereby, it could be concluded that the data follows a normal distribution. Result of the normality test for the variable X and Y are shown in Table 7.

**Table 7:** Results of normality test for variables X and Y

| S/No | Variables | Skewness Coefficient | Kurtosis value | Jarque-Bera Value | p-value | Normality Status |
|---|---|---|---|---|---|---|
| 1 | $X_1$ | -0.113335 | 2.2385 | 0.2385 | 88.76% | Normally distributed |
| 2 | $X_2$ | 0.223607 | 2.13000 | 0.358837 | 83.58% | Normally distributed |
| 3 | $X_3$ | 0.736612 | 2.7893 | 0.830329 | 66.02% | Normally distributed |
| 4 | $X_4$ | 0.576161 | 1.991481 | 0.886960 | 64.18% | Normally distributed |
| 5 | $X_5$ | -0.566391 | 2.216048 | 0.711665 | 70.06% | Normally distributed |
| 6 | $X_6$ | 0.680414 | 1.83333 | 1.204861 | 54.75% | Normally distributed |
| 7 | $X_7$ | 2.474874 | 7.125000 | 15.56836 | 0.04% | Not Normally distributed |
| 8 | $X_8$ | 0.707107 | 1.50000 | 1.593750 | 45.07% | Normally distributed |
| 9 | $X_9$ | 1.238006 | 3.170360 | 2.309870 | 31.51% | Not Normally distributed |
| 10 | Y | -1.431427 | 3.2224 | 3.2224 | 21.31% | Normally distributed |

*3.4. Residual probability plot*

To ascertain the suitability of regression method in explaining the dependence of the selected dependent variables on the independent variable, the residual probability plot was employed. To apply regression model, the residual probability plot must fluctuate around the linear mean value as presented in Figure 2.

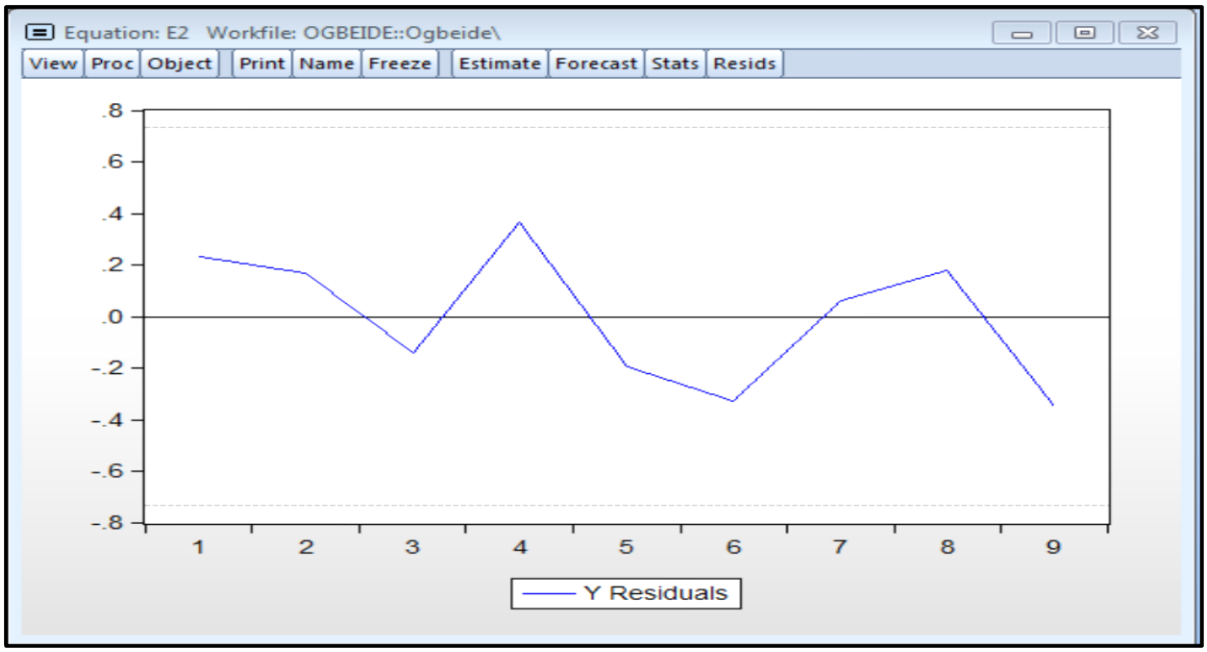


**Figure 2:** Residual probability plot

Based on the result of Figure 2, it was concluded that multiple linear regression model is suitable for this analysis. In regression analysis of data, it is pertinent to note that standard error estimation and computation of *t*-statistics are appropriate in calculating the probability (*p*-value) by which the significance of the regression model is tested. In the presence of heteroscedasticity, it is assumed that the overall standard error of regression and the t-statistics computed for each variable may not be completely adequate to estimate the resulting probability (*p*-value) of regression. In addition, the presence of serial correlation can lead to a number of issues, namely; make reported standard error and t-statistics to be invalid, and coefficient may be biased, though not necessarily inconsistent. Based on this argument, selected diagnostic statistics were conducted to verify the statistical properties of the overall regression model. The selected diagnostic statistics include; heteroscedasticity test using Breusch-Pagan Godfrey, and Variance Inflation Factor (VIF).

### *3.5. Heteroscedasticity test*

Heteroscedasticity is a diagnostic test statistics used to diagnose the adequacy of the probability (p-value) calculated for each individual variable. Hence it is important to know whether there is or there is no heteroscedasticity in the data. The null and alternate hypothesis of heteroscedasticity was formulated as follows:

$H_0$ = Presence of homoscedasticity and absence of heteroscedasticity
$H_1$ = Absence of homoscedasticity and presence of heteroscedasticity

Result of heteroscedasticity using Breusch-Pagan Godfrey is presented in Table 8.

**Table 8:** Result of heteroscedasticity test

EViews - [Equation: E2 Workfile: OGBEIDE::Ogbeide\]

File Edit Object View Proc Quick Options Add-ins Window Help

View | Proc | Object | Print | Name | Freeze | Estimate | Forecast | Stats | Resids

Heteroskedasticity Test: Breusch-Pagan-Godfrey

| | | | |
|---|---|---|---|
| F-statistic | 7.277403 | Prob. F(7,1) | 0.2782 |
| Obs*R-squared | 8.826729 | Prob. Chi-Square(7) | 0.2653 |
| Scaled explained SS | 0.031356 | Prob. Chi-Square(7) | 1.0000 |

Test Equation:
Dependent Variable: RESID^2
Method: Least Squares
Date: 12/07/20 Time: 13:59
Sample: 1 9
Included observations: 9

| Variable | Coefficient | Std. Error | t-Statistic | Prob. |
|---|---|---|---|---|
| C | -0.169766 | 0.057069 | -2.974780 | 0.2065 |
| X1 | -0.006944 | 0.002733 | -2.540837 | 0.2387 |
| X2 | 0.017513 | 0.006477 | 2.703978 | 0.2255 |
| X3 | -0.000119 | 0.008355 | -0.014198 | 0.9910 |
| X4 | 0.039412 | 0.007818 | 5.041113 | 0.1247 |
| X5 | -0.001986 | 0.007488 | -0.265221 | 0.8350 |
| X6 | 0.093439 | 0.014142 | 6.606968 | 0.0956 |
| X8 | 0.112613 | 0.031027 | 3.629536 | 0.1712 |

| | | | |
|---|---|---|---|
| R-squared | 0.980748 | Mean dependent var | 0.059984 |
| Adjusted R-squared | 0.845982 | S.D. dependent var | 0.048265 |
| S.E. of regression | 0.018942 | Akaike info criterion | -5.514361 |
| Sum squared resid | 0.000359 | Schwarz criterion | -5.339050 |
| Log likelihood | 32.81462 | Hannan-Quinn criter. | -5.892681 |
| F-statistic | 7.277403 | Durbin-Watson stat | 2.108480 |
| Prob(F-statistic) | 0.278169 | | |

Path = c:\users\ilaboya\documents | DB = none | WF = ogbeide

From the result of Table 8 it was observed that; the calculated (*p*-value) based on the *F*-statistics is 0.2782, and the calculated (*p*-value) based on Lagrange multiplier (LM) is 0.2653. Since the computed (*p*-value) based on *F*-statistics and Lagrange multiplier are greater than 0.05 ($P > 0.05$), we accept the null hypothesis of homoscedasticity and conclude that there is no heteroscedasticity in the data.

*3.6. Variance Inflation Factor (VIF)*

Variance inflation factor (VIF) measures the correlation of the dependent variables with the independent variable. Ideal VIF is 1; VIF greater than 10 is cause for alarm showing the variables are uncorrelated due to multicollinearity. Result of the calculated VIF for the selected variables is presented in Table 9.

**Table 9:** Calculated variance inflation factors

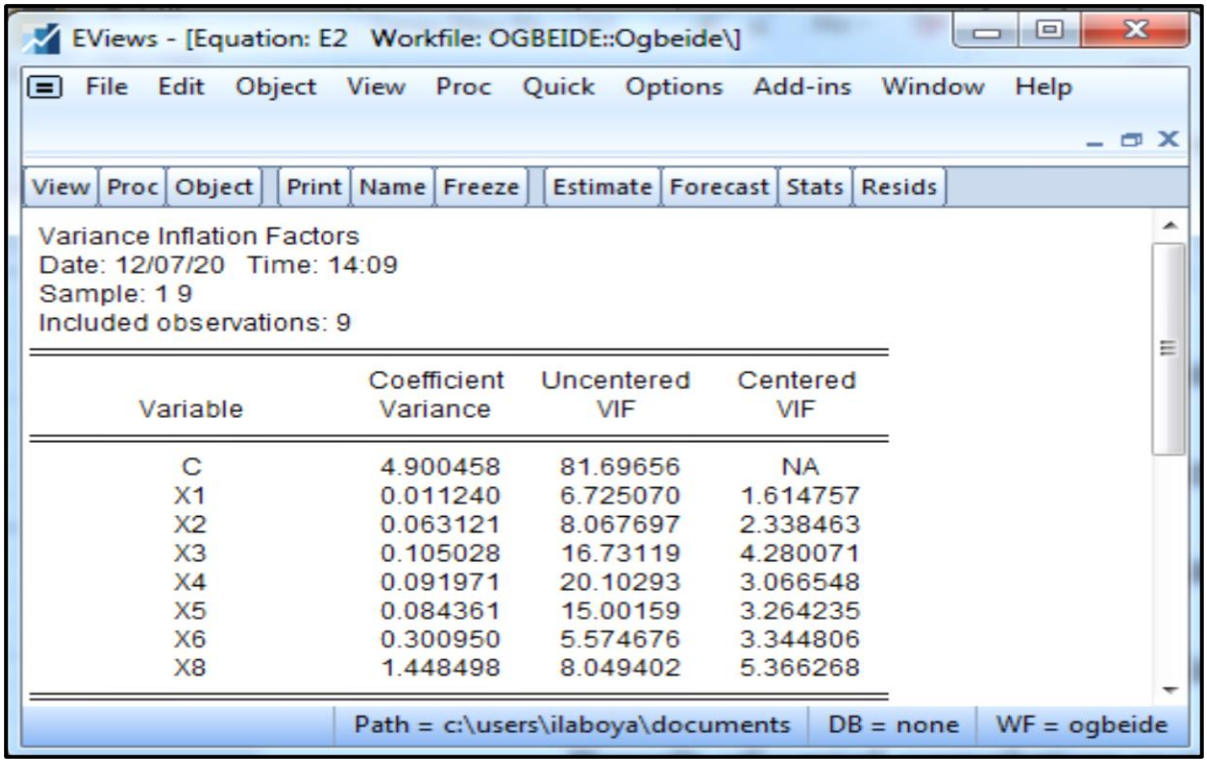


Since the computed variance inflation factors for the selected dependent variables are less than 10, it was concluded that the variables are well correlated with the independent variable, hence absence of multicollinearity. Finally, the dependence of the selected dependent variables on the independent variable was evaluated using the coded multiple regression equation function presented as:

$$(Y) = C\{X_1\ X_2\ X_3\ X_4\ X_5\ X_6\ X_8\}$$

Variable $X_7$ and $X_9$ were omitted since they are not normally distributed. The coded regression equation was implemented using Eviews and results obtained are presented in Table 10.

**Table 10:** Output of regression analysis

Equation: E4 Workfile: OGBEIDE NEW::Untitled\

View | Proc | Object | Print | Name | Freeze | Estimate | Forecast | Stats | Resids

Dependent Variable: Y
Method: Least Squares
Date: 12/07/20 Time: 15:55
Sample: 1 9
Included observations: 9

| Variable | Coefficient | Std. Error | t-Statistic | Prob. |
|---|---|---|---|---|
| C | -1.197412 | 2.213698 | -0.540911 | 0.6843 |
| X1 | 1.227930 | 0.106019 | 11.58214 | 0.0548 |
| X2 | 1.616039 | 0.251240 | 6.432265 | 0.0982 |
| X3 | 1.360726 | 0.324080 | 4.198738 | 0.1488 |
| X4 | 1.020601 | 0.303268 | 3.365344 | 0.1839 |
| X5 | 0.341867 | 0.290450 | 1.177027 | 0.4483 |
| X6 | 0.665128 | 0.548590 | 1.212433 | 0.4391 |
| X8 | 1.657477 | 1.203535 | 1.377173 | 0.3998 |

| | | | |
|---|---|---|---|
| R-squared | 0.997970 | Mean dependent var | 18.00000 |
| Adjusted R-squared | 0.983764 | S.D. dependent var | 5.766281 |
| S.E. of regression | 0.734747 | Akaike info criterion | 1.801972 |
| Sum squared resid | 0.539853 | Schwarz criterion | 1.977282 |
| Log likelihood | -0.108872 | Hannan-Quinn criter. | 1.423652 |
| F-statistic | 70.24670 | Durbin-Watson stat | 2.108480 |
| Prob(F-statistic) | 0.091620 | | |

From the result of Table 10, the following observations were made: since the adjusted R-square value of 0.983764 is in reasonable agreement with the observed coefficient of determination $R^2$ value of 0.997970, it was concluded that the regression model was reasonably adequate. Using the result of Table 10, the overall regression equation was thereafter generated and presented as follows:

$$Y = -1.1974 + 1.2279X_1 + 1.6160X_2 + 1.3607X_3 + 1.0206X_4 + 0.3419X_5 + 0.6651X_6 + 1.6575X_8 \quad (2)$$

## 4.0. Conclusion

This study shows that NDDC's completed road projects experiences time overrun as indicated below:

- 29.01% of the awarded projects were completely executed within the required duration without delay
- 12.96% of the projects experienced between 1-26 weeks' delay before final completion
- 14.81% of the projects experienced between 27-52 weeks' delay before final completion
- 19.14% of the projects experienced between 53-104 weeks' delay before final completion
- 16.15% of the projects experienced between 105-156 weeks' delay before final completion
- 3.72% of the projects experienced between 157-208 weeks' delay before final completion
- 0.62% of the projects experienced between 209-260 weeks' delay before final completion
- 1.85% of the projects experienced between 261-312 weeks' delay before final completion
- 2.47% of the projects experienced above 312 weeks' delay before final completion
- A conceptual model of time series with Number of Awarded Projects as dependent variables (Y) and Lengths of Construction delay as the independent variable (X) was developed as: $Y = -1.1974 + 1.2279X_1 + 1.6160X_2 + 1.3607X_3 + 1.0206X_4 + 0.3417X_5 + 0.6651X_6 + 1.6575X_8$

Based on the findings, the following recommendations were made:

- NDDC should evolve technologies to document and keep records of her project delivery portfolio. This will enable access to more reliable data for further studies.
- The Commission should also deploy technologies to minimize construction delay on her road projects.

**References**

Chai, C. S., Yusaf, A. M. and Habil, H. (2015). Delay mitigation in the Malaysian housing industry: A structural equation modelling approach. *Journal of construction in developing Countries*, 20(1), pp. 65 – 83.

Duerkop, S. and Hurt, M. (2017). *Transportation under threats-A PESTLE analysis for critical logistical infrastructure*, Paper presented at the 2017 AGM & Annual conference of the Nigerian Institution of Highway and Transportation Engineer, Abuja, Nigeria, 7th Dec, 2017.

Ekere, E. (2017). *We must have standards below which we cannot go,* An address by the MD/CEO of NDDC to NDDC Consultants and Contractors on September 28, 2017, Presidential Hotel, Port Harcourt.

Fregenti, E. and Cominios, D. (2012). Practice of project management – a guide to the business focused approval, Kogan Rolge Publishers.

Khan, L. (2015). Causes of delays in construction projects and their effects" (available at https.//engrligmankhan.wordpress.com), pp. 1/38-36/38.

Kikwasi, G. J. (2012). Causes and effects of delays and disruptions in construction projects in Tanzania. *Australian Journal of Construction Economics and Building Conference*, (2), pp 52-59.

Kolhe, R. and Darade, M. (2014). Detail analysis of delay in construction projects. *International Journal of Innovative Science, Engineering & Technology*, 1(10), pp. 70-72.

Lo, T. Y., Fung, I. W. H. and Tung, K. C. F. (2006). Construction delay in Hong Kong Civil Engineering Projects. *Journal of Construction Engineering and Management*, 132(6), pp. 636-649.

Memon, A. H., Rahman, I. A., Akram, M. and Ali, N. M. (2014). Significant factors causing time overrun in construction projects of Peninsular Malaysia. *Journal of Modern Applied Science*, 8(4), pp. 16-28.

Mohamad, M. R. B. (2010). The factors and effect of delay in government construction project, case study in Kuantan University, Malaysia, Patiang.

Omatsuli, T. (2014). *Sustainable Project Management,* A paper delivered at the 2014 NDDC Board and Management Retreat, March 12-13, Le Meridian Hotel, Uyo, Nigeria.

Owolabi, J. D., Amusan, L. M., Oloke, C. O., Tunji– Olayemi, P., Owolabi, D., Peter, J. and Omuh, I. (2014). Causes and effect of delay of project construction delivery time. *International Journal of Education and Research*, 2(4), pp. 197 – 208.

Pall, G. K., Bridge, A. J., Skitmore, M. and Gray, J. (2016). Comprehensive Review of Delays in Power Transmission Projects. *Inst. Eng. Technol.*, 10(14), pp. 3393–3404.

Pickavance, K. (2010). Delay and disruption in construction contracts. 4th Edition, Sweet & Mawell, London, UK

Ramli, M. Z., Malek, M. A., Muda, M. Z., Talib, Z. A., Azman, N. S., Fu'ad, N. F. S. M., Zawawi, M. H. and Katman, Y. (2018). A review of Structural Equation Model for Construction Delay Study. *International Journal of Engineering & Technology*, 7, pp. 299-306.

**Cite this article as:**

Ogbeide F. N., Ehiorobo J. O., Izinyon O. C. and Ilaboya I. R. 2021. A Qualitative Study of Time Overrun of Completed Road Projects Awarded by the Niger Delta Development Commission in the Niger Delta Region of Nigeria. *Nigerian Journal of Environmental Sciences and Technology*, 5(1), pp. 271-280. https://doi.org/10.36263/nijest.2021.01.0269

Nigerian Journal of Environmental Sciences and Technology (NIJEST)

www.nijest.com

ISSN (Print): 2734-259X | ISSN (electronic): 2734-2603

Vol 5, No. 1 March 2021, pp 281 - 289

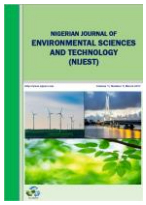

# Effect of Fallowed and Cultivated Land Use Systems on the Composition and Abundance of Soil Macroinvertebrates Assemblage in Uruk Osung Community, Akwa Ibom State, Nigeria

Akpan A. U.[1,*], Chukwu M. N.[2], Esenowo I. K.[3], Johnson M.[4] and Archibong D. E.[5]

[1,3,5]Department of Animal and Environmental Biology, University of Uyo, Akwa Ibom State, Nigeria

[2]Department of Pure and Applied Sciences, Faculty of Science, National Open University of Nigeria, Jabi-Abuja, Nigeria

[4]Department of Zoology, University of Ibadan, Ibadan, Oyo State, Nigeria

Corresponding Author: *akpanudoh@uniuyo.edu.ng

https://doi.org/10.36263/nijest.2021.01.0278

## ABSTRACT

*This study was to assess the effect of fallowed and cultivated land-use systems on the abundance of soil macroinvertebrates assemblage. Collections of soil samples were carried out fortnightly twice a month for four months. The extraction of soil macroinvertebrates was carried out using Berlese-Tullgren funnel extractor, and elutriation technique. The mean values of 6.93+/-0.25 were recorded for pH, 32.08+/-0.52$^{o}$C for temperature, 15.60+/-1.22 for moisture content, were recorded for fallowed soil, and 4.43+/-0.16 (pH), 30.95+/-0.19$^{o}$C (temperature) were recorded for cultivated soil. A total of 17 soil macroinvertebrates species comprising of 11 orders, from four classes were encountered. Out of the 517 individual soil macroinvertebrates encountered, 327 individuals representing four classes were present in the fallow land while 190 individuals representing three classes were present in the cultivated land. The most dominant species in terms of abundance in the fallowed land site included; Cryptotermes sp 67(20.49%) > Blatta sp 56(17.12%) with Hogna sp 1(0.0.30%) the least; while Cryptotermes sp. 79(41.58%) >Lasius sp 30(15.79%) > Lumbricus terrestris 21(11.05%) represents the dominant species in the cultivated soil with Paraponera sp 1(0.53%) the least. Soil temperature showed positive correlation with the abundance of Clitellata ($r = 0.851$; $p < 0.05$) and Insecta ($r = 0.826$; $p < 0.05$) and Soil pH showed positive correlation with the abundance of Diplopoda ($r = 0.911$; $p \leq 0.05$). In conclusion, it could be deduced from the study that human activities in the cultivated site perturb soil macroinvertebrates community structure which is reflected in the relative abundance of soil macroinvertebrate from the two sampling sites. The results obtained in this study could be a piece of pointing information for the conservation and management of the soil macroinvertebrates giving their functions in balancing agroecosystems.*

**Keywords:** Macro-invertebrates, Fallow land, Cultivated land, Berlese-Tullgren funnel extractor

## 1.0. Introduction

The soil represents one of the most important reservoirs of biodiversity. It is a dynamic, complex, and highly heterogeneous ecosystem that allows the development of a large fragmented number of ecological habitats. It is home to all arrays of living organisms that perform important functions for the soil ecosystem according to their niche (Menta, 2012). The health of the soil ecosystem is therefore relative to its productivity and sustainability which depends on the changing state of its physico-chemical and biological properties (Somasundaram *et al.*, 2013; Elias *et al.*, 2019; Bufebo and Elias, 2020).

According to Nanganoa *et al.* (2019), the physico-chemical and biological properties of soil ecosystems are continuously influenced by land uses. The nature of the soil structure, whether

fallowed or cultivated can exert a strong influence on the diversity and abundance of soil macroinvertebrates in a (Barrios *et al*., 2002; Barrios *et al*., 2005; Moreira *et al.,* 2008). A fallowed land system with its retaining features such as fallen logs and leaves litters provides habitats to many soil and litter-dependent arthropods. In addition, fallowed land with its stable and isolated features with little or no human disturbance over a given time often shows a high diversity and abundance of soil macro-invertebrates species composition (Lagerlöf *et al*., 2002; Rossi *et al.,* 2010). Whereas, cultivated land, with the absence of soil surface litter and tree shadings, exposes these soil macroinvertebrates to an unfavourable conditions such as changes in soil temperature and pH, loss of moisture, and predation. This degraded soil condition could lead to a reduction in the soil macroinvertebrate diversity and abundance (Rossi *et al.,* 2010).

Macroinvertebrates fauna found in soil and soil litter is known to play a crucial role in soil processes such as nutrient cycling, organic matter decomposition, and improvement of soil physical attributes such as aggregation, porosity, and water infiltration (Dangerfield and Milner, 1996; Rossi and Blanchart, 2005; Mutema *et al.,* 2013). There is scanty information on the effect of fallowed and cultivated land-use systems on the composition and abundance of soil macroinvertebrates assemblage in this part of Akwa Ibom state, herein this study to investigate the effect of fallowed and cultivated land-use systems on the composition and abundance of soil macroinvertebrate assemblage in the community.

## 2.0. Methodology

### *2.1. Study area*

The study was carried out at Uruk Osung Village in Obot Akara Local Government Area of Akwa Ibom State, South-South part of the country, Nigeria. Obot Akara Local Government Area lies between $5^0 16' 0''$ N and $7^0 36' 0''$ E. Uruk Osung is within the tropical rainforest belt characterized by a rainy and dry season - the rainy season lasting from late March to early November and the dry season from late November to early March. The forest in the area is of secondary forest mixed with oil palm trees (*Elaeis guineensis)*, and short and tall trees. The vegetation found in this area included a wide variety of grasses, herbs, and shrubs, and trees. The topsoil is of the loamy type but some areas are characterized by clay and loamy. The people living in this community are predominantly farmers specializing in the cultivation of cassava (*Manihot esculenta*), yam (*Oxalis tuberosa*), water yam (*Dioscorea alata*), pumpkin leaves (*Telfaira occidentalis*), plantain (*Musa paradisiaca)*, and Okra (*Abelmoschus esculentus*); while some are into craft making and few are civil servants.

### *2.2. Sampling sites*

The two sampling sites were located along a foot track called Afang Akang with the co-ordinates of $N5^0 12'46.3''$ and $E7^0 33' 39.4''$ (Figure 1). The fallowed land site is about 200m west of the direction from the cultivated land site. The fallowed land site is an area covered with long and dense trees such as *Guare* sp, and climbers forming a nearly closed canopy and without apparent and reported human impacts for 4years (pers. comm.). The cultivated land site is also characterized by oil palm (*Elaeis guineensis*) trees of various densities of coverage, woody shrubs such as *Chromolaena odorata* (Siam weed), and various grass undergrowth. The cultivated land-use system has the presence of human activities; conventionally tilled with hoes, cropped with melon (*Cucumismelo*), cassava (*Manihot esculenta*), yam (*Oxalis tuberosa*), water yam (*Dioscorea alata*), pumpkin leaves (*Telfaira occidentalis*), waterleaf (*Talinum triangulare*), Okra (*Abelmoschus esculentus*) and maize (*Zea mays*).

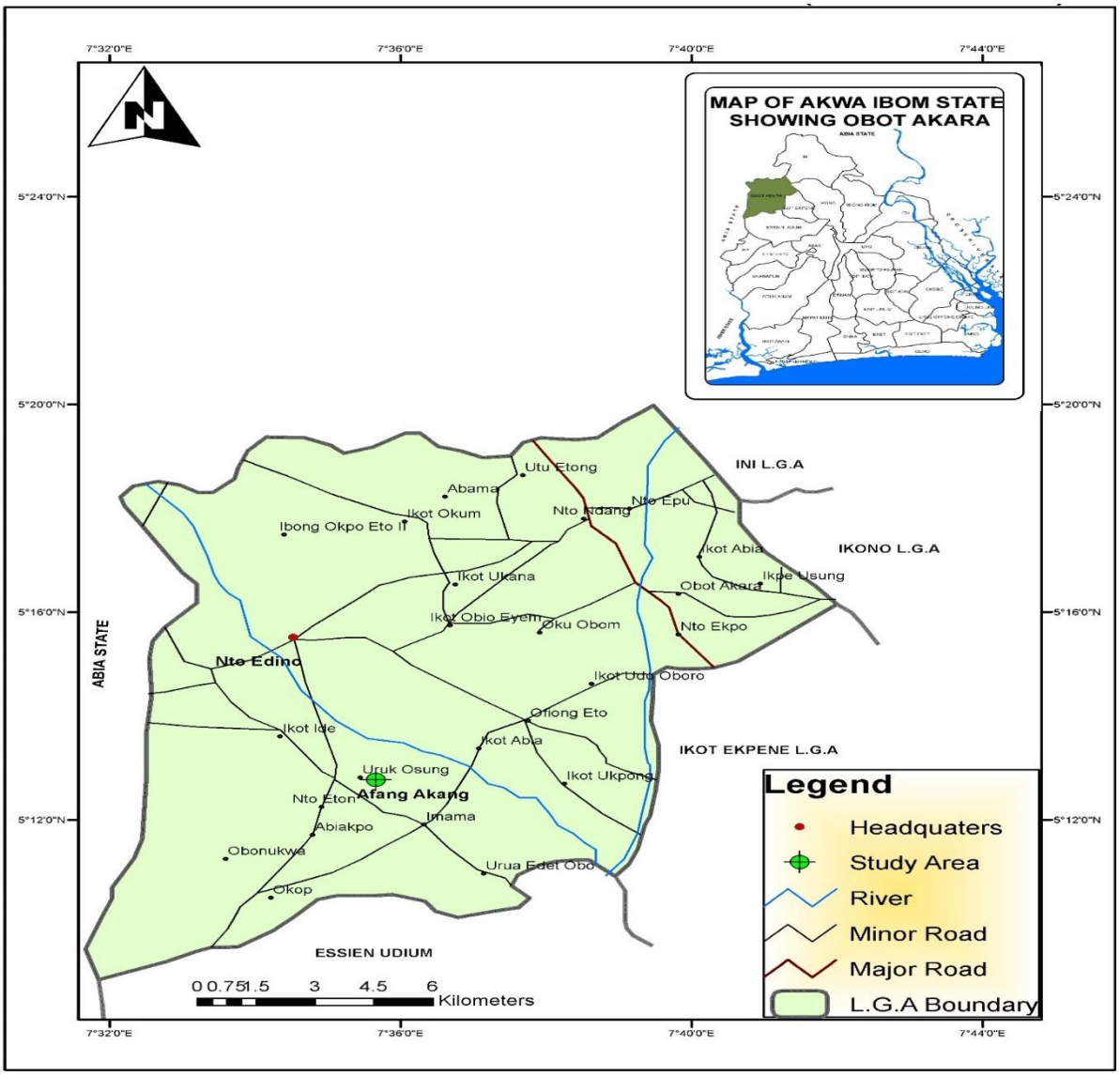


**Figure 1:** Map of Obot Akara LGA showing study area (Afang Akang) (Cartography Studio, Department of Geography and Natural Resources Management, University of Uyo, Uyo, Akwa Ibom State)

*2.3. Methods*

2.3.1 Physico-chemical parameters of soils

The soil samples from fallowed and cultivated land systems were collected and placed in separate polythene bags and taken to the Department of Animal and Environmental Biology Laboratory, the University of Uyo for determination of soil moisture content according to the method described by Jamel (2017). Soil temperature and pH were determined *in situ* with the use of mercury in a glass thermometer and buffered electronic pH meter (Kent 7020) respectively.

2.3.2. Collections of soil sample

Collections of soil samples for the extraction of soil macroinvertebrates were carried out fortnightly twice a month, for four months intervals between May and August 2016. In each of the sampling sites (fallow and cultivated), three sampling macro-plots (A, B, and C) were measured out at 10m × 10m × 10m apart from each other in a triangular transect. Each of the sample macro-plots was divided into two sampling micro-plots (A1, A2, B1, B2, C1, and C2). In each sampling micro-plots, a well-measured and marked tin container (10cm × 10cm) was used in collecting the soil samples at depth of 0-10cm (Battigelli and Marshall, 1993). The soil samples were placed into different polythene bags and labeled carefully to indicate; date of collection, sampling site, and micro-plot collected.

2.3.3. Laboratory analysis

The soil samples were taken to the Entomological Laboratory unit of the Department of Animal and Environmental Biology University of Uyo, for analysis. The elutriation technique according to Alonso-Zarazaga and Domingo-Quero (2010) was adopted to extract soil macro-invertebrates from soil litters. The soil litters were places on a transparent tray with water inside, and with the help of forceps and soft-haired brush, soil macroinvertebrates that floated, were collected and preserved. Berlese – Tullgren Funnel method was also used for the extraction of the soil macroinvertebrates; where each of the soil samples were placed in a funnel (Hopkins, 2002) sealed with a mesh wire size of 1 mm and were allowed to stand under a lighting tungsten bulb of 100watts for 72 hours. The heat energy produced from the lighting bulb extracted the soil organisms through the open narrowed lobe of the funnel. These soil organisms were collected into conical flasks containing 70% ethyl alcohol. The collected soil organisms were sorted, counted, and identified by Entomologist in the Entomological Laboratory unit of the Department of Animal and Environmental Biology and also with the aid of the key identification guides by Borror and White (1970). The scientific name and numbers of each soil macroinvertebrate species were recorded.

2.3.4. Data analysis

Microsoft Excel (version 2007) was used to determine the numerical and percentage of soil macroinvertebrate abundance. SPSS Statistical software (version 2015) was used to determine the Person correlation coefficient ($r$) between the physico-chemical parameters and the soil invertebrate abundance. PAST statistical software was used to determine the diversity indices and the canonical correspondence analysis.

## 3.0. Results and Discussion

### *3.1. Soil physico-chemical parameters*

The range, mean, and standard error of soil physic-chemical parameters measured from the two sampling sites during the study are presented in Table 1. The result of the person correlation showing the relationship between the soil physico-chemical parameters and macroinvertebrate class abundance is presented in Table 2. The result of the analysis showed that soil temperature correlated positively with the abundance of *Clitellata* at ($r$ = 0.851; $p$ < 0.05) and *Insecta* at ($r$ = 0.826; $p$ < 0.05). Similarly, soil pH correlated positively with the abundance of *Diplopoda* with ($r$ = 0.911; $p$ < 0.05). It is also worthy of note that the correlation between soil moisture and the macroinvertebrate class was non-significant at ($p$ < 0.05).

The mean pH value of the cultivated soil site shows the acidic nature of the soil which contrasts the alkaline nature of the fallowed soil. The variation in the soil pH could be due to soil exposure to environmental influences such as leaching and evaporation (Konakwan *et al*., 2015). There was a significant difference at ($p$ < 0.05) in the variation of pH values across the two contrasting soils. Furthermore, the variations observed for soil temperature and moisture in the two contrasting soils could be due to the removal of foliage from the cultivated soil which has often served the purpose of covering the topsoil from direct sunlight and evaporation processes (Alonso-Zarazaga and Domingo-Quero, 2010; Camara *et al.*, 2018).

Concerning soil macroinvertebrates composition and abundance dynamics, the correlation analysis showed positive relationships between soil temperature and pH, and macroinvertebrate classes. It was observed that soil temperature also showed a positive correlation with class Clitellata and Insecta, whereas soil pH correlated positively with class Diplopoda. This implied that the variations in soil temperature and pH affect the composition and abundance of the macro-invertebrates.

The variation of the pH range of the fallowed and cultivated soils showed that the cultivated land site tends to be more acidic than the fallowed soil. This result supports the assertion of Nanganoa *et al*. (2019), that the physico-chemical and biological properties of soil ecosystems are continuously influenced by land uses. It could also be deduced from the results that the fallowed soil with its mean characteristic pH property of 6.93±0.25 recorded a higher abundance of soil macroinvertebrates compared to the cultivated soil. This observation is consistent with the reports of Madge and Sharma (1969) that soil macro-invertebrates strive better in alkaline than acidic soil. This is because the body

fluid of these macroinvertebrates is alkaline which could be hypotonic to the acidic concentration of a degrading cultivated soil environment.

**Table 1:** The range, mean and standard error of the soil physico-chemical parameters measured during the sampling period.

| Soil Parameters | Fallowed Land | | Cultivated Land | |
|---|---|---|---|---|
| | Range | Mean ± Std. Err. | Range | Mean ± Std. Err. |
| pH | 5.26-6.95 | 6.93±0.25* | 3.20-5.10 | 4.43±0.16* |
| Moisture content | 9.50-16.50 | 15.60±1.22$^{ns}$ | 7.00-11.50 | 9.91±0.73$^{ns}$ |
| Temperature ($^{o}$C) | 30-33.5 | 32.08±0.52* | 29.00-31.5 | 30.95±0.19* |

Keys: (*) mean values are significantly different at ($p < 0.05$); (ns) = mean values not significantly different at ($p < 0.05$)

**Table 2:** Pearson correlation between variations in soil parameter and species abundance

| | Mositure | Temp. | pH | *Clitellata* | *Arachnida* | *Diplopoda* | *Insecta* |
|---|---|---|---|---|---|---|---|
| Mositure | 1 | | | | | | |
| Temp. | 0.184 | 1 | | | | | |
| | 0.727 | | | | | | |
| pH | 0.938** | 0.46 | 1 | | | | |
| | 0.006 | 0.359 | | | | | |
| Clitellata | 0.6 | 0.851* | 0.785 | 1 | | | |
| | 0.208 | 0.032 | 0.064 | | | | |
| Arachnida | 0.282 | 0.69 | 0.413 | .827* | 1 | | |
| | 0.588 | 0.13 | 0.416 | 0.042 | | | |
| Diplopoda | 0.784 | 0.664 | 0.911* | 0.820* | 0.47 | 1 | |
| | 0.065 | 0.151 | 0.011 | 0.046 | 0.347 | | |
| Insecta | 0.147 | 0.826* | 0.385 | 0.818* | 0.906* | 0.557 | 1 |
| | 0.781 | 0.043 | 0.451 | 0.047 | 0.013 | 0.251 | |

*3.2. Soil macroinvertebrates composition, abundance and diversity*

The species composition, numerical and percentage abundance of soil macroinvertebrates are presented in Table 3, while the results on the community structure of the soil macroinvertebrates classes are presented in Table 4. A total of 17 soil macroinvertebrates species comprising of 11 orders, four classes were encountered during the study period. The most abundant macroinvertebrate species in the fallowed land system were in the order; *Cryptotermes* sp 67(20.49%) > *Blatta* sp 56(17.12%) > *Lumbricus terrestris* 45(13.76%) with *Hogna* sp 1(0.0.30%) as the least; whereas the pattern encountered in the cultivated land was, *Cryptotermes sp*. 79(41.58%) > *Lasius sp* 30(15.79%) > *Lumbricus terrestris* 21(11.05), with *Paraponera sp* 1(0.53%) as the least abundant species. Notably, Class *Insecta* was observed to be higher in the two sampling land used systems with percentage abundance of 74.6% and 80.6% in the fallowed land and cultivated land respectively, whereas while Class *Arachnida* represented the least Class of soil macroinvertebrate species in the fallowed land system, they were absent in the cultivated land used system.

The result for the diversity indices of soil macroinvertebrate group across the two contrasting sampling land used systems is presented in Table 5. A total of 16 individual species were observed in the fallowed land as compared to 9 individual species recorded for the cultivated land, this means that the ratio of soil macro-invertebrate species between fallowed and the cultivated land was about 2:1. A Higher Shannon Weiner index of H = 2.332 was observed in the fallowed land compared to a lower value of 1.765 observed for the cultivated land. A similar trend was also observed for the Margalef index where a higher value of 2.591 was recorded for the fallowed land compared to the value of 1.529 recorded for the cultivated land.

In the present study, earthworm (*Lumbricus terrestris*) and termite (*Cryptotermes* sp) were dominant both in the fallowed and cultivated land than all other soil macroinvertebrate species encountered in the study. These could be attributed to their ecological niche as important drivers of soil aggregation, soil porosity, water infiltration, and resistance to erosion in any soil ecosystem (Lavelle, 1997). These activities can lead to soil structure reformation, increased aeration, water infiltration, and water availability to plants (Brown *et al*., 2004). This observation agrees with the report of Brown *et al.* (2004), who reported that termites, ants, and earthworms make up the most abundant of soil macro-invertebrates across most soil ecosystems.

*Lumbricus terrestris* in particular, plays the role of soil organic matter and cast formation enriched with soil nutrients such as nitrogen, potassium, phosphorus, and calcium which serve as plants' nutrients reservoir (Mora *et al*., 2003; Pulleman *et al*., 2004; Bossuyt *et al*., 2005). The population of *Lumbricus terrestris* in the cultivated site was less in abundance as compared to that of the fallowed site. This could be attributed to human disturbances as a result of soil cultivation practices such as deforestation, bush burning, soil tillage and the application of agrochemicals which is very detrimental to not only the *Lumbricus terrestris* population, but also to the overall population dynamics of soil macroinvertebrates in the cultivated land system.

The activities of *Cryptotermes* sp includes the construction of mounds, nests, and surface sheeting, and this brings about transportation of organic material and soil burrow, which improve drainage and aeration. Collin (1983) reported that termites engage in litter removal and breakdown to form soil nutrients, but the high abundance of termite in a cultivated land system such as encountered in this study could become a potential threat to crop yield (Rossi *et al.,* 2010). The agricultural effect of *Cryptotermes* sp has been well documented in the work of Sekammatte *et al*. (2003) and Sileshi *et al.* (2005).

The nature of a soil structure, whether fallowed or cultivated can exert a strong influence on the overall composition and abundance of soil macroinvertebrates in a given ecosystem (Barrios *et al*., 2002; Barrios *et al*., 2005). However, the higher abundance of soil macro-invertebrates observed in the fallowed land could be as a result of its stable and isolated nature with little or no human activities over time (Lagerlöf *et al*., 2002; Rossi *et. al.,* 2010). The fallowed land system has better soil covers which are necessary for the survival of soil macroinvertebrates. In addition, the soil of the fallowed land system is minimally disturbed. According to Moreira *et al.* (2008) and Rossi *et al.* (2010), these features create more favourable conditions for the development and survival of soil organisms, and the absence of soil cover and minimal soil disturbance in the cultivated land system results in soil degradation and lack of food and microhabitats which are necessary for the development and survival of the soil macroinvertebrates.

**Table 3:** The composition and abundance of soil macroinvertebrates from the two sampling sites

| | | | Abundance | | | |
|---|---|---|---|---|---|---|
| | | | Fallow land | | Cultivated land | |
| Class | Order | Species composition | Ni | (%) | Ni | (%) |
| Clitellata | Haplotaxida | *Lumbricus terrestris* | 45 | 13.76 | 21 | 11.05 |
| Arachnida | Araneae | *Hogna* sp | 1 | 0.30 | 0 | 0 |
| Diplopoda | Spirostreptida | *Archispirostreptus gigas* | 3 | 0.92 | 0 | 0 |
| | Julida | *Blaniulus guttulatus* | 34 | 10.40 | 11 | 5.79 |
| Insecta | Blattodea | *Blatta* sp | 56 | 17.12 | 12 | 6.32 |
| | Coleoptera | *Phyllophaga* sp | 21 | 6.42 | 14 | 7.37 |
| | Dermaptera | *Chelisoches* sp | 6 | 1.84 | 0 | 0 |
| | | *Forficula* sp | 17 | 5.20 | 0 | 0 |
| | Hymenoptera | *Solenopsis* sp | 15 | 4.59 | 0 | 0 |
| | | *Lasius* sp | 5 | 1.53 | 30 | 15.79 |
| | | *Paraponera* sp | 2 | 0.61 | 1 | 0.53 |
| | | *Monomorium* sp | 30 | 9.17 | 0 | 0 |
| | | *Sphex* sp | 0 | 0 | 5 | 2.63 |
| | Hemiptera | *Neotibicen* sp | 10 | 3.06 | 0 | 0 |
| | Orthoptera | *Gyllus* sp | 10 | 3.06 | 0 | 0 |
| | | *Zonocerus veriegatus* | 5 | 1.53 | 17 | 8.95 |
| | Isoptera | *Cryptotermes* sp | 67 | 20.49 | 79 | 41.58 |
| TOTAL | | | 327 | | 190 | |

Ni = Number of Individual; (%) = abundance.

**Table 4:** Community structure of soil macroinvertebrate class from the two sampling sites

| | Fallowed land | | Cultivated land | |
|---|---|---|---|---|
| Class | Numerical abundance | (%) Abundance | Numerical abundance | (%) Abundance |
| Clitellata | 45 | 13.8 | 21 | 11.1 |
| Arachnida | 4 | 1.2 | 0 | 0 |
| Diplopoda | 34 | 10.4 | 11 | 5.8 |
| Insecta | 244 | 74.6 | 153 | 80.5 |

**Table 5:** The diversity indices of the soil macro-invertebrates of the two sites

| Diversity indices | Fallowed land | Cultivated land |
|---|---|---|
| Taxa_S | 16 | 9 |
| Individuals | 327 | 190 |
| Dominance_D | 0.1212 | 0.2353 |
| Shannon_H | 2.332 | 1.765 |
| Evenness | 0.644 | 0.649 |
| Margalef index | 2.591 | 1.529 |

## 4.0. Conclusion

In conclusion, human activities such as soil cultivation practices could greatly impact negatively on the population dynamics of soil macroinvertebrates. The impact does not only caused a shift in the soil physico-chemical properties but also greats a gap in the ecosystem processes due to the decline or elimination of some soil macroinvertebrate species, which play important ecological roles in soil nutrient recycle and other soil ecosystem functions.

## References

Alonso-Zarazaga, M. A. and Domingo-Quero, T. (2010). Soil and Litter Sampling, including MSS. *ABC TAXA*, 8, pp. 173-212.

Battigelli, J. P. and Marshall, V. G. (1993). Relationships Between Soil Fauna and Soil Pollutans. In: Proceedings of the Forest Ecosystem Dynamics workshop, FRDA II report 210. Government of Canada, Province of British Columbia, pp. 31-34.

Barrios, E., Pashanasi, B., Constantino, R. and Lavelle, P. (2002). Effects of land-use system on the soil macro-fauna in western Brazilian Amazonia. *Bioliogy Fertilized Soils*, 35, pp. 338-347.

Barrios, E., Cobo, J. G., Rao, I. M., Thomas, R. J., Amezquita, E., Jimenez, J. J., Rondon, M. A. (2005). Fallow management for soil fertility recovery in tropical Andean agroecosystems in Colombia. *Agricultural Ecosystem Environment*, 110, pp. 29-42.

Borror, D. J. and White, R. E. (1970). A field guide to the Insects of America North of Mexico. 404.

Bossuyt, H., Six, J. and Hendrix, P.F. (2005). Protection of soil carbon by micro-aggregates within earthworm casts. *Soil Biology Biochemistry*, 37, pp. 251-258.

Brown, G. G., Edwards, C. A. and Brussard, L. (2004). *How earthworms affect plant growth burrowing into the mechanisms*. In: Earthworm Ecology (ed. C. A. Edwards) 13-49. CRC Press, Boca Raton, FL.

Bufebo, B. and Elias, E. (2020). Effects of land use/land cover changes on selected soil physical and chemical properties in Shenkolla watershed, south Central Ethiopia. *Advances in Agriculture*, 2020, pp. 1–8. https://doi.org/10.1155/2020/5145483.

Camara, R., Santos, G. L., Pereira, M. G., Silva, C. F., Silva, V. F. V. and Silva, R. M. (2018): Effects of natural Atlantic forest regeneration on soil fauna, Brazil. Flor@m.;25:e20160017. https://doi.org/10.1590/2179-8087.001716

Collins, N. M. (1983). Termite populations and their role in litter removal in Malaysian rainforests. In: Sutton, S.L (Eds.). In *Tropical Rainforests: Ecology and Management*, (S.L. Sutton, T.C. Whitmore and A. C. Chadwick, Eds), pp. 311-325, Blackwell Science, Oxford.

Dangerfield, J. M. and Milner, A. E. (1996). Millipede fecal pellet production in selected natural and managed habitats of Southern Africa: implications for litter dynamics. *Biotropica*, 28(1), pp. 113-120. DOI: 10.2307/2388776.

Elias, P. F., Okothc, E. M. A., and Smalingd (2019). Explaining bread wheat (Triticum aestivum) yield differences by soil properties and fertilizer rates in the highlands of Ethiopia. https://doi.org/10.1016/j.geoderma.2018.12.020.

HopKins, S. (2002). A key to springtail of Britain and Ireland, AIDGAP.

Jamel, H. (2017). To determine moisture content of soil by oven drying method. AASHO Designation: T-265. ASTM D-2216-90.

Konakwan, K, Bora, C., Ahmet, H. A., Craigh, H, B. (2015). Effect of pH on leaching mechanisms of elements rom fly as mixed soils. *Elsevier,* 140, pp. 788 – 802.

Lagerlöf, J., Goffre, B and Vincent, C. (2002). The importance of field boundaries for earthworms (Lumbricidae) in the Swedish agricultural landscape. *Agricultural Ecosystem Environment*, 89, pp. 141–151.

Lavelle, P. (1997): Faunal activities and social processes: Adaptive strategies that determines ecosystem function. *Advance Ecology Research,* 27, pp. 93-132.

Madge, D. C. and Sharma, G. D. (1969). Soil Zoology, Ibadan University Press, 26. In. Eni, G. E, Andem, BA, Oku, EE, Cletus, JU and Offem, EA (2014). Seasonal Distribution, Abundance and Diversity of Soil Arthropods in Farmlandsaround Workshops in Calabar Metropolis, Southern Nigeria. *Journal of Academia and Industrial Research (JAIR)*, 2(8), pp. 446-452.

Menta, C. (2012). Soil fauna diversity-function, soil degradation, biological indices, soil restotration. In Biodiversity Conservaton and Utilization in a Diverse World, G. A. Lameed, Ed., IntechOpen, London, Uk. 49-94.

Mora, P., Seuge, C., Chotte, J. L. and Rouland, C. (2003). Physico-chemical typology of the biogenic structures of termites and earthworms: a comparative analysis. *Biology and Fertility of Soils,* 37, pp. 245-249.

Moreira, F. M., Huising, E. J. and Bignell, D. (2008). A handbook of tropical soil biology: Sampling and characterization of below-ground biodiversity. London: Earthscan.

Mutema, M., Mafongoya, P. L., Nyagumbo, I. and Chikukura, L. (2013). Effects of crop residues and reduced tillage on macrofauna abundance. *Journal of Organic Systems*, 8(1), p. 16.

Nanganoa, L. T., Okolle, J. N., Missi, V., Tueche, J. R., Levai, L. D. and Njukeng, J. N. (2019). Impact of Different Land-Use Systems on Soil Physicochemcial Properties and Macrofauna Abundance in the Humid Tropics of Cameroon. *Applied and Environmental Soil Science*, 2019, p. 9. DOI: 10.11556/2019/5701278.

Pulleman, M. M., Six, J., Van Breemen, N. and Jongman, A. G. (2004). Soil organicmatter distribution and microaggregate characteristics as affected by agricultural management and earthworm activity. *European Journal of Soil Science*, 10, pp. 1-15.

Rossi, J. P. and Blanchart, E. (2005). Seasonal and land-use induced, variations of soil macrofauna composition in the Western Ghats, Southern India. *Soil Biology and Biochemistry*, 37(6), pp. 1093-1104. DIO:10.10161

Rossi, J. P., Celini, L., Mora, P., Mathieu, J., Lapied, E., Nahmani, J. and Lavelle, P. (2010). Decreasing fallow duration in tropical slash-and-burn agriculture alters soil macroinvertebrate diversity: a case study in southern French Guiana. *Agriculture, ecosystems & environment*, 135(1), pp. 148-154.

Sekamatte, B. M., Ogenga-Latigo, M. and Russell-Smith, A. (2003). Effects of maize and legume intercrops on termite damage to maize, activity of predatory ants and maize yield in Uganda. *Crop production*, 22, pp. 87-93.

Sileshi, G., Mafonoya, P. L., Kwesiga, F. and Nkunika, P. (2005). Termite damage to maize grown in agroforestry systems, traditional fallows and monoculture on nitrogen-limited soil in eastern Zambia. *Agricultural and Forest Entomology*, 7, pp. 61-69.

Somasuundaram, J., Singh, R. K., Parandiyal, A. K., Ali, S., Chauhau, V., Sinha, N. K., *et al*. (2013). Soil properties under different land use systems in parts of Chambal region of Rajasthan. *Journal of Agricultural Physics*, 13(2), pp. 139-147.

**Cite this article as:**
Akpan A. U., Chukwu M. N., Esenowo I. K., Johnson M. and Archibong D. E. 2021. Effect of Fallowed and Cultivated Land Use Systems on the Composition and Abundance of Soil Macro-invertebrates Assemblage in Uruk Osung Community, Akwa Ibom State, Nigeria. *Nigerian Journal of Environmental Sciences and Technology*, 5(1), pp. 281-289. https://doi.org/10.36263/nijest.2021.01.0278

**NIGERIAN JOURNAL OF ENVIRONMENTAL SCIENCES AND TECHNOLOGY**

**(NIJEST)**

## Format for Preparing Articles

Submission of a paper to NIJEST implies that the corresponding author has obtained the permission of all authors, and that all authors have read the paper and guarantee that the paper is an original research work, that the data used in carrying the research will be provided to NIJEST Editors if requested, and that the paper has not been previously published and is not currently under review for publication by another journal.

The Corresponding Author is responsible for ensuring that all figures, tables, text, and supporting materials are properly cited and, when necessary, obtaining permission for reprinting copyrighted material.

[Submit your manuscript as an attached file to the email address: editor-in-chief@nijest.com]

### Submission of Paper for Review

**A. Structure of Paper**

Paper submitted for review should generally be structured in the format given below:

Abstract
1.0 Introduction
2.0 Materials and Methods
3.0. Results and Discussion
4.0 Conclusions
Acknowledgments (If any)
References

***NOTE:*** *The abstract should be a single paragraph of not more than 300 words and summarizes the content of the paper. At the end of the abstract, 5 – 7 keywords should be provided for indexing purpose.*

**B. Paper/Article Format**

Papers accepted for publication in NIJEST, will be required to be prepared in the format for publication according to NIJEST guidelines given below:

**1. Author Affiliations**

Do not abbreviate institution names. Do not use designations such as MBA, CPA or Ph.D.

**2. Font Size and Style**

i) Paper Title: Title case, Size 16, Bold, Times New Roman
ii) Authors Name and Affiliations: Title case, Size 12, Times New Roman
iii) Main headings: Title case, Size 11, Bold, Times New Roman
iv) Sub headings: Title case, Size 11, Times New Roman
v) Document Text (Body of paper): Sentence case, Size 11, justified, Times New Roman
vi) Text within tables: Sentence case, Size 8, Times New Roman
vii) Notes to tables: Sentence case, Size 8, italic, Times New Roman
viii) Tables & Figures Heading: Title case, Size 11, Times New Roman
ix) Text within figures: Sentence or Title case, Size 8, Arial

**3. Acronyms**

The use of acronyms is allowed everywhere in the paper EXCEPT in the title or abstract. Acronyms should be defined when fist used in the paper.

**4. Tables**

Place tables in the text as you wish them to appear and in conjunction with the corresponding discussion. Tables must include a title and be numbered consecutively as “Table 1: Description” and so forth. The title must appear outside the table. Titles for tables should be in title case in a Times New Roman Font of 11. Tables must be black and white only. Do not use colour in tables. Define all variables in your table within the table or in the note to the table and in the text of the document.

**5. Figures**

Place figures in the text as you wish them to appear and in conjunction with the corresponding discussion. Figures must be numbered consecutively as “Figure 1:

Description" and so forth. Use the word "Figure" as the label. Titles for figures should be separate from the figure itself and in title case, in a Times New Roman Font of 11. Use an Arial font of 8 for text within figures.

## 6. Equations

Create Equations using the Microsoft Word Equation Tool. Number equations consecutively on the right margin. For example:

$$y = A + Bx_1 + Cx_2 + Dx_3 \quad (1)$$

## 7. References

All reference works cited in the paper must appear in a list of references that follow the formatting requirements of NIJEST given below. References not cited should not be listed. Citing and Listing of references should be according to the following:

Citing references in the body of the paper

i) For citations with one author, include author's name and year e.g. (Osamuyi, 2016). For two authors, include both authors' names e.g. (Ehiorobo and Izinyon, 2015). For citations with three or more authors, list only the first author's name followed by *et al*. e.g. (Osamuyi *et al.*, 2014)

ii) Cite references chronologically e.g. (Osamuyi *et al.* 2014; Ehiorobo and Iznyon, 2015; Osamuyi, 2016)

iii) For multiple citations with the same first author, list single-author entries by year using 2014a, 2014b, etc. For example: (Osamuyi *et al.*, 1996a).

Listing of References

In the reference section at the end of the document, include a single space between each reference. Do not indent references. For journal articles, be sure to include, author names, year of publication, article title, Journal Name, volume number, issue number and page numbers. References should appear according to the following:

i) List references with three or more authors only by year and without regard to number of authors or alphabetical rank of authors beyond the first.

ii) For articles with more than five authors, list the first five names and then *et al*.

iii) For multiple citations with the same first author published in the same year, list entries by year using 1996a, 1996b, etc. Alphabetize by second author.

iv) Sample journal article citation:

Izinyon, O.C. and Ehiorobo, J.O., (2014). L-moments approach for flood frequency analysis of river Okhuwan in Benin-Owena River basin in Nigeria. *Nigerian Journal of Technology*, 33(1), pp.10-19

v) Sample book citation:

Bond, W.R., Smith, J.T., Brown, K.L. & George, M., (1996). *Management of small firms*, McGraw-Hill, Sydney.

vi) Sample chapter-in-book citation:

Beadle, G. W., (1957). The role of the nucleus in heredity, pp. 3-22 in *The Chemical Basis of Heredity*, edited by W. D. McElroy and B. Glass. Johns Hopkins Press, Baltimore.

vii) Sample website citation:

Ehiorobo, J. (2014). *Fire Safety Engineering*. [online] Engineering Safety. Available at: http://www.firesafetyengineering.com/ehiorobo [Accessed 12 Nov. 2016].

ISSN 2734-259X
(Print)
ISSN 2734-2603
(Electronic)